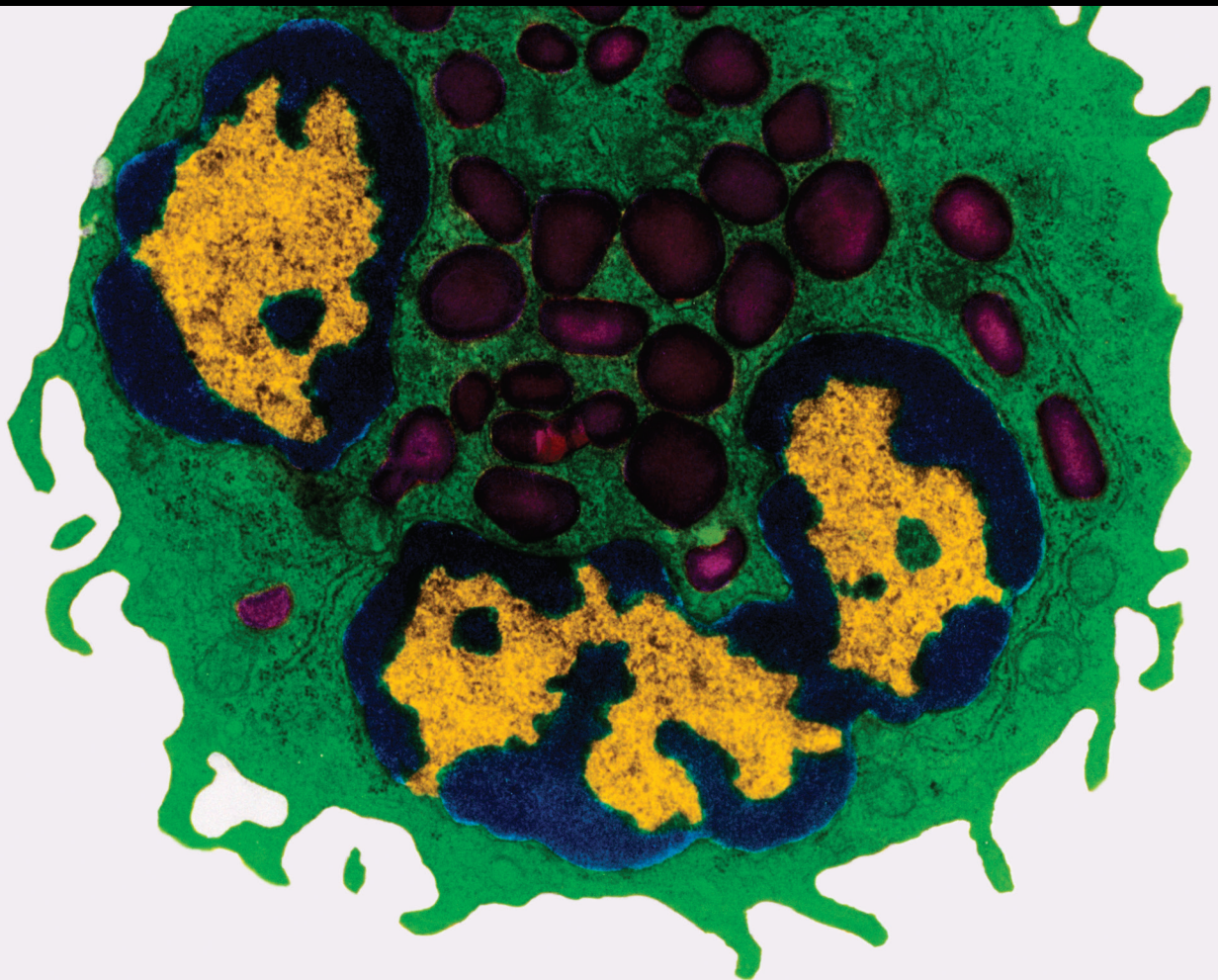


The Impact of nutrients, dietary components and derivatives on the Gut Microbiota and inflammation-related diseases, from molecular basis to therapy

Lead Guest Editor: Hongmei Jiang

Guest Editors: Guan Yang, Li Zhang, and Xiaolu Jin





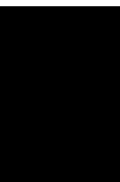
**The Impact of nutrients, dietary components
and derivatives on the Gut Microbiota and
inflammation-related diseases, from molecular
basis to therapy**

Mediators of Inflammation

The Impact of nutrients, dietary components and derivatives on the Gut Microbiota and inflammation-related diseases, from molecular basis to therapy

Lead Guest Editor: Hongmei Jiang


Guest Editors: Guan Yang, Li Zhang, and Xiaolu Jin







Copyright © 2020 Hindawi Limited. All rights reserved.

This is a special issue published in “Mediators of Inflammation.” All articles are open access articles distributed under the Creative Commons Attribution License, which permits unrestricted use, distribution, and reproduction in any medium, provided the original work is properly cited.

Chief Editor







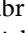
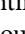
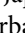
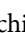
Anshu Agrawal , USA

Associate Editors

Carlo Cervellati , Italy
Elaine Hatanaka , Brazil
Vladimir A. Kostyuk , Belarus
Carla Pagliari , Brazil





Academic Editors

Amedeo Amedei , Italy
Emiliano Antiga , Italy
Tomasz Brzozowski , Poland
Daniela Caccamo , Italy
Luca Cantarini , Italy
Raffaele Capasso , Italy
Calogero Caruso , Italy
Robson Coutinho-Silva , Brazil
Jose Crispin , Mexico
Fulvio D'Acquisto , United Kingdom
Eduardo Dalmarco , Brazil
Agnieszka Dobrzyn, Poland
Ulrich Eisel , The Netherlands
Mirvat El-Sibai , Lebanon
Giacomo Emmi , Italy
Claudia Fabiani , Italy
Fabíola B Filippin Monteiro , Brazil
Antonella Fioravanti , Italy
Tânia Silvia Fröde , Brazil
Julio Galvez , Spain
Mirella Giovarelli , Italy
Denis Girard, Canada
Markus H. Gräler , Germany
Oreste Gualillo , Spain
Qingdong Guan , Canada
Tommaso Iannitti , United Kingdom
Byeong-Churl Jang, Republic of Korea
Yasumasa Kato , Japan
Cheorl-Ho Kim , Republic of Korea
Alex Kleinjan , The Netherlands
Martha Lappas , Australia
Ariadne Malamitsi-Puchner , Greece
Palash Mandal, India
Joilson O. Martins , Brazil
Donna-Marie McCafferty, Canada
Barbro N. Melgert , The Netherlands


Paola Migliorini , Italy
Vinod K. Mishra , USA
Eeva Moilanen , Finland
Elena Niccolai , Italy
Nadra Nilsen , Norway
Sandra Helena Penha Oliveira , Brazil
Michal A. Rahat , Israel
Zoltan Rakonczay Jr. , Hungary
Marcella Reale , Italy
Emanuela Roscetto, Italy
Domenico Sergi , Italy
Mohammad Shadab , USA
Elena Silvestri, Italy
Carla Sipert , Brazil
Helen C. Steel , South Africa
Saravanan Subramanian, USA
Veendamali S. Subramanian , USA
Taina Tervahartiala, Finland
Alessandro Trentini , Italy
Kathy Triantafilou, United Kingdom
Fumio Tsuji , Japan
Maria Letizia Urban, Italy
Giuseppe Valacchi , Italy
Kerstin Wolk , Germany
Soh Yamazaki , Japan
Young-Su Yi , Republic of Korea
Shin-ichi Yokota , Japan
Francesca Zimetti , Italy

Contents






The Expression Pattern and Regulatory Mechanism of the G0/G1 Switch Gene 2 (*G0S2*) in the Pathogenesis and Treatment of AChR Myasthenia Gravis (MG)

Liqun Xu , Zhibin Li, Yi Li, Zhaohui Luo , Yuebei Luo, Bo Xiao , and Huan Yang 
Research Article (11 pages), Article ID 4286047, Volume 2020 (2020)

The Potential of Food Protein-Derived Bioactive Peptides against Chronic Intestinal Inflammation

Wanying Zhu, Liying Ren, Li Zhang, Qinqin Qiao, Muhammad Zahid Farooq, and Qingbiao Xu 
Review Article (15 pages), Article ID 6817156, Volume 2020 (2020)

Protection of Fecal Microbiota Transplantation in a Mouse Model of Multiple Sclerosis

Kanglan Li , Shouchao Wei, Li Hu, Xiaojian Yin, Yingren Mai, Chunmei Jiang, Xiaoping Peng, Xingxing Cao, Zhongkai Huang, Haihong Zhou, Guoda Ma , Zhou Liu , Huiliang Li , and Bin Zhao 
Research Article (13 pages), Article ID 2058272, Volume 2020 (2020)

The Effects of Dietary Glycine on the Acetic Acid-Induced Mouse Model of Colitis

Xin Wu , Yongmin Zheng , Jie Ma , Jie Yin , and Shuai Chen 
Research Article (8 pages), Article ID 5867627, Volume 2020 (2020)



Higher Serum Neuropeptide Y Levels Are Associated with Metabolically Unhealthy Obesity in Obese Chinese Adults: A Cross-Sectional Study

Hao-Neng Tang , Fen Xiao, Ya-Ru Chen, Si-Qi Zhuang, Yue Guo, Hui-Xuan Wu, and Hou-De Zhou 
Research Article (9 pages), Article ID 7903140, Volume 2020 (2020)





Comprehensive Analysis of a circRNA-miRNA-mRNA Network to Reveal Potential Inflammation-Related Targets for Gastric Adenocarcinoma

YunXia Liu , YeFeng Xu , Feng Xiao, JianFeng Zhang, YiQing Wang, YongWei Yao, and JieWen Yang
Research Article (15 pages), Article ID 9435608, Volume 2020 (2020)


The Depletion of ABI3BP by MicroRNA-183 Promotes the Development of Esophageal Carcinoma

Hongfei Cai, Yang Li, Da Qin, Rui Wang , Ze Tang, Tianyu Lu, and Youbin Cui 
Research Article (8 pages), Article ID 3420946, Volume 2020 (2020)





Research Progress on NK Cell Receptors and Their Signaling Pathways

Yingying Chen , Dan Lu , Alexey Churov , and Rong Fu 
Review Article (14 pages), Article ID 6437057, Volume 2020 (2020)


The Pneumococcal Polysaccharide-Tetanus Toxin Native C-Fragment Conjugate Vaccine: The Carrier Effect and Immunogenicity

Rui Yu , Junjie Xu, Tao Hu , and Wei Chen 
Research Article (11 pages), Article ID 9596129, Volume 2020 (2020)



Anti-Inflammatory Effect of a Peptide Derived from the Synbiotics, Fermented *Cudrania tricuspidata* with *Lactobacillus gasseri*, on Inflammatory Bowel Disease

Jimyong Ha , Hyemin Oh , Nam Su Oh, Yeongeun Seo , Joohyun Kang, Min Hee Park, Kyung Su Kim, Shin Ho Kang, and Yohan Yoon 
Research Article (8 pages), Article ID 3572809, Volume 2020 (2020)





The Effects of Dietary Nutrition on Sleep and Sleep Disorders

Mingxia Zhao , Houzhen Tuo, Shuhui Wang, and Lin Zhao
Review Article (7 pages), Article ID 3142874, Volume 2020 (2020)



Tryptophan Metabolism, Regulatory T Cells, and Inflammatory Bowel Disease: A Mini Review

Xueyan Ding , Peng Bin, Wenwen Wu, Yajie Chang, and Guoqiang Zhu 
Review Article (10 pages), Article ID 9706140, Volume 2020 (2020)

Protein Level and Infantile Diarrhea in a Postweaning Piglet Model

Jing Gao , Jie Yin , Kang Xu, Hui Han, ZeMin Liu, ChenYu Wang, TieJun Li , and YuLong Yin 
Research Article (15 pages), Article ID 1937387, Volume 2020 (2020)




Effects of GABA Supplementation on Intestinal SIgA Secretion and Gut Microbiota in the Healthy and ETEC-Infected Weanling Piglets

Yuanyuan Zhao, Jing Wang , Hao Wang, Yonggang Huang, Ming Qi, Simeng Liao, Peng Bin, and Yulong Yin 
Research Article (17 pages), Article ID 7368483, Volume 2020 (2020)



Organ-Protective Effects and the Underlying Mechanism of Dexmedetomidine

Naren Bao  and Bing Tang 
Review Article (11 pages), Article ID 6136105, Volume 2020 (2020)



Detection and Prognosis of Prostate Cancer Using Blood-Based Biomarkers

Wei Jin , Xiang Fei, Xia Wang, Yan Song , and Fangjie Chen 
Review Article (11 pages), Article ID 8730608, Volume 2020 (2020)




Regulation of Iron Homeostasis and Related Diseases

Yikun Li, Xiali Huang, Jingjing Wang, Ruiling Huang , and Dan Wan 
Review Article (11 pages), Article ID 6062094, Volume 2020 (2020)



Dexmedetomidine Protects against Ischemia and Reperfusion-Induced Kidney Injury in Rats

Naren Bao  and Di Dai 
Research Article (8 pages), Article ID 2120971, Volume 2020 (2020)

The Enlargement of Abdominal Lymph Nodes Is a Characteristic of Autoimmune Liver Disease

Yongjuan Wang , Xiuxiu Xu, Maojuan Ran, Xiaopei Guo, Lu Zhou , Xi Wang, Bangmao Wang, and Jie Zhang 
Research Article (7 pages), Article ID 3631625, Volume 2020 (2020)

The Therapeutic Potential of MicroRNAs in Atrial Fibrillation

Xiaona Xu , Zhiqiang Zhao, and Guangping Li 
Review Article (6 pages), Article ID 3053520, Volume 2020 (2020)






Contents

Serine Deficiency Exacerbates Inflammation and Oxidative Stress via Microbiota-Gut-Brain Axis in D-Galactose-Induced Aging Mice

Fengen Wang, Hongbin Zhou, Ligang Deng, Lei Wang, Jingqing Chen , and Xihong Zhou 

Research Article (7 pages), Article ID 5821428, Volume 2020 (2020)

Effects of Shikonin on the Functions of Myeloid Dendritic Cells in a Mouse Model of Severe Aplastic Anemia

Mengying Zheng , Bingnan Liu , Yuanyuan Shao , Luogang Hua , Rong Fu , Huaquan

Wang , Ting Wang , Weiwei Qi, Zonghong Shao , and Chunyan Liu 

Research Article (10 pages), Article ID 9025705, Volume 2020 (2020)

Research Article

The Expression Pattern and Regulatory Mechanism of the G0/G1 Switch Gene 2 (*G0S2*) in the Pathogenesis and Treatment of AChR Myasthenia Gravis (MG)

Liqun Xu , Zhibin Li, Yi Li, Zhaohui Luo , Yuebei Luo, Bo Xiao , and Huan Yang 

Department of Neurology, Xiangya Hospital, Central South University, Changsha, Hunan 410008, China

Correspondence should be addressed to Bo Xiao; xiaobo_xy@126.com and Huan Yang; yangh69@126.com

Received 22 February 2020; Revised 2 June 2020; Accepted 18 July 2020; Published 30 September 2020

Guest Editor: Guan Yang

Copyright © 2020 Liqun Xu et al. This is an open access article distributed under the Creative Commons Attribution License, which permits unrestricted use, distribution, and reproduction in any medium, provided the original work is properly cited.

This study is aimed at exploring the expression pattern and methylation level of *G0S2* in the peripheral blood mononuclear cells (PBMCs) of myasthenia gravis (MG) patients with positive acetylcholine receptor (AChR) autoantibodies and revealing the relationship between the *G0S2* methylation pattern and MG. The relationship between the NFAT family members and *G0S2* was explored to reveal the regulatory mechanism of *G0S2* in the pathogenesis and treatment of AChR MG. Moreover, we attempted to demonstrate the potential therapeutic mechanism of tacrolimus in AChR MG. The relative *G0S2* expression level in the PBMCs of healthy people was compared with that in the PBMCs of AChR MG patients with quantitative real-time PCR (qRT-PCR). The methylation frequency of the *G0S2* promoter was detected by bisulfite sequencing PCR (BSP) and pyrosequencing. A dual-luciferase reporter system was used to reveal the relationship between the *G0S2* promoter and nuclear factor of activated T cells 5 (*NFAT5*). The qRT-PCR results showed that *G0S2* expression was significantly upregulated in the B cells and CD8+ T cells of AChR MG patients but not in the CD4+ T cells, and these expression differences were significantly associated with a decrease in *G0S2* methylation. *NFAT5*, which was speculated to bind to island 1 (p1) in the *G0S2* promoter, may regulate the lymphocyte balance by regulating *G0S2* gene expression but failed to affect the methylation of the *G0S2* promoter. Tacrolimus therapy-induced methylation and overexpression of *NFAT5* could significantly reduce the expression of *G0S2* in AChR MG patients. The *G0S2* gene was remarkably upregulated in the PBMCs of MG patients. *NFAT5* may affect transcription initiation and downregulate *G0S2* expression through p1 in the promoter, thus controlling *G0S2* gene expression and regulating the lymphocyte balance. Therefore, *G0S2* could be an immune regulatory factor in both AChR MG occurrence and treatment with tacrolimus.

1. Introduction

Myasthenia gravis (MG) is an autoimmune disease characterized by a transmission disorder of the neuromuscular junction. The molecular immunopathology of MG is due to the presence of circulating autoantibodies that specifically target the acetylcholine receptor (AChR), muscle-specific tyrosine kinase (MuSK), or low-density lipoprotein (LDL) receptor-related protein 4 (LRP4). Patient-derived AChR, MuSK, and LRP4 autoantibodies in MG are demonstrably pathogenic (B cells in the pathophysiology of myasthenia gravis), and patients most often harbor only one of these autoantibody specificities. In approximately 75–85% of MG

patients, AChR autoantibodies are detectable [1, 2]. The attack on postsynaptic components or functionally related molecules by AChR antibodies is regarded as the main pathogenesis of MG. Our understanding of MG immunopathology remains incomplete. It appears that the mechanism used by B cells for autoantibody production in AChR and MuSK MG differs, although details on both are needed to understand the immunopathology that will guide the development of more effective therapies [3].

It is generally agreed that the cell cycle plays an important role in regulating the clonal deletion of self-antigen-reactive lymphocytes, maintaining immune homeostasis and preventing the occurrence of autoimmune diseases [4].

Peripheral blood mononuclear cells (PBMCs) are suspended in blood plasma, which circulates these immune-related cells throughout the body [5]. Investigating PBMC disorders could represent a method of better understanding the pathogenesis of MG. Most MG patients could achieve satisfactory improvement via the application of immunosuppressive therapy, such as glucocorticoid [3]. However, the long-term use of corticosteroids is associated with severe adverse events. To prevent these side effects, a novel immunosuppressant is desired. Tacrolimus (FK-506), which is similar to cyclosporin A (CsA), is a kind of calcineurin inhibitor that can restrain calcium-dependent phosphatase calcineurin and suppress the immune response [6]. Compared to CsA, tacrolimus is more effective but has fewer side effects [7], and its benefits for MG treatment have been proven in several studies and recommended by international experts' consensus. However, until now, the therapeutic mechanism of tacrolimus on MG has not been elucidated.

A previous study suggested that cyclosporin A could downregulate the expression level of G0/G1 Switch Gene 2 (*G0S2*) in cultured human blood mononuclear cells [8]. Tacrolimus may share the same therapeutic mechanism with cyclosporin A in the treatment of MG. Thus, the *G0S2* may be a potential therapeutic site for tacrolimus. In a previous report, the *G0S2* gene was found in PBMCs and recognized as a potential tumor suppressor gene [9]. Studies on the cell cycle suggest that *G0S2* expression is related to the G0 to G1 transition; however, elevated levels of *G0S2* inhibited cell proliferation and the G0 to G1 transition [10]. Additionally, other studies have suggested that *G0S2* is significantly upregulated in the lymphocytes of immunodeficient and systemic lupus erythematosus patients [11, 12]. We screened the integration of aberrant lncRNA and mRNA expression changes in the PBMCs from MG patients in our previous study [13]. The lncRNA oebiotech_11933, which had 3 cis genes (*C1orf74*, *G0S2*, and *TRAF3IP3*), was one of the 12 differently expressed lncRNAs from the MG patients. The expression of the *G0S2* gene was significantly higher/lower in MG patients than in healthy volunteers at the mRNA level. Based on these findings, we focused on this gene and investigated the function of *G0S2*. Moreover, the promoter region of *G0S2* contains potential binding sites for nuclear factor of activated T cells (*NFAT*) [14]. Moreover, the binding sites were located in the promoter region at CpG sites, so the *NFAT* gene family members may affect the *G0S2* expression level by affecting methylation. In our study, we implemented a luciferase assay and confirmed the predicted that the inhibitory regulation of *NFAT5* and *G0S2* could be implicated in the pathophysiology of AChR MG. *NFAT5* encodes a transcription factor belonging to a family of proteins that plays a central role in regulating gene transcription during the immune response induced by osmotic stress in mammalian cells. *NFAT5* is vital to cell cycle progression and T cell proliferation [15].

In the present study, we aimed to explore the expression pattern and methylation level of *G0S2* in the PBMCs of AChR MG patients and reveal the relevant relationship between *G0S2* patterns and AChR MG. The relationships between *NFAT5* and *G0S2* in B cells and T cells were explored to reveal the different regulatory mechanisms in dif-

ferent lymphocyte subsets during the pathogenesis and treatment of MG. In addition, our future studies evaluating the effects of tacrolimus on CD8+ T cells and B cells in AChR MG patients should be particularly informative.

2. Material and Methods

2.1. Patients. This study was approved by the Ethics Committee of Xiangya Hospital (No. 201503233); all patients provided written informed consent. All experiments were performed according to the relevant guidelines and regulations. PBMC samples were obtained from MG patients with positive AChR antibodies and control patients without myopathy. Peripheral blood samples from 50 AChR MG patients and 30 healthy individuals were collected for gene expression analysis. All cell and tissue samples were used for the cell apoptosis assay and quantitative real-time PCR (qRT-PCR). MG patients ranged from 18 to 70 years old. All patients were initially treated as outpatients and did not take any immunosuppressants in the 3 months prior to the start of the study. They did not have any autoimmune diseases (ADs). The peripheral blood samples from the control group were collected from the medical examination center (MEC).

2.2. Reagents. TRIzol Reagent (Cat. No. 15596-018) and an anti-AmIg-FITC antibody were obtained from Invitrogen, Inc. SYBR® Premix Ex Taq™ (Perfect Real Time), and the Genomic DNA Extraction Kit were purchased from TaKaRa, Inc. (Otsu, Shiga, Japan). The ReverTra Ace® qPCR RT Kit was purchased from TOYOBO, Inc. The EpiTect Bisulfite Kit was purchased from Qiagen, Inc.

2.3. Monocyte Isolation. Approximately 5 mL of diluted peripheral blood (heparinized) was further diluted with Hank's buffer at a ratio of 1:3 and was slowly added to 5 mL lymphocyte separation medium (Percoll, Solarbio, Beijing) in a 15 mL centrifuge tube. The mononuclear leukocyte layer was isolated by centrifugation at 1200 rpm for 20 min. Cells at the interface were collected and slowly washed with 5 mL of sterile Hank's buffer and centrifuged at 1000 rpm for 5 min. Then, the cell pellets were washed and centrifuged 2-3 times with Hank's buffer using the same parameters. After that, magnetic beads were used to separate the CD4+ T cells from the CD19+ B cells. Total PBMCs from MG patients, PBMCs from healthy controls, CD4+ T cells from MG patients, and CD19+ B cells from MG patients were resuspended in DMEM complete medium (HyClone, USA) with 15% fetal bovine serum (Gibco, USA). The cell suspension was seeded in a culture flask (Corning, USA).

2.4. RNA Isolation and Quantitative Real-Time PCR. TRIzol Reagent (Invitrogen, Cat. No. 15596-018) was used to extract the total RNA from the peripheral blood and thymus tissues of MG subjects (with and without thymoma) and control patients according to the manufacturer's instructions. The total RNA concentrations were measured with a UV spectrophotometer. Reverse transcription was then performed with a ReverTra Ace® qPCR RT Kit (TOYOBO) after the genomic DNA was removed. (SYBR Premix Ex Taq™, TaKaRa, Otsu, Shiga, Japan) in triplicate with sequence-specific PCR

TABLE 1: Primers used in the study.

Primer name	Primer sequence (5' -3')	Utilization
G0S2-F	GAGAGGAGGAGAACGCTGAG	qRT-PCR
G0S2-R	CTTCTGGGCCATCATCTCCT	qRT-PCR
DNMT3B-F	CAAACCCAACAACACGCAAC	qRT-PCR
DNMT3B-R	ATCTTCCAGGCTGCTCTTGT	qRT-PCR
DNMT1-F	ACCAAGAACGGCATCCTGTA	qRT-PCR
DNMT1-R	GCTGCCTTTGATGTAGTCGG	qRT-PCR
NFAT1-F	AACACCAAAGTCCTGGAGATAC	qRT-PCR
NFAT1-R	AATGTCCGTCTCGCCTTTC	qRT-PCR
NFAT2-F	AATTCTCTGGTGGTTGAGATCC	qRT-PCR
NFAT2-R	TACTGGCTTCGCTTTCTCTTC	qRT-PCR
NFAT5-F	GATTCAGCCCAAGGCATACA	qRT-PCR
NFAT5-R	GCAGCTGACTAGAAGCAGAAA	qRT-PCR
NAPDH-F	GCCAAAAGGGTCATCATCTC	qRT-PCR
NAPDH-R	GTAGAGGCAGGGATGATGTTTC	qRT-PCR
G0S2-bsp-1F	TAATGTTAGGTTGTTTTGGATAAGG	BSP PCR
G0S2-bsp-1R	ACTACAACCTCTCCCAATTAATAAACTC	BSP PCR
G0S2-bsp-2F	TTTTAATTGGGAGAGTTGTAGTTGT	BSP PCR
G0S2-bsp-2R	ACCAAAAAAATCAACTCCTAAACC	BSP PCR

primers on a StepOne Plus system (Applied Biosystems, Foster City, CA, USA). The *GAPDH* gene was used as an internal control for each sample. The primer sequences are listed in Table 1. PCR amplification for all detected genes was performed in triplicate under the following conditions: initial denaturation at 95°C for 30 s, followed by 40 cycles of 95°C for 5 s and 60°C for 34 s. The relative quantification of gene expression was normalized against *GAPDH* by using the $2^{-\Delta\Delta CT}$ method.

2.5. Analysis of the *G0S2* Promoter Methylation. Genomic DNA was isolated from PBMCs. The present study selected the region from -666 bp to +31 bp of the *G0S2* genomic gene sequence as the target fragment. Bioinformatics analysis showed that there are two different CpG islands in the *G0S2* gene promoter region (island 1 (p1) and island 2 (p2) of the *G0S2* promoter). The primers for both p1 and p2 located in the *G0S2* promoter region were designed by the Methyl Primer Express version 1.0 software (Thermo Fisher Scientific, Inc.). The primer sequences are listed in Table 1.

Genomic DNA samples from the PBMCs of CD4+ T cells, CD8+ T cells, and CD19+ B cells from MG patients and healthy control, respectively, were extracted according to the instructions provided with the Genomic DNA Extraction Kit; then, the samples were analyzed by bisulfite sequencing PCR (BSP) with the EpiTect Bisulfite Kit, which detected the methylation status of the CpG islands at the *G0S2* gene promoter regions of all samples [16, 17]. PCR was used to amplify p1 and p2 in the *G0S2* promoter and was performed in a total volume of 50 μ L with the following reagents: 1 μ L cDNA template, 1 μ L G0S2-bsp-1F/R for p1 (or G0S2-bsp-2F/R for p2), 1 μ L DNA polymerase, 5 μ L 10 \times PCR buffer (Mg²⁺ plus), 4 μ L dNTP mixture, and 37 μ L

RNase-free ddH₂O. When the CpG sites in the region analyzed by methylation-specific PCR (MSP) are methylated, the methylated (M) band will appear, while the demethylated (U) band will be present when the sites are demethylated. Occasionally, both bands could be present if the sites are partially methylated. The PCR product was purified and cloned into a pMD-18T vector. The positive clones were selected and sequenced.

After confirming the exact sequence with traditional sequencing, the methylation status of the *G0S2* gene promoter region was further validated by pyrosequencing with an EpiTect Bisulfite Kit [18]. Genomic DNA from 64 MG patients and 64 healthy volunteers was modified with bisulfite reagents following the manufacturer's instructions (Zymo Research, Orange, CA). This modification resulted in a conversion of demethylated cytosine to thymine, whereas the methylated cytosine remained unchanged. A total of 20 ng of bisulfite-modified genomic DNA from each sample was subjected to PCR amplification and was directly pyrosequenced with the ABI 3700 automated sequencing system (Applied Biosystems, Carlsbad, CA) to detect the methylation level of each CpG site in the *G0S2* promoter. *G0S2* methylation was also detected by real-time quantitative-MSP (RQ-MSP) using SYBR Premix ExTaq™ according to the manufacturer's instructions to verify the pyrosequencing result. The normalized ratio (NM-G0S2) was used to assess the *G0S2* methylation in each sample and was determined using the following formula:

$$N_{M-G0S2} = (E_{M-G0S2})^{\Delta CT-G0S2(\text{control-sample})} \div (E_{ALU})^{\Delta CT-ALU(\text{control-sample})}. \quad (1)$$

2.6. Regulatory Relationship Detection between NFAT5 and the G0S2 Gene. To verify how the *NFAT5* gene regulates the expression level of *G0S2*, the *NFAT5* gene was cloned and sequenced with sequence-specific PCR primers, and the recombinant plasmid pEGFP-N1-NFAT5 was constructed. Different concentrations of pEGFP-N1-NFAT5 (100 ng and 200 ng) were transfected into the PBMCs of MG patients with lipofectamine (Lipo 2000). The control group was transfected with scrambled *G0S2* mRNA constructs, and *G0S2* promoter methylation was analyzed 48 hours after the transfection. The methylation statuses were further validated by BSP. The primer sequences used are listed in Table 1. *GAPDH* was used as an internal control. The relative quantification of gene expression was normalized against *GAPDH* by using the $2^{-\Delta\Delta CT}$ method.

2.7. Detecting the Relationship between NFAT5 and the G0S2 Gene Promoter. Dual-luciferase reporters are often employed to make relational or radiometric measurements within one experimental system. Typically, one reporter is used as an internal control, and the other reporter is normalized. To identify how the *NFAT5* gene and the promoter of *G0S2* interact, the recombinant plasmids pGL3-Basic-p1 (inserted with p1), pGL3-Basic-p2 (inserted with p2), pGL3-Basic-p12 (inserted with the continuous p1 and p2 sequences), and pEGFP-N1-NFAT5 (inserted with *NFAT5*) were constructed.

Jurkat T cells were incubated in DMEM containing 10% fetal bovine serum and placed in an incubator at 37°C and 5% CO₂. Cells in the logarithmic growth phase were counted with trypan blue and seeded in 24-well cell culture plates at 1×10^5 /well until the cells grew to 80% confluence. Then, 750 ng of the reporter plasmids pGL3-Basic-p1, pGL3-Basic-p2, and pGL3-Basic-p12 and 60 ng of pRL-TK were diluted with 50 μ L serum-free OPT1-DMEM and incubated for 5 min at room temperature. Liposomes were also cultured in 50 μ L serum-free OPT1-MEM with 2 μ L of Lipofectamine™ 2000. This plasmid and liposome mixture were incubated at room temperature for 5 min, gently mixed, and allowed to stand for 20 min at room temperature. The original medium in a 24-well plate was discarded; the plate was washed twice with PBS, and 500 μ L serum-free OPT1-DMEM was added per well. Cells were transfected with the plasmid and liposome mixture and were gently shaken and mixed. The transfection mixture was placed in a 37°C, 5% CO₂ incubator. After transfection for 24 hours, the transfected cells were subjected to a luciferase assay to detect the hLuc and hRluc activities [19, 20]. When cells positive for pGL3-Basic-p1, pGL3-Basic-p2, and pGL3-Basic-p12 were identified, liposomes, Lipofectamine™ 2000 (2 μ L), and 200 ng pEGFP-N1-NFAT5 were mixed with 50 μ L serum-free OPT1-MEM at room temperature for 20 min. The plasmid (pEGFP-N1-NFAT5) and liposome mixture was transfected into 3 positive cell lines and was gently shaken and mixed. The mixture was placed in a 37°C, 5% CO₂ incubator. After transfection for 24 hours, the transfected cells were subjected to a luciferase assay to detect the hLuc and hRluc activities [19, 20]. Each luciferase assay was

performed in triplicate, and GraphPad Prism 4.0 was used to analyze the data and generate the histograms.

2.8. Regulation of the G0S2 Expression Level. During a 3-month course of tacrolimus therapy in MG patients, the subjects received daily doses of 3-5 mg tacrolimus prior to eating [8]. The dose of tacrolimus to treat MG ranges from a fixed daily dose of 3 mg to a weight-based approach of 0.05 to 0.1 mg/kg/day. Peripheral blood samples were collected from MG patients before and after tacrolimus therapy for RNA extraction and qRT-PCR. The expression levels of *G0S2* in the PBMCs with and without tacrolimus therapy for three months were measured by qRT-PCR.

Total PBMCs were isolated from MG patients and resuspended in DMEM complete medium+15% fetal bovine serum and 1% penicillin/streptomycin in a culture flask (Corning, USA). Isolated PBMCs were treated as follows: PBMCs were cocultured with 5-aza-dC (DAC) to perform DNA demethylation; the original PBMCs were transfected with the plasmid (pEGFP-N1-NFAT5) and liposome mixture; and PBMCs were treated with DAC and transfected with the plasmid (pEGFP-N1-NFAT5) and liposome mixture. All different cells were collected for RNA extraction and qRT-PCR. The expression levels of *G0S2* in PBMCs treated with different conditions were measured by qRT-PCR.

2.9. Statistical Analyses. All result data were statistically analyzed with SPSS 13.0 software. All data with continuous variables are expressed as the mean \pm SD. Comparisons between two groups were performed by Student's *t* test. $p < 0.05$ was considered statistically significant.

3. Results

3.1. G0S2 Gene Is Upregulated in MG Patients. Previous mRNA microarray analyses of the PBMCs of MG patients [13] revealed that distinct biological pathways had diverse functions. Based on the GO biological process results, differentially expressed genes between healthy people and MG patients were annotated. As a key gene in cell cycle regulation, the expression of the *G0S2* gene was significantly higher in MG patients than in healthy volunteers at the mRNA level. Based on these findings, we focused on this gene and investigated the function of *G0S2*. The expression patterns of *G0S2* in the PBMCs of 50 MG patients and 20 healthy volunteers were determined by qRT-PCR. Compared with the mRNA microarray analysis results, the *G0S2* gene showed a more significant upregulation in the peripheral blood of MG patients. qRT-PCR revealed that the expression level of *G0S2* was sharply upregulated (up to a 2,200-fold change) in the PBMCs of MG patients (Figure 1). The expression pattern of *G0S2* in the PBMCs of MG patients suggested the involvement of *G0S2* in MG.

3.2. Association between G0S2 Methylation and Expression in MG Patients. Through sequencing and bioinformatics analysis, two CpG islands (-258 bp to +31 bp and -666 bp to -237 bp) were found in the promoter region of *G0S2* (Figure 2(a)) and were named p1 and p2. The methylation

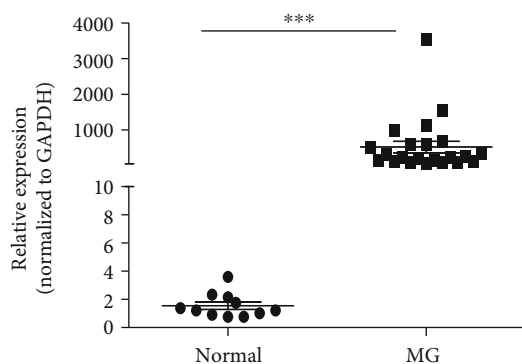


FIGURE 1: The relative expression level of *G0S2* gene in the PMBC from MG patients and normal healthy volunteers. *** $p < 0.01$ vs. control. The y -coordinate represents the relative expression level, each dot represents an individual expression result, MG means the myasthenia gravis patients, and normal means healthy volunteers. The relative expression of *G0S2* was normalized to the expression level of internal control gene GAPDH.

levels of the two CpG islands were detected by BSP. The results showed that the upstream sequence from -258 bp to +31 bp (p2) had no obvious variation in the methylation level between the MG and healthy groups. The ATG upstream sequence from -666 bp to -237 bp (p1) was clearly downregulated in MG patients compared with in healthy individuals. The methylation level of the p1 promoter was 12.25% in the PBMCs from healthy controls and downregulated to 5.16% in the MG patients ($p < 0.05$) (Figure 2(c)). Moreover, the pyrosequencing results of samples from 64 MG patients and 64 healthy volunteers showed a downward trend of the methylation level of each CpG site in p1 (Figures 2(b)–2(d)).

The total PBMCs from the control group had a 10% methylation level on the *G0S2* promoter, while the PBMCs from the MG group had a 3% methylation level on the *G0S2* promoter. It is worth mentioning that the methylation level of the *G0S2* promoter in different cell types showed a different pattern (Figure 3). The methylation level of *G0S2* in the CD4+ T cells, CD8+ T cells, and CD19+ B cells between the MG patients and healthy volunteers were analyzed, and positive results were obtained. The CD 19+ B cells from the control group had an 8.8% methylation level on the *G0S2* promoter, while the CD19+ B cells from the MG group had a 3.44% *G0S2* methylation level. The CD4+ T cells from the MG patients had a 9.76% DNA methylation level, which was equivalent to the methylation level of the CD4+ T cells from the healthy controls (9.88%). The same result was obtained for the CD8+ T cells (8.62% for the MG group vs. 9.12% for the healthy volunteers). These results indicate that the changes in the methylation level of the *G0S2* DNA promoter from PBMCs were from B cells and CD8+ T cells while the CD4+ T cell showed little change.

It is known that the methylation level of the DNA promoter region is inversely correlated with the expression level of the target gene. These results suggested that the lower methylation level of p1 may increase the expression of *G0S2* in MG patients. We also detected the expression level of *G0S2* in these samples, and a significant negative correla-

tion was found between the expression level of the *G0S2* gene and the methylation level of the *G0S2* promoter (Figure 4 and Table 2). The expression of *G0S2* in CD19+ B ($p < 0.05$) and CD8+ T ($p < 0.05$) cells from MG was upregulated comparing with that from healthy control, but the expression the *G0S2* in CD4+ T cell showed no significant change between 2 groups ($p > 0.05$). This result explains why the methylation level of the promoter decreased while the expression level increased.

3.3. NFAT5 Inhibits the Expression Level of *G0S2*. The transcription factor gene family NFAT consists of five different members, including *NFATc1*, *NFATc2*, *NFATc3*, *NFATc4*, and *NFAT5*. To verify the relationship between the NFAT family members and *G0S2*, the expression levels of the five NFAT members in MG patients were determined by qRT-PCR. We found that *NFATc1*, *NFATc2*, and *NFAT5* were downregulated in the PBMCs of MG patients (Figure 5(a)). In particular, there was a negative correlation between the expression level of *NFAT5* and the expression level of *G0S2* (Figure 6). To verify the relationship between *NFAT5* and *G0S2*, the recombinant plasmid pEGFP-N1-NFAT5 was constructed and transfected into PBMCs from MG patients. The expression level of *G0S2* after *NFAT5* overexpression was decreased by 2-fold. Moreover, the fold change depended on the concentration of the pEGFP-N1-NFAT5 recombinant plasmid (inserted next to *NFAT5*) (Figure 5(b)). The expression level of *G0S2* decreased to 0.8-fold of that of the control group when the concentration of the recombinant plasmid (inserted by *NFAT5*) was 0.5 μg and decreased to a half the control group level when the concentration was 1.0 μg . However, according to the BSP results, the methylation status of *G0S2* in transfected PBMCs from MG patients was different from that in nontransfected PBMCs from MG patients. This result suggests that *NFAT5* could downregulate the expression level of *G0S2* but not by methylating the promoter of the target gene.

3.4. NFAT5 Regulates *G0S2* by Binding to p1 in the Promoter. Our results suggest that *NFAT5* could downregulate the expression level of *G0S2*. To explain the regulatory mechanism, the recombinant plasmids pGL3-Basic-p1 (inserted by p1), pGL3-Basic-p2 (inserted by p2), pGL3-Basic-p12 (inserted by continuous p1 and p2 sequences), and pEGFP-N1-NFAT5 (inserted by *NFAT5*) were constructed. A dual-luciferase reporter system was employed to reveal the interaction between the *NFAT5* gene and the *G0S2* promoter. With increasing concentrations of pEGFP-N1-NFAT5 transfected into Jurkat T cells (pGL3-Basic-p1-, pGL3-Basic-p2-, and pGL3-Basic-p12-containing cell lines), the fluorescence of pGL3-Basic-p1- and pGL3-Basic-p12-containing cell lines progressively decreased (Figure 5(c)). The pGL3-Basic-p2-containing cell lines showed no significant changes. These results suggested that *NFAT5* could regulate the expression level of *G0S2* by binding to p1 in the promoter but showed no binding to p2 in the promoter.

3.5. Tacrolimus Therapy Reduces the Expression Level of *G0S2* in MG Patients. Tacrolimus, also named FK-506 or

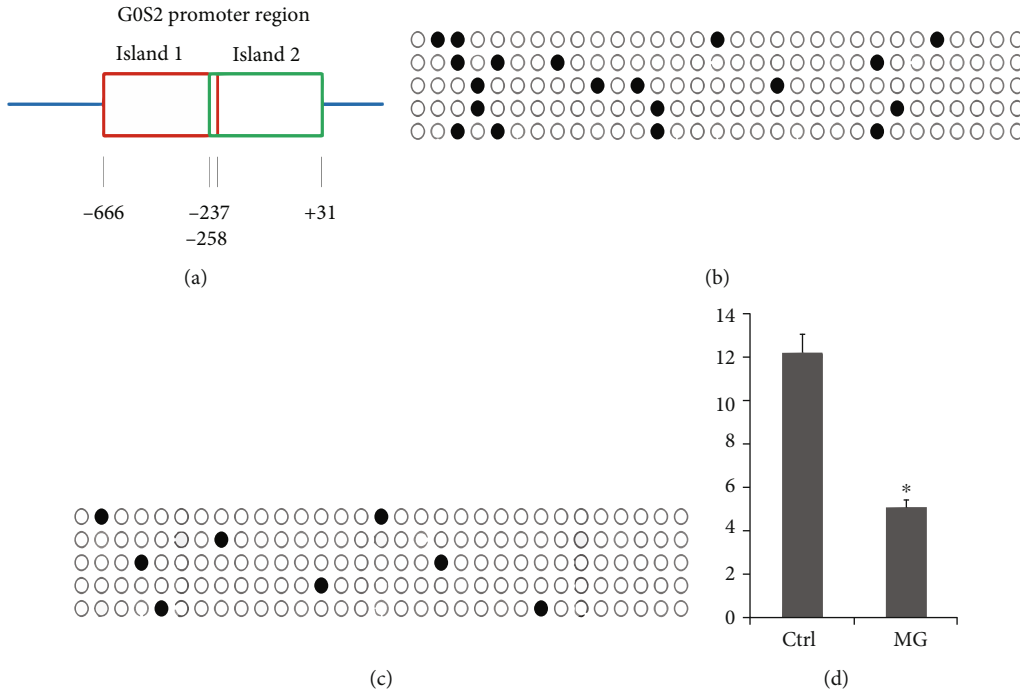


FIGURE 2: G0S2 methylation level in control and MG patients. (a) The positions of two different CpG islands in G0S2 promoter region. Box represents the different CpG islands. Number represents the positions of nucleobase. (b) G0S2 methylation density in the control group; blank circle means result which was not methylation; the black circle means methylation result. (c) G0S2 methylation density in the MG patients. Blank circle means result which was not methylated; the black circle means methylation result. (d) Normalized ratio of G0S2 methylation. MG means the myasthenia gravis patients; ctrl means healthy volunteers. The y-coordinate represents the rate of methylation result.

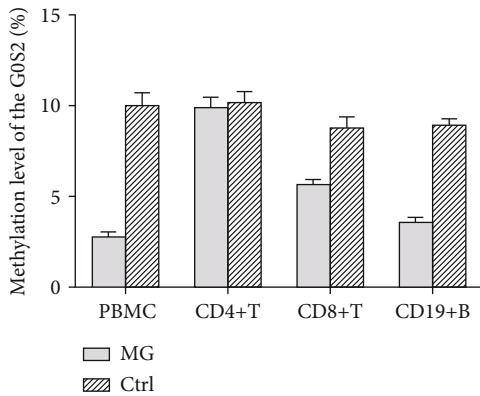


FIGURE 3: The methylation level of the G0S2 in different type of cells. The y-coordinate represents the rate of methylation result; MG means the PMBC sample from myasthenia gravis patients; control means PMBC sample from healthy volunteers. CD4+ T cell and CD19+ cells were different types of cells derived from MG PMBC sample.

fujimycin, is an immunosuppressive drug that is used to inhibit the immune system for specific reasons, such as an allogeneic organ transplant [8]. It has immunosuppressive properties similar to those of cyclosporin A but is much more potent. To explore the therapeutic effect and mechanism of tacrolimus on MG patients, we measured the expression levels of the *G0S2* transcripts in PBMCs from MG patients before and after three months of tacrolimus therapy using qRT-PCR. The expression level of *G0S2* in MG patients after

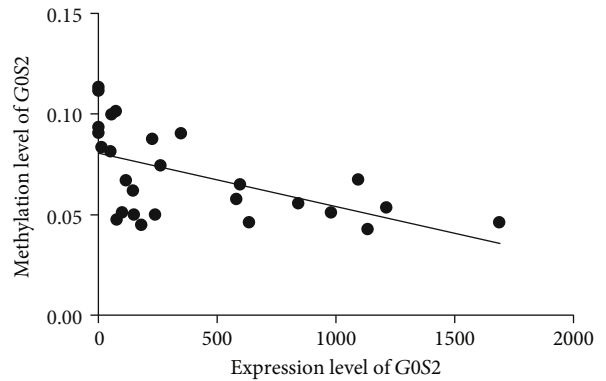


FIGURE 4: The correlation analysis between the expression level and methylation level of the G0S2. 95% confidence interval is -0.8295 to -0.3475 The y-coordinate represents rate of methylation result; each dot represents an individual expression result of G0S2. The oblique line is the fitting curve of methylation level of G0S2.

tacrolimus therapy for three months was generally downregulated compared with the expression level before treatment (Figure 7), demonstrating that tacrolimus therapy could reduce the expression of *G0S2* in MG patients. In addition, the expression level of *NFAT5* was upregulated after treatment with tacrolimus. The expression levels of *NFAT5* in the drug (tacrolimus therapy)-sensitive and nonsensitive groups showed different characteristics; the expression level of *NFAT5* in the drug-sensitive group was upregulated by 2-fold, while that in the nonsensitive groups showed no change.

TABLE 2: Fold change of G0S2 and methylation level in PBMC from the same MG patients.

	Fold change of G0S2 in PBMC from MG	Methylation level in PBMC from MG		Fold change of G0S2 in PBMC from MG	Methylation level in PBMC from MG
MG1	839.8262	0.05586734	MG14	3.16	0.09028552
MG2	261.11	0.07480559	MG15	1132.38	0.04281364
MG3	226.86	0.0878684	MG16	348.11	0.09049833
MG4	117.06	0.06729902	MG17	238.84	0.05023203
MG5	48.95	0.08162508	MG18	145.13	0.06219874
MG6	72.44	0.1017963	MG19	977.65	0.05075296
MG7	1.5	0.1118319	MG20	595.15	0.06516683
MG8	99.88	0.05115332	MG21	1211.064	0.05382841
MG9	147.86	0.05028404	MG22	1684.133	0.04635253
MG10	74.85	0.04752094	MG23	1091.28	0.06756885
MG11	14.06	0.08366191	MG24	632.5179	0.04639083
MG12	581.65	0.05811148	MG25	181.0193	0.04508229
MG13	56.93	0.1000311	MG26	1.940391	0.1133023
			MG27	2.623941	0.09335699

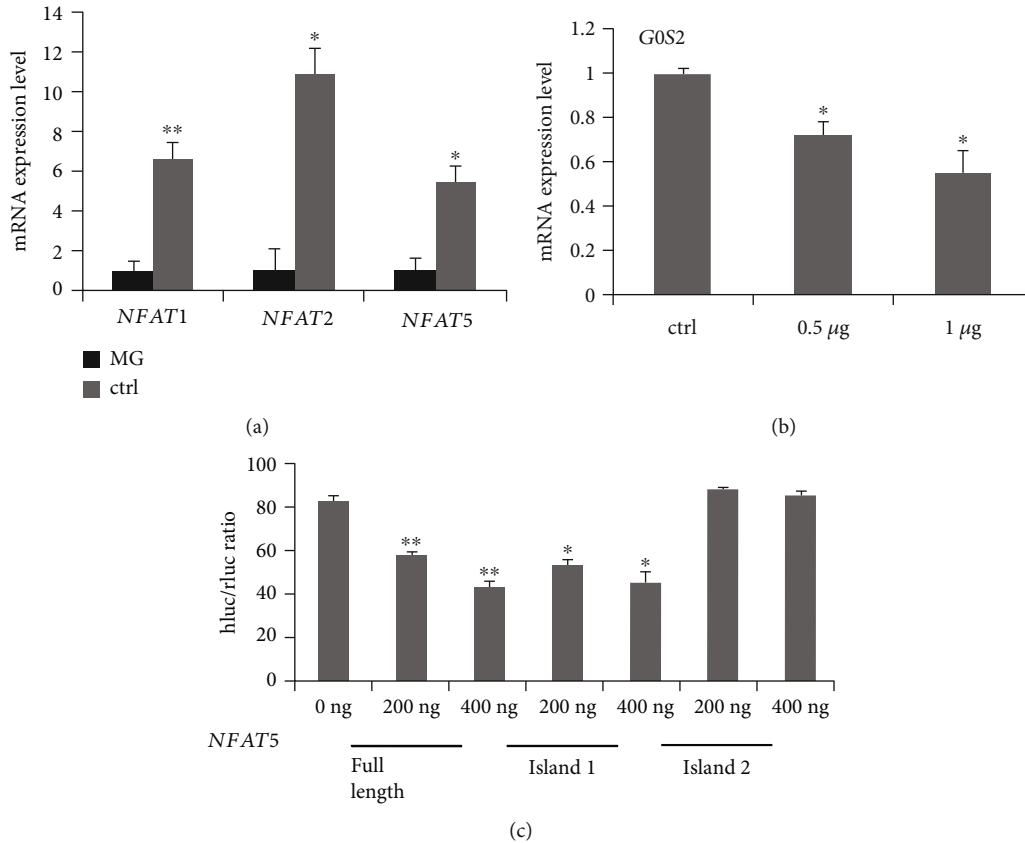


FIGURE 5: NFAT5 inhibit G0S2 expression through island 1. (a) The relative mRNA expression level of NFAT family in healthy human and MG patients. The y-coordinate represents the relative expression level, MG means the myasthenia gravis patients, and ctrl means healthy volunteers. (b) Upregulation NFAT5 inhibits G0S2 expression. The y-coordinate represents the relative expression level of G0S2; the x-coordinate represents the different concentrations P-EGF-N1-NFAT5 plasmid which were transfected into T cells. (c) NFAT5 binds island 1 of G0S2 promoter region detected by dual-Luciferase reporter. Full length represents the plasmid containing islands 1 and 2; islands 1 and 2 represent the plasmid containing the corresponding CpG island sequence from G0S2 promoter.

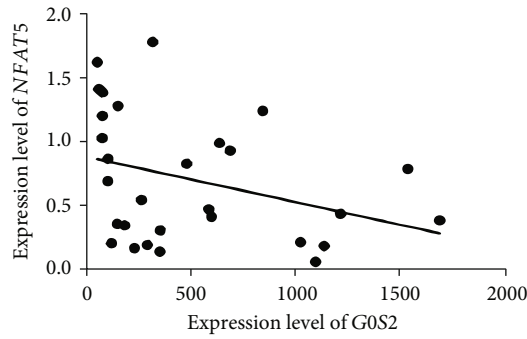


FIGURE 6: The correlation analysis between the expression level of *G0S2* and *NFAT5*. The *y*-coordinate represents expression level; each dot represents an individual expression result of *G0S2*. The oblique line is the fitting curve of expression level of *NFAT5*.

3.6. *Both Methylation and Overexpression of NFAT5 Could Reduce the Expression of G0S2*. After treatment with DAC, the expression level of the *G0S2* gene was upregulated by 20-fold (Figure 8), which means that the expression of *G0S2* in MG patients was controlled by the methylation level of *G0S2*. After demethylation of the *G0S2* promoter, the expression level of *G0S2* was upregulated. Moreover, *NFAT5* overexpression downregulated the expression level of demethylated *G0S2* genes.

4. Discussion

MG is an old disease caused by immune system disorders that can lead to muscle weakness in patients [8]. At present, the major therapies for MG are cholinesterase inhibitors, immunosuppressants, and glucocorticoid. The change in the expression pattern of *G0S2* and *NFAT5* in the PBMCs of MG patients compared with that in healthy individuals suggests an immune cell disorder. A disruption in the cell cycle of immune cells could be one reason for the immune disorder of MG patients.

The *G0S2* gene was originally discovered in PBMCs and was associated with the cell cycle. *G0S2* expression is required to accelerate the cells into the G1 phase from the G0 phase [21]. Recent studies suggest that *G0S2* is a multifunctional protein involved in subcellular localization, gene expression profiling, proliferation, differentiation, and lipid metabolism [22, 23]. In a previous study, the expression level of *G0S2* showed an obvious upward trend in the thymus of MG patients [9]. Here, the same result that the expression level of *G0S2* increased in the thymus tissues and PBMCs of MG patients was detected by qRT-PCR. The high expression level of *G0S2* (2000-fold change) in the PBMCs of MG patients and the cell cycle-associated function may suggest that *G0S2* could be an important factor in MG.

As for the different cell types, the methylation levels of *G0S2* in CD4⁺ T cells, CD8⁺ T cells, and CD 19⁺ B cell between the MG patients and healthy volunteers were analyzed. The difference between MG patients and healthy controls was most significant in B cells and least significant in CD4⁺ T cells. MG is directly mediated by autoantibodies produced by B cells, and the presence of pathogenic autoan-

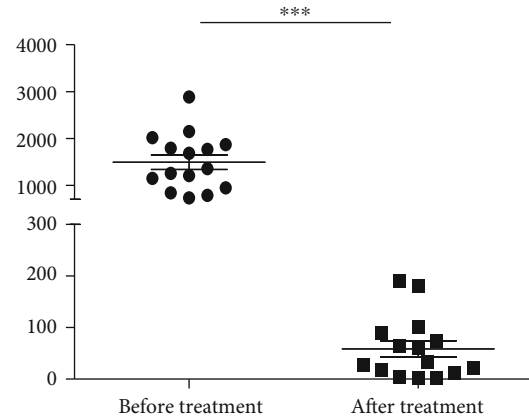


FIGURE 7: The expression of *G0S2* in the PMBC from MG patients before and after treatment with tacrolimus therapy. *** $p < 0.01$. The *y*-coordinate represents expression level; each dot or blocks represents an individual expression result of *G0S2*.

tibodies highlights the importance of B cells in MG pathophysiology, the role of upstream T cells, and their regulation with B cells. The majority of studies on the pharmacodynamic effects of tacrolimus and the NFAT family focus on T cells. This study suggests that *NFAT5* and *G0S2* may play different roles in different cell subsets.

Different subsets of immune cells that interactively work together are necessary for immune response [24]. MG is an AChR type for B cell-mediated autoimmune disorders. The production of autoantibodies clearly implicates a direct role for B cells in the disease pathogenesis. Dysregulation in immune cell types extending beyond B lineages has been documented, indicating that a combination of factors contributes to disease manifestation. Moreover, the B cell response in MG most certainly requires T cell help. Proinflammatory antigen-specific T cells are involved in AChR MG, and the pathogenic anti-AChR antibodies are high-affinity IgGs, whose synthesis requires interaction of activated CD4⁺ T cells with B cells that synthesize low-affinity anti-AChR antibodies [25]. Accordingly, CD4 T cells are the drivers in the immunopathogenesis of MG disease, and they play a multifaceted role in immunity, from promoting inflammation to inducing immune tolerance and supporting B cell function. CD8⁺ T cells are less important to disease pathophysiology in AChR MG [26], although CD8⁺ T cells from MuSK MG patients had higher frequencies of polyfunctional responses than the controls and CD4⁺ T cells had higher IL-2, TNF- α , and IL-17. In experimental autoimmune encephalomyelitis, CD8⁺ cells were shown to be both effectors and regulators. CD8⁺ cells have been implicated as suppressor or regulator T cells in other autoimmune diseases [27]. Recent studies suggest that the functions of T cells are more complicated [28]. CD8⁺ cells were also found to help B cells in antibody production through the expression of the CD40 ligand [29, 30]. The importance of CD4⁺ T cells in the pathogenesis of MG is consistent with previous data on experimental autoimmune myasthenia gravis (EAMG) and human MG [31]. However, the role of CD8⁺ T cells in MG is unclear. Another report, however, showed that both CD4⁺ and CD8⁺ cells are

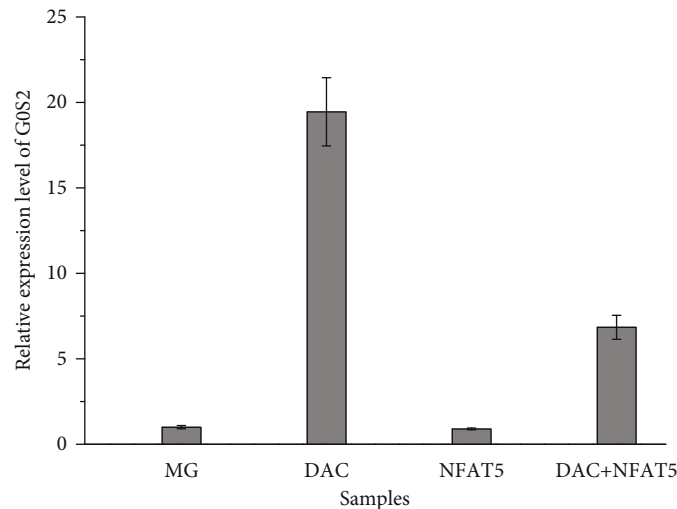


FIGURE 8: The expression level of *G0S2* in the PMBC with different treatment. MG means the PMBC sample from myasthenia gravis patients; DAC means PMBC sample cocultured with DAC(5-aza-dC) to perform DNA demethylation. NFAT5 means PMBC sample which was transfected with P-EGF-N1-NFAT5 plasmid; DAC+NFAT5 means PMBC sample which were transfected with P-EGF-N1-NFAT5 plasmid after coculturing with DAC(5-aza-dC).

essential for the development of EAMG. As the primary site of T cell development, the abnormal immune response of the thymus is closely related to the occurrence of MG [32, 33]. Recent clinical studies have shown that thymus abnormalities might have an impact on the expression of the proapoptotic factor Fas in CD4-CD8+ T cells. Indeed, an imbalance between pathogenic Th17 and Treg cells characterizes the peripheral blood of AChR MG patients and likely contributes to a loss of tolerance. Accordingly, a research group demonstrated that the proportion of Th17 cells and IL-17-producing CD8+ T cells was increased in the prethymectomy peripheral blood of MG patients compared with the controls [34].

Immunosuppressors are the main treatment for MG, especially for those who suffered severe adverse effects of glucocorticoid. Previous studies provided evidence that CYA is effective as a monotherapy or in combination with glucocorticoid in MG [35]. However, cyclosporine A also showed serious side effects. To date, cyclosporine A has been increasingly replaced by a new immunosuppressant, tacrolimus. Tacrolimus showed better efficacy with fewer side effects than cyclosporin A, which downregulated the expression level of *G0S2* in cultured blood mononuclear cells by inhibiting the activities of the calcium-dependent phosphatase calcineurin and the NFAT transcription factor family [8, 36, 37] and by suppressing the immune system. A previous study suggested that the *G0S2* gene has potential sites in the 5' arm that could bind to the NFAT gene [14]. For this reason, NFAT could regulate the expression level of *G0S2* by binding to the promoter region. In this study, all members of the NFAT gene family were detected, and only the *NFAT5* gene showed a negative correlation with *G0S2*. Furthermore, dual-luciferase reporter experiments showed that *NFAT5* could downregulate the expression of *G0S2* by binding to p1 in the promoter region of *G0S2*.

Generally, affecting the promoter region of one gene could result in DNA methylation and downregulate the gene expression level. For the first time, we found that *G0S2* methylation was significantly lower in the PBMCs of MG patients than in those of healthy controls, which indicated that the decreased *G0S2* methylation may be associated with upregulated *G0S2* expression at the mRNA level. Moreover, our work revealed that *NFAT5* could combine with p1 in the *G0S2* promoter to determine *G0S2* expression in the thymus tissues and PBMCs of MG patients. Owing to the abnormal activation of T cells in MG patients, *NFAT5* is involved in T cell activation. Our results are consistent with the findings observed in studies on other autoimmune diseases [38]. *NFAT5* binding and methylation at p1 in the *G0S2* promoter could control the expression of the *G0S2* gene to regulate the lymphocyte balance. Unfortunately, *NFAT5* showed no effect on *G0S2* methylation. *NFAT5* may affect the transcription initiation or transcriptional regulation of *G0S2* to downregulate its expression. In summary, we speculate that the expression of *G0S2* may affect the lymphocyte cell cycle and that *G0S2* expression is required to induce cells to transition from the G0 phase to the G1 phase. The interaction of T cell activation factor (NFAT) with *G0S2* may affect the number and activation of T cells, thus further affecting its influence on MG.

Like cyclosporine, tacrolimus (FK506) could inhibit the activity of calcineurin with less nephrotoxicity [39, 40]. Several reports have suggested its potential benefit in MG. Tacrolimus is used for the treatment of MG patients who are intolerant to mycophenolate mofetil, azathioprine, and cyclosporin [41]. The expression level of *G0S2* was downregulated after 3 months of tacrolimus therapy. Furthermore, tacrolimus therapy could have a positive effect, generally reducing the expression level of *G0S2* in MG patients. In addition, *G0S2* is recognized as a potential tumor suppressor

gene [9], which may explain why the side effects of tacrolimus lead to tumorigenesis. The expression of the *G0S2* gene may play an important role in maintaining the T lymphocyte balance. Therefore, the regulation of *G0S2* methylation can provide more evidence to explain the molecular mechanism of MG and offer new insights into the development of epigenetic-based therapeutic strategies for MG. Further studies are needed to develop new long-term immunosuppressive therapy strategies for MG.

Data Availability

All data, models, and code generated or used during the study appear in the submitted article.

Conflicts of Interest

The authors declare that they have no conflicts of interest.

Acknowledgments

This study was supported by a grant from the National Natural Science Foundation of China (grant number: 81501034), the Hunan Natural Science Foundation (grant number: 2015JJ3136) and the Central South University Postdoctoral Research Opening Fund.

References

- [1] S. Ragheb and R. P. Lisak, "B-cell-activating factor and autoimmune myasthenia gravis," *Autoimmune Diseases*, vol. 2011, Article ID 939520, 10 pages, 2011.
- [2] M. N. Meriglioli, "Myasthenia gravis with anti-acetylcholine receptor antibodies," *Immune-Mediated Neuromuscular Diseases*, vol. 26, pp. 94–108, 2009.
- [3] G. Beecher, B. N. Putko, A. N. Wagner, and Z. A. Siddiqi, "Therapies directed against B-cells and downstream effectors in generalized autoimmune myasthenia gravis: current status," *Drugs*, vol. 79, no. 4, pp. 353–364, 2019.
- [4] W. Mai, X. Liu, Y. Fan et al., "Up-regulated expression of Fas antigen in peripheral T cell subsets in patients with myasthenia gravis," *Clinical & Investigative Medicine*, vol. 35, no. 5, pp. 294–302, 2012.
- [5] P. Baumann, M. Perey, S. Laurian, F. Grasset, A. Steck, and J. M. Gaillard, "Distribution of tryptophan in erythrocytes, leukocytes and thrombocytes, and its binding to plasma albumin," in *Transport Mechanisms of Tryptophan in Blood Cells, Nerve Cells, and at the Blood-Brain Barrier*, pp. 165–176, Springer, 1979.
- [6] J. M. Barbarino, C. E. Staatz, R. Venkataramanan, T. E. Klein, and R. B. Altman, "PharmGKB summary: cyclosporine and tacrolimus pathways," *Pharmacogenetics and Genomics*, vol. 23, no. 10, pp. 563–585, 2013.
- [7] H.-Y. Meng, X. Li, W.-L. Jin et al., "Multiple genetic factors affecting the pharmacokinetic and pharmacodynamic processes of tacrolimus in Chinese myasthenia gravis patients," *European Journal of Clinical Pharmacology*, vol. 76, no. 5, pp. 659–671, 2020.
- [8] A. D. Cristillo, S. P. Heximer, L. Russell, and D. R. Forsdyke, "Cyclosporin A inhibits early mRNA expression of *G0/G1 switch gene 2 (G0S2)* in cultured human blood mononuclear cells," *DNA and Cell Biology*, vol. 16, no. 12, pp. 1449–1458, 1997.
- [9] A. Levinson and L. M. Wheatley, "The thymus and the pathogenesis of myasthenia gravis," *Clinical Immunology and Immunopathology*, vol. 78, no. 1, pp. 1–5, 1996.
- [10] D. Koczan, R. Guthke, H.-J. Thiesen et al., "Gene expression profiling of peripheral blood mononuclear leukocytes from psoriasis patients identifies new immune regulatory molecules," *European Journal of Dermatology*, vol. 15, no. 4, pp. 251–257, 2005.
- [11] N. Nakamura, Y. Shimaoka, T. Tougan et al., "Isolation and expression profiling of genes upregulated in bone marrow-derived mononuclear cells of rheumatoid arthritis patients," *DNA Research*, vol. 13, no. 4, pp. 169–183, 2006.
- [12] S. Kobayashi, A. Ito, D. Okuzaki et al., "Expression profiling of PBMC-based diagnostic gene markers isolated from vasculitis patients," *DNA Research*, vol. 15, no. 4, pp. 253–265, 2008.
- [13] Z. Luo, Y. Li, X. Liu et al., "Systems biology of myasthenia gravis, integration of aberrant lncRNA and mRNA expression changes," *BMC Medical Genomics*, vol. 8, no. 1, p. 13, 2015.
- [14] A. Rao, "NF-ATp: a transcription factor required for the coordinate induction of several cytokine genes," *Immunology Today*, vol. 15, no. 6, pp. 274–281, 1994.
- [15] N. Lee, D. Kim, and D. Kim, "Role of NFAT5 in the immune system and pathogenesis of autoimmune diseases," *Frontiers in Immunology*, vol. 10, p. 270, 2019.
- [16] J. D. Licchesi and J. G. Herman, "Methylation-specific PCR," in *DNA Methylation*, pp. 305–323, Springer, 2009.
- [17] M. Frommer, L. E. McDonald, D. S. Millar et al., "A genomic sequencing protocol that yields a positive display of 5-methylcytosine residues in individual DNA strands," *Proceedings of the National Academy of Sciences*, vol. 89, no. 5, pp. 1827–1831, 1992.
- [18] H. Fakhrai-Rad, N. Pourmand, and M. Ronaghi, "Pyrosequencing™: an accurate detection platform for single nucleotide polymorphisms," *Human Mutation*, vol. 19, no. 5, pp. 479–485, 2002.
- [19] Y. Z. Xu, C. Kanagaratham, S. Jancik, and D. Radzioch, "Promoter deletion analysis using a dual-luciferase reporter system," in *Gene Regulation*, pp. 79–93, Springer, 2013.
- [20] J. Y. Lee, S. Kim, D. W. Hwang et al., "Development of a dual-luciferase reporter system for in vivo visualization of MicroRNA biogenesis and posttranscriptional regulation," *Journal of Nuclear Medicine*, vol. 49, no. 2, pp. 285–294, 2008.
- [21] B. L. Heckmann, X. Zhang, X. Xie, and J. Liu, "The *G0/G1 switch gene 2 (G0S2)*: regulating metabolism and beyond," *Biochimica et Biophysica Acta (BBA) - Molecular and Cell Biology of Lipids*, vol. 1831, no. 2, pp. 276–281, 2013.
- [22] X. Yang, X. Lu, M. Lombès et al., "The *G0/G1 switch gene 2* regulates adipose lipolysis through association with adipose triglyceride lipase," *Cell Metabolism*, vol. 11, no. 3, pp. 194–205, 2010.
- [23] P. R. Chen, S. Shin, Y. M. Choi, E. Kim, J. Han, and K. Lee, "Overexpression of *G0/G1 switch gene 2* in adipose tissue of transgenic quail inhibits lipolysis associated with egg laying," *International Journal of Molecular Sciences*, vol. 17, no. 3, p. 384, 2016.
- [24] D. B. Drachman, "Myasthenia gravis," *New England Journal of Medicine*, vol. 298, no. 3, pp. 136–142, 1978.
- [25] B. M. Conti-Fine, M. Milani, and W. Wang, "CD4⁺ T cells and cytokines in the pathogenesis of acquired myasthenia gravis,"

- Annals of the New York Academy of Sciences*, vol. 1132, no. 1, pp. 193–209, 2008.
- [26] J. Yi, A. Guidon, S. Sparks et al., “Characterization of CD4 and CD8 T cell responses in MuSK myasthenia gravis,” *Journal of Autoimmunity*, vol. 52, pp. 130–138, 2014.
- [27] M. Shenoy, R. Kaul, E. Goluszko, C. David, and P. Christadoss, “Effect of MHC class I and CD8 cell deficiency on experimental autoimmune myasthenia gravis pathogenesis,” *The Journal of Immunology*, vol. 153, no. 11, pp. 5330–5335, 1994.
- [28] M. Zhao, F. Gao, X. Wu, J. Tang, and Q. Lu, “Abnormal DNA methylation in peripheral blood mononuclear cells from patients with vitiligo,” *British Journal of Dermatology*, vol. 163, no. 4, pp. 736–742, 2010.
- [29] G. X. Zhang, C. G. Ma, B. G. Xiao, M. Bakhiet, H. Link, and T. Olsson, “Depletion of CD8⁺ T cells suppresses the development of experimental autoimmune myasthenia gravis in Lewis rats,” *European Journal of Immunology*, vol. 25, no. 5, pp. 1191–1198, 1995.
- [30] X. Lian, R. Xiao, X. Hu et al., “DNA demethylation of CD40L in CD4⁺ T cells from women with systemic sclerosis: a possible explanation for female susceptibility,” *Arthritis and Rheumatism*, vol. 64, no. 7, pp. 2338–2345, 2012.
- [31] F.-D. Shi, H. Li, H. Wang et al., “Mechanisms of nasal tolerance induction in experimental autoimmune myasthenia gravis: identification of regulatory cells,” *The Journal of Immunology*, vol. 162, no. 10, pp. 5757–5763, 1999.
- [32] A. Fattorossi, A. Battaglia, A. Buzzonetti, F. Ciaraffa, G. Scambia, and A. Evoli, “Circulating and thymic CD4⁺ CD25⁺ T regulatory cells in myasthenia gravis: effect of immunosuppressive treatment,” *Immunology*, vol. 116, no. 1, pp. 134–141, 2005.
- [33] L. Gotterer and Y. Li, “Maintenance immunosuppression in myasthenia gravis,” *Journal of the Neurological Sciences*, vol. 369, pp. 294–302, 2016.
- [34] D. Gigliotti, A.-K. Lefvert, M. Jeddi-Tehrani et al., “Overexpression of select T cell receptor V β gene families within CD4⁺ and CD8⁺ T cell subsets of myasthenia gravis patients: a role for superantigen(s)?,” *Molecular Medicine*, vol. 2, no. 4, pp. 452–459, 1996.
- [35] A. Iyengar, N. Kamath, K. D. Phadke, and M. Bitzan, “Cyclosporine/ketoconazole reduces treatment costs for nephrotic syndrome,” *Indian Journal of Nephrology*, vol. 23, no. 6, pp. 419–423, 2013.
- [36] E. A. Emmel, C. L. Verweij, D. B. Durand, K. Higgins, E. Lacy, and G. Crabtree, “Cyclosporin A specifically inhibits function of nuclear proteins involved in T cell activation,” *Science*, vol. 246, no. 4937, pp. 1617–1620, 1989.
- [37] D. B. Sanders and A. Evoli, “Immunosuppressive therapies in myasthenia gravis,” *Autoimmunity*, vol. 43, no. 5–6, pp. 428–435, 2010.
- [38] D. Saggiaro, “Anti-apoptotic effect of Tax: an NF- κ B path or a CREB way?,” *Viruses*, vol. 3, no. 7, pp. 1001–1014, 2011.
- [39] L. He, Y. Peng, H. Liu et al., “Treatment of idiopathic membranous nephropathy with combination of low-dose tacrolimus and corticosteroids,” *Journal of Nephrology*, vol. 26, no. 3, pp. 564–571, 2013.
- [40] Q.-J. Chen, J. Li, S.-R. Zuo et al., “Tacrolimus decreases insulin sensitivity without reducing fasting insulin concentration: a 2-year follow-up study in kidney transplant recipients,” *Renal Failure*, vol. 37, no. 4, pp. 601–606, 2015.
- [41] J. Sieb, “Myasthenia gravis: an update for the clinician,” *Clinical & Experimental Immunology*, vol. 175, no. 3, pp. 408–418, 2014.

Review Article

The Potential of Food Protein-Derived Bioactive Peptides against Chronic Intestinal Inflammation

Wanying Zhu,¹ Liying Ren,¹ Li Zhang,¹ Qinqin Qiao,² Muhammad Zahid Farooq,³
and Qingbiao Xu^{3,4} 

¹Shanxian Central Hospital, Heze 274300, China

²College of Information Engineering, Fuyang Normal University, Fuyang 236000, China

³College of Animal Sciences and Technology, Huazhong Agricultural University, Wuhan 430070, China

⁴State Key Laboratory of Animal Nutrition, Institute of Animal Sciences, Chinese Academy of Agricultural Sciences, Beijing 100193, China

Correspondence should be addressed to Qingbiao Xu; qbxu@mail.hzau.edu.cn

Received 23 June 2020; Accepted 25 August 2020; Published 9 September 2020

Academic Editor: Hongmei Jiang

Copyright © 2020 Wanying Zhu et al. This is an open access article distributed under the Creative Commons Attribution License, which permits unrestricted use, distribution, and reproduction in any medium, provided the original work is properly cited.

Inflammation can cause various chronic diseases like inflammatory bowel diseases. Various food protein-derived bioactive peptides (BAPs) with anti-inflammatory activity have the potential to manage these diseases. The aim of this paper is to overview the mechanisms and the molecular targets of BAPs to exert anti-inflammatory activity. In this review, the *in vitro* and *in vivo* effects of BAPs on intestinal inflammation are highlighted. The mechanism, pathways, and future perspectives of BAPs as the potential sources of therapeutic treatments to alleviate intestinal inflammation are provided, including nuclear factor- κ B, mitogen-activated protein kinase, Janus kinase-signal transducer and activator of transcription, and peptide transporter 1 (PepT1), finding that PepT1 and gut microbiota are the promising targets for BAPs to alleviate the intestinal inflammation. This review provides a comprehensive understanding of the role of dietary BAPs in attenuating inflammation and gives a novel direction in nutraceuticals for people or animals with intestinal inflammation.

1. Introduction

Inflammation is a normal immune defense that is generated from the immune system responding to pathogen and infection. Inflammation can cause various chronic diseases, such as inflammatory bowel diseases (IBD), asthma, cancer, cardiovascular diseases, obesity, and diabetes [1]. The intestinal mucosa can be damaged by IBD with chronic inflammatory disorders, including ulcerative colitis (UC) and Crohn's disease (CD). UC is an inflammation of the colon mucosa and submucosa continuity affecting the rectal area, while CD is a full-thickness inflammation discontinuity affecting the terminal ileum and colon or anus [2]. Until now, the aetiology of intestinal inflammation and IBD remains unclear.

In the intestines of human and animals, dietary proteins are digested into free amino acids and peptides by enzymatic hydrolysis. Some peptides consisting of 2–20 AAs with bio-

logical function are named bioactive peptides (BAPs), such as anti-inflammation, antihypertension, antioxidation, anti-diabetics, anticancer, antimicrobics, antiadhesion, dipeptidyl peptidase IV inhibition, opioid, and immunomodulation [3]. Conventional drug treatments have adverse side effects, such as potential toxicity and immunogenicity [4]. In recent years, BAPs have attracted more and more attention to treat chronic inflammation diseases as a result of their safety [1, 5].

However, limited information of the anti-inflammatory mechanisms of the action of these BAPs is available. In this review, food protein-derived BAPs against intestinal inflammation *in vitro* and *in vivo* are discussed. Their molecular targets and the action pathways are overviewed and highlighted. Understanding of the anti-inflammatory actions of BAPs can facilitate further research on managing chronic intestinal inflammation and diseases. Therefore, the purpose of this paper is to highlight the roles of BAPs in anti-

inflammatory activity and provide future perspectives for the application of BAPs as potential sources of therapeutic management of chronic intestinal diseases.

2. Intestinal Inflammation

Inflammation can activate protective proinflammatory mediators, such as interleukin- (IL-) 1, IL-6, IL-8, IL-12, interferon- γ (INF- γ), and tumor necrosis factor- α (TNF- α) in immune responses, which include T and B lymphocytes. The activated B lymphocytes can produce antibodies, such as IgA, IgG, IgM, and IgE. The T lymphocyte cells consist of CD4⁺ and CD8⁺ T cells. CD4⁺ T cells, named helper T lymphocytes (Th), have immune regulatory function by secreting cytokines, being classified into Th1 and Th2. Th1 can release IL-2, IFN- γ , and TNF- α to promote cellular immunological response, whereas Th2 can release IL-4 and IL-10 to improve immunoresponse, while CD8⁺ T cells have the function to kill the target cells [6].

Progression of inflammation has four steps: inducers, pathways, mediators, and inflammatory response [7]. The inducers (LPS, dextran sodium sulfate (DSS), 2,4,6-trinitrobenzene sulfonic acid (TNBS), or toxicant) stimulate the sensors that can activate pathways, including nuclear factor- κ B (NF- κ B) and mitogen-activated protein kinase (MAPK). Then, inflammatory mediators (IL-8, TNF- α , monocyte chemoattractant protein-1 (MCP-1), or reactive oxygen species (ROS)) are released, leading to the inflammatory response [7]. Proinflammatory cytokines produced mainly by macrophages and mast cells lead to inflammation, while anti-inflammatory cytokines, such as IL-4, IL-10, and transforming growth factor β (TGF- β), reduce the production of procytokines in macrophage cells as agonists of toll-like receptor [7]. In *in vivo* studies, TNBS and DSS are commonly used to induce intestinal inflammation in animal models, causing immune alterations, gut physiology and morphology changes, and colitis symptoms [8]. Moreover, administration of DSS can lead to higher intraluminal IgG [9]. In UC patients, IgG production is dramatically high in the gut; therefore, IgG is an index to grade IBD. Thus, these cytokines with pathology may be the targets for BAPs to prevent chronic inflammation. In addition, it is also known that oxidative stress is associated with chronic intestinal inflammation, and it can decrease antioxidant defenses in the colonic mucosa. Additionally, ROS are released from immune cells and can be overwhelmed by oxidative stress. Therefore, antioxidative BAPs are the candidates for antioxidant defense in inflammatory gut [10], such as IRW [11], IQW [12], EAMAPK, and AVPYQP [13]. Soybean-derived lunasin can also enhance antioxidant defenses and inhibit inflammation [14, 15].

3. Anti-Inflammatory Peptides Derived from Food Proteins

In the gut of human or animals, the BAPs encrypted in parent proteins can be released by various enzymatic digestion. However, there are several classical steps toward the *in vitro* production of novel BAPs from various food protein sources:

enzymatic hydrolysis, purification by high-performance liquid chromatography, selection of most promising fraction, peptide sequencing, and final *in vitro* or *in vivo* bioactivity test (Figure 1) [5, 7, 16]. Due to their safety, the anti-inflammation potential of food-derived BAPs has become an active research area, and the intestinal tract is a main target of BAPs.

Recent knowledge of anti-inflammatory BAPs in *in vitro* studies with a concentration of 20-1000 μ M was evaluated using mammalian cells induced by TNF- α , LPS, or H₂O₂, such as murine RAW 264.7 macrophages and human intestinal epithelial cell line Caco-2 cells (Table 1). There are many food-derived BAPs that can inhibit inflammation via the MAPK or NF- κ B pathway (Table 1), such as CR, FL, HC, LL, MK [17], DEDTQAMPFR, DEDTQAMPF [18], DYKKY [19], EAMAPK, AVPYQP [13], FLV [20], GPE-TAFLR [21], GPR [22], IPAV [23], IRW [24], IQW [12], LDAVNR, MMLDF [25], MLGATSL, MSYSAGF [18], PAY [26], PRRTMMNGGR, MGPAMMRTMPG [27], QCQQAVQSAV [28], QQQQGGGSSQSQ, QEPQESQQ, QQQQGGGSSQSQK, PETMQQQQQ [29], SSEDIKE [30], VPP [31], IPP [32], VPY [33], VH, LAN, IA, AL [34], β -Ala-His [35], and pyroGlu-Leu [36]. Egg ovotransferrin-derived tripeptide IRW exhibits the anti-inflammatory effect through the NF- κ B pathway by inhibiting p65 and p50 [24]. Moreover, whey protein-derived tetrapeptide IPAV can reduce IL-8 production via the NF- κ B and MAPK pathways [23]. While BAPs have shown potential as anti-inflammatory agents in cultured cells, further *in vivo* studies and underlying mechanism are still necessary to verify their effectiveness in managing chronic inflammation [2].

4. Pathways Involved in the Inhibition of Chronic Intestinal Inflammation by BAPs

There are four possible mechanism pathways for BAPs to attenuate chronic intestinal inflammation: NF- κ B, MAPK, Janus kinase-signal transducer and activator of transcription (JAK-STAT), and peptide transporter 1 (PepT1) (Figure 2) [2, 7, 10, 20, 37-41]. Through inhibiting these pathways, BAPs can act the anti-inflammatory function in intestinal cells.

Among these pathways, the NF- κ B and MAPK pathways are two main pathways for BAPs to inhibit inflammation [7]. The NF- κ B is a key regulator of the expression and secretion of inflammatory cytokines (TNF- α , IL-1 β , IL-6, and IL-8) and also plays a vital role in the expressions of cyclooxygenase-2 (COX-2) and inducible nitric oxide synthase (iNOS) [42]. Inflammatory stimuli (IL-1 β , LPS, TNF- α , viruses, or oxidative stress) activate inhibitory κ B kinases (IKK α , IKK β , and IKK γ), leading to phosphorylation of a potential cytoplasmic transcription factor that contains an inhibitor of κ B (I κ B α , I κ B β , and I κ B γ) and I κ B α degradation [42]. NF- κ B is a family of transcription factor proteins, including five subunits: p65 (RelA), p50, p52, Rel, and RelB. After dimer p65/p50 is released into the cytosol, it can be translocated into the nucleus and initiates target gene transcription for proinflammatory factors, causing inflammation (Figure 2) [2, 42]. Many food-derived BAPs can inhibit

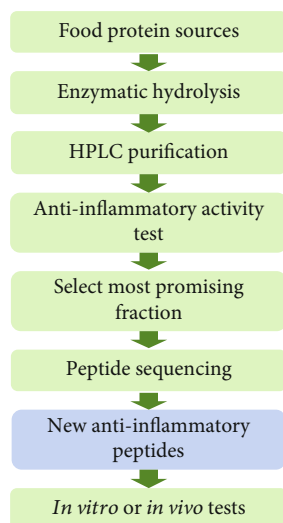


FIGURE 1: Classical steps toward the production and purification of anti-inflammatory peptides from food protein sources. HPLC: high-performance liquid chromatography. This figure was adapted from previous reports [3, 48, 81].

inflammation via this NF- κ B pathway, such as DYKKY [19], GPR [22], IRW [24], IQW [12], MLGATSL, MSYSAGF [18], pyroGlu-Leu [36], and TMKLLLVTL [43].

Another major signaling pathway, MAPK, can regulate many cellular activities, including proliferation, differentiation, death, and immune response. The stimulus and MAP3K phosphorylation can mediate the phosphorylation of the downstream MAP2K and MAPK, which contain three subfamilies: p38, extracellular signal-regulated kinases (ERK1 and ERK2), and c-Jun N-terminal kinase (JNK). In unstimulated cells, JNK mainly exists in the cytoplasm, but there is also some distribution in the nucleus. After being stimulated, JNK accumulates in the nucleus and causes the corresponding gene (IL-1 and TNF- α) expression, resulting in inflammatory response (Figure 2) [44]. Various food protein-derived BAPs can inhibit inflammation via this MAPK pathway, such as DEDTQAMPFR, DEDTQAMPF [18], FLV [20], MLGATSL, MSYSAGF [18], β -Ala-His [35], pyroGlu-Leu [36], DIKTNKPVIF [45], VPP [46], WH [41], γ -EC, and γ -EV [47].

Along with the above two pathways, the JAK-STAT pathway is also important for inflammatory response and can regulate hematopoietic cell development and inflammatory cytokines. Phosphorylation of JAK and STATs can form the dimer translocated to the nucleus [38]. BAPs can attenuate inflammation by inhibiting phosphorylation of JAK and STATs. However, the role of this pathway needs further verification for the anti-inflammation of BAPs. The translocations and activation of the substrate proteins from the above three pathways, including transcription factors in the nucleus (AP-1, ATF-2, EIK1, and c-Jun), cause the change of target genes, reducing the productions of proinflammatory cytokines, including IL-1 β , IL-2, IL-5, IL-8, IL-12, IL-13, IL-17, TNF- α , MCP-1, and IFN- γ . The overexpression of these proinflammatory mediators and the downexpression of anti-inflammatory cytokines (IL-4, IL-10, and TGF- β) can

lead to intestinal inflammation. Through regulating these pathways and cytokines, BAPs can attenuate chronic intestinal inflammation and diseases.

5. Mechanism of Food-Derived Anti-Inflammatory Peptides to Exert Bioactivities

The potential anti-inflammatory mechanisms of BAPs derived from food proteins through regulating various cytokines or systems are shown in Figure 3 [7, 48]. The secretions and expressions of proinflammatory cytokines IL-1 β , IL-2, IL-5, IL-6, IL-8, IL-12, IL-17, TNF- α , and IFN- γ can be inhibited by BAPs, as well as the activations of NF- κ B and MAPK pathways, COX-2, ROS, iNOS, and nitric oxide (NO). ROS are associated with inflammatory diseases, and NO is synthesized by NO synthase (NOS) enzyme (iNOS), and the inhibition of iNOS and ROS activities can suppress NO production. BAPs can also inhibit the expression and release of a transcription factor that drives treg phenotypic differentiation (Foxp3) and T-helper-cell-associated cytokines (Th1, Th2, and Th17) and the secretions of IgG, IgE, and IgA. On the other side, secretions and expressions of anti-inflammatory cytokines (IL-4, IL-10, and TGF- β), CD4⁺/CD8⁺, numbers of macrophages, and superoxide dismutase (SOD) activity can be increased by BAPs. In addition, the gut microbiome, which is an active topic in health, can be normalized by BAPs [7, 48]. In conclusion, these cytokines and pathways are the molecular targets and mechanisms for BAPs to regulate the intestinal inflammation of human and animals.

Milk-derived VPP and IPP can exhibit beneficial effect in an animal colitis model through anti-inflammatory action for these targets [49]. VPP also reduced TNF- α and IL-1 β expression and macrophage accumulation and activation, inhibited adipose inflammation in mice via angiotensin-converting enzyme-dependent cascade [31], and moderated monocyte adhesion to inflamed endothelia via the MAPK-JNK pathway [50]. In addition, tripeptides IRW and IQW downregulated the expression of inflammatory proteins via the NF- κ B pathway [12, 24]. Generally, these BAPs can inhibit the expression of cytokines and mediate the NF- κ B and MAPK pathways [1].

6. The *In Vivo* Studies of BAPs on Inflammation

For the *in vivo* studies of BAPs, various inflammatory models have been used, typically colitis in mice induced by DSS and TNBS. As observed in human CD, the administration of TNBS to mice can release proinflammatory cytokines, followed by infiltration of T cell CD4⁺ phenotype. In these studies, the mice with colitis were orally administered with BAPs mostly with an amount of 50-500 mg/kg body weight/day for several days to weeks (Table 2). Then, the tissues are collected for common evaluation of anti-inflammation of BAPs using morphological, immunological, and biochemical assays [51], such as body weight, colonic length, disease activity index (DAI), lymphocyte proliferation, CD4⁺/CD8⁺ determination, secretory-immunoglobulin-A

TABLE 1: The *in vitro* effects of food-derived bioactive peptides on inhibiting inflammation.

Peptides	Origin	Object	Administration	Activities	Results	Reference
CR, FL, HC, LL, MK	Egg ovotransferrin	TNF- α -induced Caco-2 cells	0.05-2 mg/mL egg white digest	Reduce IL-8 secretion and expressions of TNF- α , IL-8, IL-6, IL-1 β , and IL-12 and increase IL-10 expression	Inhibit intestinal inflammation	[17]
DEDTQAMPFR, DEDTQAMPF, MLGATSL, MSYSAGF	Egg white protein	TNF- α -induced Caco-2 cells	0.25 mg/mL peptide	Inhibit expressions of TNF- α , IL-8, IL-6, IL-1 β , IL-12, JNK, I κ B, and p38 and increase IL-10 expression	Inhibit inflammation via the MAPK pathway	[18]
DYKKY	Milk whey protein	RAW 264.7 cells	10 and 100 μ g/mL	Inhibit expressions of IL-1 β , COX-2, and TNF- α and productions of IL-1 β and TNF- α and inhibit p38, p65, and I κ B α degradation	Inhibit inflammation via the NF- κ B pathway	[19]
EAMAPK, AVPPYQ	Milk casein	H ₂ O ₂ -induced IEC-6 cells	5-150 g/mL peptide	Reduce ROS levels and increase SOD and Nrf2 activities	Antioxidation	[13]
FLV	Soybean protein	TNF- α -induced RAW 264.7 and 3T3-L1 cells	0.1-1 μ M FLV	Inhibit productions of TNF- α , IL-6, and MCP-1 and expressions of JNK, IKK, and I κ B α	Inhibit inflammation	[20]
GPETAFLR	Lupine protein	THP-1-derived macrophages	100-500 μ g/mL GPETAFLR	Reduce expressions of TNF- α , IL-1 β , and CCL2 and increase IL-10 expression	Prevent chronic inflammation	[21]
GPR	Amaranth protein	LPS-induced THP-1 and RAW 264.7 cells	1 mg/mL hydrolysate	Inhibit TNF- α secretion	Inhibit inflammation via the NF- κ B pathway	[22]
IPAV	Milk whey protein	TNF- α -induced Caco-2 cells	25-200 μ M IPAV	Reduce IL-8 and inhibit expressions of NF- κ B, ERK1/2, JNK1/2, Syk, and p38	Inhibit intestinal inflammation via PepT1	[23]
IRW	Egg ovotransferrin	TNF- α -induced human endothelial cells	50 μ M IRW	Inhibit ICAM-1, VCAM-1, MCP-1, and NF- κ B pathway	Inhibit vascular inflammation	[24]
IRW, IQW	Egg ovotransferrin	HUVECs	50 μ M IRW or IQW	Inhibit expressions of ICAM-1, VCAM-1, and NF- κ B pathway	Inhibit endothelial inflammation and oxidative stress	[12]
LDAVNR, MMLDF	Spirulina maxima	RBL-2H3 mast cells and EA.hy926 cells	200 μ M peptide	Reduce histamine release, IL-8 production, and ROS production	Inhibit inflammation	[25]

TABLE 1: Continued.

Peptides	Origin	Object	Administration	Activities	Results	Reference
Lunasin	Defatted soybean meal protein	LPS-induced RAW 264.7 cells	100 μ M lunasin	Inhibit NO and PGE2 production and COX-2 and iNOS expressions	Inhibit inflammation	[14]
PAY	Salmon protein	LPS-induced RAW 264.7 cells	0.25-0.75 mM PAY	Reduce productions or expressions of NO, PGE2, TFN- α , IL-6, IL-1 β , iNOS, and COX-2	Inhibit inflammation	[26]
PRRTRMMNGGR, MGPAMMRTMPG	Juice of cooked tuna	LPS-induced RAW 264.7 cells	100 μ g/mL hydrolysate	Inhibit secretions of IL-2, TNF- α , and IFN- γ	Inhibit inflammation	[27]
QCQQAVQSAV	Ruditapes philippinarum hydrolysate	LPS-induced RAW 264.7 cells	10-100 μ g/mL peptide	Inhibit NO production	Inhibit inflammation	[28]
QQQQGGGSQSQ, QEPQESQQ, QQQQQGGGSQSQKQ, PETMQQQQQQ	Germinated soybean protein	LPS-induced RAW 264.7 cells	2 mg/mL fraction	Inhibit NO and PGD2 production	Inhibit inflammation	[29]
SSEDIKE	Amaranth protein	Caco-2 cells	100-200 μ g/mL SSEDIKE	Reduce CCL20 and NF- κ B expressions	Inhibit inflammation	[30]
VPP	Milk casein	3T3-L1 adipocyte cells	1 mM VPP	Inhibit TNF- α expression	Inhibit inflammation via ACE-dependent cascade	[31]
VPP, IPP	Milk casein	3T3-F442A cells	50 μ M VPP or IPP	Upregulate PPAR γ , activate NF- κ B, and reduce adipokine	Inhibit inflammation	[32]
VPY	Soybean protein	Caco-2 and THP-1 cells	0.1-4 mM VPY	Inhibit IL-8 and TNF- α secretions	Treat IBD via PepT1	[33]
VH, LAN, IA, AL	Velvet antler protein from red deer	LPS-induced RAW 264.7 cells	100-500 μ g/mL peptide	Inhibit NO production	Inhibit inflammation	[34]
β -Ala-His	Meat products	H ₂ O ₂ -induced Caco-2 cells	—	Inhibit IL-8 and p38 and ERK activation	Inhibit inflammation via the MAPK and PepT1 pathways	[35]
pyroGlu-Leu	Wheat gluten	LPS-induced RAW 264.7 cells	200-800 μ g/mL peptide	Inhibit NO production, TNF- α , IL-6, and I κ B α degradation, and JNK, ERK, and p38 phosphorylation	Inhibit inflammation via the NF- κ B and MAPK pathways	[36]

3T3-L1: mouse preadipocytes; ACE: angiotensin-converting enzyme; Caco-2: human colorectal adenocarcinoma-derived intestinal epithelial cells; COX-2: cyclooxygenase-2; EA.hy926: human umbilical vein endothelial cells; PPAR γ : peroxisome proliferator-activated receptor gamma; RAW264.7: a mouse macrophage cell line; RAS: renin-angiotensin system; RBL-2H3: rat basophilic leukemia cells; ROS: reactive oxygen species; SOD: superoxide dismutase; THP-1: a human monocytic cell line; TNF- α : tumor necrosis factor α ; HUVECs: human umbilical vein endothelial cells; ICAM-1: intercellular adhesion molecule-1; IL-1 β : interleukin-1 β ; JNK: c-Jun N-terminal kinase; MAPK: mitogen-activated protein kinase; MCP-1: monocyte chemoattractant protein-1; NF- κ B: nuclear factor- κ B; NO: nitric oxide; VCAM-1: vascular cell adhesion molecule-1.

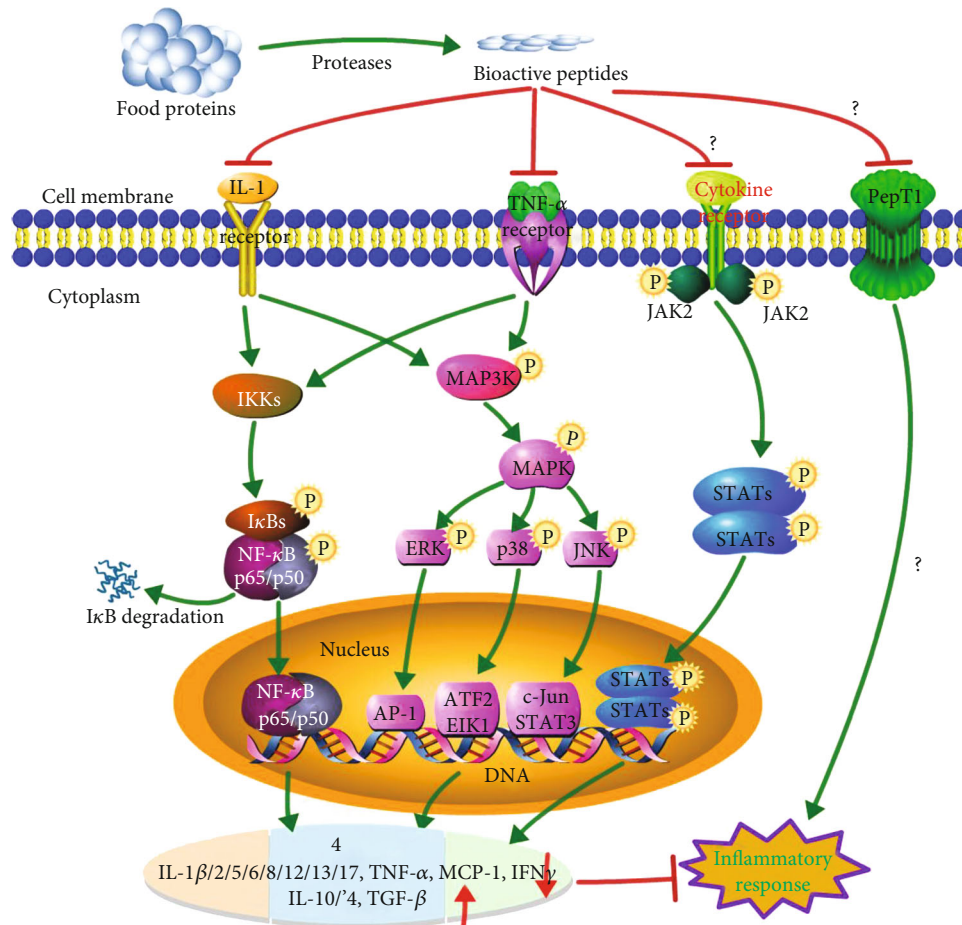


FIGURE 2: Schematic diagram of possible anti-inflammatory mechanism of bioactive peptides derived from food proteins. The anti-inflammatory activity may be via the following four pathways: NF- κ B, MAPK, JAK-STAT, and PepT1. IL-1: interleukin-1; LPS: lipopolysaccharides; MAPK: mitogen-activated protein kinase; MAP3K: MAPK kinase kinase; NF- κ B: nuclear factor-kappa B; TGF- β : transforming growth factor β ; TNF- α : tumor necrosis factor α ; JAK-STAT: Janus kinase-signal transducer and activator of transcription. This diagram was drawn using an online pathway builder tool (<http://www.proteinlounge.com>). Adapted from previous reports [2, 7, 10, 20, 37–41].

(s-IgA) measurement, immunoglobulin (IgA, IgM, and IgG) determination, and cytokine (IL-1, IL-2, IL-6, IL-8, IL-10, TNF- α , and IFN- γ) measurements (Table 2).

Numbers of BAPs derived from various food proteins (milk, plant, egg, soybean, meat, wheat, rice, potato, corn silk, fish, etc.) have been found to be well suited to treat inflammation or IBD symptoms *in vivo* (Table 2), such as Ala-Gln (AQ) [9, 52–54], DIKTNKPVIF [45], EWP [55], GLTSK [56], glycomacropeptide [57–60], lunasin [15], IRW [11, 61–63], IQW [62–64], KGHYAERVG [65], KPV [66], PTGADY [67], QCQCAVEGGL [68], QEPVL, QEPV [6], RILSILRHQNLKELQDLAL [69], SSEDIKE [70], TMKLLLVTL [43], VPP [31, 46, 71, 72], IPP [71, 72], VPY [33], WH [41], casein hydrolysates [73], soybean dipeptides and tripeptides [74], peptide P-317 [75], pyroGlu-Leu [76], β -Casofensin [77], γ -EC, and γ -EV [47]. These studies suggest that oral administration of food-derived BAPs have anti-inflammatory effects, and they can be the therapeutic agents for inflammatory-related diseases, including IBD [78].

Oral administration of dipeptide AQ reduced inflammatory cytokine expression, enhancing the mucosa recovery in

DSS-induced mice [53]. Likewise, intravenous infusion with AQ to calves with early weaned stress can increase concentrations of IgA, IgG, s-IgA, CD2⁺ and CD4⁺ lymphocytes, and CD4⁺/CD8⁺ ratio; therefore, the diarrhea occurrence was decreased [52]. Bean protein is also a rich resource for BAPs. For example, bean- and yeast extract-derived flavor peptide γ -EC and γ -EV can inhibit the inflammation in IBD mice [47]. Soybean-derived dipeptides and tripeptides decreased the colonic expressions of proinflammatory IFNG, IL-1B, IL-12B, TNF, and IL-17A and MPO activity and increased Foxp3 expression and CD4⁺CD25⁺ T cells; therefore, the colon and ileum inflammation of piglets with DSS-induced colitis was attenuated [74]. In addition, with the infusion of 150 mg/kg of egg white protein-derived EWP, weight loss, crypt distortion, IL-6 and TNF- α concentrations, and expressions of IL-1 β , IL-8, IL-17, and IFN- γ in the colon of piglets with DSS-induced colitis can be reduced, and gut barrier function was restored [55], as well as the barrier protection effects of milk-derived β -Casofensin [77] and dipeptide AQ [53]. Therefore, food-derived BAPs can contribute to disease treatment through modifying intestinal barrier function [79].

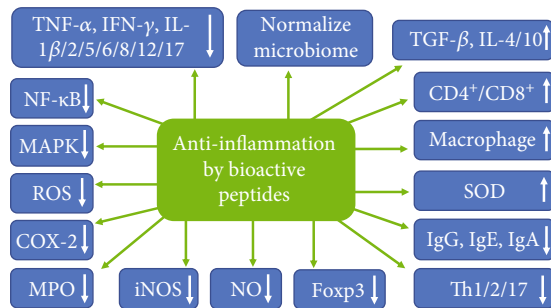


FIGURE 3: The potential mechanisms of anti-inflammatory action of food-derived bioactive peptides. CD4⁺/CD8⁺: splenic T lymphocyte subpopulations; COX-2: cyclooxygenase-2; Foxp3: a transcription factor that drives treg phenotypic differentiation; iNOS: inducible nitric synthase; IFN- γ : interferon- γ ; IL-1 β : interleukin-1 β ; MAPK: mitogen-activated protein kinase; MPO: myeloperoxidase; NF- κ B: nuclear factor- κ B; NO: nitric oxide; ROS: reactive oxygen species; SOD: superoxide dismutase; TNF- α : tumor necrosis factor α ; TGF- β : transforming growth factor β ; Th1/2/17: T-helper-cell-associated cytokine 1/2/17. This figure was adapted from previous reports [7, 48].

In DSS-induced mice, antioxidant enzyme activities and microbial diversity and abundance were increased and the colitis was attenuated by egg white protein-derived IRW and IQW [63]. Oral administration of corn silk extract-derived TMKLLLVTL suppressed IKK β activity, I κ B phosphorylation, NF- κ B activity, and IL-1 β production in LPS-induced inflammatory mice [43]. Drinking water with soybean-derived tripeptide VPY can reduce DAI, weight loss, MPO activity, and expressions of IL-1 β , IL-6, IL-17, IFN- γ , and TNF- α in colitis mice [33], suggesting that VPY can treat IBD. In addition, sardine muscle hydrolysate-derived dipeptide WH can reduce DSS-induced colitis symptoms, colonic cytokine expression, MAPK and I κ B α activation, and IL-8 secretion in colitis mice, indicating that WH can inhibit intestinal inflammation [41]. Favor peptide γ -EC and γ -EV inhibited I κ B α and JNK activation and expressions of IL-1 β , IL-6, IL-17, INF- γ , and TNF- α and increased IL-10 expression in IBD mice [47]. Moreover, tripeptide KPV reduced intestinal inflammation by decreasing IL-1 β , IL-6, IL-12, and IFN- γ expressions and attenuated colitis via PepT1 [66].

Milk protein is a rich source for BAPs, which has potential beneficial effects to the gut of humans and animals [80, 81]. Milk casein-derived VPP and IPP are two famous BAPs with antihypertensive and anti-inflammatory activities. Pro-inflammatory IL-6 and IL-1 β were reduced, and atherosclerosis was attenuated by oral administration of VPP and IPP [71]. Arterial dysfunction was attenuated by drinking water with VPP and IPP through increasing vasorelaxation and nitrite and nitrate and reducing pulse wave velocity and cardiac and renal damage [72]. It was reported that VPP attenuated inflammation via the MAPK-JNK pathway by reducing monocytes, macrophages, CD18, IL-6, and MCP-1 in adipose inflammatory mice [46]. Milk casein-derived QEPVL and QEPV reduced nitric oxide (NO) release, increased anti-inflammatory IL-4 and IL-10 production, and decreased productions of IFN- γ and TNF- α in LPS-

induced mice [6]. Milk κ -casein-derived glycomacropeptide inhibited inflammation and attenuated colitis via normalizing the inflammatory cytokine and the NF- κ B and MAPK pathways in previous studies [57–60].

From these *in vivo* studies, the evidences that the intestinal inflammation can be attenuated by oral administration of food protein-derived BAPs have been presented. As many studies have been performed recently, large-scale human and animal trials are still lacking [2]. It has been reviewed that numbers of humans or animals to be transported into the bloodstream of humans or animals to exert bioactivities [3, 81]. However, there is still limitation for such *in vivo* studies due to the possible degradation of BAPs by peptidases in the gut and plasma or insufficient absorption [82]. In the future, more studies of humans and animals are needed to evaluate the anti-inflammatory effects of BAPs, as well as the doses, times, and kinetics in the body.

7. Peptide Transporter PepT1

The peptide transporter 1 (PepT1) can transport small peptides from the intestine into the bloodstream of humans or animals [83–85], particularly di- and tripeptides, and its expression in intestinal epithelial cells is increased when the intestine is suffering from inflammation [86], indicating that PepT1 is a gateway to inflammatory response [87]. Similarly, PepT1 can transport various BAPs into intestinal epithelial cells to exert bioactivities [3, 81], such as IPAV [23], KPV [66], LKP, IQW [88], LSW [89], IWH, IW [90], and VPY [33].

It was reported that anti-inflammatory tripeptide KPV can attenuate intestinal inflammation associated with PepT1 expression, and KPV lost the anti-inflammatory function without PepT1 expression, suggesting that PepT1 mediates the anti-inflammation of KPV [66]. It was reported that soy protein-derived tripeptide VPY exerted anti-inflammatory activity in cells also through PepT1, which can transport VPY into cells [33]. In addition, pharmacological inhibition of PepT1 can counteract the inhibition of IL-8 expression mediated by peptide IPAV [23]. Moreover, the anti-inflammatory effect of meat-derived carnosine (β -Ala-His) was inhibited by dipeptide Gly-Sar, a PepT1 substrate [35]. These findings indicate that PepT1 is a promising target to treat intestinal inflammation by transporting sufficient short-chain BAPs into colonic cells [10]. In conclusion, PepT1 is a possible mechanism for the inhibition of intestinal inflammation by BAPs. However, this PepT1 pathway involved in anti-inflammation of BAPs still needs to be verified by further researches in the future (Figure 2).

8. Impact of Anti-Inflammatory Peptides on Gut Microbiota

When intestinal inflammation or IBD occurs, the gut microbial community would also change, such as the decrease of *Firmicutes* (particularly *Clostridium* groups) and the increase of *Bacteroides*, *Lactobacillus*, *Eubacterium*, and *Proteobacteria* [91]. In DSS-induced colitis mice, compositions and varieties of the gut microorganism

TABLE 2: The *in vivo* effect of bioactive peptides on inhibiting inflammation.

Peptides	Origin	Object	Administration	Activities	Results	Reference
AQ	Synthesis	Early-weaned calves	Intravenous infusion 1.01 g/kg BW/d AQ	Increase concentrations of CD2 ⁺ and CD4 ⁺ lymphocytes, CD4 ⁺ /CD8 ⁺ ratio, and IgA, IgG, and s-IgA and improve intestinal integrity	Improve gain performance and decrease diarrhea occurrence	[52]
AQ	Synthesis	DSS-induced colitis C57BL/6 mice	Inject 75 mg/kg BW/d AQ	Reduce Th1/Th2/Th17, haptoglobin, IgG, chemokine, and MPO activity	Attenuate colitis	[9]
AQ	Synthesis	DSS-induced colitis C57BL/6 mice	Inject 75 mg/kg BW/d AQ	Increase colon length, TLR4, NF- κ B activation, and expressions of mucin 2, IL-17, and TNF- α and reduce IgG, DAI, and haptoglobin	Inhibit inflammation and enhance mucosa recovery	[53]
AQ	Synthesis	DSS-induced colitis C57BL/6 mice	Inject 75 mg/kg BW/d AQ	Reduce IL-17, Th17, and macrophage	Inhibit inflammation	[54]
DIKTNKPVIF	Potato protein hydrolysate	HFD-fed SAMP8 mice	Oral and intraperitoneal injection	Reduce expressions of p-p38, FGF-2, TNF- α , and IL-6	Attenuate proinflammatory reaction via the MAPK pathway	[45]
EWP	Egg white protein	DSS-induced IBD in piglets	Infuse 150 mg/kg BW EWP for 5 days	Reduce weight loss, crypt distortion, and expressions of TNF- α , IL-6, IL-1 β , IFN- γ , IL-8, and IL-17 and restore gut barrier function	Manage IBD	[55]
GLTSK	Phaseolus vulgaris	AOM/DSS-induced colitis BALB/c mice	Oral 50 mg/kg BW/d GLTSK	Reduce DAI and neoplasms and enhance colon length	Attenuate colitis	[56]
Glycomacropeptide	Milk κ -casein	TNBS-induced ileitis rat	Oral 500 mg/kg BW/d peptide	Reduce DAI, MPO, alkaline phosphatase, iNOS, IL-1 β , IL-17, and TNF	Attenuate ileitis via reducing IL-17	[57]
Glycomacropeptide	Milk κ -casein	DSS-induced colitis C57BL/6 female mice	Gavage 500 mg/kg BW/d peptide	Reduce DAI and normalize colonic expressions of IL-1 β , IL17, IL23, IL6, TGF- β , IL10, and Foxp3	Inhibit inflammation	[58]
Glycomacropeptide	Milk κ -casein	DSS-induced colitis mice	Gavage 15 mg/d peptide	Increase BW and reduce DAI, CD4 ⁺ , IFN- γ , and MPO activity	Inhibit colitis inflammation	[59]
Glycomacropeptide	Milk κ -casein	Oxazolone-induced ulcerative colitis BALB/c mice	Oral 50 mg/kg BW/d peptide	Inhibit NF- κ B and MAPK activations and reduce serum IL-1 β , IL-5, IFN- γ , TNF- α , and IL-10 production	Attenuate colitis	[60]

TABLE 2: Continued.

Peptides	Origin	Object	Administration	Activities	Results	Reference
Lunasin	Soybean protein	LPS-induced airway inflammation mice	Intranasal 20 μ g/mice lunasin	Reduce infiltration, goblet cell metaplasia, and Th2 cytokine expression	Alleviate inflammation	[15]
IRW	Egg ovotransferrin	Spontaneously hypertensive rat	Oral 15 mg/kg BW/d IRW	Reduce ICAM-1 and VCAM-1 expression	Inhibit inflammation and hypertension via the NF- κ B pathway	[11]
IRW	Egg ovotransferrin	LPS-induced inflammatory peritonitis in rat	Oral 40 mg/kg IRW in feed	Reduce serum TNF- α and IL-6 and MPO activity, increase Shannon index, and decrease Simpson indices	Attenuate inflammation	[61]
IRW, IQW	Egg ovotransferrin	DSS-induced colitis in mice	Drink water with 30 mg/mL peptide	Increase antioxidant enzyme activities and microbial diversity and abundance	Attenuate colitis	[63]
IRW, IQW	Egg ovotransferrin	DSS-induced colitis in mice	Oral 0.03% peptide in diet	Reduce TNF- α and IL-17	Inhibit colonic inflammation	[64]
IRW, IQW	Egg ovotransferrin	Citrobacter rodentium-induced colitis in mice	Oral 0.03% peptide in diet	Regulate intestinal microorganisms	Inhibit colonic inflammation	[62]
KGHYAERVG	Rice	Autoimmune encephalitis mice	Oral 100 mg/kg peptide	Reduce productions of IL-17, IFN- γ , IL-23, and IL-12 and increase T cells	Attenuate autoimmune encephalitis	[65]
KPV	C-terminal sequence of α -melanocyte stimulating hormone	DSS- and TNBS-induced colitis in mice	Drink water with 100 μ M KPV	Decrease expressions of IL-6, IL-12, IFN- γ , and IL-1 β	Reduce intestinal inflammation via PepT1	[66]
PTGADY	Alaska pollock hydrolysates	Hydrogenated cortisone-treated mice	Oral 50-200 mg/kg BW/d hydrolysate	Increase productions of IL-2, IL-4, and IL-6	Immunomodulation	[67]
QCQCAVEGGL	Crassostrea gigas	DSS-induced colitis mice	Oral 50 mg/kg BW/d hydrolysate	Reduce IgE and increase spleen CD4 ⁺ /CD8 ⁺	Attenuate colitis	[68]
QEPVL, QEPV	Milk casein	LPS-induced mice	Oral 200 mg/kg BW/d peptide	Reduce NO release, increase IL-4 and IL-10 production, and decrease IFN- γ and TNF- α production	Inhibit inflammation	[6]
RILSILRHQNLKELQDLAL	Chromogranin A	DSS-induced colitis in mice	Intracolonic injection 2.5 mg/kg/day peptide	Reduce IL-18, active macrophages, increase TJ proteins	Attenuate colitis	[69]
SSEDIKE	Amaranth seeds	IgE-mediated food allergy mouse	Gavage 100 μ g SSEDIKE	Reduce productions of IgE, IgG, IL-5, IL-13, and NF- κ B and increase TGF- β and Foxp3 expressions	Inhibit intestinal inflammation	[70]

TABLE 2: Continued.

Peptides	Origin	Object	Administration	Activities	Results	Reference
TMKLLLVTL	Corn silk extract	LPS-induced inflammatory mice	Oral 1 mg/kg peptide	Inhibit IL- β , IKK β , and I κ B phosphorylation and NF- κ B activation	Inhibit inflammation via the IKK β -NF- κ B pathways	[43]
VPP	Milk casein	HFD-induced adipose inflammation mice	Drink water with 0.3 mg/mL VPP for 10 weeks	Reduce monocytes, macrophages, CD18, IL-6, and MCP-1	Attenuate inflammation via the MAPK-JNK pathway	[46]
VPP	Milk casein	Obesity-induced adipose inflammation C57BL/6J mice	Drink water with 0.1% VPP for 4 months	Reduce TNF- α and IL-1 β expression and macrophage accumulation and activation	Attenuate inflammation	[31]
VPP, IPP	Milk casein	Apolipoprotein E-deficient mice	Oral 60.2 or 125 μ mol/kg BW/d peptide	Reduce IL-6, IL-1 β , and oxidized low-density lipoprotein receptor	Attenuate atherosclerosis	[71]
VPP, IPP	Milk κ -casein	L-NAME-treated rats	Drink water with 0.3 mg/mL VPP or IPP	Increase vasorelaxation and nitrite and nitrate and reduce cardiac and renal damage	Attenuate arterial dysfunction	[72]
VPY	Soybean protein	DSS-induced colitis BALB/C female mice	Drink water with 1 mg/mL VPY (100 mg/kg BW/d)	Reduce DAI, weight loss, and MPO activity and expressions of TNF- α , IL-6, IL-1 β , IFN- γ , and IL-17	Treat IBD via PepT1	[33]
WH	Sardine muscle hydrolysate	DSS-induced colitis BALB/c mice	Oral 100 or 250 mg/kg BW/d WH for 14 d	Reduce DAI, cytokine expression, MAPK and I κ B α activation, and IL-8 secretion	Inhibit intestinal inflammation	[41]
Milk casein hydrolysates	Lactobacillus fermentation	TNBS-induced colitis mice	Oral 150 μ g/d hydrolysate	Reduce BW loss, microbial translocation, colonic DAI, and IFN- γ production	Treat colitis	[73]
Di- and tripeptides	Soybean protein	DSS-induced colitis pig	Infuse 250 mg/kg BW/d peptides	Reduce the expressions of IFNG, IL-1B, IL-12B, TNF, and IL-17A and MPO activity and increase Foxp3 expression and CD4 ⁺ CD25 ⁺ T cells	Attenuate colon and ileum inflammation	[74]
Peptide P-317	Cyclic analog of morphiceptin	TNBS/DSS-induced colonic mice	Intraperitoneal 0.2 or oral 2 mg/kg BW/d peptide	Inhibit TNF- α and IL-1 β expression and MPO activity	Treat IBD	[75]
pyroGlu-Leu	Wheat gluten	DSS-induced colitis mice	Gavage 0.01-10 mg/kg BW/d peptide	Reduce DAI and normalize colonic <i>Bacteroidetes</i> and <i>Firmicutes</i>	Treat IBD via gut microbiota	[76]

TABLE 2: Continued.

Peptides	Origin	Object	Administration	Activities	Results	Reference
β -Casofensin	Milk protein	NMS-induced intestinal barrier alteration rat	Oral 10 μ L/kg BW/d peptide (0.01-100 μ M)	Reduce intestinal damages and prevent neonatal stress	Protect gut barrier	[77]
γ -EC, γ -EV	Beans and yeast extracts	DSS-induced BALB/C female mice	Gavage 50 or 150 mg/kg BW/d peptide	Inhibit I κ B α and JNK activation and the expressions of TNF- α , IL-6, INF- γ , IL-1 β , and IL-17 and increase IL-10 expression	Inhibit colitis inflammation via the TNF- α pathway	[47]

ACE: angiotensin-converting enzyme; AOM: azoxymethane; BW: body weight; CD4⁺/CD8⁺: splenic T lymphocyte subpopulations; DAI: disease activity index; DSS: dextran sulfate sodium; Foxp3: a transcription factor that drives treg phenotypic differentiation; glycomacropeptide: a 64-amino acid peptide in stomach casein hydrolysis; HFD: high-fat diet; IBD: inflammatory bowel diseases; iNOS: inducible oxide nitric synthase; IFN: interferon; IKK β : inhibitory κ B kinase- β ; IL-1 β : interleukin-1 β ; KC: keratinocyte-derived chemokine; LPS: lipopolysaccharide; L-NAME: N(G)-nitro-L-arginine methyl ester hydrochloride; MCP-1: monocyte chemoattractant protein-1; MPO: myeloperoxidase; NF- κ B: nuclear factor- κ B; NMS: neonatal maternal separation; NO: nitric oxide; PPAR γ : peroxisome proliferator-activated receptor gamma; RAW264.7: a mouse macrophage cell line; SAMP8: senescence-accelerated mice prone 8; TGF- β : transforming growth factor β ; TJ: tight junction; TLR4: toll-like receptor 4; Th1/2/17: T-helper-cell-associated cytokine 1/2/17; TNBS: 2,4,6-trinitrobenzene sulfonic acid.

(*Anaerotruncus*, *Bacteroides*, *Enterobacteriaceae*, *Lactobacilli*, and *Parabacteroides*) have changed [92]. In general, when defensins decline, the abundance of bacteria from *Bacteroides* and *Firmicutes* would be increased [93].

It was reported that BAPs can exert anti-inflammation via changing the gut microbiota in several studies [62, 63, 76]. For example, oral administration of anti-inflammatory peptide pyroGlu-Leu derived from wheat gluten can normalize the population of *Bacteroidetes* and *Firmicutes* in the colon of colitis mice [76]. Shannon and Simpson indices represent species richness and species evenness, respectively. The Simpson index and the abundance of *Coprococcus-1*, *Desulfovibrio*, and *Ruminococcaceae-UCG-014* were increased by tripeptides IRW and IQW. Additionally, IQW decreased the abundance of *Bacteroides* and increased *Parabacteroides*, while the levels of *Anaerotruncus*, *Ruminiclostridium-9*, and *Oscillibacter* were increased by IRW [63]. *Firmicutes* and *Actinobacteria* species were increased, and the proportions of *Bacteroidetes* and *Proteobacteria* species were decreased by oral administration of IRW and IQW; therefore, the colonic inflammation was inhibited via regulation of intestinal microorganisms [62]. In addition, dietary dipeptide GQ changed the gut microbiota beneficially through increasing alpha diversity, bacterial loading, abundance of anaerobes and fiber-degrading bacteria (*Phylum Fibrobacteres*), and short-chain fatty acids in the gut [94].

In conclusion, the gut microbiota is a promising mechanism for BAPs to inhibit intestinal inflammation. However, the information of the mechanism underlying the effects of BAPs on gut microbiota is still lacking, and it needs more studies to explore the interaction between anti-inflammation of BAPs and gut microbiota in the future.

9. Conclusions and Future Perspectives

In this review, the mechanism and pathways of food protein-derived BAPs to exert anti-inflammatory bioactivities were

highlighted, including pathways (NF- κ B, MAPK, and JAK-STAT), PepT1, inflammatory mediators, and gut microbiota. Moreover, various *in vitro* and *in vivo* studies of BAPs on inflammation were reviewed, finding that PepT1 and gut microbiota are promising targets for the inhibition of BAPs on intestinal inflammation; however, their roles still need more further studies to be verified in the future.

The discovery of novel BAP sequences and their corresponding action mechanisms as well as gut microbiota and PepT1 involved in the mediation can provide new opportunities for better targeting of intestinal inflammation. More *in vivo* data, including pharmacokinetics and proper dosage and time of administration of BAPs, are needed before their application to humans and animals. The role of dietary BAPs in inhibiting intestinal inflammation represents a novel direction in nutraceuticals for people or animals with intestinal inflammation.

Conflicts of Interest

The authors declare that they have no competing interests.

Acknowledgments

This work was supported by grants from the State Key Laboratory of Animal Nutrition (2004DA125184F1906) and the Fundamental Research Funds for the Central Universities (2662019QD021).

References

- [1] K. Majumder, Y. Mine, and J. Wu, "The potential of food protein-derived anti-inflammatory peptides against various chronic inflammatory diseases," *Journal of the Science of Food and Agriculture*, vol. 96, no. 7, pp. 2303–2311, 2016.

- [2] S. Chakrabarti, F. Jahandideh, and J. Wu, "Food-derived bioactive peptides on inflammation and oxidative stress," *BioMed Research International*, vol. 2014, Article ID 608979, 11 pages, 2014.
- [3] Q. Xu, H. Hong, J. Wu, and X. Yan, "Bioavailability of bioactive peptides derived from food proteins across the intestinal epithelial membrane: a review," *Trends in Food Science and Technology*, vol. 86, pp. 399–411, 2019.
- [4] S. de Silva, S. Devlin, and R. Panaccione, "Optimizing the safety of biologic therapy for IBD," *Nature Reviews. Gastroenterology & Hepatology*, vol. 7, no. 2, pp. 93–101, 2010.
- [5] Z. F. Bhat, S. Kumar, and H. F. Bhat, "Antihypertensive peptides of animal origin: a review," *Critical Reviews in Food Science and Nutrition*, vol. 57, no. 3, pp. 566–578, 2017.
- [6] Z. Jiehui, M. Liuliu, X. Haihong et al., "Immunomodulating effects of casein-derived peptides QEPVL and QEPV on lymphocytes in vitro and in vivo," *Food & Function*, vol. 5, no. 9, pp. 2061–2069, 2014.
- [7] S. Guha and K. Majumder, "Structural-features of food-derived bioactive peptides with anti-inflammatory activity: a brief review," *Journal of Food Biochemistry*, vol. 43, no. 1, article e12531, 2019.
- [8] A. R. Jurjus, N. N. Houry, and J.-M. Reimund, "Animal models of inflammatory bowel disease," *Journal of Pharmacological and Toxicological Methods*, vol. 50, no. 2, pp. 81–92, 2004.
- [9] C.-C. Chu, Y.-C. Hou, M.-H. Pai, C.-J. Chao, and S.-L. Yeh, "Pretreatment with alanyl-glutamine suppresses T-helper-cell-associated cytokine expression and reduces inflammatory responses in mice with acute DSS-induced colitis," *The Journal of Nutritional Biochemistry*, vol. 23, no. 9, pp. 1092–1099, 2012.
- [10] H. Zhang, C. A. A. Hu, J. Kovacs-Nolan, and Y. Mine, "Bioactive dietary peptides and amino acids in inflammatory bowel disease," *Amino Acids*, vol. 47, no. 10, pp. 2127–2141, 2015.
- [11] K. Majumder, S. Chakrabarti, J. S. Morton et al., "Egg-derived tri-peptide IRW exerts antihypertensive effects in spontaneously hypertensive rats," *PLoS One*, vol. 8, no. 11, article e82829, 2013.
- [12] K. Majumder, S. Chakrabarti, S. T. Davidge, and J. Wu, "Structure and activity study of egg protein ovotransferrin derived peptides (IRW and IQW) on endothelial inflammatory response and oxidative stress," *Journal of Agricultural and Food Chemistry*, vol. 61, no. 9, pp. 2120–2129, 2013.
- [13] G. Pepe, E. Sommella, G. Ventre et al., "Antioxidant peptides released from gastrointestinal digestion of "Stracchino" soft cheese: characterization, in vitro intestinal protection and bioavailability," *Journal of Functional Foods*, vol. 26, pp. 494–505, 2016.
- [14] V. P. Dia, W. Wang, V. L. Oh, B. O. Lumen, and E. G. de Mejia, "Isolation, purification and characterisation of lunasin from defatted soybean flour and in vitro evaluation of its anti-inflammatory activity," *Food Chemistry*, vol. 114, no. 1, pp. 108–115, 2009.
- [15] X. Yang, J. Zhu, C.-Y. Tung et al., "Lunasin alleviates allergic airway inflammation while increases antigen-specific tregs," *PLoS One*, vol. 10, no. 2, article e0115330, 2015.
- [16] Q. Xu, N. Singh, H. Hong et al., "Hen protein-derived peptides as the blockers of human bitter taste receptors T2R4, T2R7 and T2R14," *Food Chemistry*, vol. 283, pp. 621–627, 2019.
- [17] X. Wang, Y. Zhao, Y. Yao et al., "Anti-inflammatory activity of di-peptides derived from ovotransferrin by simulated peptide-cut in TNF- α -induced Caco-2 cells," *Journal of Functional Foods*, vol. 37, pp. 424–432, 2017.
- [18] M. Zhang, Y. Zhao, Y. Yao et al., "Isolation and identification of peptides from simulated gastrointestinal digestion of preserved egg white and their anti-inflammatory activity in TNF- α -induced Caco-2 cells," *The Journal of Nutritional Biochemistry*, vol. 63, pp. 44–53, 2019.
- [19] Y. Ma, J. Liu, H. Shi, and L. Yu, "Isolation and characterization of anti-inflammatory peptides derived from whey protein," *Journal of Dairy Science*, vol. 99, no. 9, pp. 6902–6912, 2016.
- [20] S.-J. Kwak, C.-S. Kim, M.-S. Choi et al., "The soy peptide Phe-Leu-Val reduces TNF α -induced inflammatory response and insulin resistance in adipocytes," *Journal of Medicinal Food*, vol. 19, no. 7, pp. 678–685, 2016.
- [21] M. del Carmen Millán-Linares, F. Millán, J. Pedroche, and M. del Mar Yust, "GPETAFLR: a new anti-inflammatory peptide from *Lupinus angustifolius* L. protein hydrolysate," *Journal of Functional Foods*, vol. 18, pp. 358–367, 2015.
- [22] A. Montoya-Rodríguez, E. G. de Mejía, V. P. Dia, C. Reyes-Moreno, and J. Milán-Carrillo, "Extrusion improved the anti-inflammatory effect of amaranth (*Amaranthus hypochondriacus*) hydrolysates in LPS-induced human THP-1 macrophage-like and mouse RAW 264.7 macrophages by preventing activation of NF- κ B signaling," *Molecular Nutrition & Food Research*, vol. 58, no. 5, pp. 1028–1041, 2014.
- [23] M. Oyama, T. Van Hung, K. Yoda, F. He, and T. Suzuki, "A novel whey tetrapeptide IPAV reduces interleukin-8 production induced by TNF- α in human intestinal Caco-2 cells," *Journal of Functional Foods*, vol. 35, pp. 376–383, 2017.
- [24] W. Huang, S. Chakrabarti, K. Majumder, Y. Jiang, S. T. Davidge, and J. Wu, "Egg-derived peptide IRW inhibits TNF- α -induced inflammatory response and oxidative stress in endothelial cells," *Journal of Agricultural and Food Chemistry*, vol. 58, no. 20, pp. 10840–10846, 2010.
- [25] T.-S. Vo, B. Ryu, and S.-K. Kim, "Purification of novel anti-inflammatory peptides from enzymatic hydrolysate of the edible microalga *Spirulina maxima*," *Journal of Functional Foods*, vol. 5, no. 3, pp. 1336–1346, 2013.
- [26] C. B. Ahn, Y. S. Cho, and J. Y. Je, "Purification and anti-inflammatory action of tripeptide from salmon pectoral fin byproduct protein hydrolysate," *Food Chemistry*, vol. 168, pp. 151–156, 2015.
- [27] M.-L. Cheng, H.-C. Wang, K.-C. Hsu, and J.-S. Hwang, "Anti-inflammatory peptides from enzymatic hydrolysates of tuna cooking juice," *Food and Agricultural Immunology*, vol. 26, no. 6, pp. 770–781, 2015.
- [28] S.-J. Lee, E.-K. Kim, Y.-S. Kim et al., "Purification and characterization of a nitric oxide inhibitory peptide from *Ruditapes philippinarum*," *Food and Chemical Toxicology*, vol. 50, no. 5, pp. 1660–1666, 2012.
- [29] M. González-Montoya, B. Hernández-Ledesma, J. M. Silván, R. Mora-Escobedo, and C. Martínez-Villaluenga, "Peptides derived from in vitro gastrointestinal digestion of germinated soybean proteins inhibit human colon cancer cells proliferation and inflammation," *Food Chemistry*, vol. 242, pp. 75–82, 2018.
- [30] J. Moronta, P. L. Smaldini, G. H. Docena, and M. C. Añón, "Peptides of amaranth were targeted as containing sequences with potential anti-inflammatory properties," *Journal of Functional Foods*, vol. 21, pp. 463–473, 2016.

- [31] Y. Sawada, Y. Sakamoto, M. Toh et al., "Milk-derived peptide Val-Pro-Pro (VPP) inhibits obesity-induced adipose inflammation via an angiotensin-converting enzyme (ACE) dependent cascade," *Molecular Nutrition & Food Research*, vol. 59, no. 12, pp. 2502–2510, 2015.
- [32] S. Chakrabarti and J. Wu, "Milk-derived tripeptides IPP (Ile-Pro-Pro) and VPP (Val-Pro-Pro) promote adipocyte differentiation and inhibit inflammation in 3T3-F442A cells," *PLoS One*, vol. 10, no. 2, article e0117492, 2015.
- [33] J. Kovacs-Nolan, H. Zhang, M. Ibuki et al., "The PepT1-transportable soy tripeptide VPY reduces intestinal inflammation," *Biochimica et Biophysica Acta (BBA) - General Subjects*, vol. 1820, no. 11, pp. 1753–1763, 2012.
- [34] L. Zhao, X. Wang, X.-L. Zhang, and Q.-F. Xie, "Purification and identification of anti-inflammatory peptides derived from simulated gastrointestinal digests of velvet antler protein (*Cervus elaphus Linnaeus*)," *Journal of Food and Drug Analysis*, vol. 24, no. 2, pp. 376–384, 2016.
- [35] D. O. Son, H. Satsu, Y. Kiso, M. Totsuka, and M. Shimizu, "Inhibitory effect of carnosine on interleukin-8 production in intestinal epithelial cells through translational regulation," *Cytokine*, vol. 42, no. 2, pp. 265–276, 2008.
- [36] S. Hirai, S. Horii, Y. Matsuzaki et al., "Anti-inflammatory effect of pyroglutamyl-leucine on lipopolysaccharide-stimulated RAW 264.7 macrophages," *Life Sciences*, vol. 117, no. 1, pp. 1–6, 2014.
- [37] S. Li, L. Liu, G. He, and J. Wu, "Molecular targets and mechanisms of bioactive peptides against metabolic syndromes," *Food & Function*, vol. 9, no. 1, pp. 42–52, 2018.
- [38] S. Li, T. Bu, J. Zheng, L. Liu, G. He, and J. Wu, "Preparation, bioavailability, and mechanism of emerging activities of Ile-Pro-Pro and Val-Pro-Pro," *Comprehensive Reviews in Food Science and Food Safety*, vol. 18, no. 4, pp. 1097–1110, 2019.
- [39] T. Zhang, J. McCarthy, G. Wang, Y. Liu, and M. Guo, "Physicochemical properties, microstructure, and probiotic survivability of nonfat goats' milk yogurt using heat-treated whey protein concentrate as fat replacer," *Journal of Food Science*, vol. 80, no. 4, pp. M788–M794, 2015.
- [40] M. Tanaka, S. M. Hong, S. Akiyama, Q. Q. Hu, and T. Matsui, "Visualized absorption of anti-atherosclerotic dipeptide, Trp-His, in Sprague-Dawley rats by LC-MS and MALDI-MS imaging analyses," *Molecular Nutrition & Food Research*, vol. 59, no. 8, pp. 1541–1549, 2015.
- [41] Y. Kobayashi, J. Kovacs-Nolan, T. Matsui, and Y. Mine, "The anti-atherosclerotic dipeptide, Trp-His, reduces intestinal inflammation through the blockade of L-type Ca^{2+} channels," *Journal of Agricultural and Food Chemistry*, vol. 63, no. 26, pp. 6041–6050, 2015.
- [42] P. P. Tak and G. S. Firestein, "NF- κ B: a key role in inflammatory diseases," *The Journal of Clinical Investigation*, vol. 107, no. 1, pp. 7–11, 2001.
- [43] T.-Y. Ho, C.-C. Li, H.-Y. Lo, F.-Y. Chen, and C.-Y. Hsiang, "Corn silk extract and its bioactive peptide ameliorated lipopolysaccharide-induced inflammation in mice via the nuclear factor- κ B signaling pathway," *Journal of Agricultural and Food Chemistry*, vol. 65, no. 4, pp. 759–768, 2017.
- [44] P. K. Roy, F. Rashid, J. Bragg et al., "Role of the JNK signal transduction pathway in inflammatory bowel disease," *World Journal of Gastroenterology*, vol. 14, no. 2, pp. 200–202, 2008.
- [45] S. Dumeus, M. A. Shibu, W.-T. Lin et al., "Bioactive peptide improves diet-induced hepatic fat deposition and hepatocyte proinflammatory response in SAMP8 ageing mice," *Cellular Physiology and Biochemistry*, vol. 48, no. 5, pp. 1942–1952, 2018.
- [46] K. Aihara, M. Osaka, and M. Yoshida, "Oral administration of the milk casein-derived tripeptide Val-Pro-Pro attenuates high-fat diet-induced adipose tissue inflammation in mice," *The British Journal of Nutrition*, vol. 112, no. 4, pp. 513–519, 2014.
- [47] H. Zhang, J. Kovacs-Nolan, T. Kodera, Y. Eto, and Y. Mine, " γ -Glutamyl cysteine and γ -glutamyl valine inhibit TNF- α signaling in intestinal epithelial cells and reduce inflammation in a mouse model of colitis via allosteric activation of the calcium-sensing receptor," *Biochimica et Biophysica Acta (BBA) - Molecular Basis of Disease*, vol. 1852, no. 5, pp. 792–804, 2015.
- [48] M. Chalamiah, W. Yu, and J. Wu, "Immunomodulatory and anticancer protein hydrolysates (peptides) from food proteins: a review," *Food Chemistry*, vol. 245, pp. 205–222, 2018.
- [49] D. E. W. Chatterton, D. N. Nguyen, S. B. Bering, and P. T. Sangild, "Anti-inflammatory mechanisms of bioactive milk proteins in the intestine of newborns," *The International Journal of Biochemistry & Cell Biology*, vol. 45, no. 8, pp. 1730–1747, 2013.
- [50] K. Aihara, H. Ishii, and M. Yoshida, "Casein-derived tripeptide, Val-Pro-Pro (VPP), modulates monocyte adhesion to vascular endothelium," *Journal of Atherosclerosis and Thrombosis*, vol. 16, no. 5, pp. 594–603, 2009.
- [51] E. Maestri, M. Marmiroli, and N. Marmiroli, "Bioactive peptides in plant-derived foodstuffs," *Journal of Proteomics*, vol. 147, pp. 140–155, 2016.
- [52] Y. Zhou, P. Zhang, G. Deng, X. Liu, and D. Lu, "Improvements of immune status, intestinal integrity and gain performance in the early-weaned calves parenterally supplemented with l-alanyl-l-glutamine dipeptide," *Veterinary Immunology and Immunopathology*, vol. 145, no. 1–2, pp. 134–142, 2012.
- [53] Y.-C. Hou, C.-C. Chu, T.-L. Ko, C.-L. Yeh, and S.-L. Yeh, "Effects of alanyl-glutamine dipeptide on the expression of colon-inflammatory mediators during the recovery phase of colitis induced by dextran sulfate sodium," *European Journal of Nutrition*, vol. 52, no. 3, pp. 1089–1098, 2013.
- [54] Y.-C. Hou, J.-J. Liu, M.-H. Pai, S.-S. Tsou, and S.-L. Yeh, "Alanyl-glutamine administration suppresses Th17 and reduces inflammatory reaction in dextran sulfate sodium-induced acute colitis," *International Immunopharmacology*, vol. 17, no. 1, pp. 1–8, 2013.
- [55] M. Lee, J. Kovacs-Nolan, T. Archbold et al., "Therapeutic potential of hen egg white peptides for the treatment of intestinal inflammation," *Journal of Functional Foods*, vol. 1, no. 2, pp. 161–169, 2009.
- [56] D. A. Luna-Vital, E. González de Mejía, and G. Loarca-Piña, "Dietary peptides from phaseolus vulgaris L. reduced AOM/DSS-induced colitis-associated colon carcinogenesis in Balb/c mice," *Plant Foods for Human Nutrition*, vol. 72, no. 4, pp. 445–447, 2017.
- [57] P. Requena, A. Daddaoua, E. Martínez-Plata et al., "Bovine glycomacropeptide ameliorates experimental rat ileitis by mechanisms involving downregulation of interleukin 17," *British Journal of Pharmacology*, vol. 154, no. 4, pp. 825–832, 2008.
- [58] R. López-Posadas, P. Requena, R. González et al., "Bovine glycomacropeptide has intestinal antiinflammatory effects in rats

- with dextran sulfate-induced colitis," *The Journal of Nutrition*, vol. 140, no. 11, pp. 2014–2019, 2010.
- [59] M. Ortega-González, F. Capitán-Cañadas, P. Requena et al., "Validation of bovine glycomacropeptide as an intestinal anti-inflammatory nutraceutical in the lymphocyte-transfer model of colitis," *The British Journal of Nutrition*, vol. 111, no. 7, pp. 1202–1212, 2014.
- [60] Z. Ming, Y. Jia, Y. Yan, G. Pang, and Q. Chen, "Amelioration effect of bovine casein glycomacropeptide on ulcerative colitis in mice," *Food and Agricultural Immunology*, vol. 26, no. 5, pp. 717–728, 2015.
- [61] H. Jiao, Q. Zhang, Y. Lin, Y. Gao, and P. Zhang, "The ovotransferrin-derived peptide IRW attenuates lipopolysaccharide-induced inflammatory responses," *BioMed Research International*, vol. 2019, Article ID 8676410, 7 pages, 2019.
- [62] Y. Ma, S. Ding, G. Liu et al., "Egg protein transferrin-derived peptides IRW and IQW regulate citrobacter rodentium-induced, inflammation-related microbial and metabolomic profiles," *Frontiers in Microbiology*, vol. 10, p. 643, 2019.
- [63] G. Liu, W. Yan, S. Ding et al., "Effects of IRW and IQW on oxidative stress and gut microbiota in dextran sodium sulfate-induced colitis," *Cellular Physiology and Biochemistry*, vol. 51, no. 1, pp. 441–451, 2018.
- [64] Y. Ma, H. Jiang, J. Fang, and G. Liu, "IRW and IQW reduce colitis-associated cancer risk by alleviating DSS-induced colonic inflammation," *BioMed Research International*, vol. 2019, Article ID 6429845, 9 pages, 2019.
- [65] E. Shapira, B. Brodsky, E. Proscura, A. Nyska, A. Erlanger-Rosengarten, and U. Wormser, "Amelioration of experimental autoimmune encephalitis by novel peptides: involvement of T regulatory cells," *Journal of Autoimmunity*, vol. 35, no. 1, pp. 98–106, 2010.
- [66] G. Dalmasso, L. Charrier-Hisamuddin, H. T. Thu Nguyen, Y. Yan, S. Sitaraman, and D. Merlin, "PepT1-mediated tripeptide KPV uptake reduces intestinal inflammation," *Gastroenterology*, vol. 134, no. 1, pp. 166–178, 2008.
- [67] H. Hou, Y. Fan, S. Wang, L. Si, and B. Li, "Immunomodulatory activity of Alaska pollock hydrolysates obtained by glutamic acid biosensor – artificial neural network and the identification of its active central fragment," *Journal of Functional Foods*, vol. 24, pp. 37–47, 2016.
- [68] J.-W. Hwang, S.-J. Lee, Y.-S. Kim et al., "Purification and characterization of a novel peptide with inhibitory effects on colitis induced mice by dextran sulfate sodium from enzymatic hydrolysates of *Crassostrea gigas*," *Fish & Shellfish Immunology*, vol. 33, no. 4, pp. 993–999, 2012.
- [69] N. Eissa, H. Hussein, L. Kermarrec et al., "Chromofungin ameliorates the progression of colitis by regulating alternatively activated macrophages," *Frontiers in Immunology*, vol. 8, p. 1131, 2017.
- [70] J. Moronta, P. L. Smaldini, C. A. Fossati, M. C. Añon, and G. H. Docena, "The anti-inflammatory SSEDIKE peptide from Amaranth seeds modulates IgE-mediated food allergy," *Journal of Functional Foods*, vol. 25, pp. 579–587, 2016.
- [71] T. Nakamura, T. Hirota, K. Mizushima et al., "Milk-derived peptides, Val-Pro-Pro and Ile-Pro-Pro, attenuate atherosclerosis development in apolipoprotein E-deficient mice: a preliminary study," *Journal of Medicinal Food*, vol. 16, no. 5, pp. 396–403, 2013.
- [72] A. Nonaka, T. Nakamura, T. Hirota et al., "The milk-derived peptides Val-Pro-Pro and Ile-Pro-Pro attenuate arterial dysfunction in L-NAME-treated rats," *Hypertension Research*, vol. 37, no. 8, pp. 703–707, 2014.
- [73] M. B. Espeche Turbay, A. de Moreno de LeBlanc, G. Perdigon, G. Savoy de Giori, and E. M. Hebert, "β-Casein hydrolysate generated by the cell envelope-associated proteinase of *Lactobacillus delbrueckii* ssp. *lactis* CRL 581 protects against trinitrobenzene sulfonic acid-induced colitis in mice," *Journal of Dairy Science*, vol. 95, no. 3, pp. 1108–1118, 2012.
- [74] D. Young, M. Ibuki, T. Nakamori, M. Fan, and Y. Mine, "Soy-derived di- and tripeptides alleviate colon and ileum inflammation in pigs with dextran sodium sulfate-induced colitis," *The Journal of Nutrition*, vol. 142, no. 2, pp. 363–368, 2012.
- [75] M. Sobczak, P. K. Zakrzewski, A. I. Cygankiewicz et al., "Anti-inflammatory action of a novel orally available peptide 317 in mouse models of inflammatory bowel diseases," *Pharmacological Reports*, vol. 66, no. 5, pp. 741–750, 2014.
- [76] S. Wada, K. Sato, R. Ohta et al., "Ingestion of low dose pyroglutamy leucine improves dextran sulfate sodium-induced colitis and intestinal microbiota in mice," *Journal of Agricultural and Food Chemistry*, vol. 61, no. 37, pp. 8807–8813, 2013.
- [77] C. Bessette, G. Henry, S. Sekkal et al., "Oral administration of a casein matrix containing β-casofensin protects the intestinal barrier in two preclinical models of gut diseases," *Journal of Functional Foods*, vol. 27, pp. 223–235, 2016.
- [78] S. La Manna, C. Di Natale, D. Florio, and D. Marasco, "Peptides as therapeutic agents for inflammatory-related diseases," *International Journal of Molecular Sciences*, vol. 19, no. 9, p. 2714, 2018.
- [79] O. Martínez-Augustin, B. Rivero-Gutiérrez, C. Mascaraque, and F. Sánchez de Medina, "Food derived bioactive peptides and intestinal barrier function," *International Journal of Molecular Sciences*, vol. 15, no. 12, pp. 22857–22873, 2014.
- [80] Q. B. Xu, Y. D. Zhang, N. Zheng et al., "Short communication: decrease of lipid profiles in cow milk by ultra-high-temperature treatment but not by pasteurization," *Journal of Dairy Science*, vol. 103, no. 2, pp. 1900–1907, 2020.
- [81] Q. Xu, X. Yan, Y. Zhang, and J. Wu, "Current understanding of transport and bioavailability of bioactive peptides derived from dairy proteins: a review," *International Journal of Food Science and Technology*, vol. 54, no. 6, pp. 1930–1941, 2019.
- [82] L. Santiago-Lopez, A. F. Gonzalez-Cordova, A. Hernandez-Mendoza, and B. Vallejo-Cordoba, "Potential use of food protein-derived peptides in the treatment of inflammatory diseases," *Protein & Peptide Letters*, vol. 24, no. 2, pp. 137–145, 2017.
- [83] Q. Xu, Z. Liu, H. Liu et al., "Functional characterization of oligopeptide transporter 1 of dairy cows," *Journal of Animal Science and Biotechnology*, vol. 9, no. 1, p. 7, 2018.
- [84] Q. Xu, Y. Wu, H. Liu, Y. Xie, X. Huang, and J. Liu, "Establishment and characterization of an omasal epithelial cell model derived from dairy calves for the study of small peptide absorption," *PLoS One*, vol. 9, no. 3, article e88993, 2014.
- [85] Q. Xu, H. Liu, F. Zhao et al., "Mechanism of peptide absorption in the isolated forestomach epithelial cells of dairy cows," *Journal of the Science of Food and Agriculture*, vol. 99, no. 1, pp. 100–108, 2018.
- [86] S. A. Ingersoll, S. Ayyadurai, M. A. Charania, H. Laroui, Y. Yan, and D. Merlin, "The role and pathophysiological relevance of membrane transporter PepT1 in intestinal

- inflammation and inflammatory bowel disease,” *American Journal of Physiology-Gastrointestinal and Liver Physiology*, vol. 302, no. 5, pp. G484–G492, 2012.
- [87] L. Charrier and D. Merlin, “The oligopeptide transporter hPepT1: gateway to the innate immune response,” *Laboratory Investigation*, vol. 86, no. 6, pp. 538–546, 2006.
- [88] Q. Xu, H. Fan, W. Yu, H. Hong, and J. Wu, “Transport study of egg-derived antihypertensive peptides (LKP and IQW) using Caco-2 and HT29 coculture monolayers,” *Journal of Agricultural and Food Chemistry*, vol. 65, no. 34, pp. 7406–7414, 2017.
- [89] Q. Lin, Q. Xu, J. Bai, W. Wu, H. Hong, and J. Wu, “Transport of soybean protein-derived antihypertensive peptide LSW across Caco-2 monolayers,” *Journal of Functional Foods*, vol. 39, pp. 96–102, 2017.
- [90] H. Fan, Q. Xu, H. Hong, and J. Wu, “Stability and transport of spent hen-derived ACE-inhibitory peptides IWHHT, IWH, and IW in human intestinal Caco-2 cell monolayers,” *Journal of Agricultural and Food Chemistry*, vol. 66, no. 43, pp. 11347–11354, 2018.
- [91] N. A. Nagalingam and S. V. Lynch, “Role of the microbiota in inflammatory bowel diseases,” *Inflammatory Bowel Diseases*, vol. 18, no. 5, pp. 968–984, 2012.
- [92] Å. Håkansson, N. Tormo-Badia, A. Baridi et al., “Immunological alteration and changes of gut microbiota after dextran sulfate sodium (DSS) administration in mice,” *Clinical and Experimental Medicine*, vol. 15, no. 1, pp. 107–120, 2015.
- [93] N. H. Salzman, K. Hung, D. Haribhai et al., “Enteric defensins are essential regulators of intestinal microbial ecology,” *Nature Immunology*, vol. 11, no. 1, pp. 76–82, 2010.
- [94] Y. Yan, B. Xu, B. Yin et al., “Modulation of gut microbial community and metabolism by dietary glycyl-glutamine supplementation may favor weaning transition in piglets,” *Frontiers in Microbiology*, vol. 10, p. 3125, 2020.

Research Article

Protection of Fecal Microbiota Transplantation in a Mouse Model of Multiple Sclerosis

Kanglan Li ¹, Shouchao Wei,¹ Li Hu,^{1,2} Xiaojian Yin,¹ Yingren Mai,¹ Chunmei Jiang,¹ Xiaoping Peng,¹ Xingxing Cao,¹ Zhongkai Huang,³ Haihong Zhou,¹ Guoda Ma ¹, Zhou Liu ¹, Huiliang Li ⁴ and Bin Zhao ¹

¹Guangdong Key Laboratory of Age-Related Cardiac and Cerebral Diseases, Institute of Neurology, Department of Neurology, Affiliated Hospital of Guangdong Medical University, Zhanjiang, Guangdong 524001, China

²Department of Histology and Embryology, Guangdong Medical University, Zhanjiang, China

³Department of Neurosurgery, Affiliated Hospital of Guangdong Medical University, Guangdong Medical University, Zhanjiang, China

⁴Wolfson Institute for Biomedical Research, University College London, London WC1E 6BT, UK

Correspondence should be addressed to Zhou Liu; liuzhou102@126.com, Huiliang Li; huiliang.li@ucl.ac.uk, and Bin Zhao; binzhao@163.com

Received 17 April 2020; Revised 18 June 2020; Accepted 13 July 2020; Published 5 August 2020

Guest Editor: Hongmei Jiang

Copyright © 2020 Kanglan Li et al. This is an open access article distributed under the Creative Commons Attribution License, which permits unrestricted use, distribution, and reproduction in any medium, provided the original work is properly cited.

Given the growing evidence of a link between gut microbiota (GM) dysbiosis and multiple sclerosis (MS), fecal microbiota transplantation (FMT), aimed at rebuilding GM, has been proposed as a new therapeutic approach to MS treatment. To evaluate the viability of FMT for MS treatment and its impact on MS pathology, we tested FMT in mice with experimental autoimmune encephalomyelitis (EAE), a mouse model of MS. We provide evidence that FMT can rectify altered GM to some extent with a therapeutic effect on EAE. We also found that FMT led to reduced activation of microglia and astrocytes and conferred protection on the blood-brain barrier (BBB), myelin, and axons in EAE. Taken together, our data suggest that FMT, as a GM-based therapy, has the potential to be an effective treatment for MS.

1. Introduction

Multiple sclerosis (MS) commonly occurs as a progressive central nervous system (CNS) disease, characterized by inflammation, demyelination, and axonal loss in the brain and spinal cord [1]. T cell-mediated inflammatory pathology and genetic factors are closely involved in the development of MS, causing damage to myelin sheaths surrounding neuronal axons and accumulation of neurological deficits [2–4]. Environmental factors also play a driving role in the pathogenesis of MS, such as geographical latitude, vitamin D3 deficiency, early life obesity, passive smoking, Epstein-Barr virus infection, dietary habits (especially high salt and fat diet), stress, and gut microbiota (GM) [5]. Study has shown that transplanting the intestinal microbiota of autism spectrum

disorder patients into germ-free mice and that colonization of the microbiota induced typical autism spectrum disorder behaviors [6]. Germ-free mice developed severe MS symptoms after microbiota transplants from MS patients compared with transplanted healthy controls [7]. MS patient-derived microbiota resulted in a spontaneous EAE in a transgenic mouse model [8]. Human bacteria was transferred to mice can be detected and was a shift of the microbiota over time [9]. Notably, accumulating new evidence points to a link between altered intestinal microbiota and MS pathogenesis [10–15].

Investigation of GM has revealed significantly altered abundances of certain bacterial genera in MS patients compared to healthy controls [16]. Moreover, germ-free mice prove to be resistant to experimental autoimmune encephalomyelitis (EAE), a commonly used animal model of MS

[17, 18]. Together, these studies imply a causal association between GM and MS. Although the mechanisms underlying the role of GM in MS are still elusive, GM-based therapeutic strategies hold the promise of new treatments for MS.

Fecal microbiota transplantation (FMT) appears to be an effective treatment for *Clostridium difficile* infection and inflammatory bowel syndrome, able to restore GM diversity to some extent [19, 20]. Some case reports suggest that FMT may help improve symptoms of epilepsy and Parkinson's disease [21, 22]. Interestingly, one study found that after FMT treatment for constipation, three wheelchair-bound MS patients had so dramatic improvement in neurological symptoms that they regained the ability to walk unassisted [23]. Therefore, FMT has the potential to be an innovative therapy for MS. Here, we evaluate the effect of FMT on EAE and explore possible mechanisms behind it. Our data reveal that FMT can improve the clinical outcome of EAE by modulating GM, reducing glial inflammatory response and conferring protection on the blood-brain barrier (BBB), myelin, and axons.

2. Materials and Methods

2.1. Animals. Four- to five-week-old female C57BL/6 mice were purchased from Guangdong Medical Laboratory Animal Center and raised in pathogen-free conditions in an animal facility at Guangdong Medical University (GMU). Mice were allowed 1 week's habituation before being used for experiments. Animal care and all procedures complied with the guidelines of GMU Experimental Animal Ethics Committee and national laws and regulations of China for use of animals in biomedical research.

2.2. EAE Induction. EAE induction was based on a published protocol [24]. Murine myelin oligodendrocyte glycoprotein (MOG) 35–55 peptide (MOG35–55, MEVGVYRSPFSRVVHLYRNGK) was synthesized with >99% purity (SciLight Biotechnology, China). C57BL/6 mice were injected with 200 μ g MOG35–55 emulsified in 100 μ g of complete Freund's adjuvant (CFA, Sigma) and an additional 400 μ g *Mycobacterium tuberculosis* H37RA (BD Biosciences) by subcutaneous injection into the flanks. These mice were also given 400 ng pertussis toxin (List Biological Laboratories) in 100 μ l phosphate buffered saline (PBS) on the same day and 2 days later by intraperitoneal injection. In addition, MOG35–55 was administered again 1 week later. Clinical scores were recorded daily for 42 days postimmunization. Neurological function was scored on a 0–5 scale: 0, no signs of disease; 1, partial loss of tail tonicity; 2, tail paralysis; 3, ataxia and/or paresis of hind limbs; 4, complete paralysis of hind limbs; and 5, moribund or death [24]. A cumulative clinical score was the sum of all neurological function scores from onset to day 42. Day of onset was when an animal first exhibited neurological signs of disease.

2.3. Fecal Microbiota Transplantation (FMT). C57BL/6 mice (3/cage) were placed in empty autoclaved cages (no bedding) and allowed normal bowel movement. At least twelve fecal pellets were collected from each cage using sterile filter paper, promptly placed in 3 ml sterile PBS, homogenized for 2 min

with a glass pestle and spun at 800 rpm for 3 min before collecting the supernatant for transplantation. Immunized mice were randomly divided into two groups: one group (FMT group) was given 200 μ l per mouse fresh fecal supernatant via oral gavage daily for 42 consecutive days postimmunization, whereas for the other group (EAE group), fecal supernatant was replaced with sterile saline.

2.4. Sample Collection and Microbiota Analysis. Fresh feces were collected and immediately stored at -80°C . Fecal microbiota DNA was recovered with the PowerFecal DNA Kit (Qiagen). The V3–V4 region of 16S rRNA gene was amplified by using a pair of primers: 338F, 5'-ACTCCTACGGGAGG CAGCAG-3', and 806R, 5'-GGACTACHVGGGTWTCTA AT-3'. PCR amplification products were sequenced by paired-end sequencing (Majorbio, China).

2.5. Tissue Preparation. At day 42 postimmunization, mice were perfused transcardially with ice-cold saline under terminal anesthesia. Mice used for immunostaining were further perfused with 4% paraformaldehyde. Dissected brain and thoracic spinal cord tissues were fixed in 4% paraformaldehyde for 12–24 h and then immersed in 20% and 30% sucrose each for 1 day. The tissues were embedded in Tissue-Tek OCT (Sakura), frozen, and cut into 25 μ m thick spinal cord cross sections and brain coronal sections. For evaluation of BBB leakage, 4% Evans blue (Sigma) in PBS was injected into the tail vein of mice (3 μ l/g) under anesthesia two hours before perfusion.

2.6. Immunofluorescence Staining. To detect Claudin 5 expression, thoracic spinal cord sections were sealed with blocking buffer (10% sheep serum albumin and 0.3% Triton X-100 in PBS) for 30 min at 37°C , followed by incubation with anti-Claudin 5 antibody (1:200, ab15106, Abcam, USA) at 4°C overnight. For other examinations by immunostaining, brain sections were sealed with anti-Iba1 (1:100, ab153696, Abcam, USA), anti-GFAP (1:200, Cat.#12389, CST, USA), or anti-MBP (1:100, Cat.#13344, CST, USA) together with anti-NF-L antibody (1:400, Cat.#AB9568, Millipore, USA) at 4°C for 48 h. Alexa Fluor® 488-conjugated goat anti-rabbit secondary antibody (1:800, ab150077, Abcam, USA) was then added on its own or together with Alexa Fluor® 555-conjugated goat anti-mouse antibody (1:800, ab150118, Abcam, USA) for incubation at 37°C for 1 h. Nuclei were counterstained with Hoechst 33342 (Cat.#C0030, Solarbio, Beijing, China) for 10 min. Photomicrographs were taken with a confocal microscope (Leica TCS SP5 II).

2.7. Transmission Electron Microscopy. Thoracic spinal cord tissues were postfixed in osmium tetroxide and processed for transmission electron microscopy. Electron micrographs were taken with a Jem-1400 transmission electron microscope.

2.8. Western Blotting. The protein was extracted from brain tissues using an Ambion PARIS kit (Solarbio, Beijing, China) with addition of phosphatase and protease inhibitor cocktails (Roche). The Pierce BCA Protein Assay Kit (Cat.#23227,

Thermo Fisher) was used to detect protein concentrations. The proteins were separated by SDS-PAGE electrophoresis, and a blotted membrane was incubated with blocking buffer and then with anti-Claudin 5 (1:500, ab15106, Abcam, USA), anti-Iba1 (1:1000, ab153696, Abcam, USA), anti-GFAP (1:1000, Cat.#12389, CST, USA), anti-MBP (1:1000, Cat.#13344, CST, USA), or anti-NF-L (1:1000, Cat.#AB9568, Millipore, USA) primary antibody at 4°C overnight before addition of horseradish peroxidase- (HRP-) linked goat anti-rabbit (1:1000, Cat.#7074, CST, USA) or goat anti-mouse secondary antibody (1:25000, Cat.E030110-01, EarthOx, USA). Detection of β -tubulin was performed on stripped membranes with anti- β -tubulin (1:1000, ab179513, Abcam, USA) primary antibody to control for protein loading. Protein signal was visualized with the LumiGLO chemiluminescent substrate (Cat.#7003S, CST, USA), and target protein expression was normalized as fold change relative to β -tubulin expression using Photoshop for quantitative analysis.

2.9. Statistical Analysis. Statistical analysis was performed by the Mann–Whitney *U* test, followed by a linear discriminant analysis for phylum level changes. The SPSS 17.0 software was used for statistical analysis including two-way analysis of variance (ANOVA) followed by a Bonferroni test for comparing clinical scores and unpaired *t*-tests for other comparisons with means and *p* values calculated. Statistical graphs were generated with GraphPad Prism 5. *p* < 0.05 was considered statistically significant.

3. Results

3.1. FMT Modulates GM in EAE. To examine the effect of FMT on GM structure in EAE, fecal samples were collected from EAE mice (*n* = 6), FMT-treated immunized mice (*n* = 6), and normal controls (*n* = 5) 42 days postimmunization for DNA extraction and 16S rRNA gene sequencing. Acquired sequencing data were analyzed for assessment of GM diversity. We first evaluated GM α -diversity with the Shannon index, which takes account of both the richness and evenness of a microbial community. The Shannon index was significantly increased for GM in EAE mice compared to normal controls (4.38 ± 0.15 vs. 3.89 ± 0.26 , *p* = 0.008113), indicating altered GM diversity in EAE; an in-between value was discovered in FMT-treated EAE mice without statistical significance (Figure 1(a)), suggesting that FMT attenuated the increase in the Shannon index caused by the development of EAE. Therefore, these results hint that FMT is conducive to restoring altered intestinal microbiota diversity in EAE. We next evaluated GM β -diversity, which accounts for the dissimilarity between different microbial communities. Principal coordinates analysis (PCoA) of unweighted UniFrac distances showed clear clustering separation between samples from these three mouse groups on scores plot for principal component 1 (PC1, 28.91%) and PC2 (13.45%), illustrating differing GM diversity between these mouse groups (Figure 1(c)). The β -diversity distance matrix was presented for hierarchical clustering analysis to calculate the phylogenetic evolutionary relationships of each species and the distance between samples; pairwise intergroup

UniFrac distances further quantitatively detected the variation occurring on different lineages among samples. Analysis showed that FMT was closer to the control than the EAE mice on the OTU level (Figure 1(d)).

Compared with EAE mice, intestinal bacterial phyla *Bacteroidetes* (*p* = 0.0081) were more abundant in normal controls, whereas *Firmicutes* (*p* = 0.0081), *Tenericutes* (*p* = 0.0081), and *Cyanobacteria* (*p* = 0.0354) were less abundant. FMT-treated EAE mice presented changed abundances of *Verrucomicrobia* (*p* = 0.0091), four intestinal bacterial phyla *Bacteroidetes*, *Firmicutes*, *Tenericutes*, and *Cyanobacteria*, all of which that shifted towards the levels observed in normal controls (Figure 1(b)) even if it is not statistically significant. Those suggest that FMT can to a certain degree remedy altered GM structure in EAE.

To determine which bacteria was associated with the severity of the neurological function score, we performed a Spearman's correlation of bacterial abundance with EAE scores and cumulative disease scores (Figure 1(e)). Both *Lachnoclostridium* and *Unclassified_f_Lachnospiraceae* showed negative correlation in EAE scores and EAE cumulative scores. Five kinds of genus including *norank_o_Mollicutes_RF9*, *[Eubacterium]_ruminantium_group*, *unclassified_f_Ruminococcaceae*, *Turicibacter*, *Ruminococcus_1*, and *Thalassospira* were positively correlated with EAE scores and EAE cumulative scores. However, *uncultured_f_Lachnospiraceae*, *Helicobacter*, *Roseburia*, and *norank_f_Bacteroidales_S24-7_group* were found to be negatively correlated with EAE scores and cumulative scores, respectively. *Prevotellaceae_UCG-001*, *Akkermansia*, and *Ruminococcaceae_UCG-014* showed positive correlation in EAE score, as well as *Alistipes*, *unclassified_f_Veillonellaceae*, *Ruminiclostridium_6*, *Allobaculum*, and *norank_f_Clostridiales_vadinBB60_group* in cumulative scores. These results indicated that different genus of bacteria contributes differently to EAE neurological function score.

Analysis of the GM profiles of these 3 mouse groups using linear discriminant analysis (LDA) of effect size (LEfSe) identified differentially abundant bacterial taxa (LDA score threshold > 2.0), which reflected the effect of EAE and FMT treatment on the abundances of gut bacterial taxa. EAE caused a marked decrease in the abundances of 13 gut bacterial taxa (*g_norank_f_Bacteroidales_S24-7_group*, *f_Bacteroidales_S24-7_group*, *p_Bacteroidetes*, *c_Bacteroidia*, *o_Bacteroidales*, *g_Ruminococcaceae_UCG_010*, *f_Family_XIII*, *g_Eubacterium_nodatum_group*, *c_Betaproteobacteria*, *g_Parasutterella*, *f_Alcaligenaceae*, *o_Burkholderiales*, and *g_Lachnoclostridium*), made up of 1 phylum, 2 classes, 2 orders, 3 families, and 5 genera. FMT treatment for EAE decreased the abundances of 17 bacterial taxa (*p_Fimicutes*, *f_Ruminococcaceae*, *g_Alloprevotella*, *g_Alistipes*, *g_Ruminococcus_1*, *g_unclassified_f_Ruminococcaceae*, *g_Ruminococcaceae_UCG_014*, *g_Akkermansia*, *p_Verrucomicrobia*, *o_Verrucomicrobiales*, *f_Verrucomicrobiaceae*, *c_Verrucomicrobiae*, *g_Eubacterium_ruminantium_group*, *f_Staphylococcaceae*, *g_Staphylococcus*, *o_Bacillales*, and *g_Paraprevotella*) consisting of 2 phyla, 1 class, 2 orders, 3 families, and 9 genera (including *Akkermansia*) and increased the abundances of 34 bacterial taxa (*f_Rikenellaceae*, *f_Bacteroidaceae*, *g_Bacteroides*, *g_Prevotella_1*, *g_Turicibacter*, *g_Prevotellaceae_UCG_003*, *f_*

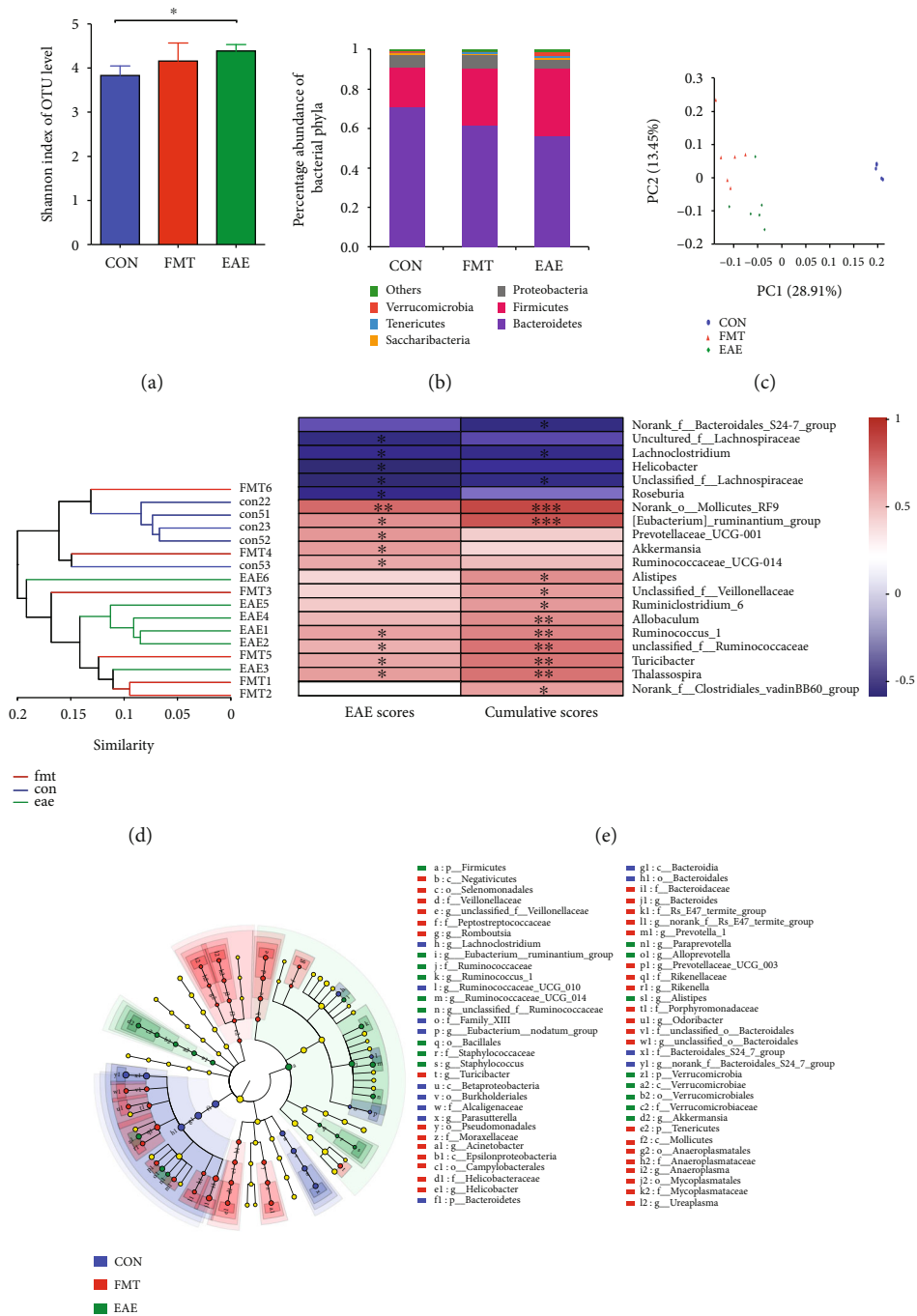


FIGURE 1: Continued.

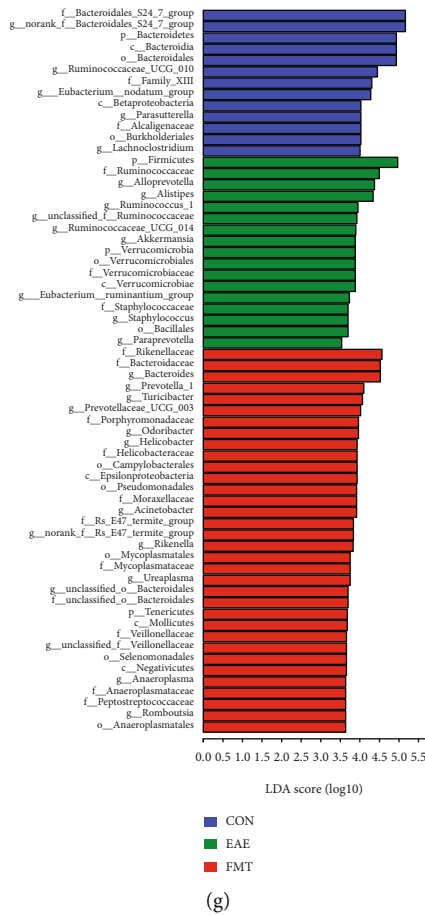


FIGURE 1: FMT modulates GM in EAE. (a) Chart of the Shannon index values for evaluation of GM α -diversity. The Shannon index for GM was significantly increased in EAE mice ($n = 6$) compared to normal controls (CON, $n = 5$); an in-between value was found in FMT-treated immunized mice (FMT; $n = 6$) without statistical significance. (b) Chart of relative abundance of gut bacterial taxa (phylum level) performed with the Mann–Whitney U test, corrected by FDR between the two groups. The figure was created by used unfiltered OUT table. (c) PCoA plot (PC1/PC2) of unweighted UniFrac distances illustrating clustering separation between samples from different mouse groups. (d) Hierarchical clustering tree on OTU level (weighted UniFrac). (e) The correlation heatmap chart performed with a Spearman’s correlation of bacterial abundance with EAE scores and cumulative scores. The R value is shown in different colors in the figure. The legend on the right is the color interval of different R values ($*0.01 < p < 0.05$ and $**0.001 < p < 0.01$). (f) LefSe cladogram showing differentially abundant gut bacterial taxa. The diameter of each dot is proportional to its effect size. Each ring (from inside to outside) represents a taxonomic level from kingdom to genus, the cladogram was made on filtered data, and only taxa with greater than 0.1% relative abundance. (g) LDA scores of abundant gut bacterial taxa (LDA score threshold >2.0). k: kingdom; p: phylum; c: class; o: order; f: family; g: genus.

Porphyromonadaceae, *g_Odoribacter*, *g_Helicobacter*, *f_Helicobacteraceae*, *o_Campylobacteriales*, *c_Epsilonproteobacteria*, *o_Pseudomonadales*, *f_Moraxellaceae*, *g_Acinetobacter*, *f_Rs_E47_termite_group*, *g_norank_f_Rs_E47_termite_group*, *g_Rikenella*, *o_Mycoplasmatales*, *f_Mycoplasmataceae*, *g_Ureaplasma*, *g_unclassified_o_Bacteroidales*, *f_unclassified_o_Bacteroidales*, *p_Tenericutes*, *c_Mollicutes*, *f_Veillonellaceae*, *g_unclassified_f_Veillonellaceae*, *o_Selenomonadales*, *c_Negativicutes*, *g_Anaeroplasmataceae*, *f_Anaeroplasmataceae*, *f_Peptostreptococcaceae*, *g_Romboutsia*, and *o_Anaeroplasmatales* increased in FMT mice) comprising 1 phylum, 3 classes, 5 orders, 11 families, and 14 genera (including *Prevotella*) in GM (Figures 1(f) and 1(g)). Taken together, these results demonstrate that FMT can modulate GM, thereby to some extent rectifying altered GM composition in EAE.

3.2. FMT Has a Therapeutic Effect on EAE. Study of human patients has revealed distinct GM in MS [25], and research with animal models of MS has discovered that modulating GM with antibiotics and probiotics can decrease EAE clinical severity [26]. To find out the effect of FMT on EAE clinical symptoms, we evaluated clinical scores of immunized mice with versus without FMT treatment. FMT-treated mice ($n = 10$) displayed alleviated clinical symptoms evidenced by significantly reduced clinical scores ($p < 0.0001$) and cumulative disease scores ($p < 0.05$) compared with EAE controls ($n = 10$) through the clinic course of EAE (Figures 2(a) and 2(b)). Furthermore, FMT treatment resulted in a delay in the onset of EAE ($p < 0.0001$, Figure 2(c)). Therefore, FMT with fecal matter from normal donors proved effective in slowing down EAE development and relieving EAE symptoms.

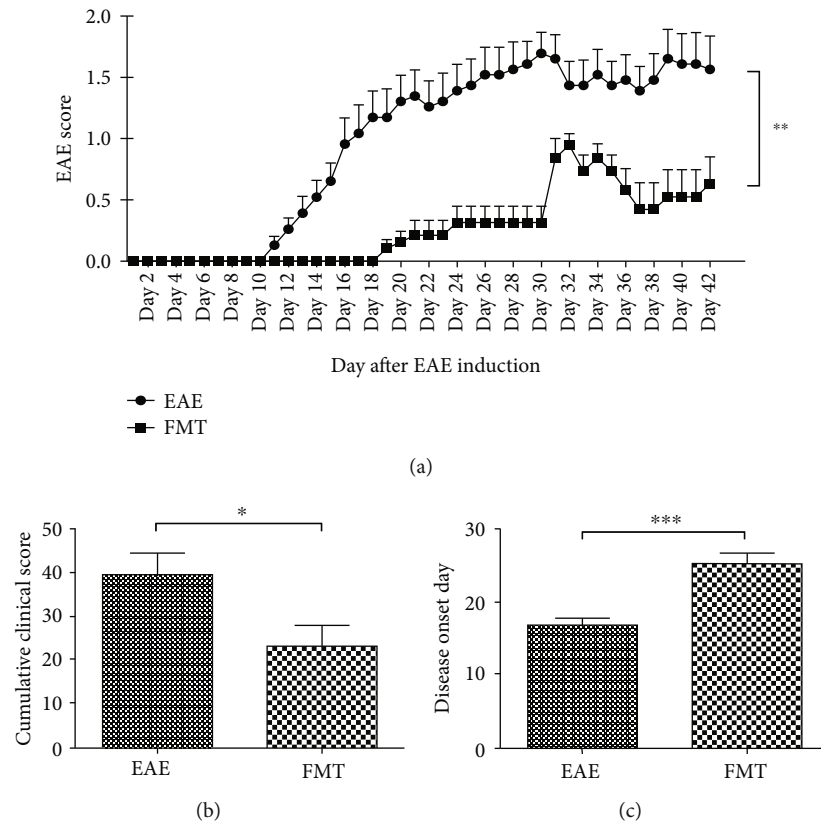


FIGURE 2: FMT has a therapeutic effect on EAE. (a) Chart of clinical scores for EAE controls and FMT-treated immunized mice after EAE induction. FMT led to decreased clinical scores through the clinical course of EAE (mean \pm SEM; $n = 10/\text{group}$; $**p < 0.01$). (b, c) Charts of cumulative clinical scores (b) and disease onset days (c) after EAE induction indicating reduced clinical severity and delayed disease onset after FMT treatment (mean \pm SEM; $n = 10/\text{group}$; $*p < 0.05$ and $***p < 0.001$).

3.3. FMT Prevents BBB Leakage in EAE. The BBB is compromised during the development of MS and EAE, allowing immune cells to infiltrate CNS and attack myelin [27]. Because GM is thought able to regulate BBB permeability [28–30], we then investigated whether FMT can help prevent BBB impairment in EAE. By Western blotting, we found that the expression of Claudin 5, a tight junction protein responsible for BBB barrier function [31], was dramatically increased in brain tissue in FMT-treated immunized mice compared to EAE controls ($n = 6$) (Figures 3(a) and 3(b)), which was further verified by immunostaining of brain sections ($n = 3$) (Figure 3(c)). In addition, Evans blue dye staining showed an appreciable reduction in dye presence in brain parenchyma after FMT treatment ($n = 1$) (Figure 3(d)). Together, these results prove that FMT treatment can lead to improved BBB integrity in EAE, preventing BBB leakage.

3.4. FMT Confers Protection on Myelin and Axons in EAE. To assess the influence of FMT on myelin and axons, we examined the expression of myelin basic protein (MBP), which is expressed in myelin, and neurofilament light chain protein (NF-L), whose release reflects axonal damage, in brain tissue. Significantly increased MBP expression and decreased NF-L

expression were detected in brain tissue in FMT-treated EAE mice compared to saline-treated controls by Western blotting (Figures 4(a)–4(c)) and by immunostaining of brain sections as well (Figure 4(d)), indicating an increase in the number of normal myelin sheaths and a decrease in myelin disintegration and axon damage after FMT treatment. Moreover, transmission electron microscopy (TEM) verified lessened demyelination and increased the presence of intact myelin sheaths in the thoracic spinal cord after FMT treatment (Figure 4(e)). All together, these data point to a protective effect conferred by FMT on myelin and axons in EAE.

3.5. FMT Alleviates Microglia and Astrocyte Activation in EAE. Microglia and astrocytes are known to contribute to the inflammatory pathology of MS [32], and some studies hint at a connection between their activation and GM composition [33, 34]. To find out the impact of FMT on microglia and astrocyte activation, we examined the expression of ionizing calcium-binding adaptor molecule 1 (Iba1, immune cells marker, which is not specific for microglia and infiltrating monocyte) and glial fibrillary acidic protein (GFAP, astrocyte marker) with Western blotting and discovered that the expression of both markers was significantly downregulated in FMT-treated EAE mice compared to

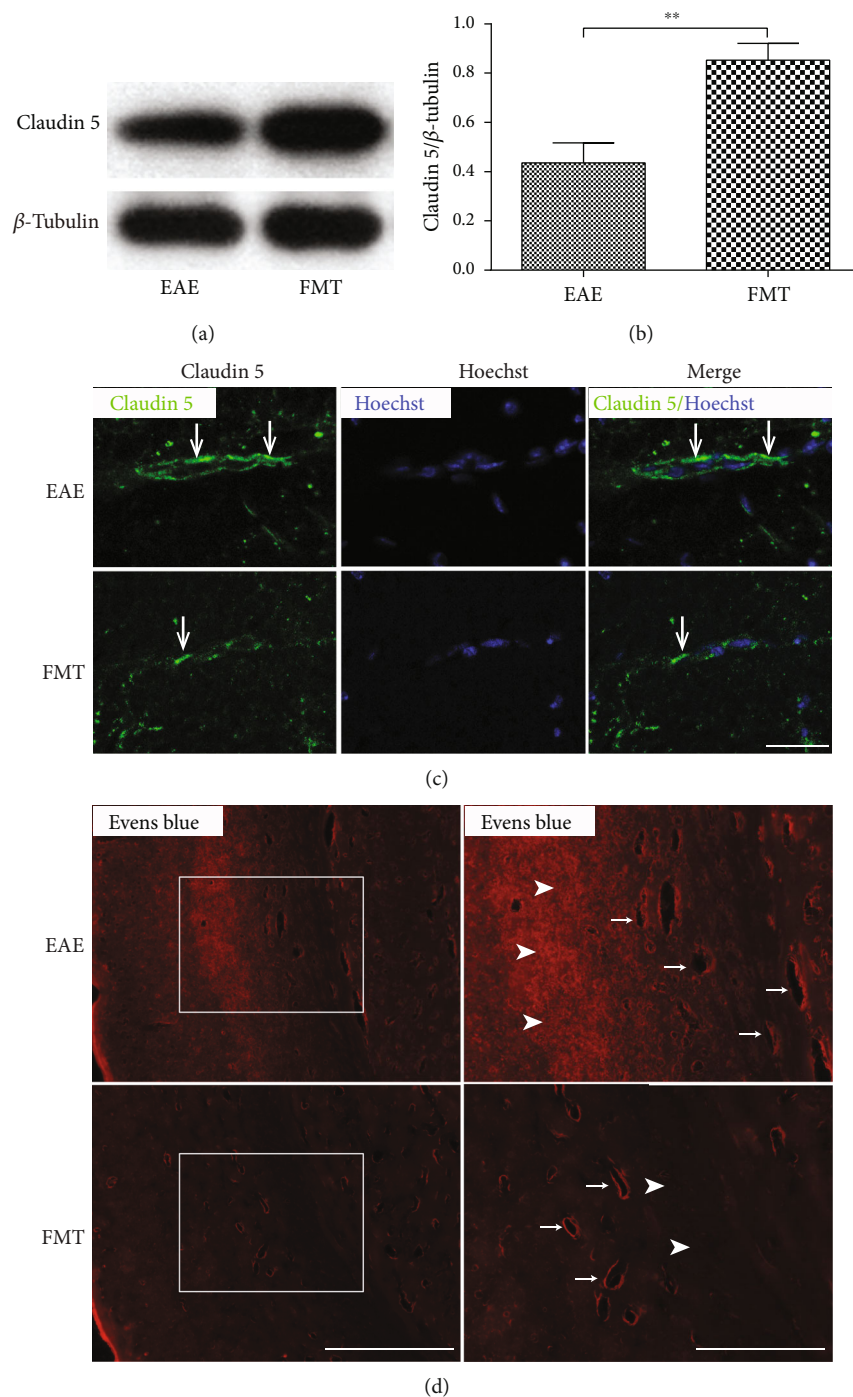


FIGURE 3: FMT prevents BBB leakage in EAE. (a) Claudin 5 expression in thoracic spinal cord tissues collected from EAE controls and FMT-treated EAE mice revealed by Western blot with β -tubulin as loading control. (b) Chart of quantified Western blot results showing increased levels of Claudin 5 expression (normalized by β -tubulin) after FMT treatment (mean \pm SEM; $n = 6$ /group; $**p < 0.01$). (c) Representative immunostaining images of Claudin 5 expression (green) in spinal cord sections. The nucleus was stained with Hoechst (blue). Scale bar: 100 μ m. (d) Representative images of Evans blue dye extravasation (red) in the subcortical white matter of brain showing the presence of dye in both blood vessels and brain parenchyma in EAE controls (upper panels) in contrast to appreciably reduced dye presence in brain parenchyma in FMT-treated EAE mice (lower panels). Each right panel shows a high magnification image of the area inside the white box (left). Scale bars: 400 μ m (left) and 200 μ m (right). Representative brain parenchyma and blood vessels are indicated by arrowheads and arrows, respectively.

saline-treated controls (Figures 5(a)–5(c)). Furthermore, decreased numbers of microglia and astrocytes were observed by immunostaining of brain sections after FMT

treatment (Figures 5(d) and 5(e)). Taken together, these data imply subdued glial inflammatory response after FMT treatment in EAE.

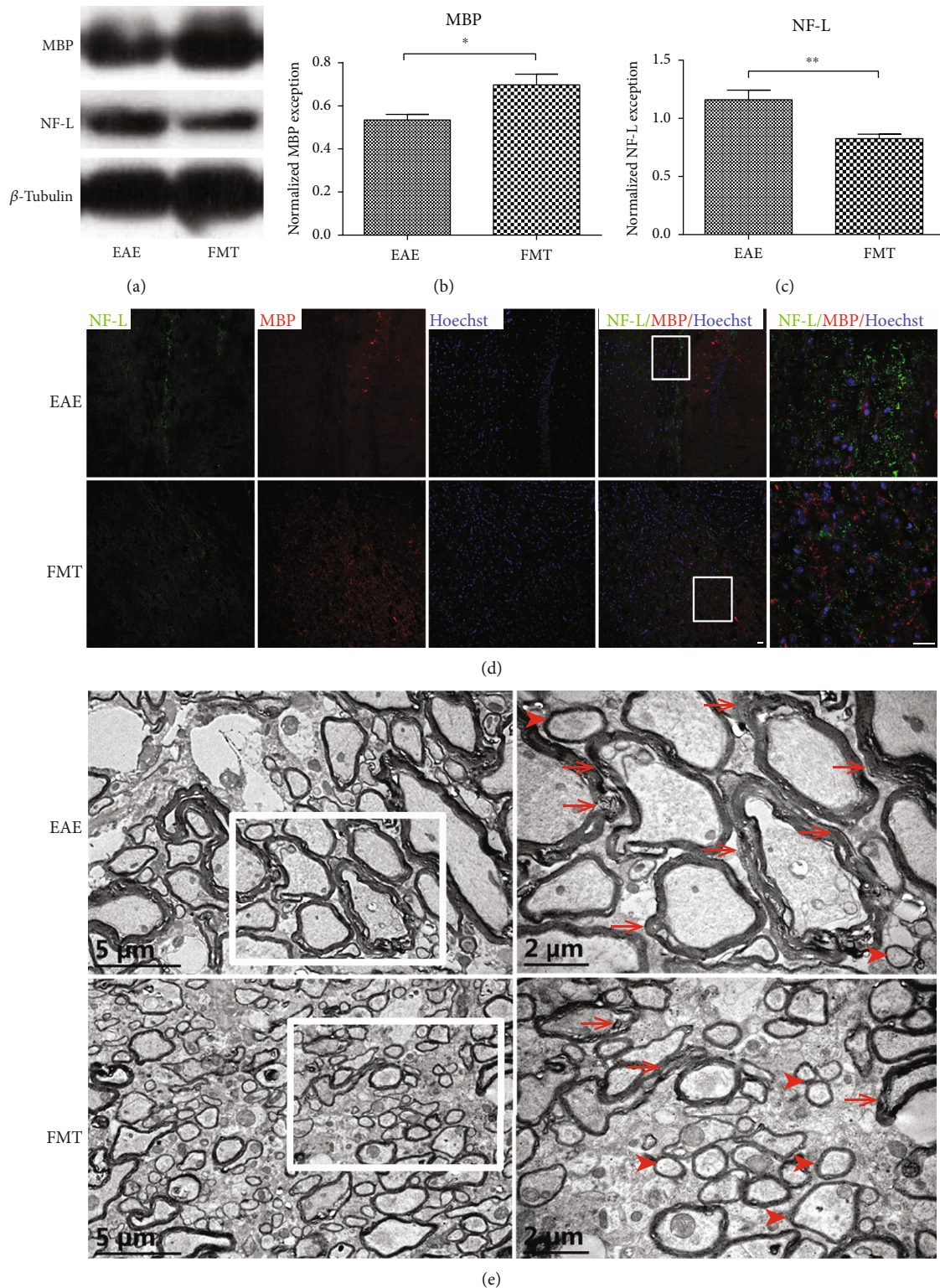


FIGURE 4: FMT confers protection on myelin and axons in EAE. (a) MBP and NF-L protein expression in the brain of EAE controls and FMT-treated EAE mice shown by Western blot with β -tubulin as loading control. (b, c) Charts of quantified Western blot results showing increased levels of MBP (b) and decreased levels of NF-L (c) expression (normalized by β -tubulin) after FMT treatment (mean \pm SEM; $n = 6$ /group; $*p < 0.05$ and $**p < 0.01$). (d) Immunofluorescence imaging of MBP (green) and NF-L (red) expression in the corpus callosum of the mouse brain. Nuclear staining was by Hoechst (blue). Each rightmost panel shows a high magnification image of the area inside the white box. Scale bar: $25 \mu\text{m}$. (e) Transmission electron microscopy (TEM) imaging of myelin sheaths in the thoracic spinal cord. Each high magnification image (right) shows the area enclosed by the white box (left). Representative normal and damaged myelin sheaths are indicated by arrowheads and arrows, respectively.

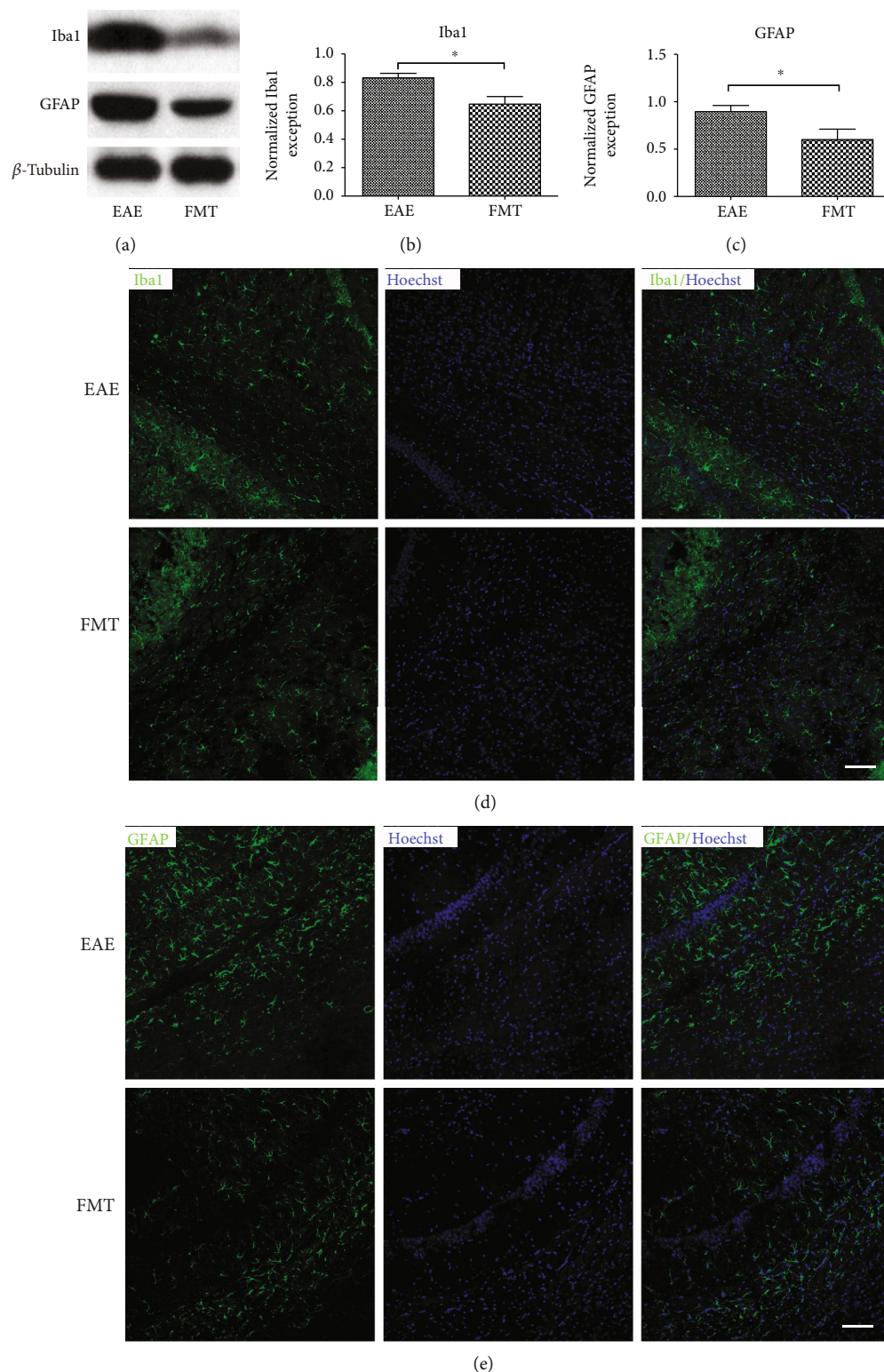


FIGURE 5: FMT alleviates immune cells and astrocyte activation in EAE. (a). Expression of Iba1 and GFAP protein in the brain of EAE controls and FMT-treated EAE mice shown by Western blot with β -tubulin as loading control. (b, c). Charts of quantified Western blot results indicating reduced levels of Iba1(b) and GFAP (c) expression (normalized by β -tubulin) after FMT treatment (mean \pm SEM; $n = 6$ /group; $*p < 0.05$). (d, e) Immunofluorescence imaging of cells expressing Iba1 (green; d) and GFAP (green; e) in brain sections with the nucleus stained by Hoechst (blue). Scale bar: 100 μ m.

4. Discussion

An increasing body of evidence reveals GM dysbiosis in MS [16, 25, 35, 36], and rebuilding GM has been proposed as an innovative approach to MS treatment. FMT appears to be the most direct way to reconstruct GM [37, 38] and is in fact an ancient treatment dating back to 1700 years ago [39]. However, whether GM can be restored back to normal by FMT remains unclear. Our data reveal a tendency for GM structure to change towards normal after FMT treatment in EAE with beneficial consequences (Figure 1).

We also found that FMT treatment for EAE markedly reduced the abundance of *Akkermansia* genus (in phylum *Verrucomicrobia*) and elevated the abundance of *Prevotella* genus (in phylum *Bacteroidetes*) in GM (Figures 1(b), 1(f), and 1(g)), which recalls the findings of decreased gut *Akkermansia* after probiotic intervention [40, 41], and increased gut *Prevotella* after disease-modifying treatment [16] and intermittent fasting in MS patients [42]. *Bacteroidetes* is one of the most abundant bacterial phyla inhabiting human gut, and the *Prevotella* genus is a dominant member of this phylum. *Bacteroidetes* ferments dietary fibers to produce short chain fatty acids (SCFAs), which take part in various physiological processes, affecting host health [43–45]. SCFAs have been found to protect the BBB from oxidative stress via nuclear factor, erythroid 2-like 2 (NFE2L2) signaling [46] and exert anti-inflammatory and neuroprotective functions [47–49]. Other favorable effects of SCFAs include attenuating myelin injury by increasing brain acetyl-CoA metabolism [50] and relieving clinical symptoms in EAE mice [49, 50]. A zwitterionic capsular polysaccharide A (PSA) produced by *Bacteroides fragilis* suppresses neuroinflammation by regulating migratory capacity of CD39⁺ CD4 T cell subsets, thus ameliorates EAE [51]. *Bacteroides fragilis* PSA⁺ regulated CNS demyelination by the induction of highly potent IL-10-producing Treg cells in EAE [52]. In addition, increased gut *Akkermansia* is associated with MS [16, 40], and probiotic treatment for MS patients resulted in decreased *Akkermansia* in GM accompanied by an anti-inflammatory peripheral response [40]. Moreover, increase of gut *Akkermansia* has been implicated in Parkinson's disease [53, 54] and advanced dementia [55]; these results showed a negative role for intestinal *Akkermansia* in CNS disorders. While *Akkermansia* is consistently elevated in MS subjects, however, it may be a compensatory change for a study has shown that transferring *Akkermansia* to mice at EAE onset can ameliorate disease [56].

So far, FMT has been tested in treating a variety of conditions including *Clostridium difficile* infection [42, 57], active ulcerative colitis [58], high-fat diet-induced steatohepatitis [59], metabolic syndrome [60], and CNS diseases such as epilepsy [21] and autism spectrum disorder [61]. Notably, applying FMT to several MS patients [62] achieved promising improvement of clinical outcome and FMT treatment for EAE mice with fecal matter from immunized mice on intermittent fasting ameliorated EAE clinical course [42]. In this study, FMT had a therapeutic effect on EAE, reducing clinical severity and delaying the onset of disease (Figure 2). Hence, our data add more

weight to the idea of using FMT as a GM-based treatment for MS.

Currently, how FMT exerts influence on MS remains unclear. Evidence from the EAE model of MS suggests a critical role for GM and its metabolites in the mechanisms behind neuroinflammation and demyelination [17, 18]. Our attempt to rectify altered GM in EAE by FMT led to alleviated neuroinflammation and reduced BBB leakage and damage to myelin and axons (Figures 3–5). These results lend support to GM's involvement in the pathogenesis of EAE and echo previous observations of GM regulating BBB integrity [28], myelination [63], and microglia activation [29, 64]. It is worth noting that two earlier studies experimented with applying FMT to EAE animals, but the fecal matter used for transplantation came from donor animals under specific experimental conditions [42, 65]. FMT from immunized donor mice on intermittent fasting resulted in reduced inflammation and demyelination in EAE recipient mice, proving that GM was part of the reason for fasting to take effect in treating EAE [42]. FMT from Albino Oxford (AO) donor rats, which are highly resistant to EAE induction, to EAE-prone Dark Agouti (DA) recipient rats from birth led to ameliorated EAE symptoms and decreased production of interleukin- (IL-) 17, a proinflammatory cytokine, in the spinal cord [65], hinting that GM can confer resistance to EAE.

Our study has limitations. Firstly, we started FMT treatment before the onset of neurological signs, which is a disadvantage from a translational point of view as treatment for MS is sought after the onset of disease. We also did not analyze the ingredients of the fecal matter used for transplantation.

5. Conclusions

In summary, our data demonstrate beneficial effects of FMT in the EAE mouse model of MS, including improved GM composition, ameliorated clinical course, subdued glial inflammatory response, and protection conferred on the BBB, myelin, and axons. Our findings suggest a causal linkage between GM and MS pathogenesis, and therefore, GM has the potential to be a new target of innovative therapies for MS. Further work is needed to unravel the mechanisms underlying the impact of FMT on gut-brain axis and formulate an ideal microbial recipe for MS treatment.

Data Availability

The raw sequences were deposited in the NCBI Sequence Read Archive (SRA) with the accession number SRP201403.

Conflicts of Interest

The authors declare that there is no conflict of interests.

Authors' Contributions

KLL, SCW, LH, XJY, YRM, CMJ, and XPP conducted the experiments. ZL, BZ, and HLL designed the experiments. Data analysis was carried out by XXC, ZKH, and HHZ. The

manuscript was written by ZL and GDM with editorial assistance of HLL. Kanglan Li, Shouchao Wei, Li Hu, and Xiaojian Yin contributed equally to this work.

Acknowledgments

This work was supported by funding from the Natural Science Foundation of China (NSFC, No. 81400986), the Natural Science Foundation of Guangdong Province (No. 2020A1515011284), the Innovation Project of Ordinary Colleges and Universities in Guangdong (No. 2019KTSCX045), the Science and Technology Planning Project of Zhanjiang (No. 2018A01021), the Medical Scientific Research Foundation of Guangdong Province (No. A2020282), the Traditional Chinese Medicine Bureau of Guangdong Province (No. 20182074), GMU (No. M2016037), and the Affiliated Hospital of GMU (BJ201515, BJ201612, and LCYJ2018A003).

References

- [1] T. Kalincik, "Multiple sclerosis relapses: epidemiology, outcomes and Management. A Systematic Review," *Neuroepidemiology*, vol. 44, no. 4, pp. 199–214, 2015.
- [2] The International Multiple Sclerosis Genetics Consortium & The Wellcome Trust Case Control Consortium 2, "Genetic risk and a primary role for cell-mediated immune mechanisms in multiple sclerosis," *Nature*, vol. 476, no. 7359, pp. 214–219, 2011.
- [3] C. Cotsapas and D. A. Hafler, "Immune-mediated disease genetics: the shared basis of pathogenesis," *Trends in Immunology*, vol. 34, no. 1, pp. 22–26, 2013.
- [4] A. Nylander and D. A. Hafler, "Multiple sclerosis," *The Journal of Clinical Investigation*, vol. 122, no. 4, pp. 1180–1188, 2012.
- [5] M. Adamczyk-Sowa, A. Medrek, P. Madej, W. Michlicka, and P. Dobrakowski, "Does the gut microbiota influence immunity and inflammation in multiple sclerosis pathophysiology?," *Journal of Immunology Research*, vol. 2017, 14 pages, 2017.
- [6] G. Sharon, N. J. Cruz, D. W. Kang et al., "Human gut microbiota from autism spectrum disorder promote behavioral symptoms in mice," *Cell*, vol. 177, no. 6, pp. 1600–1618.e17, 2019, e1617.
- [7] E. Cekanaviciute, B. B. Yoo, T. F. Runia et al., "Gut bacteria from multiple sclerosis patients modulate human T cells and exacerbate symptoms in mouse models," *Proceedings of the National Academy of Sciences of the United States of America*, vol. 114, no. 40, pp. 10713–10718, 2017.
- [8] K. Berer, L. A. Gerdes, E. Cekanaviciute et al., "Gut microbiota from multiple sclerosis patients enables spontaneous autoimmune encephalomyelitis in mice," *Proceedings of the National Academy of Sciences of the United States of America*, vol. 114, no. 40, pp. 10719–10724, 2017.
- [9] L. Wrzosek, D. Ciocan, P. Borentain et al., "Transplantation of human microbiota into conventional mice durably reshapes the gut microbiota," *Scientific Reports*, vol. 8, no. 1, p. 6854, 2018.
- [10] J. Ochoa-Repáraz, D. W. Mielcarz, L. E. Ditrio et al., "Role of gut commensal microflora in the development of experimental autoimmune encephalomyelitis," *Journal of Immunology*, vol. 183, no. 10, pp. 6041–6050, 2009.
- [11] S. Stanisavljević, J. Lukić, M. Momčilović et al., "Gut-associated lymphoid tissue, gut microbes and susceptibility to experimental autoimmune encephalomyelitis," *Beneficial Microbes*, vol. 7, no. 3, pp. 363–373, 2016.
- [12] Y. Belkaid and T. W. Hand, "Role of the microbiota in immunity and inflammation," *Cell*, vol. 157, no. 1, pp. 121–141, 2014.
- [13] N. Kamada, S. U. Seo, G. Y. Chen, and G. Nunez, "Role of the gut microbiota in immunity and inflammatory disease," *Nature Reviews. Immunology*, vol. 13, no. 5, pp. 321–335, 2013.
- [14] R. Horai, C. R. Zárate-Bladés, P. Dillenburg-Pilla et al., "Microbiota-dependent activation of an autoreactive T cell receptor provokes autoimmunity in an immunologically privileged site," *Immunity*, vol. 43, no. 2, pp. 343–353, 2015.
- [15] J. T. Van Praet, E. Donovan, I. Vanassche et al., "Commensal microbiota influence systemic autoimmune responses," *The EMBO Journal*, vol. 34, no. 4, pp. 466–474, 2014.
- [16] S. Jangi, R. Gandhi, L. M. Cox et al., "Alterations of the human gut microbiome in multiple sclerosis," *Nature Communications*, vol. 7, no. 1, p. 12015, 2016.
- [17] K. Berer, M. Mues, M. Koutrolos et al., "Commensal microbiota and myelin autoantigen cooperate to trigger autoimmune demyelination," *Nature*, vol. 479, no. 7374, pp. 538–541, 2011.
- [18] Y. K. Lee, J. S. Menezes, Y. Umesaki, and S. K. Mazmanian, "Proinflammatory T-cell responses to gut microbiota promote experimental autoimmune encephalomyelitis," *Proceedings of the National Academy of Sciences of the United States of America*, vol. 108, Supplement_1, pp. 4615–4622, 2011.
- [19] Y. T. Li, H. F. Cai, Z. H. Wang, J. Xu, and J. Y. Fang, "Systematic review with meta-analysis: long-term outcomes of faecal microbiota transplantation for *Clostridium difficile* infection," *Alimentary Pharmacology & Therapeutics*, vol. 43, no. 4, pp. 445–457, 2016.
- [20] S. Paramsothy, R. Paramsothy, D. T. Rubin et al., "Faecal microbiota transplantation for inflammatory bowel disease: a systematic review and meta-analysis," *Journal of Crohn's & Colitis*, vol. 11, no. 10, pp. 1180–1199, 2017.
- [21] Z. He, B. T. Cui, T. Zhang et al., "Fecal microbiota transplantation cured epilepsy in a case with Crohn's disease: the first report," *World Journal of Gastroenterology*, vol. 23, no. 19, pp. 3565–3568, 2017.
- [22] M. Q. Xu, H. L. Cao, W. Q. Wang et al., "Fecal microbiota transplantation broadening its application beyond intestinal disorders," *World Journal of Gastroenterology*, vol. 21, no. 1, pp. 102–111, 2015.
- [23] T. J. Borody, L. J. Brandt, and S. Paramsothy, "Therapeutic faecal microbiota transplantation: current status and future developments," *Current Opinion in Gastroenterology*, vol. 30, no. 1, pp. 97–105, 2014.
- [24] X. Zheng, X. Hu, G. Zhou et al., "Soluble egg antigen from *Schistosoma japonicum* modulates the progression of chronic progressive experimental autoimmune encephalomyelitis via Th2-shift response," *Journal of Neuroimmunology*, vol. 194, no. 1–2, pp. 107–114, 2008.
- [25] J. Chen, N. Chia, K. R. Kalari et al., "Multiple sclerosis patients have a distinct gut microbiota compared to healthy controls," *Scientific Reports*, vol. 6, no. 1, p. 28484, 2016.
- [26] W. J. van den Hoogen, J. D. Laman, and B. A. 't Hart, "Modulation of multiple sclerosis and its animal model experimental

- autoimmune encephalomyelitis by food and gut microbiota," *Frontiers in Immunology*, vol. 8, p. 1081, 2017.
- [27] S. Floris, E. L. A. Blezer, G. Schreibelt et al., "Blood-brain barrier permeability and monocyte infiltration in experimental allergic encephalomyelitis," *Brain*, vol. 127, no. 3, pp. 616–627, 2004.
- [28] V. Braniste, M. Al-Asmakh, C. Kowal et al., "The gut microbiota influences blood-brain barrier permeability in mice," *Science Translational Medicine*, vol. 6, no. 263, p. 263ra158, 2014.
- [29] D. Erny, A. L. H. de Angelis, D. Jaitin et al., "Host microbiota constantly control maturation and function of microglia in the CNS," *Nature Neuroscience*, vol. 18, no. 7, pp. 965–977, 2015.
- [30] A. F. Logsdon, M. A. Erickson, E. M. Rhea, T. S. Salameh, and W. A. Banks, "Gut reactions: how the blood-brain barrier connects the microbiome and the brain," *Experimental Biology and Medicine (Maywood, N.J.)*, vol. 243, no. 2, pp. 159–165, 2018.
- [31] J. Lv, W. Hu, Z. Yang et al., "Focusing on claudin-5: a promising candidate in the regulation of BBB to treat ischemic stroke," *Progress in Neurobiology*, vol. 161, pp. 79–96, 2018.
- [32] J. Correale and M. F. Farez, "The role of astrocytes in multiple sclerosis progression," *Frontiers in Neurology*, vol. 6, p. 180, 2015.
- [33] H.-J. Lee, Y.-H. Hwang, and D.-H. Kim, "Lactobacillus plantarum C29-Fermented soybean (DW2009) alleviates memory impairment in 5XFAD transgenic mice by regulating microglia activation and gut microbiota composition," *Molecular Nutrition & Food Research*, vol. 62, no. 20, article e1800359, 2018.
- [34] M. F. Sun, Y. L. Zhu, Z. L. Zhou et al., "Neuroprotective effects of fecal microbiota transplantation on MPTP-induced Parkinson's disease mice: gut microbiota, glial reaction and TLR4/TNF-alpha signaling pathway," *Brain, Behavior, and Immunity*, vol. 70, pp. 48–60, 2018.
- [35] S. Miyake, S. Kim, W. Suda et al., "Dysbiosis in the gut microbiota of patients with multiple sclerosis, with a striking depletion of species belonging to clostridia XIVA and IV clusters," *PLoS One*, vol. 10, no. 9, article e0137429, 2015.
- [36] H. Tremlett, D. W. Fadrosh, A. A. Faruqi et al., "Gut microbiota in early pediatric multiple sclerosis: a case-control study," *European Journal of Neurology*, vol. 23, no. 8, pp. 1308–1321, 2016.
- [37] J. S. Bajaj, G. Kakiyama, T. Savidge et al., "Antibiotic-associated disruption of microbiota composition and function in cirrhosis is restored by fecal transplant," *Hepatology*, vol. 68, no. 4, pp. 1549–1558, 2018.
- [38] B. H. Mullish, J. A. K. McDonald, M. R. Thursz, and J. R. Marchesi, "Antibiotic-associated disruption of microbiota composition and function in cirrhosis is restored by fecal transplant," *Hepatology*, vol. 68, no. 3, p. 1205, 2018.
- [39] F. Zhang, W. Luo, Y. Shi, Z. Fan, and G. Ji, "Should we standardize the 1,700-year-old fecal microbiota transplantation?," *American Journal of Gastroenterology*, vol. 107, no. 11, pp. 1755–1756, 2012.
- [40] S. K. Tankou, K. Regev, B. C. Healy et al., "A probiotic modulates the microbiome and immunity in multiple sclerosis," *Annals of Neurology*, vol. 83, no. 6, pp. 1147–1161, 2018.
- [41] S. K. Tankou, K. Regev, B. C. Healy et al., "Investigation of probiotics in multiple sclerosis," *Multiple Sclerosis*, vol. 24, no. 1, pp. 58–63, 2018.
- [42] F. Cignarella, C. Cantoni, L. Ghezzi et al., "Intermittent fasting confers protection in CNS autoimmunity by altering the gut microbiota," *Cell Metabolism*, vol. 27, no. 6, pp. 1222–1235.e6, 2018.
- [43] J. Rodríguez-Morató, N. R. Matthan, J. Liu, R. de la Torre, and C.-Y. O. Chen, "Cranberries attenuate animal-based diet-induced changes in microbiota composition and functionality: a randomized crossover controlled feeding trial," *The Journal of Nutritional Biochemistry*, vol. 62, pp. 76–86, 2018.
- [44] A. Koh, F. De Vadder, P. Kovatcheva-Datchary, and F. Backhed, "From dietary fiber to host physiology: short-chain fatty acids as key bacterial metabolites," *Cell*, vol. 165, no. 6, pp. 1332–1345, 2016.
- [45] G. den Besten, K. van Eunen, A. K. Groen, K. Venema, D. J. Reijngoud, and B. M. Bakker, "The role of short-chain fatty acids in the interplay between diet, gut microbiota, and host energy metabolism," *Journal of Lipid Research*, vol. 54, no. 9, pp. 2325–2340, 2013.
- [46] L. Hoyles, T. Snelling, U. K. Umlai et al., "Microbiome-host systems interactions: protective effects of propionate upon the blood-brain barrier," *Microbiome*, vol. 6, no. 1, p. 55, 2018.
- [47] S. M. Matt, J. M. Allen, M. A. Lawson, L. J. Mailing, J. A. Woods, and R. W. Johnson, "Butyrate and dietary soluble fiber improve neuroinflammation associated with aging in mice," *Frontiers in Immunology*, vol. 9, p. 1832, 2018.
- [48] M. Lanza, M. Campolo, G. Casili et al., "Sodium butyrate exerts neuroprotective effects in spinal cord injury," *Molecular Neurobiology*, vol. 56, no. 6, pp. 3937–3947, 2019.
- [49] M. Mizuno, D. Noto, N. Kaga, A. Chiba, and S. Miyake, "The dual role of short fatty acid chains in the pathogenesis of autoimmune disease models," *PLoS One*, vol. 12, no. 2, article e0173032, 2017.
- [50] A. C. Chevalier and T. A. Rosenberger, "Increasing acetyl-CoA metabolism attenuates injury and alters spinal cord lipid content in mice subjected to experimental autoimmune encephalomyelitis," *Journal of Neurochemistry*, vol. 141, no. 5, pp. 721–737, 2017.
- [51] Y. Wang, S. Begum-Haque, K. M. Telesford et al., "A commensal bacterial product elicits and modulates migratory capacity of CD39(+) CD4 T regulatory subsets in the suppression of neuroinflammation," *Gut Microbes*, vol. 5, no. 4, pp. 552–561, 2014.
- [52] J. Ochoa-Repáraz, D. W. Mielcarz, L. E. Ditrio et al., "Central nervous system demyelinating disease protection by the human commensal *Bacteroides fragilis* depends on polysaccharide A expression," *Journal of Immunology*, vol. 185, no. 7, pp. 4101–4108, 2010.
- [53] A. Heintz-Buschart, U. Pandey, T. Wicke et al., "The nasal and gut microbiome in Parkinson's disease and idiopathic rapid eye movement sleep behavior disorder," *Movement Disorders*, vol. 33, no. 1, pp. 88–98, 2018.
- [54] J. R. Bedarf, F. Hildebrand, L. P. Coelho et al., "Functional implications of microbial and viral gut metagenome changes in early stage L-DOPA-naive Parkinson's disease patients," *Genome Medicine*, vol. 9, no. 1, p. 39, 2017.
- [55] R. Araos, N. Andreatos, J. Ugalde, S. Mitchell, E. Mylonakis, and E. M. C. D'Agata, "Fecal microbiome among nursing home residents with advanced dementia and *Clostridium difficile*," *Digestive Diseases and Sciences*, vol. 63, no. 6, pp. 1525–1531, 2018.

- [56] S. Liu, R. M. Rezende, T. G. Moreira et al., “Oral administration of miR-30d from feces of MS patients suppresses MS-like symptoms in mice by expanding *Akkermansia muciniphila*,” *Cell Host & Microbe*, vol. 26, no. 6, pp. 779–794.e8, 2019, e778.
- [57] F. E. Juul, K. Garborg, M. Bretthauer et al., “Fecal microbiota transplantation for Primary *Clostridium difficile* Infection,” *The New England Journal of Medicine*, vol. 378, no. 26, pp. 2535–2536, 2018.
- [58] P. Moayyedi, M. G. Surette, P. T. Kim et al., “Fecal microbiota transplantation induces remission in patients with active ulcerative colitis in a randomized controlled trial,” *Gastroenterology*, vol. 149, no. 1, pp. 102–109.e6, 2015.
- [59] D. Zhou, Q. Pan, F. Shen et al., “Total fecal microbiota transplantation alleviates high-fat diet-induced steatohepatitis in mice via beneficial regulation of gut microbiota,” *Scientific Reports*, vol. 7, no. 1, p. 1529, 2017.
- [60] A. Vrieze, E. Van Nood, F. Holleman et al., “Transfer of intestinal microbiota from lean donors increases insulin sensitivity in individuals with metabolic syndrome,” *Gastroenterology*, vol. 143, no. 4, pp. 913–916.e7, 2012.
- [61] D. W. Kang, J. B. Adams, A. C. Gregory et al., “Microbiota transfer therapy alters gut ecosystem and improves gastrointestinal and autism symptoms: an open-label study,” *Microbiome*, vol. 5, no. 1, p. 10, 2017.
- [62] S. Makkawi, C. Camara-Lemarroy, and L. Metz, “Fecal microbiota transplantation associated with 10 years of stability in a patient with SPMS,” *Neurol Neuroimmunol Neuroinflamm*, vol. 5, no. 4, article e459, 2018.
- [63] A. E. Hoban, R. M. Stilling, F. J. Ryan et al., “Regulation of prefrontal cortex myelination by the microbiota,” *Translational Psychiatry*, vol. 6, no. 4, article e774, 2016.
- [64] J. F. Cryan and T. G. Dinan, “Gut microbiota: microbiota and neuroimmune signalling-Metchnikoff to microglia,” *Nature Reviews. Gastroenterology & Hepatology*, vol. 12, no. 9, pp. 494–496, 2015.
- [65] S. Stanisavljević, M. Dinić, B. Jevtić et al., “Gut microbiota confers resistance of albino Oxford rats to the induction of experimental autoimmune encephalomyelitis,” *Frontiers in Immunology*, vol. 9, p. 942, 2018.

Research Article

The Effects of Dietary Glycine on the Acetic Acid-Induced Mouse Model of Colitis

Xin Wu ¹, Yongmin Zheng ¹, Jie Ma ¹, Jie Yin ¹ and Shuai Chen ^{1,2}

¹College of Animal Science and Technology, Hunan Agriculture University, Changsha, China; Hunan Co-Innovation Center of Animal Production Safety, Changsha, Hunan 410128, China

²Scientific Observing and Experimental Station of Animal Nutrition and Feed Science in South-Central, Ministry of Agriculture, Hunan Provincial Engineering Research Center of Healthy Livestock, Key Laboratory of Agro-Ecological Processes in Subtropical Region, Institute of Subtropical Agriculture, Chinese Academy of Sciences, Changsha, Hunan 410125, China

Correspondence should be addressed to Jie Yin; yinjie2014@126.com and Shuai Chen; chenshuai@mail.com

Received 14 May 2020; Revised 3 July 2020; Accepted 9 July 2020; Published 5 August 2020

Guest Editor: Xiaolu Jin

Copyright © 2020 Xin Wu et al. This is an open access article distributed under the Creative Commons Attribution License, which permits unrestricted use, distribution, and reproduction in any medium, provided the original work is properly cited.

Inflammatory bowel disease, a gut disease that is prevalent worldwide, is characterized by chronic intestinal inflammation, such as colitis, and disorder of the gut microbiome. Glycine (Gly) is the simplest amino acid and functions as an anti-inflammatory immune-nutrient and intestinal microbiota regulator. This study aimed at investigating the effect of Gly on colitis induced in mice by intrarectal administration of 5% acetic acid (AA). Bodyweight and survival rates were monitored, and colonic length and weight, serum amino acid concentrations, intestinal inflammation-related gene expression, and colonic microbiota abundances were analyzed. The results showed that Gly dietary supplementation had no effect on the survival rate or the ratio of colonic length to weight. However, Gly supplementation reversed the AA-induced increase in serum concentrations of amino acids such as glutamate, leucine, isoleucine, and valine. Furthermore, Gly inhibited colonic gene expression of interleukin- (IL-) 1 β and promoted IL-10 expression in colitis mice. Gly supplementation also reversed the AA-induced reduction in the abundance of bacteria such as Clostridia, Ruminococcaceae, and Clostridiales. This change in the intestinal microbiota was possibly attributable to the changes in colonic IL-10 expression and serum concentrations of valine and leucine. In sum, Gly supplementation regulated the serum concentrations of amino acids, the levels of colonic immune-associated gene expression, and the intestinal microbiota in a mouse model of colitis. These findings enhance our understanding of the role of Gly in regulating metabolism, intestinal immunity, and the gut microbiota in animals afflicted with colitis.

1. Introduction

Inflammatory bowel disease (IBD), including Crohn's disease (CD) and ulcerative colitis (UC), is characterized by a loss of intestinal mucosal homeostasis associated with inappropriate and aggravated immune responses to intestinal lumen antigens [1–3]. The clinical symptoms of IBD include diarrhea, abdominal pain, bloody stools, tenderness, and abdominal mass. The increased incidence of IBD is a worldwide health-care problem [4]. It is widely believed that IBD is caused by complex interactions between genetic and environmental factors, such as immune-response disorders and microbial community changes. However, the cause of IBD remains unclear, and further research is needed [5, 6].

Several types of pharmacologically induced animal colitis models have been developed, such as dextran sulfate- (DSS-), trinitrobenzene sulfonic acid- (TNBS-), or acetic acid- (AA-) induced models [7, 8]. DSS is widely used for this purpose, as is TNBS, typically in combination with ethanol. AA causes UC (hereafter termed “colitis”) by damaging the intestinal mucosa epithelium and is a low-cost and convenient technique. Previous studies demonstrated that AA-induced colitis might be a good model with which to study the efficacy of drugs [9], so we used AA to induce colitis in this study.

Anti-inflammatory drugs such as cytokine antagonists and immunosuppressive drugs such as corticosteroids are currently used for IBD treatment [10–12]. However, long-term use of cytokine antagonists may have severe side

TABLE 1: Primers used in this study.

Gene	ID	Nucleotide sequence of primers (5'-3')	Product length
IL-1 β	NM_008361.3	ATGAAAGACGGCACACCCAC GCTTGTGCTCTGCTTGTGAG	175
IL-17	NM_010552.3	TACCTCAACCGTTCCACGTC TTCCCTCCGCATTGACAC	119
IL-10	NM_010548.2	GCCACATGCTCCTAGAGCTG CAGCTGGTCCTTTGTTTAAAA	71
IFN- γ	NM_008337.4	ATGAACGCTACACACTGCATCTTGGCTT CCTCAAACCTTGGCAATACTCATGAATGC	361
Actin	NM_007393.5	GGACTCCTATGTGGGTGACGAGG GGGAGAGCATAGCCCTCGTAGAT	366

effects [13]. Therefore, new adjuvant therapies are required to overcome the limitations of current drug therapies [14].

Many amino acids have been shown to have beneficial effects in IBD. For example, arginine reduces mucosal permeability, inhibits inflammation, and increases inducible nitric oxide synthase (iNOS) activity in mice with DSS-induced colitis [15]. It has also been shown that Gly may inhibit cytokine secretion in monocytes, macrophages, and neutrophils, and regulate T cell activities [16]. Dietary Gly prevents diarrhea, bodyweight loss, and ulceration in rats with DSS-induced IBD [17, 18]. However, the effects of Gly on AA-induced IBD in mice remain unclear.

This study aimed at investigating the effect of Gly on AA-induced colitis in mice. The results add to our knowledge of a possible role for Gly in colitis treatment.

2. Materials and Methods

2.1. Animal Model. This study was conducted following the guidelines of the Animal Welfare Committee of the Institute of Subtropical Agriculture, Chinese Academy of Sciences (2015-8A). Female six-week-old ICR (Institute for Cancer Research) mice were purchased from the SLAC laboratory animal center (Changsha, China). The mice were housed in a temperature-controlled environment with a 12 h light/dark cycle and had free access to food and water. Sixty mice were randomly divided into three groups of 20 animals: a control (Con) group (fed the basal diet), a model (Mod) group (fed the basal diet), and a model+Gly (ModGly) group (fed the basal diet supplemented with 0.1% Gly). The dose of Gly was selected following preliminary experiments. The Con group and Mod group shared the data with our previous study [19]. On the seventh day of the experiment, all of the mice were fasted for 36 h and were intrarectally treated with 5% AA (Mod and ModGly group) or saline solution (Con group). The surviving mice were monitored for 1 week after the administration of AA, and all of the mice were then sacrificed by cervical dislocation, and blood, colons, and colonic contents were collected.

2.2. Analysis of Serum Amino Acids. High-performance liquid chromatography (HPLC) was used to analyze serum amino acids. Briefly, 0.1 ml of the serum sample was thoroughly mixed with 4.9 ml of 0.01-M hydrochloric acid and then centrifuged at 5000 rpm and 4°C for 5 min. The supernatant (500 ml) was then removed and incubated at 4°C for 12 h and then homogenized with 8% salicylic acid. The resulting homogenate was centrifuged twice at 12,000 rpm

and 4°C for 10 min. Authentic standards (Sigma Chemicals) for quantifying amino acids in serum samples were prepared in 0.01-M hydrochloric acid and stored at -70°C.

2.3. RT-PCR. Total RNA was extracted from colonic tissues using the TRIZOL reagent kit (Invitrogen, USA). The PrimeScript RT kit with gDNA Eraser (Takara Bio Inc., Qingdao, China) was used to synthesize cDNA, according to the product manual. Primers (Table 1) used in this study were designed under the principles of primer design using Primer 6.0 software (PRIMER-E, New Zealand) and Oligo 5.0 software (Molecular Biology Insights, Inc., USA), based on the gene sequences of the house mouse (*Mus musculus*) on GenBank. The SYBR Premix Ex Taq kit (Takara, Japan) was used for RT-PCR analysis, and triplicate reactions were performed using the Applied Biosystems 7900HT Fast Real-Time PCR System (Thermo, USA) by the following methods: (1) initial denaturation (90°C 30 s); (2) amplification and quantification (40 cycles at 95°C 5 s, 1 cycle at 60°C 30 s). Relative gene expression was calculated with the formula $2^{-(\Delta\Delta Ct)}$.

2.4. Gut Microbiota Analysis. 16S rDNA sequencing was used for intestinal microbiota analysis, according to our previous study [20]. Digested matter in the colon cavity was collected, and the DNA was extracted from this material using a Qiagen QIAamp DNA Stool Mini kit. Illumina MiSeq sequencing was used to analyse the V3 to V4 regions of bacterial 16S rDNA, and the data analysis was performed by Anoru Genomics Technology Co., Ltd., (Beijing, China). Briefly, the library was generated and sequenced to produce 400 base pair/600 base pair single-end reads. Single-end reads were assigned to the samples based on their unique barcode and truncated by the removal of their barcode and the primer sequence. Sequence analysis and operational taxonomic unit (OTU) clustering were performed using UPARSE software (v7.0.1001, <https://drive5.com/usearch/>) following quality filtering, and sequences with more than 97% similarity were clustered to the same OTU. RDP Classifier (V2.2, Michigan State University Board of Trustees, East Lansing, MI) was used for species annotations, based on the GreenGene database. MUSCLE software (Version 3.8.31) was used to study the phylogenetic relationships of different OTUs, to examine differences in the dominant species in different samples (groups), and for multiple-sequence alignments. The abundant information in the OTUs was normalized for subsequent analysis of the alpha diversity, beta diversity, and the environmental-factor correlation analysis.

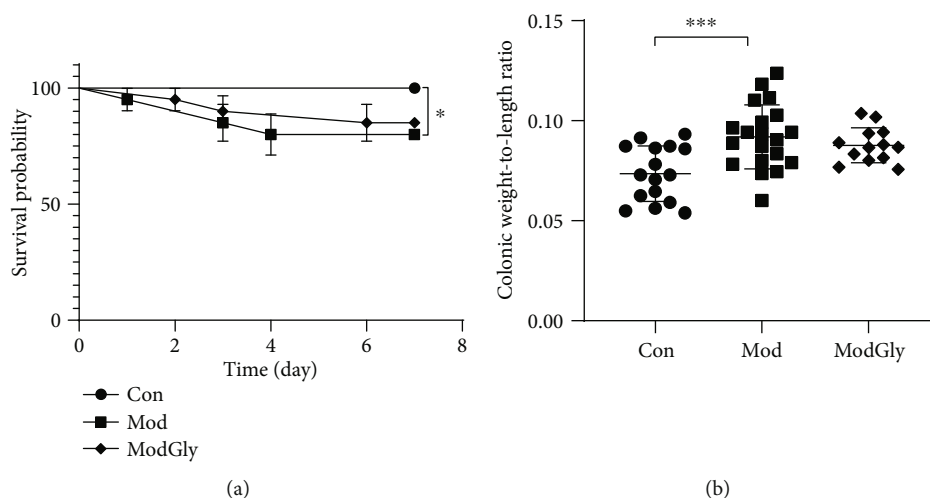


FIGURE 1: Survival proportions, the ratio of colon weight to length. (a) The survival rate was significantly lower in the Mod group than in the Con group, but was similar in the Mod and ModGly groups. (b) The colonic weight-to-length ratio was greater in the Mod group than in the Con group and was the same in the Mod and ModGly groups. The data are presented as means \pm SD; * $P < 0.05$, ** $P < 0.01$, *** $P < 0.001$.

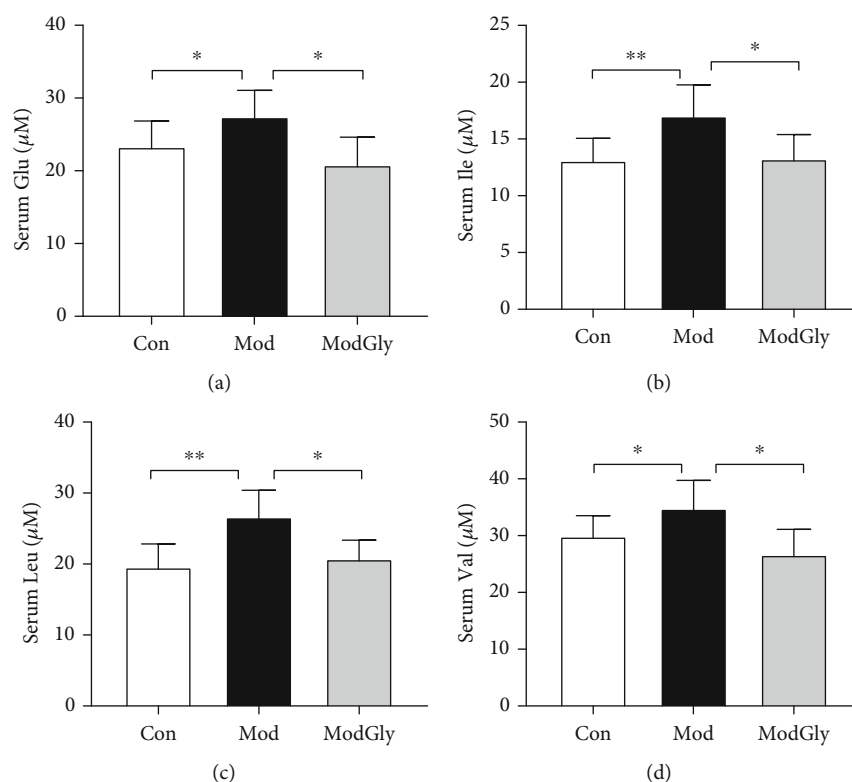


FIGURE 2: Serum amino acid profiles in the serum. The serum concentrations of Glu, glutamic acid (a), Ile, isoleucine (b), Leu, leucine (c), and Val, valine (d) were significantly higher ($P < 0.05$) in the Mod group than in the Con group and significantly lower ($P < 0.05$) in the Mod group than in the ModGly group. The data are presented as means \pm SD; * $P < 0.05$, ** $P < 0.01$, *** $P < 0.001$.

2.5. Statistical Analyses. GraphPad Prism 6.0 (GraphPad Software, Inc., La Jolla, CA) was used for statistical analyses and to create graphs. Statistical analyses between the Con and Mod groups and the Mod and ModGly groups were performed by *t*-test. Results are shown as mean \pm SD. $P < 0.05$ was considered significant; * $P < 0.05$, ** $P < 0.01$, *** $P < 0.001$.

3. Results

3.1. Survival Proportions and Ratio of Colon Weight to Length. We evaluated the effect of GLY on AA-induced colitis in mice by comparing the survival rate and the ratio of colonic weight to length. The survival rate in the Mod group was significantly lower than that in the CON group

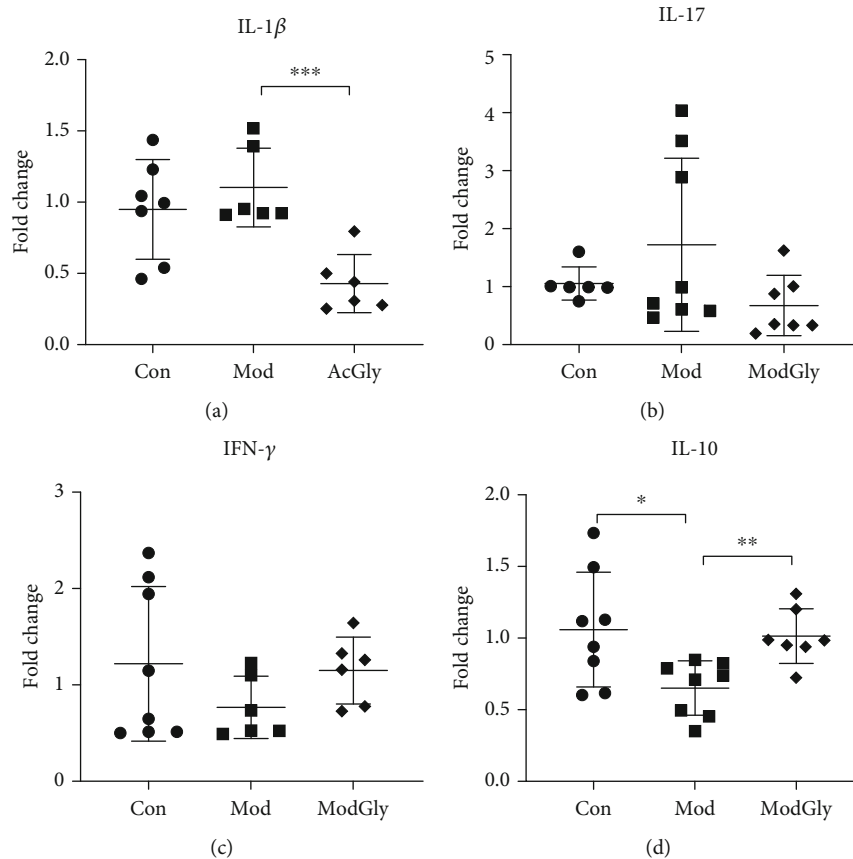


FIGURE 3: Colonic expression of IBD-associated cytokines. Real time-polymerase chain reaction analysis was used to measure the colonic expression of IL-1 β (a), IL-17 (b), IFN- γ (c), and IL-10 (d) genes. AA administration reduced IL-10 expression, whereas Gly inhibited IL-1 β expression and promoted IL-10 expression. The data are presented as means \pm SD; * P < 0.05, ** P < 0.01, *** P < 0.001.

(Figure 1(a)), and the colonic weight/length ratio was increased (P < 0.05) (Figure 1(b)). However, Gly did not affect the survival rate or the colonic weight-to-length ratio in the ModGly group (Figures 1(a)–1(b)).

3.2. Serum Amino Acid Profile. The results showed that the serum leucine (Leu), isoleucine (Ile), valine (Val), and glutamic acid (Glu) concentrations were significantly higher (P < 0.05) in the Mod group than in the CON group (Figures 2(a)–2(d)), whereas the concentrations of other amino acids were largely unchanged (data not shown). Notably, dietary Gly reduced the serum concentrations of Leu, Ile, Val, and Glu in the Mod group.

3.3. Colonic Expression of IBD-Associated Cytokines. We analyzed the gene expression of colonic proinflammatory cytokines (such as IL-1 β , IFN- γ , and IL-17) and inhibitory cytokine (IL-10). Compared with the CON group, the MOD group had significantly reduced expression of IL-10 (P < 0.05) (Figure 3(d)) but had an unaltered expression of proinflammatory cytokines (Figures 3(a)–(c)). In contrast, the ModGly group had significantly increased IL-10 expression (Figure 3(d)) and reduced IL-1 β expression (Figure 3(c)).

3.4. Intestinal Microbiota. 16sRNA was analyzed by Illumina high-throughput sequencing to examine the effect of the

experimental conditions on the gut microbiota of mice. A total of 260 OTUs were found overall, and 233 of these OTUs were present in all three groups (Figure 4(a)). Twenty-six taxa were detected at the genus level, such as *Bacteroides*, *Prevotella*, *Helicobacter*, *Akkermansia*, *Lactobacillus*, and *Sutterella* (Figure 4(b)). Clostridia, Clostridiales, and Ruminococcaceae were relatively more abundant in both the Con and ModGly groups than in the Mod group (Table 2). The prominent populations in each group were also determined based on linear discriminant analysis coupled with effect-size measurements, which revealed that Clostridia and Clostridiales were dominant in the Con group, Alcaligenaceae, Burkholderiales, and Betaproteobacteria were dominant in the Mod group, and Ruminococcaceae were dominant in the ModGly group (Figure 4(c)). A correlation analysis showed that the serum concentrations of Val and Leu were negatively correlated with the abundance of Clostridia and Clostridiales (Figure 4(d)). Moreover, colonic IL-10 expression was positively correlated with the abundance of Clostridia, Clostridiales, and IL-1 expression was negatively correlated with the abundance of Ruminococcaceae (Figure 4(e)).

4. Discussion

Previous studies have shown that body weight, survival rates, and the ratio of colon weight to colon length decreased in the

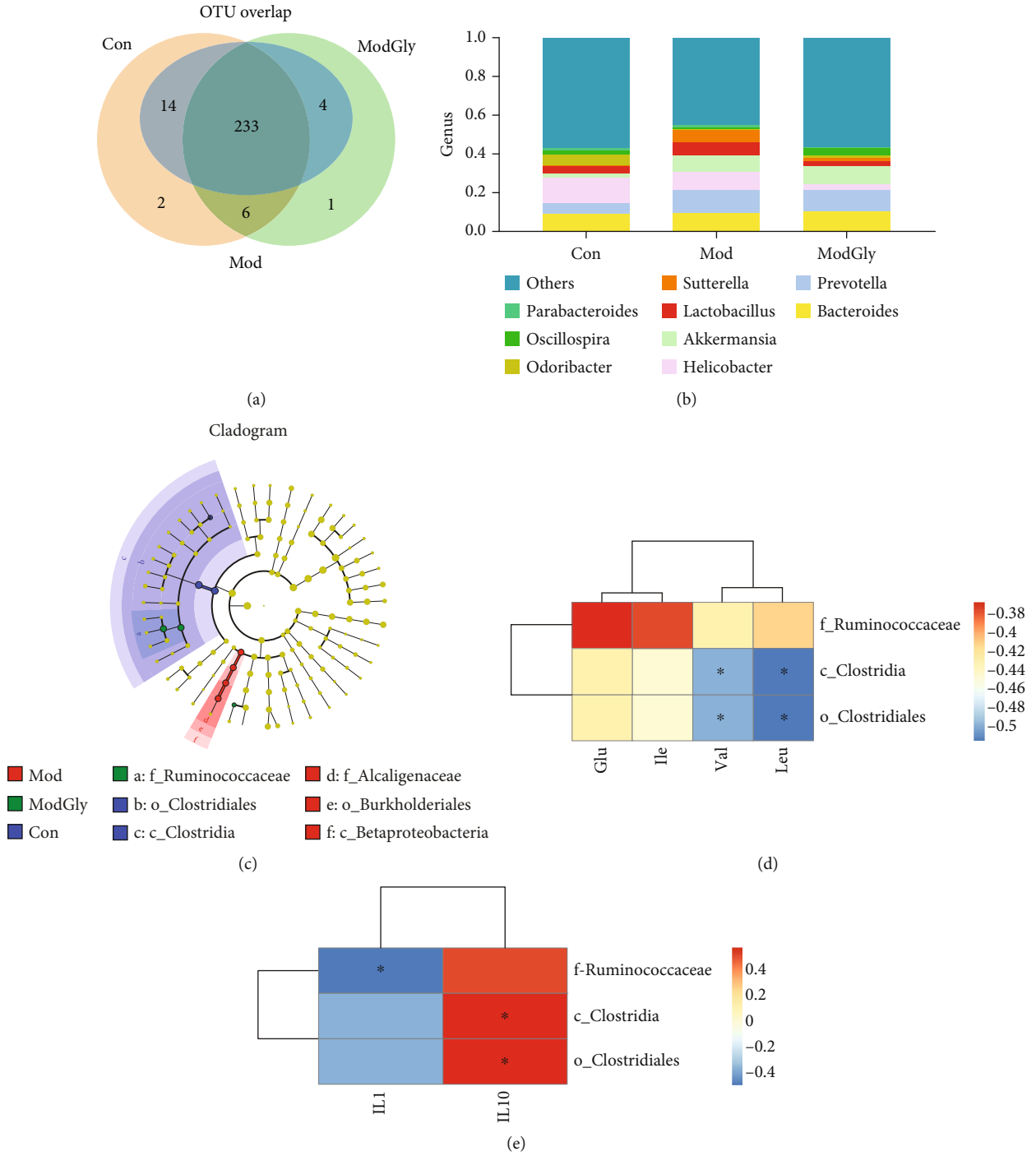


FIGURE 4: Intestinal microbiota. (a) Two hundred thirty-three OTUs were common to all three groups. (b) Relative contribution of genera in each group. (c) Prominent populations in each: Clostridia and Clostridiales in the Con group, Alcaligenaceae, Burkholderiales, and Betaproteobacteria in the Mod group, and Ruminococcaceae in the ModGly group. (d) The correlation analysis showed that serum concentrations of valine and leucine were negatively correlated with the abundance of Clostridia and Clostridiales (e); IL-10 expression was positively correlated with the abundance of Clostridia, Clostridiales, and IL-1 expression was negatively correlated with the abundance of Ruminococcaceae.

AA-induced IBD mouse model [17, 21]. It has also been shown that the expression of proinflammatory cytokines (i.e., IL-1 β , IFN- γ , and IL-17) is significantly increased in the AA-induced IBD model. Intriguingly, it has been found

that dietary supplementation Gly partially restores the above indicators in Wistar rat models of TNBS-or DSS-induced IBD [17]. However, we found that dietary Gly did not have a significant effect on survival rate and colonic weight-to-

TABLE 2: Taxa with significantly changed relative abundances at the genus level.

	Con	Mod	Gly
Clostridia	0.21380*	0.07538	0.1699#
Ruminococcaceae	0.03527*	0.01695	0.06516#
Clostridiales	0.2138*	0.07538	0.2130#

The relative abundances of Clostridia, Clostridiales, and Ruminococcaceae were significantly higher in both the Con and ModGly groups than in the Mod group. The data are presented as means \pm SD; * $P < 0.05$, Con vs. Mod; # $P < 0.05$, ModGly vs. Mod.

length ratio in the mouse model with AA-induced IBD. This different result may be attributable to the mouse model and/or the dosage of Gly we used.

Amino acids are necessary for intestinal growth and for the maintenance of mucosal integrity and barrier function [22–24]. Dietary supplementation with amino acids, such as threonine, serine, proline, and cysteine, improves mucin production, protects intestinal epithelial cells, and enhances the health of the intestinal microbiome [25–27]. Some amino acids have been suggested to be suitable as biomarkers for diagnosis and treatment in IBD, such as branched-chain amino acids (BCAAs; i.e., Leu, Ile, and Val) and tryptophan [28]. Concentrations of BCAAs and Glu have also been found to be significantly increased in a model of IBD [7], and these increases could be reversed by dietary Gly. Studies have also reported that BCAAs enhance the intestinal immune system by improving the morphological integrity of the intestinal tract and increasing the production of immunoglobulin. For example, Leu enhances cell proliferation and amino-acid transporter expression by activating the mTOR pathway [29]. However, a high concentration of BCAAs may activate the mTOR and NF- κ B pathways and thereby increase oxidative stress and inflammation. Other non-BCAAs have shown beneficial effects: for example, arginine reduces mucosal permeability, inhibits inflammation, and increases iNOS activity in mice with DSS-induced colitis [15]. Moreover, Gly inhibits cytokine secretion in monocytes, macrophages, and neutrophils and regulates T cell activities [16].

Current evidence suggests that immune disorders contribute to the IBD process via cytokine production in bowel lesions. Many proinflammatory cytokines, such as TNF- α and IL-1/6/22/23, and anti-inflammatory cytokines (such as IL-10) have been studied to determine their roles in IBD [30]. For example, it was found that IL-1 is highly activated in IBD patients and that IL-1 β activates CD4+ T cells [31]. It was also found that mice that the lack of IL-10 or IL-10R are sensitive to colitis [32], largely due to the promotion of IL-1 production.

In another study, it was found that dietary Gly supplementation could reverse the increase of colonic IL-1 β and the induction of TNF- α gene expression triggered by neutrophil-produced chemokines and inflammatory proteins secreted by macrophages [17]. Similarly, we found in this study that dietary Gly supplementation inhibited IL-1 expression and promoted IL-10 expression (as shown by

increased IL-10 mRNA abundance), suggesting the potential of Gly for IBD treatment.

The gut microbiome has been linked to many diseases, such as IBD, obesity, diabetes, and autism [33]. Some studies have reported dramatic changes in the composition of the intestinal microbial community in mice with IBD, which is in keeping with our results. Dietary supplements, such as amino acids, may regulate physiological activity via their effects on gut microbes [34, 35]. In addition, a low-Gly diet is associated with changes in gut flora [36]. In this study, we found that Gly changed the composition of the microbiota, and this has associations with serum concentrations of amino acids and colonic gene expression of IL-1 and IL-10 in IBD models.

Interestingly, *Clostridium butyricum*, a member of Clostridia and Clostridiales, has been reported to promote the growth of gut IL-10-producing innate immune cells and alleviate colitis in a mouse model by activating Treg and inhibiting activated macrophages [37]. The findings indicate that dietary Gly regulates colonic cytokine expressions, especially that of IL-10, possibly via effects on gut bacteria. However, further studies are needed to investigate this possible mechanism.

In conclusion, our data show that dietary Gly modulated serum amino acid concentrations and gut cytokine expression in AA-induced colitis mice and that this may have occurred via the regulation of the intestinal microbiota. These findings enhance our understanding of the roles of Gly in the metabolism of serum amino acids, intestinal immunity, and its effects on the intestinal microbiota of mice.

Data Availability

The data used to support the findings of this study are available from the corresponding author upon request.

Conflicts of Interest

The authors have no conflicts of interest.

Authors' Contributions

Shuai Chen and Jie Yin designed the experiment, which was performed by Xin Wu and Yongmin Zheng. Jie Ma analyzed the data and prepared tables and figures. Shuai Chen and Xin Wu prepared the manuscript. All of the authors reviewed the manuscript. Xin Wu and Yongmin Zheng contributed equally to this study.

Acknowledgments

This study was supported by the National Natural Science Foundation of China (Nos. 31772642, 31672457, and 31672433), the International Partnership Program of Chinese Academy of Sciences (161343KYSB20160008), the Hunan Provincial Science and Technology Department (2017NK2322), the China Postdoctoral Science Foundation (2018M632963), and the Key Programs of Frontier Scientific Research of the Chinese Academy of Sciences (QYZDYSSW-SMC008).



References

- [1] K. L. Glassner, B. P. Abraham, and E. M. M. Quigley, "The microbiome and inflammatory bowel disease," *The Journal of Allergy and Clinical Immunology*, vol. 145, no. 1, pp. 16–27, 2020.
- [2] G. Doherty, K. H. Katsanos, J. Burisch et al., "European Crohn's and Colitis Organisation topical review on treatment withdrawal ['exit strategies'] in inflammatory bowel disease," *Journal of Crohn's and Colitis*, vol. 12, no. 1, pp. 17–31, 2018.
- [3] M. Schirmer, A. Garner, H. Vlamakis, and R. J. Xavier, "Microbial genes and pathways in inflammatory bowel disease," *Nature Reviews Microbiology*, vol. 17, no. 8, pp. 497–511, 2019.
- [4] G. G. Kaplan, "The global burden of IBD: from 2015 to 2025," *Nature Reviews Gastroenterology & Hepatology*, vol. 12, no. 12, pp. 720–727, 2015.
- [5] H. Huang, M. Fang, L. Jostins et al., "Fine-mapping inflammatory bowel disease loci to single-variant resolution," *Nature*, vol. 547, no. 7662, pp. 173–178, 2017.
- [6] H. S. P. de Souza, "Etiopathogenesis of inflammatory bowel disease," *Current Opinion in Gastroenterology*, vol. 33, no. 4, pp. 222–229, 2017.
- [7] Y. Liu, X. Wang, and C. A. Hu, "Therapeutic potential of amino acids in inflammatory bowel disease," *Nutrients*, vol. 9, no. 9, p. 920, 2017.
- [8] N. Taghipour, N. Mosaffa, H. A. Aghdai et al., "Immunomodulatory effect of *Syphacia obvelata* in treatment of experimental DSS-induced colitis in mouse model," *Scientific Reports*, vol. 9, no. 1, article 19127, 2019.
- [9] D. Low, D. D. Nguyen, and E. Mizoguchi, "Animal models of ulcerative colitis and their application in drug research," *Drug Design, Development and Therapy*, vol. 7, pp. 1341–1357, 2013.
- [10] X. Roblin, N. Williet, G. Boschetti et al., "Addition of azathioprine to the switch of anti-TNF in patients with IBD in clinical relapse with undetectable anti-TNF trough levels and antidrug antibodies: a prospective randomised trial," *Gut*, vol. 69, no. 7, pp. 1206–1212, 2020.
- [11] T. Gjuladin-Hellon, M. Gordon, Z. Iheozor-Ejiogor, and A. K. Akobeng, "Oral 5-aminosalicylic acid for maintenance of surgically-induced remission in Crohn's disease," *Cochrane Database of Systematic Reviews*, vol. 6, article CD008414, 2019.
- [12] H. Courthion, T. Mugnier, C. Rousseaux, M. Möller, R. Gurny, and D. Gabriel, "Self-assembling polymeric nanocarriers to target inflammatory lesions in ulcerative colitis," *Journal of Controlled Release*, vol. 275, pp. 32–39, 2018.
- [13] V. Dubinsky, L. Reshef, N. Bar et al., "Predominantly antibiotic-resistant intestinal microbiome persists in patients with pouchitis who respond to antibiotic therapy," *Gastroenterology*, vol. 158, no. 3, pp. 610–624.e13, 2020.
- [14] K. Wang, X. Jin, Q. Li et al., "Propolis from different geographic origins decreases intestinal inflammation and *Bacteroides* spp. populations in a model of DSS-induced colitis," *Molecular Nutrition & Food Research*, vol. 62, no. 17, 2018.
- [15] L. A. Coburn, X. Gong, K. Singh et al., "L-arginine supplementation improves responses to injury and inflammation in dextran sulfate sodium colitis," *PLoS One*, vol. 7, no. 3, article e33546, 2012.
- [16] J. Van Den Eynden, S. SahebAli, N. Horwood et al., "Glycine and glycine receptor signalling in non-neuronal cells," *Frontiers in Molecular Neuroscience*, vol. 2, no. 9, 2009.
- [17] I. Tsune, K. Ikejima, M. Hirose et al., "Dietary glycine prevents chemical-induced experimental colitis in the rat," *Gastroenterology*, vol. 125, no. 3, pp. 775–785, 2003.
- [18] K. Sugihara, T. L. Morhardt, and N. Kamada, "The role of dietary nutrients in inflammatory bowel disease," *Frontiers in Immunology*, vol. 9, article 3183, 2019.
- [19] S. Chen, M. Wang, L. Yin et al., "Effects of dietary tryptophan supplementation in the acetic acid-induced colitis mouse model," *Food & Function*, vol. 9, no. 8, pp. 4143–4152, 2018.
- [20] S. Chen, B. Tan, Y. Xia et al., "Effects of dietary gamma-aminobutyric acid supplementation on the intestinal functions in weaning piglets," *Food & Function*, vol. 10, no. 1, pp. 366–378, 2019.
- [21] D. K. Podolsky, "Inflammatory bowel disease," *New England Journal of Medicine*, vol. 347, no. 6, pp. 417–429, 2002.
- [22] F. He, C. Wu, P. Li et al., "Functions and signaling pathways of amino acids in intestinal inflammation," *BioMed Research International*, vol. 2018, Article ID 9171905, 13 pages, 2018.
- [23] W. Tang, J. Wu, S. Jin et al., "Glutamate and aspartate alleviate testicular/epididymal oxidative stress by supporting antioxidant enzymes and immune defense systems in boars," *Science China. Life Sciences*, vol. 63, no. 1, pp. 116–124, 2020.
- [24] Q. Guo, F. Li, Y. Duan et al., "Oxidative stress, nutritional antioxidants and beyond," *Science China Life Sciences*, vol. 63, no. 6, pp. 866–874, 2020.
- [25] M. Faure, C. Mettraux, D. Moennoz et al., "Specific amino acids increase mucin synthesis and microbiota in dextran sulfate sodium-treated rats," *The Journal of Nutrition*, vol. 136, no. 6, pp. 1558–1564, 2006.
- [26] G. Guan, S. Ding, Y. Yin, V. Durairandiyar, N. A. Al-Dhabi, and G. Liu, "Macleaya cordata extract alleviated oxidative stress and altered innate immune response in mice challenged with enterotoxigenic *Escherichia coli*," *Science China Life Sciences*, vol. 62, no. 8, pp. 1019–1027, 2019.
- [27] M. Bai, H. Liu, K. Xu et al., "Compensation effects of coated cysteamine on meat quality, amino acid composition, fatty acid composition, mineral content in dorsal muscle and serum biochemical indices in finishing pigs offered reduced trace minerals diet," *Science China Life Sciences*, vol. 62, no. 11, pp. 1550–1553, 2019.
- [28] Y. Tamura, H. Ohta, Y. Kagawa et al., "Plasma amino acid profiles in dogs with inflammatory bowel disease," *Journal of Veterinary Internal Medicine*, vol. 33, no. 4, pp. 1602–1607, 2019.
- [29] M. Coëffier, S. Claeysens, M. Bensifi et al., "Influence of leucine on protein metabolism, phosphokinase expression, and cell proliferation in human duodenum," *The American Journal of Clinical Nutrition*, vol. 93, no. 6, pp. 1255–1262, 2011.
- [30] I. Marafini, S. Sedda, V. Dinallo, and G. Monteleone, "Inflammatory cytokines: from discoveries to therapies in IBD," *Expert Opinion on Biological Therapy*, vol. 19, no. 11, pp. 1207–1217, 2019.
- [31] D. S. Shouval, A. Biswas, Y. H. Kang et al., "Interleukin 1 β Mediates Intestinal Inflammation in Mice and Patients With Interleukin 10 Receptor Deficiency," *Gastroenterology*, vol. 151, no. 6, pp. 1100–1104, 2016.

- [32] J. M. Lanis, E. E. Alexeev, V. F. Curtis et al., "Tryptophan metabolite activation of the aryl hydrocarbon receptor regulates IL-10 receptor expression on intestinal epithelia," *Mucosal Immunology*, vol. 10, no. 5, pp. 1133–1144, 2017.
- [33] R. B. Sartor and G. D. Wu, "Roles for intestinal bacteria, viruses, and fungi in pathogenesis of inflammatory bowel diseases and therapeutic approaches," *Gastroenterology*, vol. 152, no. 2, pp. 327–339.e4, 2017.
- [34] S. Chen, P. Bin, W. Ren et al., "Alpha-ketoglutarate (AKG) lowers body weight and affects intestinal innate immunity through influencing intestinal microbiota," *Oncotarget*, vol. 8, no. 24, pp. 38184–38192, 2017.
- [35] S. Chen, W. K. Ren, P. Bin et al., "Alpha-ketoglutarate lowers body weight and affects intestinal immunity through intestinal microbiota," *Amino Acids*, vol. 47, no. 8, pp. 1642–1642, 2015.
- [36] V. M. Koistinen, O. Kärkkäinen, K. Borewicz et al., "Contribution of gut microbiota to metabolism of dietary glycine betaine in mice and in vitro colonic fermentation," *Microbiome*, vol. 7, no. 1, p. 103, 2019.
- [37] A. Hayashi, T. Sato, N. Kamada et al., "A single strain of *Clostridium butyricum* induces intestinal IL-10-producing macrophages to suppress acute experimental colitis in mice," *Cell Host & Microbe*, vol. 13, no. 6, pp. 711–722, 2013.

Research Article

Higher Serum Neuropeptide Y Levels Are Associated with Metabolically Unhealthy Obesity in Obese Chinese Adults: A Cross-Sectional Study

Hao-Neng Tang ^{1,2}, Fen Xiao,¹ Ya-Ru Chen,¹ Si-Qi Zhuang,² Yue Guo,¹ Hui-Xuan Wu,¹ and Hou-De Zhou ¹

¹Department of Metabolism and Endocrinology, Hunan Provincial Key Laboratory for Metabolic Bone Diseases, National Clinical Research Center for Metabolic Diseases, The Second Xiangya Hospital of Central South University, Changsha, Hunan 410011, China

²Department of Laboratory Medicine, The Second Xiangya Hospital of Central South University, Changsha, Hunan 410011, China

Correspondence should be addressed to Hou-De Zhou; houdezhou@csu.edu.cn

Received 18 June 2020; Accepted 23 July 2020; Published 4 August 2020

Guest Editor: Hongmei Jiang

Copyright © 2020 Hao-Neng Tang et al. This is an open access article distributed under the Creative Commons Attribution License, which permits unrestricted use, distribution, and reproduction in any medium, provided the original work is properly cited.

Objective. Neuropeptide Y (NPY), an orexigenic peptide known to cause hyperphagia, has been involved in the occurrence and development of obesity. However, differences in the distribution of serum NPY levels in obese phenotypes (including metabolically unhealthy obesity (MUO) phenotype and metabolically healthy obesity (MHO) phenotype) and the association of NPY with MUO phenotype have not been unequivocally established. We therefore determined associations of serum NPY levels with MUO phenotype in obese Chinese adults. **Methods.** A cross-sectional study was conducted from 400 obese adults in Hunan province, who underwent a health examination in the Second Xiangya Hospital, and 164 participants were finally enrolled in the study and divided into MHO and MUO groups. Serum NPY levels were examined; univariate and multivariate analyses as well as smooth curve fitting analyses were conducted to measure the association of NPY serum levels with the MUO phenotype. **Results.** Serum NPY levels were significantly elevated in the MUO group compared with the MHO group ((667.69 ± 292.90) pg/mL vs. (478.89 ± 145.53) pg/mL, $p < 0.001$). A threshold and nonlinear association between serum NPY levels and MUO was found ($p = 0.001$). When serum NPY levels exceeded the turning point (471.5 pg/mL), each 10 pg/mL increment in the NPY serum level was significantly associated with an 18% increased odds ratio of MUO phenotype (OR: 1.18, 95% CI: 1.07–1.29, $p = 0.0007$) after adjusted for confounders. **Conclusions.** Higher NPY serum levels were positively correlated with MUO phenotype in obese Chinese adults.

1. Introduction

Obesity is a multifactorial and chronic disease mainly caused by excess energy intake, which has caused a major global public health problem [1–3]. Life expectancy is expected to decrease as the obesity prevalence rates soar [4, 5]. More importantly, obesity typically develops because of small but long-term changes in energy balance, which causes a series of energy metabolism disorders [2]. Hence, obesity may increase the risk of premature death because of the significantly increased risk for hypertension, type 2 diabetes mellitus (T2DM), cardio-cerebrovascular diseases, and some cancers [2, 5, 6].

However, metabolic disorders are not necessarily triggered when body mass index (BMI) reaches a level indicating overweight or obesity [7, 8]. Hence, it makes sense to distinguish obese individuals with metabolic disorders from those who are metabolically healthy [5]. Obesity has two major phenotypes depending on whether it is accompanied by metabolic abnormalities. Metabolically healthy obesity (MHO) refers to an obesity phenotype with little or no metabolic abnormalities [2], while the metabolically unhealthy obesity (MUO) phenotype has at least two or more concomitant metabolic disorders [9]. There is increasing evidence that patients with MUO are more prone to have cardiovascular events than those with MHO, but the MHO phenotype is

still more likely to develop MUO phenotype than healthy people with normal weight [1, 7–9]. Thus, it is vital to identify further metabolic abnormalities in people with obesity and to explore additional risk factors.

Neuropeptide Y (NPY), one of the most powerful orexiogenic peptides, is produced in large amounts in the arcuate and dorsal medial nucleus of the hypothalamus, as well as in peripheral adipose tissue [10–12]. Excess release of NPY can lead to overeating causing excessive energy intake, subsequently precipitating a series of damaging effects resulting in diabetes, heart disease, and other illnesses [11, 13]. Our previous study [14] and other studies have found that NPY regulates fat metabolism by promoting adipocyte differentiation [15, 16], inhibiting lipolysis [17], and suppressing the beiging in white adipose tissue [18]. Overexpression of NPY in mice has been reported to cause the obesity phenotype and insulin resistance, leading to a series of metabolic disorders [19], while the use of NPY antagonists has been found to reduce obesity and metabolic imbalances in fat tissue associated with aging [17]. Therefore, NPY has an important relationship with the occurrence and development of obesity and its related complications.

Many obesity models were characterized by an increase in central nervous system NPY tone, which lead to overeating and obesity [20]. However, NPY is also involved in the development of metabolic disorders without causing overeating in mouse models [21]. Although several studies have reported the contributions of NPY to obesity [22, 23] and T2DM [24], none of them have assessed the specific effects of NPY serum levels on obesity in distinct metabolic conditions. Furthermore, research on differences in NPY levels between various obesity phenotypes has not been published.

Given that neuropeptide Y is a key orexiogenic peptide affecting on obesity, we hypothesized that high serum NPY level is an essential risk factor for the MUO phenotype, and the main purpose of the present study was to investigate differences in NPY serum levels between individuals with various obesity phenotypes and to analyze the specific association of NPY with MUO.

2. Materials and Methods

2.1. Study Subjects. A cross-sectional study was performed with 400 obese participants (aged 19 to 78 years) who were screened based on their body mass index (BMI, $\text{BMI} \geq 25.0 \text{ kg/m}^2$) [25], which was measured during a physical examination between November 2018 and February 2019 in the Second Xiangya Hospital of Central South University in China. All participants have signed informed consent form. The study was approved by the ethics committee of the Second Xiangya Hospital of Central South University (Clinicaltrials.gov ID: ChiCTR-EOC-16010194).

The major exclusion criteria in this study included (1) cancer, hematologic disease, organic heart disease, autoimmune disease, hyperthyroidism, Cushing syndrome, hyperparathyroidism, infection, history of myocardial infarction and stroke, history of tuberculosis, chronic alcohol abuse, pregnancy, and lactation; (2) diseases that may cause abnormal levels of NPY, such as psychiatric disorders and epilepsy;

(3) subjects with unqualified specimens (e.g., hemolysis); and (4) missing data on anthropometric data and metabolic components. The sample size was estimated based on confidence level ($1-\alpha$), power of test (β), tolerance (δ), and sample standard deviation (s) [26]. To estimate the sample size, a preliminary pilot study was conducted for measuring the serum NPY levels in 40 obese participants, and the sample SD was 179.6 pg/mL. Since the confidence level was 0.95, and the tolerance was 5%, a sample size of 152 individuals was estimated based on these parameters. In this study, 164 participants were eventually included based on all exclusion criteria ($n = 236$). These obese subjects were subsequently classified as two subgroups based on the presence/absence of metabolic abnormalities. Nonobese ATP III criteria [27] of components of metabolic syndrome was used for identification of metabolic abnormalities ($\text{TG} \geq 1.7 \text{ mmol/L}$, $\text{HDL-C} < 1.04 \text{ mmol/L}$ in men, $\text{HDL-C} < 1.29 \text{ mmol/L}$ in women, $\text{FBS} > 5.6 \text{ mmol/L}$, and $\text{SBP/DBP} > 130/85 \text{ mmHg}$) [28]. The presence of ≥ 2 ATP III components of metabolic syndrome in participants was defined as MUO ($n = 93$), and the presence of ≤ 1 component was defined as MHO ($n = 71$) [2, 9].

2.2. Data Collection. The anthropometric data that were collected mainly included BMI, waist circumference (WC), and waist hip rate (WHR). Systolic and diastolic blood pressure (SBP, DBP) were measured with the participant in a seated position and resting state.

All blood samples were obtained at 8 am after fasting for 10–12 hours and centrifuged at 3,000g for 5 min to separate the serum. Serum levels of triglycerides (TG), total cholesterol (TC), high-density lipoprotein cholesterol (HDL-C), low-density lipoprotein cholesterol (LDL-C), nonesterified fatty acid (NEFA), fasting blood sugar (FBS), and whole blood levels of HbA1c were tested in the Department of Laboratory Medicine of the Second Xiangya Hospital, using routine diagnostic tests [29]. Serum NPY levels (CEA879Hu 96T, CLOUD-CLONE CORP, USA) were measured with specific enzyme-linked immunosorbent assays (ELISA) with an intra-assay error $< 10\%$ and an interassay error $< 12\%$.

2.3. Statistical Analysis. We described characteristics of the subjects using means and standard deviations (SD) for normally distributed variables, median and interquartile range (IQR) for nonnormally distributed variables, and percentages for categorical variables. Independent samples t -test, Mann-Whitney U test, and χ^2 test were used for comparison of normally, nonnormally distributed continuous variables, and categorical variables, respectively. Spearman's correlation coefficient was performed for evaluating the relationship of NPY with clinic-metabolic parameters.

Univariate analyses and multiple logistic regression were used to determine the association between NPY serum levels and MUO phenotype. We began with an unadjusted model and then added some confounders defined as covariates based on their clinical implication and significance in univariate analysis ($p < 0.15$). NPY serum levels were further treated as both continuous variables in increments of 10 pg/mL and categorical variables in quartiles in all models. p values for trend were also obtained by coding NPY level categories (quartiles)

TABLE 1: Baseline characteristics of the study participants ($N = 164$).

Characteristic	All ($n = 164$)	Obesity		p^*
		MHO ($n = 71$)	MUO ($n = 93$)	
Age (years)	44.53 (14.04)	39.94 (13.09)	48.03 (13.78)	<0.001
Sex				0.488
Male	120 (73.0%)	50 (70.4%)	70 (75.3%)	
Female	44 (27.0%)	21 (29.6%)	23 (24.7%)	
BMI (kg/m^2)	28.11 (2.51)	27.78(2.38)	28.50 (2.46)	0.061
WC (cm)	92.15 (6.80)	89.23 (4.50)	94.39 (7.41)	<0.001
WHR	0.94 (0.06)	0.93 (0.06)	0.96 (0.06)	0.003
SBP (mmHg)	133.24 (18.66)	121.68 (12.17)	142.06 (17.96)	<0.001
DBP (mmHg)	81.66 (11.90)	75.08 (8.76)	86.69 (11.56)	<0.001
TG (mmol/L)	1.67 (1.12-2.78)	1.19 (0.90-1.37)	2.35 (1.73-3.33)	<0.001
TC (mmol/L)	4.83 (1.13)	4.49 (0.70)	5.09 (1.32)	<0.001
HDL-C (mmol/L)	1.18 (0.30)	1.32 (0.24)	1.08 (0.31)	<0.001
LDL-C (mmol/L)	2.88 (0.93)	2.63 (0.65)	3.07 (1.05)	<0.001
FBS (mmol/L)	5.45 (5.05-7.14)	5.08 (4.78-5.29)	6.46 (5.54-9.18)	<0.001
NEFA (mmol/L)	0.49 (0.25)	0.45 (0.15)	0.51 (0.29)	0.174
HbA1C (%)	5.60 (5.30-6.67)	5.30 (5.10-5.50)	6.40 (5.60-7.90)	<0.001
NPY(pg/mL)	585.95 (257.93)	478.89 (145.53)	667.69(292.90)	<0.001

Data were reported as the mean (SD) or median (IQR: Q1-Q3). *The t -test or Mann-Whitney U test or χ^2 test was used for comparisons between MHO group and MUO group.

MHO: metabolically healthy obese; MUO: metabolically unhealthy obese; WC: waist circumference; WHR: waist to hip measurement ratio; BMI: body mass index; SBP: systolic blood pressure; DBP: diastolic blood pressure; FBS: fasting blood sugar; TG: triglycerides; TC: total cholesterol; HDL-C: high-density lipoprotein-cholesterol; LDL-C: low-density lipoprotein-cholesterol; NEFA: nonesterified fatty acids.

as ordinal variables in the regression models. Stratified analyses and interaction analyses were further performed by gender (male, female), age (<45 years, ≥ 45 years), and BMI ($25\text{--}28 \text{ kg}/\text{m}^2$, $\geq 28 \text{ kg}/\text{m}^2$) to confirm the relationship between NPY serum levels and the MUO phenotype in the obese participants.

To explore the potential nonlinear association between NPY and MUO phenotype, smooth curve fitting analysis and a piecewise linear regression model were performed to further examine the threshold effect of NPY on MUO. All analyses were performed using Empower (R) [30]. All tests were based on a two-tailed p value of less than 0.05 as evidence of statistical significance.

3. Results

3.1. Clinical and Laboratory Characteristics of the Participants.

This analysis included 164 participants (44.53 ± 14.04 years, 73% men) of whom 43.3% and 56.7% had MHO and MUO, respectively. The baseline data of the participants were presented in Table 1. A significant difference in age was found between MHO and MUO groups, with the mean age (1 SD) of the MHO group was 39.94 (13.09) years and 48.03 (13.78) years for the MUO group. There was no significant difference in gender composition between the MHO group and MUO group, and males made up the larger percentage of both groups (70.4% of the MHO group and 75.3% of the MUO group). Compared with the MHO group, participants in the MUO group had higher WC, SBP, DBP, TG, LDL-C, TC, FBS, and HbA1c levels and lower HDL-C levels (all $p < 0.05$).

As for NPY serum levels, the trend in the distribution of the expression of NPY was similar to that of the major metabolic indicators (i.e., TG, TC, FBS, SBP, DBP, and LDL-C) between these two groups. Serum NPY level was significantly increased in MUO group compared with MHO group (667.69 (292.90) pg/mL vs. 478.89 (145.53) pg/mL, $p < 0.001$).

3.2. Univariate and Multivariate Regression Analyses of MUO's Association with Serum NPY Levels.

We first conducted univariate analyses to analyze the relationship between MUO and each variable. As shown in Table 2, positive associations were found between MUO and BMI, WC, WHR, SBP, DBP, TG, TC, LDL-C, FBS, HbA1c, and LDL-C (all $p < 0.05$), whereas a negative association was observed between MUO and HDL-C ($p < 0.001$).

Multivariate regression analyses were then conducted to analyze the specific association of serum NPY levels with MUO (Table 3). The association of NPY with MUO was measured by the odds ratio (OR). Our results showed that per 10 pg/mL increment in NPY was associated with higher risk of MUO (OR: 1.06, 95% CI: 1.03–1.08, $p < 0.0001$) in the linear modeling before adjusting for confounders (model 1). After adjusted for sex, age, BMI, WC, WHR, TC, LDL-C, and HbA1c (model 4), higher level of NPY was still independently associated with MUO (OR: 1.07, 95% CI: 1.03–1.12, $p = 0.001$).

We also observed evidence of a dose-response trend across NPY quartiles (p for trend < 0.0001) in all the models. The ORs for MUO were significantly higher in the upper

TABLE 2: Univariate analysis of variables of the participants with MUO.

Variable	OR (95% CI)	<i>p</i>
Age (years)	1.05 (1.02–1.07)	0.0004
Sex		
Male	1.0	
Female	0.78 (0.39–1.57)	0.4881
BMI (kg/m ²)	1.18 (1.02–1.35)	0.0234
WC (cm)	1.16 (1.09–1.24)	<0.0001
WHR (per 1SD)	1.64 (1.16–2.30)	0.0048
SBP (mmHg)	1.10 (1.06–1.13)	<0.0001
DBP (mmHg)	1.12 (1.08–1.16)	<0.0001
TG (mmol/L)	5.30 (2.93–9.61)	<0.0001
TC (mmol/L)	1.69 (1.24–2.32)	0.0011
HDL-C (mmol/L)	0.04 (0.01–0.15)	<0.0001
LDL-C (mmol/L)	1.77 (1.22–2.58)	0.0029
FBS (mmol/L)	11.81 (4.54–30.69)	<0.0001
NEFA (mmol/L)	4.18 (0.48–36.23)	0.1940
HbA1c (per 1%)	51.80 (11.37–235.97)	<0.0001
NPY(per 10 pg/mL)	1.06 (1.03–1.08)	<0.0001

ORs are given per year increase in age, for male vs. female, per 1 SD in WHR, per 1% in HbA1c, per 10 pg/mL in NPY, and per 1 unit in the other parameters (i.e., BMI, WC, SBP, DBP, TG, TC, HDL, LDL, FBS, and NEFA) with 95% CIs.

quartile of serum NPY levels than in the lower quartile. The third and fourth quartiles of NPY levels were associated with a 1.75 (OR: 2.75, 95% CI: 1.12–6.78, $p = 0.0278$) and 18.92 (OR: 19.92, 95% CI: 5.86–67.71, $p < 0.0001$) times higher risk of MUO compared with the first quartile in the crude model (model 1), respectively. In the analyses adjusted for sex, age, BMI, WC, and WHR (model 3), the ORs were gradually increased for MUO; the third and fourth quartiles of NPY levels were associated with a 4.41 (OR: 5.41, 95% CI: 1.15–25.39, $p = 0.0324$) and 37.99 (OR: 38.99, 95% CI: 6.18–246.01, $p < 0.0001$) times higher risk of MUO compared with the first quartile. After further adjusting for TC, LDL-C, and HbA1c (model 4), we observed that the fourth quartile of NPY was significantly positively associated with the MUO (OR: 29.85, 95% CI: 4.38–203.62, $p = 0.0005$).

Further stratified analyses and interaction analyses were conducted by sex, age, and BMI (Table 4). A gender difference and age difference were observed in the association between NPY and MUO. The level of NPY being positively associated with MUO in the male sample ($p = 0.0039$) and in participants with age ≤ 45 years ($p = 0.0041$), but the association was insignificant in the female sample ($p = 0.1906$) and in participants with age > 45 years ($p = 0.1603$). At different BMIs, NPY levels showed a positive association with MUO (25–28 kg/m², $p = 0.0166$; ≥ 28 kg/m², $p = 0.0078$). An interaction analysis revealed that the variables, i.e., age (≤ 40 years vs. > 40 years; p for the interaction = 0.4595), gender (p for the interaction = 0.3303), and BMI (25–28 vs. ≥ 28 kg/m²; p for the interaction = 0.5591), significantly modified the association between the serum NPY levels and MUO.

3.3. Analysis of the Nonlinear Relationship between NPY and MUO. After we analyzed the association between the MUO phenotype and NPY level using multivariable linear regression and found the results of quartile equidistant variables were not entirely linearly distributed, we considered whether a nonlinear relationship might exist between NPY serum levels and MUO.

Therefore, we performed smooth curve fitting after adjusted for sex, age, BMI, WC, WHR, TC, LDL-C, and HbA1c. A generalized additive model was used, and a threshold and nonlinear association was found between serum NPY levels and MUO ($p = 0.0001$, Figure 1). Threshold saturation effects were further analyzed, and the data showed that the inflection point was 471.5 pg/mL (Table 5). Specifically, no significant relationship was found between MUO and NPY when the serum NPY level was before the turning point (OR: 1, 95% CI: 0.90–1.11, $p = 0.9920$). When serum NPY level was above the inflection point, each 10 pg/mL increment in the NPY level was significantly correlated with an 18% increased OR of the MUO phenotype (OR: 1.18, 95% CI: 1.07–1.29, $p = 0.0007$).

Finally, the specific correlation between NPY and clinic-metabolic indicators in MUO population was analyzed. The results showed that NPY serum level was significantly positively correlated with TG level, but not significantly correlated with other indexes (Table S1).

4. Discussion

Our study showed the serum NPY level was remarkably higher in participants with MUO than in those with MHO. NPY was identified as a significant risk factor for MUO in this study's sample of Chinese participants who were obese. We also found a threshold effect based on the serum NPY level, and the risk of MUO associated with NPY increased significantly when the NPY serum level exceeded the threshold. To our knowledge, this may be the first epidemiologic study to provide evidence for a nonlinear relationship between NPY and MUO.

Obesity can increase the risk of some chronic diseases [1, 6, 31], and increasing number of researches have found that NPY contributes to the occurrence and development of obesity and its associated metabolic diseases through its role in the central stimulation of appetite and the regulation of peripheral fat metabolism [13, 17, 20, 21]. Several studies also have reported a link between NPY and obesity. Nyström et al. [32] found that plasma NPY levels were positively correlated with TC and LDL-C serum levels in women and that NPY may be a possible gender-specific cardiovascular risk marker. Karvonen et al. [22] reported a link between cholesterol metabolism and NPY. Ilhan et al. [24] reported that T2DM patients had increased serum NPY levels, which positively correlated with insulin levels. Several studies also showed [23, 33] that the NPY rs16147 genotype could influence changes in abdominal adiposity in overweight or obese participants with dietary interventions. However, the obese populations involved in these studies were not stratified further. Based on the combination of metabolic abnormalities in

TABLE 3: Multivariate analysis of the association of serum NPY levels with MUO.

Exposure	Model 1		Model 2		Model 3		Model 4	
	OR (95% CI)	<i>p</i>	OR (95% CI)	<i>p</i>	OR (95% CI)	<i>p</i>	OR (95% CI)	<i>p</i>
NPY levels								
Per 10 pg/mL increment	1.06 (1.03-1.08)	<0.0001	1.06 (1.03-1.08)	<0.0001	1.08 (1.04-1.12)	0.0003	1.07 (1.03-1.12)	0.0010
Quartile 1	1.0		1.0		1.0		1.0	
Quartile 2	2.05 (0.84-5.04)	0.1171	2.35 (0.90-6.14)	0.0822	3.11 (0.70-13.73)	0.1346	2.44 (0.51-11.58)	0.2628
Quartile 3	2.75 (1.12-6.78)	0.0278	2.91 (1.11-7.59)	0.0292	5.41 (1.15-25.39)	0.0324	3.93 (0.77-20.07)	0.0994
Quartile 4	19.92 (5.86-67.71)	<0.0001	22.55 (6.29-80.87)	<0.0001	38.99 (6.18-246.01)	<0.0001	29.85 (4.38-203.62)	0.0005
<i>p</i> trend	<0.0001		<0.0001		<0.0001		<0.0001	

Model 1 was unadjusted; model 2 was adjusted for sex and age; model 3 was adjusted for model 2 plus BMI, WC, and WHR; and model 4 was adjusted for model 3 plus TC, LDL-C, and HbA1c. Quartile 1: 189.32–460.89 pg/mL, quartile 2: 460.89–559.45 pg/mL, quartile 3: 559.45–659.34 pg/mL, and quartile 4: 659.34–2097.09 pg/mL.

TABLE 4: Effect size of NPY on MUO in subgroups.

Characteristic	Effect size (95% CI)	<i>p</i>	<i>p</i> for interaction
Sex			0.3303
Male	1.09 (1.03–1.16)	0.0039	
Female	1.05 (0.98–1.12)	0.1906	
Age (years)			0.4595
≤45	1.09 (1.03–1.15)	0.0041	
>45	1.05 (0.98–1.13)	0.1603	
BMI (kg/m ²)			0.5591
25–28	1.06 (1.01–1.12)	0.0166	
≥28	1.09 (1.02–1.16)	0.0078	

The effect size of association was quantified by OR and 95% CI. Adjusted for sex, age, BMI, WC, WHR, TC, LDL-C, and HbA1c except the subgroup variable.

obese individuals, obesity can be divided into MHO phenotype and MUO phenotype [5, 9].

There were significant differences between the two phenotypes in anthropometric and biochemical parameters, as shown in our study. Among these obese participants, MUO were more likely to be old compared to MHO, coincident with the research by Vasim et al. [34]. What's more, the risk of cardiovascular events among the MUO population is significantly higher than in the MHO population [1]. As for this orexigenic peptide, it is not clear whether these two obese phenotypes in these studies had the same NPY concentrations as no data on NPY serum levels were reported for individuals with MHO and MUO. In the current study, we found increased serum NPY levels in MUO participants, which was partly consistent with the previous reports of elevated NPY levels in T2DM patients [24]. As obesity-related metabolic abnormalities include not only glucose metabolic disorders but also dyslipidemia and hypertension, our results further support the positive association between NPY and metabolic disturbances reported in the existing research literature [24]. As far as our findings are concerned, although the specific mechanism remains unclear, there may be several plausible explanations for the observation elevated in serum NPY levels in the MUO participants.

First, high levels of NPY could lead to hyperphagia, which has been reported to cause a variety of metabolic diseases, such as hyperlipidemia and T2DM. Blood NPY might also come from the NPY stored in the sympathetic ganglion of the digestive tract, as ingestion stimulates the release of NPY into the blood [35]. Chronic hyperlipidemia, in turn, leads to the proliferation of NPY-containing nerve fibers in the digestive tract, leading to an increase in NPY synthesis [36]. Therefore, serum NPY synthesis can be elevated in obese participants with hyperlipidemia. Second, NPY can be secreted by adipocytes located in visceral adipose tissue and increased by insulin stimulation [12, 37]. Adipose-derived NPY can impair the insulin sensitivity of adipocytes [38] and increase the circulating levels of NPY in obese patients [39]. Short-term injections of NPY into the lateral ventricle of mice have been reported to increase their levels of insulin; specifically, the NPY inhibited endogenous glucose and induced insulin resistance [40], while the effect of diabetes-induced appetite enhancement was attenuated afterwards in NPY-targeted knockout mice [41].

The stratified analysis showed a distinct positive association between NPY levels and being male in the MUO sample. Given that Zahorska-Markiewicz et al. [42] reported lower NPY plasma concentrations among women with extreme obesity (BMI = 38.3 ± 4.4) compared with healthy subjects, there might be gender differences in terms of the relationship between NPY and obesity. It is worth noting that a possible reason for the weak association with being female in our study may be the relatively small proportion of the female participants. The *p* value of the later interaction analysis was not significant, indicating that the results of the different stratifications were consistent, and the results of the present study were reliable.

We conducted further multivariate regression to analyze the specific association between NPY and MUO. Our data showed that serum NPY levels were strongly associated with MUO, whether in the form of a continuous variable or a classified variable, after adjusting for the related confounders. Surprisingly, the present study showed a possible nonlinear relationship between serum NPY levels and MUO phenotype for the first time, by smooth curve fitting analysis. We found that NPY did not necessarily have a significant positive

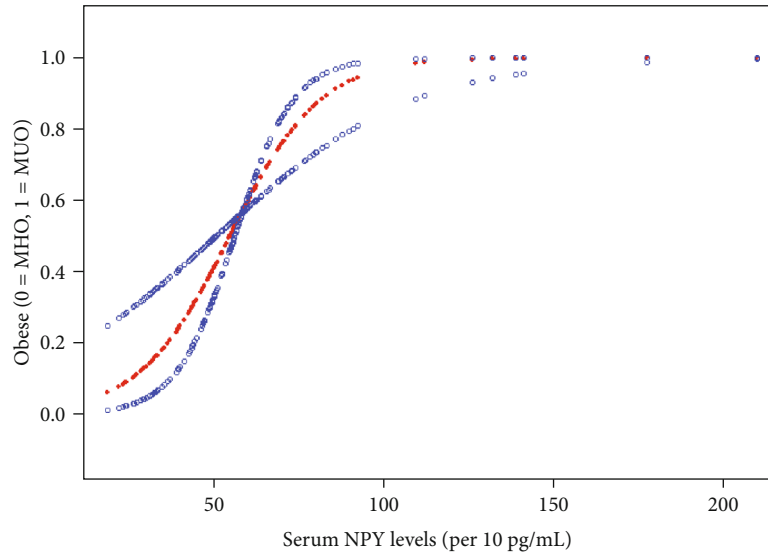


FIGURE 1: The curved lines illustrate the relationship between the serum NPY levels and MUO. A threshold and nonlinear association between serum NPY levels (per 10 pg/mL increment) and MUO was found ($p = 0.001$). The area between the two dotted lines represents the 95% CI. The blue bands represent the 95% CI for the smoothed curve fit, and the red line represents the smoothed curve fit between the variables. The model was adjusted for sex, age, BMI, WC, WHR, TC, LDL-C, and HbA1c.

TABLE 5: Analysis of the threshold effect of NPY on MUO.

Inflection point of NPY (per 10 pg/mL increment)	Effect size (OR)	95% CI	p
<471.5	1.00	(0.90–1.11)	0.9920
≥ 471.5	1.18	(1.07–1.29)	0.0007

The associated effect size was quantified by OR and 95% CI. Adjusted for sex, age, BMI, WC, WHR, TC, LDL-C, and HbA1c.

association with MUO. Only when its serum level exceeded the inflection point (471.5 pg/mL) was the increased NPY level associated with a higher risk of MUO. In other words, a high level of NPY in MHO individuals may predict the risk of subsequent metabolic disorders, such as glucose metabolism dysfunction, hyperlipidemia, and hypertension. Our previous studies found that different NPY levels had a distinct role in the proliferation and differentiation of adipocytes, and only at high concentrations can NPY promote lipid droplet synthesis and adipogenesis [13]. Therefore, from the clinical point of view, the data of our study confirmed the important value of NPY concentration segmentation.

We also analyzed the correlation between NPY level and metabolic indexes in MUO obese people. Our results showed that TG was the only index that positively correlated with NPY, which were partly consistent with the previous studies showing that NPY signal can regulate TG release, and injection of NPY into the central nervous system can increase both serum TG level and liver TG level [20, 43]. The regulatory effect of NPY on TG release may be related to the activities of enzymes involved in phospholipid synthesis, and this process is controlled by the sympathetic nerve of the liver [43]. Therefore, we speculated that the expression of phospholipid synthesis-related enzymes in MUO population may be significantly higher than that in MHO population, which needs to be further confirmed in future study.

The highlight of the present study was the stratification of obesity based on its related metabolic disorders in the analysis of NPY levels in obese participants. Compared with the goal of achieving a normal weight by losing a lot of weight, moderate weight loss might be a short-term and more achievable goal for obese individuals, as it is sufficient for the transition from the MUO phenotype to the MHO phenotype [1]. Obesity and its related metabolic abnormalities are closely related to dietary intake and the resulting energy imbalance, which is largely regulated by NPY [10]. Therefore, the analysis of the distribution of serum NPY expression in MHO and MUO participants can directly reflect the correlation between this orexigenic peptide and MUO; our data additionally underscore the potential involvement of NPY in the pathogenesis of metabolic disorders related to obesity. Furthermore, multivariate analysis and smooth curve fitting helped us find a threshold effect in the relationship between NPY and MUO phenotype. As far as we know, research on the relationship between MUO and the distinct levels of NPY has not been conducted until now. NPY serum levels in obese subjects with MHO phenotype were relatively lower than those with MUO phenotype, but it had exceeded the inflection point (471.5 pg/mL) that was first observed in this study. Since the NPY level at this level was positively associated with the MUO risk, our results provide new evidence on the view that people with MHO are still at risk for developing MUO [1, 6, 7]. A higher NPY level in participants with the MHO phenotype might serve as marker indicating a risk of occurrence of MUO in the future.

There were several limitations of the study that merit mention. First, the defining criteria for MHO are not uniform worldwide [9]; hence, the results of our present study may differ from other studies depending on variations in the defining criteria used. Second, we did not collect data on body fat distribution for some reason, which has been found

to be closely associated with obesity. Third, the participants in this study were mainly from Hunan province, so the conclusion can be mainly applicable to population in southern China, while may not be fully applicable to population in other parts of China such as northern China and western China. Additionally, we cannot draw a causal conclusion that increased NPY serum levels promote MUO development in obese Chinese adults in present study, thus, it may be meaningful and necessary to conduct a prospective research in the future. Finally, it was worth mentioning that NPY exerts biological effects via its receptors and the most well-known being NPY-Y1, NPY-Y2, and NPY-Y5 receptors which are involved in obesity [44, 45]. Since these receptors were highly distributed in the hypothalamus and peripheral tissues [44, 45], we will detect their serum levels in the future study.

5. Conclusions

In conclusion, the present study suggests that there are significant differences in serum NPY levels in obese participants with different metabolic conditions, and there is a significant association between serum NPY level and MUO. We found a nonlinear relationship between the MUO phenotype and serum NPY levels in the sample of obese Chinese adults, and higher serum NPY levels were positively associated with metabolic abnormalities in these obese individuals.

Abbreviations

NPY:	Neuropeptide Y
MHO:	Metabolically healthy obesity
MUO:	Metabolically unhealthy obesity
T2DM:	Type 2 diabetes mellitus
BMI:	Body mass index
WC:	Waist circumference
WHR:	Waist to hip measurement ratio
SBP:	Systolic blood pressure
DBP:	Diastolic blood pressure
FBS:	Fasting blood sugar
TG:	Triglyceride
TC:	Total cholesterol
HDL-C:	High-density lipoprotein cholesterol
LDL-C:	Low-density lipoprotein cholesterol
NEFA:	Nonesterified fatty acid
IQR:	Interquartile range
OR:	Odds ratio
CI:	Confidence interval.

Data Availability

The raw data supporting the conclusions of this study will be made available by the authors.

Conflicts of Interest

The authors declare no conflicts of interest.

Authors' Contributions

H.N.T. and H.D.Z. are responsible for the conceptualization of this manuscript; H.N.T., F.X., and H.X.W. are for the formal analysis; H.N.T., Y.R.C., Y.G., and S.Q.Z. for the methodology; H.N.T., Y.R.C., and H.X.W. for the software; F.X., Y.R.C., and Y.G. for the investigation; H.N.T. for the writing—original draft preparation; H.N.T., Y.R.C., Y.G., H.X.W., S.Q.Z., and H.D.Z. for the writing—review and editing; H.N.T. and H.D.Z. for the project administration; and H.N.T., Y.G., and H.D.Z. for funding acquisition. All authors have revised and approved the submitted manuscript.

Acknowledgments

We gratefully thank Dr. Xinglin Chen from the Department of Epidemiology and Biostatistics and X & Y Solutions Inc. in Boston, Massachusetts, for her contributions to the statistical analyses. We also would like to thank the native English speaking scientists of Elixigen Company (Huntington Beach, California) for editing our manuscript. This work was supported by the National Natural Scientific Foundation of China (Grant numbers 81600666, 81770880, 81970762, and 81800788), the Hunan Provincial Lifting Plan (Grant number 2017TJ-Q14), and the Hunan Provincial Science & Technology Department (Grant numbers 2018SK2134, 2017TP1006, and 2018SK52511).

Supplementary Materials

Table S1: correlations of clinical parameters and metabolism indexes with NPY levels in obese subjects with MUO phenotype. (*Supplementary Materials*)

References

- [1] N. Stefan, H. U. Häring, and M. B. Schulze, "Metabolically healthy obesity: the low-hanging fruit in obesity treatment?," *The Lancet Diabetes and Endocrinology*, vol. 6, no. 3, pp. 249–258, 2018.
- [2] F. Magkos, "Metabolically healthy obesity: what's in a name?," *The American Journal of Clinical Nutrition*, vol. 110, no. 3, pp. 533–539, 2019.
- [3] G. A. Bray, D. H. Frühbeck Gema Ryan, and W. JPH, "Management of obesity," *The Lancet*, vol. 387, pp. 1947–1956, 2016.
- [4] S. J. Olshansky, D. J. Passaro, R. C. Hershow et al., "A potential decline in life expectancy in the United States in the 21st century," *The New England Journal of Medicine*, vol. 352, no. 11, pp. 1138–1145, 2005.
- [5] M. Blüher, "The distinction of metabolically 'healthy' from 'unhealthy' obese individuals," *Current Opinion in Lipidology*, vol. 21, no. 1, pp. 38–43, 2010.
- [6] Q. P. Guo, F. N. Li, Y. H. Duan et al., "Oxidative stress, nutritional antioxidants and beyond," *Life Sciences*, vol. 63, no. 6, pp. 866–874, 2020.
- [7] D. Samocho-Bonet, V. D. Dixit, C. R. Kahn et al., "Metabolically healthy and unhealthy obese: the 2013 Stock Conference report," *Obesity Reviews*, vol. 15, no. 9, pp. 697–708, 2014.

- [8] N. Stefan, F. Schick, and H. U. Häring, "Causes, characteristics, and consequences of metabolically unhealthy normal weight in humans," *Cell Metabolism*, vol. 26, no. 2, pp. 292–300, 2017.
- [9] L. L. Roberson, E. C. Aneni, W. Maziak et al., "Beyond BMI: the "metabolically healthy obese" phenotype & its association with clinical/subclinical cardiovascular disease and all-cause mortality – a systematic review," *BMC Public Health*, vol. 14, no. 1, p. 14, 2014.
- [10] N. Erondu, I. Gantz, B. Musser et al., "Neuropeptide Y5 receptor antagonism does not induce clinically meaningful weight loss in overweight and obese adults," *Cell Metabolism*, vol. 4, no. 4, pp. 275–282, 2006.
- [11] S. P. Kalra and P. S. Kalra, "NPY and cohorts in regulating appetite, obesity and metabolic syndrome: beneficial effects of gene therapy," *Neuropeptides*, vol. 38, no. 4, pp. 201–211, 2004.
- [12] K. Yang, H. Guan, E. Arany, D. J. Hill, and X. Cao, "Neuropeptide Y is produced in visceral adipose tissue and promotes proliferation of adipocyte precursor cells via the Y1 receptor," *The FASEB Journal*, vol. 22, no. 7, pp. 2452–2464, 2008.
- [13] R. Saraf, F. Mahmood, R. Amir, and R. Matyal, "Neuropeptide Y is an angiogenic factor in cardiovascular regeneration," *European Journal of Pharmacology*, vol. 776, pp. 64–70, 2016.
- [14] H. N. Tang, X. F. Man, Y. Q. Liu et al., "Dose-dependent effects of neuropeptide Y on the regulation of preadipocyte proliferation and adipocyte lipid synthesis via the PPAR γ pathways," *Endocrine Journal*, vol. 62, no. 9, pp. 835–846, 2015.
- [15] L. E. Kuo, J. B. Kitlinska, J. U. Tilan et al., "Neuropeptide Y acts directly in the periphery on fat tissue and mediates stress-induced obesity and metabolic syndrome," *Nature Medicine*, vol. 13, no. 7, pp. 803–811, 2007.
- [16] J. Rosmaninho-Salgado, V. Cortez, M. Estrada et al., "Intracellular mechanisms coupled to NPY Y2 and Y5 receptor activation and lipid accumulation in murine adipocytes," *Neuropeptides*, vol. 46, no. 6, pp. 359–366, 2012.
- [17] S. Park, C. Fujishita, T. Komatsu et al., "NPY antagonism reduces adiposity and attenuates age-related imbalance of adipose tissue metabolism," *The FASEB Journal*, vol. 28, no. 12, pp. 5337–5348, 2014.
- [18] P. T. Chao, L. Yang, S. Aja, T. H. Moran, and S. Bi, "Knock-down of NPY expression in the dorsomedial hypothalamus promotes development of brown adipocytes and prevents diet-induced obesity," *Cell Metabolism*, vol. 13, no. 5, pp. 573–583, 2011.
- [19] L. H. Vähätalo, S. T. Ruohonen, S. Mäkelä et al., "Neuropeptide Y in the noradrenergic neurones induces obesity and inhibits sympathetic tone in mice," *Acta Physiologica (Oxford, England)*, vol. 213, no. 4, pp. 902–919, 2015.
- [20] J. M. Rojas, J. M. Stafford, S. Saadat, R. L. Printz, A. G. Beck-Sickingler, and K. D. Niswender, "Central nervous system neuropeptide Y signaling via the Y1 receptor partially dissociates feeding behavior from lipoprotein metabolism in lean rats," *American Journal of Physiology. Endocrinology and Metabolism*, vol. 303, no. 12, pp. E1479–E1488, 2012.
- [21] L. Ailanen, S. T. Ruohonen, L. H. Vähätalo et al., "The metabolic syndrome in mice overexpressing neuropeptide Y in noradrenergic neurons," *The Journal of Endocrinology*, vol. 234, no. 1, pp. 57–72, 2017.
- [22] M. K. Karvonen, U. Pesonen, M. Koulu et al., "Association of a leucine(7)-to-proline(7) polymorphism in the signal peptide of neuropeptide Y with high serum cholesterol and LDL cholesterol levels," *Nature Medicine*, vol. 4, no. 12, pp. 1434–1437, 1998.
- [23] X. Lin, Q. Qi, Y. Zheng et al., "Neuropeptide Y genotype, central obesity, and abdominal fat distribution: the POUNDS LOST trial," *The American Journal of Clinical Nutrition*, vol. 102, no. 2, pp. 514–519, 2015.
- [24] A. Ilhan, S. Rasul, A. Dimitrov et al., "Plasma neuropeptide Y levels differ in distinct diabetic conditions," *Neuropeptides*, vol. 44, no. 6, pp. 485–489, 2010.
- [25] World Health Organization Regional Office for the Western Pacific Region, International Association for the Study of Obesity, International Obesity Task Force, *The Asian-Pacific perspective: redefining obesity and its treatment*, Health Communications Australia, Sydney, 2000.
- [26] H. Ren, L. Zhang, Z. Liu, X. Zhou, and G. Yuan, "Sleep duration and apolipoprotein B in metabolically healthy and unhealthy overweight/obese phenotypes: a cross-sectional study in Chinese adults," *BMJ Open*, vol. 9, no. 2, article e023817, 2019.
- [27] T. F. Teixeira, R. D. Alves, A. P. B. Moreira, and M. C. G. Peluzio, "Main characteristics of metabolically obese normal weight and metabolically healthy obese phenotypes," *Nutrition Reviews*, vol. 73, no. 3, pp. 175–190, 2015.
- [28] S. M. Camhi and P. T. Katzmarzyk, "Differences in body composition between metabolically healthy obese and metabolically abnormal obese adults," *International Journal of Obesity*, vol. 38, no. 8, pp. 1142–1145, 2014.
- [29] H. N. Tang, C. Y. Tang, X. F. Man et al., "Plasticity of adipose tissue in response to fasting and refeeding in male mice," *Nutrition & Metabolism*, vol. 14, no. 1, p. 3, 2017.
- [30] G. P. Guan, S. J. Ding, Y. L. Yin, V. Duraipandiyani, N. A. al-Dhabi, and G. Liu, "Macleaya cordata extract alleviated oxidative stress and altered innate immune response in mice challenged with enterotoxigenic *Escherichia coli*," *Science China. Life Sciences*, vol. 62, no. 8, pp. 1019–1027, 2019.
- [31] W. J. Tang, J. Wu, S. S. Jin et al., "Glutamate and aspartate alleviate testicular/epididymal oxidative stress by supporting antioxidant enzymes and immune defense systems in boars," *Science China. Life Sciences*, vol. 63, no. 1, pp. 116–124, 2020.
- [32] F. Nyström, P. Nilsson, A. G. Olsson, B. E. Karlberg, and K. P. Öhman, "A population study of plasma neuropeptide Y: correlations with components of the metabolic syndrome," *Blood Pressure*, vol. 5, pp. 349–353, 1996.
- [33] X. Zhang, Q. Qi, J. Liang, F. B. Hu, F. M. Sacks, and L. Qi, "Neuropeptide Y promoter polymorphism modifies effects of a weight-loss diet on 2-year changes of blood pressure: the preventing overweight using novel dietary strategies trial," *Hypertension*, vol. 60, no. 5, pp. 1169–1175, 2012.
- [34] I. Vasim, M. I. Ahmad, M. Mongraw-Chaffin, and E. Z. Soliman, "Association of obesity phenotypes with electrocardiographic subclinical myocardial injury in the general population," *Clinical Cardiology*, vol. 42, no. 3, pp. 373–378, 2019.
- [35] M. J. Morris, H. S. Cox, G. W. Lambert et al., "Region-specific neuropeptide Y overflows at rest and during sympathetic activation in humans," *Hypertension*, vol. 29, no. 1, pp. 137–143, 1997.
- [36] A. L. Stewart-Lee and G. Burnstock, "Changes in vasoconstrictor and vasodilator responses of the basilar artery during maturation in the Watanabe heritable hyperlipidemic rabbit differ from those in the New Zealand White rabbit," *Arteriosclerosis and Thrombosis*, vol. 11, no. 5, pp. 1147–1155, 1991.

- [37] K. Kos, A. L. Harte, S. James et al., "Secretion of neuropeptide Y in human adipose tissue and its role in maintenance of adipose tissue mass," *American Journal of Physiology. Endocrinology and Metabolism*, vol. 293, no. 5, pp. E1335–E1340, 2007.
- [38] M. T. Gericke, T. Schröder, J. Kosacka, M. Nowicki, N. Klötting, and K. Spaniel-Borowski, "Neuropeptide Y impairs insulin-stimulated translocation of glucose transporter 4 in 3T3-L1 adipocytes through the Y1 receptor," *Molecular and Cellular Endocrinology*, vol. 348, no. 1, pp. 27–32, 2012.
- [39] A. J. Kastin and V. Akerstrom, "Nonsaturable entry of neuropeptide Y into brain," *American Journal of Physiology. Endocrinology and Metabolism*, vol. 276, no. 3, pp. E479–E482, 1999.
- [40] A. M. van den Hoek, C. van Heijningen, J. P. Schröder-van der Elst et al., "Intracerebroventricular administration of neuropeptide Y induces hepatic insulin resistance via sympathetic innervation," *Diabetes*, vol. 57, no. 9, pp. 2304–2310, 2008.
- [41] D. K. Sindelar, P. Mystkowski, D. J. Marsh, R. D. Palmiter, and M. W. Schwartz, "Attenuation of diabetic hyperphagia in neuropeptide Y-deficient mice," *Diabetes*, vol. 51, no. 3, pp. 778–783, 2002.
- [42] B. Zahorska-Markiewicz, E. Obuchowicz, M. Waluga, E. Tkacz, and Z. S. Herman, "Neuropeptide Y in obese women during treatment with adrenergic modulation drugs," *Medical Science Monitor*, vol. 7, no. 3, pp. 403–408, 2001.
- [43] J. M. Rojas, E. Bruinstroop, R. L. Printz et al., "Central nervous system neuropeptide Y regulates mediators of hepatic phospholipid remodeling and very low-density lipoprotein triglyceride secretion via sympathetic innervation," *Molecular Metabolism*, vol. 4, no. 3, pp. 210–221, 2015.
- [44] W. Zhang, M. A. Cline, and E. R. Gilbert, "Hypothalamus-adipose tissue crosstalk: neuropeptide Y and the regulation of energy metabolism," *Nutrition & Metabolism*, vol. 11, no. 1, p. 27, 2014.
- [45] W. W. Sun, P. Zhu, Y. C. Shi et al., "Current views on neuropeptide Y and diabetes-related atherosclerosis," *Diabetes & Vascular Disease Research*, vol. 14, no. 4, pp. 277–284, 2017.

Research Article

Comprehensive Analysis of a circRNA-miRNA-mRNA Network to Reveal Potential Inflammation-Related Targets for Gastric Adenocarcinoma

YunXia Liu ^{1,2}, YeFeng Xu ^{1,2}, Feng Xiao,³ JianFeng Zhang,³ YiQing Wang,^{1,2} YongWei Yao,^{1,2} and JieWen Yang^{1,2}

¹Department of Oncology, Hangzhou Third Hospital, Hangzhou, Zhejiang, China

²Affiliated Hangzhou Clinical College, Anhui Medical University, Hangzhou, Zhejiang, China

³Zhejiang Chinese Medical University, Hangzhou, Zhejiang, China

Correspondence should be addressed to YunXia Liu; zjhzylyx@163.com

Received 24 April 2020; Accepted 28 May 2020; Published 1 August 2020

Guest Editor: Xiaolu Jin

Copyright © 2020 YunXia Liu et al. This is an open access article distributed under the Creative Commons Attribution License, which permits unrestricted use, distribution, and reproduction in any medium, provided the original work is properly cited.

Gastric cancer (GC) is the most common malignancy of the stomach. This study was aimed at elucidating the regulatory network of circRNA-miRNA-mRNA and identifying the precise inflammation-related targets in GC. The expression profiles of GSE83521, GSE78091, and GSE33651 were obtained from the GEO database. Interactions between miRNAs and circRNAs were investigated by the Circular RNA Interactome, and targets of miRNAs were predicted with miRTarBase. Then, a circRNA/miRNA/mRNA regulatory network was constructed. Also, functional enrichment analysis of selected differentially expressed genes (DEGs) was performed. The inflammation-/GC-related targets were collected in the GeneCards and GenLIP3 database, respectively. And a protein-protein interaction (PPI) network of DE mRNAs was constructed with STRING and Cytoscape to identify hub genes. The genetic alterations, neighboring gene networks, expression levels, and the poor prognosis of hub genes were investigated in cBioPortal, Oncomine, and Human Protein Atlas databases and Kaplan-Meier plotter, respectively. A total of 10 DE miRNAs and 33 DEGs were identified. The regulatory network contained 26 circRNAs, 10 miRNAs, and 1459 mRNAs. Functional enrichment analysis revealed that the selected 33 DEGs were involved in negative regulation of fat cell differentiation, response to wounding, extracellular matrix- (ECM-) receptor interaction, and regulation of cell growth pathways. THBS1, FN1, CALM1, COL4A1, CTGF, and IGFBP5 were selected as inflammation-related hub genes of GC in the PPI network. The genetic alterations in these hub genes were related to amplification and missense mutations. Furthermore, the genes RYR2, ERBB2, PI3KCA, and HELZ2 were connected to hub genes in this study. The hub gene levels in clinical specimens were markedly upregulated in GC tissues and correlated with poor overall survival (OS). Our results suggest that THBS1, FN1, CALM1, COL4A1, CTGF, and IGFBP5 were associated with the pathogenesis of gastric carcinogenesis and may serve as biomarkers and inflammation-related targets for GC.

1. Introduction

Gastric cancer (GC) is one of the most common gastrointestinal malignancies in the clinic; in 2015, 1,313,000 people were diagnosed with GC, and 813,000 people died from it [1–9]. GC displays high heterogeneity with respect to histopathological and epidemiological characteristics [1, 10] and can be divided into proximal nondiffuse, diffuse, and distal nondiffuse subtypes [1, 11]. Gastric adenocarcinoma (GA)

is the primary pathological type associated with environmental factors, including a high-salt diet, infectious agents, and smoking, and this form of GC is characterized by ease of invasion and metastasis and a very low early diagnosis rate [5, 12]. Despite the tremendous efforts that have been paid in the diagnosis of GC, together with improvements in surgical techniques and targeted chemotherapy in recent years, the prognosis of patients with GC remains unsatisfactory due to the prevalence of diagnosis of the disease at advanced

stages that are often accompanied by lymphatic metastasis, which limits successful therapeutic strategies [7]. Additionally, cancer-related systemic inflammation is recognized as a flag sign of cancer-related cachexia development and progression, which results in an inappropriate systemic reaction, including fevers, weight loss, and sweats [13]. Therefore, further exploration of appropriate molecular biomarkers for early diagnosis and identification of potential inflammation-related targets of GC are urgently needed to expand the promising strategies to enhance the therapeutic efficacy and clinical prognosis in patients with GA.

Circular RNA (circRNA) is a novel type of endogenous, noncoding RNA, which is also widely expressed in different species and has been demonstrated to belong to a class of RNAs with tissue-/developmental-stage specificity, making them potential diagnostic and prognostic biomarkers [3, 14]. MicroRNAs (miRNAs) are a special type of small noncoding RNAs comprising approximately 21 nucleotides that bind to the 3'-untranslated regions (3'-UTRs) of target messenger RNAs (mRNAs) and leading to mRNA degradation or blocking of translation, which contribute to the central regulation of cell proliferation, differentiation, and apoptosis [9, 15, 16]. Recent studies have revealed that the abundance and evolutionary conservation of circRNAs play significant effects in regulating cancer progression-related processes such as metastasis, apoptosis, and invasion and that circRNAs primarily function as miRNA sponges, thereby relieving miRNA-mediated target repression. For instance, circRNA-ZFR serves as a sponge of miR-130a/miR-107 and modulates PTEN expression, resulting in the suppression of GC cell proliferation and the promotion of apoptosis [17]. Another report by Zhang et al. showed that circRNA-LARP4 inhibits cell proliferation and invasion in GC by sequestering miR-424-5p and regulating LATS1 expression [18]. Besides, it has been reported that knockdown of ciRS-133 reduced cancer cachexia by activating PRDM16 and suppressing miR-133 in tumor-implanted mice [19]. Although several circRNAs have been identified to participate in the pathogenesis of GC, it is still necessary to conduct a more comprehensive analysis of circRNA-miRNA-mRNA regulatory networks and to identify potential inflammation-related targets in GC.

In this study, we performed an integrated analysis of circRNA expression profiles in GC from the Gene Expression Omnibus (GEO) database. miRNAs and mRNAs from GEO datasets were employed to distinguish the circRNA-related dysregulated miRNAs and the miRNA-related dysregulated mRNAs, and then, a circRNA/miRNA/mRNA network was constructed to elucidate the relationships among differentially expressed (DE) circRNAs, miRNAs, and mRNAs. >GO (Gene Ontology) and KEGG (Kyoto Encyclopedia of Genes and Genomes) pathway enrichment analysis revealed the potential biological functions of selected miRNA target genes (DEGs). Besides, the inflammation-/GC-related targets were collected in the GeneCards and GenLiP3 database, respectively. Then, a PPI network of the selected DE mRNAs was constructed to identify the inflammation-related hub genes based on the value of the overall degree, node betweenness, and closeness through network topology calculations. Furthermore, genetic

alterations and neighboring gene networks were investigated by cBioPortal, and the expression transcriptional level of hub genes was explored using OncoPrint databases with subsequent validation using the Human Protein Atlas. Finally, survival analysis of hub genes was performed using the Kaplan-Meier plotter. These findings may enable us to identify novel diagnostic or prognostic biomarkers and suggested that THBS1, FN1, CALM1, COL4A1, CTGF, and IGFBP5 might be inflammation-related candidate targets for GC. The workflow of the current study is shown in Figure 1.

2. Materials and Methods

2.1. Microarray Data. We chose the circRNA expression profile GSE83521, the miRNA expression profile GSE78091, and the mRNA expression profile GSE33651 from the GEO (<http://www.ncbi.nlm.nih.gov/gds/>) database. GSE83521, which was based on Agilent GPL19978 (Agilent-069978 Arraystar Human CircRNA Microarray V1), includes 6 tumors and 6 adjacent normal mucosal tissues. GSE78091, which was based on Agilent GPL21439 (miRCURY LNA microRNA Array), includes 3 cancer tissues and 3 normal gastric mucosal tissues. The GSE33651 based on the platform of GPL2895 (Agilent, USA), including 40 gastric tumor tissue samples and 12 normal gastric tissue samples.

2.2. Data Processing. The raw data of microarray datasets were preprocessed via background correction and normalization. The box plot is a convenient way to quickly visualize the distribution of data, and we used box plots to examine and compare the distributions of expression profiles of samples after normalization. Hierarchical clustering, the most widely used clustering technique, allows us to observe the relationships between samples, and we performed a cluster analysis based on "All Targets Value-CircRNAs" in this study. DE circRNAs, miRNAs, and mRNAs were identified using GEO2R (<https://www.ncbi.nlm.nih.gov/geo/geo2r/>), an interactive online tool that permits users to compare two or more groups of samples to find out genes that are DE across experimental conditions [20]. $|\log_2(\text{fold change (FC)})| \geq 2.0$ and P value < 0.05 were used as the threshold criteria for the DE circRNAs, miRNAs, and mRNAs.

2.3. Construction of the circRNA-miRNA-mRNA Regulatory Network. DE circRNAs contain corresponding miRNA-binding sites and act as miRNA sponges. To further explore this connection, we predicted the interactions between the miRNAs and circRNAs by using the Circular RNA Interactome (<http://circinteractome.nia.nih.gov>) database [21]. Then, the circRNA-related miRNAs and DE miRNAs were intersected. miRNAs play important roles in a variety of diseases and regulate the expression of oncogenes and tumor suppressors. The regulatory relationships between miRNAs and mRNA were predicted using the miRTarBase database (<http://miRTarBase.mbc.nctu.edu.tw/>) [22]. Subsequently, the miRNA-related mRNAs and the DE mRNAs were also intersected to identify the selected DEGs by using Venny 2.1 (<https://bioinfogp.cnb.csic.es/tools/venny/index.html>). Finally, the DE circRNAs, predicted miRNAs, and mRNAs

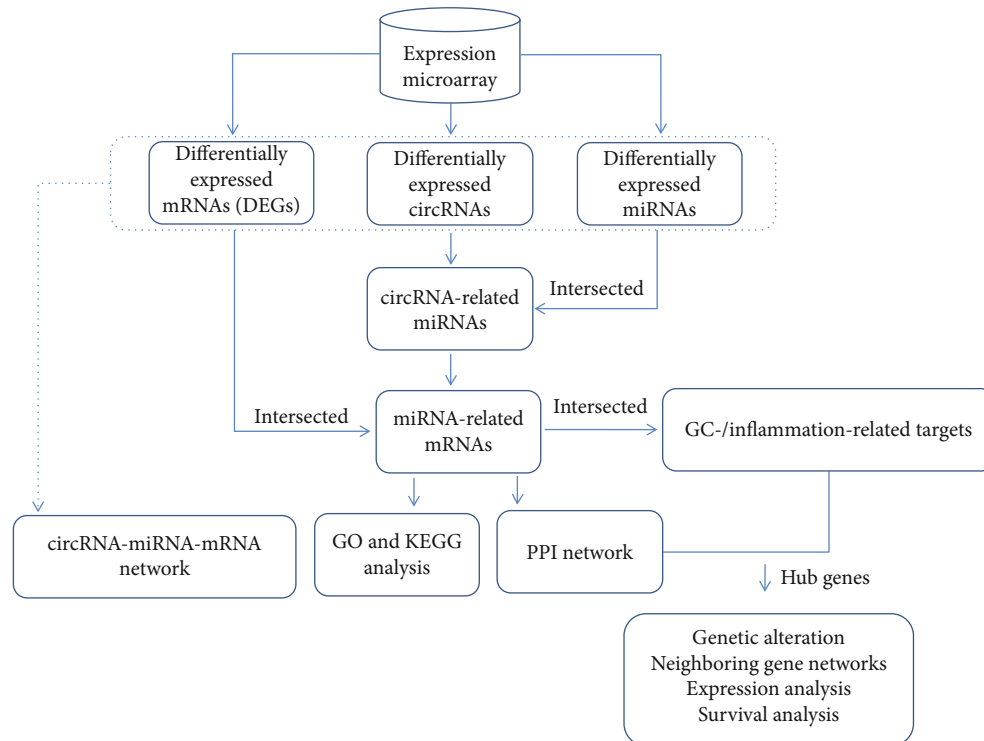


FIGURE 1: Workflow for the identification and analysis of hub genes in gastric adenocarcinoma.

were added in a circRNA/miRNA/mRNA network. Moreover, the regulatory network was visualized with Cytoscape 3.4.0 (<http://cytoscape.org>).

2.4. Functional Enrichment Analysis. GO and KEGG pathway enrichment analysis of selected DEGs was carried out using the DAVID (<http://www.david.abcc.ncifcrf.gov/>) database. GO terms (biological processes, cellular components, and molecular functions) and KEGG pathways with $P < 0.05$ were further analyzed. The enriched GO terms of selected DEGs were ranked by the enrichment scores ($-\log_{10}(P \text{ value})$).

2.5. Identification of GC and Inflammation-Related Targets. The GC-related targets and inflammation-related targets were collected from the GeneCards (<https://www.genecards.org/>) [23] and GenCLiP 3 database (<http://ci.smu.edu.cn/genclip3/analysis.php>), respectively. GenCLiP 3, a web server, is enhancing the analysis of human gene functions and regulatory networks from PubMed based on cooccurrences and natural language processing [24]. In brief, the keywords “inflammation” and “gastric cancer” were used in the GeneCards and GenCLiP 3 database to search for GC-/inflammation-related targets, respectively. Next, the inflammation-related targets of GC were analyzed with Draw Venn Diagrams (<http://bioinformatics.psb.ugent.be/webtools/Venn/>).

2.6. PPI Network and Hub Gene Identification. The associations of the selected DEGs were analyzed using STRING (<http://string-db.org/>) [25], which provides both predicted and experimental PPI interaction information, and a PPI net-

work was then constructed, which was visualized with Cytoscape software. Required confidence (combined score) ≥ 0.4 was used as the threshold criterion. Subsequently, to further analyze the more significant interactions of hub genes in the PPI network, we calculated the network topology of node degree, node betweenness, and closeness value using the Cytoscape plug-in Network Analyzer.

2.7. Exploring Cancer Genomics Data of Hub Genes Using cBioPortal. cBioPortal (<http://cbioportal.org>), an internet resource platform, is making complex cancer genomic profiles accessible to researchers and clinicians without the need for bioinformatics expertise [26, 27]. In the present study, we used cBioPortal to investigate candidate hub genes via stomach adenocarcinoma studies including 393 samples available in the database (The Cancer Genome Atlas (TCGA), Provisional). The results of the genomics datasets are shown through a concise and compact graphical summary of genomic alterations in multiple genes as heat maps, as well as multiple visualization networks of hub genes that are altered in cancer.

2.8. Oncomine Analysis and Validation. The publicly available online cancer microarray database Oncomine (<http://www.oncomine.com>), a collection of cancer microarray datasets with a comprehensive data-mining platform [28], can facilitate discovery from genome-wide expression analyses. Oncomine was chosen to explore the expression of hub genes in GC tissues compared with those in normal tissues. We chose to filter cancer vs. normal (analysis type), gastric adenocarcinoma (cancer type), clinical specimen (sample type),

and mRNA (data type) to investigate the clinical significance in GC. Derrico gastric datasets were selected because they were established based on mRNA levels and contain larger numbers of samples ($n > 50$). In Derrico datasets, the thresholds for significance were 2-fold change, P value = $1E-4$, and top 10% gene rank. The minimum, 10th, 25th, 75th, 90th, and maximum percentile data of each hub genes in both GC and normal tissues were plotted. Furthermore, the Human Protein Atlas (<http://www.proteinatlas.org>) was used to validate the immunohistochemistry of candidate hub genes. The direct links to these images in the Human Protein Atlas are as follows: <https://www.proteinatlas.org/ENSG00000137801-THBS1/tissue/stomach#img> (thrombospondin 1 (THBS1) in normal tissue); <https://www.proteinatlas.org/ENSG00000137801-THBS1/pathology/tissue/stomach+cancer#img> (THBS1 in tumor tissue); <https://www.proteinatlas.org/ENSG00000115414-FN1/tissue/stomach#img> (fibronectin 1 (FN1) in normal tissue); <https://www.proteinatlas.org/ENSG00000115414-FN1/pathology/tissue/stomach+cancer#img> (FN1 in tissue); <https://www.proteinatlas.org/ENSG00000198668-CALM1/tissue/stomach#img> (calmodulin-1 (CALM1) in normal tissue); <https://www.proteinatlas.org/ENSG00000198668-CALM1/pathology/tissue/stomach+cancer#img> (CALM1 in tumor tissue); <https://www.proteinatlas.org/ENSG00000187498-COL4A1/tissue/stomach#img> (collagen, type IV, alpha 1 (COL4A1) in normal tissue); <https://www.proteinatlas.org/ENSG00000187498-COL4A1/pathology/tissue/stomach+cancer#img> (COL4A1 in tumor tissue); <https://www.proteinatlas.org/ENSG00000118523-CTGF/tissue/stomach#img> (connective tissue growth factor (CTGF) in normal tissue); and <https://www.proteinatlas.org/ENSG00000118523-CTGF/pathology/tissue/stomach+cancer#img> (CTGF in tumor tissue).

2.9. Kaplan-Meier Plotter. The prognostic value of hub gene mRNA transcription level was measured using the Kaplan-Meier plotter (<http://www.kmplot.com>), an online open database that consists of gene expression profiles and survival information for 5,143 breast cancer, 1,816 ovarian cancer, 2,437 lung cancer, and 1,065 GC patients with mean follow-ups of 69, 40, 49, and 33 months, respectively. To evaluate the overall survival (OS) of patients with GC, we separated individuals into two groups based on median gene expression (high vs. low) and then validated their Kaplan-Meier survival curves. Hazard ratios (HRs) with 95% confidence intervals (CIs) and log-rank P values were calculated to evaluate the associations of gene expression with survival, and the number-at-risk values were displayed below the curves.

3. Results

3.1. Screening of DE circRNAs, miRNAs, and mRNA in GC. The circRNA expression profile of GSE83521 was deposited by Zhang Y from Southern Medical University, Nanfang Hospital. This dataset has 6 tumor tissue samples and 6 normal mucosal tissues. As shown in the box plot (Figure 2(a)), the median intensity values in different samples were almost similar after normalization, which showed optimal standardization. Next, the map showed the dissimilarity of circRNA

expression patterns among tissue samples (Figure 2(b)). And a total of 26 DE circRNAs were identified after the analysis of GSE83521 (Tables S1 and S2), of which 25 were upregulated and 1 was downregulated. A total of 151 DE miRNAs were detected for GSE78091 (Table S3), of which 148 were upregulated and 3 were downregulated. Furthermore, a total of 336 DE mRNAs were detected after the analysis of GSE33651 (Table S4), of which 254 were upregulated and 82 were downregulated.

3.2. Construction of the ceRNA Network. Increasing numbers of reports have shown that by acting as competing for endogenous RNAs (ceRNAs), circRNAs can compete with miRNAs to influence the stability of target mRNAs or their translation. In this study, 418 interactions were obtained between 26 DE circRNAs and 196 miRNAs (Table S5). Ten miRNAs were selected after the intersection of DE miRNAs and circRNA-related miRNAs (Figure 2(c)). The target genes of the 10 selected miRNAs were predicted using miRTarBase, and 1569 interactions were detected between these 10 selected miRNAs and 1459 miRNA-related mRNAs (Table S6). Then, thirty-three DEGs were screened after the intersection between DEGs and miRNA-related mRNAs (Figure 2(c)).

More importantly, a ceRNA network was established to uncover the connections between circRNAs, miRNAs, and mRNAs in this study. This network contained 401 circRNA-miRNA pairs and 1568 miRNA-mRNA pairs, including 26 circRNAs, 10 miRNAs, and 1459 mRNAs (Figure 3). Subsequently, the selected DEGs were analyzed with respect to their potential bioinformatics information.

3.3. Functional Enrichment Analysis of Selected DEGs. The selected 33 DEGs of the associated circRNAs were used to investigate the GO terms and KEGG pathways by using DAVID. In GO analysis, all enriched terms for the DEGs were ranked by enrichment score ($-\log_{10}(P \text{ value})$) as shown in Figure 4. The most significantly enriched GO term regarding molecular functions (Figure 4(a)) was fibronectin binding (GO:0001968, $P = 9.66E - 04$). The most significantly enriched GO terms with respect to cellular components (Figure 4(b)) were extracellular matrix (ECM) (GO:0031012, $P = 0.010291067$), fibrinogen complex (GO:0005577, $P = 0.013746239$), and nucleoplasm (GO:0005654, $P = 0.019723458$), and the top 3 most significantly enriched GO terms with respect to biological process (Figure 4(c)) were negative regulation of fat cell differentiation (GO:0045599, $P = 0.002060324$), response to wounding (GO:0009611, $P = 0.004577343$), and regulation of cell growth (GO:0001558, $P = 0.007282945$). Moreover, the ECM-receptor interaction pathway (hsa04512, $P = 0.011170014$) associated with the genes COL4A1, THBS1, and FN1 was represented as the most enriched pathway.

3.4. Analysis of the PPI Network. With the retrieving of the GeneCards and GenCLiP 3 database, we finally obtained a total of 15,784 and 16,027 genes related to GC and inflammation, respectively (Tables S7 and S8). After intersection with selected DEGs, we found that 9 DEGs may be associated

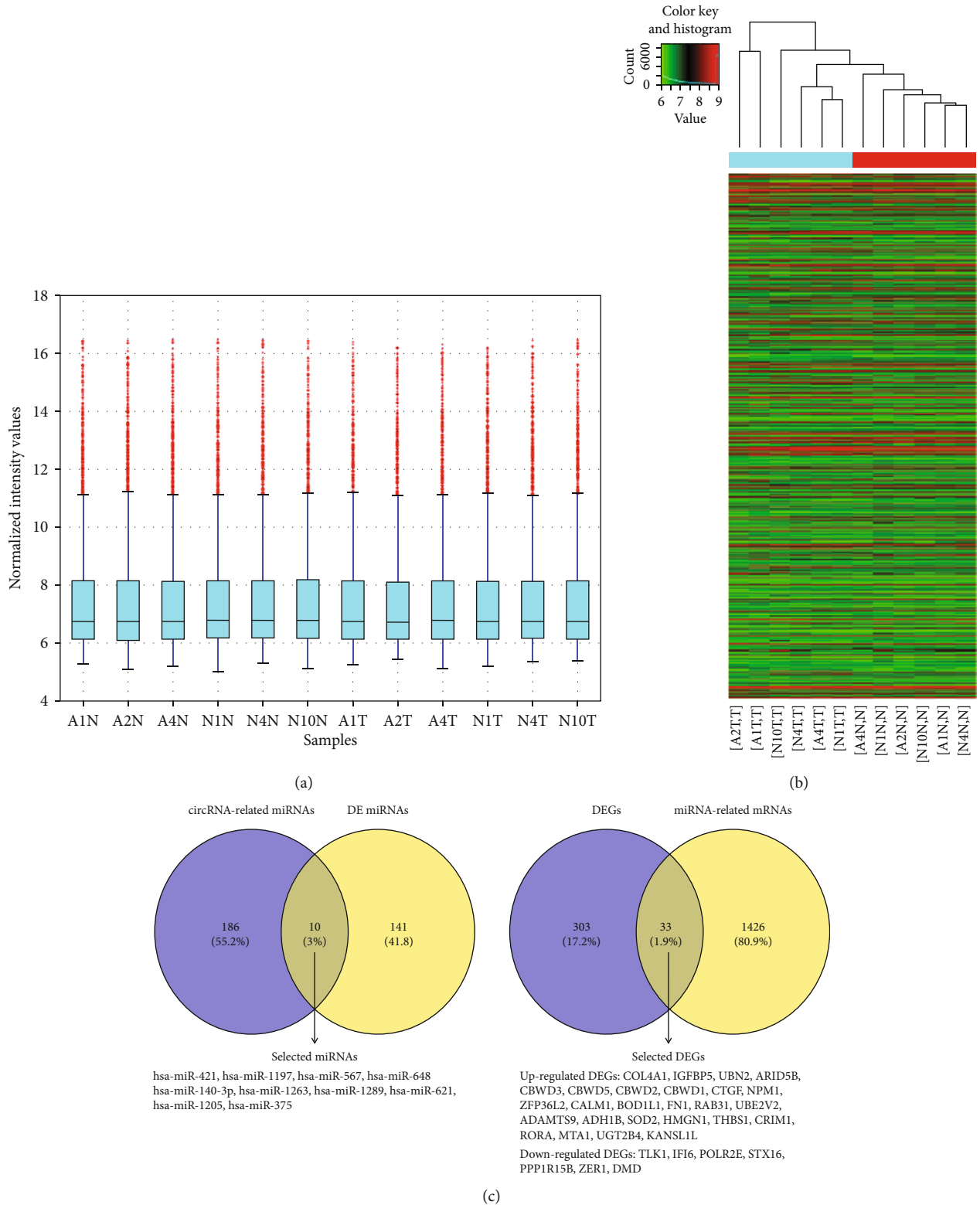


FIGURE 2: DE circRNAs in tumor tissues and adjacent normal tissues from GC patients, screening DE miRNAs and DE mRNAs, and visualization of the circRNA-miRNA-mRNA regulatory network. (a) The box plot shows variations in circRNA expression. (b) The heat map shows DE circRNAs in 6 tumors (T) and 6 normal (N) tissues. Gene expression profiles are shown in rows. “Red” suggests a high relative expression, and “green” indicates low relative expression. (c) Based on DE miRNAs and circRNA-related miRNAs, Venn diagrams were used to select the overlapping 10 miRNAs; based on DE mRNAs and miRNA-related mRNAs, Venn diagrams were used to select the overlapping 33 mRNAs.

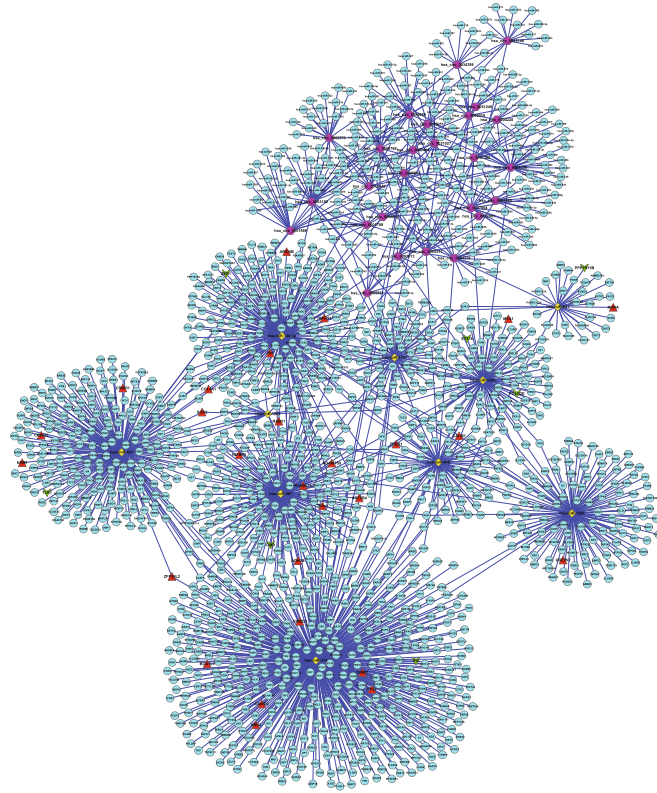


FIGURE 3: The circRNA-miRNA-mRNA regulatory network in GC. The circular nodes in blue represent mRNAs; the diamond-shaped nodes in yellow represent miRNAs, and the octagonal nodes in purple represent circRNAs. The triangular nodes in red indicate upregulated DE mRNAs, and the V nodes in green indicate downregulated DE mRNAs.

with the inflammation in the GC, including SOD2, FN1, THBS1, MTA1, NPM1, IGFBP5, COL4A1, RORA, and ADH1B (Figure 5(a)). To explore the relationships among the 33 selected DEGs, we constructed the PPI networks for genes using STRING and then visualized in Cytoscape. Degree denotes the numbers of proteins interacting with a specific protein, and a node with a high degree is deemed a hub node [29]. Hub genes are obtained by analyzing the connectivity degrees, betweenness, and closeness of the nodes in PPI networks. As presented in Figure 5(b), the genes UBN2, ARID5B, CBWD3, CBWD5, NPM1, ZFP36L2, BOD1L1, UBE2V2, CRIM1, RORA, MTA1, KANSL1L, TLK1, IFI6, PPP1R15B, and ZER1 with no interactions were removed in the STRING database. The obtained PPI networks consisted of 17 nodes and 14 edges, with 6 central node genes identified using $\text{degree} \geq 2$, and the most significant 6 node degree genes for subsequent study were THBS1 (degree = 5, closeness centrality = 1), FN1 (degree = 4, closeness centrality = 0.83), CALM1 (degree = 2, closeness centrality = 1), COL4A1 (degree = 2, closeness centrality = 0.625), CTGF (degree = 2, closeness centrality = 0.625), and insulin-like growth factor-binding protein 5 (IGFBP5, degree = 2, closeness centrality = 0.625).

3.5. Genetic Alterations in Hub Genes in GC. Combining the results of functional analysis, the aforementioned Venn Diagrams and PPI network indicated that THBS1, FN1, CALM1, COL4A1, CTGF, and IGFBP5 may play an important role in

GC as the inflammation-related targets. We further verified the genetic alterations in the selected 6 hub genes in GC patients by using the cBioPortal database. As illustrated in Figure 6, alterations ranging from 11.11% to 25.11% were found for the gene sets submitted for analysis (Figure 6(a)). cBioPortal complements existing tools, including TCGA. Multiple genetic alterations observed across each set of tumor samples from TCGA Data Portal are presented using OncoPrint to highlight the most pronounced genomic changes. The results showed that 96 cases (24%) had an alteration in at least one of the 6 queried genes. Most alterations in the THBS1 and FN1 genes were classified as missense mutations, along with a few cases of truncating mutations, amplifications, and deep deletions (Figure 6(b)). A majority of alterations in the COL4A1 gene occurred by amplification and missense mutations, with a few cases of partial missense mutations and deep deletions (Figure 6(b)). For the CALM1, CTGF, and IGFBP5 genes, missense mutations, truncating mutations, amplifications, and deep deletions occurred in select cases (Figure 6(b)).

The potential of complexity, as well as the variability of differences in interactions between hub genes in GC samples, was studied from TCGA Data Portal with multiple visualization networks generated. To identify potential interactive analysis in GC, we used THBS1, FN1, CALM1, COL4A1, CTGF, and IGFBP5 as core nodes for the network view and investigated the resulting altered networks of interest. cBioPortal was used to construct a network containing FN1,

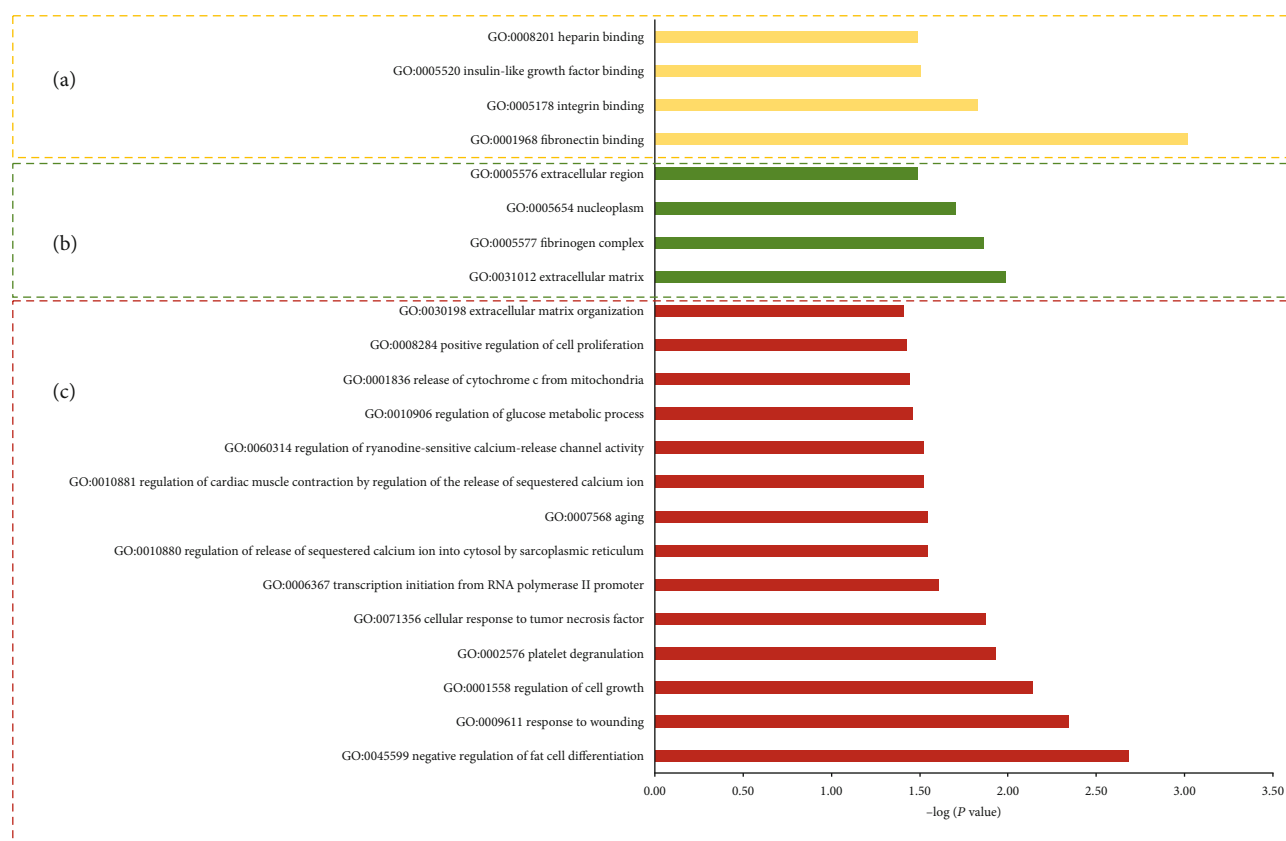


FIGURE 4: The GO term enrichment analysis on 33 selected DEGs in GC. (a) Thin yellow bars represent molecular function terms. (b) Green bars represent cell component terms. (c) Red bars represent biological processes.

CALM1, COL4A1, and CTGF in addition to THBS1 and IGFBP5 (Figure 7). The interactions between FN1 and COL4A1 were identified using a cutoff of $\geq 21.9\%$ alteration. The interactions between CALM1 and RYR2 hub genes were revealed using a cutoff of 21% alteration. ERBB2 and PIK3CA were observed with a cutoff of 18.5% alteration, and the interactions between CTGF and HELZ2 hub genes appeared when the cutoff was changed to 13% alteration (Figure 7). The results of interactive network analysis provide new perspectives on the role of hub genes, along with RYR2, ERBB2, PIK3CA, and HELZ2, with respect to the development of GC by querying multidimensional cancer genomics data in cBioPortal.

3.6. Expression and Validation of Hub Genes in GC. We also estimated the mRNA expression levels of the THBS1, FN1, CALM1, COL4A1, CTGF, and IGFBP5 in GC compared with those in normal tissues via the OncoPrint database. In Derrico datasets, which has 69 samples, the mRNA levels separated the GC cases in OncoPrint into intestinal, diffuse, and mixed types. As shown in Figure 8(a), THBS1, FN1, CALM1, COL4A1, CTGF, and IGFBP5 expression levels were markedly upregulated in mixed-type GC than in normal controls. Besides, the protein levels of these 5 genes (IGFBP5 is pending control and cancer tissue analysis) were observably higher in tumor tissues than in normal tissues,

according to the data obtained from the Human Protein Atlas (Figure 8(b)).

3.7. Survival Analysis. The Kaplan-Meier plotter was applied to predict the prognostic value of the 6 identified hub genes. According to the results, high expression levels of THBS1, FN1, CALM1, COL4A1, and IGFBP5 were closely related to the poor OS in GC patients ($P < 0.05$) (Figures 9(a)–9(e)). In contrast, low expression of CTGF was associated with poor OS in GC patients ($P < 0.05$, Figure 9(f)).

4. Discussion

GC still remains the commonest human malignancy in the world [30, 31]. Nevertheless, surgical resection is the only possible curative therapy for GC. In fact, approximately 60% of GC patients are diagnosed with metastatic and locally advanced, which results in poor prognosis due to deficiency of early detection and the loss of the opportunity for curative resection [30]. Additionally, inflammation has long been recognized to play a crucial role in the pathogenesis of cancer [13, 32]. Hence, the identification of novel diagnostic markers and inflammation-related targets and the elucidation of the underlying mechanisms of GC onset and progression have become major topics in GC research. In the current study, the circRNA expression profile GSE83521, the miRNA expression profile GSE78091, and the mRNA expression

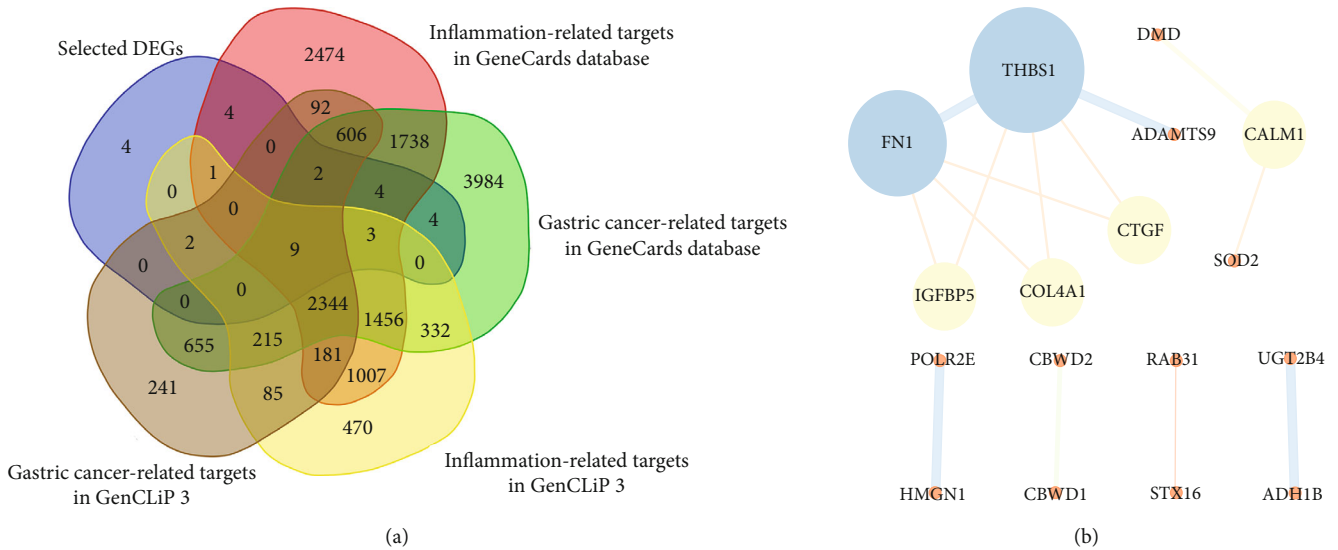


FIGURE 5: The identification of inflammation-related targets in GC by Venn diagram and PPI analysis: (a) Venn diagrams of the inflammation-related targets between the selected DEGs and the integrated GC-/inflammation-related targets in the GeneCards and GenCLiP 3 database; (b) the PPI network of 33 coexisting DEGs. Nodes represent genes, with the degree shown by the size and bright colors, and edges represent interactions between two genes, with the combined scores displayed by the size and bright colors.

profile GSE33651 were acquired from the GEO database to reanalyze DE circRNAs, miRNAs, and mRNAs between GC tissues and normal tissues using bioinformatics method to identify novel diagnostic markers and explore the inflammation-related targets for GC. In total, 26 DE circRNAs including 25 upregulated and 1 downregulated circRNAs, 151 DE miRNAs including 148 upregulated and 3 downregulated miRNAs, and 336 DE mRNAs including 254 upregulated and 82 downregulated mRNAs with $P < 0.05$ and $|\log_2 FC| \geq 2.0$ were screened; additionally, 33 DEGs were selected for further study after DE mRNA and miRNA-related mRNA intersection.

The results of functional enrichment analysis showed that the 33 DEGs were associated with the negative regulation of fat cell differentiation, response to wounding, and regulation of cell growth. Compared with the study by Gu et al. [3], which showed that the p53 signalling pathway and the Hippo signalling pathway were significantly enriched in GC, while the KEGG results indicated that the ECM-receptor interaction pathway might be involved in the development of GC in this study. Meanwhile, the results are consistent with the previous study [33]. The ECM-receptor interaction pathway has been identified in multiple cancers, and it includes “cell adhesion molecules (CAMs)” and “cell cycle” pathways [34]. Imbalances in these pathways lead to the detachment of cells from the ECM and thus enhanced metastasis, suggesting an essential role of this pathway in cancer biology [34].

circRNAs are a class of endogenous noncoding RNAs that primarily serve as miRNA sponges to regulate gene expression and are reported to play important roles in many malignant phenotypes, including the cell cycle, apoptosis, vascularization, invasion, and metastasis [35–38]. In addition, circRNAs may serve as a novel and stable biomarkers for the diagnosis of GC. Li et al. demonstrated that hsa_circ_002059, a typical

circRNA, is significantly downregulated in GC tissues compared with that in paired adjacent nontumor tissues, indicating its potential as a novel and stable biomarker for the diagnosis of GC [39]. Another study by Huang et al. found that the circRNA hsa_circ_0000745 can serve as a diagnostic marker for GC [40]. Gu et al. [3] also revealed that CCND2 might be regulated by hsa_circRNA_105039 and hsa_circRNA_104682 through hsa-miR-15a-5p. Compared with previous studies, we found that the hsa_circ_0001866/hsa_circ_0003192-hsa-miR-421-COL4A1, hsa_circ_0055521-hsa-miR-567-THBS1/IGFBP5, hsa_circ_0005217/hsa_circ_0004370-hsa-miR-648-THBS1/CALM1, hsa_circ_0007094/hsa_circ_0013048/hsa_circ_0008615/hsa_circ_0002570/hsa_circ_0001789-hsa-miR-140-3p-FN1, hsa_circ_0004339/hsa_circ_0007094/hsa_circ_0007613-hsa-miR-1205-THBS1, and hsa_circ_0007404/hsa_circ_0051246/hsa_circ_0045602/hsa_circ_0031027-hsa-miR-375-CTGF axes may play central roles in regulating the development of GC.

Further, the mechanisms underlying of the molecular targets in GC remains to be elucidated. In this study, THBS1, FN1, CALM1, COL4A1, CTGF, and IGFBP5 might be identified as the hub genes associated with inflammation in GC from the PPI network. We also identified missense mutations and amplifications as the primary genetic alterations. Additionally, survival analysis showed that high mRNA expression of THBS1, FN1, CALM1, COL4A1, and IGFBP5 was correlated with poor OS in GC patients; in contrast, high mRNA expression of CTGF was associated with poor OS in GC patients.

Thrombospondins are a family of homologous proteins that regulate cellular phenotypes and extracellular structures for tissue genesis and remodelling [41]. The first member to be identified, THBS1, is an extracellular glycoprotein that plays multifunctional roles in the cell-matrix and cell-cell interactions, angiogenesis, and tumor

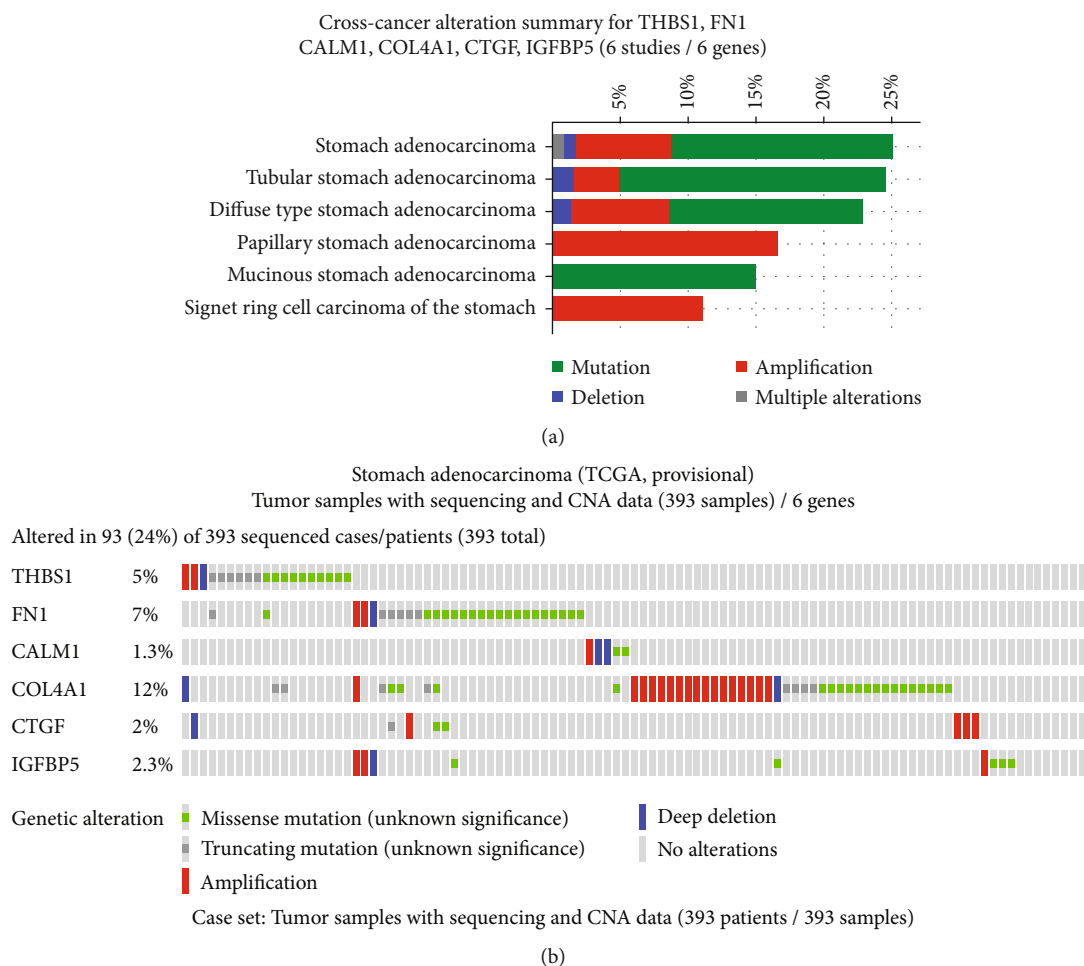


FIGURE 6: Exploring genetic alterations in THBS1, FN1, CALM1, COL4A1, CTGF, and IGFBP5 in GC by cBioPortal: (a) summary of changes within THBS1, FN1, CALM1, COL4A1, CTGF, and IGFBP5 genes in genomics datasets available for stomach adenocarcinoma (TCGA, Provisional) studies; (b) OncoPrint: a visual summary of alterations across a set of stomach adenocarcinoma samples (data are taken from TCGA Data Portal) based on a query of the 6 genes (THBS1, FN1, CALM1, COL4A1, CTGF, and IGFBP5). Distinct genomic alterations are summarized, color-coded, and presented as percent changes in particularly affected genes in individual tumor samples. Each row represents a gene, and each column represents a tumor sample. Green squares indicate missense mutations; black represents truncating mutations; red bars designate gene amplifications; blue bars represent deep deletions, and grey signifies no alterations.

progression [42–45]. THBS1 expression has been correlated with tumor angiogenesis, tumor growth, and metastasis [46]. In GC, THBS1 may play a proangiogenic and proinflammatory role due to its positive correlation with vascular endothelial growth factor (VEGF), and elevated THBS1 expression levels have been related to tumor growth and lymph node metastasis in GC [47, 48]. The function of THBS1 remains controversial, and increasing numbers of cellular assays have indicated a role for THBS1 in cell invasion and migration; nevertheless, conflicting results have been obtained in different cell types. Notably, the pleiotropic nature of THBS1, which is a multimodular and multifunctional protein, depends on environmental conditions. We noted that the expression of THBS1 was higher in cancer tissues than in adjacent normal tissues in Derrico gastric datasets from the OncoPrint database, which indicated that the results of the GSE33651 microarray were in agreement with the previous studies [43, 45].

FN1, a high molecular weight (~440 kDa) ECM cell-adhesive glycoprotein, is predominantly expressed in various cancer tissues but not in normal tissues [49] and involved in the ECM-receptor interaction, focal adhesion pathway, pathways in cancer, and the regulation of endothelial cell survival, proliferation, adhesion, migration, inflammation, and angiogenesis through the activation of the focal adhesion kinase (FAK) and downstream PI3K/Akt signalling pathways, as well as the activation of NF- κ B [50, 51]. Chen and Zheng and Zhang et al. reported that miRNA-200c binds to and inhibits the expression of FN1 to suppress the proliferation, migration, and invasion of GC cells [52, 53]. COL4A1, an essential component of the ECM that is also involved in the ECM-receptor interaction and focal adhesion pathway, has an essential role in angiogenesis, inflammation, and tumor progression [50]. Huang et al. demonstrated that COL4A1 is overexpressed in GC tissues and trastuzumab-resistant GC cells based on bioinformatics analysis [54], which is

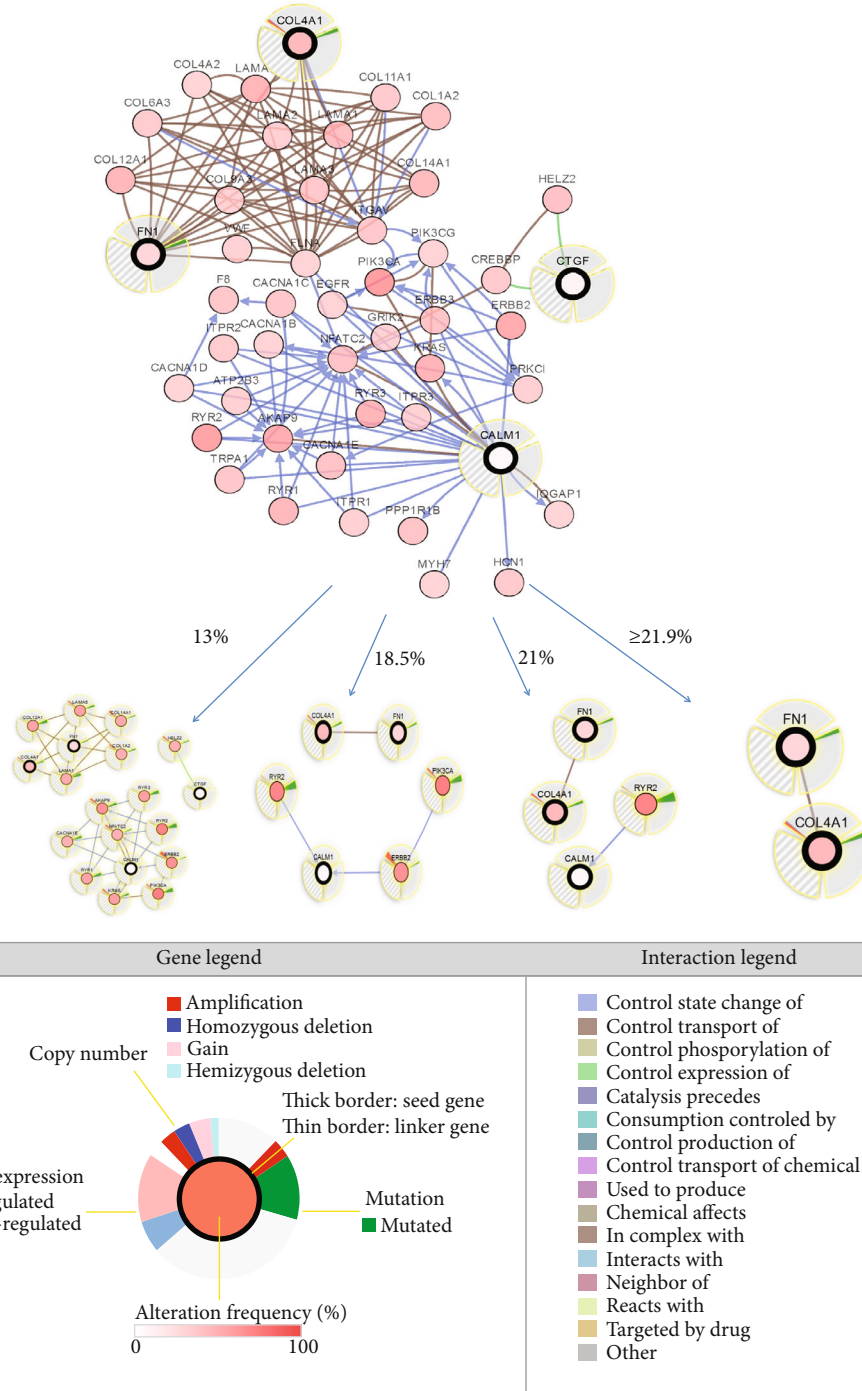


FIGURE 7: Display of neighboring genes connected to THBS1, FN1, CALM1, COL4A1, CTGF, and IGFBP5 in GC. THBS1, FN1, CALM1, COL4A1, CTGF, and IGFBP5 were used as seed genes (indicated with thick black borders) to automatically harvest all other genes identified as altered in GC. Multidimensional genomic details are shown for COL4A1, FN1, CTGF, and CALM1 seed genes. Dark red indicates an increased frequency of alterations (defined by mutation, copy number amplification, or homozygous deletion) in GC. Shown in the figure are the full and pruned networks containing all or part neighbors of all query genes generated; the neighboring genes connected to COL4A1, FN1, CTGF, and CALM1 are filtered by alteration (%).

consistent with the expression data of COL4A1 in the GSE33651 and Oncomine gastric datasets.

CALM, a ubiquitous eukaryotic calcium-binding protein that transduces much of the calcium signal [55] and plays an important role in intercellular communication,

cell movement, cell differentiation, cell proliferation, inflammation, and other physiological activities [56], is encoded by three nonallelic CALM genes (CALM1, CALM2, and CALM3). In the present study, the mRNA expression level of CALM1 was higher in GC tissues than

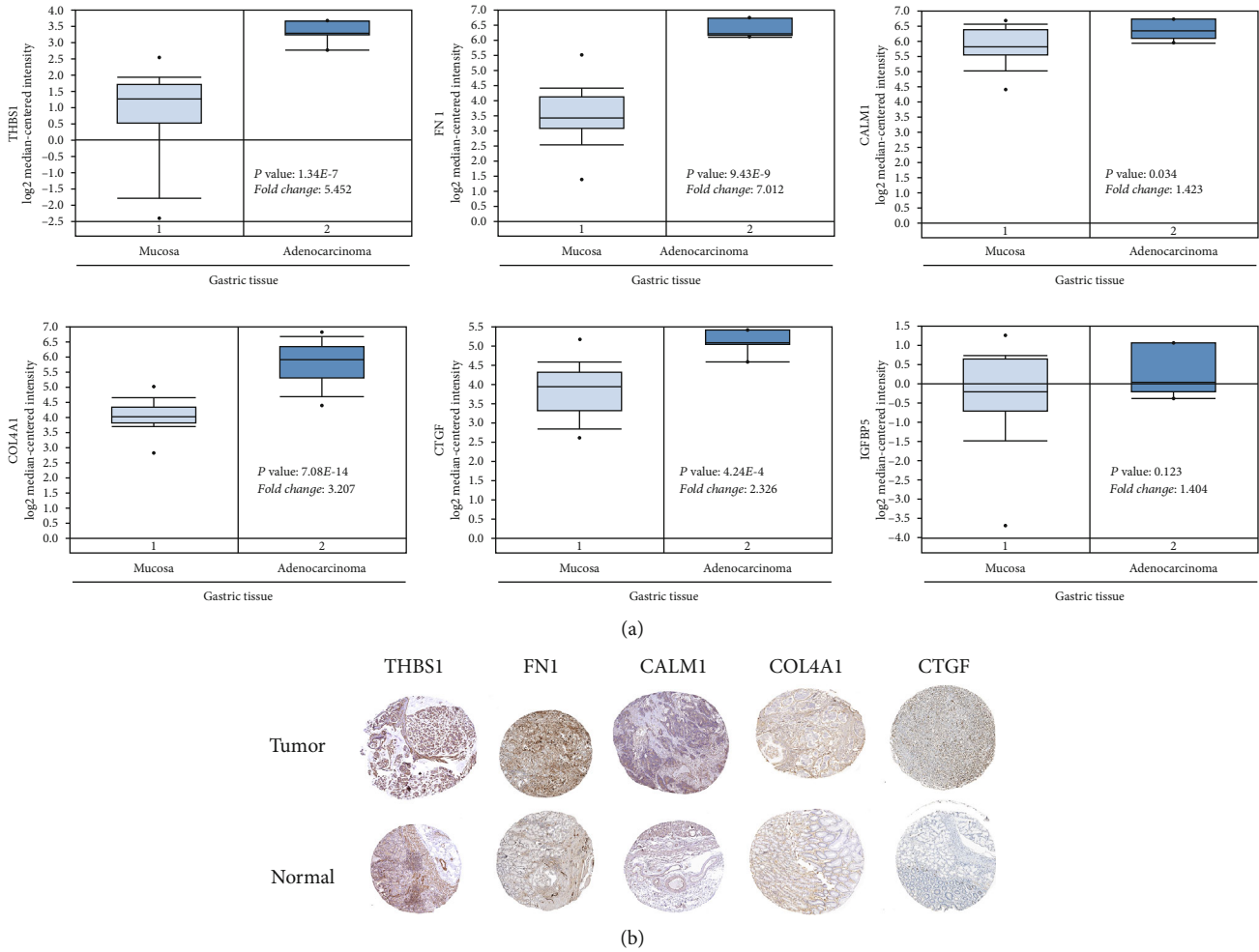


FIGURE 8: mRNA and protein expression levels of THBS1, FN1, CALM1, COL4A1, CTGF, and IGFBP5 for clinical significance in GC: (a) Oncomine data mining showing that THBS1, FN1, CALM1, COL4A1, CTGF, and IGFBP5 mRNA expression levels in Derrico datasets differ between normal mucosa and gastric adenocarcinoma tissues; (b) protein levels of THBS1 in normal tissue (staining: high; intensity: strong; quantity: >75%). Protein levels of FBXO5 in tumor tissue (staining: high; intensity: strong; quantity: >75%). Protein levels of FN1 in normal tissue (staining: low; intensity: moderate; quantity: <25%). Protein levels of FN1 in tumor tissue (staining: medium; intensity: moderate; quantity: 75%-25%). Protein levels of CALM1 in normal tissue (staining: medium; intensity: moderate; quantity: 75%-25%). Protein levels of CALM1 in tumor tissue (staining: medium; intensity: moderate; quantity: 75%-25%). Protein levels of COL4A1 in normal tissue (staining: not detectable; intensity: negative; quantity: negative). Protein levels of COL4A1 in tumor tissue (staining: medium; intensity: moderate; quantity: 75%-25%). Protein levels of CTGF in normal tissue (staining: low; intensity: moderate; quantity: rare). Protein levels of CTGF in tumor tissue (staining: low; intensity: weak; quantity: >75%).

in adjacent normal tissues. Hence, further studies of CALM1 in GC are necessary to clarify the role of CALM1 and its related molecular mechanisms in regulating physiological activities in GC.

Cyr61/CTGF/Nov (CCN) proteins are a family of matricellular proteins that consisted of an N-terminal secretory signal peptide and four structural modules and play pivotal context-dependent roles in many physiological and pathological processes according to tumor type, including inflammation [57]. CTGF (also known as CCN2) is involved in comprehensive regulatory processes in angiogenesis, chondrogenesis, osteogenesis, inflammation, fibrogenesis, diabetic nephropathy, and tumor development [58]. The Hippo signalling pathway is an emerging kinase cascade in gastrointestinal homeostasis and tumorigenesis. Kang et al. first revealed

that CTGF is the key downstream effector for the oncogenic function of YAP1 in GC and that it is highly expressed in primary tumors [59]. Jiang et al. also demonstrated that high CCN2 expression is correlated with increased lymph node metastasis, enhanced peritoneal dissemination, and short five-year survival [60]; these findings are also consistent with the expression of CTGF in GSE33651 and Oncomine GC datasets, indicating a proliferation-promoting role of CTGF in cancer.

Insulin and insulin-like growth factors (IGFs) consist of three peptide ligands (INS, IGF1, and IGF2), three specific cell surface receptors (INSR, IGF1R, and IGF2R), and ten specific IGF-binding proteins (IGFBPs; IGFBP1-7, and IGF2BP1-3) [61, 62], which are considered to play important roles in hormonal regulation, inflammation, and signal

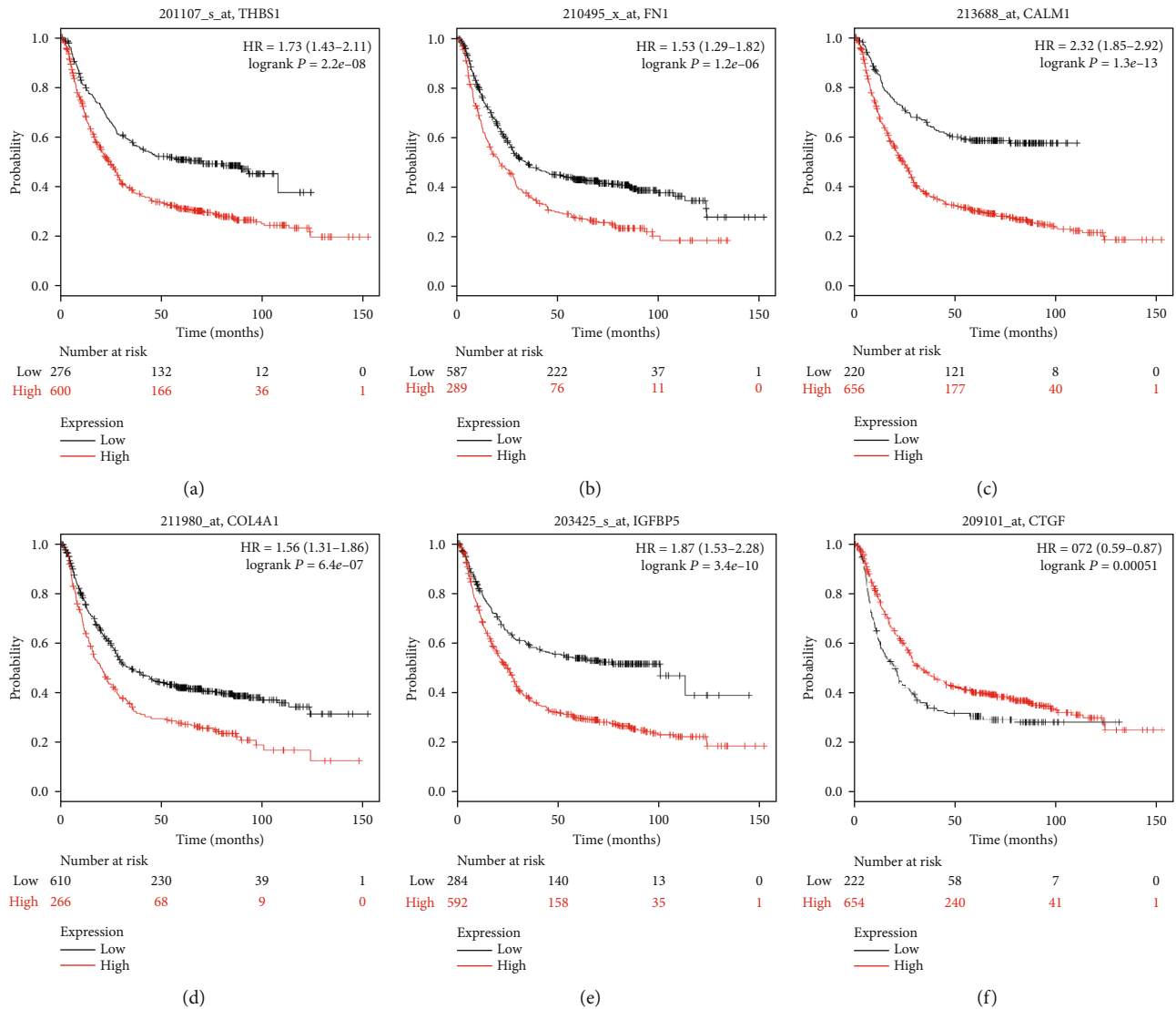


FIGURE 9: Prognostic curve for the six hub genes. The prognostic significance of the hub genes in patients with GC determined using the Kaplan-Meier plotter. Affymetrix IDs (a) 201107_s_at, (b) 210495_x_at, (c) 213688_at, (d) 211980_at, (e) 203425_s_at, and (f) 209101_at represent THBS1, FN1, CALM1, COL4A1, IGFBP5, and CTGF, respectively. Red lines represent patients with high gene expression, and black lines represent patients with low gene expression.

transduction during energy metabolism and oncogenesis [62]. IGF activity is tightly regulated by a family of IGFBPs. IGFBP5, the most conserved member of the IGFBP family, is significantly upregulated during the differentiation of several key cell lineages and in human cancer and metastatic tissues. IGFBP5 plays several outstanding roles in carcinogenesis to regulate cell growth, migration, and invasion during the development of cancer [63], but its function in the progression of cancer is controversial. Accumulating evidence has revealed that IGFBP5 can suppress tumor growth and metastasis in various tissues and under different contexts, but IGFBP5 can also function as an oncogene, promoting metastasis in a context-dependent manner [64]. Furthermore, bladder cancer [62], colorectal cancer [65], and breast cancer [66] tissues also contain high levels of IGFBP5, but few studies have explored the expression and mechanism for IGFBP5 in human GC. Our previous study has revealed that IGFBP5 exhibits a dis-

tinctly different expression pattern in GC tissues based on GSE33651 and Oncomine GC datasets.

In summary, we conducted an integrated analysis of DE circRNAs, miRNAs, and mRNAs in GC and constructed a potential circRNA-miRNA-mRNA regulatory network. We identified THBS1, FN1, CALM1, COL4A1, CTGF, and IGFBP5 as potential inflammation-related targets for the treatment of gastric adenocarcinoma. Our bioinformatics analysis represents a useful strategy to explore malignancy from a new perspective. However, future studies are required to validate the mechanisms related to the potential target genes.

Data Availability

The data used to support the findings of this study are available from the corresponding author upon request.

Conflicts of Interest

The authors declare that they have no competing interests.

Authors' Contributions

All authors participated in the preparation of the manuscript. YXL and FX conceived of and designed the study. YFX, JFZ, YQW, and YWY analyzed the transcriptomics data. YXL and JWY wrote the manuscript. All authors read and approved the final manuscript. YunXia Liu and YeFeng Xu contributed equally to this work.

Acknowledgments

This work was supported by grants from the National Natural Science Foundation of China (No. 81473505) and the Natural Science Foundation of Zhejiang Province (No. LY18H29000). The work was also supported by Hangzhou City Science and Technology Council (No. 20180533B58).

Supplementary Materials

Supplementary 1. Table S1: circRNA expression profiling data.

Supplementary 2. Table S2: differentially expressed circRNAs between tumor and normal tissues.

Supplementary 3. Table S3: differentially expressed miRNAs between tumor and normal tissues.

Supplementary 4. Table S4: differentially expressed mRNAs between tumor and normal tissues.

Supplementary 5. Table S5: circRNA-related miRNAs.

Supplementary 6. Table S6: miRNA-related mRNAs.

Supplementary 7. Table S7: GC-related genes in the GeneCards and GenCLiP 3 database.

Supplementary 8. Table S8: inflammation-related genes in the GeneCards and GenCLiP 3 database.

References

- [1] Y. Li, W. Bai, and X. Zhang, "Identifying heterogeneous subtypes of gastric cancer and subtype-specific subpaths of microRNA-target pathways," *Molecular Medicine Reports*, 2017.
- [2] X. Y. He, J. Zhao, Z. Q. Chen, R. Jin, and C. Y. Liu, "High expression of retinoic acid induced 14 (RAI14) in gastric cancer and its prognostic value," *Medical Science Monitor*, vol. 24, pp. 2244–2251, 2018.
- [3] W. Gu, Y. Sun, X. Zheng et al., "Identification of gastric cancer-related circular RNA through microarray analysis and bioinformatics analysis," *BioMed Research International*, vol. 2018, Article ID 2381680, 9 pages, 2018.
- [4] J. Chen, X. Wang, B. Hu, Y. He, X. Qian, and W. Wang, "Candidate genes in gastric cancer identified by constructing a weighted gene co-expression network," *PeerJ*, vol. 6, article e4692, 2018.
- [5] P.-L. Wu, Y.-F. He, H.-H. Yao, and B. Hu, "Martrilin-3 (MATN3) overexpression in gastric adenocarcinoma and its prognostic significance," *Medical Science Monitor*, vol. 24, pp. 348–355, 2018.
- [6] M.-J. Zhang, Y.-Y. Hong, and N. Li, "Overexpression of kin of IRRE-like protein 1 (KIRREL) in gastric cancer and its clinical prognostic significance," *Medical Science Monitor*, vol. 24, pp. 2711–2719, 2018.
- [7] Y. Xu, X. Yu, C. Wei, F. Nie, M. Huang, and M. Sun, "Overexpression of oncogenic pseudogene DUXAP10 promotes cell proliferation and invasion by regulating LATS1 and β -catenin in gastric cancer," *Journal of Experimental & Clinical Cancer Research*, vol. 37, no. 1, p. 13, 2018.
- [8] Q. N. Wu, Y. F. Liao, Y. X. Lu et al., "Pharmacological inhibition of DUSP6 suppresses gastric cancer growth and metastasis and overcomes cisplatin resistance," *Cancer Letters*, vol. 412, pp. 243–255, 2018.
- [9] Y. Huang, J. Zhu, W. Li et al., "Serum microRNA panel excavated by machine learning as a potential biomarker for the detection of gastric cancer," *Oncology Reports*, vol. 39, no. 3, pp. 1338–1346, 2018.
- [10] S. Massarrat and M. Stolte, "Development of gastric cancer and its prevention," *Archives of Iranian Medicine*, vol. 17, no. 7, pp. 514–520, 2014.
- [11] M. A. Shah, R. Khanin, L. Tang et al., "Molecular classification of gastric cancer: a new paradigm," *Clinical Cancer Research*, vol. 17, no. 9, pp. 2693–2701, 2011.
- [12] L. Zhao, H. Lei, L. Shen et al., "Prognosis genes in gastric adenocarcinoma identified by cross talk genes in disease-related pathways," *Molecular Medicine Reports*, vol. 16, no. 2, pp. 1232–1240, 2017.
- [13] M. B. Piazuolo, R. P. Riechelmann, K. T. Wilson, and H. M. S. Algood, "Resolution of gastric cancer-promoting inflammation: a novel strategy for anti-cancer therapy," *Current Topics in Microbiology and Immunology*, vol. 421, pp. 319–359, 2019.
- [14] X. Lin and Y. Chen, "Identification of potentially functional CircRNA-miRNA-mRNA regulatory network in hepatocellular carcinoma by integrated microarray analysis," *Medical Science Monitor Basic Research*, vol. 24, pp. 70–78, 2018.
- [15] J. W. Eun, et al. H. S. Kim, Q. Shen et al., "MicroRNA-495-3p functions as a tumor suppressor by regulating multiple epigenetic modifiers in gastric carcinogenesis," *Journal of Pathology*, vol. 244, no. 1, pp. 107–119, 2018.
- [16] S. Shrestha, C.-D. Yang, H.-C. Hong et al., "Integrated MicroRNA-mRNA analysis reveals miR-204 inhibits cell proliferation in gastric cancer by targeting CKS1B, CXCL1 and GPRC5A," *International Journal of Molecular Sciences*, vol. 19, no. 1, p. 87, 2018.
- [17] T. Liu, S. Liu, Y. Xu et al., "Circular RNA-ZFR inhibited cell proliferation and promoted apoptosis in gastric cancer by sponging miR-130a/miR-107 and modulating PTEN," *Cancer Research and Treatment*, vol. 50, no. 4, pp. 1396–1417, 2018.
- [18] J. Zhang, H. Liu, L. Hou et al., "Circular RNA_LARP4 inhibits cell proliferation and invasion of gastric cancer by sponging miR-424-5p and regulating LATS1 expression," *Molecular Cancer*, vol. 16, no. 1, p. 151, 2017.
- [19] H. Zhang, L. Zhu, M. Bai et al., "Exosomal circRNA derived from gastric tumor promotes white adipose browning by targeting the miR-133/PRDM16 pathway," *International Journal of Cancer*, vol. 144, no. 10, pp. 2501–2515, 2019.

- [20] S. Davis and P. S. Meltzer, "GEOquery: a bridge between the Gene Expression Omnibus (GEO) and BioConductor," *Bioinformatics*, vol. 23, no. 14, pp. 1846–1847, 2007.
- [21] D. B. Dudekula, A. C. Panda, I. Grammatikakis, S. de, K. Abdelmohsen, and M. Gorospe, "CircInteractome: a web tool for exploring circular RNAs and their interacting proteins and microRNAs," *RNA Biology*, vol. 13, no. 1, pp. 34–42, 2015.
- [22] C.-H. Chou, S. Shrestha, C.-D. Yang et al., "miRTarBase update 2018: a resource for experimentally validated microRNA-target interactions," *Nucleic Acids Research*, vol. 46, no. D1, pp. D296–D302, 2018.
- [23] G. Stelzer, N. Rosen, I. Plaschkes et al., "The GeneCards suite: from gene data mining to disease genome sequence analyses," *Current Protocols in Bioinformatics*, vol. 54, no. 1, pp. 1.30.1–1.30.33, 2016.
- [24] J. H. Wang, L. F. Zhao, H. F. Wang et al., "GenCLiP 3: mining human genes' functions and regulatory networks from PubMed based on co-occurrences and natural language processing," *Bioinformatics*, 2019.
- [25] D. Szklarczyk, A. Franceschini, S. Wyder et al., "STRING v10: protein-protein interaction networks, integrated over the tree of life," *Nucleic Acids Research*, vol. 43, no. D1, pp. D447–D452, 2015.
- [26] E. Cerami, J. Gao, U. Dogrusoz et al., "The cBio cancer genomics portal: an open platform for exploring multidimensional cancer genomics data," *Cancer Discovery*, vol. 2, no. 5, pp. 401–404, 2012.
- [27] J. Gao, B. A. Aksoy, U. Dogrusoz et al., "Integrative analysis of complex cancer genomics and clinical profiles using the cBioPortal," *Science Signaling*, vol. 6, no. 269, p. p11, 2013.
- [28] D. R. Rhodes, S. Kalyana-Sundaram, V. Mahavisno et al., "OncoPrint 3.0: genes, pathways, and networks in a collection of 18,000 cancer gene expression profiles," *Neoplasia*, vol. 9, no. 2, pp. 166–180, 2007.
- [29] P. V. Missiuro, K. Liu, L. Zou et al., "Information Flow Analysis of Interactome Networks," *PLoS Computational Biology*, vol. 5, no. 4, p. e1000350, 2009.
- [30] R. Li, C. Zhuang, S. Jiang et al., "TTGFB1 predicts a poor prognosis and correlates EMT phenotype in gastric cancer," *Journal of Cancer*, vol. 8, no. 18, pp. 3764–3773, 2017.
- [31] B. Li, L. Wang, Z. Li et al., "miR-3174 contributes to apoptosis and autophagic cell death defects in gastric cancer cells by targeting ARHGAP10," *Molecular Therapy - Nucleic Acids*, vol. 9, pp. 294–311, 2017.
- [32] K. Echizen, O. Hirose, Y. Maeda, and M. Oshima, "Inflammation in gastric cancer: Interplay of the COX-2/prostaglandin E2 and Toll-like receptor/MyD88 pathways," *Cancer Science*, vol. 107, no. 4, pp. 391–397, 2016.
- [33] Q. Liu, W. Zhang, Z. Wu et al., "Construction of a circular RNA-microRNA-messengerRNA regulatory network in stomach adenocarcinoma," *Journal of Cellular Biochemistry*, vol. 121, no. 2, pp. 1317–1331, 2019.
- [34] M. Krupp, et al. T. Maass, J. U. Marquardt et al., "The functional cancer map: a systems-level synopsis of genetic deregulation in cancer," *BMC Medical Genomics*, vol. 4, no. 1, 2011.
- [35] Y. Wang, Y. Mo, Z. Gong et al., "Circular RNAs in human cancer," *Molecular Cancer*, vol. 16, no. 1, p. 25, 2017.
- [36] Y. Zhang, J. Li, J. Yu et al., "Circular RNAs signature predicts the early recurrence of stage III gastric cancer after radical surgery," *Oncotarget*, vol. 8, no. 14, pp. 22936–22943, 2017.
- [37] J. Zhu, J. Ye, L. Zhang et al., "Differential expression of circular RNAs in glioblastoma multiforme and its correlation with prognosis," *Translational Oncology*, vol. 10, no. 2, pp. 271–279, 2017.
- [38] Y. Zhong, Y. du, X. Yang et al., "Circular RNAs function as ceRNAs to regulate and control human cancer progression," *Molecular Cancer*, vol. 17, no. 1, p. 79, 2018.
- [39] P. Li, S. Chen, H. Chen et al., "Using circular RNA as a novel type of biomarker in the screening of gastric cancer," *Clinica Chimica Acta*, vol. 444, pp. 132–136, 2015.
- [40] M. Huang, Y.-R. He, L.-C. Liang, Q. Huang, and Z.-Q. Zhu, "Circular RNA hsa_circ_0000745 may serve as a diagnostic marker for gastric cancer," *World Journal of Gastroenterology*, vol. 23, no. 34, pp. 6330–6338, 2017.
- [41] C. B. Carlson, J. Lawler, and D. F. Mosher, "Structures of thrombospondins," *Cellular and Molecular Life Sciences*, vol. 65, no. 5, pp. 672–686, 2008.
- [42] B.-B. Hong, S. Q. Chen, Y. L. Qi, J. W. Zhu, and J. Y. Lin, "Association of THBS1 rs1478605 T > C in 5' -untranslated regions with the development and progression of gastric cancer," *Biomedical Reports*, vol. 3, no. 2, pp. 207–214, 2015.
- [43] H. Kashiwara, M. Shimada, K. Yoshikawa et al., "Correlation between thrombospondin-1 expression in non-cancer tissue and gastric carcinogenesis," *Anticancer Research*, vol. 37, no. 7, pp. 3547–3552, 2017.
- [44] S. Eto, K. Yoshikawa, M. Shimada et al., "The relationship of CD133, histone deacetylase 1 and thrombospondin-1 in gastric cancer," *Anticancer Research*, vol. 35, no. 4, pp. 2071–2076, 2015.
- [45] T. Huang, L. Wang, D. Liu et al., "FGF7/FGFR2 signal promotes invasion and migration in human gastric cancer through upregulation of thrombospondin-1," *INTERNATIONAL JOURNAL OF ONCOLOGY*, vol. 50, no. 5, pp. 1501–1512, 2017.
- [46] Z.-Q. Zhou, et al. W.-H. Cao, J.-J. Xie et al., "Expression and prognostic significance of THBS1, Cyr61 and CTGF in esophageal squamous cell carcinoma," *BMC Cancer*, vol. 9, no. 1, 2009.
- [47] T. Nakao, N. Kurita, M. Komatsu et al., "Expression of thrombospondin-1 and Ski are prognostic factors in advanced gastric cancer," *International Journal of Clinical Oncology*, vol. 16, no. 2, pp. 145–152, 2011.
- [48] X. D. Lin, S. Q. Chen, Y. L. Qi, J. W. Zhu, Y. Tang, and J. Y. Lin, "Overexpression of thrombospondin-1 in stromal myofibroblasts is associated with tumor growth and nodal metastasis in gastric carcinoma," *Journal of Surgical Oncology*, vol. 106, no. 1, pp. 94–100, 2012.
- [49] L. Xiang, G. Xie, J. Ou, X. Wei, F. Pan, and H. Liang, "The extra domain a of fibronectin increases VEGF-C expression in colorectal carcinoma involving the PI3K/AKT signaling pathway," *PLoS One*, vol. 7, no. 4, article e35378, 2012.
- [50] H. Zhang, X. Teng, Z. Liu, L. Zhang, and Z. Liu, "Gene expression profile analyze the molecular mechanism of CXCR7 regulating papillary thyroid carcinoma growth and metastasis," *Journal of Experimental & Clinical Cancer Research*, vol. 34, no. 1, p. 16, 2015.
- [51] Y. H. Wang, Y. Y. Dong, W. M. Wang et al., "Vascular endothelial cells facilitated HCC invasion and metastasis through the Akt and NF- κ B pathways induced by paracrine cytokines," *Journal of Experimental & Clinical Cancer Research*, vol. 32, no. 1, p. 51, 2013.

- [52] H.-B. Chen and H.-T. Zheng, "MicroRNA-200c represses migration and invasion of gastric cancer SGC-7901 cells by inhibiting expression of fibronectin 1," *European Review for Medical and Pharmacological Sciences*, vol. 21, no. 8, pp. 1753–1758, 2017.
- [53] H. Zhang, Z. Sun, Y. Li, D. Fan, and H. Jiang, "MicroRNA-200c binding to FN1 suppresses the proliferation, migration and invasion of gastric cancer cells," *Biomedicine & Pharmacotherapy*, vol. 88, pp. 285–292, 2017.
- [54] R. Huang, W. Gu, B. Sun, and L. Gao, "Identification of COL4A1 as a potential gene conferring trastuzumab resistance in gastric cancer based on bioinformatics analysis," *Molecular Medicine Reports*, 2018.
- [55] H. Kobayashi, S. Saragai, A. Naito, K. Ichio, D. Kawauchi, and F. Murakami, "Calm1 signaling pathway is essential for the migration of mouse precerebellar neurons," *Development*, vol. 142, no. 2, pp. 375–384, 2015.
- [56] R. M. Hanley, S. Shenolikar, J. Pollack, D. Steplock, and E. J. Weinman, "Identification of calcium-calmodulin multifunctional protein kinase II in rabbit kidney," *Kidney International*, vol. 38, no. 1, pp. 63–66, 1990.
- [57] T.-Y. Cheng, M.-S. Wu, K.-T. Hua, M. L. Kuo, and M. T. Lin, "Cyr61/CTGF/Nov family proteins in gastric carcinogenesis," *World Journal of Gastroenterology*, vol. 20, no. 7, pp. 1694–1700, 2014.
- [58] C. C. Chen and L. F. Lau, "Functions and mechanisms of action of CCN matricellular proteins," *The International Journal of Biochemistry & Cell Biology*, vol. 41, no. 4, pp. 771–783, 2009.
- [59] W. Kang, T. Huang, Y. Zhou et al., "miR-375 is involved in Hippo pathway by targeting YAP1/TEAD4-CTGF axis in gastric carcinogenesis," *Cell Death & Disease*, vol. 9, no. 2, p. 92, 2018.
- [60] C.-G. Jiang, L. Lv, F.-R. Liu et al., "Downregulation of connective tissue growth factor inhibits the growth and invasion of gastric cancer cells and attenuates peritoneal dissemination," *Molecular Cancer*, vol. 10, no. 1, p. 122, 2011.
- [61] D. Sachdev and D. Yee, "Disrupting insulin-like growth factor signaling as a potential cancer therapy," *Molecular Cancer Therapeutics*, vol. 6, no. 1, pp. 1–12, 2007.
- [62] Y. Neuzillet, E. Chapeaublanc, C. Krucker et al., "IGF1R activation and the in vitro antiproliferative efficacy of IGF1R inhibitor are inversely correlated with IGFBP5 expression in bladder cancer," *BMC Cancer*, vol. 17, no. 1, p. 636, 2017.
- [63] J. Wang, N. Ding, Y. Li et al., "Insulin-like growth factor binding protein 5 (IGFBP5) functions as a tumor suppressor in human melanoma cells," *Oncotarget*, vol. 6, no. 24, pp. 20636–20649, 2015.
- [64] R. C. Baxter, "IGF binding proteins in cancer: mechanistic and clinical insights," *Nature reviews Cancer*, vol. 14, no. 5, pp. 329–341, 2014.
- [65] L. Yu, Y. Lu, X. Han et al., "microRNA -140-5p inhibits colorectal cancer invasion and metastasis by targeting ADAMTS5 and IGFBP5," *Stem Cell Research & Therapy*, vol. 7, no. 1, p. 180, 2016.
- [66] M. Akkiprik, İ. Peker, T. Özmen et al., "Identification of differentially expressed IGFBP5-related genes in breast cancer tumor tissues using cDNA microarray experiments," *Genes*, vol. 6, no. 4, pp. 1201–1214, 2015.

Research Article

The Depletion of ABI3BP by MicroRNA-183 Promotes the Development of Esophageal Carcinoma

Hongfei Cai, Yang Li, Da Qin, Rui Wang , Ze Tang, Tianyu Lu, and Youbin Cui 

Department of Thoracic Surgery, The First Hospital of Jilin University, 71 Xinmin Street, Changchun 130021, China

Correspondence should be addressed to Youbin Cui; cuiyb@jlu.edu.cn

Received 21 May 2020; Revised 8 July 2020; Accepted 13 July 2020; Published 26 July 2020

Guest Editor: Hongmei Jiang

Copyright © 2020 Hongfei Cai et al. This is an open access article distributed under the Creative Commons Attribution License, which permits unrestricted use, distribution, and reproduction in any medium, provided the original work is properly cited.

Background. Esophageal cancer (EC), as a serious threat to human life and health, is one of the most common cancers around the world. Many studies have suggested that many microRNAs are involved in tumorigenesis and progression. **Methods.** To search for a novel and promising predictive therapeutic target or biomarker to achieve the goal of the early diagnosis and treatment of EC, we used the EC cell lines Eca-109 and KYSE-150 and normal human esophageal epithelial cells (HEECs) to investigate the effect of ABI3BP on EC. **Results.** We found that ABI family member 3 binding protein (ABI3BP) was downregulated in EC and suppressed the proliferation, activity, migration, and invasion of EC cells. ABI3BP was downregulated by miR-183, which plays the role of an oncogene. **Conclusion.** ABI3BP and miR-183 can be considered potential biomarkers for the diagnosis of patients with EC and can be effective targets for antitumor therapy.

1. Introduction

Esophageal cancer (EC) is one of the most common malignancies and ranks eighth in prevalence throughout the world. It also remains the sixth leading cause of death due to carcinoma. EC, because of its high malignancy potential, poor prognosis, and high mortality, is one of the most serious gastrointestinal malignancies. It has been shown that its global incidence has increased sharply by more than 6-fold. The number of new cases of EC was more than 572,000 in 2018 and nearly 440,000 deaths occurred. EC poses a serious threat to human life and health worldwide [1–5]. In the past few years, with the rapid progress in surgery, chemotherapy, and preoperative radiotherapy, the survival rate has been effectively improved to some extent in patients with EC. Unfortunately, because the early symptoms of EC are not apparent, an increasing number of patients with EC are diagnosed when they are at an advanced stage and the tumor cannot be removed surgically. In addition, the poor prognosis of patients with EC is seriously affected by resistance to chemotherapy and radiotherapy as well as tumor metastasis and recurrence [6, 7]. Recent studies have reported that the

5-year survival rate and the median survival time of patients with EC are 15–20% and 1.5 years, respectively [7, 8]. Although some new treatments, such as systemic treatment, nivolumab, novel targeted therapies, and immune checkpoint inhibition, have been used recently, there are still many limitations [7, 9–12]. Therefore, it is urgent to develop new treatment methods to improve the prognosis of EC patients.

An increasing number of studies have indicated that miRNAs (miRs) play a crucial role in tumorigenesis and progression and are useful and important diagnostic and prognostic markers in human cancers [13–17]. A great number of miRNAs are also involved in the development and progression of EC. For instance, miR-377 has been proven to be significantly downregulated in both the serum and tumor tissues of patients with esophageal squamous cell carcinoma (ESCC) and was shown to be located in the chromosome 14q32 region. Moreover, the survival rate of patients is positively correlated with the expression level of miR-377. miR-377 inhibited the occurrence, growth, angiogenesis, and metastasis of ESCC by targeting the expression of CD133 and VEGF, thus acting as a tumor suppressor [18]. miR-873 has a crucial effect on the growth and metastasis of EC by targeting

the DEC2 gene [19]. miR-183 was found to be involved in the pathogenesis of ESCC [20]. The above studies revealed the regulatory role of miRNAs in the occurrence, growth, and metastasis of EC and their roles as tumor suppressors or tumor promoters.

ABI3BP is an ArgBP/E3B1/Avi2/NESH family protein that is well known to be involved in the negative regulation of cell movement and metastasis through its effects on membrane folding and lamellar formation and was proven to be an SRC homologous (SH3) adaptor molecule [21, 22]. ABI3BP was considered to have a tumor-suppressive effect in thyroid cancer [23]. The online Gene Expression Profiling Interactive Analysis [24] database showed that the expression level of ABI3BP may be negatively associated with EC, while the miR-183-3p expression level may be positively correlated with EC. Moreover, ABI3BP is a potential target gene of miR-183. Taken together, the evidence suggests that ABI3BP restoration could exert inhibitory effects on EC cell growth and play a crucial role in mediating the pathogenesis, development, and/or progression of EC, indicating the possible treatment of EC by inhibiting miR-183 or enhancing ABI3BP.

2. Materials and Methods

2.1. Cell Culture. Eca-109 (KG189, KeyGEN Bio, Jiangsu, China), KYSE-150 (KG532, KeyGEN Bio, Jiangsu, China), and human normal esophageal epithelial cells (KG161, KeyGEN Bio, Jiangsu, China) were cultured in DMEM which containing 10% FBS, penicillin (100 U/ml), and streptomycin (0.1 mg/ml) in a cell incubator (5% CO₂, 37°C). When the cells entered the logarithmic growth stage and the cell density reaches 80%~90%, the culture medium was removed, washing by PBS (10 ml) for three times, in addition to trypsin (0.25%), and was used for digestion in 37°C for 1 min. After the cells became round, fresh culture medium was added to stop digestion, and the pipette was used for repeated blowing and beating to form single-cell suspension. Then, cells were centrifuged with 2000 rpm for 2 min and used for follow-up research studies.

2.2. Cell Transfection. Cells were inoculated in a 6-well plate for culture. For the cells grown to 80%, the culture medium was replaced with a nonantibiotic culture medium 2 hours before transfection for further transfection. Prepare the transfection complex; dissolve the siRNA oligomer (2.5 g) or plasmid (2.5 g) into 250 living room culture solution free of serum and antibiotics. The culture medium with no serum and no antibiotics was diluted to 250 living room Lipofectamine 2000 and incubated for five minutes at room temperature (RT). The above diluted Lipofectamine 2000 and siRNA/plasmid were mixed and incubated at RT for twenty minutes. Add the above mixture (500 livl/hole) to the incubator plate for 6 hours. The cells were replaced with a complete culture medium and continued for 24 hours/48 hours for subsequent research studies [25, 26].

2.3. CCK8 Assay. After 24 h cell transfection, trypsin digested the cells to prepare cell suspension. These cells were cultured in 96-well plates in an incubator at a thickness of 2000/well.

When cultivating for 0, 24, 48, and 72 h, respectively, add 10 living room CCK8 reagent to each well of the 96-well plate, and continue to cultivate for 1 hour. After the incubation, the absorbance value of OD450 nm in each well was detected with an enzyme marker, and the cell proliferation curve was plotted according to the absorbance value [27, 28].

2.4. Transwell Invasion Assay. Matrigel was diluted with serum-free precooling medium and placed at the bottom of the upper chamber of the Transwell chamber for incubation at 37°C for five hours. The basement membrane was rehydrated with the culture medium which is serum-free. Twenty-four hours later after transfection, trypsin was used to digest the cells and serum-free culture medium was preparing cell suspension. Take out the Transwell chamber, and wipe the remaining cells in the chamber by cotton swabs after incubation during all night.

Wash these cells by PBS for three times, and then fix with 4% paraformaldehyde for thirty minutes. After that, the cells were treated with 0.1% crystal violet for 20 min. Then, wash it by PBS for three times, and select randomly for three fields for counting under the microscope (100x).

2.5. Flow Cytometry Assay. Twenty-four hours later after transfection with the cells, replace the culture medium by the serum-free medium to culture for twenty-four hours. The cells were cultured followed by trypsin digestion fluid without EDTA and collected by centrifugation. The density of cell was controlled to $1-5 \times 10^6$ /ml. Using a pipette, 100 living room cell suspension was absorbed into the flow tube. After adding 5 living room cells Annexin V/FITC, cultivate it out of light for five minutes at RT. Add 10 livl PI dye solution and 400 livl PBS to the flow tube, and then conduct apoptosis detection on the flow cytometer. The data obtained were analyzed using FlowJo software.

2.6. Wound Healing Assay. After 24 h cell transfection, trypsin was used to digest the cells to prepare cell suspension as described above. Then, cells were cultured at 37°C for twelve hours in 6-well plates, and the cell density was controlled to about 5×10^5 per well. The sterilized suction head was used to cut a wound in the middle of each hole of the 6-hole plate, and the photos were taken after PBS washing for 2 times (Nikon Eclipse Ti-S, 20x). Culture was continued for 24 h, and the wound was photographed again. Five photos were taken for each well. ImageJ software was used to image the wounds taken twice before and after, and the wound closure was measured.

2.7. Dual-Luciferase Reporter Assay. Mouse ABI3BP mRNA and miR-183-3p were synthesized by GENEWIZ (Suzhou, China) and subcloned in pmirGLO and pCMV plasmids. Dual-luciferase reporter assay kit was purchased from Beyotime Biotechnology (Shanghai, China).

The cells were cultured as described above. After digested into single-cell suspension, the cells were divided into 2 groups and cultured in a 24-well plate. Transfection was carried out when the cell density reached about 70-80%. The cells were transfected with pmirGLO-ABI3BP+pCMV-NC and pmirGLO-ABI3BP+pCMV-miR-183-3p, respectively, by using

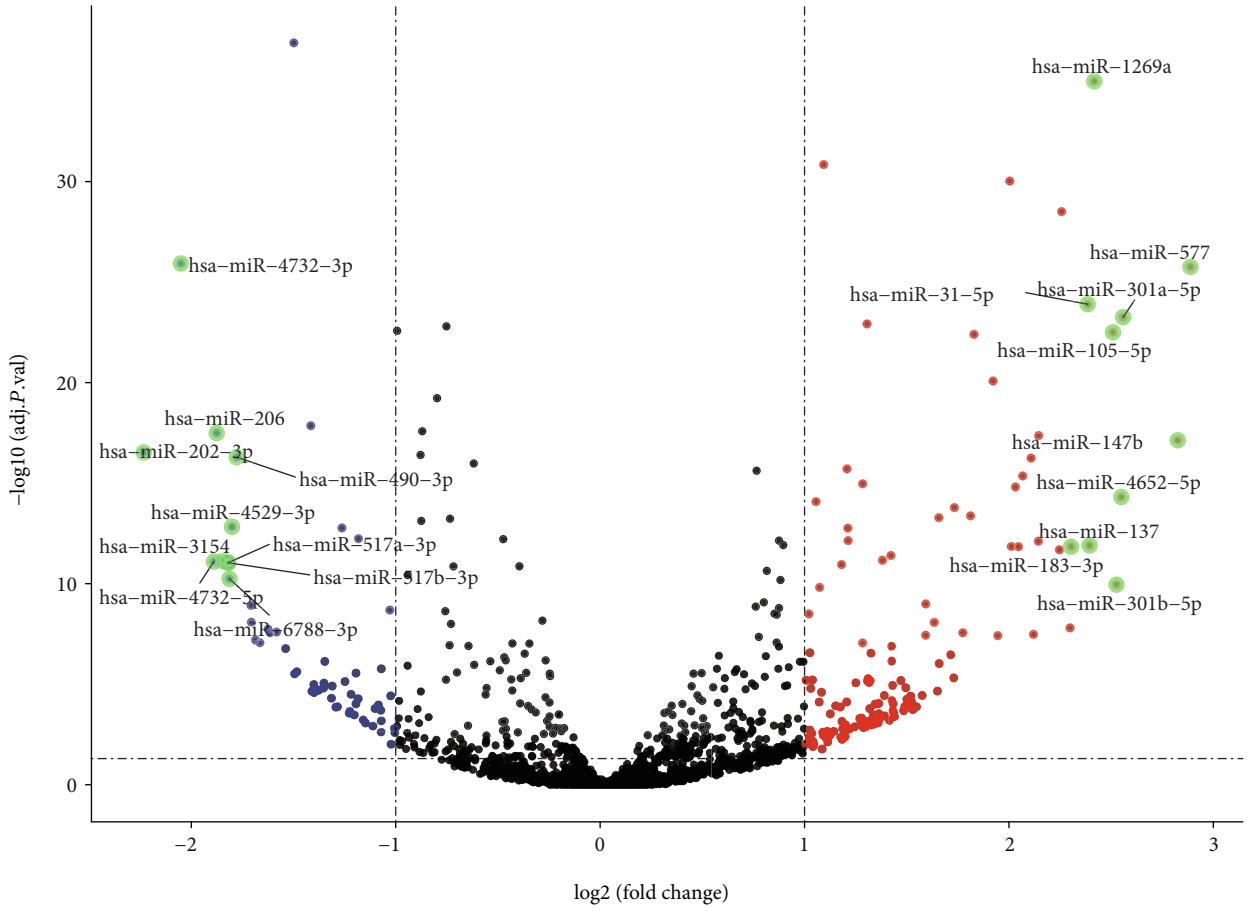


FIGURE 1: The expression of miRNAs in EC tissues and normal tissues from GEPIA analysis. The top 10 variation miRNAs were marked in the map.

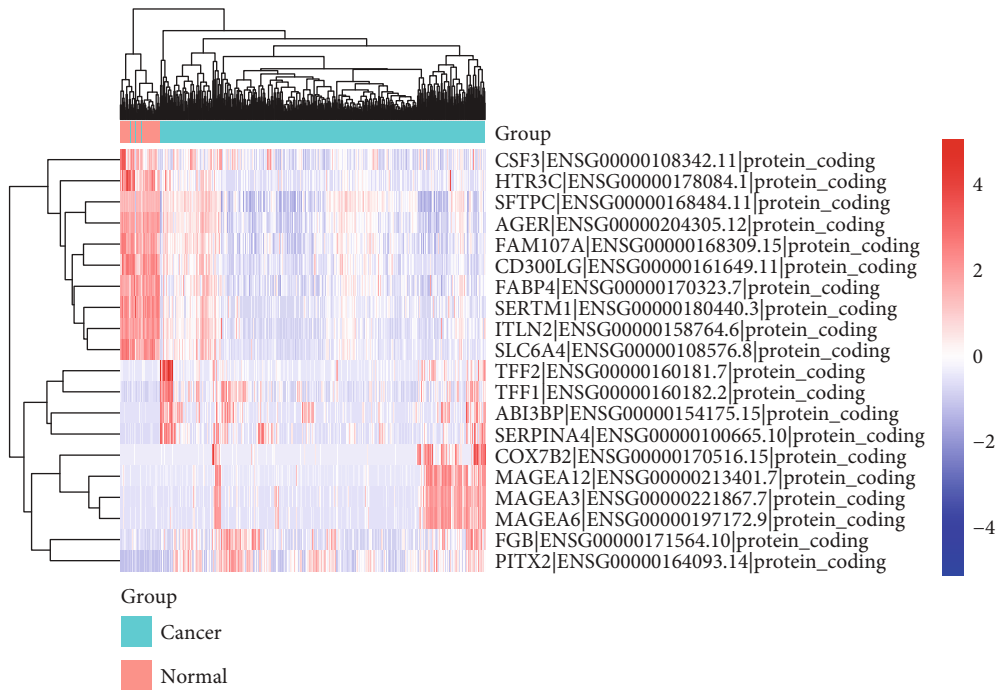


FIGURE 2: The expression of mRNAs in EC tissues and normal tissues from GEPIA analysis. The top 10 variation mRNAs were showed in the heat map.

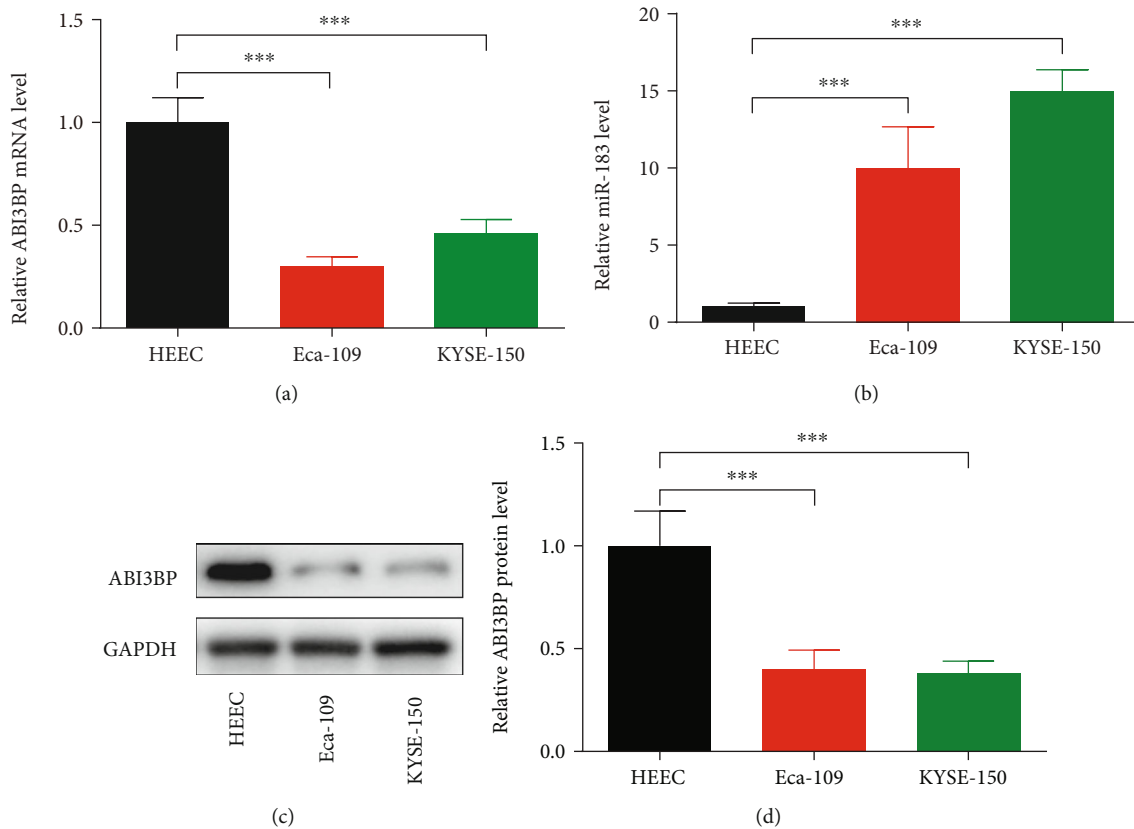


FIGURE 3: The expression levels of ABI3BP and miR-183 in HEEC, Eca-109, and KYSE-150 cells. Three kinds of cells were cultured and harvested when growing to 80-90%. Total mRNA or protein was extracted and detected by real-time PCR or Western blot analysis. (a) Relative ABI3BP mRNA level was detected by using RT-PCR. Five independent experiments ($n = 5$) were repeated for each cell line. (b) Relative miR-183-3p level was detected by using RT-PCR. Five independent experiments ($n = 5$) were repeated for each cell line. (c) Relative ABI3BP protein level was detected by Western blot. Five independent experiments ($n = 5$) were repeated for each cell line. (d) Quantitative analysis of (c). *** $P < 0.001$, one-way ANOVA with post hoc.

Lipofectamine™ 3000 Transfection Reagent (L3000001, Thermo Fisher). Then, the cells were cultured for 48 hours in normal condition. Then, the cells were collected and the fluorescence values of the cells in each group were immediately determined according to the protocol provided in the kit.

2.8. Statistical Analysis. Three independent repeated experiments were carried out in this study. The experimental data were expressed as mean \pm SEM using GraphPad Prism 7.0 software for analyzing. Student's t -test or single-factor ANOVA was used to analyze the differences between groups, and the value of P less than 0.05 was considered statistically significant.

3. Results

3.1. ABI3BP and miR-183 Are Related to EC. Through the online Gene Expression Profiling Interactive Analysis database, our team analyzed public data and found that the ABI3BP expression level may be negatively correlated with EC, while the miR-183-3p expression level may be positively correlated with EC (Figures 1 and 2). According to previous studies, miR-183 participates in the pathogenesis of ESCC [20], while ABI3BP is related to gallbladder cancer, thyroid

tumors, and lung cancer [29–32]. These results strongly suggest that ABI3BP and miR-183 could regulate EC development.

Then, the mRNA expression levels of ABI3BP and miR-183 in KYSE-150 and Eca-109 cells and HEECs were detected by RT-PCR. The results revealed that, compared with those in HEECs, the expression levels of ABI3BP were markedly downregulated in KYSE-150 and Eca-109 cells (Figure 3(a)); furthermore, miR-183 was significantly upregulated (Figure 3(b)), suggesting that the expression of ABI3BP and miR-183 were altered in ECs. The protein level of ABI3BP was also detected in the three cell lines, which showed that ABI3BP was significantly downregulated in KYSE-150 and Eca-109 cells (Figures 3(c) and 3(d)).

3.2. ABI3BP Is a Target of miR-183-3p in EC Cells. The potential target gene of miR-183-3p was predicted using an online bioinformatics database (TargetScan). Our team found that ABI3BP contains binding sites that might interact with miR-183-3p and may possibly be a target gene of miR-183-3p (Figure 4(a)). To further verify the above hypothesis, we constructed a dual-luciferase reporter gene and transfected it into Eca-109 cells. The results suggested that miR-183-3p

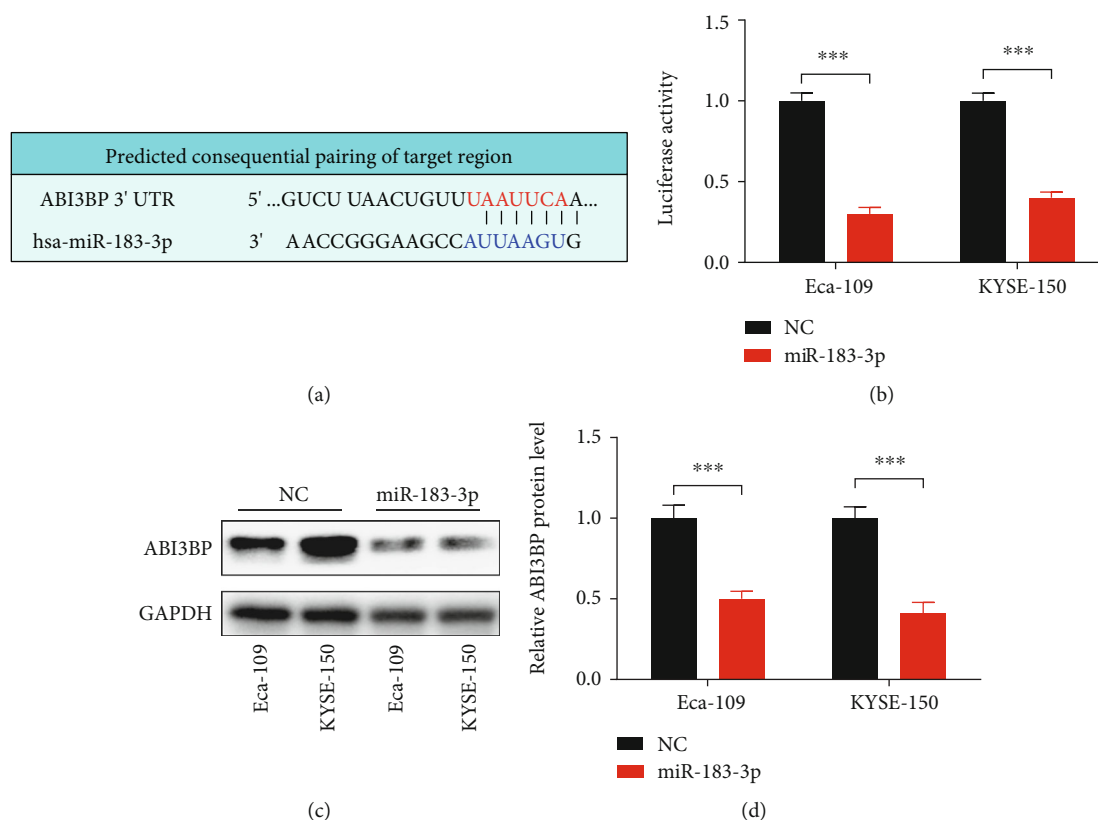


FIGURE 4: ABI3BP may be one of the targets of miR-183 in Eca-109 and KYSE-150 cells. (a) Predicted consequential pairing site of ABI3BP mRNA and miR-183-3p. (b) Dual-luciferase reporter assay was performed to detect the luciferase activity of ABI3BP mRNA and miR-183-3p. Three independent experiments ($n = 3$) were repeated. (c) Two kinds of cells were cultured and harvested when growing to 80-90%. Total protein was extracted and detected by Western blot analysis. Relative ABI3BP protein level was detected by Western blot under miR-183-3p overexpression condition. Five independent experiments ($n = 5$) were repeated for each cell line. (d) Quantitative analysis of (c). *** $P < 0.001$, Student's t -test.

markedly decreased the luciferase activity of ABI3BP (Figure 4(b)). Therefore, miR-183-3p can bind to ABI3BP, which may be its target gene. To further verify this result, we transfected miR-183-3p mimics into the cells and detected the expression levels of ABI3BP in Eca-109 cells. The result suggested that the expression levels of ABI3BP protein were markedly reduced after transfection (Figures 4(c) and 4(d)), which further proved that ABI3BP was a target of miR-183-3p.

3.3. ABI3BP and miR-183 Modulate the Apoptosis and Proliferation of EC Cells. To further explore the functions of ABI3BP and miR-183 in EC, we designed experiments to detect the apoptosis and proliferation of Eca-109 cells under ABI3BP or miR-183 overexpression conditions. The flow cytometry assay revealed that ABI3BP could obviously increase the rate of apoptosis, while miR-183 could significantly reduce the rate of apoptosis (Figures 5(a) and 5(b)), which suggested that ABI3BP plays a role as a tumor suppressor and that miR-183 is an oncogene. The CCK8 assay indicated that the viability of Eca-109 cells was markedly decreased by ABI3BP and increased by miR-183 (Figure 5(c)). All these results are consistent with the database results (Figures 1 and 2).

3.4. ABI3BP and miR-183 Modulate the Migration and Invasion of EC Cells. Next, we detected the invasion and migration of EC cells under ABI3BP or miR-183 overexpression conditions. In the wound healing assay, ABI3BP markedly reduced the migration of EC cells, while miR-183 markedly promoted EC cell migration (Figures 6(a) and 6(b)). Additionally, the Transwell invasion assay showed that ABI3BP could significantly inhibit the invasion of EC cells, while miR-183 promoted EC cell invasion (Figures 6(c) and 6(d)).

4. Discussion

Despite the rapid progress in surgery, chemotherapy, and preoperative radiotherapy techniques for EC made in recent years, unfortunately, an increasing number of patients with EC are diagnosed when they are at an advanced stage and the tumor cannot be removed surgically because the early symptoms of EC are not obvious. In addition, the poor prognosis of patients with EC is seriously affected by resistance to chemotherapy and radiotherapy as well as tumor metastasis and recurrence. Numerous lncRNAs and microRNAs have been proven to play a crucial role in tumor development

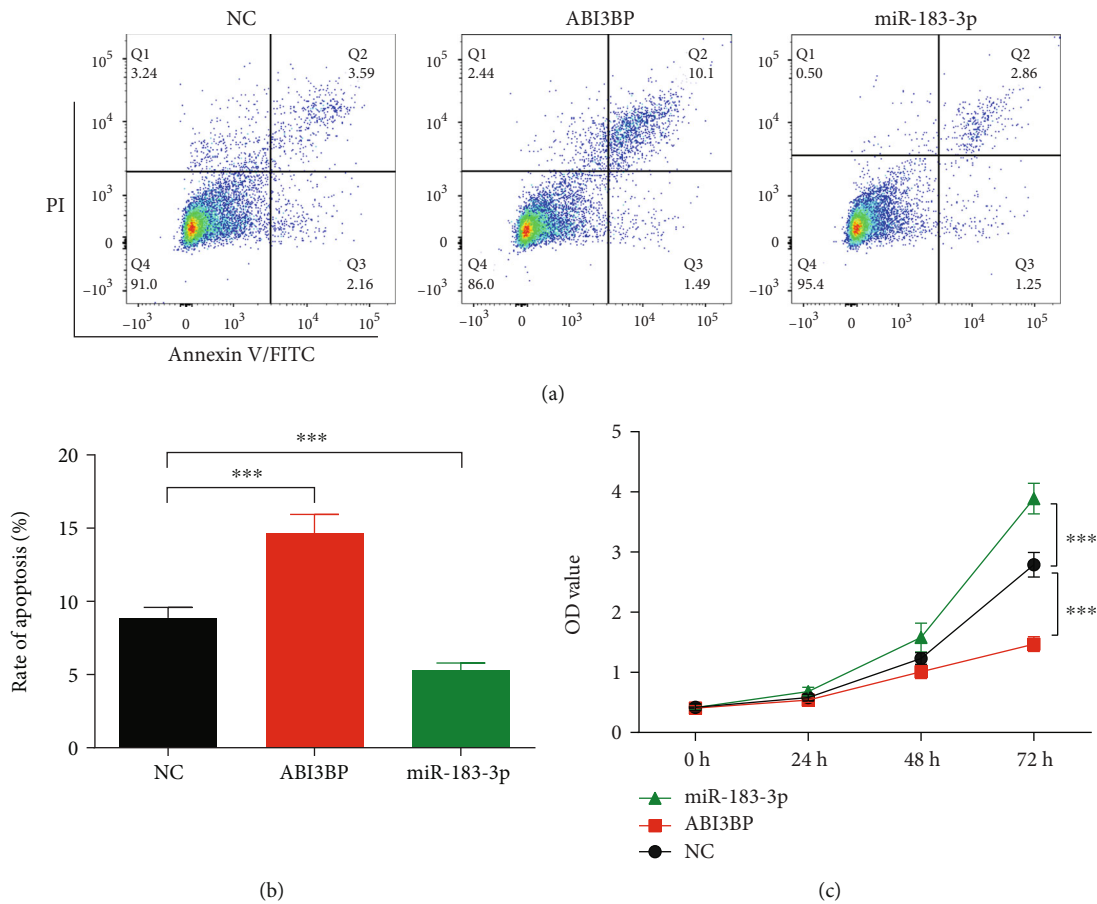


FIGURE 5: ABI3BP and miR-183 modulate the apoptosis and proliferation in EC cells. (a) After being transfected with ABI3BP or miR-183 for 24 h, flow cytometry assay was performed to detect the rate of apoptosis in Eca-109 cells under ABI3BP or miR-183 overexpression conditions. Three independent experiments ($n = 3$) were repeated for each group. (b) Quantitative analysis of Figure 5(a). (c) After being transfected with ABI3BP or miR-183 for 24 h, CCK8 assay was performed to assess the proliferation of Eca-109 under ABI3BP or miR-183 overexpression conditions. $n = 5$ for each group. *** $P < 0.001$, one-way ANOVA with post hoc and two-way ANOVA with post hoc.

and drug resistance and can be used as potential biomarkers for tumor diagnosis and prognosis and as molecular therapeutic targets [33–35].

Human ABI3BP was originally identified as a novel NESH-binding protein that is involved in tumor cell migration and mobility [36]. Through its interaction with NESH, ABI3BP may exert a great effect on the progression of tumor cells. In fact, the expression level of ABI3BP mRNA was markedly decreased in human lung cancer cell lines and clinical samples. Although the molecular mechanisms of tumorigenesis and progression are not well understood, the progression of tumorigenesis is closely related to the cell cycle. For example, p53, RB, or p19ARF, all of which are tumor suppressor proteins, play important roles in the cell cycle. It has been reported that the expression of ABI3BP is downregulated in gallbladder cancer tissues, and ABI3BP is a downstream target of metastasis-associated lung adenocarcinoma transcript 1 [29]. Studies have confirmed the tumor-suppressive effect of ABI3BP, suggesting that the ectopic expression of ABI3BP can impair the growth characteristics of cancer cells and induce senescence [23]. Depletion of ABI3BP could induce oncogenic transformation [37]. ABI3BP recovery was highlighted as an important factor

associated with thyroid tumors that inhibited tumor growth and invasion and promoted cell senescence [32]. In addition, ABI3BP was reported to show decreased expression in lung cancer cell lines, suggesting that ABI3BP could be a biomarker for lung cancer progression [31].

Here, in our study, we found that there is a low level of ABI3BP expression in EC cells and a high level of miR-183 expression. Additionally, we found that ABI3BP is one of the targets of miR-183. Together, the results indicated that miR-183 reduced ABI3BP protein levels and thus promoted EC development by enhancing cell proliferation, migration, and invasion and inhibiting apoptosis.

We showed for the first time that ABI3BP is downregulated in EC, revealing the role of ABI3BP as a tumor suppressor gene in the progression of EC growth and metastasis at the cellular level. It was further proven that miR-183 is an upstream regulatory molecule of ABI3BP. The molecular mechanism of the promotion by miR-183 of the growth and metastasis of EC cells mediated by regulating ABI3BP was demonstrated. In our future work, the mechanism of ABI3BP involved in its tumor-suppressive effects will be studied in detail, and ABI3BP will be explored as an effective target for tumor diagnosis and as a biomarker.

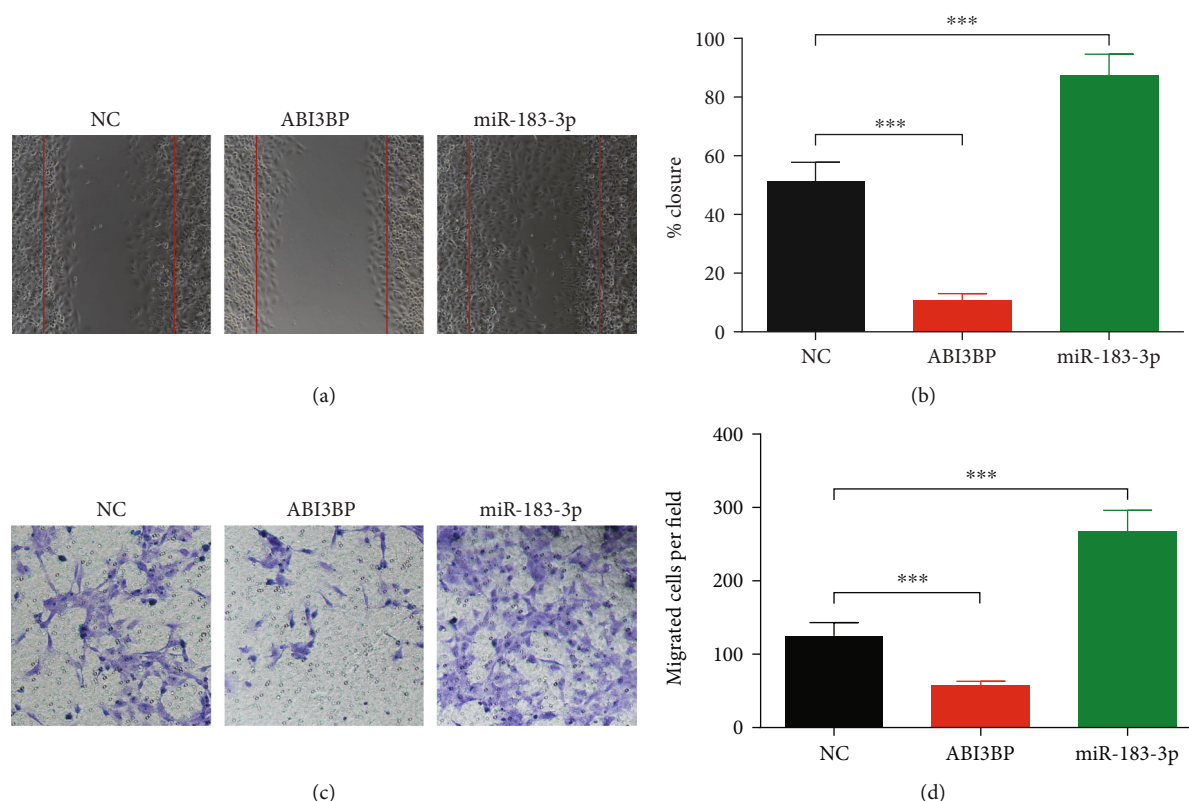


FIGURE 6: ABI3BP and miR-183 modulate the migration and invasion in EC cells. (a) After being transfected with ABI3BP or miR-183 for 24 h, the migration ability of EC cells was assessed by wound healing assay. Five independent experiments ($n = 5$) were repeated for each group. (b) Quantitative analysis of (a). (c) After being transfected with ABI3BP or miR-183 for 24 h, the invasion ability of EC cells was assessed by Transwell assays. Five independent experiments ($n = 5$) were repeated for each group. (d) Quantitative analysis of (b). *** $P < 0.001$, one-way ANOVA with post hoc.

5. Conclusions

ABI3BP plays the role of a tumor suppressor gene in the progression of EC growth and metastasis at the cellular level. miR-183 is an upstream regulatory molecule of ABI3BP. ABI3BP and miR-183 can be considered potential biomarkers for the diagnosis and prediction of the progression and prognosis of EC patients and can be effective targets for antitumor therapy.

Data Availability

The data in the manuscript are original and available.

Conflicts of Interest

The authors declare that there is no conflict of interest regarding the publication of this article.

Acknowledgments

This study was supported by the Jilin Province Health Committee Youth Science and Technology Backbone Training Program (2018Q029) and the Youth Fund of the First Hospital of Jilin University (No. JDYY11202022).

References

- [1] F. Bray, J. Ferlay, I. Soerjomataram, R. L. Siegel, L. A. Torre, and A. Jemal, "Global cancer statistics 2018: GLOBOCAN estimates of incidence and mortality worldwide for 36 cancers in 185 countries," *CA: a Cancer Journal for Clinicians*, vol. 68, no. 6, pp. 394–424, 2018.
- [2] J. Lagergren, E. Smyth, D. Cunningham, and P. Lagergren, "Oesophageal cancer," *Lancet*, vol. 390, no. 10110, pp. 2383–2396, 2017.
- [3] G. K. Malhotra, U. Yanala, A. Ravipati, M. Follet, M. Vijayakumar, and C. Are, "Global trends in esophageal cancer," *Journal of Surgical Oncology*, vol. 115, no. 5, pp. 564–579, 2017.
- [4] E. C. Smyth, J. Lagergren, R. C. Fitzgerald et al., "Oesophageal cancer," *Nature Reviews Disease Primers*, vol. 3, no. 1, p. 17048, 2017.
- [5] M. Arnold, J. Ferlay, M. I. van Berge Henegouwen, and I. Soerjomataram, "Global burden of oesophageal and gastric cancer by histology and subsite in 2018," *Gut*, p. gutjnl-2020-321600, 2020.
- [6] F. L. Huang and S. J. Yu, "Esophageal cancer: risk factors, genetic association, and treatment," *Asian Journal of Surgery*, vol. 41, no. 3, 2016.
- [7] H. Hirano and K. Kato, "Systemic treatment of advanced esophageal squamous cell carcinoma: chemotherapy,

- molecular-targeting therapy and immunotherapy,” *Japanese Journal of Clinical Oncology*, vol. 49, no. 5, pp. 412–420, 2019.
- [8] A. K. Rustgi and H. B. el-Serag, “Esophageal carcinoma,” *New England Journal of Medicine*, vol. 371, no. 26, pp. 2499–2509, 2014.
- [9] E. C. Smyth and F. Lordick, “Nivolumab for previously treated squamous oesophageal carcinoma,” *The Lancet Oncology*, vol. 20, no. 11, pp. 1468–1469, 2019.
- [10] E. Smyth and P. C. Thuss-Patience, “Immune checkpoint inhibition in gastro-oesophageal cancer,” *Oncology Research and Treatment*, vol. 41, no. 5, pp. 272–280, 2018.
- [11] S. Pasquali, G. Yim, R. S. Vohra et al., “Survival after neoadjuvant and adjuvant treatments compared to surgery alone for resectable esophageal carcinoma: a network meta-analysis,” *Annals of Surgery*, vol. 265, no. 3, pp. 481–491, 2017.
- [12] T. van den Ende, E. Smyth, M. C. C. M. Hulshof, and H. W. M. van Laarhoven, “Chemotherapy and novel targeted therapies for operable esophageal and gastroesophageal junctional cancer,” *Best Practice & Research Clinical Gastroenterology*, vol. 36–37, pp. 45–52, 2018.
- [13] A. Ventura and T. Jacks, “MicroRNAs and cancer: short RNAs go a long way,” *Cell*, vol. 136, no. 4, pp. 586–591, 2009.
- [14] J. H. Song and S. J. Meltzer, “MicroRNAs in pathogenesis, diagnosis, and treatment of gastroesophageal cancers,” *Gastroenterology*, vol. 143, no. 1, pp. 35–47.e2, 2012.
- [15] Y.-X. Fang and W.-Q. Gao, “Roles of microRNAs during prostatic tumorigenesis and tumor progression,” *Oncogene*, vol. 33, no. 2, pp. 135–147, 2014.
- [16] F. J. Kohlhapp, A. K. Mitra, E. Lengyel, and M. E. Peter, “MicroRNAs as mediators and communicators between cancer cells and the tumor microenvironment,” *Oncogene*, vol. 34, no. 48, pp. 5857–5868, 2015.
- [17] L. L. Mei, Y. T. Qiu, B. Zhang, and Z. Z. Shi, “MicroRNAs in esophageal squamous cell carcinoma: potential biomarkers and therapeutic targets,” *Cancer Biomarkers*, vol. 19, no. 1, pp. 1–9, 2017.
- [18] B. Li, W. W. Xu, L. Han et al., “MicroRNA-377 suppresses initiation and progression of esophageal cancer by inhibiting CD133 and VEGF,” *Oncogene*, vol. 36, no. 28, pp. 3986–4000, 2017.
- [19] Y. Liang, P. Zhang, S. Li, H. Li, S. Song, and B. Lu, “MicroRNA-873 acts as a tumor suppressor in esophageal cancer by inhibiting differentiated embryonic chondrocyte expressed gene 2,” *Biomedicine & pharmacotherapy = Biomedicine & pharmacotherapie*, vol. 105, pp. 582–589, 2018.
- [20] L. H. Ren, W. X. Chen, S. Li et al., “MicroRNA-183 promotes proliferation and invasion in oesophageal squamous cell carcinoma by targeting programmed cell death 4,” *British Journal of Cancer*, vol. 111, no. 10, pp. 2003–2013, 2014.
- [21] Y. Ichigotani, K. Fujii, M. Hamaguchi, and S. Matsuda, “In search of a function for the E3B1/Abi2/Argbp1/NESH family (review),” *International Journal of Molecular Medicine*, vol. 9, no. 6, pp. 591–595, 2002.
- [22] K. Miyazaki, S. Matsuda, Y. Ichigotani et al., “Isolation and characterization of a novel human gene (NESH) which encodes a putative signaling molecule similar to e3B1 protein,” *Biochimica et Biophysica Acta*, vol. 1493, no. 1–2, pp. 237–241, 2000.
- [23] F. R. Latini, J. P. Hemerly, B. C. G. Freitas, G. Oler, G. J. Riggins, and J. M. Cerutti, “ABI3 ectopic expression reduces in vitro and in vivo cell growth properties while inducing senescence,” *BMC Cancer*, vol. 11, no. 1, p. 11, 2011.
- [24] Z. Tang, C. Li, B. Kang, G. Gao, C. Li, and Z. Zhang, “GEPIA: a web server for cancer and normal gene expression profiling and interactive analyses,” *Nucleic Acids Research*, vol. 45, no. W1, pp. W98–W102, 2017.
- [25] L. Wang, F. Zhu, H. Yang et al., “Epidermal growth factor improves intestinal morphology by stimulating proliferation and differentiation of enterocytes and mTOR signaling pathway in weaning piglets,” *Science China Life Sciences*, vol. 63, no. 2, pp. 259–268, 2020.
- [26] Q. Guo, F. Li, Y. Duan et al., “Oxidative stress, nutritional antioxidants and beyond,” *Science China Life Sciences*, vol. 63, no. 6, pp. 866–874, 2020.
- [27] G. Guan, S. Ding, Y. Yin, V. Duraipandiyan, N. A. al-Dhabi, and G. Liu, “Macleaya cordata extract alleviated oxidative stress and altered innate immune response in mice challenged with enterotoxigenic *Escherichia coli*,” *Science China Life Sciences*, vol. 62, no. 8, pp. 1019–1027, 2019.
- [28] L. Zou, X. Xiong, H. Yang et al., “Identification of microRNA transcriptome reveals that miR-100 is involved in the renewal of porcine intestinal epithelial cells,” *Science China Life Sciences*, vol. 62, no. 6, pp. 816–828, 2019.
- [29] N. Lin, Z. Yao, M. Xu et al., “Long noncoding RNA MALAT1 potentiates growth and inhibits senescence by antagonizing ABI3BP in gallbladder cancer cells,” *Journal of Experimental & Clinical Cancer Research*, vol. 38, no. 1, p. 244, 2019.
- [30] N. Uekawa, K. Terauchi, A. Nishikimi, J. I. Shimada, and M. Maruyama, “Expression of TARSH gene in MEFs senescence and its potential implication in human lung cancer,” *Biochemical and Biophysical Research Communications*, vol. 329, no. 3, pp. 1031–1038, 2005.
- [31] K. Terauchi, J. Shimada, N. Uekawa, T. Yaoi, M. Maruyama, and S. Fushiki, “Cancer-associated loss of TARSH gene expression in human primary lung cancer,” *Journal of Cancer Research and Clinical Oncology*, vol. 132, no. 1, pp. 28–34, 2006.
- [32] F. R. M. Latini, J. P. Hemerly, G. Oler, G. J. Riggins, and J. M. Cerutti, “Re-expression of ABI3-binding protein suppresses thyroid tumor growth by promoting senescence and inhibiting invasion,” *Endocrine-Related Cancer*, vol. 15, no. 3, pp. 787–799, 2008.
- [33] P. Han, J. W. Li, B. M. Zhang et al., “The lncRNA CRNDE promotes colorectal cancer cell proliferation and chemoresistance via miR-181a-5p-mediated regulation of Wnt/ β -catenin signaling,” *Molecular Cancer*, vol. 16, no. 1, p. 9, 2017.
- [34] T. Gutschner, G. Richtig, M. Haemmerle, and M. Pichler, “From biomarkers to therapeutic targets—the promises and perils of long non-coding RNAs in cancer,” *Cancer & Metastasis Reviews*, vol. 37, no. 1, pp. 83–105, 2018.
- [35] X. Hou, J. Wen, Z. Ren, and G. Zhang, “Non-coding RNAs: new biomarkers and therapeutic targets for esophageal cancer,” *Oncotarget*, vol. 8, no. 26, pp. 43571–43578, 2017.
- [36] Y. Ichigotani, S. Yokozaki, Y. Fukuda, M. Hamaguchi, and S. Matsuda, “Forced expression of NESH suppresses motility and metastatic dissemination of malignant cells,” *Cancer Research*, vol. 62, no. 8, pp. 2215–2219, 2002.
- [37] T. Wakoh, N. Uekawa, K. Terauchi et al., “Implication of p53-dependent cellular senescence related gene, TARSH in tumor suppression,” *Biochemical and Biophysical Research Communications*, vol. 380, no. 4, pp. 807–812, 2009.

Review Article

Research Progress on NK Cell Receptors and Their Signaling Pathways

Yingying Chen ¹, Dan Lu ¹, Alexey Churov ², and Rong Fu ¹

¹Department of Hematology, General Hospital of Tianjin Medical University, China

²Institute of Biology, Karelian Research Centre, Russian Academy of Sciences, Petrozavodsk, Russia

Correspondence should be addressed to Alexey Churov; achurov@yandex.ru and Rong Fu; furong8369@tmu.edu.cn

Received 15 March 2020; Revised 25 May 2020; Accepted 20 June 2020; Published 24 July 2020

Guest Editor: Guan Yang

Copyright © 2020 Yingying Chen et al. This is an open access article distributed under the Creative Commons Attribution License, which permits unrestricted use, distribution, and reproduction in any medium, provided the original work is properly cited.

Natural killer cells (NK cells) play an important role in innate immunity. NK cells recognize self and nonself depending on the balance of activating receptors and inhibitory receptors. After binding to their ligands, NK cell receptors trigger subsequent signaling conduction and then determine whether NK is activated or inhibited. Furthermore, NK cell response includes cytotoxicity and cytokine release, which is tightly related to the activation of NK cell-activating receptors and the inhibition of inhibitory receptors on the surfaces of NK cells. The expression and function of NK cell surface receptors also alter in virus infection, tumor, and autoimmune diseases and influence the occurrence and development of diseases. So, it is important to understand the mechanism of recognition between NK receptors and their ligands in pathological conditions and the signaling pathways of NK cell receptors. This review mainly summarizes the research progress on NK cell surface receptors and their signal pathways.

1. Introduction

NK cells are crucial immune cells and enormously contribute to the innate immunity. NK cells can differentiate self from nonself by activating receptors and inhibitory receptors. NK cells exhibit natural cell cytotoxicity and directly destroy tumor cells or virally infected cells. Besides, NK cells play crucial roles in regulating various hematopoietic, inflammatory, and immune responses by secreting cytokines and chemokines [1, 2]. Therefore, it is necessary to understand the function of different surface NK cell receptors and their mechanisms of action. This article will summarize the existing research on NK cell receptors as well as their signaling pathways.

2. The Classification of NK Cell Receptors

Dozens of NK cell receptors have been discovered to date. These can be classified into the immunoglobulin superfamily (Ig-SF) and C-type lectin superfamily (CL-SF) according to their structure [3]. The Ig-SF includes killer cell immunoglobulin receptors (KIRs) [3, 4], leucocyte

immunoglobulin-like receptors (LILRs/LIRs) [5], and natural cytotoxic receptors (NCRs) [6]. The CL-SF mainly includes killer cell lectin-like receptors (KLRs) [7].

NK cell receptors can be divided into two types according to functional classification [8]: inhibitory receptors and activating receptors. Inhibitory receptors mainly include KIR-2DL, KIR-3DL, CD94/NKG2A, and TIGIT. Activating receptors mainly contain KIR-2DS, KIR-3DS, NCR (NKp46, NKp44, and NKp30), NKG2D, 2B4, CD226, CD94/NKG2C, etc. In this volume, we will discuss NK cell receptors, respectively.

3. Inhibitory Receptors

NK cells express various inhibitory receptors. Most of inhibitory receptors, by identifying MHC class I molecules, conduct inhibitory signals to suppress NK cell function and participate in autoimmune tolerance under physiological conditions to avoid killing normal cells. In addition, some non-MHC-restricted inhibitory receptors are also focused on the immune escape of tumor cells and virally infected cells under pathological conditions.

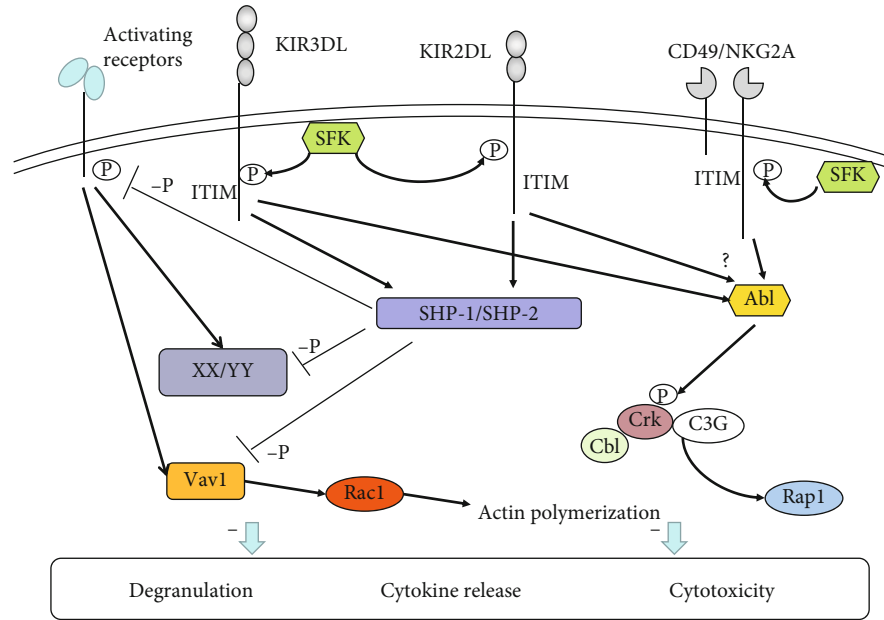


FIGURE 1: Signaling pathways of inhibitory receptors in NK cells. After KIR2DL, KIR3DL, and CD49/NKG2A bind to their corresponding ligands, the ITIM sequences are phosphorylated by Src-family kinase (SFK). Furthermore, the phosphorylated ITIM recruits SHP-1/SHP-2, which downregulates the phosphorylation level of the downstream signaling molecules (XX/YY) of activating receptors, including Vav1, thereby inhibiting NK cell function. In addition, Crk binds to Abl and is phosphorylated by Abl, which separates Crk from the Cbl-Crk-C3G complex, further inhibiting NK cell function.

3.1. Inhibitory Killer Cell Immunoglobulin Receptors (IKIRs).

KIRs belong to the Ig-SF. According to the structure of extracellular region, KIRs are divided into two categories, namely, KIR2D with two Ig-like domains and KIR3D with three Ig-like domains. KIR2DL and KIR3DL are inhibitory receptors that have longer intracellular tails with the immunoreceptor tyrosine-based inhibitory motifs (ITIMs) [4]. Other members are defined as an S to reflect their short ITIM-lacking intracellular region (KIR2DS and KIR3DS), which associate with adaptor proteins through the transmembrane region. These adaptor proteins help to deliver activating signals by means of immunoreceptor tyrosine-based activating motifs (ITAMs) in their intracellular region [9, 10]. The majorities of KIRs are highly specific for classic MHC-I molecules (HLA-A, HLA-B, and HLA-C) [4]. For instance, KIR2DL1, KIR2DL2, and KIR2DL3 are specific receptors for HLA-C molecules, and KIR3DL1 and KIR3DL2 can combine with HLA-A or HLA-B. Unlike other KIRs, KIR2DL4 recognizes both soluble and membrane HLA-G. However, in endosomes, only when KIR2DL4 binds to soluble HLA-G can the signals be transmitted [11].

When the inhibitory receptor recognizes its corresponding ligand, Src-family kinase (SFK) mediates the phosphorylation of ITIM sequences in the inhibitory receptor immediately [12]. After phosphorylation, ITIMs activate protein tyrosine phosphatases (PT-Pases), mainly including Src homology region 2-containing protein tyrosine phosphatase-1 (SHP-1) and Src homology region 2-containing protein tyrosine phosphatase-2 (SHP-2) [13–15]. As an effector molecule of inhibitory receptor, SHP-1 downregulates multiple activating signal molecules by dephosphorylation [16, 17] (Figure 1). Thus, SHP-1 plays

a crucial role in initiating inhibitory signals and blocking activating signals, and the substrates of SHP-1 need to be further identified. During the repression of NK cells by ITIM-containing receptors, the tyrosine phosphorylation level of multiple proteins is downregulated [17]. Previously, it was viewed that the directly identified substrate of SHP-1 is Vav1. Vav1 can promote rac1-dependent cytoskeletal rearrangement, synapse formation, and receptor aggregation. However, SHP-1-catalyzed dephosphorylation of Vav1 does not depend on actin polymerization in inhibitory signaling [18]. This may suggest that ITIM-containing inhibitory receptors' repression of NK cell activation before the actin-dependent signals occurs and even before tyrosine phosphorylation of activating receptors [8, 18]. In 2016, researchers found that LAT and PLC γ 1/2 served as the substrates of SHP-1 when NK cells were inhibited by MHC-restricted inhibitory receptor KIR2DL1 [19]. Besides, LAT could be ubiquitinated by c-Tcbl and Cbl-b and degraded in inhibitory condition of NK cells [19]. They also confirmed that LAT:PLC γ 1/2 complexes were necessary for degranulation and cytotoxicity of NK cells [19]. ITIM-containing receptors of NK cells are also involved in the downstream pathways when transmitting inhibitory signals. Peterson and Long found that when NK cells interacted with target cells expressing the MHC-I molecules, the adaptor Crk could associate with tyrosine kinase Abl and be phosphorylated [20]. Crk binding to Abl and phosphorylation are essential steps for the separation of Crk from the Cbl-Crk-C3G complex, a part of the activating signal pathway. These results point out that phosphorylation also plays a significant role in NK cell inhibitory signaling pathways (Figure 1). Overall, NK cell inhibitory receptors induce Vav1, LAT,

and PLC γ 1/2 dephosphorylation and Crk phosphorylation, which inhibit the NK cell activation signal and eventually inhibit NK cell activity. Moreover, inhibitory receptors, which recognize the MHC-I molecules, can provide a license for NK cell responsiveness [21]. The functions of inhibitory receptors, whatever inhibition or licensing, require the participation of activating receptor signal molecules. Therefore, the downstream molecules of SHP-1 and SHP-2 need to be observed further, and much work remains to be done in how inhibitory receptors conduct inhibitory signals and inhibit NK cell function. The connection between inhibitory receptors and activating receptors remains to be investigated further.

KIR2DL4 only carries a single ITIM in the intracellular tail, and its transmembrane region contains an arginine residue, which suggests that KIR2DL4 has dual functions of inhibition and activation [22]. Although functional KIR2DL4 is mainly located in endosomes, studies have demonstrated that IL-2 can transiently upregulate the expression levels of KIR2DL4 on NK cell surfaces, *in vitro*, and it is closely related to the NK cell function [23]. Further research showed that KIR2DL4 on the NK cell surface noncovalently associated with Fc ϵ RI γ via arginine residues and then activated ITAM signal transduction [24]. KIR2DL4 is expressed in endosomes and is associated with proinflammatory and angiogenic functions through the DNA-PKCs-Akt-NF- κ B signaling pathway [11, 25]. Studies found that KIR2DL4 can connect to SHP-1 and SHP-2 through pull-down experiments, suggesting that KIR2DL4 has inhibitory potential [22]. Moreover, other studies showed that the ITIMs of KIR2DL4 could inhibit the cytotoxic effect of NK cells, while functionally mutated SHP-1 did not block the cytotoxic effect of KIR2DL4 completely [15], suggesting that the phosphorylated ITIM of KIR2DL4 recruits SHP-2 instead of SHP-1. Further research showed that the tyrosine residue of the mutated ITIM motif did not thoroughly abrogate the function of KIR2DL4, which may be related to SHP-2 binding to the mutated ITIMs and nonphosphorylated ITIMs of KIR2DL4 on NK cells [15]. These results suggest that KIR inhibitory signal transduction is partially independent of SHP-1 or phosphotyrosine. Similarly, KIR2DL5 has typical ITIM sequences and an atypical ITIM in the intracellular region and can recruit both SHP-1 and SHP-2 simultaneously [26]. The cytotoxicity of NK cells can be suppressed by functionally mutated SHP-2 instead of functionally mutated SHP-1. These studies indicate that KIR2DL5 might have a more obvious inhibitory function [15]. In addition, KIR3DL1 directly binds to SHP-2 through conformational changes in the intracellular region, inhibiting target cell conjugation and cytotoxicity function [14, 27].

3.2. CD94/NKG2A and LIRs. Killer cell lectin-like receptor (KLR, CD49/NKG2) is a heterodimeric receptor that combines CD94 with different NKG2 family members through disulfide bonds [28]. KLR can be detected on most NK cell membranes. The NKG2A intracellular segment contains an ITIM, which transduces inhibitory signals [7]. The NKG2C intracellular segment is shorter and does not contain ITIM sequences, but it can bind to the ITAM-containing adaptor

proteins to conduct activation signals [29]. The ligands of both CD49/NKG2A and CD49/NKG2C are types of the non-classical MHC molecule, HLA-E [30]. Under normal conditions, HLA-E has a greater affinity for NKG2A than for NKG2C. Under stress, the HLA-E molecules of “stressed” cells bind to the polypeptide containing heat shock protein 60 (HSP60), which decreases HLA-E affinity with NKG2A and increases affinity with NKG2C, thus activating NK cells [31]. Other studies have shown that NKG2A is associated with immune escape. Senescent dermal fibroblasts express HLA-E, which binds to the NKG2A and suppresses the immune reaction of senescent cells [32]. CD94/NKG2A could inhibit the synergistic effect of activating receptors NKG2D and 2B4 [33, 34]. Moreover, CD94/NKG2A complex could inhibit the CD16-dependent activation of Syk and ERK [35]. Those results showed that the activation signals of NK cells can be blocked by inhibitory receptors in multiple levels.

LIRs belong to the Ig-SF, which have ITIM sequences transmitting inhibitory signals in intracellular regions [5]. LIRs contain multiple members such as LIR1, also named Ig-like transcript 2 (LIT2), LIR2/ILT4, etc. The ligands of LIR1/ILT2 are multiple MHC class I molecules (HLA-A, HLA-B, and HLA-G) [36–38] and UL18 glycoprotein from human cytomegalovirus [5]. The signaling pathways of LIRs and CD49/NKG2A are similar to IKIR inhibitory signaling pathways [8, 13], which can recruit SHP-1 to block the activating signals. The role of LIRs and CD94/NKG2A is to establish a threshold for NK cell activation to protect the normal cells. However, when the host is in a pathological state, the expression and function of those inhibitory receptors are abnormal, which would not be conducive to disease development. Scientists can research targeted drugs to restore the cytotoxicity of NK cells according to the mechanism of those inhibitory receptors.

3.3. ITIM-Containing Non-MHC Ligand Receptors. Besides the above receptors, NK cells still express many other intracellular ITIM-containing receptors on the surface [13, 39]: NKR-P1 (CD161), KLRG1, Siglec-7 (CD328), LAIR-1 (CD305), CEACAM-1, PILR α , TACTILE (CD96), TIGIT, etc. Among them, TIGIT, a non-MHC-I molecule-dependent inhibitory receptor, can recognize CD113, CD112, and CD155. And TIGIT is correlated to the maturation of NK cells and NK cell-mediated autoimmune tolerance [40].

4. Activating Receptors

There are multiple MHC-dependent or MHC-independent activating receptors on NK cells such as NKG2D, NCRs, and 2B4. Under physiological conditions, inhibitory receptors play a leading role in preventing NK cells from killing normal cells. However, when the MHC class I molecules on target cells are attenuated or absent, or the specific ligands directly recognize activating receptors, the inhibitory signal is weakened and the activation signal is enhanced, resulting in NK cells exhibiting killing effects. Activating receptors cannot activate NK cells on their own, except for CD16.

Therefore, the activation of NK cells requires the synergy of multiple receptors.

4.1. Natural Cytotoxic Receptor (NCR). NCRs are specific surface markers of NK cells, as well as major activating receptors of NK cells. The NCR family includes three members: NKp46 (NCR1, CD335), NKp44 (NCR2, CD336), and NKp30 (NCR3, CD337) [6].

NKp46-encoding genes are on human chromosome 19. The intracellular region of NKp46 does not have ITAM sequences. However, the transmembrane region of NKp46 contains an arginine residue that takes charge of associating with adaptors, Fc ϵ RI γ and CD3 ζ , which can conduct activating signals [41]. The ligands of NKp46 include [42] (1) tumor cell ligands, such as ligands from melanoma and myeloma (but most of the tumor cell ligands are still unknown); (2) viral ligands, such as hemagglutinin (HA), hemagglutinin neuraminidase (HN); (3) bacterial ligands, such as vimentin on the mycobacterium tuberculosis-infected cell surfaces; and (4) parasitic ligands, such as Plasmodium falciparum erythrocyte membrane protein (PfEMP1). In addition, NKp46 can also identify complement factor P and unknown ligands on the hepatic stellate cells and pancreatic B cells, inhibit liver fibrosis, and participate in the pathogenesis of type I diabetes. All of the mature NK cells express NKp46 which acts a crucial role in triggering NK cell killing. The expression of NKp46 is related to the cytotoxic effect of NK cells [43]. The binding of NKp46 with the ligand can promote the killing ability of NK cells, increase the secretion of IFN- γ and TNF- α , and participate in the process of anti-infective immunity and killing tumor cells.

NKp46 transmits activating signals through ITAM-related receptors, which is similar to how most activating signals of NK cells are transmitted. The ITAM-containing adaptor proteins mainly include DAP12, FcR γ , DAP10, and CD3 ζ . NK cells can constitutively express the type I transmembrane proteins Fc ϵ RI γ , CD3 ζ , and DAP12. After binding to the ligands, NKp46 associates with the adaptor proteins CD3 ζ and Fc ϵ RI γ [42]. Then, the ITAMs of adaptors are phosphorylated, which may be mediated by Src-family kinases such as Lck and Fyn [44]. Through the SH2 domain, the phosphorylated ITAM recruits and activates tyrosine kinases such as Syk and/or ZAP70 [45, 46]. The tyrosine kinases activate transmembrane adaptor proteins such as LAT and NTAT, leading to the activation of downstream molecules such as phospholipase C (PLC γ), phosphatidylinositol-3-OH kinase (PI3K), and Vav1, Vav2, and Vav3. PLC γ further causes Ca $^{2+}$ influx; PI3K and Vav1 recruit the small G protein Rac1 and induce cascade phosphorylation through the PAK1-MEK-Erk signaling pathway, further activating the MAPK signaling pathway and other reactions [9, 47–51]. Ultimately, these signaling cascades promote actin cytoskeleton rearrangement, degranulation, cytotoxicity, and the gene expression of cytokine or chemokine (Figure 2). NKp46 acts as a coactivation receptor which triggers NK cell cytotoxicity by synergistic effects with other activating receptors. Researches confirmed that NKp46 could coengage with 2B4, CD2, NKG2D, and DNAM-1, transmitting activation signals to enhance the Ca $^{2+}$ flux of NK cells

further [52, 53]. However, we still do not know if synergistic signals of NKp46 and other coactivation receptors are the same as the synergistic signals of NKG2D and 2B4.

The coding genes of NKp30 and NKp44 are both on human chromosome 6. The ligands of NKp30 contain the following [42]: (1) tumor cell ligands, such as B7-H6, BAG6/BAT3 (BCL2-associated athanogene 6/nuclear HLA-B-associated transcript-3 protein), and galectin-3; (2) viral ligands, such as HA of vaccinia virus and poxvirus and pp65 of human cytomegalovirus; and (3) parasitic ligands, such as Plasmodium falciparum erythrocyte membrane protein (PfEMP1). In addition, all NCRs, including NKp30, can recognize heparan sulfate glycosaminoglycans (HS-GAGs), which are significantly upregulated in tumor cells. The expression and signal transduction of NKp30 are similar to those of NKp46. NKp30 makes synergistic reaction with NKp46 and NKp44 in triggering the cytotoxicity of NK cells. Delahaye et al.'s group transfected NK cell lines with NKp30a, NKp20b, and NKp30c separately and found that NKp30a and NKp30b were immunostimulating subtypes that could mediate the production of Th1 cytokines, while NKp30c enhanced the secretion of IL-10 and transmitted suppressive signals through the rapid phosphorylation of p38 MAPK [54]. Overall, NKp30 plays an important role in anti-infection immunity and antitumor immunity and is involved in tumor immune escape mechanisms. However, how it works still needs to be explored. Studies have found that soluble BAG6, a specific ligand of NKp30, could be detected in chronic lymphocytic leukemia (CLL), and the plasma levels of soluble BAG6 were higher at the advanced disease stages [55]. Then, they found that the soluble BAG6 released from CLL cells could inhibit the cytotoxicity of NK cells [55]. In contrast, exosomal BAG6 could enhance the killing function of NK cells [55]. As we all know that tumor microenvironment can influence the antitumor effect of NK cells, so the phenomenon that one molecule plays opposite acts on increasing the complexity of antitumor immunity. This may provide a new idea for increasing the NK cell killing effects as immunotherapeutic strategies.

NKp44 is only expressed on activated NK cell surfaces as a specific marker of activated NK cells. NKp44 ligands include the following [42]: (1) tumor cell ligands, such as proliferating cell nuclear antigen (PCNA), platelet-derived growth factor DD (PDGF-DD), nidogen-1, and NKp44L (NKp44L, an isomer of mixed-lineage leukemia-5 protein (MLL5), is expressed in tumor cells and transformed cells that can improve cell sensitivity to the cytotoxicity of NK cells [56]); (2) viral ligands, such as HA and HN; and (3) bacterial ligands, such as Mycobacterium tuberculosis cell wall components. Furthermore, some subtypes of HLA-DP are also ligands of NKp44 [57]. The transmembrane region of NKp44 contains Lys residues that can associate with KAPA P/DAP12 and transmit activation signals through the ITAM of KAPAP/DAP12. DNAX-activation protein of 12 kDa (DAP12; also named as killer cell-activating receptor-associated protein (KARAP)) is an adaptor protein containing a single ITAM in its intracellular domain [9, 10, 58]. The tyrosine residues in ITAM domain are rapidly phosphorylated under the action of the tyrosine kinase Syk after

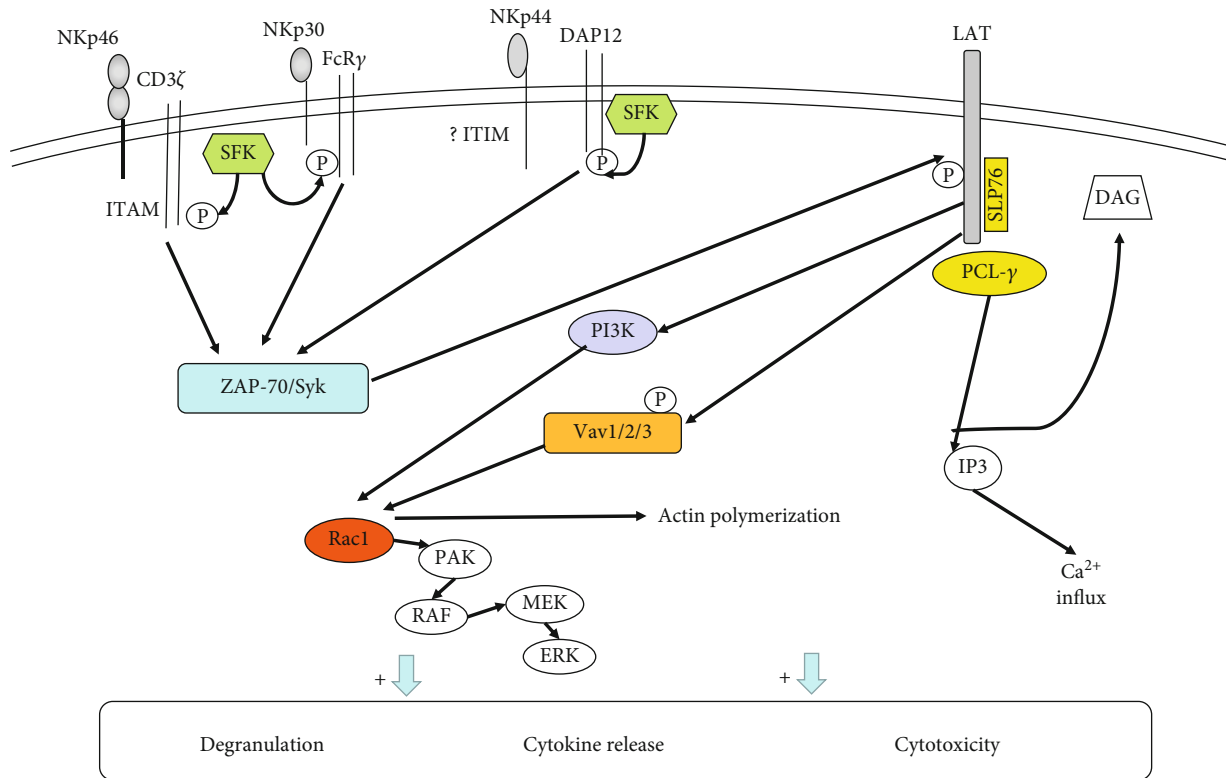


FIGURE 2: Model of signaling pathways by NCRs. After binding to their ligand, NKp46 and NKp30 associate with the adaptors FcεRIγ and/or CD3ζ, while NKp44 binds to DAP12. Furthermore, ITAMs in the adaptor protein intracellular regions are phosphorylated by SFK. Phosphorylated ITAMs activate the tyrosine kinases Syk and/or ZAP70. This recruits and activates downstream molecules such as PLCγ, PI3K, and Vav1/2/3 with the help of LAT. PLCγ further causes Ca²⁺ influx. PI3K and Vav1 can recruit the small G protein Rac1 and activate the MAPK signaling pathway through cascade phosphorylation of the PAK1–MEK–Erk signaling pathway. In addition, the intracellular region of NKp44 contains an ITIM sequence that may be related to inhibitory signaling, but the specific mechanism is not yet clear.

NKp44 receives stimulation. Further phosphorylation of the ITAM recruits Syk and ZAP-70. This pathway mediates downstream signal transduction and then activates NK cell function [9, 45] (Figure 2). Research has found that the intracellular domain of NKp44 contains a sequence consistent with the ITIM sequence [59]. Further studies have shown that this special sequence of NKp44 could be efficiently phosphorylated, but it was not able to inhibit NK cell function by recruiting of SHP-1, SHP-2, and SHIP [59]. Next, it still needs more researches to explore the mechanism of ITIM sequence as well as the phosphorylation of NKp44 and its function in signal conduction. Another study found that tumor cells could overexpress PCNA, which can associate with HLA I molecules forming an inhibitory ligand complex. NKp44 can recognize the complex ligand and suppress the NK cell killing activity through its ITIM sequences [60, 61].

The expression of NCRs can be influenced by many factors, such as cytokines, drugs, disease status, and epigenetic changes. For example, IL-2 increases the expression of NKp46 as well as enhances the killing effect of NK cells [62]. On the other hand, transforming growth factor-β (TGF-β) can downregulate the transcriptional level of NKp30 [63]. Drugs can also affect NCR expression. For instance, prolactin can upregulate the expression of NKp30 and NKp46, whereas corticosteroids have the opposite effect

[64]. Meanwhile, the expression level of NCR on NK cells and the expression level of NCR ligands on tumor cells were related to the cytotoxicity of NK cells [42]. Furthermore, studies have found that multiple genes associated with NK cell surface receptors are upregulated following epigenetic changes [65]. TCRβ⁺NKp46⁺ cells increase in the spleen, liver, and bone marrow of Ezh2^{-/-} mice, and human NK cells that expressed NKp46 also increase when selectively inhibiting Ezh2 activity, in vitro [66]. Further investigations on the influence factors of NK cell-activating receptors will be beneficial for understanding the roles of NK cells in various diseases and provide more ideas for NK cell-based immunotherapies in cancer.

4.2. NKG2D. NKG2D is a member of CL-SF and effects in activation signal transduction. It is a major activating receptor expressed on NK cells and CD8⁺ T cells in a dimer form [67]. The coding genes of NKG2D are located on chromosome 12 [67]. NKG2D can recognize multiple ligands such as MHC class I chain-related molecules (MICA and MICB) and human cytomegalovirus ULL6-binding proteins (ULBP1, ULBP2, ULBP3, ULBP4, ULBP5, and ULBP6) [67–70]. There are two different adaptor proteins, DAP10 and DAP12, both of which can associate with NKG2D and mediate activation via two different signaling pathways [71].

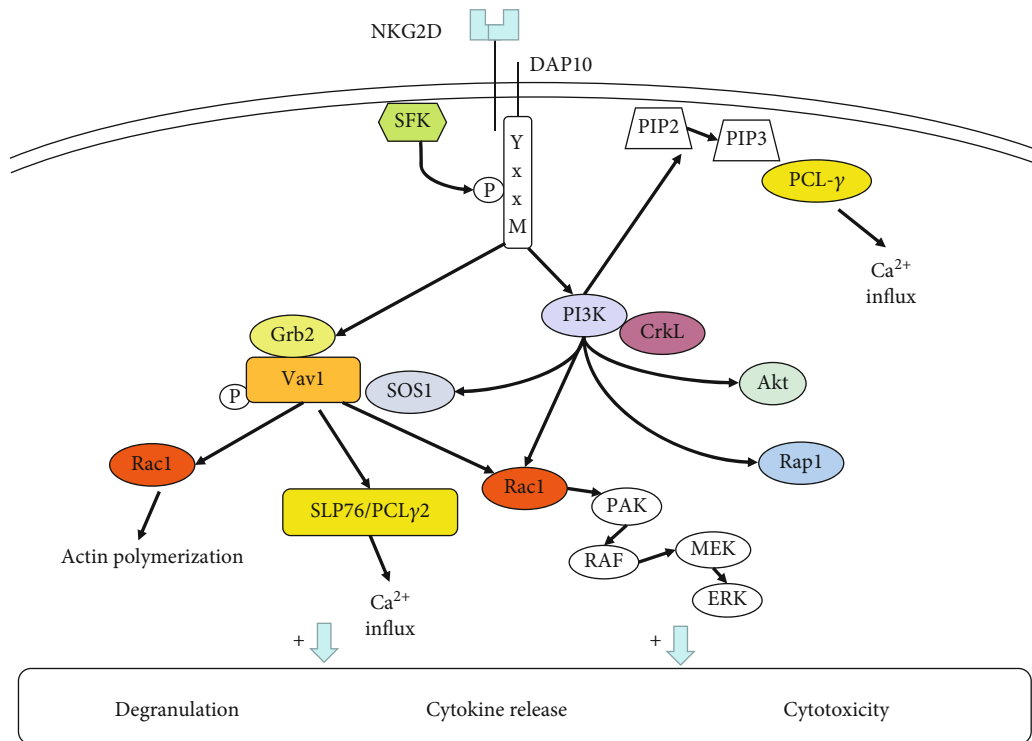


FIGURE 3: NKG2D signaling pathways. After DAP10 associates with NKG2D, it can bind to PI3K and the Grb2-Vav-1-SOS1 complex. The Grb2-Vav-1-SOS1 complex activates SLP76, PLC γ 2, and Rac1. Rac1 can activate the MAPK signaling pathway and promote actin polymerization. SLP76/PLC γ 2 causes Ca²⁺ influx. Furthermore, it leads to cellular degranulation and secretion of cytokines. PI3K can recruit PCL- γ , Rac1, and Akt signaling molecules to activate NK cell function. In addition, PI3K can recruit the SOS1-Grb2-Vav1 complex via SOS1 and recruit the small Ras-family GTPase Rap1 with the help of CrkL to achieve cytotoxicity.

Studies have shown that there are two NKG2D splicing variants in mouse NK cells [72]. Resting NK cells express the longer protein (NKG2DL), which can associate with DAP10 only [73]. In contrast, activated NK cells express the shorter protein (NKG2DS) which can associate with either DAP10 or DAP12. Human NK cells express NKG2DL simply, so the intracellular tail of human NKG2D associates with DAP10 exclusively.

As a critical activating receptor, through noncovalent binding to the adaptor protein DAP10, NKG2D can achieve multiple forms of signal transduction through phosphorylation by activating mitogen-activated protein kinase (MAPK) and Janus kinase (Jak)/signal transducer and activation of transcription (STAT) signaling [68, 74]. The intracellular segment of DAP10 contains a YxxM motif, which can bind to p85 PI3K, Grb2, and Shc [9]. Experimental results indicated that after the cross-linking of DAP10 and NKG2D, DAP10 could bind p85 PI3K and the Grb2-Vav-1-SOS1 complex to activate Akt/PKB [75–77]. However, there is no evidence that DAP10 can recruit Syk and/or ZAP-70 [75]. This indicated that DAP10 might transmit activation signals through different pathways than DAP12 and Fc ϵ RI γ . After DAP10 recruits PI3K and the Grb2-Vav1 complex, SLP76 and PLC γ 2 are activated [51, 75, 77]. Activation signals eventually promote Ca²⁺ influx, cellular degranulation, and secretion of cytokines. Giurisato et al. reported that PI3K catalyzed the generation of PIP3, which can recruit the SOS1-Grb2-Vav1 complex via SOS1 [78].

Segovis et al. found that the interaction between p85 PI3K and the adaptor protein CrkL was required for NK cell activation [79]. PI3K and CrkL can further recruit the small Ras-family GTPase Rap1, which is necessary for NKG2D-mediated cytotoxicity, conjugate formation, and MTOC polarization [79] (Figure 3).

The expression and function of NKG2D are modulated by multiple factors. The ligands of NKG2D can affect the function of NKG2D. MICA can upregulate the expression of NKG2D and downregulate the expression of the inhibitory receptors NKG2A, NKG2B, and KIR2DL1. And then, NKG2D stimulates the cytotoxicity of NK cells on tumor cells. In contrast, soluble MICA can suppress the expression of NKG2D and inhibitory receptors [80]. Similarly, soluble ULBP also downregulate NKG2D expression on NK cells [80]. The soluble NKG2D ligands (NKG2DL) released from tumor cells may be a means of tumor immune escape in tumor microenvironment. In contrast, the binding of NKG2D to NKG2DL on the tumor cells can promote the killing effect of NK cells on tumor cells. However, tumor cells can change the expression of NKG2DL with various mechanisms to escape the attack mediated by NKG2D [81]. Martinet et al. showed that tumor cells secreted PGE2, inhibiting the activating signals of NKG2D, NCR, and CD16 on NK cells, thereby inhibiting tumor cells from being attacked by NK cells [82]. The mechanism may be related to the activation of EP2/EP4 receptors on NK cells via PGE2, which activates type I PKA and leads to Csk phosphorylation. Csk

mediates Lck inactivation, preventing it from allowing activating receptors to bind to adaptor proteins, and then inhibits the transmission of activating signals. Sustained activation of NKG2D on NK cells decreases the reaction of other receptors, such as CD16 and NKp46 [83]. Otherwise, when NKG2D is combined with the natural receptor MICB, it will cause rapid endocytosis and degradation of NKG2D and DAP10 [84]. Studies have found that epigenetic changes regulate the expression and function of NKG2D [66]. Researchers found that higher levels of NKG2D on NK cells compared to wild type could be detected during Ezh2 deletion or inhibition of Ezh2 activity [66]. Researchers established an NKG2D-deficient mouse model (*Klrk1*^{-/-}) and found that NKG2D deficiency affected maturation of NK subsets, leading to decreased NK cell numbers [85]. Using the *Klrk1*^{-/-} mouse model, researchers have found that Ezh2 activity inhibition can enhance the NK cell development, which requires the NKG2D expression [66]. Furthermore, inhibition of Ezh2 activity can upregulate the NKG2D-dependent cytotoxicity [66].

NKG2D activates NK cells by cooperating with other activating receptors, such as CD16, NKp46, and 2B4 [53, 86]. The synergistic activation signals will be introduced below. It is noteworthy that activation of NK cells is tightly associated with the signals of coactivation receptors. NKG2D also participates in regulating the function of other receptors. In 2018, Jelencic et al. found that *Klrk1*^{-/-} mice had a stronger ability to inhibit tumor and cytomegalovirus infection during NK cell development than wild-type mice [87]. Subsequently, they found that deficiency of NKG2D or DAP12 could downregulate CD3 γ and ZAP70, resulting in the upregulation of NCR1 signals [87]. This indicated that NKG2D can regulate the expression of NCR1 by setting an activation threshold.

4.3. CD244 (2B4). 2B4 belongs to the signaling lymphocytic activation molecule (SLAM) family of CD2-related receptors [88]. It is expressed on all NK cells, CD8⁺ T cells, monocytes, and other immune cells [89]. 2B4 takes part in NK cell activation and participates in leukocyte differentiation [89, 90]. The specific ligand of 2B4 is CD48, which is also a member of CD2 subfamily. CD48 is generally expressed on hematopoietic-origen cells and parts of EBV-infected B cells. The intracellular region of 2B4 contains immunoreceptor tyrosine-based switch motifs (ITSMs), which are composed of TxYxxV/1 [91]. The SH-2-containing adaptor proteins SAP, EAT-2 (human), and ERT (rat) can associate with ITSM sequences [91, 92]. The binding of 2B4 to ligands causes ITSMs to undergo tyrosine phosphorylation under the action of SFK and recruits adaptor proteins. In humans, the ligand is mainly SAP. SAP combines with ITSMs to recruit FynT [93, 94]. FynT phosphorylates downstream proteins such as PLC γ and Vav1 [95]. The 2B4-SAP complex can trigger NK cell activation. Otherwise, SAP is capable of promoting the combination of EAT2 and 2B4, which indicates that SAP plays a crucial role in EAT2-related signal pathways [96]. Some studies showed that EAT-1 suppressed the cytotoxicity and IFN- γ secretion of NK cells [97]. In contrast, some studies proved that EAT-2 may be capable of promot-

ing NK cell cytotoxicity, granule polarization, and degranulation by the activation of PLC γ , Ca²⁺, and Erk [98, 99]. Overexpression of EAT-2 can enhance the NK cell antitumor activity [100]. The function of EAT-2 may be correlated to the environment of NK cells. When SAP is absent, 2B4 can conduct inhibitory signals through recruiting SHP-1, SHP-2, SHIP, and Csk and block NK cell activity [98, 101] (Figure 4). Research has proven that 2B4 can dephosphorylate P27 by activating the SHP-2 signaling pathway, which plays an important role in maintaining the development of leukemia-initiating stem cells [102]. However, there is much work to be done about how do SHP-1 and SHP-2 work in the 2B4 signal pathway. Does 2B4 conduct inhibitory signals through SHP-1 or SHP-2? It is needed to mention that deletion or functional mutation of SAP can result in a severe hereditary immunodeficiency disease, X-linked lymphoproliferative disease (XLP). SAP function loss results in a decrease in NK cell anti-infection ability in XLP patients, and patients are having difficulty to control Epstein-Barr virus infection [103]. Current studies suggest that 2B4 exhibits different effects during NK cell development and maturation. In the early stage of NK cell maturation, 2B4 only inhibited NK cells and blocked the killing activity of NK cells, suggesting that 2B4 contains potential suppression effect [104]. After NK cells mature, the function of 2B4 depends on the balance between different signaling molecule complexes. Studies have shown that the function of 2B4 is influenced by several factors: the expression density of 2B4, the expression level of its ligands, and the relative content of certain adaptor molecules [105].

Similar to NKG2D, 2B4 acts as an NK cell coreceptor in combination with its ligand CD48 to take effect [106]. Its function of transmitting signals in most cases relies on the participation of other activating receptors, such as NCRs, NKG2D, and CD226. Then, 2B4 and the coactivation receptor activate NK cell cytotoxic effect and IFN- γ production synergistically and play an important part in antiviral and antitumor immunity. But how does synergistic signal transmit? Researchers found that coactivation receptors, NKG2D and 2B4 or 2B4 and DNAM-1, could conduct synergistic signals by phosphorylating Vav1 and then, PLC γ 2 and ERK were phosphorylated [33]. Further, phosphorylated PLC γ 2 and ERK induced the Ca²⁺ mobilization, cytotoxic degranulation, and the secretion of INF- γ [33]. NKG2D and 2B4 each one activated alone could phosphorylate Vav1, but only NKG2D and 2B4 synergy could induce degranulation [33], which may be associated with the ubiquitination in Vav1 induced by c-Cbl. c-Cbl could inhibit the activation of NK cells through a Vav1-dependent way, and consequently, synergy of coactivation receptors is required to overcome negative regulation of c-Cbl [33]. On the other hand, the activation signals from different coactivation receptors need to be integrated before Vav1, which need the phosphorylation of adaptor protein SLP76 by each coactivation receptor [107] (Figure 5). The phosphorylation of SLP76 in Y113 could be induced by the cross-linking of 2B4, and the phosphorylation of SLP76 in Y128 could be induced by the cross-linking of NKG2D or DNAM-1 [107]. For Y113 or Y128, each tyrosine phosphorylation of SLP76 was required

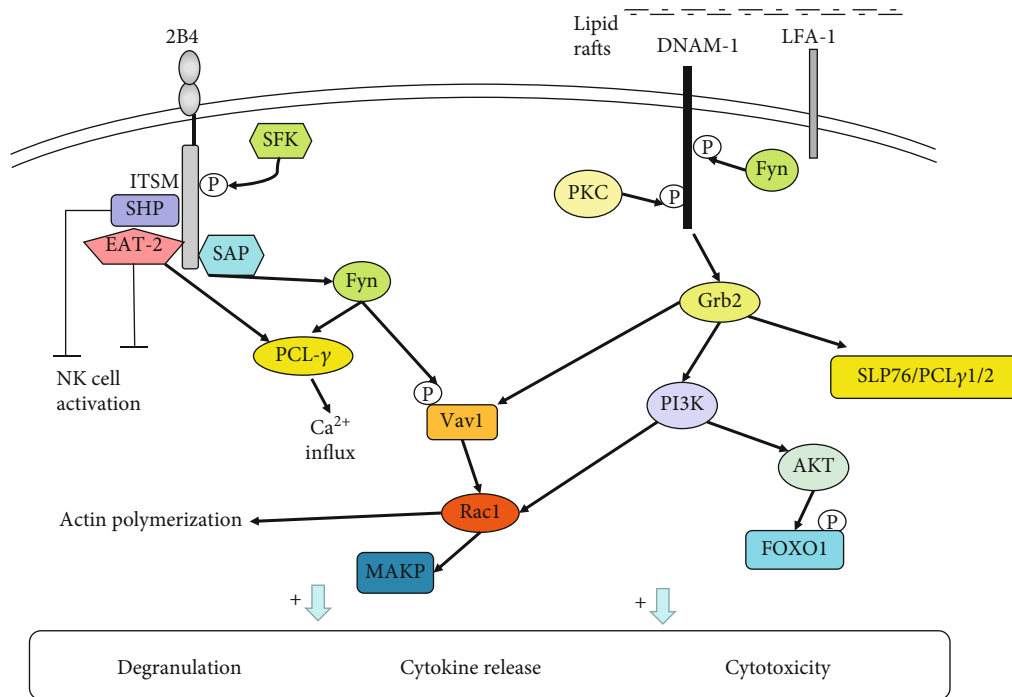


FIGURE 4: Signaling pathways of 2B4 and DNAM-1. Binding of 2B4 to CD48 promotes ITSM phosphorylation and recruits the adaptor SAP. SAP combines with ITSM to recruit Fyn, and Fyn phosphorylates the downstream proteins PLC γ and Vav1 to activate NK cells. 2B4 can also recruit the phosphatases SHP-1/SHP-2 in the absence of SAP, transmitting inhibitory signals. The 2B4-EAT2 complex may have opposite functions in NK cells. DNAM-1 binds to its ligand, and it is phosphorylated by PKC and Fyn, which promotes the interaction between DNAM-1 and LFA-1. Eventually, DNAM-1 is recruited to the lipid raft and binds to the adaptor Grb2. Binding of DNAM-1 to Grb2 enables PI3K, Vav1, SLP76, and PLC γ 1/2 to be recruited and then activates the AKT and ERK signaling pathways, thus triggering degranulation and calcium mobilization. In addition, activated AKT catalyzes FOXO1 phosphorylation. Phosphorylated FOXO1 is transferred from the nucleus to the intracellular space, where it is inactivated and degraded, regulating NK cell cytotoxicity and exerting antitumor effects.

for the synergistic activation of NK cells [107]. Therefore, the cooperation of NKG2D, 2B4, and DNAM-1 is necessary for NK cell activation. But how coactivation receptors phosphorylate the SLP76 still needs to be researched. Researchers found that the phosphorylation of SLP76 induced by 2B4 was Fyn-dependent, whereas the phosphorylation of SLP76 in Y128 induced by NKG2D was SYK-independent. Thus, there is much work required to be done about the signals for synergistic activation of NK cells, in the future.

NK-T-B antigen (NTB-A) belongs to the SLAM family and can be detected on all NK cells, T cells, and B cells [88]. The action mechanism of NTB-A is analogous to 2B4 [108]. It also plays a synergic effect with activating receptors to assist in the NK cell activation. Studies have shown that 2B4 and NTB-A can straightly recognize the HA of influenza virus via sialylation and induce the killing function of NK cells through costimulation. The virus can counteract this process by neuraminidase (NA), which indicates the action of 2B4 and NTB-A in antiviral immunity [109].

4.4. DNAM-1 (CD226). The DNAX-activating molecule (DNAM-1) gene is located on chromosome 18. DNAM-1 belongs to the Ig-SF and is expressed on the surfaces of NK cells, T cells, and monocytes, which participated in the formation of immunological synapses. It can transmit activating signals through synergetic effects with lymphocyte function-

associated antigen 1 (LFA-1) or 2B4. The ligands of DNAM-1 are CD112 (nectin-2, PRR2) and CD155 (PVR, Necl4), which are expressed in some immune cells such as monocytes, DCs, activated CD4⁺ T cells, and tumor tissue [110]. In DNAM-1-mediated cytotoxicity, PVR is the main ligand. In addition to DNAM-1, PVR can also interact with CD96 (TACTILE) and TIGIT. Under normal conditions, autologous cells express low levels of PVR, and TIGIT combined with PVR inhibits NK cell activation. However, during tumor formation, malignant cells highly express PVR, which can bind to DNAM-1 and CD96 activating the antitumor effects of NK cells [39, 111, 112].

The intracellular region of DNAM-1 contains a special signaling structure, which has four tyrosine residues Y293, Y300, Y322 (equivalent to Y319 in the murine orthologue), and Y325 and one serine residue, S329 (equivalent to Y326 in the murine orthologue) [113]. In a mouse model, the phosphorylation of Y319 and S326 has been shown to play a key role in DNAM-1 signaling pathways. DNAM-1 associates with LFA-1, which induces tyrosine kinase Fyn to phosphorylate Y319 on CD226. LFA-1 and DNAM-1 can physically bind during the process of immune synapse formation [113]. When LFA-1 is deficient, NK cells lose the killing function mediated by CD226 [113]. The phosphorylation of Y319 on DNAM-1 is very important for the function of LFA-1, and LFA-1 can promote the tyrosine kinase Fyn to phosphorylate

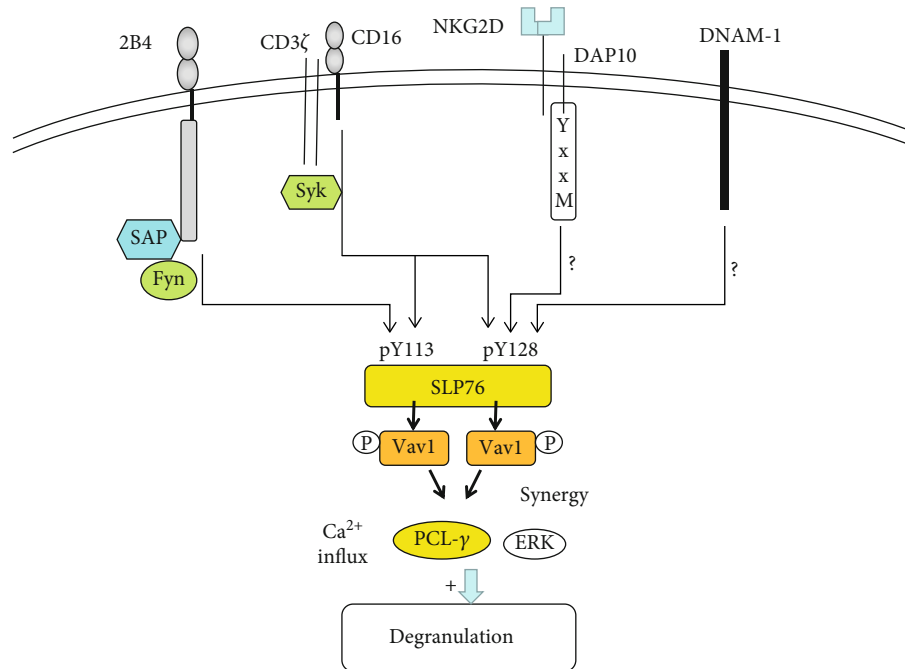


FIGURE 5: Synergistic activation of coactivation receptors is Vav1-dependent; NK cells promote the cytotoxicity and the secretion of INF- γ by the synergistic effects of NKG2D and 2B4 and 2B4 and DNAM-1. After coactivation receptors engaged, synergistic signals are integrated at SLP76. The phosphorylation of SLP76 induced by 2B4 was Fyn-dependent, whereas the phosphorylation of SLP76 in Y128 induced by NKG2D or DNAM-1 was SYK-independent. In contrast, CD16 can phosphorylate both Y113 and Y128 of SLP76 and sufficient to induce NK cell action on itself. Phosphorylated SLP76 associates with Vav1, resulting in phosphorylation of PLC γ 2 and ERK, which promotes degranulation and INF- γ secretion of NK cells.

Y319 on DNAM-1 in turn [114]. When the immune synapse is established between NK cells and target cells, LFA-1 binds to ICAM-1 in the target cells. At the same time, DNAM-1 of NK cells binds to its ligand, and S326 in the intracellular region of DNAM-1 is phosphorylated by PKC, which promotes LFA-1 to interact with DNAM-1 via Y319 phosphorylated by tyrosine kinase Fyn in the intracellular region of DNAM-1 [113, 114]. Eventually, DNAM-1 is recruited to the lipid raft as well as aggregates at the immune synapse site where a large number of signals occur. Furthermore, DNAM-1 binds to adaptor Grb2 through phosphorylated Y319 cooperating with N321. Binding of DNAM-1 to Grb2 enables PI3K, Vav1, SLP76, and PLC γ 1/2 to be recruited and then activates the AKT and ERK signaling pathways, triggering degranulation and Ca²⁺ mobilization [39, 107, 114, 115]. Consequently, NK cell function is activated (Figure 4). In addition, the intracellular region of the DNAM-1 molecule also contains motifs for binding to the isoforms of actin-binding protein 4.1G. 4.1G is an important molecule in the membrane cytoskeleton structure, which can interact with the membrane-associated guanylate kinase (MAGUK) homologue, and plays a part in the formation and anchoring of membrane protein complexes [116]. MAGUK molecules provide multiple functional domains to cluster multiple molecules related to activation such as membrane protein receptors, adhesion molecules, and intracellular signaling proteins at synapses, cell junctions, and polarized membrane functional regions [116]. The binding of these two protein families to the DNAM-1 molecule may

be related to the formation of the cytoskeleton, the clustering of CD226 molecule, the narrowing of CD226 and LFA-1 molecules, and the entry of CD226 into lipid rafts [116].

DNAM-1 is a costimulatory receptor that plays an important role in antitumor and antiviral immunity. A study has shown that DNAM-1 can phosphorylate FOXO1 by activating AKT. Thus, FOXO1 is transferred from the nucleus to the intracellular space, where it will be inactivated and degraded, regulating NK cytotoxicity and playing an antitumor role [117]. In addition, one issue that deserves attention is that the functional status of DNAM-1 is strongly related to the expression extent of its ligand and inhibitory receptors, CD96 (TACTILE), TIGIT, and PVRIG [39]. The interaction and balance between these receptors are complicated, and we will not introduce it here.

4.5. Activating Killer Cell Immunoglobulin Receptors (AKIRs) and CD94/NKG2C. AKIRs are subtypes of KIRs with a shorter intracellular tail, and they conduct activation signals to activate NK cells. AKIRs can be divided into KIR2DS and KIR3DS the same as IKIRs. Their intracellular region does not contain ITIMs, but the transmembrane region can be noncovalently bound to adaptor proteins containing ITAM sequences [4]. CD94/NKG2C does not contain ITIMs in the intracellular region, but it has the ability of transmitting activation signals through noncovalently binding to adaptor proteins. KIR2DS, KIR3DS, and CD94/NKG2C are MHC-dependent activating receptors. KIR2DS1, KIR2DS2, and KIR2DS4 can recognize HLA-C.

KIR3DS1 can recognize HLA-B. The ligand of CD94/NKG2C is HLA-E [30]. The adaptor protein of KIR2DS, KIR3DS, and CD94/NKG2C is DAP12, and their phosphorylation and downstream signaling pathways are the same as those described for NCRs [9, 10].

In addition, the activating receptors associated with NK cell function include CD16 (FcRII) recognizing antigen-antibody complexes, Tim-3 binding to galectin-9, NKp80 binding to activation-induced C-type lectin (AICL), CD28 recognizing CD80 (B7-1) and CD86 (B7-2), and CD2 binding to CD48 and CD58 (LFA-3) [8].

5. Conclusion

Activation and inhibition of NK cell function require the interactions between receptors and their corresponding ligands and are also closely related to the interactions between receptors. Understanding the mechanisms of function of NK cell receptor and its mediated signaling pathway is helpful in exploring the mysteries of NK cell function. Knowing more about how NK cells function regulation can help scientists to discover more about the role of NK cells in the pathogenesis of lots of immune diseases, as well as provide more strategies in NK cell immunotherapies. Although MHC-restricted inhibitory receptors need more extensive researches in regulating NK cell cytotoxicity and cytokine secretion, some targeted drugs have been explored for the effectiveness in solid tumors and hematological tumors, such as anti-KIR and anti-NKG2A mAbs [118]. NK cell-based immunotherapies are feasible because of the antigen-unrestricted cytotoxicity of NK cells on tumor cells. However, the expression of NK cell-activating receptors and specific ligands has individual difference in different patients. Thus, it is necessary to distinguish the individual difference and find out the inherent law of NK cell receptors in different diseases, in the future. Studying on the mechanism of NK cells in anti-infection immunity and antitumor immunity can provide more theoretical basis for exploring new targets of tumor and virus therapy. NK cells as innate immune cells also play parts in autoimmune reaction. Thereby, changes in the NK cell function and quantity participate in the pathogenesis of multiple autoimmune diseases. Our group found that NK cells had high expression of activating receptors NKp46 and NKG2D, low-expression of inhibitory receptor NKG2A, and increased cytotoxicity in patients with severe aplastic anemia (SAA) [119]. Thus, we speculated that NK cells suppressed the function of CD8⁺ T cells and played immunoregulation roles in the pathogenesis of SAA. Next, we want to start from the signal pathway, gene, epigenetic, and other aspects to explore the specific mechanism of NK cell receptors and function changes in SAA. In the future, we should pay more attention to the relationship between NK cells and different diseases, as well as how do those NK cell inhibitory receptors and activating receptors change and act. Ultimate goals are to provide new treatment breakthroughs applied in clinic by the researches of mechanism.

Conflicts of Interest

The authors report no conflicts of interest.

Authors' Contributions

Yingying Chen and Dan Lu contributed equally to this work and should be considered co-first authors.

Acknowledgments

This work was supported by the National Natural Science Foundation of China (81770110, 81970115, 81800120, 81870101, 81800119, 81600093, 81700117, 81900125, and 81970116) and Natural Science Foundation of Tianjin City (16JCZDJC35300, 17JCQNJC11500, 18JCYBJC91700, and 18ZXDBSY00140).

References

- [1] L. L. Lanier, "Natural killer cells: roundup," *Immunological Reviews*, vol. 214, no. 1, pp. 5–8, 2006.
- [2] W. E. Seaman, "Natural killer cells and natural killer T cells," *Arthritis and Rheumatism*, vol. 43, no. 6, pp. 1204–1217, 2000.
- [3] S. Radaev and P. D. Sun, "Structure and function of natural killer cell surface receptors," *Annual Review of Biophysics and Biomolecular Structure*, vol. 32, no. 1, pp. 93–114, 2003.
- [4] M. Colonna, "Specificity and function of immunoglobulin superfamily NK cell inhibitory and stimulatory receptors," *Immunological Reviews*, vol. 155, no. 1, pp. 127–133, 1997.
- [5] D. Cosman, N. Fanger, L. Borges et al., "A novel immunoglobulin superfamily receptor for cellular and viral MHC class I molecules," *Immunity*, vol. 7, no. 2, pp. 273–282, 1997.
- [6] C. Bottino, R. Biassoni, R. Millo, L. Moretta, and A. Moretta, "The human natural cytotoxicity receptors (NCR) that induce HLA class I-independent NK cell triggering," *Human Immunology*, vol. 61, no. 1, pp. 1–6, 2000.
- [7] M. Carretero, C. Cantoni, T. Bellón et al., "The CD94 and NKG2-A C-type lectins covalently assemble to form a natural killer cell inhibitory receptor for HLA class I molecules," *European Journal of Immunology*, vol. 27, no. 2, pp. 563–567, 1997.
- [8] C. Watzl and E. O. Long, "Signal transduction during activation and inhibition of natural killer cells," *Current Protocols in Immunology*, vol. 11, pp. 9–11, 2010.
- [9] L. L. Lanier, "DAP10- and DAP12-associated receptors in innate immunity," *Immunological Reviews*, vol. 227, no. 1, pp. 150–160, 2009.
- [10] L. L. Lanier, B. C. Corliss, J. Wu, C. Leong, and J. H. Phillips, "Immunoreceptor DAP12 bearing a tyrosine-based activation motif is involved in activating NK cells," *Nature*, vol. 391, no. 6668, pp. 703–707, 1998.
- [11] S. Rajagopalan and E. O. Long, "KIR2DL4 (CD158d): an activation receptor for HLA-G," *Frontiers in Immunology*, vol. 3, 2012.
- [12] B. A. Binstadt, K. M. Brumbaugh, C. J. Dick et al., "Sequential involvement of Lck and SHP-1 with MHC-recognizing

- receptors on NK cells inhibits FcR-initiated tyrosine kinase activation," *Immunity*, vol. 5, no. 6, pp. 629–638, 1996.
- [13] E. O. Long, "Negative signaling by inhibitory receptors: the NK cell paradigm," *Immunological Reviews*, vol. 224, no. 1, pp. 70–84, 2008.
- [14] S. Yusa and K. S. Campbell, "Src homology region 2-containing protein tyrosine phosphatase-2 (SHP-2) can play a direct role in the inhibitory function of killer cell Ig-like receptors in human NK cells," *Journal of Immunology*, vol. 170, no. 9, pp. 4539–4547, 2003.
- [15] S. Yusa, T. L. Catina, and K. S. Campbell, "SHP-1- and phosphotyrosine-independent inhibitory signaling by a killer cell Ig-like receptor cytoplasmic domain in human NK cells," *Journal of Immunology*, vol. 168, no. 10, pp. 5047–5057, 2002.
- [16] A. K. Purdy and K. S. Campbell, "Natural killer cells and cancer. Regulation by the killer cell Ig-like receptors (KIR)," *Zhongguo Fei Ai Za Zhi*, vol. 13, no. 7, pp. 731–736, 2010.
- [17] M. C. Sweeney, A.-S. Wavreille, J. Park, J. P. Butchar, S. Tridandapani, and D. Pei, "Decoding protein-protein interactions through combinatorial chemistry: sequence specificity of SHP-1, SHP-2, and SHIP SH2 domains," *Biochemistry*, vol. 44, no. 45, pp. 14932–14947, 2005.
- [18] C. C. Stebbins, C. Watzl, D. D. Billadeau, P. J. Leibson, D. N. Burshtyn, and E. O. Long, "Vav1 dephosphorylation by the tyrosine phosphatase SHP-1 as a mechanism for inhibition of cellular cytotoxicity," *Molecular and Cellular Biology*, vol. 23, no. 17, pp. 6291–6299, 2003.
- [19] O. Matalon, S. Fried, A. Ben-Shmuel et al., "Dephosphorylation of the adaptor LAT and phospholipase C- γ by SHP-1 inhibits natural killer cell cytotoxicity," *Science Signaling*, vol. 9, no. 429, p. ra54, 2016.
- [20] M. E. Peterson and E. O. Long, "Inhibitory receptor signaling via tyrosine phosphorylation of the adaptor Crk," *Immunity*, vol. 29, no. 4, pp. 578–588, 2008.
- [21] S. Kim, J. Poursine-Laurent, S. M. Truscott et al., "Licensing of natural killer cells by host major histocompatibility complex class I molecules," *Nature*, vol. 436, no. 7051, pp. 709–713, 2005.
- [22] M. Faure and E. O. Long, "KIR2DL4 (CD158d), an NK cell-activating receptor with inhibitory potential," *Journal of Immunology*, vol. 168, no. 12, pp. 6208–6214, 2002.
- [23] A. Kikuchi-Maki, S. Yusa, T. L. Catina, and K. S. Campbell, "KIR2DL4 is an IL-2-regulated NK cell receptor that exhibits limited expression in humans but triggers strong IFN- γ production," *Journal of Immunology*, vol. 171, no. 7, pp. 3415–3425, 2003.
- [24] A. Kikuchi-Maki, T. L. Catina, and K. S. Campbell, "Cutting edge: KIR2DL4 transduces signals into human NK cells through association with the Fc receptor gamma protein," *Journal of Immunology*, vol. 174, no. 7, pp. 3859–3863, 2005.
- [25] S. Rajagopalan, M. W. Moyle, I. Joosten, and E. O. Long, "DNA-PKcs Controls an Endosomal Signaling Pathway for a Proinflammatory Response by Natural Killer Cells," *Science Signaling*, vol. 3, no. 110, p. ra14, 2010.
- [26] S. Yusa, T. L. Catina, and K. S. Campbell, "KIR2DL5 can inhibit human NK cell activation via recruitment of Src homology region 2-containing protein tyrosine phosphatase-2 (SHP-2)," *Journal of Immunology*, vol. 172, no. 12, pp. 7385–7392, 2004.
- [27] H. Cheng, V. Schwell, B. R. Curtis, R. Fazlieva, H. Roder, and K. S. Campbell, "Conformational changes in the cytoplasmic region of KIR3DL1 upon interaction with SHP-2," *Structure*, vol. 27, no. 4, pp. 639–650.e2, 2019, e2.
- [28] C. Chang, A. Rodríguez, M. Carretero, M. López-Botet, J. H. Phillips, and L. L. Lanier, "Molecular characterization of human CD94: a type II membrane glycoprotein related to the C-type lectin superfamily," *European Journal of Immunology*, vol. 25, no. 9, pp. 2433–2437, 1995.
- [29] L. L. Lanier, B. Corliss, J. Wu, and J. H. Phillips, "Association of DAP12 with activating CD94/NKG2C NK cell receptors," *Immunity*, vol. 8, no. 6, pp. 693–701, 1998.
- [30] V. M. Braud, D. S. J. Allan, C. A. O'Callaghan et al., "HLA-E binds to natural killer cell receptors CD94/NKG2A, B and C," *Nature*, vol. 391, no. 6669, pp. 795–799, 1998.
- [31] J. Michaëlsson, C. T. de Matos, A. Achour, L. L. Lanier, K. Kärre, and K. Söderström, "A signal peptide derived from hsp60 binds HLA-E and interferes with CD94/NKG2A recognition," *The Journal of Experimental Medicine*, vol. 196, no. 11, pp. 1403–1414, 2002.
- [32] B. I. Pereira, O. P. Devine, M. Vukmanovic-Stejić et al., "Senescent cells evade immune clearance via HLA-E-mediated NK and CD8⁺ T cell inhibition," *Nature Communications*, vol. 10, no. 1, p. 2387, 2019.
- [33] H. S. Kim, A. Das, C. C. Gross, Y. T. Bryceson, and E. O. Long, "Synergistic signals for natural cytotoxicity are required to overcome inhibition by c-Cbl ubiquitin ligase," *Immunity*, vol. 32, no. 2, pp. 175–186, 2010.
- [34] Y. T. Bryceson, H. G. Ljunggren, and E. O. Long, "Minimal requirement for induction of natural cytotoxicity and intersection of activation signals by inhibitory receptors," *Blood*, vol. 114, no. 13, pp. 2657–2666, 2009.
- [35] G. Palmieri, V. Tullio, A. Zingoni et al., "CD94/NKG2-A inhibitory complex blocks CD16-triggered Syk and extracellular regulated kinase activation, leading to cytotoxic function of human NK cells," *Journal of Immunology*, vol. 162, no. 12, pp. 7181–7188, 1999.
- [36] T. Gonen-Gross, H. Achdout, R. Gazit et al., "Complexes of HLA-G protein on the cell surface are important for leukocyte Ig-like receptor-1 function," *Journal of Immunology*, vol. 171, no. 3, pp. 1343–1351, 2003.
- [37] D. C. Jones, V. Kosmoliaptis, R. Apps et al., "HLA class I allelic sequence and conformation regulate leukocyte Ig-like receptor binding," *Journal of Immunology*, vol. 186, no. 5, pp. 2990–2997, 2011.
- [38] M. Ryu, Y. Chen, J. Qi et al., "LILRA3 binds both classical and non-classical HLA class I molecules but with reduced affinities compared to LILRB1/LILRB2: structural evidence," *PLoS One*, vol. 6, no. 4, article e19245, 2011.
- [39] L. Martinet and M. J. Smyth, "Balancing natural killer cell activation through paired receptors," *Nature Reviews Immunology*, vol. 15, no. 4, pp. 243–254, 2015.
- [40] Y. He, H. Peng, R. Sun et al., "Contribution of inhibitory receptor TIGIT to NK cell education," *Journal of Autoimmunity*, vol. 81, pp. 1–12, 2017.
- [41] I. H. Westgaard, S. F. Berg, J. T. Vaage et al., "Rat NKp46 activates natural killer cell cytotoxicity and is associated with FcepsilonR1gamma and CD3zeta," *Journal of Leukocyte Biology*, vol. 76, no. 6, pp. 1200–1206, 2004.

- [42] A. D. Barrow, C. J. Martin, and M. Colonna, "The natural cytotoxicity receptors in health and disease," *Frontiers in Immunology*, vol. 10, p. 909, 2019.
- [43] S. Sivori, M. Vitale, L. Morelli et al., "p46, a novel natural killer cell-specific surface molecule that mediates cell activation," *The Journal of Experimental Medicine*, vol. 186, no. 7, pp. 1129–1136, 1997.
- [44] F. Fasbender, M. Claus, S. Wingert, M. Sandusky, and C. Watzl, "Differential requirements for Src-family kinases in SYK or ZAP70-mediated SLP-76 phosphorylation in lymphocytes," *Frontiers in Immunology*, vol. 8, p. 789, 2017.
- [45] D. W. McVicar, L. S. Taylor, P. Gosselin et al., "DAP12-mediated signal transduction in natural killer cells. A dominant role for the Syk protein-tyrosine kinase," *The Journal of Biological Chemistry*, vol. 273, no. 49, pp. 32934–32942, 1998.
- [46] K. M. Brumbaugh, B. A. Binstadt, D. D. Billadeau et al., "Functional role for Syk tyrosine kinase in natural killer cell-mediated natural cytotoxicity," *The Journal of Experimental Medicine*, vol. 186, no. 12, pp. 1965–1974, 1997.
- [47] S. Kumar, "Natural killer cell cytotoxicity and its regulation by inhibitory receptors," *Immunology*, vol. 154, no. 3, pp. 383–393, 2018.
- [48] M. Cella, K. Fujikawa, I. Tassi et al., "Differential requirements for Vav proteins in DAP10- and ITAM-mediated NK cell cytotoxicity," *The Journal of Experimental Medicine*, vol. 200, no. 6, pp. 817–823, 2004.
- [49] I. Tassi and M. Colonna, "The cytotoxicity receptor CRACC (CS-1) recruits EAT-2 and activates the PI3K and phospholipase C γ signaling pathways in human NK cells," *Journal of Immunology*, vol. 175, no. 12, pp. 7996–8002, 2005.
- [50] A. T. Ting, R. A. Schoon, R. T. Abraham, and P. J. Leibson, "Interaction between protein kinase C-dependent and G protein-dependent pathways in the regulation of natural killer cell granule exocytosis," *The Journal of Biological Chemistry*, vol. 267, no. 33, pp. 23957–23962, 1992.
- [51] J. L. Upshaw, R. A. Schoon, C. J. Dick, D. D. Billadeau, and P. J. Leibson, "The isoforms of phospholipase C-gamma are differentially used by distinct human NK activating receptors," *Journal of Immunology*, vol. 175, no. 1, pp. 213–218, 2005.
- [52] L. Zamaï, G. Del Zotto, F. Buccella et al., "Understanding the synergy of NKp46 and co-activating signals in various NK cell subpopulations: paving the way for more successful NK-cell-based immunotherapy," *Cells*, vol. 9, no. 3, p. 753, 2020.
- [53] Y. T. Bryceson, M. E. March, H. G. Ljunggren, and E. O. Long, "Synergy among receptors on resting NK cells for the activation of natural cytotoxicity and cytokine secretion," *Blood*, vol. 107, no. 1, pp. 159–166, 2006.
- [54] N. F. Delahaye, S. Rusakiewicz, I. Martins et al., "Alternatively spliced NKp30 isoforms affect the prognosis of gastrointestinal stromal tumors," *Nature Medicine*, vol. 17, no. 6, pp. 700–707, 2011.
- [55] K. S. Reiners, D. Topolar, A. Henke et al., "Soluble ligands for NK cell receptors promote evasion of chronic lymphocytic leukemia cells from NK cell anti-tumor activity," *Blood*, vol. 121, no. 18, pp. 3658–3665, 2013.
- [56] F. Baychelier, A. Sennepin, M. Ermonval, K. Dorgham, P. Debré, and V. Vieillard, "Identification of a cellular ligand for the natural cytotoxicity receptor NKp44," *Blood*, vol. 122, no. 17, pp. 2935–2942, 2013.
- [57] A. Niehrs, W. F. Garcia-Beltran, P. J. Norman et al., "A subset of HLA-DP molecules serve as ligands for the natural cytotoxicity receptor NKp44," *Nature Immunology*, vol. 20, no. 9, pp. 1129–1137, 2019.
- [58] C. Cantoni, C. Bottino, M. Vitale et al., "NKp44, a triggering receptor involved in tumor cell lysis by activated human natural killer cells, is a novel member of the immunoglobulin superfamily," *The Journal of Experimental Medicine*, vol. 189, no. 5, pp. 787–796, 1999.
- [59] K. S. Campbell, S. Yusa, A. Kikuchi-Maki, and T. L. Catina, "NKp44 triggers NK cell activation through DAP12 association that is not influenced by a putative cytoplasmic inhibitory sequence," *Journal of Immunology*, vol. 172, no. 2, pp. 899–906, 2004.
- [60] B. Rosental, M. Brusilovsky, U. Hadad et al., "Proliferating cell nuclear antigen is a novel inhibitory ligand for the natural cytotoxicity receptor NKp44," *Journal of Immunology*, vol. 187, no. 11, pp. 5693–5702, 2011.
- [61] N. C. Horton, S. O. Mathew, and P. A. Mathew, "Novel interaction between proliferating cell nuclear antigen and HLA I on the surface of tumor cells inhibits NK cell function through NKp44," *PLoS One*, vol. 8, no. 3, article e59552, 2013.
- [62] A. Campos, N. López, A. Pera et al., "Expression of NKp30, NKp46 and DNAM-1 activating receptors on resting and IL-2 activated NK cells from healthy donors according to CMV-serostatus and age," *Biogerontology*, vol. 16, no. 5, pp. 671–683, 2015.
- [63] R. Castriconi, C. Cantoni, M. Della Chiesa et al., "Transforming growth factor beta 1 inhibits expression of NKp30 and NKG2D receptors: consequences for the NK-mediated killing of dendritic cells," *Proceedings of the National Academy of Sciences of the United States of America*, vol. 100, no. 7, pp. 4120–4125, 2003.
- [64] E. Mavoungou, M. K. Bouyou-Akotet, and P. G. Kremsner, "Effects of prolactin and cortisol on natural killer (NK) cell surface expression and function of human natural cytotoxicity receptors (NKp46, NKp44 and NKp30)," *Clinical and Experimental Immunology*, vol. 139, no. 2, pp. 287–296, 2005.
- [65] Y. Li, J. Wang, J. Yin et al., "Chromatin state dynamics during NK cell activation," *Oncotarget*, vol. 8, no. 26, pp. 41854–41865, 2017.
- [66] J. Yin, J. W. Leavenworth, Y. Li et al., "Ezh2 regulates differentiation and function of natural killer cells through histone methyltransferase activity," *Proceedings of the National Academy of Sciences*, vol. 112, no. 52, pp. 15988–15993, 2015.
- [67] L. L. Lanier, "NKG2D receptor and its ligands in host defense," *Cancer Immunology Research*, vol. 3, no. 6, pp. 575–582, 2015.
- [68] C. L. Sutherland, N. J. Chalupny, K. Schooley, T. VandenBos, M. Kubin, and D. Cosman, "UL16-binding proteins, novel MHC class I-related proteins, bind to NKG2D and activate multiple signaling pathways in primary NK cells," *Journal of Immunology*, vol. 168, no. 2, pp. 671–679, 2002.
- [69] R. A. Eagle, G. Flack, A. Warford et al., "Cellular expression, trafficking, and function of two isoforms of human ULBP5/RAET1G," *PLoS One*, vol. 4, no. 2, article e4503, 2009.
- [70] R. A. Eagle, J. A. Traherne, J. R. Hair, I. Jafferji, and J. Trowsdale, "ULBP6/RAET1L is an additional human NKG2D ligand," *European Journal of Immunology*, vol. 39, no. 11, pp. 3207–3216, 2009.

- [71] S. Gilfillan, E. L. Ho, M. Cella, W. M. Yokoyama, and M. Colonna, "NKG2D recruits two distinct adapters to trigger NK cell activation and costimulation," *Nature Immunology*, vol. 3, no. 12, pp. 1150–1155, 2002.
- [72] T. Nabekura, D. Gotthardt, K. Niizuma et al., "Cutting edge: NKG2D signaling enhances NK cell responses but alone is insufficient to drive expansion during mouse cytomegalovirus infection," *Journal of Immunology*, vol. 199, no. 5, pp. 1567–1571, 2017.
- [73] B. Rabinovich, J. Li, M. Wolfson et al., "NKG2D splice variants: a reexamination of adaptor molecule associations," *Immunogenetics*, vol. 58, no. 2-3, pp. 81–88, 2006.
- [74] B. Meresse, Z. Chen, C. Ciszewski et al., "Coordinated induction by IL15 of a TCR-independent NKG2D signaling pathway converts CTL into lymphokine-activated killer cells in celiac disease," *Immunity*, vol. 21, no. 3, pp. 357–366, 2004.
- [75] D. D. Billadeau, J. L. Upshaw, R. A. Schoon, C. J. Dick, and P. J. Leibson, "NKG2D-DAP10 triggers human NK cell-mediated killing via a Syk-independent regulatory pathway," *Nature Immunology*, vol. 4, no. 6, pp. 557–564, 2003.
- [76] J. Wu, Y. Song, A. B. Bakker et al., "An activating immunoreceptor complex formed by NKG2D and DAP10," *Science*, vol. 285, no. 5428, pp. 730–732, 1999.
- [77] J. L. Upshaw, L. N. Arneson, R. A. Schoon, C. J. Dick, D. D. Billadeau, and P. J. Leibson, "NKG2D-mediated signaling requires a DAP10-bound Grb2-Vav1 intermediate and phosphatidylinositol-3-kinase in human natural killer cells," *Nature Immunology*, vol. 7, no. 5, pp. 524–532, 2006.
- [78] E. Giurisato, M. Cella, T. Takai et al., "Phosphatidylinositol 3-kinase activation is required to form the NKG2D immunological synapse," *Molecular and Cellular Biology*, vol. 27, no. 24, pp. 8583–8599, 2007.
- [79] C. M. Segovis, R. A. Schoon, C. J. Dick, L. P. Nacusi, P. J. Leibson, and D. D. Billadeau, "PI3K links NKG2D signaling to a CrkL pathway involved in natural killer cell adhesion, polarity, and granule secretion," *Journal of Immunology*, vol. 182, no. 11, pp. 6933–6942, 2009.
- [80] G. Chitadze, J. Bhat, M. Lettau, O. Janssen, and D. Kabelitz, "Generation of soluble NKG2D ligands: proteolytic cleavage, exosome secretion and functional implications," *Scandinavian Journal of Immunology*, vol. 78, no. 2, pp. 120–129, 2013.
- [81] S. Duan, W. Guo, Z. Xu et al., "Natural killer group 2D receptor and its ligands in cancer immune escape," *Molecular Cancer*, vol. 18, no. 1, p. 29, 2019.
- [82] L. Martinet, C. Jean, G. Dietrich, J. J. Fournié, and R. Poupot, "PGE2 inhibits natural killer and gamma delta T cell cytotoxicity triggered by NKR and TCR through a cAMP-mediated PKA type I-dependent signaling," *Biochemical Pharmacology*, vol. 80, no. 6, pp. 838–845, 2010.
- [83] N. Hanaoka, B. Jabri, Z. Dai et al., "NKG2D initiates caspase-mediated CD3 ζ degradation and lymphocyte receptor impairments associated with human cancer and autoimmune disease," *Journal of Immunology*, vol. 185, no. 10, pp. 5732–5742, 2010.
- [84] P. Roda-Navarro and H. T. Reyburn, "The traffic of the NKG2D/Dap10 receptor complex during natural killer (NK) cell activation," *The Journal of Biological Chemistry*, vol. 284, no. 24, pp. 16463–16472, 2009.
- [85] B. Zafirova, S. Mandarić, R. Antulov et al., "Altered NK cell development and enhanced NK cell-mediated resistance to mouse cytomegalovirus in NKG2D-deficient mice," *Immunity*, vol. 31, no. 2, pp. 270–282, 2009.
- [86] F. M. Wensveen, V. Jelencic, and B. Polic, "NKG2D: a master regulator of immune cell responsiveness," *Frontiers in Immunology*, vol. 9, p. 441, 2018.
- [87] V. Jelencić, M. Šestan, I. Kavazović et al., "NK cell receptor NKG2D sets activation threshold for the NCR1 receptor early in NK cell development," *Nature Immunology*, vol. 19, no. 10, pp. 1083–1092, 2018.
- [88] M. Claus, "Regulation of NK cell activity by 2B4, NTB-A and CRACC," *Frontiers in Bioscience*, vol. 13, no. 13, pp. 956–965, 2008.
- [89] M. H. Brown, K. Boles, P. A. van der Merwe, V. Kumar, P. A. Mathew, and A. N. Barclay, "2B4, the natural killer and T cell immunoglobulin superfamily surface protein, is a ligand for CD48," *The Journal of Experimental Medicine*, vol. 188, no. 11, pp. 2083–2090, 1998.
- [90] H. Pahima, P. G. Puzovio, and F. Levi-Schaffer, "2B4 and CD48: a powerful couple of the immune system," *Clinical Immunology*, vol. 204, pp. 64–68, 2019.
- [91] L. Agresta, K. H. N. Hoebe, and E. M. Janssen, "The emerging role of CD244 signaling in immune cells of the tumor microenvironment," *Frontiers in Immunology*, vol. 9, p. 2809, 2018.
- [92] A. Veillette, "Immune regulation by SLAM family receptors and SAP-related adaptors," *Nature Reviews. Immunology*, vol. 6, no. 1, pp. 56–66, 2006.
- [93] B. Chan, A. Lanyi, H. K. Song et al., "SAP couples Fyn to SLAM immune receptors," *Nature Cell Biology*, vol. 5, no. 2, pp. 155–160, 2003.
- [94] S. Latour, R. Roncagalli, R. Chen et al., "Binding of SAP SH2 domain to FynT SH3 domain reveals a novel mechanism of receptor signalling in immune regulation," *Nature Cell Biology*, vol. 5, no. 2, pp. 149–154, 2003.
- [95] Z. Dong, D. Davidson, L. A. Pérez-Quintero, T. Kurosaki, W. Swat, and A. Veillette, "The adaptor SAP controls NK cell activation by regulating the enzymes Vav-1 and SHIP-1 and by enhancing conjugates with target cells," *Immunity*, vol. 36, no. 6, pp. 974–985, 2012.
- [96] S. Meinke and C. Watzl, "NK cell cytotoxicity mediated by 2B4 and NTB-A is dependent on SAP acting downstream of receptor phosphorylation," *Frontiers in Immunology*, vol. 4, 2013.
- [97] R. Roncagalli, J. E. R. Taylor, S. Zhang et al., "Negative regulation of natural killer cell function by EAT-2, a SAP-related adaptor," *Nature Immunology*, vol. 6, no. 10, pp. 1002–1010, 2005.
- [98] T. J. Wilson, L. I. Garner, C. Metcalfe, E. King, S. Margraf, and M. H. Brown, "Fine specificity and molecular competition in SLAM family receptor signalling," *PLoS One*, vol. 9, no. 3, article e92184, 2014.
- [99] L.-A. Pérez-Quintero, R. Roncagalli, H. Guo, S. Latour, D. Davidson, and A. Veillette, "EAT-2, a SAP-like adaptor, controls NK cell activation through phospholipase C γ , Ca $^{2+}$, and Erk, leading to granule polarization," *The Journal of Experimental Medicine*, vol. 211, no. 4, pp. 727–742, 2014.
- [100] Y. A. Aldhamen, S. S. Seregin, C. F. Aylsworth, S. Godbehere, and A. Amalfitano, "Manipulation of EAT-2 expression promotes induction of multiple beneficial regulatory and effector functions of the human innate immune system as a novel immunomodulatory strategy," *International Immunology*, vol. 26, no. 5, pp. 291–303, 2014.

- [101] P. Eissmann, L. Beauchamp, J. Wooters, J. C. Tilton, E. O. Long, and C. Watzl, "Molecular basis for positive and negative signaling by the natural killer cell receptor 2B4 (CD244)," *Blood*, vol. 105, no. 12, pp. 4722–4729, 2005.
- [102] F. Zhang, X. Liu, C. Chen et al., "CD244 maintains the proliferation ability of leukemia initiating cells through SHP-2/p27kip1 signaling," *Haematologica*, vol. 102, no. 4, pp. 707–718, 2017.
- [103] D. Pende, R. Meazza, S. Marcenaro, M. Aricò, and C. Bottino, "2B4 dysfunction in XLP1 NK cells: more than inability to control EBV infection," *Clinical Immunology*, vol. 204, pp. 31–36, 2019.
- [104] S. Sivori, M. Falco, E. Marcenaro et al., "Early expression of triggering receptors and regulatory role of 2B4 in human natural killer cell precursors undergoing in vitro differentiation," *Proceedings of the National Academy of Sciences of the United States of America*, vol. 99, no. 7, pp. 4526–4531, 2002.
- [105] L. K. Chlewicki, C. A. Velikovskiy, V. Balakrishnan, R. A. Mariuzza, and V. Kumar, "Molecular basis of the dual functions of 2B4 (CD244)," *Journal of Immunology*, vol. 180, no. 12, pp. 8159–8167, 2008.
- [106] S. Sivori, S. Parolini, M. Falco et al., "2B4 functions as a co-receptor in human NK cell activation," *European Journal of Immunology*, vol. 30, no. 3, pp. 787–793, 2000.
- [107] H. S. Kim and E. O. Long, "Complementary phosphorylation sites in the adaptor protein SLP-76 promote synergistic activation of natural killer cells," *Science Signaling*, vol. 5, no. 232, p. ra49, 2012.
- [108] G. Katz, S. M. Krummey, S. E. Larsen, J. R. Stinson, and A. L. Snow, "SAP facilitates recruitment and activation of LCK at NTB-A receptors during restimulation-induced cell death," *Journal of Immunology*, vol. 192, no. 9, pp. 4202–4209, 2014.
- [109] A. Duev-Cohen, Y. Bar-On, A. Glasner et al., "The human 2B4 and NTB-A receptors bind the influenza viral hemagglutinin and co-stimulate NK cell cytotoxicity," *Oncotarget*, vol. 7, no. 11, pp. 13093–13105, 2016.
- [110] C. Bottino, R. Castriconi, D. Pende et al., "Identification of PVR (CD155) and Nectin-2 (CD112) as cell surface ligands for the human DNAM-1 (CD226) activating molecule," *The Journal of Experimental Medicine*, vol. 198, no. 4, pp. 557–567, 2003.
- [111] B. Sanchez-Correa, I. Valhondo, F. Hassouneh et al., "DNAM-1 and the TIGIT/PVRIG/TACTILE axis: novel immune checkpoints for natural killer cell-based cancer immunotherapy," *Cancers*, vol. 11, no. 6, p. 877, 2019.
- [112] S. Tahara-Hanaoka, K. Shibuya, Y. Onoda et al., "Functional characterization of DNAM-1 (CD226) interaction with its ligands PVR (CD155) and nectin-2 (PRR-2/CD112)," *International Immunology*, vol. 16, no. 4, pp. 533–538, 2004.
- [113] K. Shibuya, L. L. Lanier, J. H. Phillips et al., "Physical and functional association of LFA-1 with DNAM-1 adhesion molecule," *Immunity*, vol. 11, no. 5, pp. 615–623, 1999.
- [114] Z. Zhang, N. Wu, Y. Lu, D. Davidson, M. Colonna, and A. Veillette, "DNAM-1 controls NK cell activation via an ITT-like motif," *The Journal of Experimental Medicine*, vol. 212, no. 12, pp. 2165–2182, 2015.
- [115] L. Cifaldi, M. Doria, N. Cotugno et al., "DNAM-1 activating receptor and its ligands: how do viruses affect the NK cell-mediated immune surveillance during the various phases of infection?," *International Journal of Molecular Sciences*, vol. 20, no. 15, p. 3715, 2019.
- [116] K. J. Ralston, S. L. Hird, X. Zhang et al., "The LFA-1-associated molecule PTA-1 (CD226) on T cells forms a dynamic molecular complex with protein 4.1G and human discs large," *The Journal of Biological Chemistry*, vol. 279, no. 32, pp. 33816–33828, 2004.
- [117] X. Du, P. de Almeida, N. Manieri et al., "CD226 regulates natural killer cell antitumor responses via phosphorylation-mediated inactivation of transcription factor FOXO1," *Proceedings of the National Academy of Sciences of the United States of America*, vol. 115, no. 50, pp. E11731–E11740, 2018.
- [118] N. Kim and H. S. Kim, "Targeting checkpoint receptors and molecules for therapeutic modulation of natural killer cells," *Frontiers in Immunology*, vol. 9, p. 2041, 2018.
- [119] T. Chen, T. Zhang, C. Liu et al., "NK cells suppress CD8(+) T cell immunity via NKG2D in severe aplastic anemia," *Cellular Immunology*, vol. 335, pp. 6–14, 2019.

Research Article

The Pneumococcal Polysaccharide-Tetanus Toxin Native C-Fragment Conjugate Vaccine: The Carrier Effect and Immunogenicity

Rui Yu ¹, Junjie Xu,¹ Tao Hu ², and Wei Chen ¹

¹Laboratory of Vaccine and Antibody Engineering, Beijing Institute of Biotechnology, Beijing 100071, China

²State Key Laboratory of Biochemical Engineering, Institute of Process Engineering, Chinese Academy of Sciences, Beijing 100190, China

Correspondence should be addressed to Tao Hu; thu@home.ipe.ac.cn and Wei Chen; cw0226@foxmail.com

Received 27 April 2020; Accepted 15 June 2020; Published 4 July 2020

Guest Editor: Hongmei Jiang

Copyright © 2020 Rui Yu et al. This is an open access article distributed under the Creative Commons Attribution License, which permits unrestricted use, distribution, and reproduction in any medium, provided the original work is properly cited.

The encapsulated bacteria, as *Streptococcus pneumoniae*, *Haemophilus influenzae* type b, and *Neisseria meningitidis*, cause serious morbidity and mortality worldwide. The capsular polysaccharide (PS), which could elicit a weak T cell-independent immune response, is a vital virulence determinant. One of the strategies to improve the PS-specific immunogenicity is to conjugate PS with a nontoxic carrier protein. Tetanus toxoid (TT) and CRM₁₉₇ are the typical carrier proteins for the PS conjugate vaccines. TT is the inactivated tetanus toxin manipulated with formaldehyde, which suffers from the pollution from residual formaldehyde and the incomplete detoxification. CRM₁₉₇ has the disadvantage of low-yield purification with the requirement of sophisticated culture conditions. Thus, a novel carrier protein without these disadvantages is highly required. The tetanus toxin native C-fragment (Hc) is safe, low-cost, and highly immunogenic with easy purification, which can act as a promising carrier protein. Pneumococcal serogroups 14 and 23F were major epidemic causes of pneumococcal infections. In the present study, the capsular PSs (PS14 and PS23F) were conjugated with Hc, TT, and CRM₁₉₇, respectively. TT- and CRM₁₉₇-based conjugates acted as controls for Hc-based conjugates (PS14-Hc and PS23F-Hc). The structural properties of Hc were not fundamentally changed after conjugated with PS. PS14-Hc and PS23F-Hc could potentiate sound PS-specific antibody levels comparable to the controls. Thus, Hc exhibited a practical carrier effect to help the pneumococcal conjugate vaccines perform good immunogenicities.

1. Introduction

The encapsulated bacteria with capsular polysaccharide (PS), as *Streptococcus pneumoniae*, *Haemophilus influenzae* type b, and *Neisseria meningitidis*, cause serious morbidity and mortality worldwide [1]. Due to the increasing bacterial resistance to antibiotics, effective vaccinations are urgently required to protect from the encapsulated bacteria-caused diseases [2, 3]. Capsular PS is an important virulence determinant of the encapsulated bacteria and has been used as an antigen for preventive vaccine development [4, 5]. However, the PS vaccines elicit weak T cell-independent immune responses without long-term immunological memories, particularly in children and the old [6, 7].

The conjugate vaccines have been produced by covalent conjugation of the antigenic PS with a nontoxic carrier protein to enhance the immunogenicity of PS vaccines [8–10]. After priming with the carrier protein, the immune response of PS improved by increasing the number of T lymphocytes [11, 12]. The carrier protein can also anchor PS to the B cell MHC-II, which makes the carbohydrate moiety present to T cell and eliciting T cell-dependent response to PS [13, 14]. Thus, the conjugate vaccines have been demonstrated to be immunogenic and capable of inducing immunological memory and high avidity [15].

Tetanus toxoid (TT) is one of the most commonly used carrier proteins, and TT-based conjugate vaccines have been developed to confer protection against meningococcal and pneumococcal diseases [16]. However, TT is derived from

Clostridium tetani and inactivated with formaldehyde, which suffers from residual toxic formaldehyde [17]. *C. tetani* can resist the inactivation of formaldehyde by forming spores, so it cannot guarantee that TT is completely nontoxic [17]. Besides, TT-based conjugate vaccine showed high rates of irritability, crying, and fever.

Cross-reactive material 197 (CRM₁₉₇) is a carrier protein used in approved conjugate vaccines, such as Prevnar (Pfizer) against *S. pneumoniae* [13]. It does not require detoxification with formaldehyde, thus preserves T-helper epitopes and provides more lysyl side chains for conjugation [18]. However, CRM₁₉₇ is classically purified from the culture supernatant of *C. diphtheriae* C7 (β 197) strain, which suffers from low yield and requires sophisticated culture conditions [19]. Thus, a candidate carrier protein without the disadvantages of the two proteins is urgently needed for the conjugate vaccines.

The native C-fragment of tetanus toxin (Hc) is a well-defined protein that retains many properties such as low allergenicity, low toxicity, binding activities to gangliosides, and immunogenic potency [20]. Due to its advantages in production, characterization, and homogeneity, Hc is a good substitute for TT in the production of tetanus antitoxin [21, 22]. Moreover, Hc could be purified with high yield by a three-step purification based on affinity chromatography.

Pneumococcal serogroups 14 and 23F have been proved to be a leading cause of pneumococcal infections, and their capsular PSs (PS14 and PS23F) are essential virulence determinants [23, 24]. In the present study, PS14 and PS23F were conjugated with Hc, TT, and CRM₁₉₇, respectively. The carrier effect of Hc to enhance the immunogenicity of the conjugate pneumococcal vaccines was thus evaluated. TT-based and CRM₁₉₇-based conjugates acted as controls for Hc-based ones (PS14-Hc and PS23F-Hc). PS14-Hc and PS23F-Hc were both proved to potentiate a strong PS-specific humoral immunity. The biophysical and immunological properties of PS14-Hc and PS23F-Hc were investigated. The study could rationalize the carrier effect of Hc to enhance the immunogenicity of the conjugate pneumococcal vaccines.

2. Materials and Methods

2.1. Materials and Animals. 2-iminothiolane (IT), bovine serum albumin (BSA), 5,5'-dithio-bis-(2-nitrobenzoic acid), and *N*-(2-aminoethyl) maleimide (AM) were purchased from Sigma (USA). Horseradish peroxidase- (HRP-) conjugated goat anti-mouse antibodies (including HRP-IgM, HRP-IgG, HRP-IgG1, and HRP-IgG2a) were products of Abcam (USA). Pneumococcal PS serogroups 14 and 23F, CRM₁₉₇, and TT were products of Hualan Biological Engineering Inc. (China). Hc was prepared as described previously [20].

BALB/c (15-20 g, female) were purchased from Beijing Vital River Laboratory Animal Technologies Co. Ltd. The mice were provided with enough food and water and raised under a comfortable environment. The mouse experiments were approved by the Institutional Animal Care and Use Committee of Beijing Laboratory Animal Research Center

(identification code: ZSBD-2017-A034-3R). All operations performed on mice were according to approved methods. The mice were euthanized at the end of the experiment, and all efforts were made to reduce the pain.

2.2. Activation of PS. 4 mg/ml PS14 or PS23F with a volume of 20 ml was added to the 20 mM acetate buffer (pH 5.8), which contained 10 mM sodium periodate to conduct an oxidation reaction for 40 minutes (Figure 1). The oxidized PS14 or PS23F with a concentration of 3 mg/ml and a volume of 20 ml, NaCNBH₃ with a concentration of 10 mg/ml and a volume of 2 ml, and AM with a concentration of 6 mg/ml and a volume of 10 ml were mixed and incubated in 20 mM phosphate buffer (PB buffer, pH 7.4) at 2~8°C overnight. The activated PS was subsequently dialyzed to 20 mM PB buffer (pH 7.4).

2.3. Preparation of PS14-Hc and PS23F-Hc. Hc with a concentration of 3 mg/ml and a volume of 6 ml was added into 20 mM PB buffer (pH 7.4) containing 36 nmol of IT. After being incubated at 2~8°C overnight, the free IT was removed by extensive dialysis using 20 mM PB buffer (pH 7.4). The activated PS14 (2 mg/ml, 4.5 ml) or PS23F (2 mg/ml, 4.5 ml) was incubated with the resultant Hc derivative at 2~8°C overnight, respectively. The resultant conjugates were referred to as PS14-Hc and PS23F-Hc, respectively.

2.4. Preparation of PS14-TT and PS23F-TT. TT with a concentration of 3 mg/ml and a volume of 9 ml was added into 20 mM PB buffer (pH 7.4) containing 11 nmol of IT. After being incubated at 2~8°C overnight, the free IT was removed by extensive dialysis using 20 mM PB buffer (pH 7.4). The activated PS14 (2 mg/ml, 4.5 ml) or PS23F (2 mg/ml, 4.5 ml) was incubated with the resultant Hc derivative at 2~8°C overnight, respectively. PS14-TT and PS23F-TT were referred to as the resultant conjugates, respectively.

2.5. Preparation of PS14-CRM and PS23F-CRM. CRM₁₉₇ with a concentration of 3 mg/ml and a volume of 6 ml was added into 20 mM PB buffer (pH 7.4) containing 16 nmol of IT. After being incubated at 2~8°C overnight, the free IT was removed by extensive dialysis using 20 mM PB buffer (pH 7.4). The activated PS14 (2 mg/ml, 4.5 ml) or PS23F (2 mg/ml, 4.5 ml) was incubated with the resultant Hc derivative at 2~8°C overnight, respectively. PS14-CRM and PS23F-CRM were referred to as the resultant conjugates, respectively.

2.6. Purification of the Conjugates. The purification of the six conjugates was performed by a Superdex 200 column (1.6 cm × 60 cm, GE Healthcare, USA) with a method of size exclusion chromatography (SEC). The column was equilibrated and eluted by 20 mM PB buffer (pH 7.4) with a flow rate of 2.0 ml/min. Then, the target conjugates were collected.

2.7. Quantitative Assay. The phenol-sulfuric acid method was used to determine the total PS contents of the conjugates. A quantitative method for the determination of unconjugated PS in conjugates was established. The method was based on the ethanol precipitation of TT. The thiolation

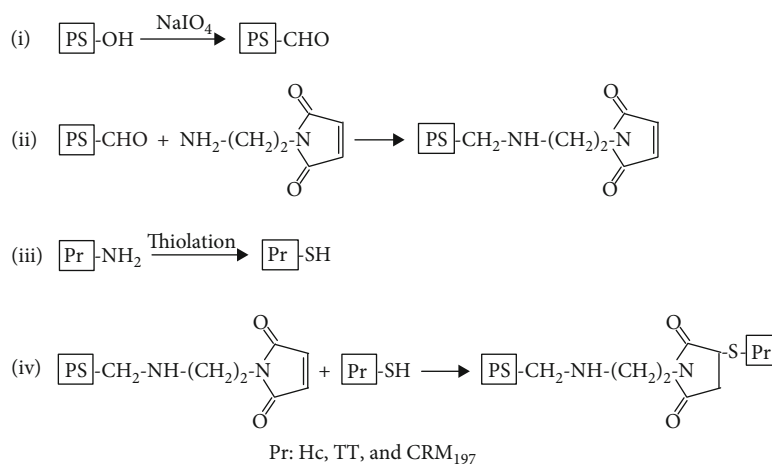


FIGURE 1: Schematic representation of the conjugates. PS was introduced with maleimide groups by incubation with AM. The carrier proteins were thiolated and reacted with the activated PS.

degree of TT was detected by 5,5'-dithiobis (2-nitrobenzoic acid). Using BSA as the standard, TT contents in the conjugates were determined by bicinchoninic acid. Then, the mass ratios of PS/TT of the conjugate vaccines were obtained.

2.8. Dynamic Light Scattering. Using a Wyatt DynaPro Titan TC instrument (Santa Barbara, CA, USA), the molecular radii of the six conjugates were calculated at 25°C. Before the analysis, the samples were centrifuged at 12,000 g for 10 min in 20 mM PB buffer (pH 7.4) with a concentration of 1 mg/ml.

2.9. Intrinsic Fluorescence Spectroscopy. The conjugates were prepared at a protein concentration of 0.15 mg/ml in 20 mM PB buffer (pH 7.4). Using a fluorescence spectropolarimeter (Hitachi, Japan), the intrinsic fluorescence spectra of the six conjugates were recorded. The emission fluorescence intensities were between 300 nm and 400 nm with excitation at 280 nm. The emission and excitation slit widths were both 2.5 nm.

2.10. Circular Dichroism Spectroscopy. Far-UV circular dichroism (CD) spectra of the six conjugates were detected by the spectropolarimeter (Jasco, Japan) with the wavelengths from 260 nm to 190 nm. The length of cuvettes used in this detection was 0.2 cm path. All the protein concentrations of the conjugates in 20 mM PB buffer (pH 7.4) were 0.15 mg/ml.

2.11. Immunization. BALB/c mice (female, six weeks old) were randomly divided into eight groups with the name of PS14, PS23F, PS14-TT, PS23F-TT, PS14-Hc, PS23F-Hc, PS14-CRM, and PS23F-CRM, respectively. Each group has six mice. The mice were intraperitoneally injected with different vaccines on days 0, 14, and 28, respectively. All the vaccines contained 2 µg/ml of PS in a volume of 0.5 ml. The tail vein blood of mice was taken on days 14, 28, and 42. The sera of mice were stored at -20°C after separation.

2.12. Antibody Titers. The anti-PS antibody titers of IgG, IgG1, IgG2a, and IgM were determined by ELISA assay

[25]. Briefly, PS14-BSA or PS23F-BSA (2 µg PS/ml) was prepared as the previous description [26] and used to coat the 96-well plates 100 µl per well at 2 ~ 8°C overnight. The plates were washed four times with PBS plus 0.1% Tween 20 (PBST). The serum serially 2-fold diluted from 1:100 was added to the well and incubated at 37°C for 1 h followed by being washed four times. 100 µl per well of anti-mouse HRP-IgG, IgG1, IgG2a, or IgM was added and then incubated at 37°C for 1 h. After four times washing by PBST, TMB substrate was added to the 96-well plates with a volume of 100 µl per well and incubated for 5 min at room temperature. 50 µl of 2 M H₂SO₄ was used to stop the reaction. The values of OD₄₅₀ were recorded.

2.13. Statistical Analysis. GraphPad Prism 5 software (GraphPad Software, USA) was used to analyze the results. The differences between the groups of mice were compared by one-way ANOVA. The values of $P < 0.05$ (*) represented the statistically significant, and $P < 0.01$ (**) represented the highly statistically significant between the experimental groups.

3. Results

3.1. Purification of the PS-Protein Conjugates. A Superdex 200 column (1.6 cm × 60 cm, GE) was used to purify the six conjugates based on SEC. As a result in Figure 2(a), PS14-Hc was first eluted as a broad symmetric peak at 55.3 ml, followed by a single peak of the unconjugated Hc. The reaction mixture containing PS14-CRM showed a chromatographic behavior similar to PS14-Hc, and the elution peak of PS14-CRM was at 52.4 ml (Figure 2(b)). In contrast, PS14-TT was first eluted as a significant peak at 45.2 ml, followed by a small peak of the unconjugated TT (Figure 2(c)). As a result in Figure 2(d), PS23F-Hc was eluted at the peak of 44.9 ml. Similarly, there also appeared two elution peaks of the reaction mixture of PS23F-CRM and the target elution peak was at 44.4 ml (Figure 2(e)). The reaction mixture containing PS23F-TT was eluted as a single peak at 42.4 ml (Figure 2(f)).

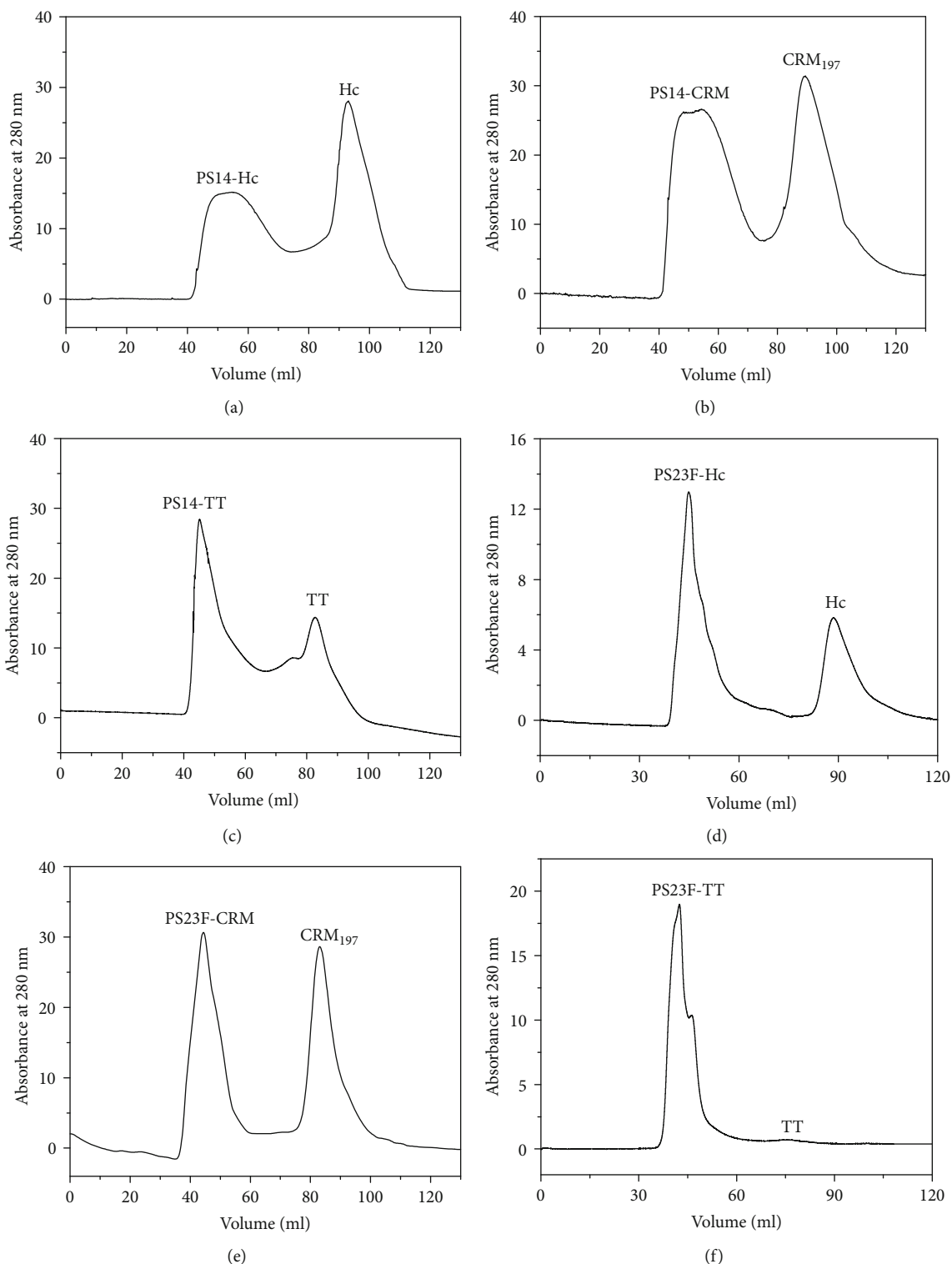


FIGURE 2: Purification of the conjugates. PS14-Hc (a), PS14-CRM (b), PS14-TT (c), PS23F-Hc (d), PS23F-CRM (e), and PS23F-TT (f) were purified by a Superdex 200 column (1.6 cm × 60 cm) at room temperature.

The elution peaks of the six conjugates appeared in the turn of PS23F-TT, PS23F-CRM, PS23F-Hc, PS14-TT, PS14-CRM, and PS14-Hc, which were proportional to the apparent molecular weights (MWs) of the conjugates. The PS23F-based conjugates were eluted more first than the

PS14-based ones; due to that, PS23F showed higher MW than PS14. The CRM₁₉₇-based conjugates were eluted earlier than the Hc-based ones and later than the TT-based ones. This result was due to that CRM₁₉₇ displayed an Mw higher than Hc and lower than TT.

3.2. Molecular Radius Detection. The molecular radii of the carrier proteins and the conjugates were measured by dynamic light scattering. The molecular radii of TT, Hc, and CRM₁₉₇ were 6.9 nm, 4.7 nm, and 5.2 nm, respectively. The molecular radii of PS14-TT and PS23F-TT were 11.9 nm and 14.3 nm, respectively. The molecular radii of PS14-Hc and PS23F-Hc were 10.3 nm and 12.4 nm, respectively. The molecular radii of PS14-CRM and PS23F-CRM were 10.8 nm and 12.9 nm, respectively. This analysis is consistent with the SEC result (Figure 2).

3.3. Quantitative Analysis. Free carrier proteins were not detected in the six conjugates. In contrast, the free PS14 ratios in PS14-Hc, PS14-TT, and PS14-CRM were 3.9%, 2.8%, and 3.3% (*w/w*), respectively. The free PS23F ratios in PS23F-Hc, PS23F-TT, and PS23F-CRM were 3.6%, 4.2%, and 3.0% (*w/w*), respectively. The PS14/protein ratios (*w/w*) of PS14-Hc, PS14-TT, and PS14-CRM were 0.56, 1.39, and 0.65, respectively. The PS23F/protein ratios (*w/w*) of PS23F-Hc, PS23F-TT, and PS23F-CRM were 0.62, 1.48, and 0.77, respectively. Due to the MWs of TT (140 kDa), Hc (50 kDa), and CRM₁₉₇ (62 kDa), the PS14/protein and PS23F/protein ratios (mol/mol) of the six conjugates were comparable with each other.

3.4. Intrinsic Fluorescence Analysis. Due to Trp and Tyr residues, proteins have intrinsic fluorescence. As a result in Figure 3(a), Hc showed a unimodal curve with a maximum wavelength of 328 nm. The emission fluorescence intensities of PS14-Hc and PS23F-Hc were slightly lower than that of Hc with an inapparent change of the maximum wavelength. As shown in Figure 3(b), CRM₁₉₇ displayed a unimodal curve with a maximum wavelength of 332 nm. The emission fluorescence intensities of PS14-CRM and PS23F-CRM were comparable to that of CRM₁₉₇, accompanied by no shift in the maximum wavelength. As a result in Figure 3(c), TT exhibited a unimodal curve with a maximum wavelength of 327 nm. The curve of PS14-TT or PS23F-TT was almost overlapped with that of TT. Thus, the conjugation of PS14 and PS23F did not fundamentally change the Trp and Tyr environment of the carrier proteins. In other words, the conformations of the carrier proteins did not change when binding with PS.

3.5. Secondary Structure Analysis. Far-UV circular dichroism (CD) spectroscopy was used to measure the secondary structures of the six conjugates. As a result in Figure 4, Hc, CRM₁₉₇, and TT all showed typical CD spectra. As a result in Figure 4(a), the CD spectra of PS16-Hc or PS23F-Hc were almost overlapped on that of Hc. Similarly, the CD spectra of PS16-CRM and PS23F-CRM were essentially coincided with that of CRM₁₉₇ (Figure 4(b)). The CD spectra of PS16-TT and PS23F-TT were close to that of TT (Figure 4(c)). Thus, the secondary structures of Hc, CRM₁₉₇, and TT were not essentially altered upon conjugation with PS.

3.6. PS14-Specific Antibodies. ELISA assay was used to measure the PS14-specific antibody titers in mice. As a result in Figure 5(a), the IgG titers of PS14-specific antibodies in the four groups were all very low after the first vaccina-

tion (day 14). The PS14 group showed a 2.8-fold increase in the PS14-specific IgG titers after the second immunization (day 28) compared with the first immunization (~1:270). The third vaccination (day 42) could not further booster the IgG titers. However, the PS14-specific IgG titers of the PS14-Hc group showed a 4.2-fold increase after the second immunization (day 28), which was higher than those of the PS14 group ($P < 0.01$). The third vaccination could not further booster the IgG titers. The IgG titers of the PS14-TT ($1 : 1.7 \times 10^3$) and PS14-CRM groups ($1 : 1.4 \times 10^3$) were not significantly different from the PS14-Hc group on day 42 ($1 : 1.1 \times 10^3$, $P > 0.05$). Thus, Hc could act as a capable carrier protein to enhance the PS14-specific IgG titers like CRM₁₉₇ and TT.

As shown in Figure 5(b), the four groups all showed low PS14-specific IgG1 titers after the first immunization (day 14). As a marker of the Th2 pathway, IgG1 titer of the PS14 group could hardly be detected after the second and third vaccination. In contrast, the PS14-Hc group got a 2.4-fold increase of the specific IgG1 titers after the second (~1:180) vaccination and a 5.2-fold increase of the specific IgG1 titers after the third (~1:380) vaccinations. The IgG1 titers of the PS14-TT (~1:900) and PS14-CRM groups ($1 : 1.3 \times 10^3$) were both higher than that of the PS14-Hc group on day 42 (~1:380, $P < 0.05$).

As a result in Figure 5(c), the PS14-specific IgG2a titers of the PS14 group were almost undetectable upon the three vaccinations. As a sign of the Th1 immune pathway, the IgG2a titers of the other three groups were undetectable upon initial vaccination and significantly increased upon the second and third vaccinations. In particular, the PS14-Hc group showed significantly higher IgG2a titers on day 42 ($1 : 1.1 \times 10^3$) than those of the PS14-TT group (~1:430) ($P < 0.05$) and PS14-CRM groups (~1:190) ($P < 0.01$). The ratios of IgG2a/IgG1 in the PS14-Hc, PS14-TT, and PS14-CRM groups on day 42 were 2.90, 0.48, and 0.15, respectively. Thus, the Th1/Th2 bias of the PS14-Hc group was significantly different from the PS14-TT and PS14-CRM groups. It is suggested that Hc could stimulate stronger cellular immunity than TT and CRM₁₉₇ as a carrier protein.

As a result in Figure 5(d), the IgM titers in the four groups were low upon initial vaccination and significantly increased upon the second vaccination. The third vaccination could not further booster the IgG titers. Moreover, the PS14-specific IgM titers of the four groups were comparable to each other upon the three vaccinations. Besides, the IgG/IgM ratios of the PS14-Hc, PS14-TT, and PS14-CRM groups on day 42 were 1.1, 1.4, and 1.4, respectively. These ratios were higher than those at the first vaccination (1.0, 0.8, and 1.0). This result suggested that the conjugation of PS14 with the carrier proteins shifted more response from IgM to IgG.

3.7. PS23F-Specific Antibodies. As a result in Figure 6(a), all groups showed low IgG titers of the PS23F-specific antibodies after the first immunization (day 14). The PS23F group did not booster the PS23F-specific IgG titers after the second and third immunizations compared with the initial vaccination of PS23F. Compared to the first immunization of PS23F-Hc (~1:480), the IgG titers of the PS23F-Hc group

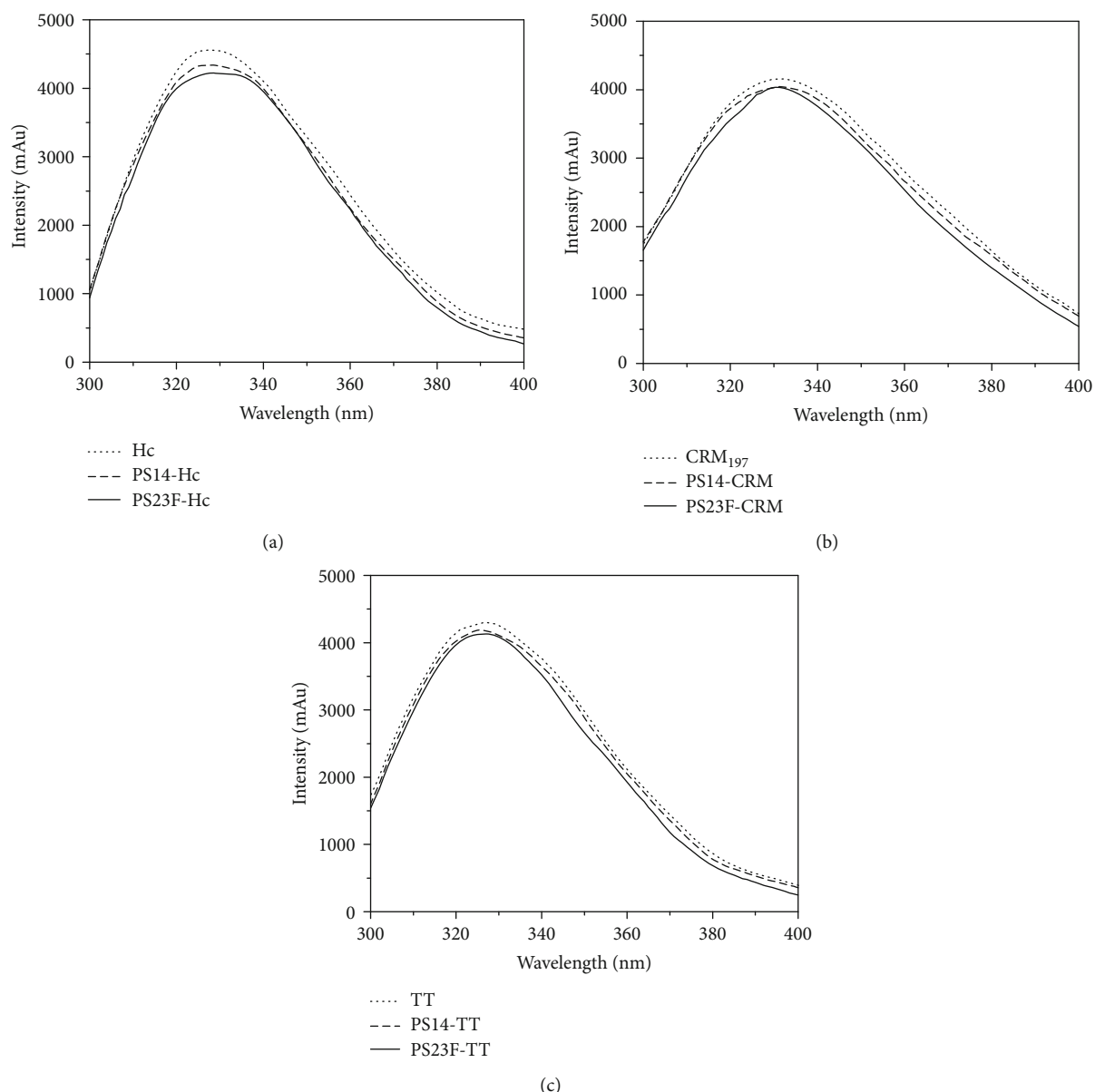


FIGURE 3: Fluorescence analysis of the conjugates. The intrinsic fluorescence emission spectra of the Hc-based conjugates (a), the CRM₁₉₇-based conjugates (b), and the TT-based conjugates (c) were recorded from 300 to 400 nm.

showed a 3.6-fold increase upon the second immunization and a 7.8-fold increase upon the third immunization. Moreover, the PS23F-specific IgG titers of the PS23F-Hc group were higher than those of the PS23F group ($P < 0.01$). Thus, the immunogenicity of PS23F-Hc was substantial after two doses with a positive booster response observed after the second dose. The PS23F-specific IgG titers of the PS23F-TT ($1 : 1.0 \times 10^3$) and PS23F-CRM groups ($1 : 2.8 \times 10^3$) on day 42 were both lower than those of the PS23F-Hc group ($1 : 3.7 \times 10^3$) ($P < 0.05$). Thus, Hc showed a more powerful carrier effect than TT and CRM₁₉₇ on the PS23F-specific IgG titers.

As a result in Figure 6(b), all the groups showed low IgG1 titers of the PS23F-specific antibodies after the initial vaccination. The second and third vaccinations could significantly

increase the IgG1 titers of the three conjugate groups ($P < 0.05$). Particularly, the IgG1 titers of the PS23F-Hc group (4.2×10^3) were lower than those of the PS23F-TT group (5.8×10^3) and higher than those of the PS23F-CRM groups (2.5×10^3) ($P > 0.05$) on day 42.

As a result in Figure 6(c), the PS23F-specific IgG2a titers of the PS23F group were undetectably low after all three vaccinations. The Th1-type IgG2a titers of the other three groups were undetectable upon initial vaccination and slightly increased upon the second ($P < 0.05$) and third vaccinations ($P < 0.05$). Moreover, the IgG2a titers of the three groups on the third vaccination did not display a significant difference ($P > 0.05$). The ratios of IgG2a/IgG1 in the PS23F-Hc, PS23F-TT, and PS23F-CRM groups on day 42 were 0.03, 0.02, and 0.03, respectively. Thus, the PS23F-specific antibody

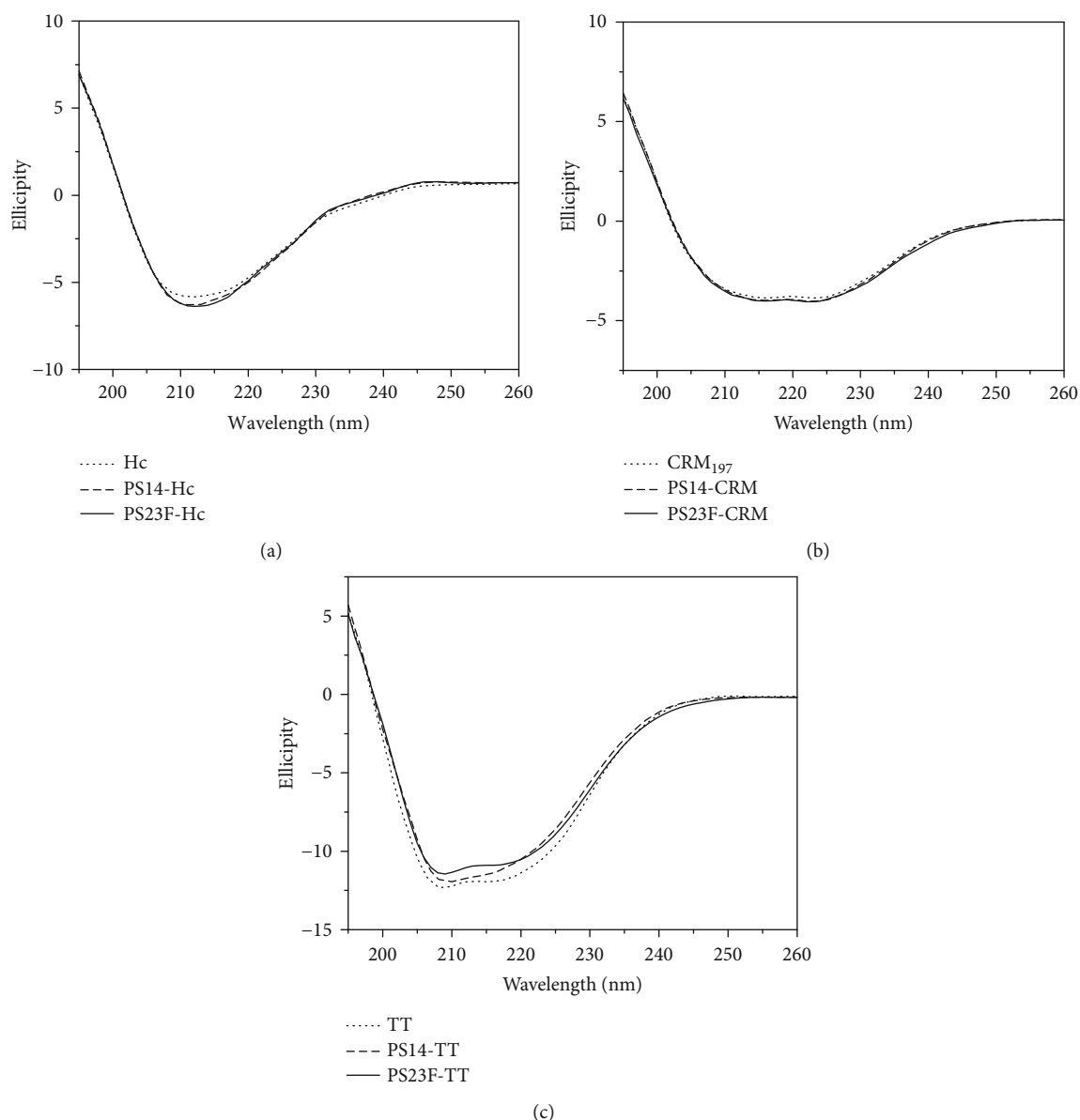


FIGURE 4: Circular dichroism analysis of the conjugates. The far-UV circular dichroism spectra of the Hc-based conjugates (a), the CRM₁₉₇-based conjugates (b), and the TT-based conjugates (c) were recorded from 260 to 190 nm.

response of the three groups was predominantly in the form of IgG1.

As a result in Figure 6(d), the IgM titers of the four groups were low upon initial vaccination. The second and third vaccinations could not significantly booster the IgG titers. Moreover, the PS23F-specific IgM titers of the four groups were comparable to each other upon the three vaccinations. Besides, the IgG/IgM ratios of the PS23F-Hc, PS23F-TT, and PS23F-CRM groups on the third vaccination were 3.1, 0.9, and 2.9, respectively. These ratios were higher than those at the first vaccination (0.6, 0.5, and 0.6). This result suggested that conjugation of the carrier proteins changed the response of IgM to IgG, which was a typical reaction of the conjugate vaccines.

4. Discussion

Hc was a safe, effective, and low-cost protein with robust immunogenic potency. Pneumococcal serogroups 14 and 23F were the major causes of invasive pneumococcal disease in children and older persons. The three carrier proteins (Hc, TT, and CRM₁₉₇) were covalently conjugated with PS14 and PS23F in the present study. The six conjugates were used to investigate the carrier effect of Hc on the immunogenicity of PS14 and PS23F.

As T cell-independent antigens, PS14 and PS23F both have some repeating B cell epitopes. The T-helper cell epitopes of a carrier protein can activate the protein-specific CD4⁺ T cells, which may provide help to B cells in the

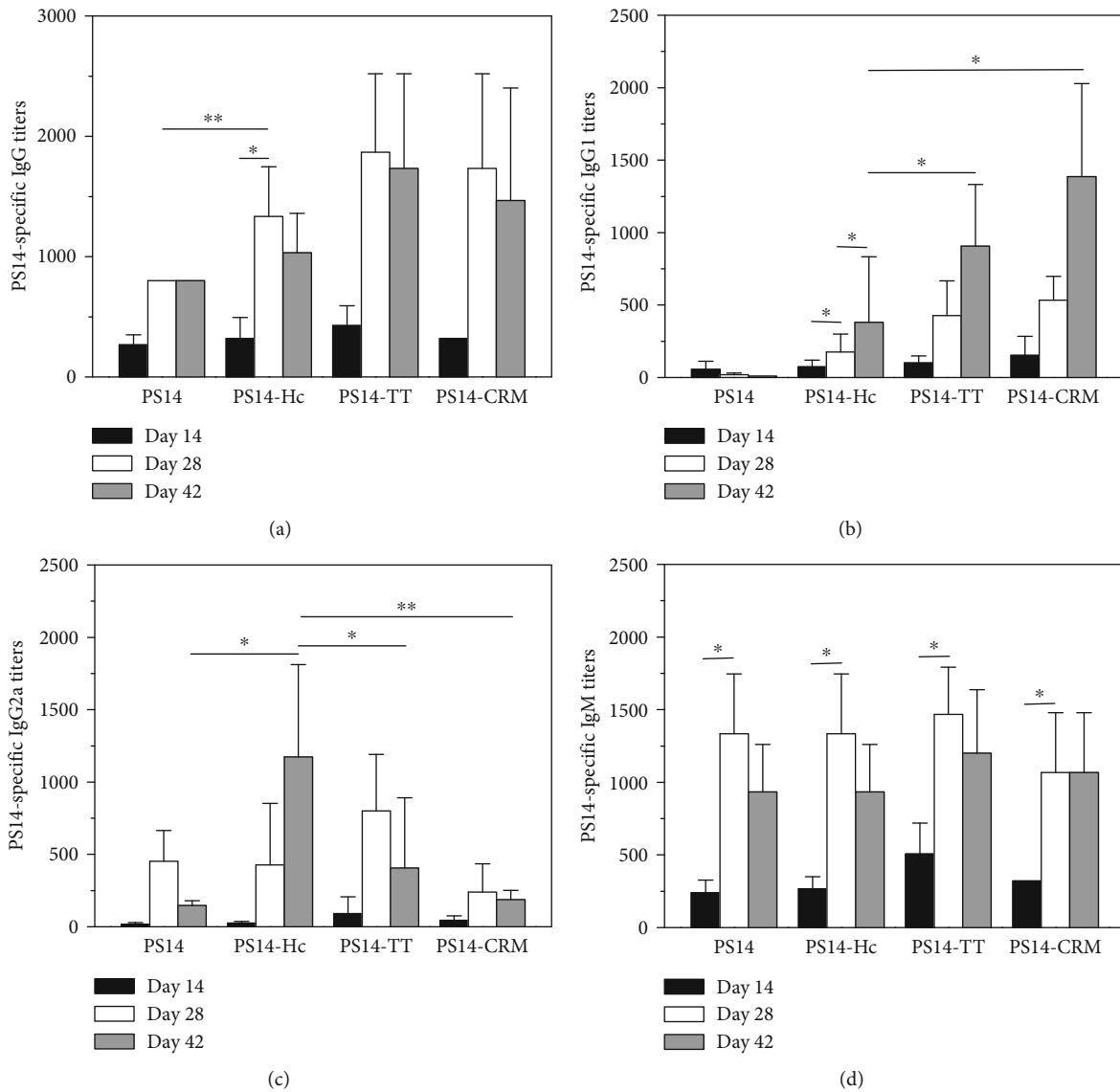


FIGURE 5: PS14-specific antibody titers elicited by the PS14-based conjugates. The measurements of PS14-specific IgG (a), IgG1 (b), IgG2a (c), and IgM (d) were carried out using ELISA. Blood samples after immunization on days 42 were obtained for antibody measurement. Each sample was measured three times. Bar represented mean \pm S.D. from 6 mice per group.

internalization and process of the conjugate and presentation of peptides in MHC class II molecules [26]. The PS-specific B cells can induce its differentiation towards plasma or memory cells and elicit significant intensity of PS-specific antibody response [27]. Acquired protective immunity to *S. pneumonia* mainly due to the PS-specific antibodies naturally obtained against invasive pneumococcal diseases. Thus, the PS-specific antibody response of the conjugates was investigated in this study.

The conjugate vaccines were formed by PS, and the carrier proteins covalently conjugated. Several factors may affect the PS-specific antibody titers of the conjugates, such as the conjugation method, immunization protocol, carrier protein, PS antigen, and PS/protein molar ratio. The conjugation method, immunization protocol, and PS antigen were identical for the six conjugates. The PS14- and PS23F-based conjugates showed comparable PS/pro-

tein molar ratios. Thus, the carrier protein was the major differential factor of the conjugate vaccines.

In the present study, PS14-Hc and PS23F-Hc were demonstrated to potentiate a robust PS-specific antibody response at the levels comparable to the TT- and CRM₁₉₇-based controls. Hc possessed multiple T-helper cell epitopes and exhibited a practical carrier effect on the immunogenicity of the conjugate vaccine, given the high levels of PS-specific antibodies that were measured. This result indicated a sufficient potency of Hc as a carrier protein. The PS14-specific IgG response after three doses was higher than the PS14-specific IgM response. A similar pattern was observed for PS23F-specific immune reactions. This result indicated that the two antigens were changed to T cell-dependent antigens by Hc.

Different from the protein vaccine, the antibody titers of the specific polysaccharide induced by the conjugate vaccine

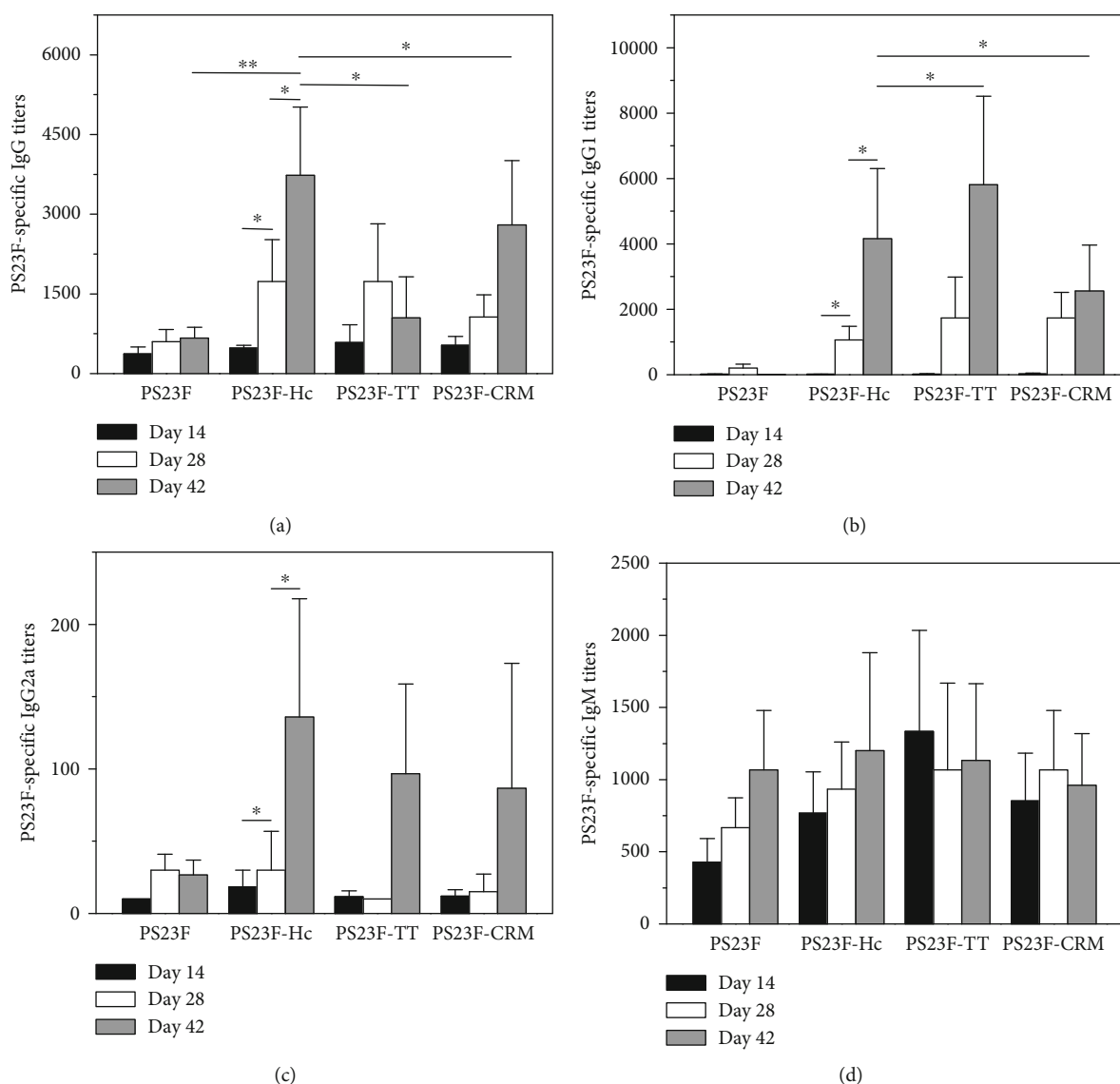


FIGURE 6: PS23F-specific antibody titers elicited by the PS23F-based conjugates. The measurements of PS23F-specific IgG (a), IgG1 (b), IgG2a (c), and IgM (d) were carried out using ELISA. Blood samples after immunization on days 42 were obtained for antibody measurement. Each sample was measured three times. Bar represented mean \pm S.D. from 6 mice per group.

in animals do not seem high. Zhang et al. studied the immunogenicity of the 13 valent *Streptococcus pneumoniae* polysaccharide conjugate vaccine without adjuvants in rhesus monkeys. The results showed that the antibody titer for different polysaccharide types was 1:95.1 ~ 1:538.2 [28]; Shen et al. studied the antibody titers of NIH mice immunized intraperitoneally with *Streptococcus pneumoniae* capsular polysaccharide-tetanus toxoid conjugate vaccine for three times. The results showed that the antibody titers against 18C and 23F polysaccharide were 1:373.29 and 1:422.24, respectively [29]. In our study, the antibody titers of 14 and 23F polysaccharide in mice immunized with Hc conjugate vaccine three times can reach 1:1100 and 1:3700, which is much higher than that reported in previous literatures. It is speculated that the conjugate vaccines have strong immunogenicities and good protective activities.

TT and CRM197 are the typical carrier proteins for meningococcal and pneumococcal conjugate vaccines. Fluorescence spectroscopy data confirmed that Hc, CRM₁₉₇, and TT all assumed mostly no conformational changes after conjugation with PS. In the population with preexisting immunity of TT or CRM₁₉₇, the undesirable antibodies can decrease the effectiveness of the conjugate vaccines with carrier protein TT or CRM₁₉₇. Thus, Hc is an ideal candidate carrier to avoid this problem.

5. Conclusion

In summary, conjugation with Hc significantly increased the immunogenicity of pneumococcal PS14 and PS23F. The carrier effect of Hc was comparable to TT and CRM₁₉₇. Thus, Hc could act as a capable carrier protein for the development

of capsular PS conjugate vaccines to prevent encapsulated bacterial infection. This study lends credence to the notion that it is vital to select an appropriate carrier to enable the epitopes of PS for the induction of proper antibody response.

Data Availability

All the data are available from Dr. Rui Yu yurui1102@139.com upon request.

Additional Points

Highlights. This is the first report about tetanus toxin native C-fragment (Hc), which is safe, low-cost, highly immunogenic, and easy to purify, used as the carrier protein of polysaccharide binding vaccine.

Conflicts of Interest

The authors declare that they have no conflicts of interest with the contents of this article.

Authors' Contributions

Rui Yu and Tao Hu conceptualized and designed the study; Rui Yu did the experiments and analyzed the data; Junjie Xu drafted the article and revised it critically for important intellectual content; Tao Hu and Wei Chen finally approved the version to be submitted.

Acknowledgments

This study was financially supported by the National Key Research and Development Project of China (2018YFA0900804) and the National Natural Science Foundation of China (31970875 and 81703445).

References

- [1] M. Sadarangani, "Protection against invasive infections in children caused by encapsulated bacteria," *Frontiers in Immunology*, vol. 9, p. 2674, 2018.
- [2] H. Ziane, V. Manageiro, E. Ferreira et al., "Serotypes and antibiotic susceptibility of *Streptococcus pneumoniae* isolates from invasive pneumococcal disease and asymptomatic carriage in a pre-vaccination period in Algeria," *Frontiers in Microbiology*, vol. 7, 2016.
- [3] R. Baxter, A. Yee, L. Aukes et al., "Risk of underlying chronic medical conditions for invasive pneumococcal disease in adults," *Vaccine*, vol. 34, no. 36, pp. 4293–4297, 2016.
- [4] G. Lesinski and M. A. Julie Westerink, "Vaccines against polysaccharide antigens," *Current Drug Target - Infectious Disorders*, vol. 1, no. 3, pp. 325–334, 2001.
- [5] C. J. Lee, L. H. Lee, C. S. Lu, and A. Wu, "Bacterial polysaccharides as vaccines—immunity and chemical characterization," *Advances in Experimental Medicine and Biology*, vol. 491, pp. 453–471, 2001.
- [6] C. C. Daniels, P. D. Rogers, and C. M. Shelton, "A review of pneumococcal vaccines: current polysaccharide vaccine recommendations and future protein antigens," *Journal of Pediatric Pharmacology and Therapeutics*, vol. 21, no. 1, pp. 27–35, 2016.
- [7] C. S. Kuo, C. W. Lu, Y. K. Chang et al., "Effectiveness of 23-valent pneumococcal polysaccharide vaccine on diabetic elderly," *Medicine*, vol. 95, no. 26, article e4064, 2016.
- [8] X. Chang, W. Yu, S. Ji, L. Shen, A. Tan, and T. Hu, "Conjugation of PEG-hexadecane markedly increases the immunogenicity of pneumococcal polysaccharide conjugate vaccine," *Vaccine*, vol. 35, no. 13, pp. 1698–1704, 2017.
- [9] D. Wu, S. Ji, and T. Hu, "Development of pneumococcal polysaccharide conjugate vaccine with long spacer arm," *Vaccine*, vol. 31, no. 48, pp. 5623–5626, 2013.
- [10] M. Xu, X. Xing, Z. Wu, Y. Du, and T. Hu, "Molecular shape and immunogenicity of meningococcal polysaccharide group A conjugate vaccine," *Vaccine*, vol. 33, no. 43, pp. 5815–5821, 2015.
- [11] G. Ada and D. Isaacs, "Carbohydrate-protein conjugate vaccines," *Clinical Microbiology and Infection*, vol. 9, no. 2, pp. 79–85, 2003.
- [12] M. E. Pichichero, "Protein carriers of conjugate vaccines: characteristics, development and clinical trials," *Human vaccines & immunotherapeutics*, vol. 9, no. 12, pp. 2505–2523, 2013.
- [13] M. van der Linden, G. Falkenhorst, S. Perniciaro, C. Fitzner, and M. Imöhl, "Effectiveness of pneumococcal conjugate vaccines (PCV7 and PCV13) against invasive pneumococcal disease among children under two years of age in Germany," *PLoS One*, vol. 11, no. 8, article e0161257, 2016.
- [14] T. Zhang, W. Yu, Y. Wang, and T. Hu, "Moderate PEGylation of the carrier protein improves the polysaccharide-specific immunogenicity of meningococcal group A polysaccharide conjugate vaccine," *Vaccine*, vol. 33, no. 28, pp. 3208–3214, 2015.
- [15] C. G. Whitney, M. M. Farley, J. Hadler et al., "Decline in Invasive Pneumococcal Disease after the Introduction of Protein–Polysaccharide Conjugate Vaccine," *New England Journal of Medicine*, vol. 348, no. 18, pp. 1737–1746, 2003.
- [16] M. Knuf, F. Kowalzik, and D. Kieninger, "Comparative effects of carrier proteins on vaccine-induced immune response," *Vaccine*, vol. 29, no. 31, pp. 4881–4890, 2011.
- [17] M. Tontini, F. Berti, M. R. Romano et al., "Comparison of CRM₁₉₇, diphtheria toxoid and tetanus toxoid as protein carriers for meningococcal glycoconjugate vaccines," *Vaccine*, vol. 31, no. 42, pp. 4827–4833, 2013.
- [18] G. Giannini, R. Rappuoli, and G. Ratti, "The amino-acid sequence of two non-toxic mutants of diphtheria toxin: CRM₄₅ and CRM₁₉₇," *Nucleic Acids Research*, vol. 12, no. 10, pp. 4063–4069, 1984.
- [19] R. Rappuoli, "Isolation and characterization of *Corynebacterium diphtheriae* nontandem double lysogens hyperproducing CRM₁₉₇," *Applied and Environmental Microbiology*, vol. 46, no. 3, pp. 560–564, 1983.
- [20] R. Yu, L. Hou, C. Yu et al., "Enhanced expression of soluble recombinant tetanus neurotoxin Hc in *Escherichia coli* as a tetanus vaccine candidate," *Immunobiology*, vol. 216, no. 4, pp. 485–490, 2011.
- [21] R. Yu, T. Fang, S. Liu et al., "Comparative immunogenicity of the tetanus toxoid and recombinant tetanus vaccines in mice, rats, and cynomolgus monkeys," *Toxins*, vol. 8, no. 7, p. 194, 2016.
- [22] R. Yu, S. Yi, C. Yu et al., "A conformational change of C fragment of tetanus neurotoxin reduces its ganglioside-binding

- activity but does not destroy its immunogenicity," *Clinical and Vaccine Immunology*, vol. 18, no. 10, pp. 1668–1672, 2011.
- [23] H. Keyserling, C. Bosley, S. Starr, B. Watson, D. Laufer, and E. Anderson, "Immunogenicity of type 14 conjugate vaccine in infants," *Pediatric Research*, vol. 35, p. 184A, 1994.
- [24] R. Dagan, R. Melamed, M. Muallem et al., "Reduction of nasopharyngeal carriage of pneumococci during the second year of life by a heptavalent conjugate pneumococcal vaccine," *The Journal of Infectious Diseases*, vol. 174, no. 6, pp. 1271–1278, 1996.
- [25] W. Yu and T. Hu, "Conjugation with an inulin-chitosan adjuvant markedly improves the immunogenicity of Mycobacterium tuberculosis CFP10-TB10.4 fusion protein," *Molecular Pharmaceutics*, vol. 13, no. 11, pp. 3626–3635, 2016.
- [26] K. Pobre, M. Tashani, I. Ridda, H. Rashid, M. Wong, and R. Booy, "Carrier priming or suppression: understanding carrier priming enhancement of anti-polysaccharide antibody response to conjugate vaccines," *Vaccine*, vol. 32, no. 13, pp. 1423–1430, 2014.
- [27] F. Y. Avci, X. Li, M. Tsuji, and D. L. Kasper, "A mechanism for glycoconjugate vaccine activation of the adaptive immune system and its implications for vaccine design," *Nature Medicine*, vol. 17, no. 12, pp. 1602–1609, 2011.
- [28] Z. H. A. N. G. Ming-hua, S. H. I. Ji-chun, C. A. O. Xin, R. E. N. Tao, X.-l. Tang, and H. A. N. Fei, "Studies on preparation and immunogenicity of 13-valent pneumococcal polysaccharide conjugate vaccines," *International Journal of Biological Macromolecules*, vol. 36, no. 3, pp. 118–122, 2013.
- [29] S. H. E. N. Rong, C. H. E. N. Xiao-hang, R. E. N. Ke-ming, K. O. N. G. Su-juan, W. A. N. G. Jian-hong, and Z. H. A. N. G. Yong, "Antibody responses induced with Streptococcus pneumoniae capsular polysaccharide-tetanus toxoid conjugates by two immune routes in mice," *Chinese Journal of Biologicals*, vol. 19, no. 4, pp. 387–390, 2006.

Research Article

Anti-Inflammatory Effect of a Peptide Derived from the Synbiotics, Fermented *Cudrania tricuspidata* with *Lactobacillus gasseri*, on Inflammatory Bowel Disease

Jimyeong Ha ¹, Hyemin Oh ², Nam Su Oh,³ Yeongeun Seo ², Joo Hyun Kang,² Min Hee Park,⁴ Kyung Su Kim,⁴ Shin Ho Kang,⁴ and Yohan Yoon ^{1,2}

¹Risk Analysis Research Center, Sookmyung Women's University, Seoul 04310, Republic of Korea

²Department of Food and Nutrition, Sookmyung Women's University, Seoul 04310, Republic of Korea

³Department of Food Science and Biotechnology, Korea University, Sejong 30019, Republic of Korea

⁴R&D Center, Seoul Dairy Cooperative, Ansan 15407, Republic of Korea

Correspondence should be addressed to Yohan Yoon; yoon@sookmyung.ac.kr

Received 23 March 2020; Revised 5 June 2020; Accepted 8 June 2020; Published 4 July 2020

Guest Editor: Li Zhang

Copyright © 2020 Jimyeong Ha et al. This is an open access article distributed under the Creative Commons Attribution License, which permits unrestricted use, distribution, and reproduction in any medium, provided the original work is properly cited.

The objective of this study was to evaluate the effects of peptides derived from synbiotics on improving inflammatory bowel disease (IBD). Five-week-old male C57BL/6 mice were administered with dextran sulfate sodium (DSS) via drinking water for seven days to induce IBD (IBD group). The mice in the IBD group were orally administered with PBS (IBD-PBS-positive control), *Lactobacillus gasseri* 505 (IBD-Pro), fermented powder of CT extract with *L. gasseri* 505 (IBD-Syn), β -casein: LSQSKVLPVPQKAVPYQRDMP (IBD-Pep 1), or α_{s2} -casein: VYQHQAAMKPWIQPKTKVIPYVRYL (IBD-Pep 2) (both peptides are present in the synbiotics) for four more days while inducing IBD. To confirm IBD induction, the weights of the animals and the disease activity index (DAI) scores were evaluated once every two days. Following treatment of probiotics, synbiotics, or peptides for 11 days, the mice were sacrificed. The length of the small and large intestines was measured. The expression of the proinflammatory cytokines IL-1 β , IL-6, TNF- α , and COX-2 in the large intestine was measured. Large intestine tissue was fixed in 10% formalin and stained with hematoxylin and eosin for histopathological analysis. The body weights decreased and DAI scores increased in the IBD group, but the DAI scores were lower in the IBD-Pep 2 group than those in the IBD group treated with PBS, Pro, Syn, or Pep 1. The lengths of the small and large intestines were shorter in the IBD group than in the group without IBD, and the expression levels of the proinflammatory cytokines were lower ($p < 0.05$) in the IBD-Pep 2 group than those in the IBD-PBS-positive control group. In addition, histopathological analysis showed that IBD was ameliorated in the Pep 2-treated group. These results indicate that Pep 2 derived from α_{s2} -casein was effective in alleviating IBD-associated inflammation. Thus, we showed that these peptides can alleviate inflammation in IBD.

1. Introduction

Inflammatory bowel disease (IBD) is a chronic inflammation in the intestine, and the number of IBD patients has increased by 12 to 14.5 times, especially for pediatric patients [1, 2]. IBD is caused by abnormal immune responses and dysbiosis of intestinal bacteria [3, 4]. Thus, it is necessary to study how to improve immune responses and dysbiosis.

Probiotics are living organisms that are beneficial to the health of the host when ingested in moderate quantities [5, 6]. Lactic acid bacteria are representative probiotics that have various health-beneficial functions, such as normalization of intestinal flora and enhancement of immunity, as well as antioxidative and anti-inflammatory activities [7, 8]. Other studies [9, 10] have shown that indigestible food ingredients can help the growth of beneficial microorganisms in the

intestine, especially probiotic strains, and improve human health. Thus, the effect of the combination of probiotics and prebiotics, called synbiotics, has been investigated on the basis of the hypothesis that synbiotics have better functional benefits than probiotics or prebiotics alone [11, 12].

Lactobacillus gasseri is a facultative anaerobic bacterium that is abundant in human and animal gastrointestinal tracts [13, 14]. They are used in diverse fermented dairy products and probiotics because they have immunomodulatory, antibacterial, and antihypertensive activities [15, 16]. *Cudrania tricuspidata* (CT) has been used in Asia as a medicine for antibacterial and anticancer therapy [17, 18] and was found to have a prebiotic effect by promoting the growth of beneficial bacteria in the intestine through its noncarbohydrate components comprising polyphenols [19].

Therefore, the objective of this study was to examine the effects of probiotics (*L. gasseri*), synbiotics (*L. gasseri*+CT extract), and peptides separated from the synbiotics on IBD improvements.

2. Materials and Methods

2.1. Animal. Five-week-old male C57BL/6 mice were purchased from Orient Bio Inc. (Seongnam, Gyeonggi, Korea) and adapted at 20–30°C and 40–60% humidity for a week. The mice were then divided into six experimental groups, as presented in Table 1. The animal experiment (SMWU-IACUC-1709-020) was approved by the Institute of Animal Care and Use Committee at Sookmyung Women’s University.

2.2. Induction of IBD and Treatment. Mice were treated with 1–2% dextran sulfate sodium (DSS; MP Biomedicals Korea, Songpa-gu, Seoul, Korea) via the drinking water to induce IBD for 7 days; these mice comprised the IBD group. The negative control group received normal drinking water. Starting from day 0, the negative control mice were orally administered with phosphate-buffered saline (PBS: pH 7.4; 0.2 g KH_2PO_4 , 1.5 g $\text{Na}_2\text{HPO}_4 \cdot 7\text{H}_2\text{O}$, 8.0 g NaCl, and 0.2 g KCl, in 1 L distilled water) using feeding needles once a day for 7 days. The IBD group was further divided in the following subgroups: the IBD-PBS group—orally administered with PBS; the IBD-Pro group—administered with probiotics (*L. gasseri* 505; Oh et al., 2016); the IBD-Syn group—administered with synbiotics (fermented powder of CT extract with *L. gasseri* 505); the IBD-Pep 1 group—administered with Pep 1; and the IBD-Pep 2 group—administered with Pep 2. Administration took place once a day for 7 days using feeding needles, as shown in Table 1. The oral administration continued for 4 more days without the DSS in the drinking water (Table 1). The two peptides Pep 1 and Pep 2, separated from the synbiotics as shown in Table 2 [19], were provided by Seoul Milk Central Research Institute (Ansan-si, Gyeonggi, Korea). The mice were fasted for 18 h and anesthetized with isoflurane (Hana pharm Co., Ltd., Hwaseong, Gyeonggi, Korea) for sacrifice. The intestines were rapidly removed, and the length of the small and large intestines was measured. They were then stored at -70°C . Parts of the large intestine tissues were fixed in 10% formalin solution (HISKO, Gunpo-si, Korea) for histopathological analysis.

TABLE 1: Experimental groups.

Groups	Drinking water	Oral injection	<i>n</i>
Negative control	General water	PBS	8
IBD-PBS-positive control	DSS	PBS	8
IBD-Pro	DSS	Probiotics ¹	8
IBD-Syn	DSS	Synbiotics ²	8
IBD-Pep 1	DSS	Peptide1 ³	8
IBD-Pep 2	DSS	Peptide2 ⁴	8

¹Using *Lactobacillus gasseri* 505 injected in mice at a concentration of 10^8 CFU/kg bw/day. ²Preparation of fermentation powders by using *Lactobacillus gasseri* 505 and *Cudrania tricuspidata* extract injected in mice at a concentration of 1500 mg/kg. ^{3,4}Peptides isolated from fermentation powders injected in mice at a concentration of 20 mg/kg.

2.3. Measurement of Body Weight and Observation of Fecal Conditions. The body weight of the mice was measured every 2 days. The disease activity index (DAI) scores were graded by observing the viscosity of feces and the presence or absence of blood in feces for 11 days from the first day of DSS water administration. The value was calculated according to the Hamers et al. [20].

2.4. Measurement of Nitric Oxide and Inflammatory Cytokine Concentrations in Serum. The blood samples were centrifuged at $94\times g$ for 10 min to separate the serum. The serum (80 μl) and the same volume of Griess reagent (Promega, Madison, WI, USA) were added to a 96-well plate and then incubated at room temperature for 10 min. The absorbance was measured with the Take3 system in Epoch™ Microplate Spectrophotometer (BioTek Instruments, Inc., Winooski, VT, USA) at 540 nm, and the concentrations of NO were calculated based on the quantitative curve of NaNO_2 standard solution. In addition, the concentrations of inflammatory cytokines productions in the serum were measured using the ProcartaPlex™ mouse Th1/Th2 cytokine panel (11 plex) (Thermo Fisher Scientific, Waltham, MA, USA).

2.5. Measurement of Proinflammatory Cytokine mRNA Levels in the Large Intestine Tissue. Total mRNA was extracted from large intestine tissues using the RNeasy Mini Kit (Qiagen, Hilden, Germany) according to the manufacturer’s instructions. The mRNA of large intestine tissues was quantified using the Take3 system in Epoch™ Microplate Spectrophotometer (BioTek Instruments). For quantitative real-time reverse transcription polymerase chain reaction (qRT-PCR) analysis, cDNA was synthesized using QuantiTect Reverse Transcription Kit (Qiagen) according to the manufacturer’s instructions. The primers used in qRT-PCR for IL-1 β , IL-6, and COX-2 are listed in Table 3, and the primers for TNF- α were purchased from Qiagen (Mm_Tnf_1_SG QuantiTect Primer Assay, Cat. no. QT00104006). qRT-PCR was performed on a Rotor-Gene Q instrument (Qiagen), using a Rotor-Gene SYBR® Green PCR Kit (Qiagen) according to the manufacturer’s instructions. Relative fold changes of gene expression levels were analyzed using the $-2^{\Delta\Delta\text{Ct}}$ method [24].

TABLE 2: Peptide information.

Groups	<i>m/z</i> peptide	Protein	Sequence	Reference
Pep 1	2479.2	β -casein	LSQSKVLPVPQKAVPYPQRDMP	[19]
Pep 2	3115.4	α_{s2} -casein	VYQHQBKAMKPWVQPKTKVIPYVRYL	

TABLE 3: Primers for quantitative real-time reverse transcription polymerase chain reaction.

Primer	Sequence (5' to 3')	Reference
Cytokine related primers		
IL-1 β	F: AAC CTG CTG GTG TGT GAC GTT C R: CAG CAC GAG GCT TTT TTG TTG T	[21]
IL-6	F: ACC AGA GGA AAT TTT GAA TAG GC R: TGA TGC ACT TGC AGA AAA CA	[22]
COX-2	F: TGT ATC CCC CCA CAG TCA AAG ACA C R: GTG CTC CCG AAG CCA GAT GG	[23]

2.6. Histopathological Analysis of the Large Intestine Tissue.

The fixed large intestine tissue samples were washed with distilled water and dehydrated using alcohol. They were fixed with paraffin, and these samples were then placed on slides and stained with hematoxylin and eosin (H&E). Histopathological analysis was performed at 200 magnification. The results were determined by referring to the international harmonization of nomenclature and diagnostic criteria (INHAND) standard, and the specimen lesions were compared.

2.7. Statistical Analysis. Experimental data were analyzed using the general linear procedure of SAS[®] version 9.4 (SAS Institute, Inc., Cary, NC, USA). The least square mean comparisons among the treatment groups were performed by a pairwise *t*-test at $\alpha = 0.05$.

3. Results

3.1. Effects of Peptides on Mouse Weight and DAI. After 4 days of oral administration of 1% DSS, no obvious changes in fecal state, such as the presence of blood and diarrhea, were then observed. Thus, the DSS concentration was increased to 2% for 3 days, and bloody stool and diarrhea were observed. The body weight of the group treated with 2% DSS (IBD group) decreased, while that of the negative control group increased steadily (Table 4). The DAI scores were calculated using the fecal conditions (Table 5). As a result, the DAI scores for the negative control and the IBD group were 0 and 2, respectively (Table 6). The body weights in the IBD-Pro, IBD-Syn, IBD-Pep 1, or IBD-Pep 2 groups were not obviously different from that in the IBD-PBS-positive control group. The DAI scores (0.5-1.5) of the IBD-Pro, IBD-Pep 1, and IBD-Pep 2 groups were generally lower than that of the IBD-PBS-positive control group

TABLE 4: Weight change by dextran sulfate sodium autogenous feeding.

Groups	Initial weight (g)	Weight before sacrifice (g)
Negative control	21.5 \pm 0.6 ^{A,a}	22.3 \pm 0.8 ^{A,b}
IBD-PBS-positive control	21.3 \pm 1.0 ^{A,a}	15.4 \pm 1.4 ^{C,b}
IBD-Pro	21.2 \pm 1.0 ^{A,a}	17.4 \pm 1.3 ^{B,b}
IBD-Syn	21.4 \pm 1.5 ^{A,a}	16.0 \pm 1.0 ^{C,b}
IBD-Pep 1	21.1 \pm 0.6 ^{A,a}	15.0 \pm 0.6 ^{C,b}
IBD-Pep 2	20.9 \pm 0.6 ^{A,a}	16.3 \pm 1.2 ^{B,C,b}

^{A,B,C}Values within the same column with different superscript letters are significantly different ($p < 0.05$). ^{a,b}Values within the same row with different superscript letters are significantly different ($p < 0.05$).

TABLE 5: Scoring table for disease activity index.

Symptoms/score	Characteristics
Stool consistency	
0	Normal feces
1	Loose stool
2	Watery diarrhea
3	Slimy diarrhea, little blood
4	Severe watery diarrhea with blood
Blood in stool	
0	Negative
2	Positive
4	Gross bleeding

TABLE 6: Measurement of disease activity index using feces conditions the day after dextran sulfate sodium stops supplying and before sacrifice.

Groups	DAI scores	
	The day after DSS supply stopped	Before sacrifice
Negative control	0	0
IBD-PBS-positive control	3.5	2
IBD-Pro	2	1.5
IBD-Syn	2	2
IBD-Pep 1	4	1
IBD-Pep 2	2.5	0.5

(DAI = 2), especially for the IBD-Pep 2 group (DAI = 0.5) (Table 6). The DAI score of the IBD-Pep 2 group was very close to that of the negative control (Table 6). Therefore, the Pep 2 (α_{s2} -casein) separated from synbiotics could improve intestinal inflammation.

3.2. Comparisons of Small and Large Intestine Lengths. Yoon et al. [25] showed that the lengths of the small and large intestines tended to be shorter in mice with IBD. Similarly, we found that the lengths of the small and large intestines were shorter in the IBD-PBS-positive control, IBD-Pro, IBD-Syn, IBD-Pep 1, and IBD-Pep 2 groups than those in the negative control group, and the lengths of the large intestines in the IBD-PBS-positive control group were the shortest (Table 7).

3.3. Nitric Oxide and Inflammatory Cytokine Levels in Serum. The NO level was the highest in the positive control group, but the NO levels of the groups treated with IBD-Pro, IBD-Syn, and IBD-Pep 1, were significantly lower ($p < 0.05$) than that of the positive control (Figure 1). It indicates that the levels of inflammation were improved, when probiotics, synbiotics, and Pep1 were treated to the mice having intestinal inflammation. In serum inflammatory cytokines (IFN- γ , IL-6, and TNF- α), these cytokines were less secreted in all treatment groups, compared to the positive control (Figure 2). In particular, IFN- γ was lower ($p < 0.05$) in the IBD-Pep 2 group, and IL-6 was lower ($p < 0.05$) in the IBD-Pro and IBD-Pep 1 groups than those of the positive group. TNF- α was significantly lower ($p < 0.05$) in the IBD-Pro, IBD-Syn, and IBD-Pep 2 groups than that of the positive group (Figure 2).

3.4. mRNA Levels of Inflammatory Cytokine in Large Intestine Tissue. Many studies have reported that the expression levels of IL-1 β and TNF- α are increased in IBD patients [26]. We evaluated the mRNA levels of the proinflammatory cytokines such as IL-1 β , IL-6, TNF- α , and COX-2 in the intestine of DSS-treated mice (IBD group), and the levels in the large intestine were increased ($p < 0.05$), indicating that DSS treatment obviously induced IBD (Figure 3). The mRNA levels of these inflammatory markers in large intestine tissues were significantly decreased ($p < 0.05$) in the IBD-Pep 2 group, compared to the IBD-PBS-positive control group. In addition, the mRNA levels of IL-6, TNF- α , and COX-2, but not IL-1 β , were significantly decreased in the IBD-Pro and IBD-Pep 1 groups ($p < 0.05$) (Figure 3). Therefore, probiotics, Pep 1, and Pep 2 are efficient in inhibiting proinflammatory cytokine expression.

3.5. Histopathological Features of Large Intestine Tissue. IBD was mainly observed in the large intestine, and thus, histopathological features of jejunum tissue were examined. Jejunum inflammation was found in the IBD-PBS-positive control, IBD-Pro, IBD-Syn, and IBD-Pep 1 groups, compared to the negative control group (Figure 4). The degree of lesions was obviously lower in the IBD-Pep 2 treatment group than those in the IBD-PBS-positive control group and the other treatment groups (Figure 4). Therefore, α_s2 -casein (Pep 2) treatment results in the reduction of colorectal lesions in IBD mice.

4. Discussions

Bauer et al. [27] have suggested that DSS-induced IBD mice are characterized by weight loss, and Okayasu et al. [28] have suggested that weight loss and bloody stool are hallmarks of

TABLE 7: Differences in small and large intestine lengths among the groups (unit: cm).

Treatment	Small intestine	Large intestine
Negative control	38.24 \pm 1.55 ^A	7.37 \pm 0.75 ^A
IBD-PBS positive control	36.54 \pm 1.15 ^B	4.73 \pm 0.53 ^C
IBD-Pro	36.03 \pm 1.34 ^B	5.38 \pm 0.57 ^{B,C}
IBD-Syn	36.51 \pm 1.45 ^B	5.09 \pm 0.54 ^{B,C}
IBD-Pep 1	35.25 \pm 1.21 ^B	4.75 \pm 0.33 ^{B,C}
IBD-Pep 2	37.39 \pm 1.78 ^{A,B}	5.43 \pm 0.68 ^B

^{A,B,C}Values within the same column with different superscript letters are significantly different ($p < 0.05$).

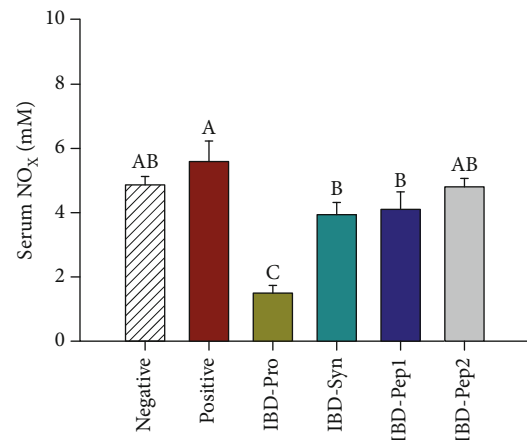


FIGURE 1: Serum nitric oxide (NO) concentration. ^{A,B}Values are significantly different ($p < 0.05$).

IBD. According to these studies, our results indicate that IBD was induced in the mice by 2% DSS treatment (Table 4), and the length of the small and large intestines became shorter by 2% DSS treatment, which is found in IBD patients [29]. The DAI scores were also low in the IBD-Pep 1 and IBD-Pep 2 treatment groups, indicating that the inflammation was improved by Pep 1 and Pep 2 (Table 6).

NO level in serum is used as an important biomarker for active IBD patients [30]. When the inflammatory reaction of the colon occurs, the productions of cytokines such as TNF- α and IFN- γ induced third isoform inducible (iNOS) to increase the production of NO. TNF- α and IL-6 in the serum are related to intestinal disease, and all are upregulated in IBD patients [31]. Increased TNF- α due to intestinal disease stimulates the secretion of IFN- γ in IBD patients [32]. In our study, the inflammatory response was alleviated when the probiotics, synbiotics, and Pep 1 were orally administered to mice which had the IBD. TNF- α , IFN- γ , and IL-6 secretions were generally lowered (Figure 2) by probiotics, Pep 1, and Pep 2 treatments. This result indicates that the treatments of probiotics, synbiotics, Pep 1, and Pep 2 can reduce NO and the inflammatory cytokines in serum.

Colonic lesions occur in IBD patients, and inflammatory cells infiltrate the lesion areas to produce proinflammatory cytokines [33]. However, the use of probiotics downregulates the expression of proinflammatory cytokines, limiting inflammatory reactions such as immune cell infiltration of

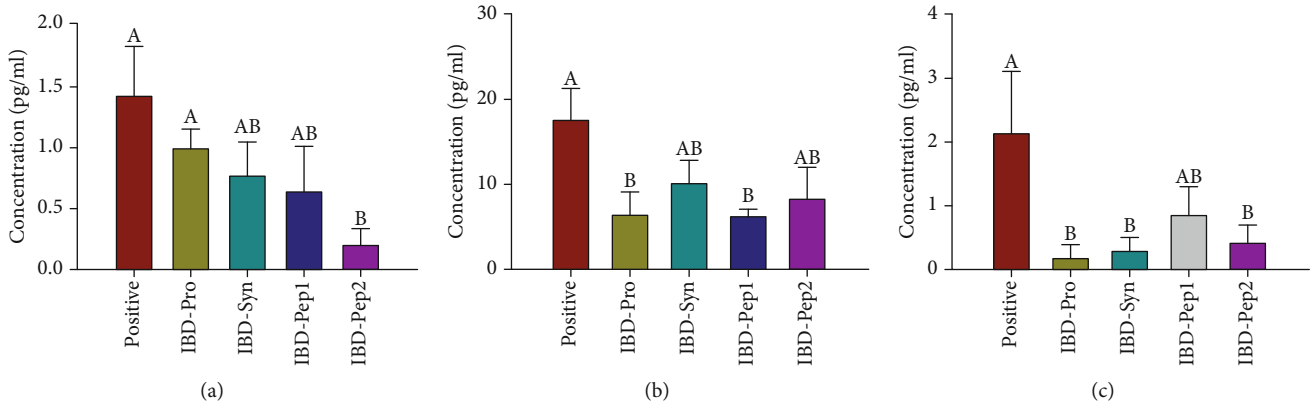


FIGURE 2: Inflammatory cytokine levels in the serum: (a) IFN- γ , (b) IL-6, and (c) TNF- α . ^{A,B}Values are significantly different ($p < 0.05$).

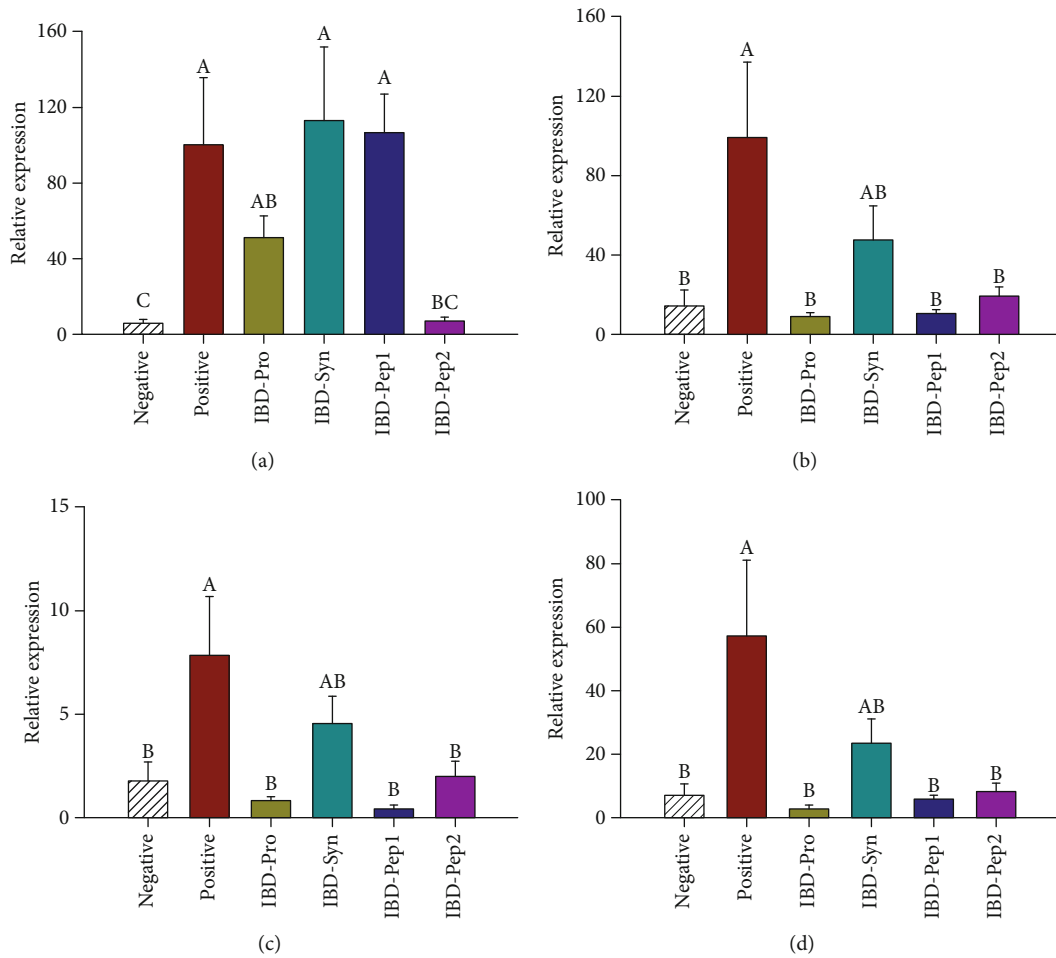


FIGURE 3: Inflammatory cytokine mRNA levels in the large intestine tissue: (a) IL-1 β , (b) IL-6, (c) TNF- α , and (d) COX-2. ^{A,B,C}Values are significantly different ($p < 0.05$).

mucous membranes [34]. Thus, the mRNA levels of proinflammatory cytokines such as IL-1 β , IL-6, TNF- α , and COX-2 in the large intestine tissue were also measured in our study. As a result, the proinflammatory cytokines in the IBD-Pro, IBD-Pep 1, and IBD-Pep 2 were significantly

reduced, compared to positive control. Also, in the histopathology results, the level of lesion in the jejunum was clearly reduced, especially in the IBD-Pep 2 group. This result indicates that probiotics, Pep 1, and Pep 2 reduce the inflammatory cytokine levels and Pep 2 reduces the level of lesion.

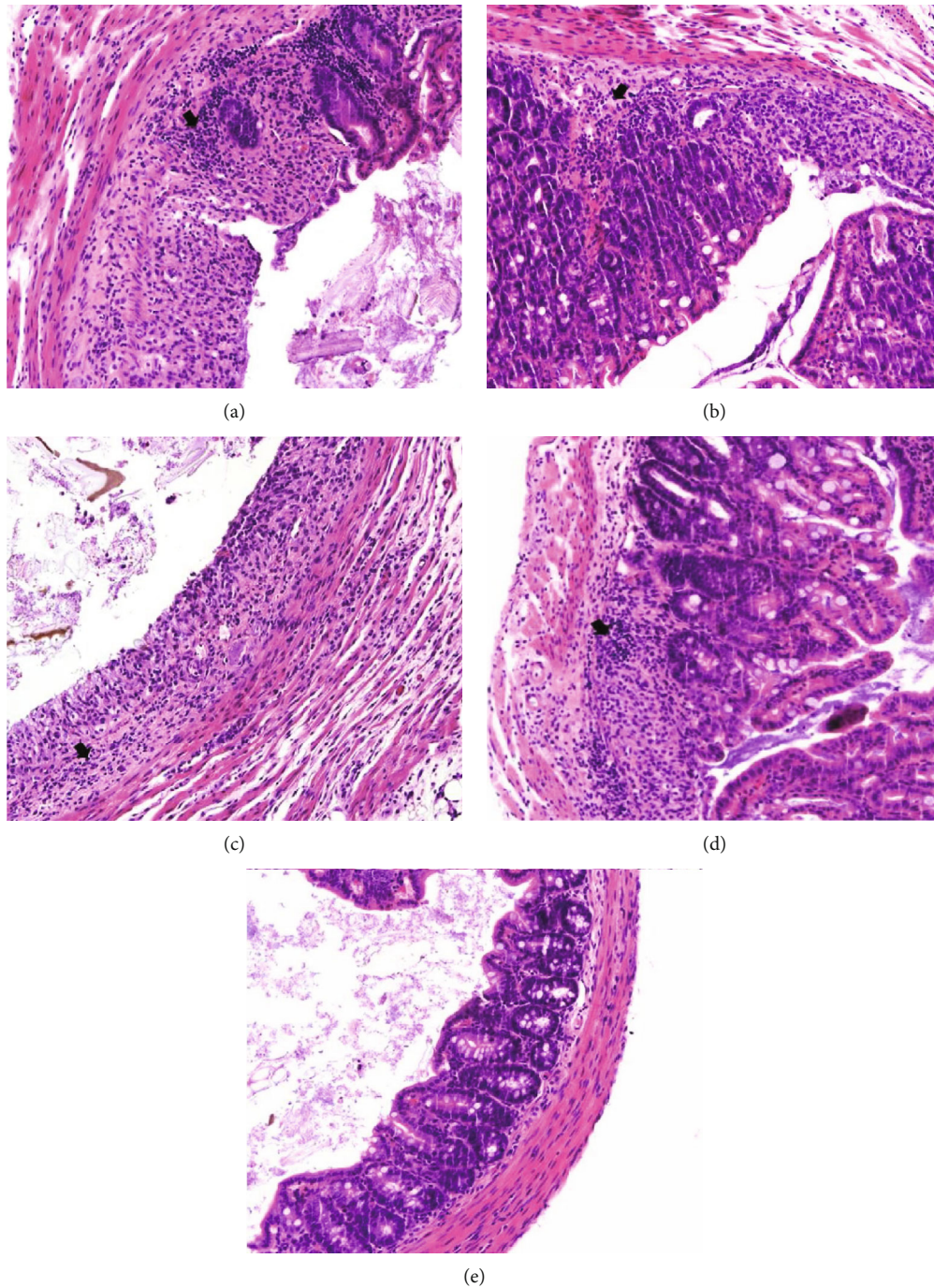


FIGURE 4: Histopathological features of jejunum of the IBD group of mice treated with PBS (a; IBD-PBS-positive group), probiotics (b; IBD-Pro), synbiotics (c; IBD-Syn), peptide 1 (d; IBD-Pep 1), and peptide 2 (e; IBD-Pep 2). Hematoxylin and eosin- (H&E-) stained sections of a mouse large intestine are shown. Black arrows indicate inflammation of the colitis mucosa. Magnifications: $\times 200$.

5. Conclusions

In conclusion, Pep 2, which contains the α_{s2} -casein sequence of VYQHQAAMKPWIQPKTKVIPYVRYL separated from the synbiotics (fermented *CT* extract with *L. gasseri* 505), was commonly involved to improve the intestinal inflammation factors such as the DAI score, proinflammatory cytokine levels, and histopathological result. Therefore, Pep 2 could be

used as a supplement for improving inflammation in IBD patients. However, a human application study should be conducted to confirm this effect.

Data Availability

The data used to support the findings of this study are available from the corresponding author upon request.

Conflicts of Interest

The authors declare no conflicts of interest.

Acknowledgments

This study was supported by the “Development and Production of Natural Synbiotic Foods for Improving Pediatric Inflammatory Bowel Disease and Gut Microbiota” (Project No. 117069), Korea Institute of Planning and Evaluation for Technology in Food, Agriculture, Forestry, and Fisheries.


References

- [1] J. Cosnes, C. Gower-Rousseau, P. Seksik, and A. Cortot, “Epidemiology and natural history of inflammatory bowel diseases,” *Gastroenterology*, vol. 140, no. 6, pp. 1785–1794.e4, 2011.
- [2] J. D. Lewis, E. Z. Chen, R. N. Baldassano et al., “Inflammation, antibiotics, and diet as environmental stressors of the gut microbiome in pediatric Crohn’s disease,” *Cell Host & Microbe*, vol. 18, no. 4, pp. 489–500, 2015.
- [3] D. C. Rubin, A. Shaker, and M. S. Levin, “Chronic intestinal inflammation: inflammatory bowel disease and colitis-associated colon cancer,” *Frontiers in Immunology*, vol. 3, no. 107, pp. 1–10, 2012.
- [4] K. Matsuoka and T. Kanai, “The gut microbiota and inflammatory bowel disease,” in *Seminars in immunopathology (Vol. 37, No. 1, pp. 47-55)*, Springer, Berlin Heidelberg, 2015.
- [5] U. Andersson, C. Bränning, S. Ahrné et al., “Probiotics lower plasma glucose in the high-fat fed C57BL/6J mouse,” *Beneficial Microbes*, vol. 1, no. 2, pp. 189–196, 2010.
- [6] M. E. A. Afjeh, R. Pourahmad, B. Akbari-adergani, and M. Azin, “Use of glucose oxidase immobilized on magnetic chitosan nanoparticles in probiotic drinking yogurt,” *Food Science of Animal Resources*, vol. 39, no. 1, pp. 73–83, 2019.
- [7] C. S. Stancu, G. M. Sanda, M. Deleanu, and A. V. Sima, “Probiotics determine hypolipidemic and antioxidant effects in hyperlipidemic hamsters,” *Molecular Nutrition & Food Research*, vol. 58, no. 3, pp. 559–568, 2014.
- [8] E. Alshammari, M. Patel, M. Sachidanandan, P. Kumar, and M. Adnan, “Potential evaluation and health fostering intrinsic traits of novel probiotic strain *Enterococcus durans* F3 isolated from the gut of fresh water fish catla catla,” *Food Science of Animal Resources*, vol. 39, no. 5, pp. 844–861, 2019.
- [9] M. T. Liong, “Roles of probiotics and prebiotics in colon cancer prevention: postulated mechanisms and in-vivo evidence,” *International Journal of Molecular Sciences*, vol. 9, no. 5, pp. 854–863, 2008.
- [10] A. Wasilewski, M. Zielińska, M. Storr, and J. Fichna, “Beneficial effects of probiotics, prebiotics, synbiotics, and psychobiotics in inflammatory bowel disease,” *Inflammatory Bowel Diseases*, vol. 21, no. 7, pp. 1674–1682, 2015.
- [11] P. Markowiak and K. Śliżewska, “Effects of probiotics, prebiotics, and synbiotics on human health,” *Nutrients*, vol. 9, no. 9, p. 1021, 2017.
- [12] N. S. Oh, K. Kim, S. Oh, and Y. Kim, “Enhanced production of galactooligosaccharides enriched skim milk and applied to potentially synbiotic fermented milk with *Lactobacillus rhamnosus* 4B15,” *Food Science of Animal Resources*, vol. 39, no. 5, pp. 725–741, 2019.
- [13] R. Wall, G. Fitzgerald, S. Å.©. Hussey et al., “Genomic diversity of cultivable *Lactobacillus* populations residing in the neonatal and adult gastrointestinal tract,” *FEMS Microbiology Ecology*, vol. 59, no. 1, pp. 127–137, 2007.
- [14] M. A. Azcarate-Peril, E. Altermann, Y. J. Goh et al., “Analysis of the genome sequence of *Lactobacillus gasseri* ATCC 33323 reveals the molecular basis of an autochthonous intestinal organism,” *Applied and Environmental Microbiology*, vol. 74, no. 15, pp. 4610–4625, 2008.
- [15] M. Olivares, M. P. Díaz-Ropero, N. Gómez et al., “Oral administration of two probiotic strains, *Lactobacillus gasseri* CECT5714 and *Lactobacillus coryniformis* CECT5711, enhances the intestinal function of healthy adults,” *International Journal of Food Microbiology*, vol. 107, no. 2, pp. 104–111, 2006.
- [16] K. Selle and T. R. Klaenhammer, “Genomic and phenotypic evidence for probiotic influences of *Lactobacillus gasseri* on human health,” *FEMS Microbiology Reviews*, vol. 37, no. 6, pp. 915–935, 2013.
- [17] H. J. Kim, J. Y. Cha, M. L. Choi, and Y. S. Cho, “Antioxidative activities by water-soluble extracts of *Morus alba* and *Cudrania tricuspidata*,” *Applied Biological Chemistry*, vol. 43, no. 2, pp. 148–152, 2000.
- [18] J. Y. Joung, J. Y. Lee, Y. S. Ha et al., “Enhanced microbial, functional and sensory properties of herbal yogurt fermented with Korean traditional plant extracts,” *Korean Journal for Food Science of Animal Resources*, vol. 36, no. 1, pp. 90–99, 2016.
- [19] N. S. Oh, J. Y. Lee, S. Oh et al., “Improved functionality of fermented milk is mediated by the synbiotic interaction between *Cudrania tricuspidata* leaf extract and *Lactobacillus gasseri* strains,” *Applied Microbiology and Biotechnology*, vol. 100, no. 13, pp. 5919–5932, 2016.
- [20] A. A. Hamers, L. van Dam, J. M. Duarte et al., “Deficiency of nuclear receptor Nur77 aggravates mouse experimental colitis by increased NFκB activity in macrophages,” *PLoS One*, vol. 10, no. 8, article e0133598, 2015.
- [21] S. M. Lim, J. J. Jeong, K. H. Woo, M. J. Han, and D. H. Kim, “*Lactobacillus sakei* OK67 ameliorates high-fat diet-induced blood glucose intolerance and obesity in mice by inhibiting gut microbiota lipopolysaccharide production and inducing colon tight junction protein expression,” *Nutrition Research*, vol. 36, no. 4, pp. 337–348, 2016.
- [22] M. Song, H. W. Baik, S. G. Hong, and M. K. Sung, “Wheat bran arabinoxylan supplementation alleviates 5-fluorouracil induced mucositis and myelosuppression in BALB/c mice,” *Journal of Functional Foods*, vol. 21, pp. 312–320, 2016.
- [23] Y. W. Shin, E. A. Bae, S. S. Kim, Y. C. Lee, and D. H. Kim, “Effect of ginsenoside Rb1 and compound K in chronic oxazolone-induced mouse dermatitis,” *International Immunopharmacology*, vol. 5, no. 7-8, pp. 1183–1191, 2005.
- [24] K. J. Livak and T. D. Schmittgen, “Analysis of relative gene expression data using real-time quantitative PCR and the 2^{-ΔΔCT} method,” *Methods*, vol. 25, no. 4, pp. 402–408, 2001.
- [25] J. W. Yoon, S. I. Ahn, J. W. Jhoo, and G. Y. Kim, “Antioxidant activity of yogurt fermented at low temperature and its anti-inflammatory effect on DSS-induced colitis in mice,” *Food Science of Animal Resources*, vol. 39, no. 1, pp. 162–176, 2019.
- [26] E. J. Choi and W. Y. So, “The differential impact of high-intensity swimming exercise and inflammatory bowel disease on IL-1β, TNF-α, and COX-2 gene expression in the small intestine and colon in mice,” *Journal of Men’s Health*, vol. 14, no. 2, pp. e22–e29, 2018.

- [27] C. Bauer, P. Diewell, C. Mayer et al., "Colitis induced in mice with dextran sulfate sodium (DSS) is mediated by the NLRP3 inflammasome," *Gut*, vol. 59, no. 9, pp. 1192–1199, 2010.
- [28] I. Okayasu, S. Hatakeyama, M. Yamada, T. Ohkusa, Y. Inagaki, and R. Nakaya, "A novel method in the induction of reliable experimental acute and chronic ulcerative colitis in mice," *Gastroenterology*, vol. 98, no. 3, pp. 694–702, 1990.
- [29] H. Sann, J. . Erichsen, M. Hessmann, A. Pahl, and A. Hoffmeyer, "Efficacy of drugs used in the treatment of IBD and combinations thereof in acute DSS-induced colitis in mice," *Life Sciences*, vol. 92, no. 12, pp. 708–718, 2013.
- [30] N. Avdagić, A. Zaćiragić, N. Babić et al., "Nitric oxide as a potential biomarker in inflammatory bowel disease," *Bosnian Journal of Basic Medical Sciences*, vol. 13, no. 1, pp. 5–9, 2013.
- [31] F. Sanchez-Muñoz, A. Dominguez-Lopez, and J. K. Yamamoto-Furusho, "Role of cytokines in inflammatory bowel disease," *World journal of gastroenterology: WJG*, vol. 14, no. 27, pp. 4280–4288, 2008.
- [32] S. Lebel-Binay, A. Berger, F. Zinzindohoue et al., "Interleukin-18: biological properties and clinical implications," *European Cytokine Network*, vol. 11, no. 1, pp. 15–26, 2000.
- [33] D. J. B. Marks and A. W. Segal, "Innate immunity in inflammatory bowel disease: a disease hypothesis," *The Journal of Pathology*, vol. 214, no. 2, pp. 260–266, 2008.
- [34] I. G. Je, D. G. Lee, D. G. Jeong et al., "The probiotic, ID-JPL934, attenuates dextran sulfate sodium-induced colitis in mice through inhibition of proinflammatory cytokines expression," *Journal of Medicinal Food*, vol. 21, no. 9, pp. 858–865, 2018.

Review Article

The Effects of Dietary Nutrition on Sleep and Sleep Disorders

Mingxia Zhao ¹, Houzhen Tuo,¹ Shuhui Wang,¹ and Lin Zhao²

¹Department of Neurology, Beijing Friendship Hospital, Capital Medical University, Beijing, China

²Department of Cardiology, Beijing Anzhen Hospital, Capital Medical University, Beijing, China

Correspondence should be addressed to Mingxia Zhao; debbiezhao@126.com

Received 8 April 2020; Revised 21 May 2020; Accepted 2 June 2020; Published 25 June 2020

Guest Editor: Hongmei Jiang

Copyright © 2020 Mingxia Zhao et al. This is an open access article distributed under the Creative Commons Attribution License, which permits unrestricted use, distribution, and reproduction in any medium, provided the original work is properly cited.

Sleep disorder significantly affects the life quality of a large number of people but is still an underrecognized disease. Dietary nutrition is believed to play a significant impact on sleeping wellness. Many nutritional supplements have been used trying to benefit sleep wellness. However, the relationship between nutritional components and sleep is complicated. Nutritional factors vary dramatically with different diet patterns and depend significantly on the digestive and metabiotic functions of each individual. Moreover, nutrition can profoundly affect the hormones and inflammation status which directly or indirectly contribute to insomnia. In this review, we summarized the role of major nutritional factors, carbohydrates, lipids, amino acids, and vitamins on sleep and sleep disorders and discussed the potential mechanisms.

1. Introduction

The body maintains a biological rhythm called circadian rhythm which oscillate in cycles of 24 hours. This normal circadian rhythm orchestrates normal physiological cycles happening each day [1]. Sleep disorder is a highly prevalent disease that disrupts the normal circadian rhythm which negatively impacts psychological well-being and physical health [2]. There are several types of sleep disorders, among which insomnia, obstructive sleep apnoea (OSA), and circadian rhythm disorders are more frequently studied [3]. Sleep disorders are not only associated with decreased life quality and work efficiency but also with increased medical and psychiatric problems [4]. It is considered a risk factor for many diseases including cardiovascular events [5, 6], hypertension [7, 8], and type 2 diabetes [9]. Sleep wellness of children is associated with their physiological and mental health as well as cognition development and behaviors [10].

The circadian rhythm is controlled by both the internal genetic components of biological clock (clock genes) and external factors including those from nutrition and environment. Diet is believed to play an important role in the regulation of sleep wellness [11]. The mechanism for diet in the regulation of sleep is a very complex question that could be demonstrated through the following pathways. First, diet

components can directly affect sleep. For example, caffeine which is contained in caffeinated coffee or tea causes a decrease in total sleep time and quality, as well as an increase in sleep induction time [12]. Caffeine is chemically related to adenosine, which is a sleep-inducing agent. It is believed that caffeine works by reversibly antagonizing the sleep-inducing adenosine receptors ($A_{2A}R$) in the brain, although other pathways may coexist [13]. Melatonin is a well-recognized sleep inducer which conveys information of the daily cycle of light and darkness to the body. Melatonin activates two receptors, MT1 and MT2, both are G-protein-coupled receptors to mediate its effects on sleep induction and circadian rhythm. Thus, food containing melatonin can directly have an effect on sleep [14]. Secondly, many nutritional metabolites can be bioactive in sleep regulation directly or through the regulation of other relating factors as discussed below. It should be noted that nutrition could significantly alter the commensal microbiota which could affect the metabolic generation of metabolites [15]. Thirdly, long-term nutritional factors could alter the inflammation status which is also closely related with insomnia. This has been supported by substantial number of studies that sleep disturbance is related with altered circulating inflammatory cytokines (especially C-reactive protein and interleukine 6) and glucocorticoids [16–20]. The relationship of diet patterns and inflammation status has been reviewed

previously [21], thus is no longer a focus of current review. It is worth to mention that with the establishment of the link between chronic inflammation and many major diseases of modern society, this area is receiving more and more research interests. However, the mechanism of inflammation on sleep wellness is still a complex question which requires more investigation.

The past decades have seen a dramatic increase in literature on the role of diet/nutrition on sleep. However, although huge in quantity, many of which sleep are observational with a limited sample size and often had contradictory results. This makes those studies based on clinical interventions more valuable to unveil the role of each nutritional components. Moreover, due to the complex nutritional component of food, studies involving refined nutrition components provided better insights to that particular nutrition. Thus, this review summarized the knowledge on the nutritional components on sleep with more preferential focus on those studies with clinical interventions and refined nutrition.

2. Carbohydrates

Instead of studying each refined carbohydrate, the overall dietary glycemic index (GI) based on their effects on postprandial blood glucose levels is normally used to study the impact of carbohydrate on diseases [22]. High-GI diet has been shown to be associated with stroke [23], cancer [24], and certain chronic diseases [25]. The consumption of high-GI food caused a rapid increase in blood glucose level which results in compensatory insulin increase and a series of downstream humoral effects. The studies on the role of carbohydrates on sleep have mixed results. Afaghi et al. reported that healthy sleepers (12 healthy adults ranging from 18-35 years old) taking carbohydrate-based high-GI meal 4 h before bedtime resulted in a significant shortening of sleep onset latency (SOL, 48.6% reduction) when compared to individuals taking a low-GI meal [26]. The result is supported by another study that low-carbohydrate intake was associated with difficulty maintaining sleep [27]. However, other studies, including a recently published by Gangwisch et al., suggested that high glycemic index and glycemic load diets is a risk factor for insomnia [28]. This prospective study of a much larger population of postmenopausal women population demonstrated that high-GI diet was associated with increased insomnia incidence over 3 years, and higher intakes of dietary added sugars, starch, and nonwhole/refined grains each were associated with higher incidence of insomnia. Moreover, they found higher fiber content in food as well as nonjuice fruit were associated with a lower prevalence and incidence of insomnia. This conclusion is consistent with a previous study that high intake of confectionary is related with poor sleep quality among middle-aged female Japanese workers [29]. Supporting this concept, a study on short-term consumption of a very low-carbohydrate (VLC) diet over 48 h comparing to a control mixed diet on sleep indices suggested promotes SWS (deep sleep stage) and reduces the percentage of REM sleep ("dreaming" sleep) [30].

Although not completely solved, the potential mechanisms behind the relationship of carbohydrate and insomnia

has been suggested. Food with high GI could alter the ratio of tryptophan relative to other large neutral amino acids (LNAAs including tyrosine, phenylalanine, leucine, isoleucine, valine, and methionine) in the circulation [31]. It does so through the effect of insulin which increased following consumption of high-GI food [31]. Insulin promotes the selective uptake of LNAAs by the muscles leading to higher tryptophan to LNAAs ratio. Since tryptophan competes with LNAAs for transportation into the brain [32], this change in ratio may lead to increased tryptophan in the brain [26]. Tryptophan is the precursor for serotonin which induces sleep. Brain serotonin levels could indeed increase after ingestion of carbohydrate [33]. This mechanism was used to explain the observations that high-GI diet benefits sleeping [26]. However, this theory has been challenged by the recent publication by Gangwisch et al. who suggested that this theory may not be realistic as it required the meal to contain only carbohydrate. If the meal contains as little as 5% protein, this can prevent the increase of tryptophan concentrations [28]. Moreover, the increase of serotonin is not necessarily associated with melatonin whose production is regulated by the presence of darkness [28]. Instead, they proposed that hyperglycemia induced after high-GI diet and resulting compensatory hyperinsulinemia could induce the release of autonomic counterregulatory hormones including adrenaline, cortisol, glucagon, and growth hormone which contributed to insomnia [28, 34]. Moreover, high-GI diets have also been shown to stimulate inflammatory immune responses [35] and lead to alternations in intestinal microbiome which may also profoundly affect sleep quality [15].

It should be noted that these abovementioned studies are performed in different populations with dramatically different sample sizes and experiment designs, so the results may be comparable to each other. Nevertheless, more studies are needed to address the relationship between high-carbohydrate diet and insomnia from a mechanistic aspect.

3. Fatty Acids

Fatty acids are another major component of human diet, including saturated fat and unsaturated fat [36]. High consumption of saturated fat increases low-density lipoprotein (LDL) cholesterol levels and is related with increased risks for diseases like cardiovascular diseases [37] and diabetes [38]. Among unsaturated fats, omega-3 polyunsaturated fatty acids (PUFAs) including α -linolenic acid (ALA), eicosapentaenoic acid (EPA), and docosahexaenoic acid (DHA) have been extensively studied on their effects to human health. Contrary to saturated fat, consumption of omega-3 PUFA is known to prevent the risks of cardiovascular diseases [39] and stroke [40]. The relationship between fatty acids and sleep wellness has also been studied and is reviewed [41].

3.1. Saturated Fatty Acids. Animal fat contains almost exclusively saturated fatty acids. Processed foods including those deep fried in hydrogenated oil are also high in saturated fat content. Consumption of saturated fat is a major risk factor for cardiovascular disease and diabetes as has been suggested by many scientific societies [42].

The studies on the role of saturated fatty acids on sleep are relatively rare. In a study of normal weighted adults, it is concluded that higher saturated fat intake during the day was associated with a shortened duration of slow wave sleep and more arousals during the night [43]. Another study of 459 postmenopausal women investigated the relationships among nutrients in the diet and objective sleep. The authors concluded that total sleep time as measured by actigraphy was negatively associated with intake of total fat and saturated fat [44]. From these limited studies, it seems that the consumption of saturated fatty acids deteriorates sleeping wellness. This is also true if diabetes is induced due to the long-term consumption of saturated fatty acids, as diabetes is often associated with sleeping problems [45].

3.2. Omega-3 PUFA. Omega-3 PUFA is a type of polyunsaturated fatty acid with good reputation for health. Compared to animal fats which are largely saturated, fish and vegetable contain significant portion of unsaturated fat. Omega-3 fats are important for the development of the brain. The deficiency in DHA in the developing brain will lead to problems in neurogenesis, associated with altered learning and visual problems [46]. In addition, omega-3 fats are considered anti-inflammatory, consumption of which can reduce the inflammation in the body that benefit a number of chronic diseases [47]; thus, omega-3 fats are commonly used as nutritional supplements to prevent cardiovascular problems and stroke.

Studies have suggested that diet deficient in omega-3 PUFA disturbed nocturnal sleep though affecting the melatonin rhythm and circadian clock functions [48]. There is also a positive relation between omega-3 fatty acid composition in gluteal adipose tissue and sleep wellness including slow wave sleep and rapid eye movement sleep among obese patients with obstructive sleep apnoea syndrome [49]. A study of healthy children has reported that higher blood DHA level is associated with significantly improved sleep wellness [50]. In their subsequent randomized controlled trial (RCT) of DHA supplementation (with 600 mg/day for 16 weeks), significant group differences were observed including sleep duration increased by 58 min and fewer and shorter night-wakings in the treatment group versus the placebo group [50]. Other than children, the effect of DHA on sleep was also reported in adolescents, as higher plasma DHA was associated with earlier sleep timing and longer weekend sleep [51].

Although the prevailing results suggested the beneficial role of omega-3 PUFA on sleep, a report raised opposite findings stating high-EPA fish oil supplements is likely associated with disturbance of sleeping after successful treatment of depression; the symptoms disappeared after cessation of supplementation [52]. However, such negative reports on omega-3 fat are rare. Although fish is a source of omega-3 fat, the results are mixed when it comes to the impact of fish consumption to sleeping wellness. A positive correlation is found between better sleep quality and oily fish consumption in a population of over 40 years old [53]. Moreover, a study of 95 male adults consuming Atlantic salmon three times per week from September to February gave a positive impact on sleep in general and also on daily functioning effect on resting HRV and EPA+DHA, but not on vitamin D status

[54]. However, in a two-armed randomized controlled trial, there was no significant differences in mental health and sleep for the fish eating group compared with the meat eating group in kids of 4-6 years old [10].

3.3. Omega-6 PUFA. Omega-6 PUFA are another type of polyunsaturated fatty acid that is abundant in vegetable oil like corn, primrose seed, and soybean oil. Compared to the general consensus on the beneficial role of omega-3 fat on sleep, the roles of omega-6 are not as clear. Omega-6 fat serves as precursors of potent lipid mediators called eicosanoids. For example, arachidonic acid is the precursor for at least three groups of lipid mediators including, prostaglandins (PGs), thromboxanes, and leukotrienes [55]. Generally speaking, eicosanoids derived from omega-6 displayed a proinflammatory function while eicosanoids derived from omega-3 PUFA showed more anti-inflammatory tendency. The metabolism of omega-6 fatty acids and generation of eicosanoids as well as how they influence inflammatory responses have been reviewed [55].

The prostaglandin derivatives of arachidonic acid PGD_2 and PGE_2 are very important factors regulating sleep. PGD_2 has been experimentally tested as an effective sleep promoter on different animal models [56–58]. This humoral factor is gradually accumulated in the brain while awake and circulates in the cerebrospinal fluid as a sleep hormone. In contrast to the sleep-inducing role of PGD_2 , PGE_2 has a strong awakening effect in rats and suppresses sleep [59]. Considering the contrasting results of PGD_2 and PGE_2 on sleep induction, it would be interesting to know the results of increased omega-6 PUFA supplement, especially when arachidonic acid is provided. However, despite the well-established role of PGD_2 and PGE_2 in sleep regulation, studies on the consumption of their precursor omega-6 PUFA on sleep wellness are rare. In a bioinformatics study, lower arachidonic acid biosynthesis was seen in the insomnia group, suggesting that lower production of arachidonic acid may be associated with a high incidence of insomnia [60].

No studies directly supply omega-6 fatty acids to study their role on sleep. However, the ratio of omega-6 to omega-3 essential fatty acids (EFA) is commonly used to describe the fatty acid composition in the nutrition field. It is believed that a diet with omega-6/omega-3 ratio of approximately 1 is recommend, whereas this ratio has increased steadily over the past few decades (currently ~15:1). This imbalance is associated with many chronic inflammatory diseases such as nonalcoholic fatty liver disease, cardiovascular disease, obesity, inflammatory bowel disease (IBD), and rheumatoid arthritis. [55]. A 4-week double-blind study including 100 Alzheimer patients indicated supplement of compound comprising a 4:1 ratio of omega-6/omega-3 fatty acids improves sleep compared to placebo [61]. However, the mechanism of action is not clear; it is possible that the effect is indirect through the regulation of inflammation status.

4. Amino Acids

Amino acids are the building blocks of proteins. There are hundreds of naturally occurring amino acids and most of

which can be found in the human diet. Numerous studies on the role of amino acids on sleep wellness and insomnia have been performed in the past decades. Current review only focuses on the most important amino acids in sleeping, including tryptophan, glutamine, tyrosine, and gamma-aminobutyric acid (GABA).

4.1. Tryptophan. Tryptophan is the substrate for serotonin which has been intensively studied on its role on sleep for many decades [20]. Although the role of serotonin on sleep has been under debate, there is a general agreement that serotonin is a major sleep mediator which first increases wakefulness but then increases NREM sleep [20]. Considering the role of serotonin, it has been indicated that supplementation of tryptophan (1 g or more) produces an increase in subjective sleepiness and a decreased time to sleep especially in subjects with mild insomnia [62]. A random double-blind experiment on healthy adults suggested that tryptophan consistently reduced sleep latency which is associated with blood levels [63]. Recently, a Japanese study of younger aged population concluded that tryptophan ingested during breakfast is required for children to keep a morning-type diurnal rhythm and maintain high quality sleep [64]; however, this study did not involve supplementation of tryptophan, instead they calculated the tryptophan-index based on food they consume.

4.2. Gamma-Aminobutyric Acid and Glutamine. Gamma-aminobutyric acid (GABA) is a bioactive amino acid with which does not form proteins. This amino acid has received significant research interests due to its effects on many metabolic disorders [65]. The production of GABA is through the decarboxylation of L-glutamate catalyzed by glutamate decarboxylase. Food fermented by lactic acid bacteria or yeast normally contains an increased level of GABA. Numerous physiological functions about GABA have been reported and reviewed in [65]. In particular, the sleep-promoting function of GABA has been appreciated [66].

There are many studies showing the sleep-promoting effect of GABA, for example, Byun et al. reported a study of 40 patients with insomnia receiving 4 weeks of GABA (300 mg/day) have decreased sleep latency and increased sleep efficacy [66]. The mechanisms of sleep induction by GABA through their receptors have been reviewed [67]. GABA receptor agonists have also been used to induce sleeping [68].

Glutamine is also a nonessential amino acid which can be used for the synthesis of GABA, a known inhibitory neurotransmitter and sleep inducer. Thus, it has been hypothesized and sometime taken for granted that the supplement of glutamine can benefit sleep. However, since glutamine is nonessential, this can be generated by the body. The beneficiary effects of glutamine supplementation, if exists, still need scientific confirmation.

4.3. Tyrosine. Tyrosine is a nonessential amino acid whose metabolite is norepinephrine (NE) which is a neurotransmitter. NE is released at its lowest levels during sleep and rises during wakefulness. The level of NE dramatically increases during situations of stress or danger, which is called the fight-or-flight response. NE is long known for its role in main-

taining general arousal [69] which has also been confirmed using mouse models. Dopamine β -hydroxylase knockout mice, which lack norepinephrine displayed increased overall sleep and require stronger stimuli to wake up after sleep deprivation [70]. The precursor for NE dopamine (DA) also inhibits adrenergic receptor signaling and blocks the synthesis of melatonin through α 1B-D4 and β 1-D4 receptor heteromers [71]. The supplementation of tyrosine has been used in many cognitive/behavioral studies but yielding significantly varied results [72]. Magill et al. reported that supplementation of tyrosine 150 mg/kg following overnight sleep deprivation improved working memory, reasoning, and vigilance [73]. However, the role of tyrosine supplement on sleep disorders are not well studied. Considering the significant roles of tyrosine metabolites during sleep, it would be worthwhile to study this topic.

5. Vitamins

5.1. Vitamin D. Vitamin D is a fat-soluble vitamin which is crucial for the absorption of calcium and many other biological effects. The most important vitamin D3 and D2 can both be synthesized by the body in the presence of sunshine or obtained from the diet. Fatty fish is a major source of dietary vitamin D. Multiple studies have studied the role of vitamin D on sleep. A meta-analysis including 9 studies (6 cross-sectional, 2 case-control, and 1 cohort studies) aimed at clarifying the association between vitamin D and sleep disorder risk [74]. Overall, the study concluded that vitamin D deficiency is associated with a higher risk of sleep disorders including poor sleep quality, short sleep duration, and sleepiness [74]. When examining each individual studies, most studies indeed suggested positive correlation of vitamin D intake and sleep quality. Moreover, there is an association between serum vitamin D levels and obstructive sleep apnoea syndrome [75]. The mechanism regarding the role of vitamin D in sleep is yet to be confirmed, possibly related with inflammation and oxidative stress [75].

5.2. Vitamin C. Vitamin C found in most citrus fruits and vegetables has been shown to be protective of the brain against memory losses associated with sleep deprivation [76]. A study compared people with short sleep and those with longer sleep and concluded that the vitamin C are among those consumed less by short sleepers [77]. A cross-sectional study of adults in the UK suggested there is a relationship between fruit/vegetable intake and sleep wellness, and long sleepers have high plasma levels of vitamin C [78]. However, other than that, literature actually does not have much evidence supporting the relationship of vitamin C and sleep wellness.

5.3. Vitamin B6/B12. Vitamin B6 (pyridoxine) is widely distributed in food that serves as a coenzyme in hundreds of enzymatic reactions. A randomized, double-blind, placebo-controlled study of vitamin B6 and B vitamins on the effects on dreaming and sleep showed no significant differences in the B6-treated group compared with the placebo in terms of time awake during the night, sleep quality, or tiredness on waking. However, the B complex-treated

group showed significantly lower self-rated sleep quality and significantly higher tiredness on waking. The authors suggested that vitamin B6 supplementation had no detrimental effects on sleep quality [79].

The effects of vitamin B12 on sleep is also controversial. A case report suggested successful vitamin B12 treatment for a free-running sleep-wake rhythm and delayed sleep phase syndrome [80]. However, a multicenter double-blind study challenged this conclusion showing that 3 mg vitamin B12 administered over 4 weeks is not effective for delayed sleep phase syndrome [81]. However, on animal models, intravenously administered vitamin B12 promotes effects on the sleep of rat, especially during the light period [82].

6. Concluding Remarks

It is easy to believe that dietary nutrition plays an important role in sleep wellness. Using diet management to improve sleep is a possible, convenient, and inexpensive strategy. Indeed, some nutritional components or their metabolites have been experimentally proved to be beneficial. However, many other are only hypothetical and lack solid scientific evidence. It is more complicated when it comes to the relationship of the consumption of a particular food and sleep wellness, due to complex composition of food, as well as the absorptive and metabolic abilities of each individual. Moreover, a majority of the studies are observational or cross-sectional, many of which included limited sample size and results from literature often conflict with each other. This field needs more high-quality cohort studies and randomized controlled trials (RCTs) to further confirm the contribution of dietary nutrition to sleep wellness. In addition, better animal models to mimic clinical situations are also of great importance.

Conflicts of Interest

The authors have declared that no conflict of interest exists.

Acknowledgments

The authors would like to thank Dr. Donglei Sun from University of Maryland College Park for his advice.

References



- [1] C. Dibner, U. Schibler, and U. Albrecht, "The mammalian circadian timing system: organization and coordination of central and peripheral clocks," *Annual Review of Physiology*, vol. 72, no. 1, pp. 517–549, 2010.
- [2] W. R. Pigeon, "Diagnosis, prevalence, pathways, consequences & treatment of insomnia," *The Indian Journal of Medical Research*, vol. 131, pp. 321–332, 2010.
- [3] L. A. Panossian and A. Y. Avidan, "Review of sleep disorders," *The Medical Clinics of North America*, vol. 93, no. 2, pp. 407–425, 2009, ix.
- [4] D. Leger and V. Bayon, "Societal costs of insomnia," *Sleep Medicine Reviews*, vol. 14, no. 6, pp. 379–389, 2010.
- [5] P. M. Ridker, N. Rifai, L. Rose, J. E. Buring, and N. R. Cook, "Comparison of C-reactive protein and low-density lipoprotein cholesterol levels in the prediction of first cardiovascular events," *The New England Journal of Medicine*, vol. 347, no. 20, pp. 1557–1565, 2002.
- [6] P. M. Ridker, J. E. Buring, N. R. Cook, and N. Rifai, "C-reactive protein, the metabolic syndrome, and risk of incident cardiovascular events: an 8-year follow-up of 14 719 initially healthy American women," *Circulation*, vol. 107, no. 3, pp. 391–397, 2003.
- [7] H. D. Sesso, J. E. Buring, N. Rifai, G. J. Blake, J. M. Gaziano, and P. M. Ridker, "C-reactive protein and the risk of developing hypertension," *JAMA*, vol. 290, no. 22, pp. 2945–2951, 2003.
- [8] J. E. Gangwisch, "A review of evidence for the link between sleep duration and hypertension," *American Journal of Hypertension*, vol. 27, no. 10, pp. 1235–1242, 2014.
- [9] E. J. Brunner, M. Kivimäki, D. R. Witte et al., "Inflammation, insulin resistance, and diabetes—Mendelian randomization using CRP haplotypes points upstream," *PLoS Medicine*, vol. 5, no. 8, p. e155, 2008.
- [10] M. Hysing, I. Kvestad, M. Kjelleveid et al., "Fatty fish intake and the effect on mental health and sleep in preschool children in FINS-KIDS, a randomized controlled trial," *Nutrients*, vol. 10, no. 10, p. 1478, 2018.
- [11] M. P. St-Onge, A. Mikic, and C. E. Pietrolungo, "Effects of diet on sleep quality," *Advances in Nutrition*, vol. 7, no. 5, pp. 938–949, 2016.
- [12] L. Shilo, H. Sabbah, R. Hadari et al., "The effects of coffee consumption on sleep and melatonin secretion," *Sleep Medicine*, vol. 3, no. 3, pp. 271–273, 2002.
- [13] Z. L. Huang, Y. Urade, and O. Hayaishi, "The role of adenosine in the regulation of sleep," *Current Topics in Medicinal Chemistry*, vol. 11, no. 8, pp. 1047–1057, 2011.
- [14] K. Peuhkuri, N. Sihvola, and R. Korpela, "Dietary factors and fluctuating levels of melatonin," *Food & Nutrition Research*, vol. 56, no. 1, p. 17252, 2017.
- [15] C. Gerard and H. Vidal, "Impact of gut microbiota on host glycemic control," *Frontiers in Endocrinology*, vol. 10, p. 29, 2019.
- [16] M. R. Irwin, R. Olmstead, and J. E. Carroll, "Sleep disturbance, sleep duration, and inflammation: a systematic review and meta-analysis of cohort studies and experimental sleep deprivation," *Biological Psychiatry*, vol. 80, no. 1, pp. 40–52, 2016.
- [17] J. Fernandez-Mendoza, J. H. Baker, A. N. Vgontzas, J. Gaines, D. Liao, and E. O. Bixler, "Insomnia symptoms with objective short sleep duration are associated with systemic inflammation in adolescents," *Brain, Behavior, and Immunity*, vol. 61, pp. 110–116, 2017.
- [18] S. Floam, N. Simpson, E. Nemeth, J. Scott-Sutherland, S. Gautam, and M. Haack, "Sleep characteristics as predictor variables of stress systems markers in insomnia disorder," *Journal of Sleep Research*, vol. 24, no. 3, pp. 296–304, 2015.
- [19] A. N. Vgontzas, E. O. Bixler, H.-M. Lin et al., "Chronic insomnia is associated with nyctohemeral activation of the hypothalamic-pituitary-adrenal axis: clinical implications," *The Journal of Clinical Endocrinology & Metabolism*, vol. 86, no. 8, pp. 3787–3794, 2001.
- [20] L. Imeri and M. R. Opp, "How (and why) the immune system makes us sleep," *Nature Reviews Neuroscience*, vol. 10, no. 3, pp. 199–210, 2009.
- [21] L. Galland, "Diet and inflammation," *Nutrition in Clinical Practice*, vol. 25, no. 6, pp. 634–640, 2010.

- [22] M. L. Neuhouser, L. F. Tinker, C. Thomson et al., "Development of a glycemic index database for food frequency questionnaires used in epidemiologic studies," *The Journal of Nutrition*, vol. 136, pp. 1604–1609, 2006, 6.
- [23] D. Yu, X. Zhang, X. O. Shu et al., "Dietary glycemic index, glycemic load, and refined carbohydrates are associated with risk of stroke: a prospective cohort study in urban Chinese women," *The American Journal of Clinical Nutrition*, vol. 104, no. 5, pp. 1345–1351, 2016.
- [24] G. C. Kabat, J. M. Shikany, S. A. A. Beresford et al., "Dietary carbohydrate, glycemic index, and glycemic load in relation to colorectal cancer risk in the Women's Health Initiative," *Cancer Causes & Control*, vol. 19, no. 10, pp. 1291–1298, 2008.
- [25] A. W. Barclay, P. Petocz, J. McMillan-Price et al., "Glycemic index, glycemic load, and chronic disease risk—a meta-analysis of observational studies," *The American Journal of Clinical Nutrition*, vol. 87, no. 3, pp. 627–637, 2008.
- [26] A. Afaghi, H. O'Connor, and C. M. Chow, "High-glycemic-index carbohydrate meals shorten sleep onset," *The American Journal of Clinical Nutrition*, vol. 85, no. 2, pp. 426–430, 2007.
- [27] E. Tanaka, H. Yatsuya, M. Uemura et al., "Associations of protein, fat, and carbohydrate intakes with insomnia symptoms among middle-aged Japanese workers," *Journal of Epidemiology*, vol. 23, no. 2, pp. 132–138, 2013.
- [28] J. E. Gangwisch, L. Hale, M.-P. St-Onge et al., "High glycemic index and glycemic load diets as risk factors for insomnia: analyses from the Women's Health Initiative," *The American Journal of Clinical Nutrition*, vol. 111, no. 2, pp. 429–439, 2020.
- [29] R. Katagiri, K. Asakura, S. Kobayashi, H. Suga, S. Sasaki, and the Three-generation Study of Women on Diets and Health Study Group, "Low intake of vegetables, high intake of confectionary, and unhealthy eating habits are associated with poor sleep quality among middle-aged female Japanese workers," *Journal of Occupational Health*, vol. 56, no. 5, pp. 359–368, 2014.
- [30] A. Afaghi, H. O'Connor, and C. M. Chow, "Acute effects of the very low carbohydrate diet on sleep indices," *Nutritional Neuroscience*, vol. 11, no. 4, pp. 146–154, 2013.
- [31] R. J. Wurtman, J. J. Wurtman, M. M. Regan, J. M. McDermott, R. H. Tsay, and J. J. Brey, "Effects of normal meals rich in carbohydrates or proteins on plasma tryptophan and tyrosine ratios," *The American Journal of Clinical Nutrition*, vol. 77, no. 1, pp. 128–132, 2003.
- [32] W. H. Oldendorf and J. Szabo, "Amino acid assignment to one of three blood-brain barrier amino acid carriers," *American Journal of Physiology-Legacy Content*, vol. 230, no. 1, pp. 94–98, 1976.
- [33] J. D. Fernstrom and R. J. Wurtman, "Brain serotonin content: increase following ingestion of carbohydrate diet," *Science*, vol. 174, no. 4013, pp. 1023–1025, 1971.
- [34] S. Gais, J. Born, A. Peters et al., "Hypoglycemia counterregulation during sleep," *Sleep*, vol. 26, no. 1, pp. 55–59, 2003.
- [35] Y. Kim, J. Chen, M. D. Wirth, N. Shivappa, and J. R. Hebert, "Lower dietary inflammatory index scores are associated with lower glycemic index scores among college students," *Nutrients*, vol. 10, no. 2, p. 182, 2018.
- [36] B. White, "Dietary fatty acids," *American Family Physician*, vol. 80, no. 4, pp. 345–350, 2009.
- [37] L. Hooper, N. Martin, A. Abdelhamid, and G. Davey Smith, "Reduction in saturated fat intake for cardiovascular disease," *Cochrane Database of Systematic Reviews*, no. 6, article CD011737, 2015.
- [38] P. K. Luukkonen, S. Sädevirta, Y. Zhou et al., "Saturated fat is more metabolically harmful for the human liver than unsaturated fat or simple sugars," *Diabetes Care*, vol. 41, no. 8, pp. 1732–1739, 2018.
- [39] T. Aung, J. Halsey, D. Kromhout et al., "Associations of omega-3 fatty acid supplement use with cardiovascular disease risks: meta-analysis of 10 trials involving 77 917 individuals," *JAMA Cardiology*, vol. 3, no. 3, pp. 225–234, 2018.
- [40] H. Saber, M. Y. Yakoob, P. Shi et al., "Omega-3 fatty acids and incident ischemic stroke and its atherothrombotic and cardioembolic subtypes in 3 US cohorts," *Stroke*, vol. 48, no. 10, pp. 2678–2685, 2017.
- [41] S. Yehuda, S. Rabinovitz, and D. I. Mostofsk, "Essential fatty acids and sleep: mini-review and hypothesis," *Medical Hypotheses*, vol. 50, no. 2, pp. 139–145, 1998.
- [42] F. M. Sacks, A. H. Lichtenstein, J. H. Y. Wu et al., "Dietary fats and cardiovascular disease: a presidential advisory from the American Heart Association," *Circulation*, vol. 136, no. 3, pp. e1–e23, 2017.
- [43] M. P. St-Onge, A. Roberts, A. Shechter, and A. R. Choudhury, "Fiber and saturated fat are associated with sleep arousals and slow wave sleep," *Journal of Clinical Sleep Medicine*, vol. 12, no. 1, pp. 19–24, 2016.
- [44] M. A. Grandner, D. F. Kripke, N. Naidoo, and R. D. Langer, "Relationships among dietary nutrients and subjective sleep, objective sleep, and napping in women," *Sleep Medicine*, vol. 11, no. 2, pp. 180–184, 2010.
- [45] S. Surani, V. Brito, A. Surani, and S. Ghamande, "Effect of diabetes mellitus on sleep quality," *World Journal of Diabetes*, vol. 6, no. 6, pp. 868–873, 2015.
- [46] S. M. Innis, "Dietary omega 3 fatty acids and the developing brain," *Brain Research*, vol. 1237, pp. 35–43, 2008.
- [47] P. C. Calder, "n-3 polyunsaturated fatty acids, inflammation, and inflammatory diseases," *The American Journal of Clinical Nutrition*, vol. 83, no. 6, pp. 1505S–1519S, 2006.
- [48] M. Lavialle, G. Champeil-Potokar, J. M. Alessandri et al., "An (n-3) polyunsaturated fatty acid-deficient diet disturbs daily locomotor activity, melatonin rhythm, and striatal dopamine in Syrian hamsters," *The Journal of Nutrition*, vol. 138, no. 9, pp. 1719–1724, 2008.
- [49] C. Papandreou, "Independent associations between fatty acids and sleep quality among obese patients with obstructive sleep apnoea syndrome," *Journal of Sleep Research*, vol. 22, no. 5, pp. 569–572, 2013.
- [50] P. Montgomery, J. R. Burton, R. P. Sewell, T. F. Spreckelsen, and A. J. Richardson, "Fatty acids and sleep in UK children: subjective and pilot objective sleep results from the DOLAB study—a randomized controlled trial," *Journal of Sleep Research*, vol. 23, no. 4, pp. 364–388, 2014.
- [51] E. C. Jansen, D. A. Conroy, H. J. Burgess et al., "Plasma DHA is related to sleep timing and duration in a cohort of Mexican adolescents," *The Journal of Nutrition*, vol. 150, no. 3, pp. 592–598, 2020.
- [52] L. B. Blanchard and G. C. McCarter, "Insomnia and exacerbation of anxiety associated with high-EPA fish oil supplements after successful treatment of depression," *Oxford Medical Case Reports*, vol. 2015, no. 3, pp. 244–245, 2015.
- [53] O. H. Del Brutto, R. M. Mera, J. E. Ha, J. Gillman, M. Zambrano, and P. R. Castillo, "Dietary fish intake and sleep quality: a population-based study," *Sleep Medicine*, vol. 17, pp. 126–128, 2016.

- [54] A. L. Hansen, L. Dahl, G. Olson et al., "Fish consumption, sleep, daily functioning, and heart rate variability," *Journal of Clinical Sleep Medicine*, vol. 10, no. 5, pp. 567–575, 2014.
- [55] E. Patterson, R. Wall, G. F. Fitzgerald, R. P. Ross, and C. Stanton, "Health implications of high dietary omega-6 polyunsaturated fatty acids," *Journal of Nutrition and Metabolism*, vol. 2012, Article ID 539426, 16 pages, 2012.
- [56] S. Sri Kantha, H. Matsumura, E. Kubo et al., "Effects of prostaglandin D₂, lipoxins and leukotrienes on sleep and brain temperature of rats," *Prostaglandins, Leukotrienes, and Essential Fatty Acids*, vol. 51, no. 2, pp. 87–93, 1994.
- [57] Z. Huang, Y. Urade, and O. Hayaishi, "Prostaglandins and adenosine in the regulation of sleep and wakefulness," *Current Opinion in Pharmacology*, vol. 7, no. 1, pp. 33–38, 2007.
- [58] S. Inoue, K. Honda, Y. Komoda, K. Uchizono, R. Ueno, and O. Hayaishi, "Differential sleep-promoting effects of five sleep substances nocturnally infused in unrestrained rats," *Proceedings of the National Academy of Sciences of the United States of America*, vol. 81, no. 19, pp. 6240–6244, 1984.
- [59] O. Hayaishi, "Sleep-wake regulation by prostaglandins D₂ and E₂," *The Journal of Biological Chemistry*, vol. 263, no. 29, pp. 14593–14596, 1988.
- [60] L. Xie, B. Liu, T. Xiang et al., "Gut microbiota as a subjective measurement for auxiliary diagnosis of insomnia disorder," *Frontiers in Microbiology*, vol. 10, p. 1770, 2019.
- [61] S. Yehuda, S. Rabinovitz, R. L. Carasso, and D. I. Mostofsky, "Essential fatty acids preparation (SR-3) improves Alzheimer's patients quality of life," *The International Journal of Neuroscience*, vol. 87, no. 3-4, pp. 141–149, 2009.
- [62] E. Hartmann, "Effects of L-tryptophan on sleepiness and on sleep," *Journal of Psychiatric Research*, vol. 17, no. 2, pp. 107–113, 1982.
- [63] C. F. P. George, T. W. Millar, P. J. Hanly, and M. H. Kryger, "The effect of L-tryptophan on daytime sleep latency in normals: correlation with blood levels," *Sleep*, vol. 12, no. 4, pp. 345–353, 1989.
- [64] T. Harada, M. Hirotsu, M. Maeda, H. Nomura, and H. Takeuchi, "Correlation between breakfast tryptophan content and morningness-eveningness in Japanese infants and students aged 0–15 yrs," *Journal of Physiological Anthropology*, vol. 26, no. 2, pp. 201–207, 2007.
- [65] M. Diana, J. Quílez, and M. Rafecas, "Gamma-aminobutyric acid as a bioactive compound in foods: a review," *Journal of Functional Foods*, vol. 10, pp. 407–420, 2014.
- [66] J. I. Byun, Y. Y. Shin, S. E. Chung, and W. C. Shin, "Safety and efficacy of gamma-aminobutyric acid from fermented rice germ in patients with insomnia symptoms: a randomized, double-blind trial," *Journal of Clinical Neurology*, vol. 14, no. 3, pp. 291–295, 2018.
- [67] C. Gottesmann, "GABA mechanisms and sleep," *Neuroscience*, vol. 111, no. 2, pp. 231–239, 2002.
- [68] N. L. Harrison, "Mechanisms of sleep induction by GABA(A) receptor agonists," *The Journal of Clinical Psychiatry*, vol. 68, Supplement 5, pp. 6–12, 2007.
- [69] C. W. Berridge, B. E. Schmeichel, and R. A. Espana, "Noradrenergic modulation of wakefulness/arousal," *Sleep Medicine Reviews*, vol. 16, no. 2, pp. 187–197, 2012.
- [70] M. S. Hunsley and R. D. Palmiter, "Norepinephrine-deficient mice exhibit normal sleep-wake states but have shorter sleep latency after mild stress and low doses of amphetamine," *Sleep*, vol. 26, no. 5, pp. 521–526, 2003.
- [71] S. González, D. Moreno-Delgado, E. Moreno et al., "Circadian-related heteromerization of adrenergic and dopamine D₄ receptors modulates melatonin synthesis and release in the pineal gland," *PLoS Biology*, vol. 10, no. 6, p. e1001347, 2012.
- [72] B. J. Jongkees, B. Hommel, S. Kuhn, and L. S. Colzato, "Effect of tyrosine supplementation on clinical and healthy populations under stress or cognitive demands—a review," *Journal of Psychiatric Research*, vol. 70, pp. 50–57, 2015.
- [73] R. A. Magill, W. F. Waters, G. A. Bray et al., "Effects of tyrosine, phentermine, caffeined-amphetamine, and placebo on cognitive and motor performance deficits during sleep deprivation," *Nutritional Neuroscience*, vol. 6, no. 4, pp. 237–246, 2013.
- [74] Q. Gao, T. Kou, B. Zhuang, Y. Ren, X. Dong, and Q. Wang, "The association between vitamin D deficiency and sleep disorders: a systematic review and meta-analysis," *Nutrients*, vol. 10, no. 10, p. 1395, 2018.
- [75] K. Archontogeorgis, E. Nena, N. Papanas, and P. Steiropoulos, "The role of vitamin D in obstructive sleep apnoea syndrome," *Breathe*, vol. 14, no. 3, pp. 206–215, 2018.
- [76] N. M. Mhaidat, K. H. Alzoubi, O. F. Khabour, N. H. Tashtoush, S. A. Banihani, and K. K. Abdul-razzak, "Exploring the effect of vitamin C on sleep deprivation induced memory impairment," *Brain Research Bulletin*, vol. 113, pp. 41–47, 2015.
- [77] M. A. Grandner, N. Jackson, J. R. Gerstner, and K. L. Knutson, "Dietary nutrients associated with short and long sleep duration. Data from a nationally representative sample," *Appetite*, vol. 64, pp. 71–80, 2013.
- [78] E. A. Noorwali, J. E. Cade, V. J. Burley, and L. J. Hardie, "The relationship between sleep duration and fruit/vegetable intakes in UK adults: a cross-sectional study from the National Diet and Nutrition Survey," *BMJ Open*, vol. 8, no. 4, article e020810, 2018.
- [79] D. J. Aspy, N. A. Madden, and P. Delfabbro, "Effects of vitamin B₆ (pyridoxine) and a B complex preparation on dreaming and sleep," *Perceptual and Motor Skills*, vol. 125, no. 3, pp. 451–462, 2018.
- [80] M. Okawa, K. Mishima, T. Nanami et al., "Vitamin B₁₂ treatment for sleep-wake rhythm disorders," *Sleep*, vol. 13, no. 1, pp. 15–23, 1990.
- [81] M. Okawa, K. Takahashi, K. Egashira et al., "Vitamin B₁₂ treatment for delayed sleep phase syndrome: a multi-center double-blind study," *Psychiatry and Clinical Neurosciences*, vol. 51, no. 5, pp. 275–279, 1997.
- [82] H. Y. Chang, H. Sei, and Y. Morita, "Effects of intravenously administered vitamin B₁₂ on sleep in the rat," *Physiology & Behavior*, vol. 57, no. 6, pp. 1019–1024, 1995.

Review Article

Tryptophan Metabolism, Regulatory T Cells, and Inflammatory Bowel Disease: A Mini Review

Xueyan Ding ^{1,2,3} Peng Bin,^{1,2,3} Wenwen Wu,^{1,2,3} Yajie Chang,^{1,2,3}
and Guoqiang Zhu ^{1,2,3}

¹College of Veterinary Medicine, Yangzhou University, Yangzhou 225009, China

²Jiangsu Co-Innovation Center for Important Animal Infectious Diseases and Zoonoses, Yangzhou 225009, China

³Joint International Research Laboratory of Agriculture and Agri-Product Safety, the Ministry of Education of China, Yangzhou University, Yangzhou, Jiangsu 225009, China

Correspondence should be addressed to Guoqiang Zhu; yzgzhu@yzu.edu.cn

Received 8 April 2020; Accepted 26 May 2020; Published 12 June 2020

Guest Editor: Xiaolu Jin

Copyright © 2020 Xueyan Ding et al. This is an open access article distributed under the Creative Commons Attribution License, which permits unrestricted use, distribution, and reproduction in any medium, provided the original work is properly cited.

Inflammatory bowel disease (IBD) is a chronic inflammatory disorder of the gastrointestinal tract resulting from the homeostasis imbalance of intestinal microenvironment, immune dysfunction, environmental and genetic factors, and so on. This disease is associated with multiple immune cells including regulatory T cells (Tregs). Tregs are a subset of T cells regulating the function of various immune cells to induce immune tolerance and maintain intestinal immune homeostasis. Tregs are correlated with the initiation and progression of IBD; therefore, strategies that affect the differentiation and function of Tregs may be promising for the prevention of IBD-associated pathology. It is worth noting that tryptophan (Trp) metabolism is effective in inducing the differentiation of Tregs through microbiota-mediated degradation and kynurenine pathway (KP), which is important for maintaining the function of Tregs. Interestingly, patients with IBD show Trp metabolism disorder in the pathological process, including changes in the concentrations of Trp and its metabolites and alteration in the activities of related catalytic enzymes. Thus, manipulation of Treg differentiation through Trp metabolism may provide a potential target for prevention of IBD. The purpose of this review is to highlight the relationship between Trp metabolism and Treg differentiation and the role of this interaction in the pathogenesis of IBD.

1. Introduction

Inflammatory bowel disease (IBD) is an autoimmune disease with high incidence and unclear etiology, mainly including ulcerative colitis (UC), Crohn's disease (CD), and indeterminate colitis (IC) [1]. UC is an ulcerative bowel disease that only occurs in the colon with a slow and occult onset, and usually, it has a tendency to recur. CD is a chronic, proliferative, and transmural inflammatory disease that can invade any part of the gastrointestinal tract in a discontinuous manner [2]. IBD can seriously lower the quality of lives of patients and significantly increase the risk to colon cancer that result from the proneoplastic effects of chronic intestinal inflammation [3]. A variety of factors, such as genetic, environmental, and microbial factors, are all known to be responsible for

the occurrence of IBD [4, 5]. In addition, multiple immune cells like macrophages, dendritic cells (DCs), and lymphoid cells play important roles in the development of IBD, and the turbulence in the differentiation and function of certain T lymphocytes [e.g., regulatory T cells (Tregs)] could contribute to the pathogenesis of IBD [6, 7]. Hence, the thorough understanding of precise regulation of Tregs may be helpful to perceive IBD-related pathology.

Usually, the generation, differentiation, and function of Tregs are significantly affected by the availability of amino acids in the local microenvironment. Depletion of certain essential amino acids from the local milieu results in the generation of Tregs [8–10]. For example, low concentrations of Trp inhibit T cell growth but enhance Treg production through mTOR-dependent mechanisms [11]. In the gastro-

intestinal tract, Trp undergoes several different metabolic pathways, and Trp metabolism can influence the differentiation and function of Tregs. Trp catabolism is a tolerogenic effector system in Treg function, and its modulation is thought to function as a general mechanism of action of Tregs that express T-lymphocyte antigen-4 (CTLA-4) [12]. In addition, Trp starvation and Trp catabolites could induce the generation of a regulatory phenotype in naive CD4⁺ T cells, and previous studies indicated that there is a close relationship between indoleamine 2,3-dioxygenase (IDO) activity and the occurrence of Tregs [12–14]. Notably, Trp metabolism disorder is also associated with the development and progression of IBD [15–17]. For example, the decreased Trp concentration and increased kynurenine (Kyn) concentration are observed in the IBD patients, and the activity of IDO is also altered as well [18–23]. Thus, regulation of Tregs through altering Trp metabolism may provide potential targets for prevention of IBD.

Herein, we provide an in-depth review highlighting the understanding of the regulatory roles of Trp metabolism in Treg differentiation and discuss the availability of manipulating Trp metabolism to Tregs, which further prevent or ameliorate IBD.

2. Tregs and IBD

2.1. The Mechanism of Action of Tregs in IBD. In normal intestinal mucosa, effector cells and Tregs are in a state of dynamic equilibrium. Tregs play an important role in maintaining intestinal homeostasis and can significantly suppress immune responses to maintain autoimmune tolerance and immune stability through multiple ways, such as cell-cell contact or cytokine-dependent mechanism [24].

2.1.1. Cell-Cell Contact Mechanism. CD4⁺CD25⁺ Tregs can constitutively express inhibitory regulatory molecules such as cytotoxic CTLA-4, transforming growth factor β (TGF- β) and glucocorticoid-induced TNF receptor (GITR), which can bind to the corresponding receptors and transmit inhibition signals to prevent excessive activation of target immune cells [25]. The binding is capable of inhibiting the expression of IL-2R α chain and reduce the reactivity of target cells to IL-2, thereby inhibiting the proliferation of effector T cells (Teffs). A variety of ligand-receptors including costimulatory molecules such as CTLA-4, GITR, OX40 (CD134), and lymphocyte activation gene 3 (LAG-3) are involved in this process [26–29]. Thus, costimulatory molecule receptors play a significant role in the activation process of Tregs. Studying the mechanisms of their abnormal expression and on how to regulate the signaling pathways may bring new light for a deeper understanding of the mechanism of action of Tregs. In addition, Tregs also express programmed death receptors and ligands, which stabilize the relationship between Tregs and antigen presenting cells (APCs) while promoting the differentiation of inducible regulatory T cells (iTregs) [30]. Moreover, Tregs can downregulate the expression levels of costimulatory molecules CD80 and CD86 on DCs and affect the function of DCs, thereby achieving immunosuppressive effects [31].

2.1.2. Cytokine-Dependent Mechanism. Tregs can achieve their functions by releasing inhibitory cytokines such as interleukin-10 (IL-10), TGF- β , and interleukin-35 (IL-35). High mRNA expression of IL-10 and TGF- β was found in the CD4⁺CD25⁺ Tregs *in vitro*, and CD4⁺CD25⁺ Tregs can directly secrete IL-10 and TGF- β under appropriate stimulation [32]. In the CD4⁺CD45RB^{high} T-induced IBD model, TGF- β and IL-10 play an important role in the protective effect of Tregs on IBD. CD4⁺CD25⁺ Tregs isolated from TGF- β knockout mice or CD4⁺CD45RB^{low} T cells derived from IL-10 knockout mice lost their anti-IBD function [33, 34]. IL-35 is a heterodimeric cytokine comprising Epstein-Barr virus-induced gene 3 (Ebi3) and IL-12 alpha (IL-12 α) chain, which was expressed in Foxp3⁺ Tregs, and Tregs lacking Ebi3 or IL-12 α lost their inhibition in the T cell metastatic colitis model. Exogenous IL-35 inhibits T cell proliferation, and the vector encoding IL-35 achieves *in vitro* inhibitory activity by retroviral transduction into Teffs [35]. More potential mechanisms of action of Tregs in IBD have not been established. Nevertheless, strategies that induce the generation of a regulatory phenotype may be a treatment option in preventing or improving the pathological process of IBD.

2.2. Tregs Are Associated with the Development and Progression of IBD. Available evidence suggests that Tregs play an important role in the development and immune regulation of IBD (Figure 1). It has been demonstrated that Tregs maintain intestinal homeostasis and reduce tissue damage during the progression of IBD by inhibiting the responsiveness of immune cells [36, 37]. Changes in the number, phenotype, and inhibitory function of Tregs may contribute to the pathogenesis of IBD. For example, Tregs from mice deficient in cytotoxic CTLA-4, IL-35, IL-10, or LAG-3 are unable to effectively suppress T cell proliferation and fail to prevent chronic T cell-mediated colitis *in vivo* [28, 29, 35, 38]. In addition, Tregs in the inflamed mucosa or periphery blood of patients with IBD or animal models are considerably different [39, 40]. For example, Maul et al. found that CD4⁺CD25⁺ Tregs were reduced in peripheral blood during the active phase of IBD, while the frequency of Tregs at the mucosal level was higher than healthy controls [41]. Moreover, the frequency of Foxp3⁺ Tregs was found to be significantly lower in patients with active IBD [42]. In addition, Wang et al. [6] suggest that insufficient Tregs in peripheral blood may be associated with the recurrence of IBD. However, there are still reports that Tregs fail to exert the inhibition function in the context of IBD [43, 44], which might be explained by the individual differences of patients. Therefore, understanding Tregs in IBD can be helpful in monitoring the cellular immune status of IBD patients and opening up new immunotherapeutic approaches for the treatment of IBD.

Mechanistically, Tregs could be considered as therapeutic targets for controlling IBD (Figure 1). Fortunately, many cases of IBD have been successfully cured or alleviated by manipulating Tregs in animal models or patients [45–56]. For example, Treg transfer is sufficient to alleviate experimental colitis including IBD, and tTregs and iTregs can work together [57–60]. Tregs and IL-10 producing Tr1 cells have

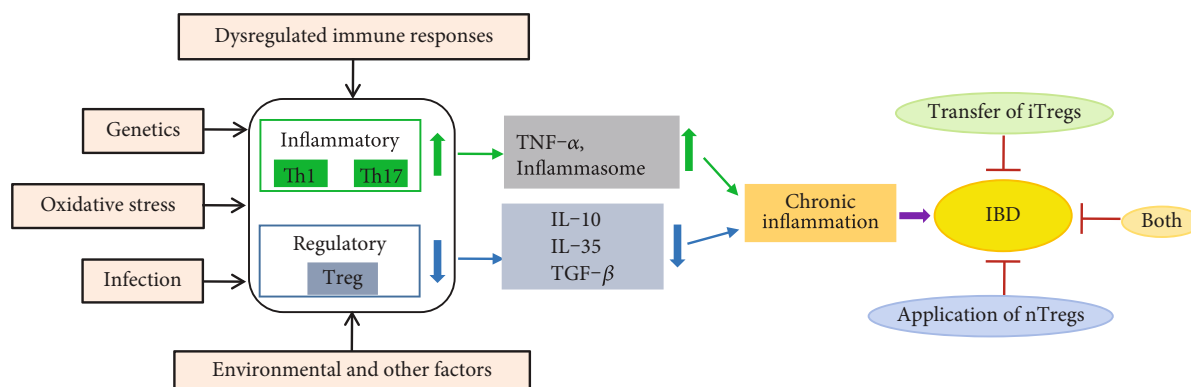


FIGURE 1: The occurrence of IBD and its relationship with Tregs. The pathophysiology of IBD is multifactorial and not completely understood, but genetic components, dysregulated immune responses, oxidative stress, and inflammatory mediators are known to be involved. Tregs are related to the occurrence and development of IBD, and IBD can be cured or alleviated by inducing the generation of Tregs or direct administration of Tregs. Treg: regulatory T cell; TNF- α : tumor necrosis factor α ; TNF- β : tumor necrosis factor β ; iTregs: inducible regulatory T cells; nTregs: natural regulatory T cells; IBD: inflammatory bowel disease.

the potential to prevent or cure colitis, which is supported by a favourable safety profile in phase I clinical trials [61]. However, it should not be overlooked that Treg-based therapies may be attached by some adverse reactions. For example, excessive Treg activity may simultaneously weaken the protective immunity against pathogens and tumors, which could be reduced by controlling the antigen specificity of Tregs [62]. In addition, the phenotype of the original population and culture conditions are also critical for achieving maximum purity of therapeutic Tregs and ensuring phenotypic stability [63, 64]. Therefore, before developing new strategies to improve Treg function, it is very important to study the detailed mechanism of how Tregs function to limit potential negative side effects. It would be meaningful to explore whether it can be more effective when Treg-based therapy is combined with other therapies.

3. Trp Metabolism in the Differentiation and Function of Tregs

3.1. Trp Metabolism in the Gut. Trp is ubiquitous in many foods and has important physiological functions. Once in the gastrointestinal tract, Trp enters several different metabolic pathways by host or intestinal microbiota [65]. We mainly focus on microbial-mediated degradation, KP, and serotonin pathway. About 4-6% of Trp undergoes microbial degradation, by which intestinal microbes directly convert Trp into several molecules, including indoles and its derivatives [66]. Notably, KP is the major route for Trp catabolism which is mediated by the rate-limiting enzyme IDO1. KP can produce Kyn and its downstream products such as quinolinic acid (QA), niacin, nicotinamide adenine dinucleotide (NAD), and kynurenic acid (KA) [67, 68]. KP metabolites are associated with many biological processes involved in neurotransmission, inflammation, and immune responses. In addition to KP, approximately 1-2% of the dietary Trp is converted to serotonin mediated by tryptophan hydroxylase 1 (Tph1) [69]. There is evidence of the importance of serotonin in regulating gastrointestinal function [70, 71]. Collectively, Trp and its metabolites are essential

for the development and maintenance of human and animal health, and all these metabolic pathways work together to maintain the homeostasis.

3.2. Trp Promotes Treg Differentiation through Microbiota-Mediated Degradation. Intestinal microorganisms can directly catabolize Trp into indoles and its derivatives, which play an important role in regulating intestinal immune tolerance [72]. Most indoles and its derivatives, such as indole-3-aldehyde (IAld), indole-3-acid-acetic (IAA), indole-3-propionic acid (IPA), indole-3-acetaldehyde (IAAld), and indoleacrylic acid (IA), are the ligands of aryl hydrocarbon receptor (AhR) (Figure 2).

AhR is a ligand-activated transcription factor that is widely found in immune cells and intestinal epithelial cells, and it is sensitive to certain environmental chemicals and plays an important role in the immune response. Previous work demonstrated the importance of AhR in the differentiation and function of Tregs and Tefs by controlling the production of IL-10 and IL-22 [73-77]. Indole and its derivatives infiltrate into intestinal epithelial cells and deposit in the host circulatory system, which could be recognized by immune cells and then activated AhR signaling pathway. It has been well demonstrated that AhR signaling can induce the proliferation of CD4⁺CD25⁺Foxp3⁺ Tregs (Figure 2), which play an indispensable role in adaptive immune tolerance, such as inhibiting the immune function of activated T cells [78-80]. Collectively and mechanistically indole and its derivatives derived from Trp regulate the differentiation of Tregs through AhR-ligand-Treg axis, thereby affecting the function of Tregs [81-90].

3.3. Trp Promotes Treg Differentiation through KP. KP is the main pathway of Trp catabolism, through which Kyn and other metabolites are produced, such as KA, anthranilic acid (AA), 3-hydroxykynurenine (3-HK), xanthurenic acid (XA), and QA [91-93]. Some KP metabolites bind to AhR to induce FoxP3 expression and promote the generation and differentiation of FoxP3⁺ Tregs [75, 94-97] (Figure 2). In addition, 3-HK and the downstream product pyridine-2-3-

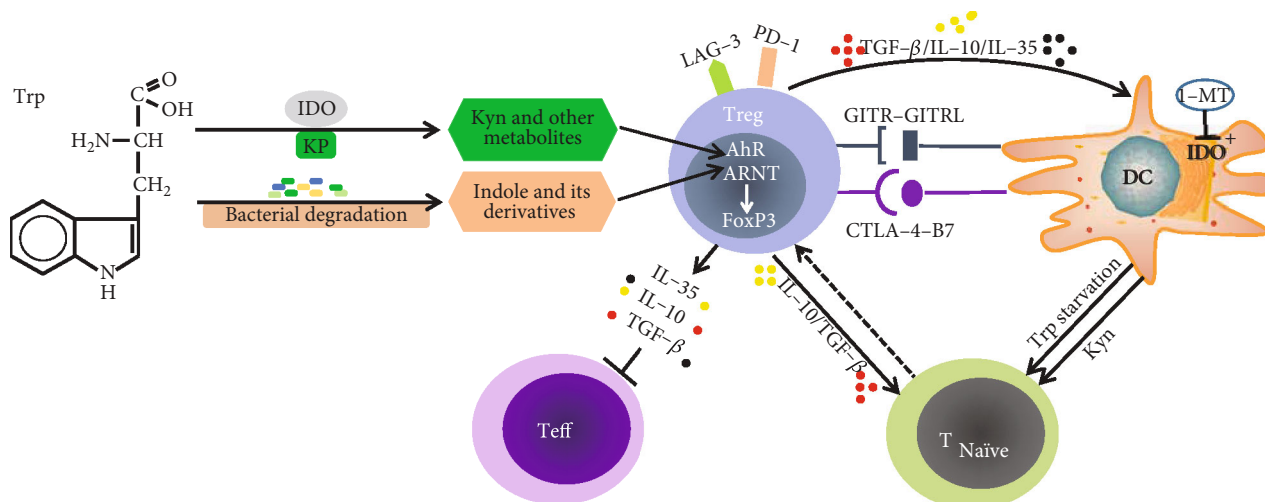


FIGURE 2: The schematic representation of Trp metabolism and its influence on Tregs. Trp metabolism produces AhR ligands through KP and microbial-mediated degradation, which affects the generation of Tregs. The relationship between IDO and Tregs is bidirectional, because they can regulate each other via DCs. CTLA-4, GITR, IL-10, IL-35, TGF- β , and IFN- γ are main components of the regulatory responses. Trp: tryptophan; IDO: indoleamine 2, 3-dioxygenase; KP: kynurenine pathway; Kyn: kynurenine; Treg: regulatory T cell; AhR: aryl hydrocarbon receptor; ARNT: aryl hydrocarbon receptor nuclear translocator; FoxP3: forkhead box P3; IL-35: interleukin-35; IL-10: interleukin-10; TGF- β : transforming growth factor beta; GITR: glucocorticoid-induced TNF receptor; CTLA-4: cytotoxic T-lymphocyte antigen-4; DC: dendritic cell; 1-MT: 1-Methyl-tryptophan.

dioic acid can trigger the activity of Tregs. This is consistent with the long-term synergistic effect of Trp deficiency, and high Kyn induced the transformation of naive CD4⁺ T cells into Tregs [12].

Since IDO is the main enzyme that catalyzes Trp to produce Kyn and other metabolites, the level of IDO expression is important for KP [98, 99]. IDO is expressed in APCs, and its immunoregulatory function is mainly achieved by DCs. IDO suppresses CD4⁺ T cell function by inhibiting cell proliferation, inducing apoptosis and promoting cell differentiation into Tregs. This is achieved by degrading Trp in the microenvironment where immune responses occur [100, 101]. Francesca et al. found that there was a positive regulatory loop by which Tregs expand their own population through the IDO mechanism. In contrast, the activity of IDO enzyme can be inhibited by 1-Methyl-tryptophan (1-MT) [102, 103]. Therefore, manipulating the activity of IDO or the application of synthetic Kyn could provide an idea for the therapeutic agents of IBD [104]. Later, it was discovered that the relationship between IDO and Tregs was bidirectional [96] (Figure 2). IDO can induce the production of Tregs, and the increase of Tregs can in turn induce the expression of IDO [105]. Given the complex relationship between IDO and Tregs, combining IDO blockade with other immunotherapies may be beneficial to overcome the shortcomings of immune counterregulation.

Likewise, serotonin has been reported to be involved in the pathogenesis of experimental colitis [106, 107]. Therefore, Trp metabolism in the gut is a target that can be considered, such as using either molecules targeting a specific pathway or exploiting bacteria affecting Trp metabolism as probiotics. However, the complicated interactions between microbes and hosts need to be elucidated to achieve better therapeutic effects. Moreover, the metabolic pathways

influencing Treg differentiation and function are amenable for modulation in therapeutic settings, thus providing the clinician with potentially valuable tools in the fight against immune-mediated diseases. At the same time, the deviation between diseases and models requires further investigation to refine targets and therapeutic interventions.

4. Modulation of Trp Metabolism in Tregs for IBD

Because Trp metabolism has an important effect on Treg differentiation and function, measures that target Trp metabolism may reduce the severity of IBD, but the possibility deserves further exploration. However, most investigations about effects of Trp metabolism on Treg differentiation were conducted *in vitro* with mouse Tregs; it is not known if Trp metabolism has similar effects in human Treg differentiation *in vitro* or *in vivo*. Indeed, accumulating evidence suggests that Trp promotes intestinal integrity and function, and its metabolism has an important effect on spontaneous and induced IBD models [108–111]. Trp and its metabolism show a high correlation with the etiology of IBD (Figure 3). Usually, Trp deficiency could contribute to the development of IBD or aggravate disease activity [17, 112]. Patients with IBD have lower levels of Trp in serum and feces than healthy subjects [18, 19, 113–115]. Moreover, some Trp metabolites and metabolic enzymes are also found to be significantly different in patients and healthy volunteers [20, 116–118]. Increased Kyn and Kyn/Trp ratios were observed in IBD patients indicating that Trp metabolism along the KP is increased in active IBD [20, 21]. In addition, consumption of Trp metabolites in the intestinal tract may affect the severity of IBD. For example, the concentration of the AhR agonist IAA in feces of IBD patients was significantly reduced [19].

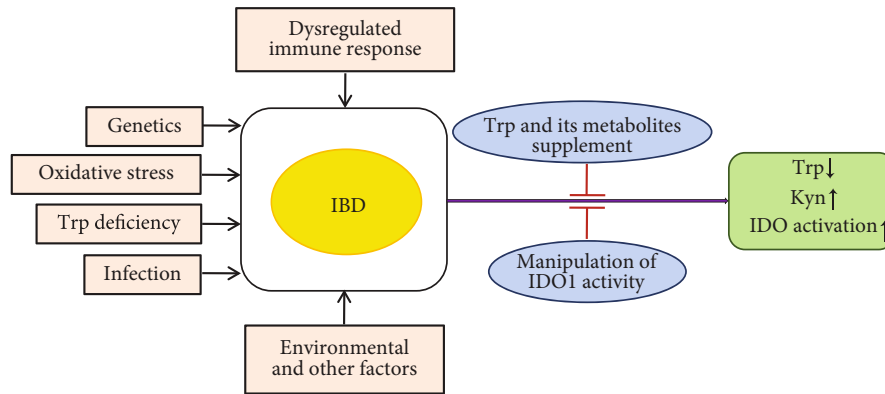


FIGURE 3: Effects of Trp and its metabolism on the etiology of IBD. Trp deficiency could contribute to the development of IBD, and patients with IBD have lower Trp levels, higher Kyn levels, and elevated IDO expression. Trp: tryptophan; IBD: inflammatory bowel disease; IDO1: indoleamine 2,3-dioxygenase-1; Kyn: kynurenine.

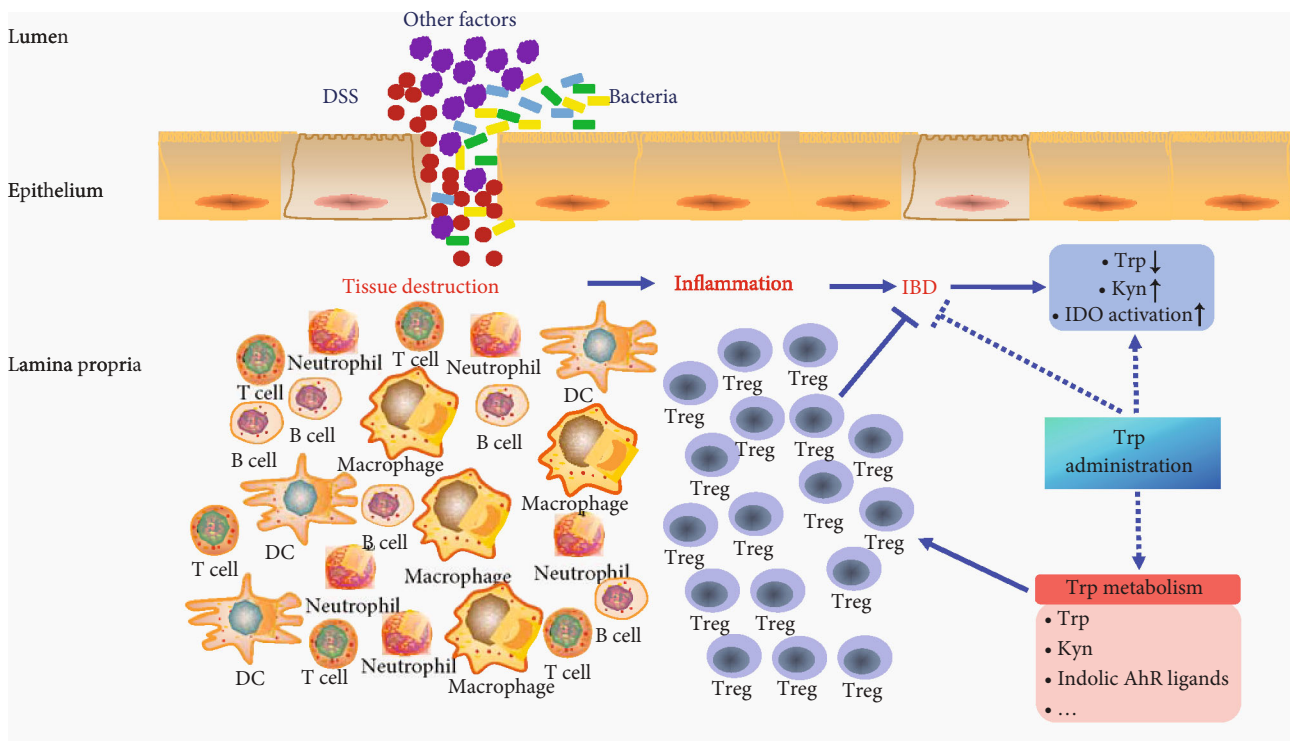


FIGURE 4: Overview of the relationship among Trp metabolism, Tregs, and IBD. DSS: dextran sodium sulfate; Treg: regulatory T cell; IBD: inflammatory bowel disease; Trp: tryptophan; Kyn: kynurenine; IDO: indoleamine 2,3-dioxygenase; AhR: aryl hydrocarbon receptor.

Also, the content of IPA in circulating serum from patients with active colitis was selectively diminished compared to healthy subjects [119, 120]. However, IDO1 levels in the intestine are higher in patients with IBD, although the role of IDO1 in colitis is somewhat controversial [22, 23]. Besides, the content of serotonin in the intestine has changed dramatically in human IBD and animal models of colitis, which suggests that serotonin plays an important role in the occurrence and development of intestinal inflammation [107, 121, 122].

Conversely, dietary supplementation with Trp and Trp metabolites could alleviate symptoms such as weight loss, fecal hemorrhage, and colonic structural damage in experimental mouse colitis (Figure 3) [72, 106]. The protective

effect of Trp administration on IBD may be achieved by reducing proinflammatory cytokines and activating apoptosis initiators, while another anticolitis mechanism may be antioxidative or nitration stress [106, 123]. For example, dietary supplementation of 0.5% Trp inhibited colonic inflammatory symptoms and proinflammatory cytokine secretion in mice by activating AhR [124]. Mice or piglets fed a Trp-supplemented diet had reduced inflammation and decreased severity of dextran sodium sulfate- (DSS-) induced colitis [112, 123, 125], whereas mice fed a low-Trp diet became susceptible to chemically induced inflammation. In addition, the administration of Trp metabolites, such as Kyn, indole, and IPA, were observed to ameliorate colonic

inflammation in mice [119, 120, 126]. Simultaneously, manipulation of IDO1 activity has great potential as treatment for IBD [127]. Moreover, indirect manipulation of the gut microbiota affecting Trp metabolism could be considered to develop new therapeutic drugs that target IBD individuals. For example, the use of *Lactobacillus* (a kind of bacterium that degrades Trp into AhR agonists) lightened the severity of colitis in mice, and probiotics can serve as a supportive therapy for patients with intestinal disorders [125]. Collectively, Trp and its metabolites can be used as biomarkers and promising targets for the treatment of IBD, but further investigation is necessary to validate the effectiveness and feasibility [17, 128]. Therefore, the levels of Trp and its metabolites in patients with IBD need to be analyzed to assess their impact on the progression of IBD.

Collectively, patients with IBD have lower Trp levels, higher Kyn levels, and elevated IDO expression. This is positively correlated with reduced Tregs in IBD. Thus, manipulation of Treg differentiation through these metabolites may be a promising strategy for the treatment of IBD.

5. Conclusions and Future Perspectives

In summary, Tregs are associated with the development of IBD and strategies to manipulate Treg differentiation by Trp metabolism may lead to new therapeutic approaches for the treatment of IBD (Figure 4). Therefore, it is important for researchers to elucidate the exact regulatory mechanism of Trp metabolism in Tregs during the development of IBD. Fortunately, Trp and its metabolites are known to be beneficial for IBD patients and related animal models, although it is unclear whether they regulate the progression of IBD by precisely affecting the differentiation and function of Tregs. Considering that other metabolic pathways also regulate the proliferation and function of Tregs (such as the CD39-CD73-adenosine pathway), combining Trp metabolism with other metabolic pathways will be a better strategy for preventing IBD-related pathologies. At the same time, the manipulation of metabolic pathways in Tregs can be combined with traditional drugs that affect Treg function to achieve better preventive and therapeutic effects. But at present, very satisfactory results have not been achieved in the treatment of IBD. Therefore, an in-depth study of the role of immune cells and amino acid metabolism in IBD will provide a more meaningful basis for the early diagnosis, effective treatment, and progression evaluation of IBD, which will be a serious challenge in the medical field.

Conflicts of Interest

The authors declare that they have no conflicts of interest.

Authors' Contributions

Xueyan Ding, Peng Bin, and Guoqiang Zhu conceptualized the idea. Xueyan Ding and Peng Bin performed literature search and wrote and revised the manuscript. Xueyan Ding, Peng Bin, Wenwen Wu, Yajie Chang, and Guoqiang Zhu revised the manuscript. All authors agreed to the final version

of the manuscript. Xueyan Ding and Peng Bin contributed equally to this work.

Acknowledgments

This work was supported by the Postgraduate Research & Practice Innovation Program of Jiangsu Province (grant KYCX19_2116), the Programs from Ministry of Science and Technology of the People's Republic of China (grants 2016YFD0500905 and 2017YFD0500203), and the Chinese National Science Foundation (grants 30771603, 31072136, 31270171, 31502075, and 31672579).

References

- [1] M. Guindi and R. H. Riddell, "Indeterminate colitis," *Journal of Clinical Pathology*, vol. 57, no. 12, pp. 1233–1244, 2004.
- [2] R. Hodson, "Inflammatory bowel disease," *Nature*, vol. 540, no. 7634, p. S97, 2016.
- [3] R. W. Stidham and P. D. R. Higgins, "Colorectal cancer in inflammatory bowel disease," *Clinics in Colon and Rectal Surgery*, vol. 31, no. 3, pp. 168–178, 2018.
- [4] J. Wehkamp, M. Götz, K. Herrlinger, W. Steurer, and E. F. Stange, "Inflammatory bowel Disease: Crohn's disease and ulcerative colitis," *Deutsches Aerzteblatt Online*, vol. 113, no. 5, pp. 72–82, 2016.
- [5] N. Goyal, A. Rana, A. Ahlawat, K. R. V. Bijjem, and P. Kumar, "Animal models of inflammatory bowel disease: a review," *Inflammopharmacology*, vol. 22, no. 4, pp. 219–233, 2014.
- [6] Y. Wang, X. P. Liu, Z. B. Zhao, J. H. Chen, and C. G. Yu, "Expression of CD4⁺ forkhead box P 3 (FOXP3)⁺ regulatory T cells in inflammatory bowel disease," *Journal of Digestive Diseases*, vol. 12, no. 4, pp. 286–294, 2011.
- [7] G. Muzes, B. Molnar, and F. Sipos, "Regulatory T cells in inflammatory bowel diseases and colorectal cancer," *World Journal of Gastroenterology*, vol. 18, no. 40, pp. 5688–5694, 2012.
- [8] H. Hörig, G. C. Spagnoli, L. Filgueira et al., "Exogenous glutamine requirement is confined to late events of T cell activation," *Journal of Cellular Biochemistry*, vol. 53, no. 4, pp. 343–351, 1993.
- [9] M. Munder, K. Eichmann, and M. Modolell, "Alternative metabolic states in murine macrophages reflected by the nitric oxide synthase/arginase balance: competitive regulation by CD4⁺ T cells correlates with Th1/Th2 phenotype," *The Journal of Immunology*, vol. 160, no. 11, pp. 5347–5354, 1998.
- [10] M. Munder, "Suppression of T-cell functions by human granulocyte arginase," *Blood*, vol. 108, no. 5, pp. 1627–1634, 2006.
- [11] R. Metz, S. Rust, J. B. DuHadaway et al., "IDO inhibits a tryptophan sufficiency signal that stimulates mTOR: a novel IDO effector pathway targeted by D-1-methyl-tryptophan," *OncoImmunology*, vol. 1, no. 9, pp. 1460–1468, 2014.
- [12] F. Fallarino, U. Grohmann, S. You et al., "The combined effects of tryptophan starvation and tryptophan catabolites down-regulate T cell receptor ζ -chain and induce a regulatory phenotype in naive T cells," *Journal of Immunology*, vol. 176, no. 11, pp. 6752–6761, 2006.
- [13] A. Curti, S. Pandolfi, B. Valzasina et al., "Modulation of tryptophan catabolism by human leukemic cells results in

- the conversion of CD25⁻ into CD25⁺ T regulatory cells," *Blood*, vol. 109, no. 7, pp. 2871–2877, 2006.
- [14] F. Li, R. Zhang, S. Li, and J. Liu, "IDO1: an important immunotherapy target in cancer treatment," *International Immunopharmacology*, vol. 47, pp. 70–77, 2017.
- [15] W. W. Wang, S. Y. Qiao, and D. F. Li, "Amino acids and gut function," *Amino Acids*, vol. 37, no. 1, pp. 105–110, 2009.
- [16] S. Chen, M. Wang, L. Yin et al., "Effects of dietary tryptophan supplementation in the acetic acid-induced colitis mouse model," *Food & Function*, vol. 9, no. 8, pp. 4143–4152, 2018.
- [17] S. Nikolaus, B. Schulte, N. Al-Massad et al., "Increased tryptophan metabolism is associated with activity of inflammatory bowel diseases," *Gastroenterology*, vol. 153, no. 6, pp. 1504–1516.e2, 2017.
- [18] T. Hisamatsu, S. Okamoto, M. Hashimoto et al., "Novel, objective, multivariate biomarkers composed of plasma amino acid profiles for the diagnosis and assessment of inflammatory bowel disease," *Plo S one*, vol. 7, no. 1, p. e31131, 2012.
- [19] B. Lamas, M. L. Richard, V. Leducq et al., "CARD9 impacts colitis by altering gut microbiota metabolism of tryptophan into aryl hydrocarbon receptor ligands," *Nature Medicine*, vol. 22, no. 6, pp. 598–605, 2016.
- [20] A. M. Wolf, D. Wolf, H. Rumpold et al., "Overexpression of indoleamine 2,3-dioxygenase in human inflammatory bowel disease," *Clinical Immunology*, vol. 113, no. 1, pp. 47–55, 2004.
- [21] M. A. Sofia, M. A. Ciorba, K. Meckel et al., "Tryptophan metabolism through the kynurenine pathway is associated with endoscopic inflammation in ulcerative colitis," *Inflammatory Bowel Diseases*, vol. 24, no. 7, pp. 1471–1480, 2018.
- [22] G. Matteoli, E. Mazzini, I. D. Iliev et al., "Gut CD103+ dendritic cells express indoleamine 2,3-dioxygenase which influences T regulatory/T effector cell balance and oral tolerance induction," *Gut*, vol. 59, no. 5, pp. 595–604, 2010.
- [23] M. A. Ciorba, E. E. Bettonville, K. G. McDonald et al., "Induction of IDO-1 by immunostimulatory DNA limits severity of experimental colitis," *Journal of Immunology*, vol. 184, no. 7, pp. 3907–3916, 2010.
- [24] P.-F. Hou, L.-J. Zhu, Y. Pan, X.-C. Sun, and J. Pu, "Relation entre les cellules T regulatrices et la radiotherapie," *Cancer/Radiothérapie*, vol. 24, no. 1, pp. 81–84, 2020.
- [25] B. Langhans, H. D. Nischalke, B. Krämer et al., "Role of regulatory T cells and checkpoint inhibition in hepatocellular carcinoma," *Cancer Immunology, Immunotherapy*, vol. 68, no. 12, pp. 2055–2066, 2019.
- [26] F. Fallarino, U. Grohmann, K. W. Hwang et al., "Modulation of tryptophan catabolism by regulatory T cells," *Nature Immunology*, vol. 4, no. 12, pp. 1206–1212, 2003.
- [27] K. Uraushihara, T. Kanai, K. Ko et al., "Regulation of murine inflammatory bowel disease by CD25⁺ and CD25⁻ CD4⁺ glucocorticoid-induced TNF receptor family-related gene+ regulatory T cells," *The Journal of Immunology*, vol. 171, no. 2, pp. 708–716, 2014.
- [28] S. Read, V. Malmstrom, and F. Powrie, "Cytotoxic T lymphocyte-associated antigen 4 plays an essential role in the function of CD25⁺ CD4⁺ regulatory cells that control intestinal inflammation," *The Journal of Experimental Medicine*, vol. 192, no. 2, pp. 295–302, 2000.
- [29] C. T. Huang, C. J. Workman, D. Flies et al., "Role of LAG-3 in regulatory T cells," *Immunity*, vol. 21, no. 4, pp. 503–513, 2004.
- [30] S. Dai, R. Jia, X. Zhang, Q. Fang, and L. Huang, "The PD-1/PD-Ls pathway and autoimmune diseases," *Cellular Immunology*, vol. 290, no. 1, pp. 72–79, 2014.
- [31] X. Chen, Y. Du, Q. Hu, and Z. M. Huang, "Tumor-derived CD4 + CD25 + regulatory T cells inhibit dendritic cells function by CTLA-4," *Pathology - Research and Practice*, vol. 213, no. 3, pp. 245–249, 2017.
- [32] M. C. E. Guedes, M. J. Arroz, C. Martins, M. Angelo-Dias, R. D. Proença, and L. M. Borrego, "Regulatory T cells and IL-17A levels in noninfectious uveitis," *Graefe's Archive for Clinical and Experimental Ophthalmology*, vol. 258, no. 6, pp. 1269–1278, 2020.
- [33] M. M. Shull, I. Ormsby, A. B. Kier et al., "Targeted disruption of the mouse transforming growth factor- β 1 gene results in multifocal inflammatory disease," *Nature*, vol. 359, no. 6397, pp. 693–699, 1992.
- [34] C. Asseman, S. Mauze, M. W. Leach, R. L. Coffman, and F. Powrie, "An essential role for interleukin 10 in the function of regulatory T cells that inhibit intestinal inflammation," *Journal of Experimental Medicine*, vol. 190, no. 7, pp. 995–1004, 1999.
- [35] L. W. Collison, C. J. Workman, T. T. Kuo et al., "The inhibitory cytokine IL-35 contributes to regulatory T-cell function," *Nature*, vol. 450, no. 7169, pp. 566–569, 2007.
- [36] M. C. Fantini, A. Rizzo, D. Fina et al., "IL-21 regulates experimental colitis by modulating the balance between Treg and Th17 cells," *European Journal of Immunology*, vol. 37, no. 11, pp. 3155–3163, 2007.
- [37] A. Yamada, R. Arakaki, M. Saito, T. Tsunematsu, Y. Kudo, and N. Ishimaru, "Role of regulatory T cell in the pathogenesis of inflammatory bowel disease," *World Journal of Gastroenterology*, vol. 22, no. 7, pp. 2195–2205, 2016.
- [38] E. G. Schmitt, D. Haribhai, J. B. Williams et al., "IL-10 produced by induced regulatory T cells (iTregs) controls colitis and pathogenic ex-iTregs during immunotherapy," *The Journal of Immunology*, vol. 189, no. 12, pp. 5638–5648, 2012.
- [39] C. G. Mayne and C. B. Williams, "Induced and natural regulatory T cells in the development of inflammatory bowel disease," *Inflammatory Bowel Diseases*, vol. 19, no. 8, pp. 1772–1788, 2013.
- [40] M. C. Kullberg, V. Hay, A. W. Cheever et al., "TGF- β 1 production by CD4⁺ CD25⁺ regulatory T cells is not essential for suppression of intestinal inflammation," *European Journal of Immunology*, vol. 35, no. 10, pp. 2886–2895, 2005.
- [41] J. Maul, C. Loddenkemper, P. Mundt et al., "Peripheral and Intestinal Regulatory CD4⁺ CD25^{high} T Cells in Inflammatory Bowel Disease," *Gastroenterology*, vol. 128, no. 7, pp. 1868–1878, 2005.
- [42] M. Takahashi, K. Nakamura, K. Honda et al., "An inverse correlation of human peripheral blood regulatory T cell frequency with the disease activity of ulcerative colitis," *Digestive Diseases and Sciences*, vol. 51, no. 4, pp. 677–686, 2006.
- [43] N. Holmén, A. Lundgren, S. Lundin et al., "Functional CD4⁺ CD25^{high} regulatory T cells are enriched in the colonic mucosa of patients with active ulcerative colitis and increase with disease activity," *Inflammatory Bowel Diseases*, vol. 12, no. 6, pp. 447–456, 2006.
- [44] Q. T. Yu, M. Saruta, A. Avanesyan, P. R. Fleshner, A. H. Banham, and K. A. Papadakis, "Expression and functional characterization of FOXP3⁺ CD4⁺ regulatory T cells in

- ulcerative colitis," *Inflammatory Bowel Diseases*, vol. 13, no. 2, pp. 191–199, 2007.
- [45] F. Powrie, M. W. Leach, S. Mauze, L. B. Caddie, and R. L. Coffman, "Phenotypically distinct subsets of CD₄⁺ T cells induce or protect from chronic intestinal inflammation in C. B-₁₇-scid mice," *International Immunology*, vol. 5, no. 11, pp. 1461–1471, 1993.
- [46] F. Powrie, R. Correa-Oliveira, S. Mauze, and R. L. Coffman, "Regulatory interactions between CD45RB^{high} and CD45RB^{low} CD4⁺ T cells are important for the balance between protective and pathogenic cell-mediated immunity," *The Journal of Experimental Medicine*, vol. 179, no. 2, pp. 589–600, 1994.
- [47] C. Mottet, H. H. Uhlig, and F. Powrie, "Cutting edge: cure of colitis by CD4⁺CD25⁺ regulatory T cells," *Journal of Immunology (Baltimore, Md. : 1950)*, vol. 170, no. 8, pp. 3939–3943, 2003.
- [48] R. Hontecillas and J. Bassaganya-Riera, "Peroxisome proliferator-activated receptor γ is required for regulatory CD4⁺ T cell-mediated protection against colitis," *Journal of Immunology*, vol. 178, no. 5, pp. 2940–2949, 2007.
- [49] D. Ishikawa, A. Okazawa, D. Corridoni et al., "Tregs are dysfunctional *in vivo* in a spontaneous murine model of Crohn's disease," *Mucosal Immunology*, vol. 6, no. 2, pp. 267–275, 2013.
- [50] M. Mohammadnia-Afrouzi, A. Zavarán Hosseini, A. Khalili, S. Abediankenari, V. Hosseini, and I. Maleki, "Decrease of CD4⁺CD25⁺CD127^{low}FoxP3⁺ regulatory T cells with impaired suppressive function in untreated ulcerative colitis patients," *Autoimmunity*, vol. 48, no. 8, pp. 556–561, 2015.
- [51] M. C. Fantini and G. Monteleone, "Update on the therapeutic efficacy of Tregs in IBD," *Inflammatory Bowel Diseases*, vol. 23, no. 10, pp. 1682–1688, 2017.
- [52] J. Cho, S. Kim, D. H. Yang et al., "Mucosal immunity related to FOXP3⁺ regulatory T cells, Th17 cells and cytokines in pediatric inflammatory bowel disease," *Journal of Korean medical science*, vol. 33, no. 52, 2018.
- [53] Y. Lu, N. M. Kim, Y. W. Jiang et al., "Cambogin suppresses dextran sulphate sodium-induced colitis by enhancing Treg cell stability and function," *British Journal of Pharmacology*, vol. 175, no. 7, pp. 1085–1099, 2018.
- [54] R. N. Fedorak, A. Gangl, C. O. Elson et al., "Recombinant human interleukin 10 in the treatment of patients with mild to moderately active Crohn's disease," *Gastroenterology*, vol. 119, no. 6, pp. 1473–1482, 2000.
- [55] A. Majowicz, S. van der Marel, A. A. te Velde et al., "Murine CD4⁺CD25⁻ cells activated *in vitro* with PMA/ionomycin and anti-CD3 acquire regulatory function and ameliorate experimental colitis *in vivo*," *BMC gastroenterology*, vol. 12, no. 1, 2012.
- [56] P. Desreumaux, A. Foussat, M. Allez et al., "Safety and efficacy of antigen-specific regulatory T-cell therapy for patients with refractory Crohn's disease," *Gastroenterology*, vol. 143, no. 5, pp. 1207–1217.e2, 2012.
- [57] N. Ohkura, M. Hamaguchi, H. Morikawa et al., "T cell receptor stimulation-induced epigenetic changes and Foxp3 expression are independent and complementary events required for Treg cell development," *Immunity*, vol. 37, no. 5, pp. 785–799, 2012.
- [58] F. Karlsson, N. E. Martinez, L. Gray, S. Zhang, I. Tsunoda, and M. B. Grisham, "Therapeutic evaluation of ex vivo-generated versus natural regulatory T-cells in a mouse model of chronic gut inflammation," *Inflammatory Bowel Diseases*, vol. 19, no. 11, pp. 2282–2294, 2013.
- [59] D. Haribhai, W. Lin, B. Edwards et al., "A central role for induced regulatory T cells in tolerance induction in experimental colitis," *Journal of Immunology (Baltimore, Md. : 1950)*, vol. 182, no. 6, pp. 3461–3468, 2009.
- [60] C. Asseman, S. Fowler, and F. Powrie, "Control of experimental inflammatory bowel disease by regulatory T cells," *American Journal of Respiratory and Critical Care Medicine*, vol. 162, supplement_3, pp. S185–S189, 2000.
- [61] P. Trzonkowski, M. Bieniaszewska, J. Juścińska et al., "First-in-man clinical results of the treatment of patients with graft versus host disease with human ex vivo expanded CD4⁺CD25⁺CD127⁻ T regulatory cells," *Clinical Immunology*, vol. 133, no. 1, pp. 22–26, 2009.
- [62] A. Cebula, M. Seweryn, G. A. Rempala et al., "Thymus-derived regulatory T cells contribute to tolerance to commensal microbiota," *Nature*, vol. 497, no. 7448, pp. 258–262, 2013.
- [63] M. Feuerer, J. A. Hill, K. Kretschmer, H. von Boehmer, D. Mathis, and C. Benoist, "Genomic definition of multiple ex vivo regulatory T cell subphenotypes," *Proceedings of the National Academy of Sciences of the United States of America*, vol. 107, no. 13, pp. 5919–5924, 2010.
- [64] J. B. Canavan, C. Scottà, A. Vossenkämper et al., "Developing *in vitro* expanded CD45RA⁺ regulatory T cells as an adoptive cell therapy for Crohn's disease," *Gut*, vol. 65, no. 4, pp. 584–594, 2016.
- [65] J. D. Fernstrom, "A perspective on the safety of supplemental tryptophan based on its metabolic fates," *The Journal of nutrition*, vol. 146, no. 12, pp. 2601s–2608s, 2016.
- [66] M. T. Yokoyama and J. R. Carlson, "Microbial metabolites of tryptophan in the intestinal tract with special reference to skatole," *The American Journal of Clinical Nutrition*, vol. 32, no. 1, pp. 173–178, 1979.
- [67] I. Cervenka, L. Z. Agudelo, and J. L. Ruas, "Kynurenines: tryptophan's metabolites in exercise, inflammation, and mental health," *Science*, vol. 357, no. 6349, article eaaf9794, 2017.
- [68] P. J. Kennedy, J. F. Cryan, T. G. Dinan, and G. Clarke, "Kynurenine pathway metabolism and the microbiota-gut-brain axis," *Neuropharmacology*, vol. 112, Part B, pp. 399–412, 2017.
- [69] D. A. Bender, "Biochemistry of tryptophan in health and disease," *Molecular Aspects of Medicine*, vol. 6, no. 2, pp. 101–197, 1983.
- [70] J. Gao, K. Xu, H. Liu et al., "Impact of the gut microbiota on intestinal immunity mediated by tryptophan metabolism," *Frontiers in cellular and infection microbiology*, vol. 8, p. 13, 2018.
- [71] T. Nedi, P. J. White, I. M. Coupar, and H. R. Irving, "Effect of the 5-HT₄ receptor agonist tegaserod on the expression of GRK2 and GRK6 in the rat gastrointestinal tract," *BMC research notes*, vol. 11, no. 1, p. 362, 2018.
- [72] D. Keszthelyi, F. J. Troost, and A. A. M. Masclee, "Understanding the role of tryptophan and serotonin metabolism in gastrointestinal function," *Neurogastroenterology and Motility*, vol. 21, no. 12, pp. 1239–1249, 2009.
- [73] L. Apetoh, F. J. Quintana, C. Pot et al., "The aryl hydrocarbon receptor interacts with c-Maf to promote the differentiation of type 1 regulatory T cells induced by IL-27," *Nature Immunology*, vol. 11, no. 9, pp. 854–861, 2010.

- [74] R. Gandhi, D. Kumar, E. J. Burns et al., "Activation of the aryl hydrocarbon receptor induces human type 1 regulatory T cell-like and Foxp3⁺ regulatory T cells," *Nature Immunology*, vol. 11, no. 9, pp. 846–853, 2010.
- [75] F. J. Quintana, A. S. Basso, A. H. Iglesias et al., "Control of T_{reg} and T_H17 cell differentiation by the aryl hydrocarbon receptor," *Nature*, vol. 453, no. 7191, pp. 65–71, 2008.
- [76] A. Yeste, I. D. Mascanfroni, M. Nadeau et al., "IL-21 induces IL-22 production in CD4⁺ T cells," *Nature communications*, vol. 5, no. 1, 2014.
- [77] I. D. Mascanfroni, M. C. Takenaka, A. Yeste et al., "Metabolic control of type 1 regulatory T cell differentiation by AHR and HIF1- α ," *Nature Medicine*, vol. 21, no. 6, pp. 638–646, 2015.
- [78] Q. Lv, C. Shi, S. Qiao et al., "Alpinetin exerts anti-colitis efficacy by activating AhR, regulating miR-302/DNMT-1/CREB signals, and therefore promoting Treg differentiation," *Cell death & disease*, vol. 9, no. 9, p. 890, 2018.
- [79] J. Xue, Q. Zhao, V. Sharma et al., "Aryl hydrocarbon receptor ligands in cigarette smoke induce production of interleukin-22 to promote pancreatic fibrosis in models of chronic pancreatitis," *Gastroenterology*, vol. 151, no. 6, pp. 1206–1217, 2016.
- [80] R. Fuertig, D. Azzinnari, G. Bergamini et al., "Mouse chronic social stress increases blood and brain kynurenine pathway activity and fear behaviour: both effects are reversed by inhibition of indoleamine 2,3-dioxygenase," *Brain, Behavior, and Immunity*, vol. 54, pp. 59–72, 2016.
- [81] Z. Huang, Y. Jiang, Y. Yang et al., "3,3'-Diindolylmethane alleviates oxazolone-induced colitis through Th2/Th17 suppression and Treg induction," *Molecular Immunology*, vol. 53, no. 4, pp. 335–344, 2013.
- [82] J. A. Goettel, R. Gandhi, J. E. Kenison et al., "AHR activation is protective against colitis driven by T cells in humanized mice," *Cell Reports*, vol. 17, no. 5, pp. 1318–1329, 2016.
- [83] W. H. Kim, H. S. Lillehoj, and W. Min, "Indole treatment alleviates intestinal tissue damage induced by chicken coccidiosis through activation of the aryl hydrocarbon receptor," *Frontiers in immunology*, vol. 10, 2019.
- [84] A. K. Ehrlich, J. M. Pennington, W. H. Bisson, S. K. Kolluri, and N. I. Kerkvliet, "TCDD, FICZ, and other high affinity AhR ligands dose-dependently determine the fate of CD4⁺ T cell differentiation," *Toxicological Sciences*, vol. 161, no. 2, pp. 310–320, 2018.
- [85] A. K. Ehrlich and N. I. Kerkvliet, "Is chronic AhR activation by rapidly metabolized ligands safe for the treatment of immune-mediated diseases?," *Current opinion in Toxicology*, vol. 2, pp. 72–78, 2017.
- [86] S. Punj, P. Kopparapu, H. S. Jang et al., "Benzimidazoisoquinolines: a new class of rapidly metabolized aryl hydrocarbon receptor (AhR) ligands that induce AhR-dependent Tregs and prevent murine graft-versus-host disease," *PloS one*, vol. 9, no. 2, p. e88726, 2014.
- [87] A. K. Ehrlich, J. M. Pennington, X. Wang et al., "Activation of the aryl hydrocarbon receptor by 10-cl-BBQ prevents insulinitis and effector T cell development independently of Foxp3⁺ regulatory T cells in nonobese diabetic mice," *The Journal of Immunology*, vol. 196, no. 1, pp. 264–273, 2015.
- [88] P. B. Busbee, M. Rouse, M. Nagarkatti, and P. S. Nagarkatti, "Use of natural AhR ligands as potential therapeutic modalities against inflammatory disorders," *Nutrition Reviews*, vol. 71, no. 6, pp. 353–369, 2013.
- [89] N. I. Kerkvliet, L. B. Stepan, W. Vorachek et al., "Activation of aryl hydrocarbon receptor by TCDD prevents diabetes in NOD mice and increases Foxp3⁺ T cells in pancreatic lymph nodes," *Immunotherapy*, vol. 1, no. 4, pp. 539–547, 2009.
- [90] N. B. Marshall and N. I. Kerkvliet, "Dioxin and immune regulation: emerging role of aryl hydrocarbon receptor in the generation of regulatory T cells," *Annals of the New York Academy of Sciences*, vol. 1183, no. 1, pp. 25–37, 2010.
- [91] P. Terness, T. M. Bauer, L. Röse et al., "Inhibition of allogeneic T cell proliferation by indoleamine 2,3-dioxygenase-expressing dendritic cells: mediation of suppression by tryptophan metabolites," *The Journal of Experimental Medicine*, vol. 196, no. 4, pp. 447–457, 2002.
- [92] A. Curti, S. Trabanelli, C. Onofri et al., "Indoleamine 2,3-dioxygenase-expressing leukemic dendritic cells impair a leukemia-specific immune response by inducing potent T regulatory cells," *Haematologica*, vol. 95, no. 12, pp. 2022–2030, 2010.
- [93] Y. Chen and G. J. Guillemin, "Kynurenine pathway metabolites in humans: disease and healthy states," *International Journal of Tryptophan Research*, vol. 2, pp. 1–19, 2009.
- [94] H. Kawasaki, H. W. Chang, H. C. Tseng et al., "A tryptophan metabolite, kynurenine, promotes mast cell activation through aryl hydrocarbon receptor," *Allergy*, vol. 69, no. 4, pp. 445–452, 2014.
- [95] M. Veldhoen, K. Hirota, A. M. Westendorf et al., "The aryl hydrocarbon receptor links T_H17-cell-mediated autoimmunity to environmental toxins," *Nature*, vol. 453, no. 7191, pp. 106–109, 2008.
- [96] P. Puccetti and U. Grohmann, "IDO and regulatory T cells: a role for reverse signalling and non-canonical NF- κ B activation," *Nature Reviews Immunology*, vol. 7, no. 10, pp. 817–823, 2007.
- [97] J. D. Mezrich, J. H. Fechner, X. Zhang, B. P. Johnson, W. J. Burlingham, and C. A. Bradfield, "An interaction between kynurenine and the aryl hydrocarbon receptor can generate regulatory T cells," *Journal of Immunology*, vol. 185, no. 6, pp. 3190–3198, 2010.
- [98] S. Li, X. Han, N. Lyu et al., "Mechanism and prognostic value of indoleamine 2,3-dioxygenase 1 expressed in hepatocellular carcinoma," *Cancer Science*, vol. 109, no. 12, pp. 3726–3736, 2018.
- [99] L. I. Greene, T. C. Bruno, J. L. Christenson et al., "A role for tryptophan-2,3-dioxygenase in CD8 T-cell suppression and evidence of tryptophan catabolism in breast cancer patient plasma," *Molecular Cancer Research*, vol. 17, no. 1, pp. 131–139, 2019.
- [100] N. J. C. King and S. R. Thomas, "Molecules in focus: indoleamine 2,3-dioxygenase," *The International Journal of Biochemistry & Cell Biology*, vol. 39, no. 12, pp. 2167–2172, 2007.
- [101] A. Curti, S. Trabanelli, V. Salvestrini, M. Baccarani, and R. M. Lemoli, "The role of indoleamine 2,3-dioxygenase in the induction of immune tolerance: focus on hematology," *Blood*, vol. 113, no. 11, pp. 2394–2401, 2009.
- [102] M. D. Sharma, D. Y. Hou, Y. Liu et al., "Indoleamine 2,3-dioxygenase controls conversion of Foxp3⁺ Tregs to TH17-like cells in tumor-draining lymph nodes," *Blood*, vol. 113, no. 24, pp. 6102–6111, 2009.
- [103] M. D. Sharma, D. Y. Hou, B. Baban et al., "Reprogrammed Foxp3⁺ Regulatory T Cells Provide Essential Help to Support Cross-presentation and CD8⁺ T Cell Priming in Naive Mice," *Immunity*, vol. 33, no. 6, pp. 942–954, 2010.

- [104] F. Fallarino, U. Grohmann, S. You et al., "Tryptophan catabolism generates autoimmune-preventive regulatory T cells," *Transplant Immunology*, vol. 17, no. 1, pp. 58–60, 2006.
- [105] B. Sawitzki, C. I. Kingsley, V. Oliveira, M. Karim, M. Herber, and K. J. Wood, "IFN- γ production by alloantigen-reactive regulatory T cells is important for their regulatory function in vivo," *The Journal of Experimental Medicine*, vol. 201, no. 12, pp. 1925–1935, 2005.
- [106] T. Shizuma, H. Mori, and N. Fukuyama, "Protective effect of tryptophan against dextran sulfate sodium- induced experimental colitis," *The Turkish Journal of Gastroenterology*, vol. 24, no. 1, pp. 30–35, 2013.
- [107] J.-E. Ghia, N. Li, H. Wang et al., "Serotonin has a key role in pathogenesis of experimental colitis," *Gastroenterology*, vol. 137, no. 5, pp. 1649–1660, 2009.
- [108] Y. Liu, X. Wang, and C. A. Hu, "Therapeutic potential of amino acids in inflammatory bowel disease," *Nutrients*, vol. 9, no. 9, p. 920, 2017.
- [109] P. Rutgeerts, S. Vermeire, and G. Van Assche, "Biological therapies for inflammatory bowel diseases," *Gastroenterology*, vol. 136, no. 4, pp. 1182–1197, 2009.
- [110] J. Yin, M. Conlon, and S. W. Kim, "Nutrients and inflammatory diseases," *Mediators of inflammation*, vol. 2017, Article ID 6134909, 2 pages, 2017.
- [111] X. Bao, Z. Feng, J. Yao, T. Li, and Y. Yin, "Roles of Dietary Amino Acids and Their Metabolites in Pathogenesis of Inflammatory Bowel Disease," *Mediators of inflammation*, vol. 2017, Article ID 6869259, 9 pages, 2017.
- [112] T. Hashimoto, T. Perlot, A. Rehman et al., "ACE2 links amino acid malnutrition to microbial ecology and intestinal inflammation," *Nature*, vol. 487, no. 7408, pp. 477–481, 2012.
- [113] M. Ooi, S. Nishiumi, T. Yoshie et al., "GC/MS-based profiling of amino acids and TCA cycle-related molecules in ulcerative colitis," *Inflammation research*, vol. 60, no. 9, pp. 831–840, 2011.
- [114] Y. Shiomi, S. Nishiumi, M. Ooi et al., "GCMS-based metabolomic study in mice with colitis induced by dextran sulfate sodium," *Inflammatory Bowel Diseases*, vol. 17, no. 11, pp. 2261–2274, 2011.
- [115] R. Schicho, A. Nazyrova, R. Shaykhtudinov, G. Duggan, H. J. Vogel, and M. Storr, "Quantitative metabolomic profiling of serum and urine in DSS-induced ulcerative colitis of mice by ^1H NMR spectroscopy," *Journal of Proteome Research*, vol. 9, no. 12, pp. 6265–6273, 2010.
- [116] C. M. Forrest, P. Youd, A. Kennedy, S. R. Gould, L. G. Darlington, and T. W. Stone, "Purine, kynurenine, neopterin and lipid peroxidation levels in inflammatory bowel disease," *Journal of Biomedical Science*, vol. 9, no. 5, pp. 436–442, 2002.
- [117] C. M. Forrest, S. R. Gould, L. G. Darlington, and T. W. Stone, "Levels of purine, kynurenine and lipid peroxidation products in patients with inflammatory bowel disease," *Advances in Experimental Medicine and Biology*, vol. 527, pp. 395–400, 2003.
- [118] L. Zhou, H. Chen, Q. Wen, and Y. Zhang, "Indoleamine 2,3-dioxygenase expression in human inflammatory bowel disease," *European Journal of Gastroenterology & Hepatology*, vol. 24, no. 6, pp. 695–701, 2012.
- [119] E. E. Alexeev, J. M. Lanis, D. J. Kao et al., "Microbiota-derived indole metabolites promote human and murine intestinal homeostasis through regulation of interleukin-10 receptor," *The American Journal of Pathology*, vol. 188, no. 5, pp. 1183–1194, 2018.
- [120] C. M. Whitfield-Cargile, N. D. Cohen, R. S. Chapkin et al., "The microbiota-derived metabolite indole decreases mucosal inflammation and injury in a murine model of NSAID enteropathy," *Gut Microbes*, vol. 7, no. 3, pp. 246–261, 2016.
- [121] S. C. Bischoff, R. Mailer, O. Pabst et al., "Role of serotonin in intestinal inflammation: knock-out of serotonin reuptake transporter exacerbates 2,4,6-trinitrobenzene sulfonic acid colitis in mice," *American Journal of Physiology. Gastrointestinal and Liver Physiology*, vol. 296, no. 3, pp. G685–G695, 2009.
- [122] A. Rapalli, S. Bertoni, V. Arcaro et al., "Dual role of endogenous serotonin in 2,4,6-trinitrobenzene sulfonic acid-induced colitis," *Frontiers in pharmacology*, vol. 7, 2016.
- [123] C. J. Kim, J. A. Kovacs-Nolan, C. Yang, T. Archbold, M. Z. Fan, and Y. Mine, "L-Tryptophan exhibits therapeutic function in a porcine model of dextran sodium sulfate (DSS)-induced colitis," *The Journal of Nutritional Biochemistry*, vol. 21, no. 6, pp. 468–475, 2010.
- [124] J. Islam, S. Sato, K. Watanabe et al., "Dietary tryptophan alleviates dextran sodium sulfate-induced colitis through aryl hydrocarbon receptor in mice," *The Journal of Nutritional Biochemistry*, vol. 42, pp. 43–50, 2017.
- [125] T. Zelante, R. G. Iannitti, C. Cunha et al., "Tryptophan catabolites from microbiota engage aryl hydrocarbon receptor and balance mucosal reactivity via interleukin-22," *Immunity*, vol. 39, no. 2, pp. 372–385, 2013.
- [126] J. M. Lanis, E. E. Alexeev, V. F. Curtis et al., "Tryptophan metabolite activation of the aryl hydrocarbon receptor regulates IL-10 receptor expression on intestinal epithelia," *Mucosal Immunology*, vol. 10, no. 5, pp. 1133–1144, 2017.
- [127] A. Acovic, M. Gazdic, N. Jovicic et al., "Role of indoleamine 2,3-dioxygenase in pathology of the gastrointestinal tract," *Therapeutic advances in gastroenterology*, vol. 11, p. 175628481881533, 2018.
- [128] L. Etienne-Mesmin, B. Chassaing, and A. T. Gewirtz, "Tryptophan: a gut microbiota-derived metabolites regulating inflammation," *World Journal of Gastrointestinal Pharmacology and Therapeutics*, vol. 8, no. 1, pp. 7–9, 2017.

Research Article

Protein Level and Infantile Diarrhea in a Postweaning Piglet Model

Jing Gao ^{1,2,3,4,5}, Jie Yin ^{1,2,3,4,5}, Kang Xu,^{1,2,3,4,5} Hui Han,^{1,2,3,4,5} ZeMin Liu,^{1,2,3,4,5}
ChenYu Wang,^{1,2,3,4,5} TieJun Li ^{1,2,3,4} and YuLong Yin ^{1,2,3,4,5,6}

¹Key Laboratory of Agro-ecological Processes in Subtropical Region, Institute of Subtropical Agriculture, Chinese Academy of Sciences, China

²National Engineering Laboratory for Pollution Control and Waste Utilization in Livestock and Poultry Production, Ministry of Agriculture, Changsha, Hunan 410125, China

³Hunan Provincial Engineering Research Center for Healthy Livestock and Poultry Production, Ministry of Agriculture, Changsha, Hunan 410125, China

⁴Scientific Observing and Experimental Station of Animal Nutrition and Feed Science in South-Central, Ministry of Agriculture, Changsha, Hunan 410125, China

⁵University of Chinese Academy of Sciences, Beijing 100039, China

⁶College of Life Science, Hunan Normal University, Changsha, Hunan, China

Correspondence should be addressed to Jing Gao; gaojing.he@163.com

Received 15 February 2020; Accepted 8 April 2020; Published 31 May 2020

Guest Editor: Xiaolu Jin

Copyright © 2020 Jing Gao et al. This is an open access article distributed under the Creative Commons Attribution License, which permits unrestricted use, distribution, and reproduction in any medium, provided the original work is properly cited.

Infantile diarrhea is a serious public health problem around worldwide and results in millions of deaths each year. The levels and sources of dietary protein are potential sources of diarrhea, but the relationship between the pathogenesis causes of infantile diarrhea and protein intake remains poorly understood. Many studies have indicated that the key to understanding the relationship between the protein in the diet and the postweaning diarrhea of piglets is to explore the influences of protein sources and levels on the mammalian digestion system. The current study was designed to control diarrhea control by choosing different protein levels in the diet and aimed at providing efficient regulatory measures for infantile diarrhea by controlling the protein levels in diets using a postweaning piglets model. To avoid influences from other protein sources, casein was used as the only protein source in this study. Fourteen piglets (7.98 ± 0.14 kg, weaned at 28 d) were randomly allotted to two dietary treatments: a control group (Cont, containing 17% casein) and a high protein group (HP, containing 30% casein). The experiment lasted for two weeks and all animals were free to eat and drink water ad libitum. The diarrhea score (1 = normal; 3 = watery diarrhea) and growth performance were recorded daily. The results showed that the piglets in HP group had persistent diarrhea during the whole study, while no diarrhea was noticed in the control groups. Also, the feed intake and body weights were reduced in the HP groups compared with the other group ($P < 0.05$). The diarrhea-related mRNA abundances were analyzed by real-time PCR; the results showed that HP treatment markedly decreased the expression of aquaporin (AQP, $P < 0.05$) and the tight junction protein ($P < 0.05$), but increased inflammatory cytokines ($P < 0.01$) than those in control group. In addition, the Adenosine 5'-monophosphate (AMP)-activated protein kinase (AMPK) signaling pathway ($P < 0.01$) was inhibited in the HP group. Intestinal microbiota was tested by 16S sequencing, and we found that the HP group had a low diversity compared the other group. In conclusion, despite being highly digestible, a high casein diet induced postweaning diarrhea and reduced the growth performance of the postweaning piglets. Meanwhile, AQP, tight junction protein, and intestinal immune were compromised. Thus, the mechanism of how a highly digestible protein diet induces diarrhea might be associated with the AMPK signaling pathway and intestinal microbiome.

1. Introduction

In many countries, people are still struggling against infection, allergy, and a lack of powerful nutritional control for the infantile diarrhea [1]. Infantile diarrhea is usually distinguished as acute for diarrhea continuing exist for about 2 weeks or acting as a chronic disease if the diarrhea lasts beyond 2 weeks [2]. Diarrhea disease induces high morbidity and mortality in children younger than five years [3]. Generally speaking, gastrointestinal illnesses are a major cause of infantile diarrhea, which induces severe morbidity and mortality among young children. Further, most gastrointestinal illnesses are closely associated with gut microbiota and their products [4]. The composition of the gastrointestinal microbiota is affected by dietary nutrition intake, for example, the three main nutritional components, proteins, carbohydrates, and fats [5]. Protein is the most essential component of tissues in animals and humans, and, unlike carbohydrates, high concentrations of dietary protein intakes could result in several deleterious metabolites in the gut [6]. Amounts of researches that aimed at figure out the effects of protein on infantile and model animals have showed that the concentration and sources of dietary proteins are potential causes of diarrhea in mammals [7]. Members of the aquaporins (AQP) family act as water and ion transporters and complete the rapid transportation of water through membranes in the intestinal tract in the human body; water, via sensitive AQPs, is essential in the migration via diarrhea. While as Zonula occluden-1 (ZO-1) and occludin can dynamically affect intercellular permeability. We chose these markers to illustrate the characteristics of diarrhea.

To better understand nutritional control on the development of an individual infantile diarrhea, piglets' model has been chosen as an experimentally analog to human diets. The chosen animal model has been indicated the effects of high protein levels in daily diets on diarrhea, including reduced growth performance, severely watery feces, and gastrointestinal dysfunction. In this work, we have investigated two postweaning piglets' diets that reflected protein's effects on diarrhea. These diets included a control group (Cont, containing 17% casein) and a high protein group (HP, containing 30% casein) that led to an excessive intake of protein compared to that shown in infantile diarrhea. These piglet models provide an approach for clarifying the relationship between infantile protein intake level and its growth performance.

2. Methods

2.1. Experiment Designed. Our experiment was proceeded in compliance with the Chinese guidelines for animal welfare. Experimental protocol and approved by the Animal Care and Use Committee of the Chinese Academy of Sciences, and the ethical approval code is ISA2017030523.

A total of fourteen piglets weaned piglets (Duroc Landrace Large White, 7.98 ± 0.14 kg, weaned at 28 d) were randomly divided into 2 treatments of 7 replicates each and one piglet one metabolism cage.

Diets (Table 1) according to NRC 2012 were formulated to provide 17% casein protein (CP, containing 17% casein)

TABLE 1: The composition level of basal diet. *Premix contained the following per kilogram of the diet: sepiolite, 6.043 g; $\text{FeSO}_4 \cdot \text{H}_2\text{O}$, 516 mg; pig vitamin, 750 mg; $\text{MnSO}_4 \cdot \text{H}_2\text{O}$ 250 mg; CoO, 500 mg; $\text{ZnSO}_4 \cdot \text{H}_2\text{O}$, 212 mg; $\text{CuSO}_4 \cdot 5\text{H}_2\text{O}$, 600 mg; Na_2SeSO_3 , 30 mg; ZnO; VB4 1000 mg.

Diets	17% casein	30% casein
Ingredients		
Casein	19.11	33.72
Corn starch	63.39	45.44
Soybean oil	2	0
Sucrose	5	5
Bran	5	5
Stone power	2	2
Salt	0.5	0.5
Calcium bicarbonate	2	2
Sepiolite	0	5.34
Vitamin-mineral premix	1	1
Calculate analysis		
Crude protein	16.998	29.994
L-Lysine	1.313	2.317
L-(Methionine+cysteine)	0.568	1.001
L-Threonine	0.72	1.271
L-Tryptophane	0.254	0.448
Total energy	15.305	15.387

and a high protein (HP, containing 30% casein), and animals were fed three times per day. The diets were devoid of antibiotics or growth promoters and satisfied all essential amino acids level or exceeded the standard of NRC.

The experiment lasted for two weeks and piglets housed individually in temperature-controlled incubators. All animals were free to diets and drinking water. Piglets were weighed at the starting and ending of the whole test, while feed intake was recorded every day to calculate average daily gain (ADG), average daily feed intake (ADFI), and gain to feed ratio (G: F ratio).

2.2. Diarrhea Score. During the whole feeding trial period, diarrhea score (1 = normal; 2 = semiwatery diarrhea; 3 = watery diarrhea) was recorded twice a day (10:00, 16:00) by counting the number of pigs with diarrhea per metabolism cage.

2.3. Fecal Fluid Content Determination. When all the piglets of HP group suffered to diarrhea, faeces of each piglet were individually collected in 50 ml centrifuge tube (Sigma), recorded the total weight of each faeces as initiate weight. Collected faeces were baked at 98°C for 3 days, recorded the net weight of faeces. Fecal fluid content was calculated using the formula $W\% = W_{\text{initiate}} - W_{\text{net}}$.

2.4. Slaughter Procedure. Before the end day of the trail, all piglets fasted overnight and were slaughtered by an intravenous injection of sodium pentobarbital (50 mg/kg BW, Sigma) in the last day of the trial.

TABLE 2: Primers used in this experiment. F: forward; R: reverse.

Accession no.	Gene	Primers	Product length (bp)
NM_001167633.1	AMPK1	F: CCTTCGGCAAAGTGAAGGTTG R: TGCAGCATAGTTGGGTGAGC	467
XM_003353439.1	ZO-1	F: GAGGATGGTCACACCGTGGT R: GGAGGATGCTGTTGTCTCGG	169
NM_001163647.1	Occludin	F: TCCTGGGTGTGATGGTGTTC R: CGTAGAGTCCAGTCACCGCA	144
NM_214454.1	AQP1	F: TTGGGCTGAGCATTGCCACGC R: CAGCGAGTTCAGGCCAAGGGAGTT	221
NM_001110172.1	AQP3	F: CACCTCCATGGGCTTCAACT R: TGCCCATTCGCATCTACTCC	278
NM_001110423.1	AQP4	F: CCGGCGGCCTTTATGAGTAT R: TTCTGTTGTCATCCGCCTCC	123
NM_001110424.1	AQP5	F: TGAGTCCGAGGAGGATTGGG R: GAGGCTTCGCTGTCATCTGTTT	147
NM_001113438.1	AQP7	F: AGGCACTTCAGCAGACATCTAA R: TGGCGTGATCATCTTGGAGG	106
NM_001112683.1	AQP8	F: GGTGCCATCAACAAGAAGACG R: CCGATAAAGAACCTGATGAGCC	227
NM_001128454.1	AQP10	F: AGACAGCCTCCATCTTTGCC R: GTACCCACAGTTGACACCCATG	212
NM_001112682.1	AQP11	F: CGTCTGGAGTTTCTGGCTACC R: CCTGTCCCTGACGTGATACTTG	313
XM_003124280.3	β -Actin	F: CTGCGGCATCCACGAAACT R: AGGGCCGTGATCTCCTTCTG	147
NM_001206359.1	GAPDH	F: AAGGAGTAAGAGCCCCTGGA R: TCTGGGATGGAAACTGGAA	140
NM_214399.1	IL-6	F: GCTGCAGTCACAGAACGAGT R: CAGGTGCCCCAGCTACATTA	118
NM_213867.1	IL-8	F: TGCAGAACTTCGATGCCAGT R: ACAGTGGGGTCCACTCTCAA	97
NM_214022.1	TNF- α	F: GCCCTTCCACCAACGTTTTTC R: CAAGGGCTCTTGATGGCAGA	97

ZO-1: Zonula occluden-1; β -Actin: beta-actin; AQP: aquaporins; IL-6: interleukin-6; IL-8: interleukin-8; TNF α : tumor necrosis factor alpha.

Blood sampled from the anterior vena cava were collected; serum samples were breakaway form the blood after centrifugation 10 min at 3000 x g and under 4°C. Then, all samples were held at -80°C for analysis.

After slaughtered and cut a midline abdominal incision, gastric, distal ileum, and colon contents were collected. The entire intestinal tract was taking and cut into several segments; 1 cm of ileum was fixed in 4% paraformaldehyde for morphometric analysis.

2.5. Gut Morphological Analysis. Fixed tissues were sectioned at 5 mm thickness and stained with haematoxylin and eosin using standard paraffin embedding procedures. 7 intact, well-oriented crypt-villus units were chosen to calculate the ratio of villous height: crypt depth with a light microscope which was loaded with an image analysis system (AxioScope A1, Carl Zeiss, Jena, Germany).

2.6. Serum Amino Acids. Serum samples from anterior vena cava were collected for further analysis of amino acid concentration (His, Ser, Arg, Gly, Asp, Glu, Thr, Ala, Pro, Cys, Lys, Tyr, Met, Val, Ile, Leu, Phe, and Trp) by High-speed Amino Acid Analyzer L-8900 (Hitachi, Japan).

2.7. Total RNA from Ileum and Real-Time RT-PCR Assays (RT-PCR). Total RNA from ileum tissue samples was extracted from liquid nitrogen frozen and chop tissues with TRIZOL reagent (Invitrogen, USA), then added in DNase I (Invitrogen, USA) [8] [9]. The reverse transcription was proceeded at 37°C for 15 min, 95°C 5 sec. Primers applied in our experiment were designed by Primer 5.0 according to the pig gene sequence (Table 2). And we chose β -actin (the house-keeping gene) to normalize target gene levels. The PCR cycling condition was 36 cycles at 94°C for 40 sec, 60°C for 30 sec, and 72°C for 35 sec. The relative expression was a ratio

TABLE 3: The diarrhea rate depending on the diarrhea score.

Index	17% casein	30% casein	SEM	P value
Diarrhea rate	13%	96%	0.0812	<0.01

of the target gene compared to the control gene using the formula $2^{-(\Delta\Delta Ct)}$, where $\Delta\Delta Ct = (Ct_{\text{Target}} - Ct_{\beta - \text{actin}})_{\text{treatment}} - (Ct_{\text{Target}} - Ct_{\beta - \text{actin}})_{\text{control}}$. Relative expression was normalized and expressed as a ratio to the expression in the control group [10, 11].

2.8. 16S rRNA Sequencing and Characterization of Microbiota. Total colon digest genome DNA was extracted by QIAamp DNA Stool Mini Kit according to the manufacturer's instructions, and using sterile water diluted DNA to $1 \text{ ng}/\mu\text{L}$ for further study. Distinct region 16SV3-V4 of 16S rRNA genes were amplified using specific primer with index codes on it. All PCR reactions were in the Phusion® High-Fidelity PCR Master Mix (New England Biolabs) condition. PCR products mixed 1X loading buffer (contained SYB green), then used electrophoresis on 2% agarose gel for verification. Picked bright strap between 400 and 450 bp and purified strap with Qiagen Gel Extraction Kit (Qiagen, Germany) for the next experiment.

Used the Ion Plus Fragment Library Kit 48 rxns (Thermo Scientific) following manufacturer's recommendations created sequencing libraries. Then, the library was sequenced on an Ion S5TM XL platform, and 400 bp/600 bp single-end reads were produced. Additionally, the sequencing libraries were appraised by Qubit@ 2.0 Fluorometer (Thermo Scientific) and Agilent Bioanalyzer 2100 system. Raw sequences are available in the NCBI SRA with accession numbers PRJNA600085.

Cut off the low-quality reads by Cutadapt (V1.9.1, <http://cutadapt.readthedocs.io/en/stable/>), and cut off the barcode and primer sequence to generate paired-end reads [12]. And merged paired-end reads by FLASH (V1.2.7, <http://ccb.jhu.edu/software/FLASH/>), to avoid the overlap reads generated the opposite end of the same DNA fragment; then, raw tags generated. Using Uparse software (Uparse v7.0.1001) analyzed the high-quality sequences [13]. Sequences were inducted to OTU at $\geq 97\%$ for further annotation. And taxonomic data was assigned to every representative sequence based on RDP classifier (Version 2.2).

In order to check the phylogenetic relationship of each OTUs and to detect different dominant species between different treatment groups, several sequence alignments were proceeded by the MUSCLE software (Version 3.8.31) [14, 15]. OTUs abundance information were conducted by a standard of sequence number parallel to the sample with the least sequences. Alpha (complexity of species diversity) and beta (differences of samples in species complexity) diversity analysis were both conducted according to this output normalized data. To perform alpha diversity, Observed-species, Chao1 (species richness estimator), Shannon (diversity indices), Simpson (diversity indices), ACE (community richness), and Good-coverage (sequencing depth) were calculated with QIIME (Version 1.7.0), and all these indices in our samples were displayed with the R software (Version

2.15.3) [16]. To perform beta diversity, weighted and unweighted unifrac were calculated with QIIME (Version 1.7.0) [16]. Cluster analysis was preceded by principal component analysis (PCA), which was applied to reduce the dimension of the original variables using the FactoMineR package and ggplot2 package in the R software (Version 2.15.3).

Principal Coordinate Analysis (PCoA) was functioned as principal coordinates and visualized from complex, multidimensional data. A distance matrix from weighted or unweighted unifrac calculated result was converted to a new set of orthogonal axes, and basing on the maximum variation factor is demonstrated by the first principal coordinate, and the second maximum one by the second principal coordinate, and persist in the end. PCoA analysis was conducted by WGCNA package, stat packages, and ggplot2 package in the R software (Version 2.15.3). Arithmetic Means (UPGMA) Clustering analysis was used for a type of hierarchical clustering method (to interpret the distance matrix using average linkage) called unweighted pair-group, which is basing on QIIME software [17].

2.9. Statistical Analysis. Data analysis was done according to the one-way analysis of variance (ANOVA), used Levene's test, and within the student's *t* test (IBM SPSS 21.0 software IIME software (Version 1.7.0)) to make sure the homogeneity of variances.

3. Results

3.1. Growth Performance, Diarrhea Ratio and Diarrhea Index in Piglets. It was showed that high protein level feed could induce persistent diarrhea during the whole study, while no diarrhea was noticed in control piglets ($P < 0.05$) (Table 3) (Figure 1(a)). Also, the body weight (BW) ($P < 0.05$), food intake (FI) ($P < 0.05$), average daily gain (ADG) ($P < 0.05$), average daily feed intake (ADFI) ($P < 0.05$), and feed efficiency (G:F ratio) ($P < 0.05$) were reduced in HP groups compared with the control piglets (Figures 1(b)–1(f)).

3.2. Intestinal Morphology. The ileum intestinal morphological analysis results of the piglets are shown in Figures 2(a) and 2(b). The height of the villus, depth of the crypt, and the ratio of villus and crypt are shown in Figure 2(c). The results showed that a high protein level diet significantly decreased the height of the ileum villus and increased the depth of the ileum crypt, compared with the control piglets ($P < 0.05$).

3.3. Serum Amino Acids. In our experiment, we collected serum samples from anterior vena cava and test amino acid contents, and the result showed that Arg, Gly, Lys, Tyr, Val, Ile, Leu, Thr, Phe, and Trp ($P < 0.05$) significantly reduced in HP piglets compared with the control group (Table 4).

3.4. Relative Gene Expression of Tight Junction Proteins. Provide high casein level feed to piglets decreased the relative expression of ZO-1 and occludin in the ileum ($P < 0.05$), compared with the control group (Figures 3(a) and 3(b)).

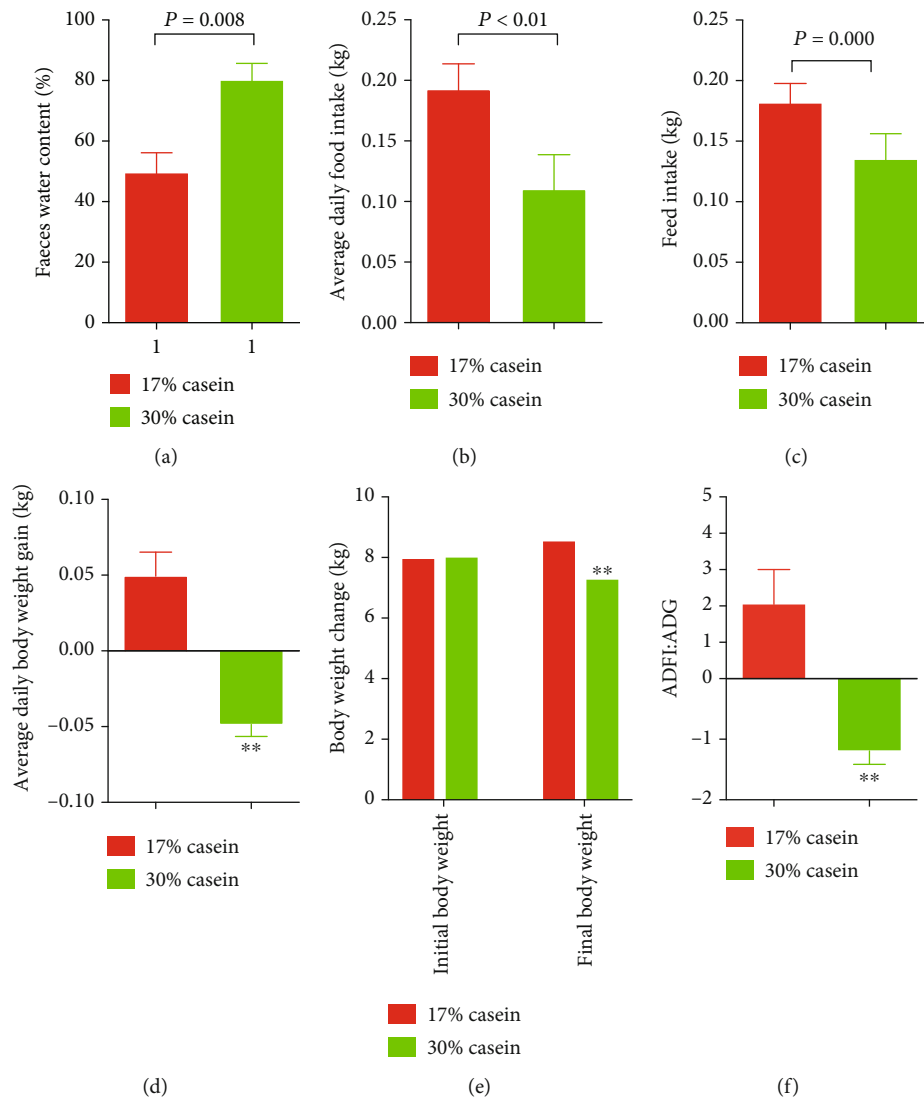


FIGURE 1: Effects of high casein level diet on the faeces water content and growth performance of piglets. (a) Faeces water content. (b) Body weight change. (c) Feed intake. (d) ADG (average daily gain of body weight). (e) ADFI (average daily feed intake). (f) The ratio of ADFI/ADG. Values are expressed as the mean \pm SEM, $n = 6$.

3.5. Tight Junction Proteins Protein Expressions. ZO-1 and occludin protein expression levels were tested in the high casein piglets and control piglets using Western blot analysis. However, in ileum, the protein expression of ZO-1 and occludin was increased in high casein group piglets compared with the control piglets, which was in contrast to the expression of the mRNA ($P < 0.05$) (Figures 3(c) and 3(d)).

3.6. Relative Gene Expression of Aquaporin Protein Family. Aquaporins (AQP) family were called as water and ion channels which took charge of the rapid transport of water across membranes in the intestinal tract in the human body, and played a key role in the management of water homeostasis [18, 19]. In the intestinal tract, there are several types that are indicated to expressions, such as AQP1, AQP3, AQP4, AQP5, AQP8, and AQP10. And almost all of these AQP in mammalian appear to be highly participated for the trans-

port of water. As expected, we found that the relative mRNA expression of AQP1 ($P < 0.05$), AQP3 ($P < 0.05$), AQP8 ($P < 0.05$), and AQP10 (Figures 4(a)–4(d)) in ileum was strongly decreased in high casein group piglets, while the difference of relative mRNA expression of AQP4 and AQP5 (Figures 4(e) and 4(f)) between HP and cont in ileum was not noticed.

3.7. Aquaporins Protein Expressions. Using Western blot analysis, we found the protein expression of AQP1 ($P < 0.05$) and AQP3 ($P < 0.05$) was decreased in high casein group compared with the control group piglets (Figures 4(g) and 4(h)).

3.8. Relative Gene Expression of Proinflammatory Cytokines. When fed high casein level diet to weaned piglets, the relative gene expression of proinflammatory cytokines TNF α in

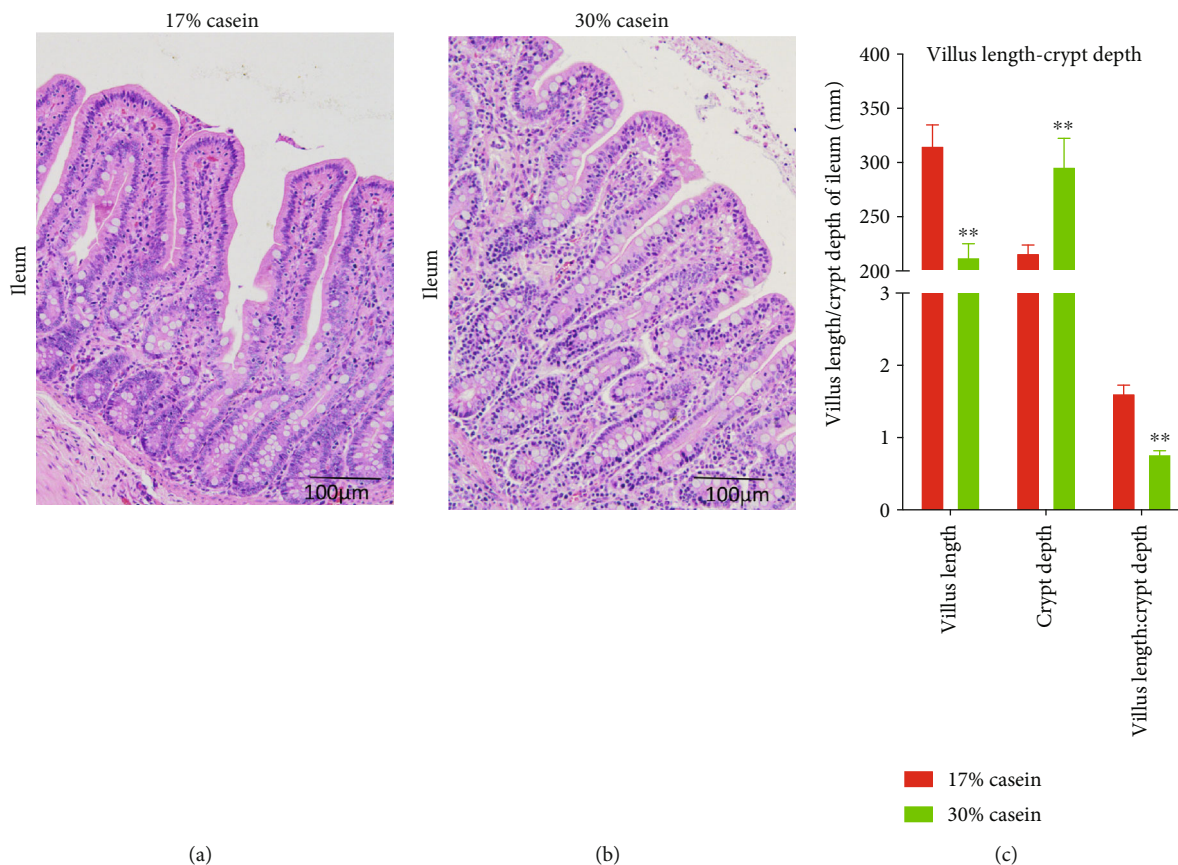


FIGURE 2: Effects of high casein level diet on morphometrics. Effects of high casein level diet on morphometrics in the ileum in weaning piglets. Representative staining of the ileum mucosal morphology of piglets (magnification: 100x). (a) Ileum morphometrics of control group. (b) Ileum morphometrics of high casein group. (c) Ratio of villus height/crypt depth of control and high casein group. Values are expressed as the mean \pm SEM. **Means the difference was significant ($P < 0.01$), $n = 6$.

ileum were increased ($P < 0.05$); consistent with $\text{TNF}\alpha$, we also found that the relative gene expression of IL-6 and IL-8 increased. And using western blot analysis, however, the protein expression of IL-6 increased, whereas the protein expression of $\text{TNF}\alpha$ decreased ($P < 0.05$) (Figures 5(a)–5(e)).

3.9. The Difference in Intestinal Microbiota Diversity and Composition Influenced by High Protein Level. The hypervariable V3 and V4 regions of 16S rRNA genes were sequenced from colon content, and about an average of $79,920 \pm 5,250$ reads were detected by each sample. Picked pairwise identity threshold $\geq 97\%$, we got an average of 690 ± 100 operational taxonomic units (OTUs) each sample. Alpha-diversity, including observed-species, Chao1 (species richness estimator), Shannon (diversity indices), Simpson (diversity indices), ACE (community richness), Good-coverage (sequencing depth) were calculated between the microbiomes (Figures 6(a)–6(d)). However, compared to the control piglets, high casein diet seems suppressed the colon microbiota diversity, but the difference showed insignificant (PD, 47.08 ± 3.24 vs. 54.91 ± 2.71 , $p = 0.09$; H, 5.98 ± 0.23 vs. 6.0 ± 0.18 , $p = 0.95$; chao1, 514.3 ± 38.14 vs. 601 ± 29.78 , $p = 0.1$). In order to test the differences between the microbiomes by beta-diversity, we conducted Principal

Component Analysis (PCoA), which obtained weighted and unweighted UniFrac distance metric matrices produced for the sample set (Figures 6(e) and 6(f)). And the result of unweighted UniFrac distances in two group piglets indicated that the difference of microbial community structure in two groups showed insignificant (Figure 6).

The total microbial composition for high casein feed showed differences at both the genus and phylum levels (Figures 6(g) and 6(h)). The three largest genera represented in the control dataset *Ruminococcaceae-UCG-002*, *Ruminococcaceae-UCG-005*, and *Ruminococcaceae-UCG-014*, but turned out *Ruminococcaceae-UCG-002*, *Fusobacterium*, and *Ruminococcaceae-UCG-005* in high casein diet piglets, and the difference of *Fusobacterium* was statistically significant after t test ($P < 0.01$). And more importantly, the three largest phyla represented in the control dataset *Firmicutes*, *Bacteroidetes*, and *Proteobacteria*, whereas *Firmicutes*, *Bacteroidetes*, and *Fusobacteria* in high casein group, same with the result in genera level, the high casein diet significant increased colon *Fusobacteria* ($P < 0.01$). The obvious differences were additionally vitrified by LEfSe analysis, which based on linear discriminant analysis (LDA) to detect bacterial taxa, and it turned out that the sequences are largely abundant in the high casein diet group (data not shown).

TABLE 4: Effects of high casein level diet on anterior vena cava serum amino acid concentrations in weaning pigs.

Item	17% casein	30% casein
Histone	11.28 ± 1.62	9.08 ± 0.62
Serine	18.49 ± 2.54	13.64 ± 0.56
Arginine	32.36 ± 3.96	21.07 ± 1.07 *
Glycine	66.58 ± 10.90	35.83 ± 2.48 *
Aspartate	9.06 ± 1.28	7.32 ± 0.30
Glutamate	93.45 ± 15.89	59.15 ± 2.72
Threonine	34.05 ± 7.58	5.73 ± 0.58 *
Alanine	48.92 ± 8.63	43.20 ± 2.36
Proline	33.55 ± 7.62	16.86 ± 0.78
Cysteine	3.73 ± 1.14	2.60 ± 0.20
Lysine	44.41 ± 7.42	23.42 ± 0.68 *
Tyrosine	20.29 ± 4.81	6.48 ± 0.44 *
Methionine	5.57 ± 1.09	2.93 ± 0.14
Valine	43.98 ± 7.54	17.85 ± 0.93 *
Isoleucine	23.14 ± 3.57	10.89 ± 0.51 *
Leucine	29.99 ± 4.95	13.86 ± 0.75 *
Phenylalanine	20.51 ± 2.03	13.69 ± 1.72 *
Tryptophan	6.70 ± 1.59	1.03 ± 0.06 *

Values are mg/l. Serum amino acid levels were determined by HPLC Ultimate 3000 and 3200 Q TRAP LC-MS/MS. Data are presented as mean ± SEM, $n = 6$. *Within a row, means the difference is significant ($P < 0.05$).

4. Relative Gene Expression and Protein Expression of AMPK

According to the real-time RT-PCR assays, high casein level diet decreased the relative gene expression of the target of AMPK signal pathway-AMPK α ($P < 0.05$), which indicated that high casein level diet inhibited AMPK signal pathway than low casein diet (Figure 7).

5. Discussion

The potential positives of balanced nutrition for the clinical treatment of diarrheal have been researched for many years. To select an appropriate method of nutritional management, the function of the digestive-absorptive metabolism was the first to be studied. Secondly, the reestablishment of the normal physiology of the small intestine needs following with interest.

The high casein level diet of weaning-piglets follows a well-established animal model of postweaning diarrhea. Infantile and early weaned piglets are extremely easy susceptible to intestinal infection according to many factors, resulting in enteric diarrhea. Many parts of the world lack sufficient nutritional control for infantile diarrhea. Because of the immaturity of their digestive systems and immune systems, the weaning period is critical for young humans and swine. When newborns and piglets have diarrhea after being weaned, highly morbidity and mortality were generally

occurred [19, 20]. During this period, the composition and level of dietary feeding is a key factor in decreasing the diarrhea incidence [21, 22] (for example, the ingests of the three main nutritional components, proteins, carbohydrates, and fats [5]). Protein is the most essential component of tissues in animals, and, unlike carbohydrates, high level of dietary protein intakes could result in several deleterious metabolites in the gut [22]. Both the severity and incidence chance of diarrhea may be increased in piglets fed diets high in protein level [23].

The maintenance of the normal state of the intestinal epithelium is important to the activities of key physiological processes, such as digestion, absorption, and immune responses. Morphometric results of the small intestine, including the villous height, crypt depth, and the ratio of the villous and crypt, can represent gut health [24]. And increased villous height reflects a larger absorptive area, and a deeper crypt implies a great villous epithelial breakdown, causing some pathogenic inflammation [25]. Previous studies showed that the ratio of villous height and crypt depth was decreased with increased protein dietary level. Further, an early report showed that the intestinal mucosa, given an abundance level of protein, was suffered easily attacked [26, 27] in piglets. In line with the published results, our study shows that the villous height and crypt depth increased, while the ratio of the ileum decreased in high casein group.

Dietary protein is a foundational essential nutrient. Protein levels can influence growth performance and are involved in several pathways, such as the immune system and the assimilation system, in humans and mammalian animals, particularly in elderly adults who need protein to provide nutrition to supporting their growth [11, 28]. After ingestion, dietary protein is hydrolyzed by pepsin and other proteases and formatted into di- and tripeptides and free amino acids (AAs). The imbalanced composition of AA in mammals causes AA antagonism, resulting in reduced food intake and impaired growth [29]. Imbalanced of essential amino acids (EAAs) such as threonine, lysine [30], tyrosine, valine, leucine, glutamine, glycine [31], arginine [32], and tryptophan [33], imbalance in the body induced harmful effects on the health, growth, and development of the animals [34]. In our experiment, we collected serum samples from the anterior vena cava and tested amino acid contents. The results showed that Arg, Gly, Lys, Tyr, Val, Ile, Leu, Thr, Phe, and Trp ($P < 0.05$) were significantly reduced in HP piglets compared with the control group.

Cytokines are closely associated with the immune-inflammatory responses, such as regulating the integrity of the intestinal barrier [35]. Previous studies showed that, in piglets, weaning increased inflammatory cytokines in the intestine. For example, IL-6, IL-8, and TNF α could increase the intestinal epithelial, thereby inhibiting the functions of epithelial cells [24, 36, 37]. In our study, a high casein protein level diet increased the ileum's inflammatory responses. IL-6, IL-8, and TNF α were significantly increased with the high dietary protein levels, which may partially explain how high protein level diets postweaning diarrhea. Except for the observation that TNF α increased protein expression levels, the clear mechanism behind this phenomenon remains

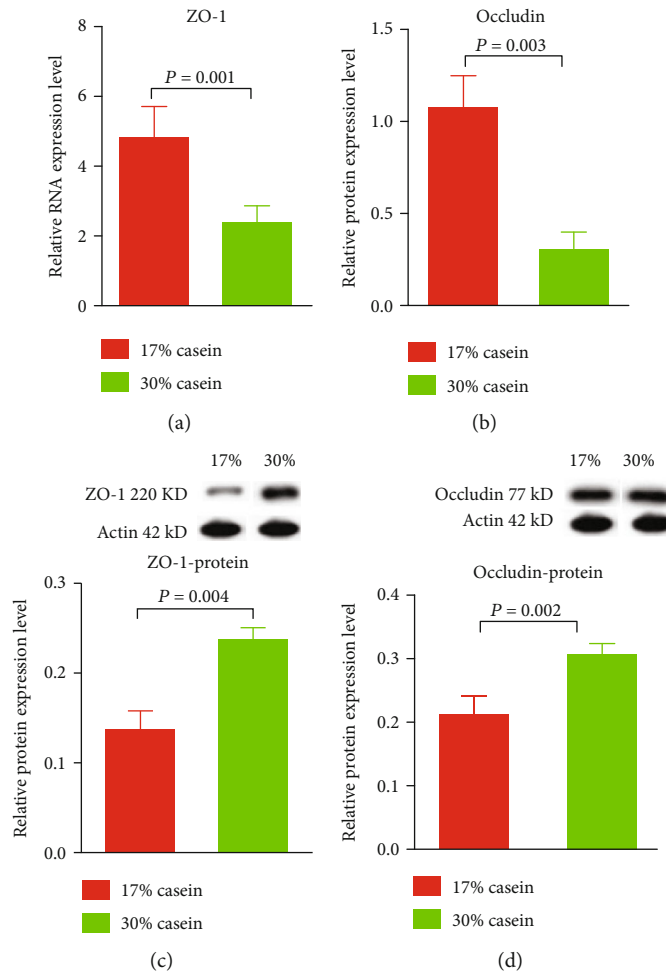


FIGURE 3: Effects of high casein level diet on the relative gene expression of tight junction protein in ileum. (a) The relative gene expression of ZO-1 in ileum in weaning piglets. (b) The relative gene expression of occludin in ileum in weaning piglets. (c) The protein expression of ZO-1 in ileum in weaning piglets. (d) The protein expression of occludin in ileum in weaning piglets. Values are expressed as the mean \pm SEM. $n = 6$.

unknown. More studies are needed to determine the reasons for the reason.

The present study investigated the nutritional control on the health and development of postweaning diarrhea. Nutrition was shown to replicate the characteristic side effects of high protein level in daily diets on diarrhea including reduced growth performance, and severely watery feces. The high severity and incidence of diarrhea among weaned piglets given the HP diet suggests that high levels of dietary protein triggered postweaning diarrhea, which may be attributed to the fermentation of undigested protein and the dysfunction of tight junction proteins and aquaporins. Importantly, high protein level diets inhibited the AMPK signal pathway, which promotes the incidence and severity of diarrhea. To further illustrate the possible underlying mechanisms of the postweaning diarrhea for a further step, the relative mRNA expression and protein expression of tight junction proteins, which could be regulated by dietary protein, were detected. As we mentioned before, proinflammatory agents can significantly affect intestinal integrity [38]. Our result shows that the expression of IL-6, IL-8, and TNF α in the high casein group realized upregulation, thereby

launching the intestinal tight junction barrier and enhancing the permeability of intestinal epithelial cells. As reported, the intestinal barrier includes the proteins ZO-1, occludin, and claudin-1 [39]. The increased expression of IL-6, IL-8, and TNF α may also affects the expression of ZO-1 and occludin. In our study, with higher dietary casein, IL-6, IL-8, and TNF α expression increased in the ileum. Further, the expression of ZO-1 and occludin at the transcriptional level decreased in ileum of piglets, which is consistent with the previous study. To some extent, the abnormal tight junction protein expression could have contributed to postweaning diarrhea [40, 41].

The intestinal epithelium can regulate the absorption of nutrients and fluids, mainly point electrolyte and water absorption and secretion. Diarrhea is closely associated with the disorders of water absorption and secretion [42]. Therefore, to investigate whether a high protein level diet is associated with the potential mechanisms for cellular osmotic homeostasis in a diarrhea animal model, the expression level and potential function of AQP were determined in our study.

Aquaporins, water, and ion channel proteins have been reported to be of vital importance in water balance. Members of the aquaporins (AQP) family were acted as water and ion

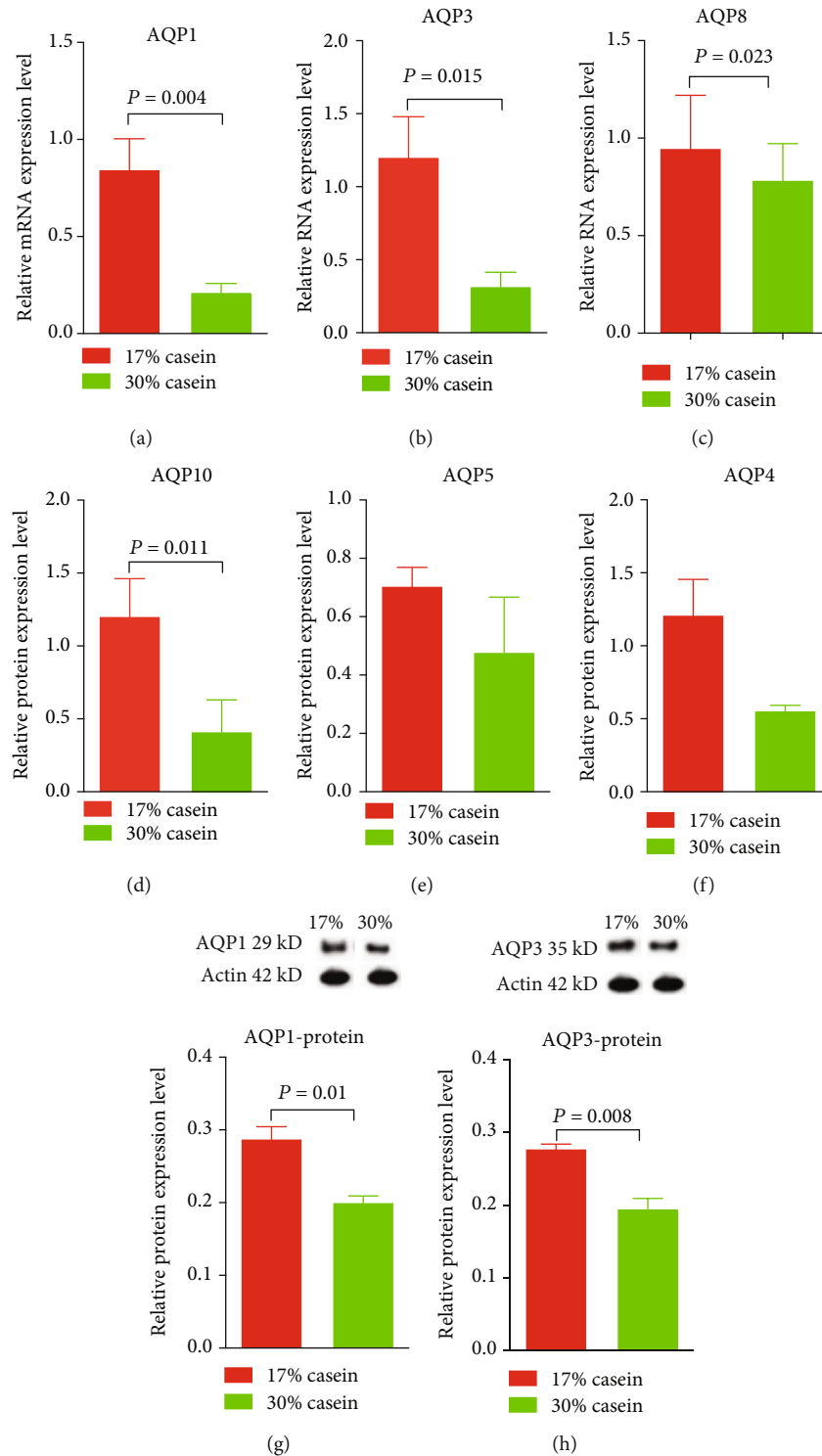


FIGURE 4: Effects of high casein level diet on the relative gene expression of aquaporins family protein in ileum. (a) The relative gene expression of aquaporins1 (AQP1) in ileum in weaning piglets. (b) The relative gene expression of aquaporins 3 (AQP3) in ileum in weaning piglets. (c) The relative gene expression of aquaporins 8 (AQP8) in ileum in weaning piglets. (d) The relative gene expression of aquaporins 10 (AQP10) in ileum in weaning piglets. (e) The relative gene expression of aquaporins 5 (AQP5) in ileum in weaning piglets. (f) The relative gene expression of aquaporins4 (AQP4) in ileum in weaning piglets. (g) The protein expression of AQP-1 in ileum in weaning piglets. (h) The protein expression of AQP3 in ileum in weaning piglets. Values are expressed as the mean \pm SEM. $n = 6$.

transporters and realized the rapid transportation of water through membranes in the intestinal tract in the human body. They are also an integral part of the management of

water homeostasis [43]. Several aquaporins exist in the intestinal tract, such as AQP1, AQP3, AQP4, AQP5, AQP6, AQP8, AQP10, and AQP11. Almost all AQPs in mammals

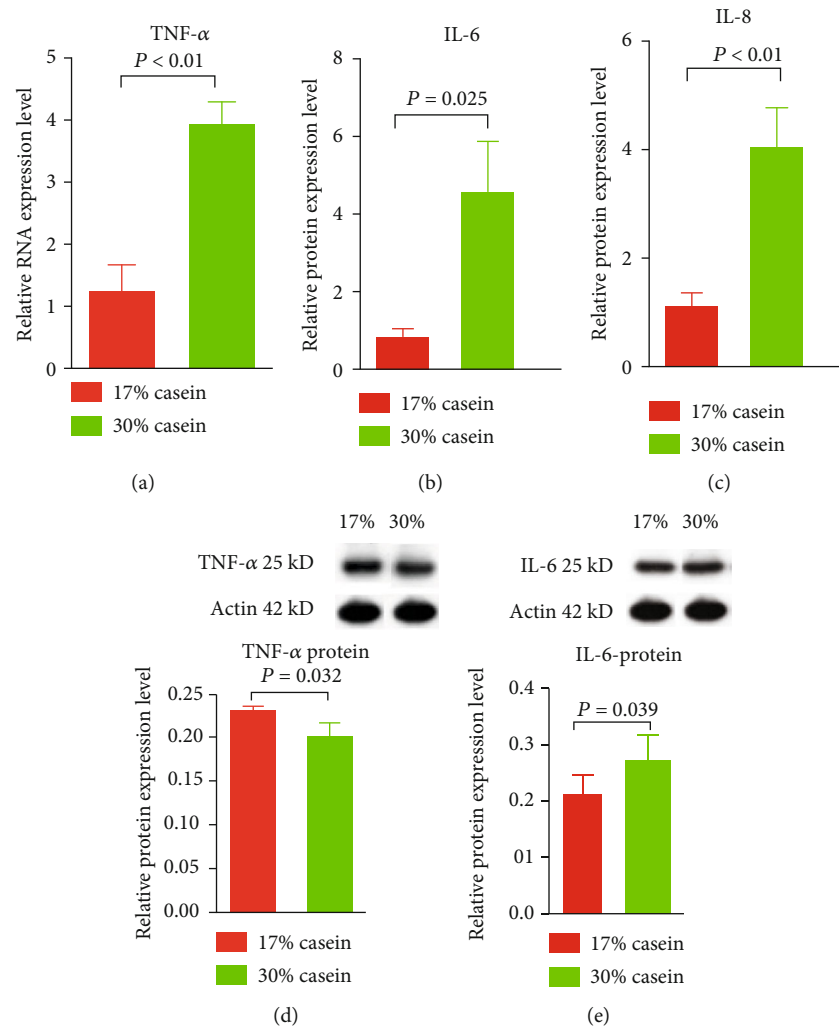


FIGURE 5: Effects of high casein level diet on the relative gene expression and protein expression of proinflammatory cytokines in ileum. (a) The relative gene expression of TNF α in ileum in weaning piglets. (b) The relative gene expression of IL-6 in ileum in weaning piglets. (c) The relative gene expression of IL-8 in ileum in weaning piglets. (d) The protein expression of TNF α in ileum in weaning piglets. (e) The protein expression of IL-6 in ileum in weaning piglets. Values are expressed as the mean \pm SEM. $n = 6$.

seem to be highly discriminating for the transport of water [44]. Moreover, several AQPs have been demonstrated to be downregulated under different types of diarrhea [45].

Accordingly, we found that the expression of AQP1, AQP3, and AQP10 in the ileum was significantly decreased in piglets given a high casein level diet, while the expression of AQP8 was decreased at the mRNA level but remained the same at the protein level. The inhibition of AQP1, AQP3, AQP8, and AQP10 in the ileum has shown the imbalance of water absorption and secretion. With a high casein diet, the expression of some aquaporins becomes inhibited, thereby increasing the fecal water content, and ultimately inducing diarrhea [46, 47]. AQPs played an important role in the transition during diarrhea in many tissues. Among these AQPs, a high protein level diet has a significant influence on the mRNA levels of AQPs in the ileum. Generally speaking, the water transport through the epithelium across the small intestine is regulated by all these AQPs. However, under stress and bacterial infection (e.g., *Fusobacterium*) conditions, AQP1, AQP3, AQP8, and AQP10 are mainly

responsible for the maintaining of water homeostasis in the gastrointestinal tract [48]. Also, under a high protein level diet, AQP1, AQP3, AQP8, and AQP10 in the ileum were downregulated, thus interrupting the intestinal permeability during diarrhea. Previous studies have indicated that in the intestine, AQPs act as an alleviator of the dehydration and ions loss by completing a rapid reflow of luminal water back to the body [49]. This activity is possibly explained by the decreased AQP expression in the control group, whose dietary protein level is only 17% higher than that in the high protein group. Importantly, new studies have shown that the intestinal inflammatory response has a striking effect on the inhibition of AQP expression over the postweaning diarrhea period. Therefore, a deeper experimental design is needed to obtain more effective information on the effects of high protein level diets associated with the expression of AQPs and their interactions in the intestine.

The intestinal microbiota serves as an indispensable role in maintaining a host's health by inhibiting the composition of pathogens, supporting the development of a healthy

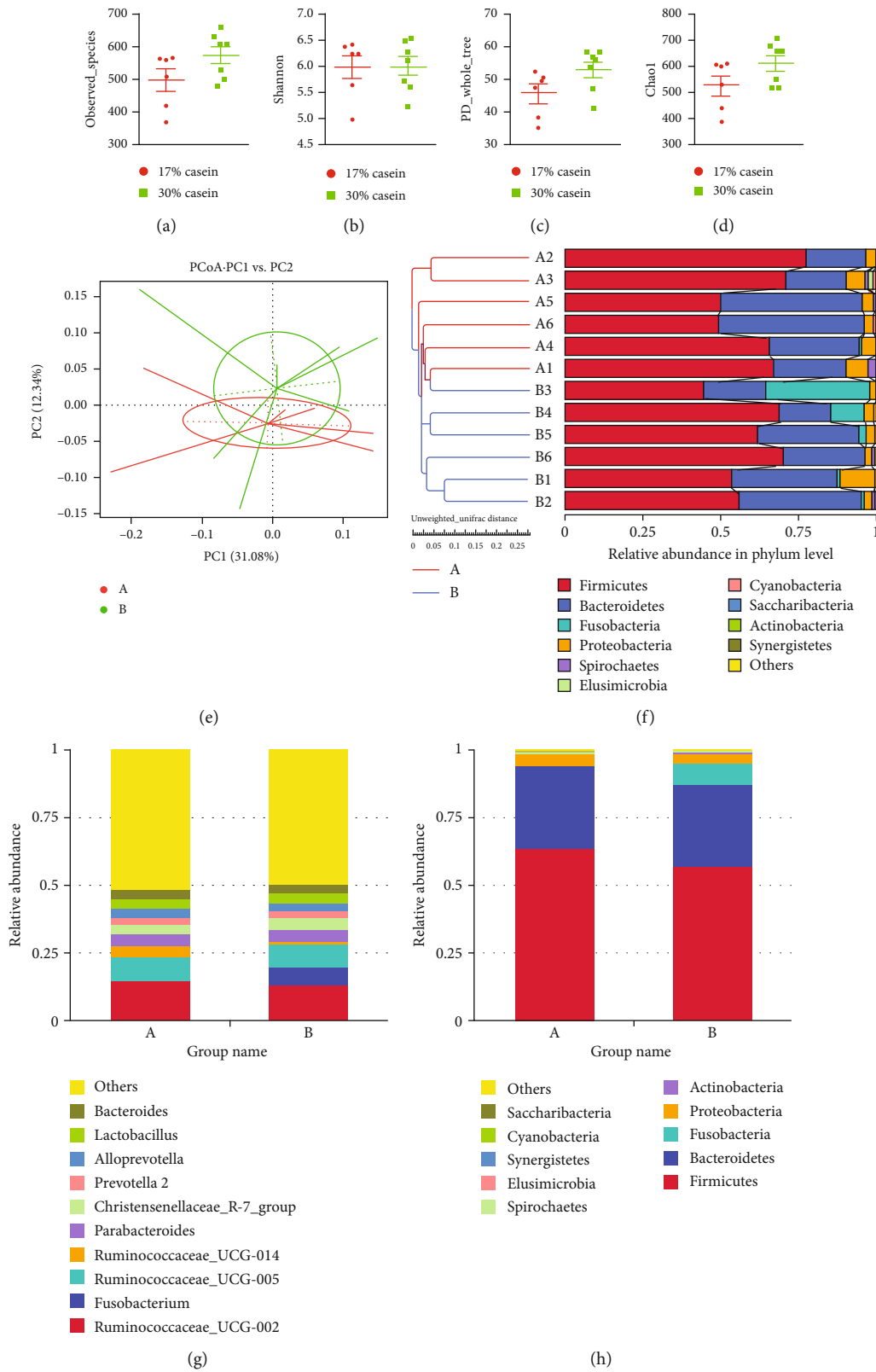


FIGURE 6: Effects of high casein diet on gut microbial diversity and unweighted UniFrac distances. (a) Observed species. (b) Phylogenetic Diversity (PD). (c) Shannon H index. (d) Chao1 index. (e) Principal Component Analysis (PCoA) of intestinal microbiomes. (f) Comparison of unweighted UniFrac distances between pairs of samples. Data were expressed as the mean \pm SEM ($n = 6$); (g, h) 16S RNA bacterial sequences represent in colon samples. A represents control group; B represents high casein diet group. Each figure values of relative abundance of the ten most abundant bacterial groups: genus (g) and phylum (h) found in the colon microbiota ($n = 6$).

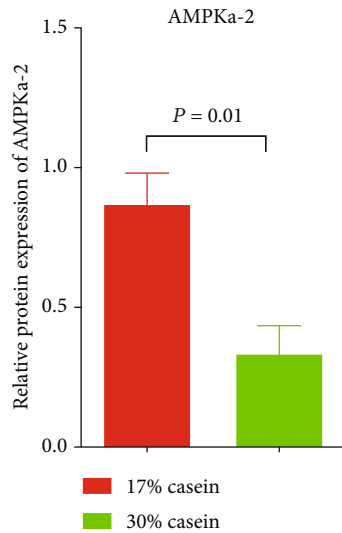


FIGURE 7: Effects of high casein level diet on the relative gene expression of target of AMPK signal pathway-AMPK α -2 in ileum. Values expressed the mean \pm SEM. $n = 6$.

intestinal microbiota, and promoting a beneficial immune system, as well as metabolites for host epithelial cells [50]. In mammals, several studies have showed that production metabolized by the intestinal microbiota somehow affects host metabolism. Piglets are susceptible to various pathogens because of their unstable gut microbiota and immature immune systems [51]. Although the relationship between intestinal microbiota and microbial metabolites in pigs is a research hot spot, we have not confirmed the clear connections, through functional and clinically associated symptoms, between high casein levels and postweaning diarrhea. This is the first study to show a tight correlation between *Fusobacterium* and postweaning diarrhea. *Fusobacterium* is one of the most effective infectious factors that causes intestinal inflammation in piglets. Members of the genus *Fusobacterium* are a group of commensal Gram-negative anaerobes belonging to the phylum *Fusobacteria*. They are usually found in the human oral cavity and are closely associated with periodontal diseases [52]. In our study, we performed a 16S-rRNA gene analysis on colon content samples from all 14 piglets. We discovered that *Fusobacterium* was much richer in the colons of the high casein group piglets than in those of the control group at both the phylum and genus levels. Increasing the abundance of *Fusobacterium* in the colon microbiota seems to act as an important aggravating factor for postweaning diarrhea in piglets. This novel finding may contribute to improved control strategies for infantile diarrhea and postweaning diarrhea in pigs. Clinical studies test on human diarrheal diseases have indicated that *Fusobacterium* can be detected in the colonic tissue of patients within inflammatory bowel disease [53]. And some papers also suggest that *Fusobacterium* is closely associated with the severity of diarrhea in humans and in piglets' model [54, 55]. Species belonging to the *Fusobacterium* genus are closely associated with periodontal diseases. Additionally, some species from the *Fusobacterium* genus act as a cause of colorectal cancer [56]. However, few studies have reported the relationship between

Fusobacterium genus and diarrhea. Thus, it remains unclear if *Fusobacterium* is induced by the postweaning diarrhea associated with high protein levels in dietary feed. The potential effect of *Fusobacterium* as a pathogenic bacterium has been reported in multiple observations [57]. The specific enrichment of *Fusobacterium* could be due to the following mechanism. The fermentation of undigested protein could engender a failure in the function of the microvilli that grow on the surfaces of intestinal epithelial cells, thereby stimulating the susceptibility to *Fusobacterium* infection. *Fusobacteria* occupy a dominant genus status and are positively populated due to their ability to affix to and invade intestinal cells, thus influencing important function and the metabolic pathways of the gastrointestinal tract, which may induce severe diarrhea in piglet. However, for the time being, this hypothesis remains unsubstantiated.

Recent studies have demonstrated that AMPK participates in the manipulation of water and ion transport, particularly, the expression of transport proteins, including the AQPs and ion transporters in the intestinal epithelium [58, 59]. Importantly, in our experiment, we found that the expression of AMPK was decreased, this may be accompanied by the inhibited expression of aquaporin.

6. Conclusion

Our study investigated the nutritional control on the health and development of postweaning diarrhea and indicated that high casein level diet resulted in growth performance, severely watery feces, and a significant diarrhea symptom. And this may be attributed to the fermentation of undigested protein and dysfunction of tight junction protein and aquaporins. Importantly, high protein level diets inhibited AMPK signal pathway, which is promoting the incidence and severity of diarrhea.

Abbreviations

Cont:	Control group
HP:	High protein group
AMPK:	Adenosine 5'-monophosphate (AMP)-activated protein kinase
BW:	Body weight
FI:	Food intake
ADG:	Average daily gain
ADFI:	Average daily feed intake
G:F ratio:	Gain: Feed ratio
ENA:	Essential amino acids
AQP:	Aquaporins
β -Actin:	Beta-actin
ZO-1:	Zonula occluden-1
IL-6:	Interleukin-6
IL-8:	Interleukin-8
TNF α :	Tumor necrosis factor alpha.

Data Availability

The data used to support the findings of this study are available from the corresponding author upon request.

Conflicts of Interest

The authors declare no competing financial interest. The founding sponsors had no role in the design of the study; in the collection, analyses, or interpretation of data; in the writing of the manuscript; and in the decision to publish the results.

Authors' Contributions

All the authors contributed extensively to the work presented in this manuscript. JG mainly completed this review. JG performed the literature search and wrote the manuscript. KX, HH, JY, ZML, CYW, TL, and YY conceived the work and critically revised it. YY revised the manuscript. All authors read and approved the final manuscript.

Acknowledgments

Funding was provided by the Key R&D Program of Guangxi Zhuang Autonomous region (2019AB19003), the Key Programs of frontier scientific research of the Chinese Academy of Sciences (QYZDY-SSW-SMC008), the National Natural Science Foundation of China (31872371) and the Key R&D Program of Hunan Province (2017NK2321), the Earmarked Fund for China Agriculture Research System (CARS-35), the Hunan Provincial Science and Technology Department (2018TP1031).

References

- [1] G. A. Mensah, G. A. Roth, U. K. Sampson et al., "Mortality from cardiovascular diseases in sub-Saharan Africa, 1990-2013: a systematic analysis of data from the Global Burden of Disease Study 2013," *Cardiovascular Journal of Africa*, vol. 26, no. 2, pp. S6-10, 2015.
- [2] M. J. A. Nabuurs, "Weaning piglets as a model for studying pathophysiology of diarrhea," *The Veterinary Quarterly*, vol. 20, pp. 42-45, 1998.
- [3] D. Cameron, Q. S. Hock, M. Kadim et al., "Probiotics for gastrointestinal disorders: proposed recommendations for children of the Asia-Pacific region," *World Journal of Gastroenterology*, vol. 23, no. 45, pp. 7952-7964, 2017.
- [4] M.-C. Arrieta, L. T. Stiemsma, N. Amenogbe, E. M. Brown, and B. Finlay, "The intestinal microbiome in early life: health and disease," *Frontiers in Immunology*, vol. 5, p. 427, 2014.
- [5] K. Qiu, X. Zhang, N. Jiao et al., "Dietary protein level affects nutrient digestibility and ileal microbiota structure in growing pigs," *Animal Science Journal*, vol. 89, no. 3, pp. 537-546, 2018.
- [6] K. E. Garcia, T. C. R. de Souza, G. M. Landin, A. A. Barreyro, M. G. B. Santos, and J. G. G. Soto, "Microbial fermentation patterns, diarrhea incidence, and performance in weaned piglets fed a low protein diet supplemented with probiotics," *Food and Nutrition Sciences*, vol. 5, no. 18, pp. 1776-1786, 2014.
- [7] Z. Weizman, M. Binsztok, D. Fraser, R. J. Deckelbaum, and E. Granot, "Intestinal protein loss in acute and persistent diarrhea of early childhood," *Journal of Clinical Gastroenterology*, vol. 34, no. 4, pp. 427-429, 2002.
- [8] A. Burokas, S. Arboleya, R. D. Moloney et al., "Targeting the microbiota-gut-brain axis: prebiotics have anxiolytic and antidepressant-like effects and reverse the impact of chronic stress in mice," *Biological Psychiatry*, vol. 82, no. 7, pp. 472-487, 2017.
- [9] W. Zhou, K. Ullman, V. Chowdry et al., "Molecular investigations on the prevalence and viral load of enteric viruses in pigs from five European countries," *Veterinary Microbiology*, vol. 182, pp. 75-81, 2016.
- [10] F. Stämmler, J. Gläsner, A. Hiergeist et al., "Adjusting microbiome profiles for differences in microbial load by spike-in bacteria," *Microbiome*, vol. 4, no. 1, p. 28, 2016.
- [11] Y. Wu, Z. Jiang, C. Zheng et al., "Effects of protein sources and levels in antibiotic-free diets on diarrhea, intestinal morphology, and expression of tight junctions in weaned piglets," *Animal Nutrition*, vol. 1, no. 3, pp. 170-176, 2015.
- [12] K. P. Aßhauer, B. Wemheuer, R. Daniel, and P. Meinicke, "Tax4Fun: predicting functional profiles from metagenomic 16S rRNA data," *Bioinformatics*, vol. 31, no. 17, pp. 2882-2884, 2015.
- [13] R. C. Edgar, "UPARSE: highly accurate OTU sequences from microbial amplicon reads," *Nature Methods*, vol. 10, no. 10, pp. 996-998, 2013.
- [14] R. C. Edgar, "MUSCLE: multiple sequence alignment with high accuracy and high throughput," *Nucleic Acids Research*, vol. 32, no. 5, pp. 1792-1797, 2004.
- [15] C. Quast, E. Pruesse, P. Yilmaz et al., "The SILVA ribosomal RNA gene database project: improved data processing and web-based tools," *Nucleic Acids Research*, vol. 41, no. Database issue, pp. D590-D596, 2013.
- [16] J. Kuczynski, J. Stombaugh, W. A. Walters, A. González, J. G. Caporaso, and R. Knight, "Using QIIME to analyze 16S rRNA gene sequences from microbial communities," *Current Protocols in Bioinformatics*, vol. 36, no. 1, pp. 10.7.1-10.7.20, 2012.
- [17] G.-J. Hua, C.-L. Hung, C.-Y. Lin, F.-C. Wu, Y.-W. Chan, and C. Y. Tang, "MGUPGMA: a fast UPGMA algorithm with multiple graphics processing units using NCCL," *Evolutionary Bioinformatics Online*, vol. 13, 2017.
- [18] T. Matsuzaki, Y. Tajika, A. Ablimit, T. Aoki, H. Hagiwara, and K. Takata, "Aquaporins in the digestive system," *Medical Electron Microscopy*, vol. 37, no. 2, pp. 71-80, 2004.
- [19] J. A. Guttman, F. N. Samji, Y. Li, W. Deng, A. Lin, and B. B. Finlay, "Aquaporins contribute to diarrhoea caused by attaching and effacing bacterial pathogens," *Cellular Microbiology*, vol. 9, no. 1, pp. 131-141, 2007.
- [20] S. Lin, X. Yang, P. Yuan et al., "Undernutrition shapes the gut microbiota and bile acid profile in association with altered gut-liver FXR signaling in weaning pigs," *Journal of Agricultural and Food Chemistry*, vol. 67, no. 13, pp. 3691-3701, 2019.
- [21] R. Gresse, F. Chaucheyras-Durand, M. A. Fleury, T. van de Wiele, E. Forano, and S. Blanquet-Diot, "Gut microbiota dysbiosis in postweaning piglets: understanding the keys to health," *Trends in Microbiology*, vol. 25, no. 10, pp. 851-873, 2017.
- [22] J. K. Htoo, B. A. Araiza, W. C. Sauer et al., "Effect of dietary protein content on ileal amino acid digestibility, growth performance, and formation of microbial metabolites in ileal and cecal digesta of early-weaned pigs^{1,2}," *Journal of Animal Science*, vol. 85, no. 12, pp. 3303-3312, 2007.
- [23] R. O. Ball and F. X. Aherne, "Influence of dietary nutrient density, level of feed intake and weaning age on young pigs. II. Apparent nutrient digestibility and incidence and severity of diarrhea," *Canadian Veterinary Journal La Revue Veterinaire Canadienne*, vol. 67, pp. 1105-1115, 1987.

- [24] F. Han, L. Hu, Y. Xuan et al., "Effects of high nutrient intake on the growth performance, intestinal morphology and immune function of neonatal intra-uterine growth-retarded pigs," *The British Journal of Nutrition*, vol. 110, no. 10, pp. 1819–1827, 2013.
- [25] J. R. Pluske, M. J. Thompson, C. S. Atwood, P. H. Bird, I. H. Williams, and P. E. Hartmann, "Maintenance of villus height and crypt depth, and enhancement of disaccharide digestion and monosaccharide absorption, in piglets fed on cows' whole milk after weaning," *The British Journal of Nutrition*, vol. 76, no. 3, pp. 409–422, 1996.
- [26] F. Wu, X. Xiong, H. Yang et al., "Expression of proteins in intestinal middle villus epithelial cells of weanling piglets," *Frontiers in Bioscience*, vol. 22, no. 4, pp. 539–557, 2017.
- [27] H. M. van Beers-Schreurs, M. J. Nabuurs, L. Vellenga, H. Kalsbeek-van der Valk, T. Wensing, and H. J. Breukink, "Weaning and the weanling diet influence the villous height and crypt depth in the small intestine of pigs and alter the concentrations of short-chain fatty acids in the large intestine and blood," *The Journal of Nutrition*, vol. 128, no. 6, pp. 947–953, 1998.
- [28] S. Ghosh, "Protein quality in the first thousand days of life," *Food and Nutrition Bulletin*, vol. 37, no. 1, pp. S14–S21, 2016.
- [29] G. Wu, "Amino acids: metabolism, functions, and nutrition," *Amino Acids*, vol. 37, no. 1, pp. 1–17, 2009.
- [30] J. Yin, H. Han, Y. Li et al., "Lysine restriction affects feed intake and amino acid metabolism via gut microbiome in piglets," *Cellular Physiology and Biochemistry*, vol. 44, no. 5, pp. 1749–1761, 2017.
- [31] Y. Liu, X. Wang, H. Wu et al., "Glycine enhances muscle protein mass associated with maintaining Akt-mTOR-FOXO1 signaling and suppressing TLR4 and NOD2 signaling in piglets challenged with LPS," *American Journal of Physiology Regulatory, Integrative and Comparative Physiology*, vol. 311, no. 2, pp. R365–R373, 2016.
- [32] X. Ma, M. Han, D. Li et al., "L-Arginine promotes protein synthesis and cell growth in brown adipocyte precursor cells via the mTOR signal pathway," *Amino Acids*, vol. 49, no. 5, pp. 957–964, 2017.
- [33] J. Gao, K. Xu, H. Liu et al., "Impact of the gut microbiota on intestinal immunity mediated by tryptophan metabolism," *Frontiers in Cellular and Infection Microbiology*, vol. 8, p. 13, 2018.
- [34] G. Wu, F. W. Bazer, Z. Dai, D. Li, J. Wang, and Z. Wu, "Amino acid nutrition in animals: protein synthesis and beyond," *Annual Review of Animal Biosciences*, vol. 2, pp. 387–417, 2014.
- [35] R. Al-Sadi, M. Boivin, and T. Ma, "Mechanism of cytokine modulation of epithelial tight junction barrier," *Frontiers in Bioscience*, vol. 14, pp. 2765–2778, 2009.
- [36] R. Al-Sadi, D. Ye, M. Boivin et al., "Interleukin-6 modulation of intestinal epithelial tight junction permeability is mediated by JNK pathway activation of claudin-2 gene," *PLoS One*, vol. 9, no. 3, article e85345, 2014.
- [37] J. Xu, X. Chen, S. Yu, Y. Su, and W. Zhu, "Effects of early intervention with sodium butyrate on gut microbiota and the expression of inflammatory cytokines in neonatal piglets," *PLoS One*, vol. 11, no. 9, article e0162461, 2016.
- [38] Y. Wu, C. Zhu, Z. Chen et al., "Protective effects of *Lactobacillus plantarum* on epithelial barrier disruption caused by enterotoxigenic *Escherichia coli* in intestinal porcine epithelial cells," *Veterinary Immunology and Immunopathology*, vol. 172, pp. 55–63, 2016.
- [39] A. Buckley and J. R. Turner, "Cell biology of tight junction barrier regulation and mucosal disease," *Cold Spring Harbor Perspectives in Biology*, vol. 10, no. 1, 2018.
- [40] H. R. Wardill and J. M. Bowen, "Chemotherapy-induced mucosal barrier dysfunction: an updated review on the role of intestinal tight junctions," *Current Opinion in Supportive and Palliative Care*, vol. 7, no. 2, pp. 155–161, 2013.
- [41] Q. F. Zong, Y. J. Huang, L. S. Wu, Z. C. Wu, S. L. Wu, and W. B. Bao, "Effects of porcine epidemic diarrhea virus infection on tight junction protein gene expression and morphology of the intestinal mucosa in pigs," *Polish Journal of Veterinary Sciences*, vol. 22, no. 2, pp. 345–353, 2019.
- [42] M. F. Kagnoff, "The intestinal epithelium is an integral component of a communications network," *The Journal of Clinical Investigation*, vol. 124, no. 7, pp. 2841–2843, 2014.
- [43] M. Camilleri, P. Carlson, V. Chedid, P. Vijayvargiya, D. Burton, and I. Busciglio, "Aquaporin expression in colonic mucosal biopsies from irritable bowel syndrome with diarrhea," *Clinical and Translational Gastroenterology*, vol. 10, no. 4, article e00019, 2019.
- [44] M. Abir-Awan, P. Kitchen, M. M. Salman, M. Conner, A. Conner, and R. Bill, "Inhibitors of mammalian aquaporin water channels," *International Journal of Molecular Sciences*, vol. 20, no. 7, p. 1589, 2019.
- [45] N. Ikarashi, R. Kon, and K. Sugiyama, "Aquaporins in the colon as a new therapeutic target in diarrhea and constipation," *International Journal of Molecular Sciences*, vol. 17, no. 7, p. 1172, 2016.
- [46] N. Ikarashi, R. Kon, T. Iizasa et al., "Inhibition of aquaporin-3 water channel in the colon induces diarrhea," *Biological & Pharmaceutical Bulletin*, vol. 35, no. 6, pp. 957–962, 2012.
- [47] N. Ikarashi, "The elucidation of the function and the expression control mechanism of aquaporin-3 in the colon," *Yakugaku Zasshi*, vol. 133, no. 9, pp. 955–961, 2013.
- [48] J. E. C. Krone, A. K. Agyekum, M. ter Borgh, K. Hamonic, G. B. Penner, and D. A. Columbus, "Characterization of Urea Transport Mechanisms in the Intestinal Tract of Growing Pigs," *American Journal of Physiology Gastrointestinal and Liver Physiology*, vol. 317, no. 6, pp. G839–G844, 2019.
- [49] C. Zhu, Z. Chen, and Z. Jiang, "Expression, Distribution and Role of Aquaporin Water Channels in Human and Animal Stomach and Intestines," *International Journal of Molecular Sciences*, vol. 17, no. 9, p. 1399, 2016.
- [50] M. Minty, T. Canceil, M. Serino, R. Burcelin, F. Tercé, and V. Blasco-Baque, "Oral microbiota-induced periodontitis: a new risk factor of metabolic diseases," *Reviews in Endocrine & Metabolic Disorders*, vol. 20, no. 4, pp. 449–459, 2019.
- [51] L. Jiang, C. Feng, S. Tao et al., "Maternal imprinting of the neonatal microbiota colonization in intrauterine growth restricted piglets: a review," *Journal of Animal Science and Biotechnology*, vol. 10, no. 1, p. 88, 2019.
- [52] J. Sabino, R. P. Hirten, and J. F. Colombel, "Review article: bacteriophages in gastroenterology—from biology to clinical applications," *Alimentary Pharmacology & Therapeutics*, vol. 51, no. 1, pp. 53–63, 2020.
- [53] E. A. Alhinai, G. E. Walton, and D. M. Commane, "The role of the gut microbiota in colorectal cancer causation," *International Journal of Molecular Sciences*, vol. 20, no. 21, p. 5295, 2019.

- [54] Z. Tan, W. Dong, Y. Ding, X. Ding, Q. Zhang, and L. Jiang, "Changes in cecal microbiota community of suckling piglets infected with porcine epidemic diarrhea virus," *PLoS One*, vol. 14, no. 7, article e0219868, 2019.
- [55] C. Zhang, Y. Liu, S. Chen et al., "Effects of intranasal pseudorabies virus AH02LA infection on microbial community and immune status in the ileum and colon of piglets," *Viruses*, vol. 11, no. 6, p. 518, 2019.
- [56] M. S. R. Shirazi, K. Z. K. Al-Alo, M. H. Al-Yasiri, Z. M. Lateef, and A. Ghasemian, "Microbiome Dysbiosis and Predominant Bacterial Species as Human Cancer Biomarkers," *Journal of Gastrointestinal Cancer*, 2019.
- [57] S. H. Wong and J. Yu, "Gut microbiota in colorectal cancer: mechanisms of action and clinical applications," *Nature Reviews Gastroenterology & Hepatology*, vol. 16, no. 11, pp. 690–704, 2019.
- [58] F. Lang and M. Foller, "Regulation of ion channels and transporters by AMP-activated kinase (AMPK)," *Channels*, vol. 8, pp. 20–28, 2013.
- [59] L. He, N. Huang, H. Li et al., "AMPK/ α -ketoglutarate axis regulates intestinal water and ion homeostasis in young pigs," *Journal of Agricultural and Food Chemistry*, vol. 65, no. 11, pp. 2287–2298, 2017.

Research Article

Effects of GABA Supplementation on Intestinal SIgA Secretion and Gut Microbiota in the Healthy and ETEC-Infected Weaning Piglets

Yuanyuan Zhao,^{1,2} Jing Wang^{1,2,3}, Hao Wang,¹ Yonggang Huang,³ Ming Qi,² Simeng Liao,² Peng Bin,⁴ and Yulong Yin^{1,2,3}

¹Guangdong Provincial Key Laboratory of Animal Nutrition Control, Institute of Subtropical Animal Nutrition and Feed, College of Animal Science, South China Agricultural University, Guangzhou, China

²Hunan International Joint Laboratory of Animal Intestinal Ecology and Health, Laboratory of Animal Nutrition and Human Health, College of Life Sciences, Hunan Normal University, Changsha 410081, China

³College of Animal Science and Technology, Hunan Agricultural University, Changsha, 410128 Hunan, China

⁴Jiangsu Co-Innovation Center for Important Animal Infectious Diseases and Zoonoses, Joint International Research Laboratory of Agriculture and Agri-Product, Safety of Ministry of Education of China, College of Veterinary Medicine, Yangzhou University, Yangzhou, China

Correspondence should be addressed to Jing Wang; jingwang90@g.ucla.edu and Yulong Yin; yinyulong@isa.ac.cn

Received 10 March 2020; Accepted 2 April 2020; Published 26 May 2020

Guest Editor: Xiaolu Jin

Copyright © 2020 Yuanyuan Zhao et al. This is an open access article distributed under the Creative Commons Attribution License, which permits unrestricted use, distribution, and reproduction in any medium, provided the original work is properly cited.

Pathogenic enterotoxigenic *Escherichia coli* (ETEC) has been considered a major cause of diarrhea which is a serious public health problem in humans and animals. This study was aimed at examining the effect of γ -aminobutyric acid (GABA) supplementation on intestinal secretory immunoglobulin A (SIgA) secretion and gut microbiota profile in healthy and ETEC-infected weaning piglets. A total of thirty-seven weaning piglets were randomly distributed into two groups fed with the basal diet or supplemented with 40 mg·kg⁻¹ of GABA for three weeks, and some piglets were infected with ETEC at the last week. According to whether ETEC was inoculated or not, the experiment was divided into two stages (referred as CON1 and CON2 and GABA1 and GABA2). The growth performance, organ indices, amino acid levels, and biochemical parameters of serum, intestinal SIgA concentration, gut microbiota composition, and intestinal metabolites were analyzed at the end of each stage. We found that, in both the normal and ETEC-infected piglets, jejunal SIgA secretion and expression of some cytokines, such as IL-4, IL-13, and IL-17, were increased by GABA supplementation. Meanwhile, we observed that some low-abundance microbes, like *Enterococcus* and *Bacteroidetes*, were markedly increased in GABA-supplemented groups. KEGG enrichment analysis revealed that the nitrogen metabolism, sphingolipid signaling pathway, sphingolipid metabolism, and microbial metabolism in diverse environments were enriched in the GABA1 group. Further analysis revealed that alterations in microbial metabolism were closely correlated to changes in the abundances of *Enterococcus* and *Bacteroidetes*. In conclusion, GABA supplementation can enhance intestinal mucosal immunity by promoting jejunal SIgA secretion, which might be related with the T-cell-dependent pathway and altered gut microbiota structure and metabolism.

1. Introduction

Postweaning is a critical stage in swine husbandry, because inappropriate management procedures in this stage may cause health problems in the swine industry and lead to significant economic losses [1]. Weaning piglets are quite

vulnerable to a variety of environmental stressors [2] and pathogens (e.g., enterotoxigenic *Escherichia coli* (ETEC)) [3], which could induce severe diarrhea and pose great threat to the health of weaning piglets. To deal with these problems, antibiotics have been used extensively to prevent pathogen infections. However, the widespread use of antibiotics in

farm animals has been proved to cause severe problems like pathogenic drug resistance [4]. Thus, it is necessary to develop effective nutritional regulatory strategies to enhance intestinal immunity and prevent intestinal infection in weaning piglets.

Immunoglobulin A (IgA) secreted by plasma cells is the most abundant immunoglobulin in the body and is of critical importance in intestinal mucosal immunity [5]. The function of SIgA in intestinal mucosal immunity includes immune exclusion, antigen presentation, and interaction with gut commensals [6–10]. Therefore, it is clear that SIgA plays a critical role in maintaining intestinal mucosal immunity and preventing intestinal infection. A previous study reported that the fecal SIgA concentration in piglets reached the peak within a few days after birth [11]. After that, it constantly decreased to a relatively low level in about 10 days [11]. From then on, the fecal SIgA concentration in piglets remained low until at least 50 days of age [11]. This suggests that lack of SIgA might be an underlying reason why weaning piglets are so susceptible to numerous stressors and pathogens.

Current studies revealed that dietary amino acid supplementation, such as glutamine, arginine, and leucine, is an effective way to promote intestinal immunity and health [12–16]. Gamma-aminobutyric acid (GABA) is a well-known neurotransmitter generated through the decarboxylation of glutamic acid (Glu) catalyzed by glutamic acid decarboxylase (GAD) and also has critical roles in the immune system [17, 18]. Recent years have witnessed a growing interest in the application of GABA in animal husbandry. For instance, dietary GABA supplementation reduced the negative influences of weaning stress on weaning piglets by reducing aggressive behavior and regulating endocrine hormones [19]. For chicks under beak trimming stress, the supplementation of GABA significantly improves the immune response of chicks [20]. Our previous study also revealed that GABA supplementation can modulate the intestinal functions, including intestinal immunity, intestinal amino acid profiles, and gut microbiota in weaning piglets [21]. Furthermore, recent studies reported that GABA could alleviate intestinal pathogenic infection through attenuating epithelial cell apoptosis and promoting host Th17 responses [22, 23]. Moreover, a previous study found that intestinal microbiota-derived GABA also could increase intestinal IL-17 expression by activating mechanistic target of rapamycin complex 1- (mTORC1-) ribosomal protein S6 kinase 1 (S6K1) signaling in the context of ETEC or *Citrobacter rodentium* infection and drug-induced intestinal inflammation [24]. These studies have raised the possibility that GABA supplementation has great prospect in improving intestinal immunity and preventing intestinal infection through metabolism of intestinal microbiota in weaning piglets.

Therefore, this study is mainly aimed at examining the effects of dietary GABA supplementation on the growth performance, intestinal SIgA secretion, gut microbiota profiles, and metabolism in the normal and ETEC-infected weaning piglets. In total, we confirmed that the increased SIgA production is likely to be related to the activation of the T-cell-dependent pathway and altered intestinal microbial metabolism.

2. Materials and Methods

2.1. Bacterial Strain. An enterotoxigenic *Escherichia coli* F4-producing strain W25K (O149:K91, K88ac; LT, STb, EAST), which was isolated from a piglet with diarrhea [25], was used in the present study.

2.2. Piglets and Experiment Design. All procedures adopted in this experiment were approved by the Animal Welfare Committee of the Institute of Subtropical Agriculture, Chinese Academy of Sciences. A total of thirty-seven Duroc × Landrace × Yorkshire weaning piglets (5.82 ± 0.86 kg) were enrolled in the experiment at 21 d of age. The piglets were housed individually in an environmentally controlled nursery with hard plastic slatted flooring. All animals had free access to drinking water. The room temperature was maintained at $25 \pm 2^\circ\text{C}$ throughout the whole experiment. The composition and nutrient levels of the diets met the nutrient requirements for weaning piglets according to recommendations of the NRC (2012). The experiment lasted for three weeks and was divided into two stages. The first two weeks are the first stage, and the last week is the second stage. At the beginning of the experiment, all piglets were randomly distributed into two groups: (1) control group (CON, basal diet, $n = 18$) and (2) GABA group (GABA, basal diet with $40 \text{ mg}\cdot\text{kg}^{-1}$ of GABA supplementation, $n = 19$). On the 14th day of the experiment, 6 pigs in each group were slaughtered for sampling, and the remaining piglets were fed with ETEC to construct the infection model. Seven days after the modeling, 6 pigs were slaughtered for sampling in each group. According to whether or not ETEC was inoculated, it was divided into two stages: uninfected and infected (referred as CON1 and CON2 and GABA1 and GABA2). At the last day of every stage, six piglets from each group were randomly selected and sacrificed after anesthesia. Before being sacrificed, 10 mL blood was taken from the anterior vena cava and serum samples were obtained by centrifugation at $2000 \times g$ for 10 min at 4°C and stored at -80°C . The liver, kidney, spleen, heart, and lung were obtained and weighed for calculating the relative weight of each organ. Samples from the same positions of the jejunum, ileum, colon, and feces were collected and immediately snap-frozen in liquid nitrogen and stored at -80°C for RNA extraction, determination of cytokine concentration, microbiota, and metabolite analysis.

2.3. Growth Performance and Organ Indices. Body weight and feed intake were recorded at the end of the first stage and the end of the whole experiment. The average daily gain and average daily feed intake were calculated with the ratio of total bodyweight gain to experimental days and the ratio of feed intake to experimental days. The feed conversion ratio is referred to as the ratio of the feed intake to the body weight gain.

2.4. Serum Amino Acid Analysis. Serum free amino acids were analyzed by high-performance liquid chromatography (HPLC) according to the manufacturer's instructions. The preprocessing of the samples was conducted as following description. In brief, firstly, 2 mL of serum samples was

TABLE 1: Serum amino acid profiles of piglets in stages 1 and 2.

	CON1	GABA1	<i>P</i> value (1)	CON2	GABA2	<i>P</i> value (2)
Taurine	53 ± 6.62	47.09 ± 3.93	0.464	77.05 ± 12.9	84.51 ± 9.47	0.652
Aspartic acid	12.9 ± 12.9	7.11 ± 1.22*	0.016	11.46 ± 2.91	11.11 ± 1.54	0.918
Threonine	27.82 ± 7.32	22.05 ± 5.6	0.547	28.68 ± 5.29	33.65 ± 7.71	0.608
Serine	48.89 ± 4.44	44.34 ± 2.2	0.388	46.72 ± 5.11	43.74 ± 7.44	0.749
Glutamic acid	119.99 ± 8.85	106.94 ± 12.61	0.419	130.03 ± 10.46	115.37 ± 10.49	0.346
Sarcosine	1.47 ± 0.43	1.77 ± 0.25	0.567	1.71 ± 0.45	1.75 ± 0.54	0.957
α-Aminoadipic acid	26.12 ± 3.03	26.13 ± 2.76	0.998	21.3 ± 4.17	22.79 ± 2.82	0.775
Glycine	368.99 ± 41.85	326.62 ± 28.04	0.423	234.47 ± 40.5	210.24 ± 66.01	0.762
Alanine	179.52 ± 18.95	143.21 ± 17.19	0.187	132.82 ± 19.87	124.6 ± 17.84	0.765
Citrulline	18.83 ± 0.78	22.88 ± 2.08	0.115	16.3 ± 1.4	14.79 ± 0.69	0.364
2-Aminobutanoic acid	4.12 ± 1.3	3.86 ± 0.73	0.866	10.94 ± 4.99	12.97 ± 3.13	0.738
Valine	57.92 ± 9.09	57.29 ± 5.27	0.954	72.64 ± 17.19	75.41 ± 7.8	0.888
Cysteine	11.97 ± 2.04	7.52 ± 1.16	0.095	12.47 ± 2.45	15.2 ± 3	0.498
Methionine	7.68 ± 0.87	7.57 ± 0.59	0.916	6.91 ± 0.78	7.29 ± 0.37	0.672
Cystathionine	7.75 ± 0.98	8.29 ± 1.09	0.720	6.01 ± 0.87	8.68 ± 1.24	0.112
Isoleucine	31.79 ± 3.12	33.52 ± 3.65	0.727	44.11 ± 9.79	54.03 ± 5.82	0.408
Leucine	59.29 ± 3.2	63.65 ± 2.31	0.298	61.87 ± 8.29	67.57 ± 3.78	0.551
Tyrosine	31.27 ± 3.21	36.63 ± 3.21	0.265	29.22 ± 2.03	26.57 ± 1.53	0.322
Phenylalanine	36.57 ± 2.39	38.35 ± 1.56	0.548	51.35 ± 8.64	56.15 ± 4.54	0.636
β-Alanine	7.82 ± 0.72	6.27 ± 0.5	0.112	6.38 ± 1.41	6.09 ± 1.04	0.874
3-Aminoisobutyric acid	0.26 ± 0.07	0.32 ± 0.09	0.597	0.23 ± 0.08	0.22 ± 0.06	0.915
γ-Aminobutyric acid	0.06 ± 0.02	0.05 ± 0.02	0.761	0.07 ± 0.02	0.04 ± 0.02	0.380
Ethanolamine	2.39 ± 0.25	2.22 ± 0.12	0.553	2.5 ± 0.19	2.68 ± 0.2	0.521
Hydroxylysine	1.21 ± 0.59	2.98 ± 0.77	0.099	1.16 ± 0.34	3.3 ± 1.61	0.245
Ornithine	31.15 ± 2.43	30.07 ± 1.74	0.726	32.15 ± 3.84	27.19 ± 1.59	0.273
Lysine	1.74 ± 11.02	93.03 ± 8.84	0.762	70.334 ± 7.35	78.54 ± 5.77	0.402
1-Methyl-L-histidine	6.01 ± 2.31	6.02 ± 1.74	1.000	4.77 ± 1.41	4.18 ± 1.41	0.773
Histidine	24.48 ± 1.99	32.26 ± 2.45*	0.034	22.91 ± 2.95	23.62 ± 1.33	0.832
3-Methyl-L-histidine	4.3 ± 0.38	5.59 ± 0.46	0.059	5.68 ± 1.23	5.83 ± 0.48	0.915
Carnosine	10.51 ± 1.38	12.03 ± 0.96	0.389	6.01 ± 1.3	4.31 ± 0.89	0.307
Arginine	84.21 ± 7.29	87.61 ± 7.76	0.756	105.45 ± 17.44	106.34 ± 5.2	0.962
Proline	103.14 ± 5.08	95.3 ± 4.36	0.269	94.64 ± 12.63	84.46 ± 9.65	0.537

Means with * are significantly different from the control group ($P < 0.05$).

centrifuged at 3000 rpm for 5 minutes. Then 1 mL of supernatants was mixed with 0.8% sulfosalicylic acid solution. After being incubated at 4°C for 15 minutes, the mixtures were then centrifuged at 10,000 rpm for 10 minutes and filtered by a 0.22 μm filter membrane before being analyzed by HPLC.

2.5. Serum Biochemical Analysis. Serum biochemical parameters were determined by the Biochemical Analytical Instrument (Beckman CX4) according to the instructions of manufacturer. And corresponding kits were bought from Roche (Shanghai, China).

2.6. Immunohistochemistry Analysis. The jejunum, ileum, and colon samples were fixed in 4% buffered paraformaldehyde for 24 hours at room temperature and embedded in paraffin and sectioned at a thickness of 3 mm. After being heated at 60°C for 30 to 60 minutes, the sections were dewaxed in xylene (10 min, twice) and then rehydrated in a descending ethanol scale (100%, 95%, 85%, and 75%, 5 min every time). After being washed by distilled water for 5 minutes, the sections were soaked in a 0.01 M citrate buffer (pH = 6.0) and heated to boiling by a microwave oven for 25 minutes. When it had been cooled down and washed by PBS, 3% H₂O₂ was added into the buffer to inactivate the

TABLE 2: Serum biochemistry parameters of piglets in stages 1 and 2.

	CON1	GABA1	P value (1)	CON2	GABA2	P value (2)
Total protein	46.933 ± 0.750	45.8 ± 1.035	0.398	48.433 ± 1.410	47.267 ± 1.506	0.584
Albumin	37.75 ± 1.628	39.7167 ± 1.148	0.349	34.833 ± 1.114	31.200 ± 0.733*	0.024
Alanine aminotransferase	31.85 ± 3.609	30.0833 ± 1.537	0.667	40.017 ± 8.316	43.217 ± 3.088	0.730
Aspartate aminotransferase	55.5 ± 9.549	53 ± 7.024	0.838	56.167 ± 10.058	51.500 ± 6.479	0.706
Alkaline phosphatase	309.833 ± 23.494	380.667 ± 49.876	0.239	199.333 ± 32.278	170.500 ± 20.343	0.470
Lactate dehydrogenase	555.167 ± 70.002	532.5 ± 25.160	0.770	612.667 ± 72.638	524.333 ± 46.760	0.335
Blood urea nitrogen	1.8333 ± 0.233	2.1333 ± 0.265	0.416	2.817 ± 1.009	2.617 ± 0.547	0.866
Glucose	5.6 ± 0.259	4.9667 ± 0.362	0.189	3.833 ± 0.549	4.467 ± 0.506	0.146
Ca	2.7017 ± 0.051	2.915 ± 0.070*	0.036	2.632 ± 0.171	2.493 ± 0.082	0.490
P	2.208 ± 0.099	2.025 ± 0.191	0.420	2.868 ± 0.150	2.480 ± 0.107	0.064
Triglyceride	0.422 ± 0.030	0.405 ± 0.015	0.637	0.638 ± 0.178	0.845 ± 0.151	0.398
Cholesterol	1.821 ± 0.102	1.675 ± 0.119	0.373	2.127 ± 0.111	2.563 ± 0.202	0.096
High-density lipoprotein cholesterol	0.702 ± 0.054	0.580 ± 0.029	0.084	0.562 ± 0.099	0.520 ± 0.068	0.767
Low-density lipoprotein cholesterol	0.897 ± 0.099	0.832 ± 0.086	0.630	1.245 ± 0.112	1.648 ± 0.195	0.110
D-Lactic acid	8.967 ± 0.789	7.417 ± 0.320	0.114	9.763 ± 0.820	8.06 ± 0.683	0.143
Blood ammonia	172.567 ± 8.083	193.35 ± 6.764	0.078	299.367 ± 16.071	263.017 ± 5.825	0.075
Immunoglobulin M	0.067 ± 0.014	0.080 ± 0.012	0.481	0.172 ± 0.112	0.167 ± 0.090	0.973
Diamine oxidase	1.2 ± 0.157	1.433 ± 0.203	0.257	1.767 ± 0.275	1.500 ± 0.197	0.451

Means with * are significantly different from the control group ($P < 0.05$).

endogenous enzymes. The treated slides were incubated with primary antibodies (IgA, ab112746, Abcam), diluted at the ratio of 1:100, overnight at 4°C. Washed in PBS, the slides were incubated in 50~100 µL biotinylated secondary antibodies and HRP-conjugated peroxidase at 37°C for 30 minutes. The chromogen was 3,39-diaminobenzidine free base (DAB).

2.7. ELISA. Equal amounts of samples were applied to examine IgA levels of the jejunum, ileum, and colon, as well as IFN- γ , IL-1 β , IL-10, IL-13, IL-17, IL-4, and TNF- α levels of the jejunum by commercially available ELISA kits (Cusabio Biotech Company Limited, Wuhan, China) in accordance with the manufacturer's instructions.

2.8. Real-Time Quantitative PCR. Total RNA of ground jejunum tissue was isolated using the TRIzol reagent (Invitrogen, Carlsbad, CA, USA). The synthesis of complementary DNA was accomplished with the PrimeScript RT reagent kit with gDNA Eraser (Takara Bio Inc., Qingdao, China). RT-PCR was performed in duplicate with an ABI 7900 PCR system (ABI Biotechnology, MD, USA). Primers for the selected genes were designed using the Oligo 5.0 software (Molecular Biology Insights, Inc., USA) and Primer 6.0 software (PRIMER-e, New Zealand) and listed in Supplementary Table 1. β -Actin was used as an internal control to normalize target gene transcript levels. Relative expression of target genes was calculated by the $2^{-\Delta\Delta C_t}$ method [21]. The relative gene expression was expressed as a ratio of the expression of the GABA group to the controls.

2.9. Gut Microbiota Analysis. 16S rRNA sequencing and general data analyses were performed by a commercial company (Novogene, Beijing, China). In brief, total genome DNA from samples was extracted using the CTAB/SDS method. The V3-V4 regions were amplified using the specific primer with the barcode. All PCR reactions were carried out in 30 µL reactions with 15 µL of Phusion® High-Fidelity PCR Master Mix (New England Biolabs), 0.2 µM of the forward and reverse primers, and about 10 ng template DNA. Thermal cycling consisted of the initial denaturation at 98°C for 1 min, followed by 30 cycles of denaturation at 98°C for 10 s, annealing at 50°C for 30 s, and elongation at 72°C for 30 s, and finally 72°C for 5 min. PCR products were mixed in equidensity ratios. Then, mixture PCR products were purified with the GeneJET™ Gel Extraction Kit (Thermo Scientific). Sequencing libraries were generated using Ion Plus Fragment Library Kit 48 rxns (Thermo Scientific) following the manufacturer's recommendations. The library quality was assessed on the Qubit 2.0 Fluorometer (Thermo Scientific). At last, the library was sequenced on an Ion S5™ XL platform and 400 bp/600 bp single-end reads were generated. After the quality control, clean reads were obtained from single-end reads. Sequences analyses were performed by Uparse software (Uparse v7.0.1001). Sequences with $\geq 97\%$ similarity were assigned to the same OTUs. Representative sequence for each OTU was screened for further annotation. Alpha indices (ACE, Chao1, observed species, Shannon, and Simpson) are applied in analyzing complexity of species diversity for a sample. Principal Coordinate Analysis (PCoA) was performed to get principal coordinates and visualize from complex, multidimensional data.

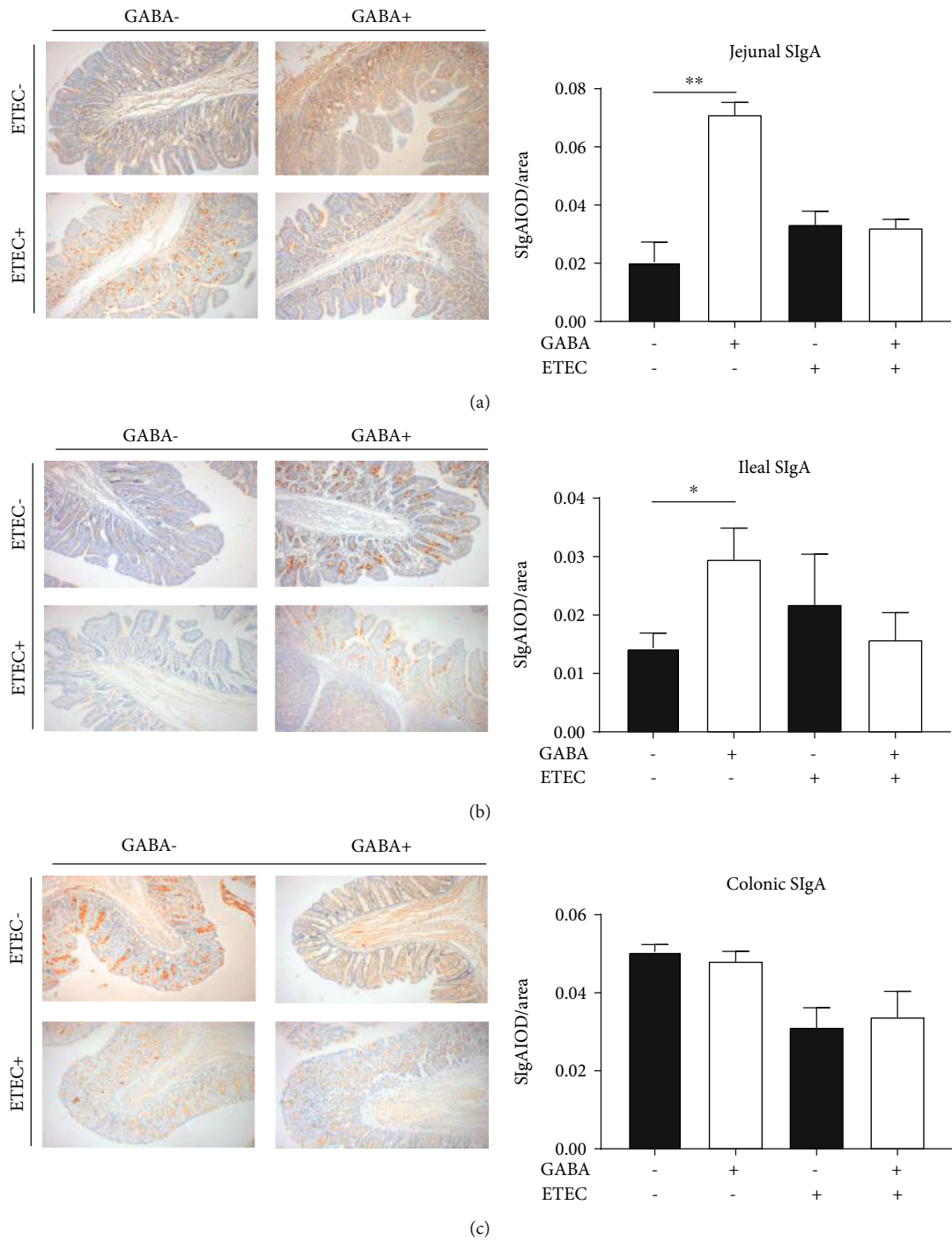


FIGURE 1: Continued.

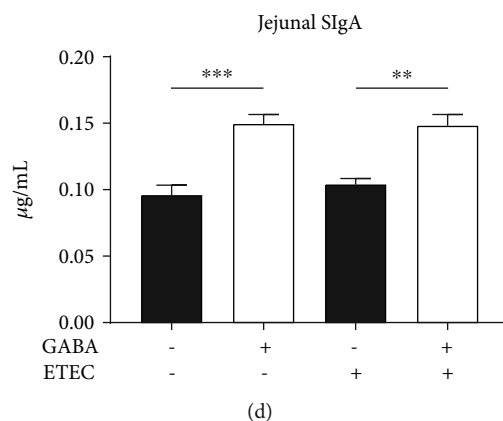


FIGURE 1: Dietary GABA promoted the production of SIgA in the intestine of piglets. Immunohistochemistry analysis of the IgA levels in the (a) jejunum, (b) ileum, and (c) colon of piglets in stage 1 and stage 2. (d) ELISA test of the jejunal SIgA level of piglets in stage 1 and stage 2. Data ($n = 6$) are presented as mean \pm SEM and analyzed by the unpaired t -test with Welch's correction or Mann-Whitney U test. Differences were denoted as follows: * $P < 0.05$, ** $P < 0.01$, and *** $P < 0.001$.

2.10. Metabolite Profiling Analysis. Untargeted metabolomics of piglet feces was performed by a commercial company (Novogene, Beijing, China). Preparation of samples could be briefly concluded as follows: dry completely in a vacuum concentrator without heating; add 60 μL methoxyamination hydrochloride (20 mg/mL in pyridine) incubated for 30 min at 80°C; and add 80 μL of the N,O-bis(trimethylsilyl)trifluoroacetamide reagent (1% trimethylchlorosilane, v/v) to the sample aliquots, incubated for 1.5 h at 70°C. All samples were analyzed by a gas chromatograph system coupled with a Pegasus HT time-of-flight mass spectrometer (GC-TOF-MS). GC-TOF-MS analysis was performed using an Agilent 7890 gas chromatograph system coupled with a Pegasus HT time-of-flight mass spectrometer. The system utilized a DB-5MS capillary column coated with 5% diphenyl cross-linked with 95% dimethylpolysiloxane (30 m \times 250 μm inner diameter, 0.25 μm film thickness; J&W Scientific, Folsom, CA, USA). A 1 μL aliquot of the analyte was injected in splitless mode. Helium was used as the carrier gas, the front inlet purge flow was 3 mL min^{-1} , and the gas flow rate through the column was 1 mL min^{-1} . The initial temperature was kept at 50°C for 1 min, then raised to 310°C at a rate of 20°C min^{-1} , then kept for 6 min at 310°C. The injection, transfer line, and ion source temperatures were 280, 280, and 250°C, respectively. The energy was -70 eV in electron impact mode. The mass spectrometry data were acquired in full-scan mode with the m/z range of 50-500 at a rate of 12.5 spectra per second after a solvent delay of 4.78 min. Chroma TOF 4.3X software of LECO Corporation and LECO-Fiehn Rtx5 database were used for raw peak exacting, data baseline filtering and calibration of the baseline, peak alignment, deconvolution analysis, peak identification, and integration of the peak area. Both mass spectrum match and retention index match were considered in metabolite identification.

2.11. Microbiome-Metabolome Association Analysis. Pearson statistical method was used to calculate the correlation coefficients (ρ) and P values of the contents of differential metabolites and relative abundances of differential bacteria.

The absolute value of ρ bigger than 0.6 and P value smaller than 0.05 were considered significant. Scatterplot and heat map of correlation analysis were drawn according to the results of Pearson statistical method.

2.12. Statistical Analyses. Data are shown as mean \pm Standard Error of Mean (SEM). First, the D'Agostino-Pearson omnibus normality test (Prism 7.0) and Kolmogorov-Smirnov test (Prism 7.0) were applied to examine whether the data were in Gaussian distribution. If the data were in Gaussian distribution with equal variance, it would be analyzed by the unpaired t -test (Prism 7.0). If the data were in Gaussian distribution but with unequal variance, it would be analyzed by the unpaired t -test with Welch's correction (Prism 7.0). If the data were not in Gaussian distribution, it would be analyzed by the nonparametric test (Mann-Whitney U test, Prism 7.0). Differences with $P < 0.05$ were considered significant.

3. Results

3.1. GABA Supplementation Has No Effect on the Growth Performance and Organ Indices in Weanling Piglets. No significant difference was observed in the body weight gain, average daily gain, average daily feed intake, and feed conversion ratio between the CON1 and GABA1 groups (Fig. S1A). The growth performances of ETEC-infected piglets were not markedly influenced by GABA supplementation (Fig. S1B). In the first stage, organ indices had no difference between the CON1 and GABA1 groups (Table S2). From the perspective of the whole experiment, the organ indices of the GABA group were all higher than those of the CON group but without significant differences (Table S2).

3.2. GABA Supplementation Has Little Effect on the Serum Amino Acid Profile and Biochemical Indices. Compared with the CON1 group, the aspartic acid level in serum of the GABA1 group was significantly decreased ($P < 0.05$), while the histidine level in serum increased ($P < 0.05$) (Table 1).

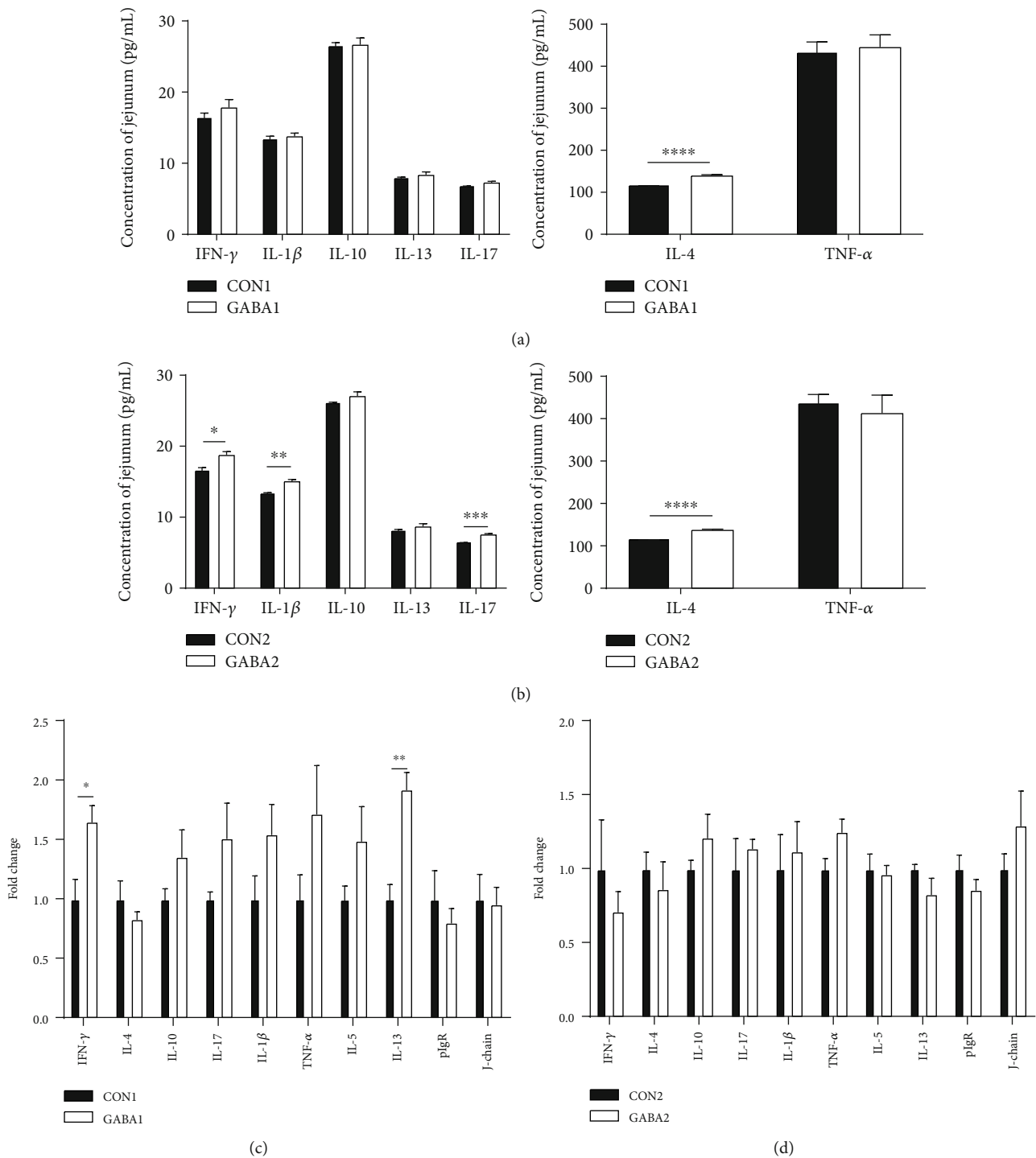


FIGURE 2: GABA promoted RNA expression and production of cytokines. (a) Jejunal concentrations of cytokines in normal piglets; (b) jejunal concentrations of cytokines in ETEC-infected piglets; (c) mRNA expression levels of cytokines in normal piglets; (d) mRNA expression levels of cytokines in ETEC-infected piglets. Data ($n = 6$) are presented as mean \pm SEM and analyzed by the unpaired t -test with Welch's correction or Mann-Whitney U test. Differences were denoted as follows: * $P < 0.05$, ** $P < 0.01$, *** $P < 0.001$, and **** $P < 0.0001$.

However, there was no difference in amino acid levels of serum between the CON2 and GABA2 groups (Table 1). As for the serum biochemical parameters, the calcium level in the serum of the GABA1 group was higher than that of the CON1 group ($P < 0.05$) (Table 2). For the ETEC-infected piglets, the albumin level in the serum was decreased in the

GABA2 group compared with the CON2 group ($P < 0.05$) (Table 2).

3.3. GABA Supplementation Promotes Intestinal SIgA Production. To examine the effect of GABA supplementation on intestinal SIgA secretion, the jejunum, ileum, and colon

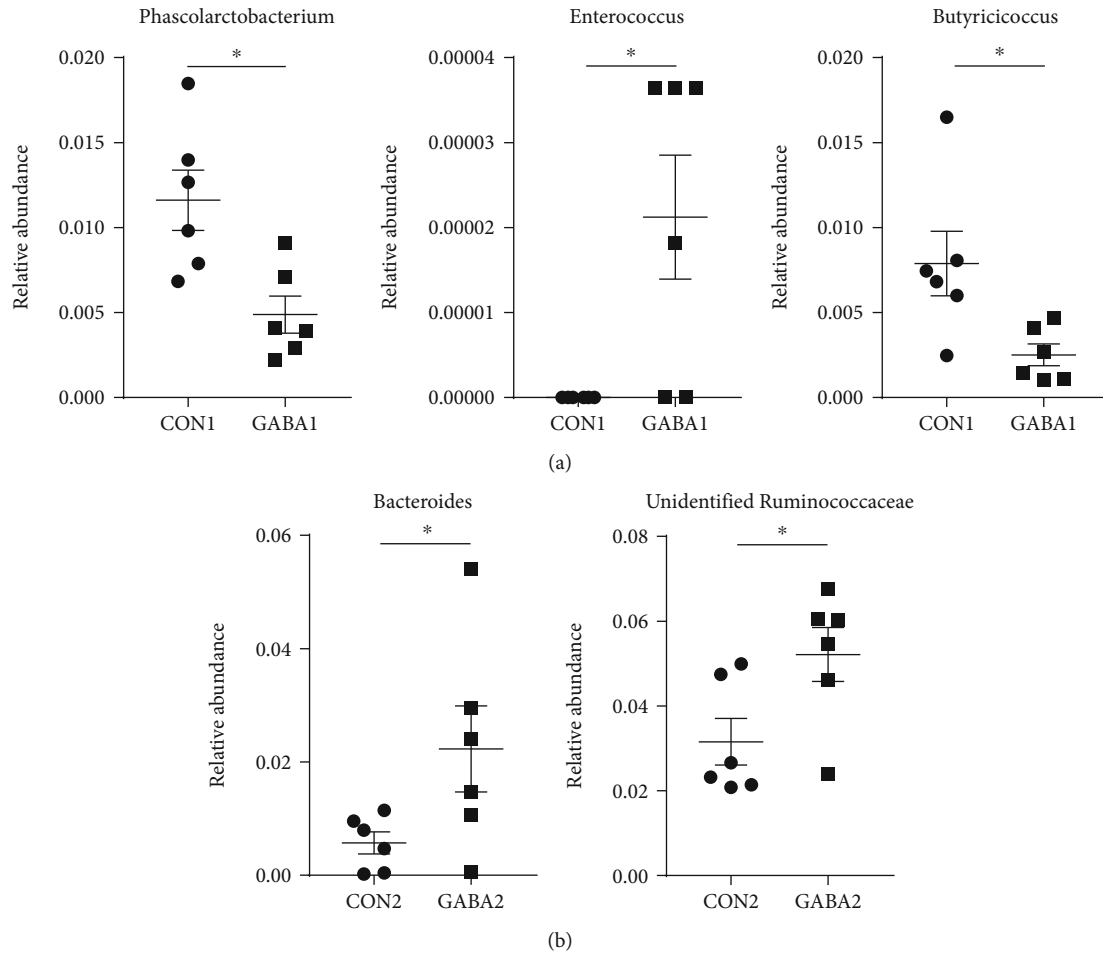


FIGURE 3: GABA altered the relative abundance of gut microbiota. (a) Relative abundance of *Phascolarctobacterium*, *Enterococcus*, and *Butyrivicoccus* in normal piglets. (b) Relative abundance of *Bacteroides* and unidentified *Ruminococcaceae* in ETEC-infected piglets. Data are presented as mean \pm SEM and analyzed by the unpaired *t*-test with Welch's correction or Mann-Whitney *U* test. Differences were denoted as follows: * $P < 0.05$.

were applied to the immunohistochemistry analysis. As the results show, GABA1 significantly improved the jejunal ($P < 0.01$) and ileal ($P < 0.05$) SIgA levels compared to CON1 (Figures 1(a) and 1(b)). However, GABA supplementation had no effect on the jejunal and ileal SIgA levels in ETEC-infected piglets (Figures 1(a) and 1(b)). With regard to the colonic SIgA level, neither healthy nor ETEC-infected piglets were affected by GABA supplementation (Figure 1(c)). Results from ELISA analysis further verified that GABA supplementation increased the jejunal SIgA secretion in both healthy piglets and infected piglets ($P < 0.01$) (Figure 1(d)).

3.4. GABA Supplementation Improves the Expression of SIgA-Related Cytokines, Especially in ETEC-Infected Piglets. To explore the underlying mechanisms of the regulating effect of GABA supplementation on jejunal SIgA production, the protein levels and mRNA expression of cytokines in the jejunum of piglets were examined. The results of ELISA analysis showed that the jejunal concentration of IL-4 in the GABA1 group was much higher than that in the CON1 group

($P < 0.0001$) (Figure 2(a)). Compared with the CON2 group, GABA2 improved the jejunal concentrations of IL-4 ($P < 0.0001$), IFN- γ ($P < 0.01$), IL-1 β ($P < 0.01$), and IL-17 ($P < 0.001$) (Figure 2(b)). Compared with the CON1 group, the mRNA expression of jejunal IFN- γ ($P < 0.05$) and IL-13 ($P < 0.01$) was significantly increased in the GABA1 group, while no significant alterations in the mRNA expression of any jejunal cytokines were observed in the GABA2 group (Figures 2(c) and 2(d)).

3.5. GABA Supplementation Alters the Relative Abundances of Gut Bacteria. To examine if GABA supplementation increased intestinal SIgA production through modulating gut microbiota, the fecal microbiota of piglets was analyzed by bacterial 16S rRNA sequencing (V3-V4 regions). An average of 85,463 raw reads was generated for each sample. After removing the low-quality sequences, 80,121 clean tags were clustered into OTUs for the following analysis, based on the 97% similarity level. As shown in Table S3, no matter in the healthy piglets or the ETEC-infected piglets, GABA supplementation had no effect on the diversity indices

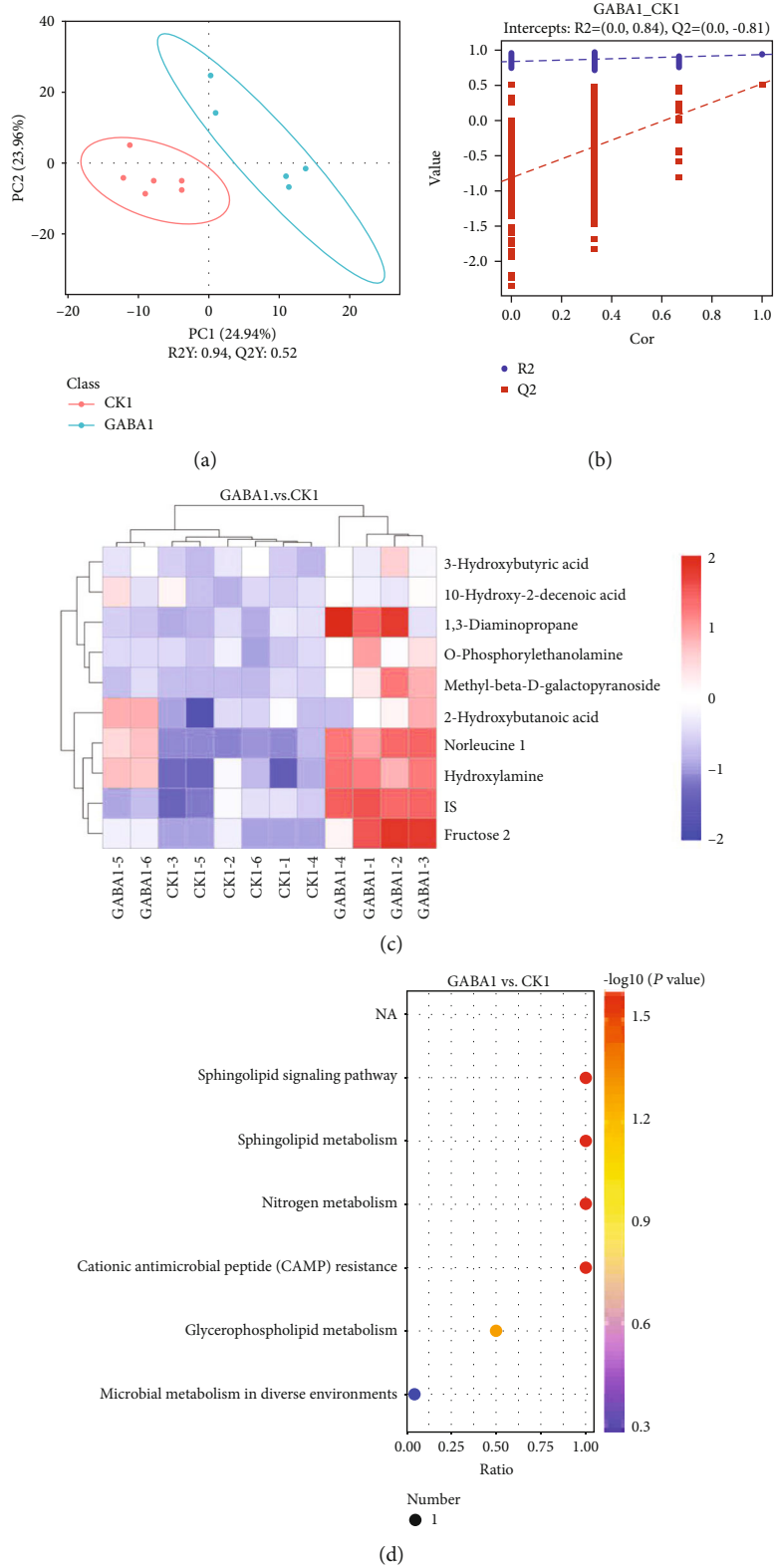


FIGURE 4: GABA highly changes the metabolism of gut microbiota in healthy piglets. (a) GABA1 vs. CON1 PLS-DA score plot; (b) GABA1 vs. CON1 PLS-DA valid plot; (c) heat map of significant variables; (d) scatterplot of KEGG enrichment analysis. The ratio in the scatterplot means the ratio of the number of altered metabolites to the number of all metabolites in this pathway. The CK group in this figure means the CON group.

TABLE 3: Significant variables responsible for group separation of the CON1 group and GABA1 group.

Metabolites	RT	VIP	P value	Fold change
2-Hydroxybutanoic acid	8.39152,0	1.0943912	0.0219111	2.08685768
1,3-Diaminopropane	15.2455,0	1.5156162	0.0389701	3.578994496
IS	16.6102,0	1.0352327	0.0446863	2.116515269
O-Phosphorylethanolamine	16.7466,0	1.1989025	0.0272898	2.718830077
Methyl-beta-D-galactopyranoside	17.4716,0	2.662989	0.0125204	8.738756131
3-Hydroxybutyric acid	8.87752,0	1.0999058	0.0356118	2.488895428
Fructose 2	17.7379,0	8.2363709	0.0037375	15.0103342
10-Hydroxy-2-decenoic acid	19.8381,0	1.1643369	0.0498178	2.53080591
Norleucine 1	11.1259,0	5.3345447	0.0008329	21.17542765
Hydroxylamine	8.2099,0	1.7659162	0.0021158	3.131884356

RT: retention time (min); VIP: variable importance in the projection of the PLS-DA first principal component; P value: *t*-test significance; fold change: GABA1 group to CON1 group.

(Shannon and Simpson) or the richness indices (Chao1, ACE, and observed species). In addition, PCoA revealed that the gut microbiota composition of piglets basically was little affected by GABA treatment (Figs. S2F and S2L). The relative abundances of the top ten strains in the phylum, class, order, family, and genus level were not significantly altered by GABA supplementation (Figs. S2A to S2E). The same goes for the gut microbiota of ETEC-infected piglets (Figs. S2G to S2K). However, when the scope was not limited to the top ten strains anymore, there were some low-abundance strains that were markedly altered by GABA supplementation. In normal piglets, the relative abundances of *Phascolarctobacterium* ($P < 0.05$) and *Butyricicoccus* ($P < 0.05$) were decreased by GABA, while the relative abundance of *Enterococcus* ($P < 0.05$) was increased (Figure 3(a)). In ETEC-infected piglets, GABA supplementation increased the relative abundance of *Bacteroides* ($P < 0.05$) and an unidentified *Ruminococcaceae* ($P < 0.05$) (Figure 3(b)). These results suggested that GABA supplementation affected the relative abundances of certain low-abundance bacteria in weanling piglets.

3.6. GABA Supplementation Modulates Metabolism of Gut Microbiota, Especially in Normal Weanling Piglets. The fecal metabolites were analyzed to examine whether GABA supplementation altered the metabolism of intestinal microbiota in weanling piglets. Firstly, a PLS-DA analysis was applied to have a better view of the different metabolic patterns in normal piglets. As shown in the PLS-DA score plot, the CON1 group and GABA1 group were distributed separately (Figure 4(a)). Quality of the resulting discriminant models suggested that the model was available and had good fitness and prediction (Figure 4(b)). Significant variables responsible for group separation were selected using the variable importance in the projection (VIP) statistic of the first principal component of the PLS-DA model (threshold > 1), together with the *P* value of Student's *t*-test (threshold < 0.05). As listed in Table 3, 10 metabolites were markedly upregulated in the GABA1 group. These metabolites were identified as potential markers: 2-hydroxybutanoic acid ($P < 0.05$), 1,3-diaminopropane ($P < 0.05$), IS ($P < 0.05$),

O-phosphorylethanolamine ($P < 0.05$), methyl-beta-D-galactopyranoside ($P < 0.05$), 3-hydroxybutyric acid ($P < 0.05$), fructose 2 ($P < 0.01$), 10-hydroxy-2-decenoic acid ($P < 0.05$), norleucine 1 ($P < 0.01$), and hydroxylamine ($P < 0.01$) (Figure 4(c)). The results of KEGG enrichment analysis were presented as a scatterplot which showed that GABA markedly altered the sphingolipid signaling pathway, sphingolipid metabolism, nitrogen metabolism, cationic antimicrobial peptide (CAMP) resistance, glycerophospholipid metabolism, and microbial metabolism in diverse environments (Figure 4(d)).

In the PLS-DA score plot, the GABA2 group and CON2 group were not separated from each other (Figure 5(a)). Only 4 metabolites were significantly altered: 1,2,4-benzenetriol ($P < 0.01$) and methyl-beta-D-galactopyranoside ($P < 0.05$) were upregulated, and oleic acid ($P < 0.05$) and DL-dihydrospingosine 1 ($P < 0.05$) were downregulated (Figure 5(c)). The results of VIP statistic and fold changes are listed in Table 4. The scatterplot suggested that GABA significantly affected the longevity regulating pathway-worm in ETEC-infected piglets (Figure 5(d)).

We identified the specific metabolites related with enriched KEGG pathways and found that, in healthy piglets, all enriched KEGG pathways were related with O-phosphorylethanolamine or hydroxylamine (Table 5). In ETEC-infected piglets, two metabolites, oleic acid and 1,2,4-benzenetriol (Table 6), might mediate the effect of GABA supplementation on gut microbial metabolism in ETEC infection.

3.7. There Are Significant Correlations between Differential Metabolites and Altered Low-Abundance Bacteria. We performed a microbiome-metabolome association analyses to examine the possible correlation between the altered low-abundance bacteria and the changed microbial metabolites. The results showed that hydroxylamine was positively correlated with *Enterococcus* ($|\rho| > 0.6$) (Figure 6(b)) but negatively correlated with *Phascolarctobacterium* ($|\rho| > 0.6$) (Figure 6(c)) and *Butyricicoccus* ($|\rho| > 0.6$) in healthy piglets (Figure 6(d)). The absolute values of the correlation coefficient between other observed differential metabolites, O-phosphorylethanolamine, and *Enterococcus*

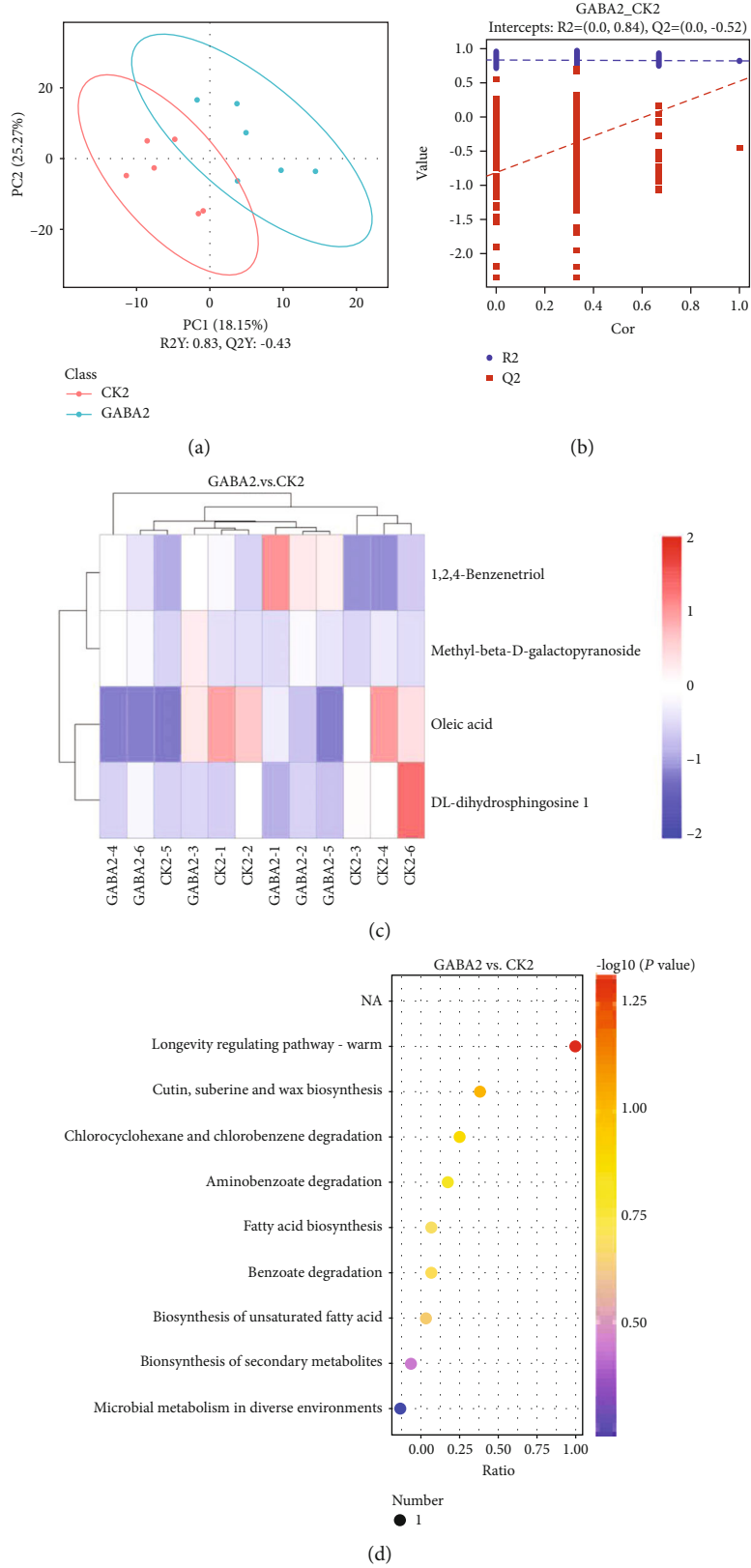


FIGURE 5: GABA regulated the metabolism of gut microbiota in ETEC-infected piglets. (a) GABA2 vs. CON2 PLS-DA score plot; (b) GABA2 vs. CON2 PLS-DA valid plot; (c) heat map of significant variables; (d) scatterplot of KEGG enrichment analysis. The ratio in the scatterplot means the ratio of the number of altered metabolites to the number of all metabolites in this pathway. The CK group in this figure means the CON group.

TABLE 4: Significant variables responsible of the CON2 group and GABA2 group.

Metabolites	RT	VIP	P value	Fold change
1,2,4-Benzenetriol	14.717,0	1.331900147	0.005181206	2.074787321
Methyl-beta-D-galactopyranoside	17.4716,0	2.865360744	0.030532857	7.741120774
Oleic acid	21.1446,0	1.239038753	0.038381941	0.520647409
DL-dihydrosphingosine 1	23.2836,0	2.333778351	0.03935667	0.271034926

RT: retention time (min); VIP: variable importance in the projection of the PLS-DA first principal component; P value: *t*-test significance; fold change: GABA1 group to CON1 group.

TABLE 5: Enriched KEGG pathway and related differential metabolites in normal piglets.

Map ID	Map title	Metabolite
map00600	Sphingolipid metabolism	O-Phosphorylethanolamine
map00910	Nitrogen metabolism	Hydroxylamine
map01503	Cationic antimicrobial peptide (CAMP) resistance	O-Phosphorylethanolamine
map04071	Sphingolipid signaling pathway	O-Phosphorylethanolamine
map00564	Glycerophospholipid metabolism	O-Phosphorylethanolamine
map01120	Microbial metabolism in diverse environments	Hydroxylamine

Map ID: ID of the enriched KEGG pathway; map title: title of the enriched KEGG pathway; metabolite: specific differential metabolites related with the corresponding enriched KEGG pathway.

TABLE 6: Enriched KEGG pathway and related differential metabolites in ETEC-infected piglets.

Map ID	Map title	Metabolite
map04212	Longevity regulating pathway-worm	Oleic acid
map00073	Cutin, suberine, and wax biosynthesis	Oleic acid
map00361	Chlorocyclohexane and chlorobenzene degradation	1,2,4-Benzenetriol
map00627	Aminobenzoate degradation	1,2,4-Benzenetriol
map00061	Fatty acid biosynthesis	Oleic acid
map00362	Benzoate degradation	1,2,4-Benzenetriol
map01040	Biosynthesis of unsaturated fatty acids	Oleic acid
map01060	Biosynthesis of plant secondary metabolites	Oleic acid
map01120	Microbial metabolism in diverse environments	1,2,4-Benzenetriol

Map ID: ID of the enriched KEGG pathway; map title: title of the enriched KEGG pathway; metabolite: specific differential metabolites related with the corresponding enriched KEGG pathway.

and *Phascolarctobacterium* were lower than 0.6 (Figure 6(a)). In addition, we also found 1,2,4-benzenetriol in the colon was positively correlated with *Bacteroides* (Figures 7(a) and 7(b)), and oleic acid was negatively correlated with an unidentified *Ruminococcaceae* (Figures 7(a) and 7(c)).

4. Discussion

As a multifunctional neurotransmitter, GABA has received a lot of attention for its essential role in conducting neural signals, improving sleep quality, and alleviating hot stress [17, 26, 27]. Dietary GABA supplementation improves the growth performance, serum parameters, feed intake, and immune function of various animals, such as broilers, lambs, and cows [27–29]. However, consistent with our results, there is no direct evidence which revealed that GABA supplementation contributed to the growth of weaning piglets in previous studies [19, 21]. But previous studies and our results both demonstrated that GABA could modify intestine

immunity and metabolism condition [21, 22]. In the present study, 40 mg·kg⁻¹ of GABA supplementation decreased the aspartic acid level but increased the histidine level in the serum of normal piglets, while there are no significant changes in serum amino acid contents of ETEC-infected piglets. Aspartic acid can be metabolized to glutamate, which is the precursor of GABA, through transamination [30]. Glutamate could also degrade to histidine [31]. GABA supplementation does not affect the serum glutamate concentration maybe due to the inhibition of absorption of aspartic acid and the promotion of glutamate degradation to histidine in piglets. Surprisingly, GABA supplementation increases the calcium concentration of serum in normal piglets but decreases the albumin content of serum in ETEC-infected piglets. Serum albumin represents the main determinant of plasma oncotic pressure [32], and serum calcium is closely related to calcium and phosphorus metabolism. Therefore, GABA may affect the plasma oncotic pressure and calcium and phosphorus metabolism.

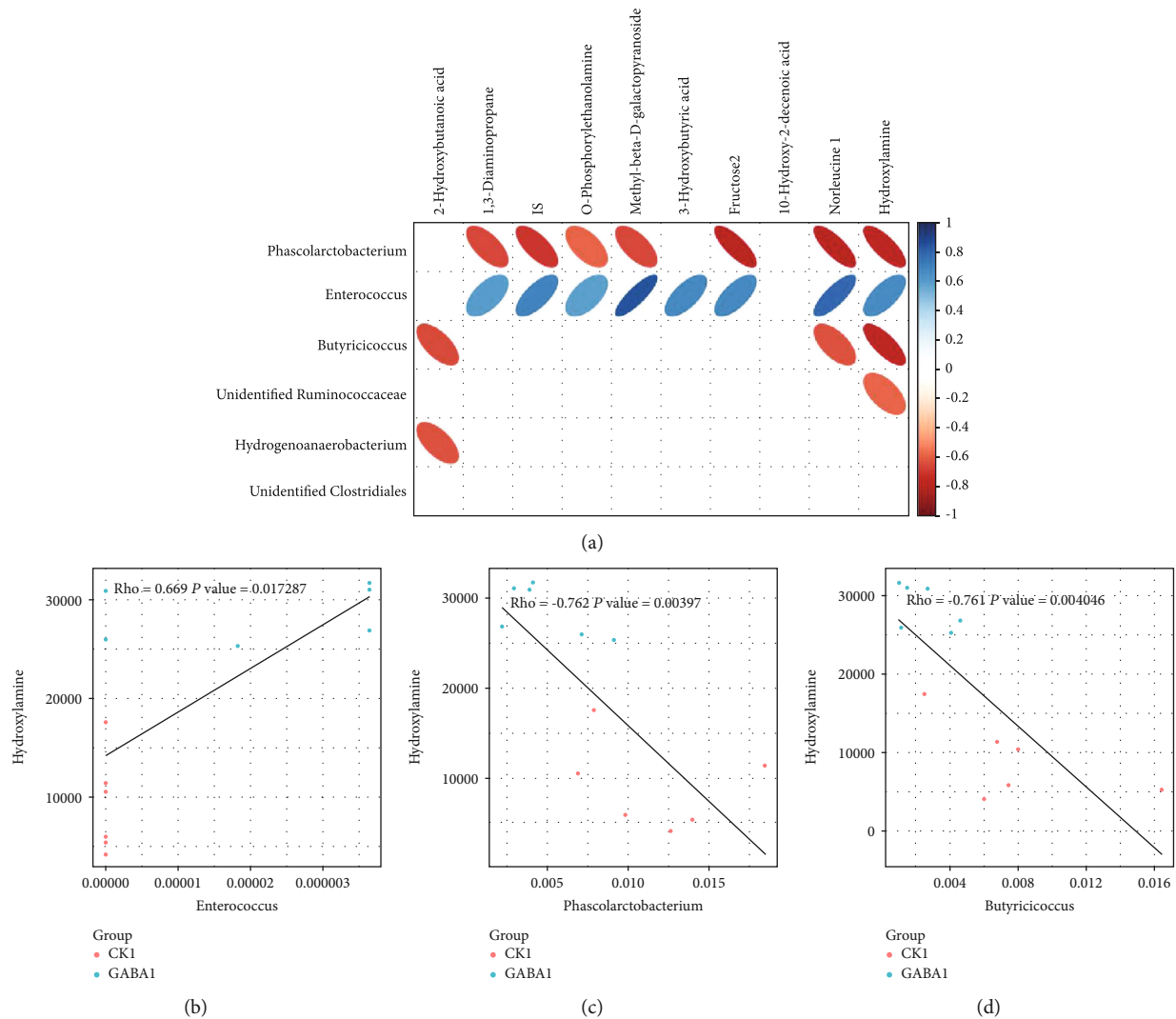


FIGURE 6: The relationship between gut microbiota and metabolites in healthy piglets. (a) Correlation analysis heat map of differential bacteria and differential metabolites in normal piglets; (b) correlation analysis scatterplot of the content of hydroxylamine and the abundance of *Enterococcus* in normal piglets; (c) correlation analysis scatterplot of the content of hydroxylamine and the abundance of *Phascolarctobacterium* in normal piglets. The CK group in this figure means the CON group.

SIgA is a 400 kDa molecule composed of the secretory components, J-chain and dimeric IgA [33]. As a major component of the intestinal immune barrier, SIgA plays an important role in maintaining intestinal health by clearing pathogenic microorganisms and interacting with intestinal commensal microorganisms [5, 34, 35]. Furthermore, the host may discriminate symbionts from pathogens by recognizing the coating of commensal bacteria by SIgA [36]. Thus, enough SIgA secretion in the gut is essential for the intestinal homeostasis. However, piglets, especially weaning piglets, are unable to get maternal immunoglobulins and usually cannot secrete enough SIgA because of their underdeveloped intestinal immune system [11]. Interestingly, in the current study, results of the ELISA and immunohistochemistry analyses confirmed that GABA supplementation increases the jejunal and ileal SIgA levels in normal piglets. Various Th2 cytokines, such as transforming growth factor- (TGF-) β 1, interleukin- (IL-) 4, IL-5, IL-6, IL-10, and IL-13, can promote the

immature B cells differentiated into IgA-secreting plasma cells [13]. To further verify our results about jejunal SIgA secretion and explore the underlying effects of GABA supplementation on cytokine production, we examined the SIgA-secreting cytokines in mRNA and protein levels. We found that jejunal concentrations of IFN- γ , IL-1 β , IL-4, and IL-17 were upregulated by GABA treatment in ETEC-infected piglets. IL-1 β mediates the host inflammatory response to prevent infection [37]. IFN- γ not only can activate macrophages to enhance phagocytosis of pathogenic bacteria [38] but also is implicated in the induction of pIgR synthesis and dimeric IgA binding [39]. Differentiation of B cells into plasma cells secreting IgA occurs upon interactions with T-cells in the lamina propria in an environment rich in IL-4 and other Th2 cytokines [39]. Moreover, IL-17 is an IgA-inducing cytokine that can increase pIgR expression and therefore the rate of SIgA secreted into the lumen [40]. In total, our study provided evidences that GABA

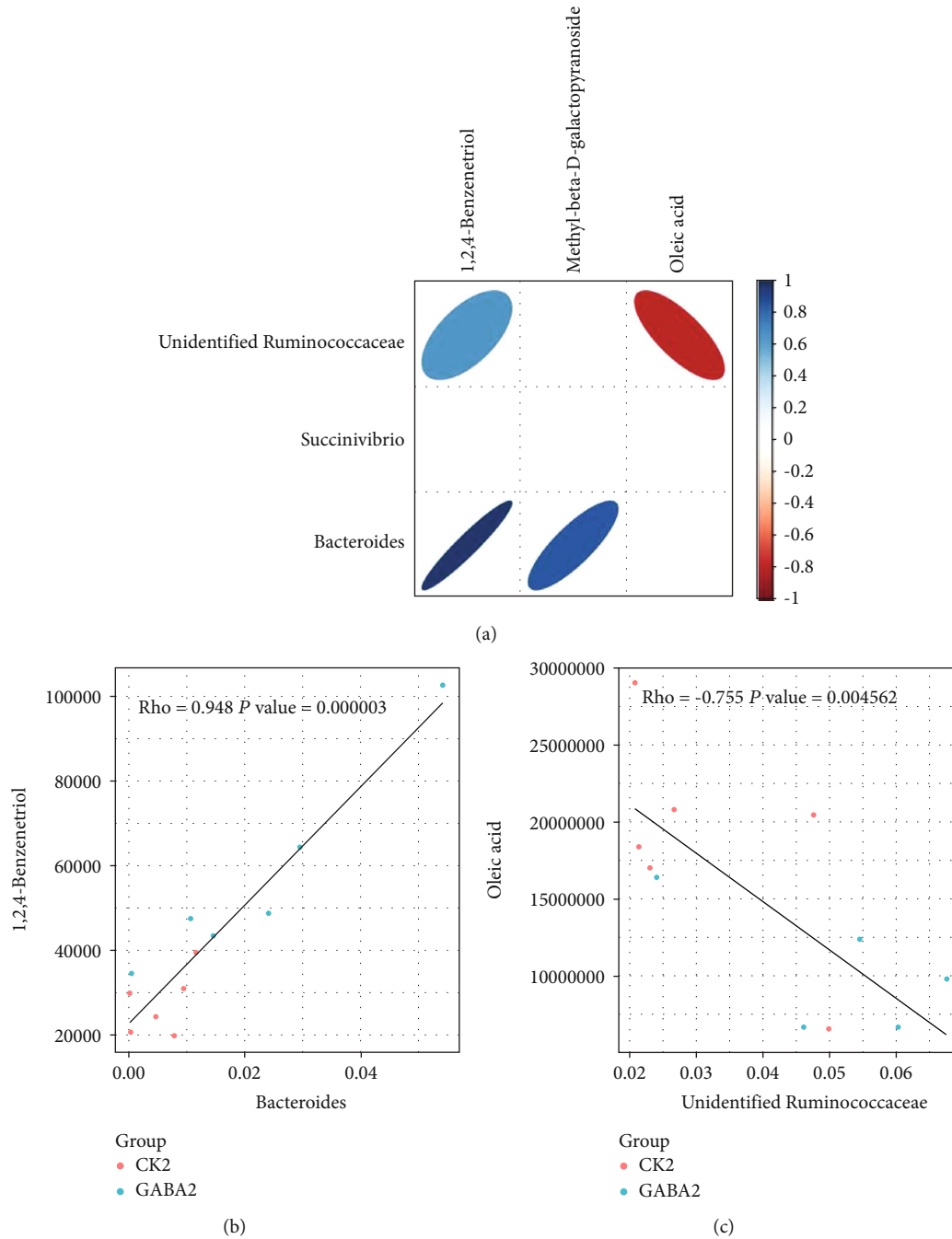


FIGURE 7: The relationship between gut microbiota and metabolites in ETEC-infected piglets. (a) Correlation analysis heat map of differential bacteria and differential metabolites in ETEC-infected piglets; (b) correlation analysis scatterplot of the content of 1,2,4-benzenetriol and the abundance of *Bacteroides* in ETEC-infected piglets; (c) correlation analysis scatterplot of the content of oleic acid and the abundance of unidentified *Ruminococcaceae* in ETEC-infected piglets. The CK group in this figure means the CON group.

enhances intestinal immunity by promoting SIgA secretion, and this might be the result of elevated levels of Th2 cytokines which further promotes the maturation of IgA-secreting plasma cells.

An extensive body of the literature has confirmed the interaction between SIgA and gut microbiota [13, 35, 41–43]. Interestingly, we detected several noteworthy strains altered by GABA supplementation. For example, GABA supplementation increased the relative abundance of *Enterococ-*

cus, which has been widely proposed to be a probiotics that could be applied in porcine, murine, chicken, and even human models [44–47]. Feeding *Enterococcus faecium* significantly increases the intestinal SIgA level and promotes the proliferation of IgA⁺ cells in chicken and murine models [48–50]. Moreover, feeding dehydrated *Enterococcus faecium* increases the concentration of IL-4 in jejunal mucosa and decreases intestinal colonization of *Escherichia coli* in broilers [51]. Therefore, our results suggested GABA

supplementation might enhance the SIgA secretion of intestine through increasing the relative abundance of *Enterococcus*.

The metabolite produced by gut microbes also exerts crucial roles in the health maintenance and modulation of physiologic function [52–56]. In the present study, we identified two metabolites, O-phosphorylethanolamine and hydroxylamine, which are significantly enriched by GABA supplementation in normal piglets. Interestingly, the content of hydroxylamine is positively correlated with the abundance of *Enterococcus* and associated with two enriched KEGG pathways: nitrogen metabolism and microbial metabolism in diverse environments. These results provided stronger implication that *Enterococcus* might play a key role in mediating the effect of GABA on intestinal SIgA secretion. On the other hand, the sphingolipid signaling pathway and sphingolipid metabolism are also enriched by GABA supplementation in normal piglets. Brown et al. demonstrated that sphingolipid produced by *Bacteroides* species can promote symbiosis with the host [57]. Meanwhile, the elevated abundance of *Bacteroides* in ETEC-infected piglets suggested that GABA supplementation might also affect SIgA secretion through *Bacteroides* and sphingolipid. However, the changes in microbial metabolism of ETEC-infected piglets are not as significant and organized as those in normal piglets. This could be attributed to the interference of ETEC infection, and further studies will be needed to clarify this issue.

In conclusion, although GABA supplementation had little effect on the growth performance, organ indices, serum amino acid profile, and serum biochemistry, it enhances intestinal immunity by promoting jejunal SIgA secretion. In addition, we observed interesting alterations in gut microbiota and microbial metabolism, which implies the potential mechanisms underlying the promotion of GABA supplementation on SIgA secretion. Our study provides insight into functional patterns of dietary supplementation on gut microbiome and host immune response and stresses the possibility of GABA utilization on intestinal health improvement.

Data Availability

The data used to support the findings of this study are included within the article.

Conflicts of Interest

There are no conflicts between the authors to declare.

Authors' Contributions

Y. Yin and J. Wang devised the experiment. Y. Zhao, J. Wang, and Y. Huang conducted the experiment. Y. Zhao analyzed the data and prepared all tables, figures, and manuscript. H. Wang, M. Qi, S. Liao, and P. Bin revised the manuscript. J. Wang and Y. Yin approved the final version of manuscript.

Acknowledgments

This study was funded from the National Key R&D Program (2017YFD0500503 and 2018YFD0500600), the National Natural Science Foundation of China (31922079, 31872365, and 31790411), the Key Programs of Frontier Scientific Research of the Chinese Academy of Sciences (QYZDY-SSW-SMC008), the Earmarked Fund for China Agriculture Research System (CARS-35), and the project funded by China Postdoctoral Science Foundation (BX20180096).

Supplementary Materials

Supplementary Table 1: primers used in this study. Supplementary Table 2: organ indices of piglets in stages 1 and 2. Supplementary Table 3: gut microbial alpha diversity indices of piglets in stages 1 and 2. Figure S1: dietary GABA did not affect the growth performance of piglets. Growth performance of piglets in (A) stage 1 and (B) stage 2. Data are presented as mean \pm SEM, analyzed by the unpaired *t*-test with Welch's correction or Mann–Whitney *U* test. Figure S2: dietary GABA had little effect on the composition of gut microbiota. (A–E) The relative abundances of main strains in the phylum, class, order, family, and genus level in normal piglets; (F) PCoA of gut microbiota in normal piglets; (G, H) the relative abundances of main strains in the phylum, class, order, family, and genus level in ETEC-infected piglets; (F) PCoA of gut microbiota in ETEC-infected piglets. (*Supplementary Materials*)

References

- [1] Y. Tang, J. Li, S. Liao et al., "The effect of dietary protein intake on immune status in pigs of different genotypes," *Food and Agricultural Immunology*, vol. 29, no. 1, pp. 776–784, 2018.
- [2] C. S. Pohl, J. E. Medland, E. Mackey et al., "Early weaning stress induces chronic functional diarrhea, intestinal barrier defects, and increased mast cell activity in a porcine model of early life adversity," *Neurogastroenterology & Motility*, vol. 29, no. 11, article e13118, 2017.
- [3] K. Katsuda, M. Kohmoto, K. Kawashima, and H. Tsunemitsu, "Frequency of enteropathogen detection in suckling and weaned pigs with diarrhea in Japan," *Journal of Veterinary Diagnostic Investigation*, vol. 18, no. 4, pp. 350–354, 2006.
- [4] G. Guan, S. Ding, Y. Yin, V. Duraipandiyar, N. A. al-Dhabi, and G. Liu, "Macleaya cordata extract alleviated oxidative stress and altered innate immune response in mice challenged with enterotoxigenic *Escherichia coli*," *Science China Life Sciences*, vol. 62, no. 8, pp. 1019–1027, 2019.
- [5] P. Chairatana and E. M. Nolan, "Defensins, lectins, mucins, and secretory immunoglobulin A: microbe-binding biomolecules that contribute to mucosal immunity in the human gut," *Critical Reviews in Biochemistry and Molecular Biology*, vol. 52, no. 1, pp. 45–56, 2017.
- [6] B. Corthésy, "Multi-faceted functions of secretory IgA at mucosal surfaces," *Frontiers in Immunology*, vol. 4, p. 185, 2013.
- [7] A. J. Macpherson, M. B. Geuking, and K. McCoy, "Homeland security: IgA immunity at the frontiers of the body," *Trends in Immunology*, vol. 33, no. 4, pp. 160–167, 2012.

- [8] N. J. Mantis, N. Rol, and B. Corthesy, "Secretory IgA's complex roles in immunity and mucosal homeostasis in the gut," *Mucosal Immunology*, vol. 4, no. 6, pp. 603–611, 2011.
- [9] O. Pabst, "New concepts in the generation and functions of IgA," *Nature Reviews Immunology*, vol. 12, no. 12, pp. 821–832, 2012.
- [10] R. Herich, "Is the role of IgA in local immunity completely known?," *Food and Agricultural Immunology*, vol. 28, no. 2, pp. 223–237, 2016.
- [11] K. Ushida, C. Kameue, T. Tsukahara, K. Fukuta, and N. Nakanishi, "Decreasing traits of fecal immunoglobulin A in neonatal and weaning piglets," *The Journal of Veterinary Medical Science*, vol. 70, no. 8, pp. 849–852, 2008.
- [12] W. Ren, K. Wang, J. Yin et al., "Glutamine-induced secretion of intestinal secretory immunoglobulin A: a mechanistic perspective," *Frontiers in Immunology*, vol. 7, p. 503, 2016.
- [13] M. Wu, H. Xiao, G. Liu et al., "Glutamine promotes intestinal SIgA secretion through intestinal microbiota and IL-13," *Molecular Nutrition & Food Research*, vol. 60, no. 7, pp. 1637–1648, 2016.
- [14] B. Song, C. Zheng, C. Zha et al., "Dietary leucine supplementation improves intestinal health of mice through intestinal SIgA secretion," *Journal of Applied Microbiology*, vol. 128, no. 2, pp. 574–583, 2020.
- [15] W. Ren, J. Yin, J. Duan et al., "Mouse intestinal innate immune responses altered by enterotoxigenic *Escherichia coli* (ETEC) infection," *Microbes and Infection*, vol. 16, no. 11, pp. 954–961, 2014.
- [16] G. Liu, W. Ren, J. Fang et al., "L-Glutamine and L-arginine protect against enterotoxigenic *Escherichia coli* infection via intestinal innate immunity in mice," *Amino Acids*, vol. 49, no. 12, pp. 1945–1954, 2017.
- [17] L. K. Bak, A. Schousboe, and H. S. Waagepetersen, "The glutamate/GABA-glutamine cycle: aspects of transport, neurotransmitter homeostasis and ammonia transfer," *Journal of Neurochemistry*, vol. 98, no. 3, pp. 641–653, 2006.
- [18] Y. Peng, "The immunological function of GABAergic system," *Frontiers in Bioscience*, vol. 22, no. 7, pp. 1162–1172, 2017.
- [19] Y. H. Li, F. Li, M. Liu et al., "Effect of γ -aminobutyric acid on growth performance, behavior and plasma hormones in weaned pigs," *Canadian Journal of Animal Science*, vol. 95, no. 2, pp. 165–171, 2015.
- [20] W. Y. Xie, X. Y. Hou, F. B. Yan, G. R. Sun, R. L. Han, and X. T. Kang, "Effect of γ -aminobutyric acid on growth performance and immune function in chicks under beak trimming stress," *Animal Science Journal*, vol. 84, no. 2, pp. 121–129, 2013.
- [21] S. Chen, B. Tan, Y. Xia et al., "Effects of dietary gamma-aminobutyric acid supplementation on the intestinal functions in weaning piglets," *Food & Function*, vol. 10, no. 1, pp. 366–378, 2019.
- [22] W. Ren, Y. Liao, X. Ding et al., "Slc6a13 deficiency promotes Th17 responses during intestinal bacterial infection," *Mucosal Immunology*, vol. 12, no. 2, pp. 531–544, 2019.
- [23] Y. Xia, S. Chen, Y. Zhao et al., "GABA attenuates ETEC-induced intestinal epithelial cell apoptosis involving GABAAR signaling and the AMPK-autophagy pathway," *Food & Function*, vol. 10, no. 11, pp. 7509–7522, 2019.
- [24] W. Ren, J. Yin, H. Xiao et al., "Intestinal microbiota-derived GABA mediates interleukin-17 expression during enterotoxigenic *Escherichia coli* infection," *Frontiers in Immunology*, vol. 7, p. 685, 2017.
- [25] W. Ren, G. Liu, J. Yin et al., "Draft genome sequence of enterotoxigenic *Escherichia coli* strain W25K," *Genome Announcements*, vol. 2, no. 3, 2014.
- [26] A. Yamatsu, Y. Yamashita, I. Maru, J. Yang, J. Tatsuzaki, and M. Kim, "The improvement of sleep by oral intake of GABA and Apocynum venetum leaf extract," *Journal of Nutritional Science and Vitaminology*, vol. 61, no. 2, pp. 182–187, 2015.
- [27] H. Hu, X. Bai, A. A. Shah et al., "Dietary supplementation with glutamine and γ -aminobutyric acid improves growth performance and serum parameters in 22- to 35-day-old broilers exposed to hot environment," *Journal of Animal Physiology and Animal Nutrition*, vol. 100, no. 2, pp. 361–370, 2016.
- [28] D. M. Wang, B. Chacher, H. Y. Liu, J. K. Wang, J. Lin, and J. X. Liu, "Effects of γ -aminobutyric acid on feed intake, growth performance and expression of related genes in growing lambs," *Animal*, vol. 9, no. 3, pp. 445–448, 2015.
- [29] D. M. Wang, C. Wang, H. Y. Liu, J. X. Liu, and J. D. Ferguson, "Effects of rumen-protected γ -aminobutyric acid on feed intake, lactation performance, and antioxidative status in early lactating dairy cows," *Journal of Dairy Science*, vol. 96, no. 5, pp. 3222–3227, 2013.
- [30] K. Birsoy, T. Wang, W. W. Chen, E. Freinkman, M. Abu-Remaileh, and D. M. Sabatini, "An essential role of the mitochondrial electron transport chain in cell proliferation is to enable aspartate synthesis," *Cell*, vol. 162, no. 3, pp. 540–551, 2015.
- [31] N. Kanarek, H. R. Keys, J. R. Cantor et al., "Histidine catabolism is a major determinant of methotrexate sensitivity," *Nature*, vol. 559, no. 7715, pp. 632–636, 2018.
- [32] G. Fanali, A. di Masi, V. Trezza, M. Marino, M. Fasano, and P. Ascenzi, "Human serum albumin: from bench to bedside," *Molecular Aspects of Medicine*, vol. 33, no. 3, pp. 209–290, 2012.
- [33] J. M. Woof and M. W. Russell, "Structure and function relationships in IgA," *Mucosal Immunology*, vol. 4, no. 6, pp. 590–597, 2011.
- [34] C. R. Stokes, J. F. Soothill, and M. W. Turner, "Immune exclusion is a function of IgA," *Nature*, vol. 255, no. 5511, pp. 745–746, 1975.
- [35] C. Lindner, B. Wahl, L. Föhse et al., "Age, microbiota, and T cells shape diverse individual IgA repertoires in the intestine," *The Journal of Experimental Medicine*, vol. 209, no. 2, pp. 365–377, 2012.
- [36] P. J. Sansonetti, "To be or not to be a pathogen: that is the mucosally relevant question," *Mucosal Immunology*, vol. 4, no. 1, pp. 8–14, 2011.
- [37] S. Han, H. Yu, F. Yang, S. Qiao, and P. He, "Effect of dietary supplementation with hyperimmunized hen egg yolk powder on diarrhoea incidence and intestinal health of weaned pigs," *Food and Agricultural Immunology*, vol. 30, no. 1, pp. 333–348, 2019.
- [38] D. Ren, D. Wang, H. Liu, M. Shen, and H. Yu, "Two strains of probiotic *Lactobacillus* enhance immune response and promote naive T cell polarization to Th1," *Food and Agricultural Immunology*, vol. 30, no. 1, pp. 281–295, 2019.
- [39] R. Nelson, S. Katayama, Y. Mine, J. Duarte, and C. Matar, "Immunomodulating effects of egg yolk low lipid peptic digests in a murine model," *Food and Agricultural Immunology*, vol. 18, no. 1, pp. 1–15, 2007.

- [40] M. Levkut, E. Husáková, K. Bobíková et al., "Inorganic or organic zinc and MUC-2, IgA, IL-17, TGF- β 4 gene expression and sIgA secretion in broiler chickens," *Food and Agricultural Immunology*, vol. 28, no. 5, pp. 801–811, 2017.
- [41] J. R. Catanzaro, J. D. Strauss, A. Bielecka et al., "IgA-deficient humans exhibit gut microbiota dysbiosis despite secretion of compensatory IgM," *Scientific Reports*, vol. 9, no. 1, 2019.
- [42] A. J. Macpherson, B. Yilmaz, J. P. Limenitakis, and S. C. Ganal-Vonarburg, "IgA function in relation to the intestinal microbiota," *Annual Review of Immunology*, vol. 36, pp. 359–381, 2018.
- [43] M. Auteri, M. G. Zizzo, and R. Serio, "GABA and GABA receptors in the gastrointestinal tract: from motility to inflammation," *Pharmacological Research*, vol. 93, pp. 11–21, 2015.
- [44] B. C. B. Beirão, M. Ingberman, C. Fávoro et al., "Effect of an *Enterococcus faecium* probiotic on specific IgA following live *Salmonella* Enteritidis vaccination of layer chickens," *Avian Pathology*, vol. 47, no. 3, pp. 325–333, 2018.
- [45] J. Benyacoub, P. F. Pérez, F. Rochat et al., "*Enterococcus faecium* SF68 enhances the immune response to *Giardia intestinalis* in mice," *The Journal of Nutrition*, vol. 135, no. 5, pp. 1171–1176, 2005.
- [46] S. Kreuzer, P. Machnowska, J. Ałmus et al., "Feeding of the probiotic bacterium *Enterococcus faecium* NCIMB 10415 differentially affects shedding of enteric viruses in pigs," *Veterinary Research*, vol. 43, no. 1, p. 58, 2012.
- [47] I. S. Surono, F. P. Koestomo, N. Novitasari, F. R. Zakaria, and K. Yulianasari, "Novel probiotic *Enterococcus faecium* IS-27526 supplementation increased total salivary sIgA level and bodyweight of pre-school children: a pilot study," *Anaerobe*, vol. 17, no. 6, pp. 496–500, 2011.
- [48] K. Bobíková, V. Revajová, V. Karaffová, M. Levkutová, and M. Levkut, "IgA gene expression and quantification of cecal IgA+, IgM+, and CD4+ cells in chickens treated with EFAL41 and infected with *Salmonella* Enteritidis," *Acta Histochemica*, vol. 117, no. 7, pp. 629–634, 2015.
- [49] A. P. A. Hendrickx, D. van de Kamer, and R. J. L. Willems, "Primary murine mucosal response during cephalosporin-induced intestinal colonization by *Enterococcus faecium*," *MicrobiologyOpen*, vol. 7, no. 5, article e00602, 2018.
- [50] E. Husáková, K. Bobíková, and D. Stašová, "Total IgA in spleen, bursa and intestine of chickens pretreated with *E. faecium* AL41 and challenged with *Salmonella* Enteritidis PT4," *Food and Agricultural Immunology*, vol. 26, no. 3, pp. 366–370, 2014.
- [51] G. T. Cao, X. F. Zeng, A. G. Chen et al., "Effects of a probiotic, *Enterococcus faecium*, on growth performance, intestinal morphology, immune response, and cecal microflora in broiler chickens challenged with *Escherichia coli* K88," *Poultry Science*, vol. 92, no. 11, pp. 2949–2955, 2013.
- [52] L. Fandriks, "Roles of the gut in the metabolic syndrome: an overview," *Journal of Internal Medicine*, vol. 281, no. 4, pp. 319–336, 2017.
- [53] A. L. Jonsson and F. Backhed, "Role of gut microbiota in atherosclerosis," *Nature Reviews. Cardiology*, vol. 14, no. 2, pp. 79–87, 2017.
- [54] L. Lin and J. Zhang, "Role of intestinal microbiota and metabolites on gut homeostasis and human diseases," *BMC Immunology*, vol. 18, no. 1, p. 2, 2017.
- [55] T. S. Postler and S. Ghosh, "Understanding the holobiont: how microbial metabolites affect human health and shape the immune system," *Cell Metabolism*, vol. 26, no. 1, pp. 110–130, 2017.
- [56] J. L. Sonnenburg and F. Backhed, "Diet-microbiota interactions as moderators of human metabolism," *Nature*, vol. 535, no. 7610, pp. 56–64, 2016.
- [57] E. M. Brown, X. Ke, D. Hitchcock et al., "Bacteroides-derived sphingolipids are critical for maintaining intestinal homeostasis and symbiosis," *Cell Host & Microbe*, vol. 25, no. 5, pp. 668–680.e7, 2019.

Review Article

Organ-Protective Effects and the Underlying Mechanism of Dexmedetomidine

Naren Bao  and Bing Tang 

Department of Anesthesiology, The First Hospital of China Medical University, 155 Nanjing North Street, Shenyang, China

Correspondence should be addressed to Bing Tang; btang@cmu.edu.cn

Received 3 March 2020; Revised 13 April 2020; Accepted 16 April 2020; Published 9 May 2020

Guest Editor: Xiaolu Jin

Copyright © 2020 Naren Bao and Bing Tang. This is an open access article distributed under the Creative Commons Attribution License, which permits unrestricted use, distribution, and reproduction in any medium, provided the original work is properly cited.

Dexmedetomidine (DEX) is a highly selective α_2 adrenergic receptor (α_2 AR) agonist currently used in clinical settings. Because DEX has dose-dependent advantages of sedation, analgesia, antianxiety, inhibition of sympathetic nervous system activity, cardiovascular stabilization, and significant reduction of postoperative delirium and agitation, but does not produce respiratory depression and agitation, it is widely used in clinical anesthesia and ICU departments. In recent years, much clinical study and basic research has confirmed that DEX has a protective effect on a variety of organs, including the nervous system, heart, lungs, kidneys, liver, and small intestine. It acts by reducing the inflammatory response in these organs, activating antiapoptotic signaling pathways which protect cells from damage. Therefore, based on wide clinical application and safety, DEX may become a promising clinical multiorgan protection drug in the future. In this article, we review the physiological effects related to organ protection in α_2 AR agonists along with the organ-protective effects and mechanisms of DEX to understand their combined application value.

1. Introduction

Dexmedetomidine (DEX) is a highly selective α_2 adrenergic receptor (α_2 AR) agonist currently used in the clinic which binds in ratio to the adrenergic receptor— $\alpha_2:\alpha_1$ is close to 1620:1. In 1999, the United States Drug and Food Administration (FDA) approved DEX for sedation and analgesia in short-term intensive care [1]. In 2008, DEX was approved by the FDA for pre- and intraoperative sedation in nontracheal intubation patients. It was then approved, in 2009, for sedating patients under general anesthesia, endotracheal intubation, and mechanical ventilation. Because DEX has the dose-dependent advantages of sedation, analgesia, anti-anxiety, inhibition of sympathetic nervous system activity, cardiovascular stabilization, and significant reduction of postoperative delirium and agitation, but does not produce respiratory depression and agitation, it is widely used in clinical anesthesia and the ICU.

In recent years, much clinical and basic research has confirmed that DEX has a protective effect on a variety of organs, including the nervous system, heart, lungs, kidneys, liver, and small intestine. It reduces inflammatory response, activating antiapoptotic signaling pathways which protect cells from damage. Therefore, based on wide clinical application and safety, DEX may become a promising clinical multiorgan protection drug in the future. In this article, we review the physiological effects related to organ protection in α_2 AR agonists along with the organ-protective effects and mechanisms of DEX to understand their combined application value.

2. Main Physiological Effects and Molecular Mechanisms Related to Organ Protection by α_2 AR Agonists

In the body, α_2 adrenoceptors (α_2 AR) have three subtypes including α_2A , α_2B , and α_2C . These are widely distributed

in the central and peripheral nervous systems, autonomic ganglia, vital organs, and blood vessels [2, 3]. The main physiological effects and molecular mechanisms involved in organ protection by $\alpha 2$ ARs are summarized as follows.

2.1. Sedative and Hypnotic Effects. Central norepinephrine has the effect of maintaining brain arousal. $\alpha 2$ AR agonists activate the $\alpha 2$ AR located in the locus coeruleus of the brainstem, producing an inhibition of adenylate cyclase activity and reduction of cyclic adenosine monophosphate. They also promote the outflow of potassium ions and inhibit the inflow of calcium ions in nerve endings, which leads to hyperpolarization of the cell membrane. This inhibits the discharge of neurons in the locus coeruleus and the release of norepinephrine. All these effects produce sedation and hypnosis [4].

2.2. Analgesic Effect. $\alpha 2$ AR agonists produce analgesic effects in multiple sites. In the brain, they bind to the $\alpha 2$ AR in the brainstem locus coeruleus to stop the transmission of pain signals. In the spinal cord, they activate $\alpha 2$ AR in the presynaptic membranes of neurons in the posterior horn and the postsynaptic membranes of intermediate neurons to open the potassium ion channel. Thus, promotion of potassium ion outflow and inhibition of calcium ion inflow lead to the cell membrane's hyperpolarization, ultimately inhibiting the transmission of pain signals to the brain. In the periphery, they inhibit the activation of nociceptive neurons by A δ and C-type nerve fibers along with the release of the nociceptive neurotransmitter P and other nociceptive peptides [5].

2.3. Antisymphathetic Effects. $\alpha 2$ AR agonists can activate the $\alpha 2$ AR of the brainstem locus coeruleus to inhibit the release of norepinephrine through negative feedback. This can inhibit sympathetic nerve excitability, reduce plasma catecholamine concentration, stabilize hemodynamics, reduce blood pressure and heart rate, and produce antisymphathetic effects [6].

2.4. Affects G Protein and Intracellular Signaling. $\alpha 2$ ARs belong to the G protein-coupled receptors (GPCRs) across the cell membrane and have the general biological properties of G protein. GPCRs are extensively expressed throughout the body. When they are activated, GPCRs interact with their cognate G protein. They transmit extracellular stimulation into the cell by amplifying transduction and triggering a series of intracellular responses. G proteins, being heterotrimeric, are composed of three subunits: α , β , and γ . The enormous quantities of G protein families—e.g., 18 α subunits, 12 β subunits, and 5 γ subunits—indicate that the signal transduction pathway triggered by GPCR is very intricate [7]. The G proteins activating adenylate cyclase are called Gs, and other inhibitors are called Gi. $\alpha 2$ ARs are classic inhibitory GPCRs [8, 9] which couple to the pertussis toxin-sensitive inhibitory G protein (Gai) and produce a multifarious biological effect in multiple organs. However, the molecular mechanism after $\alpha 2$ AR receptor activation is not clear. At present, some believe that $\alpha 2$ AR directly inhibits the AC-cAMP-PKA pathway through Gai proteins and the phosphorylation of the cAMP response element-binding protein (CREB) [10, 11]. Additionally, the separation of

the G $\beta\gamma$ subunit from Gai activates the PI3K/Akt pathway, phospholipase C, ERK, etc. [9, 12–14]. Both of the pathways mentioned above ultimately lead to the activation of NF- κ B [9]. However, some others point out that $\alpha 2$ ARs can couple both physically and functionally to Gs, producing diametrically opposite physiological effects under high concentrations of agonist and high receptor expression. Moreover, this Gs coupling is subtype-selective [15, 16]. In fact, it seems to be inconsistent with the physiological effects of $\alpha 2$ AR as a GPCR; most clinical researchers show that DEX produces anti-inflammatory and organ-protective effects by inhibiting NF- κ B. Based on the results of the above discussion, we speculate that DEX may couple with Gs to stimulate AC-cAMP-PKA pathways or affect PI3K/Akt pathways, etc., thus inhibiting NF- κ B in situations such as inflammation and ischemia, or applications within a certain concentration range.

2.5. Inhibits the Activity of Adenylyl Cyclase (AC). Cyclic adenosine monophosphate (cAMP), an important intracellular functional regulator, regulates the target protein activity by controlling its phosphorylation. AC is the main factor in regulating the amount of intracellular cAMP, and a change in its activity directly leads to cAMP synthesis change. Studies have pointed out that agonistic $\alpha 2$ AR has the ability to inhibit AC activity in order to reduce intracellular cAMP [17]. However, others have suggested that low-dose $\alpha 2$ AR agonists reduce cAMP levels by inhibiting AC activity and vice versa. Pohjanoksa and his colleagues believe that $\alpha 2$ AR-related AC regulation depends on the $\alpha 2$ AR density and the activity of AC at the time [18]. Thus, it can be seen that the effect of $\alpha 2$ AR agonists on the activity of AC has a subtle dual-direction regulation effect, which is related to the physical condition [16, 18, 19]. The main molecular mechanisms governing organ protection by $\alpha 2$ AR agonists are shown in Figure 1.

3. The Main Biological Effects of Using Dexmedetomidine for Organ Protection

3.1. Anti-Inflammatory. In addition to the main biological effects of $\alpha 2$ AR agonists, DEX has confirmed the anti-inflammatory effect of $\alpha 2$ AR agonists by reducing the inflammatory cytokine (such as TNF- α and IL-6) in vitro, in vivo, and in clinical experiments [20, 21]. Since then, DEX's organ-protective effects as an anti-inflammatory have become a popular topic. In summary, the anti-inflammatory effects of DEX function through the following means: inhibition of TLR4/NF- κ B [13, 22–24], JAK2-STAT3 [25, 26], and NF- κ B/COX-2 [27] pathways. DEX also promotes the release of acetylcholine (ACh) through an antisymphathetic effect; this combines with $\alpha 7$ nAChR on immune cytomembranes and exerts anti-inflammatory effects via the cholinergic pathway (as in Figure 1) [13, 26, 28].

3.2. Antiapoptotic. With the advancement of DEX research in recent years, researchers have found that DEX also has an antiapoptotic effect. The antiapoptosis function of DEX is achieved by activating the PI3K/Akt signaling pathway [29],

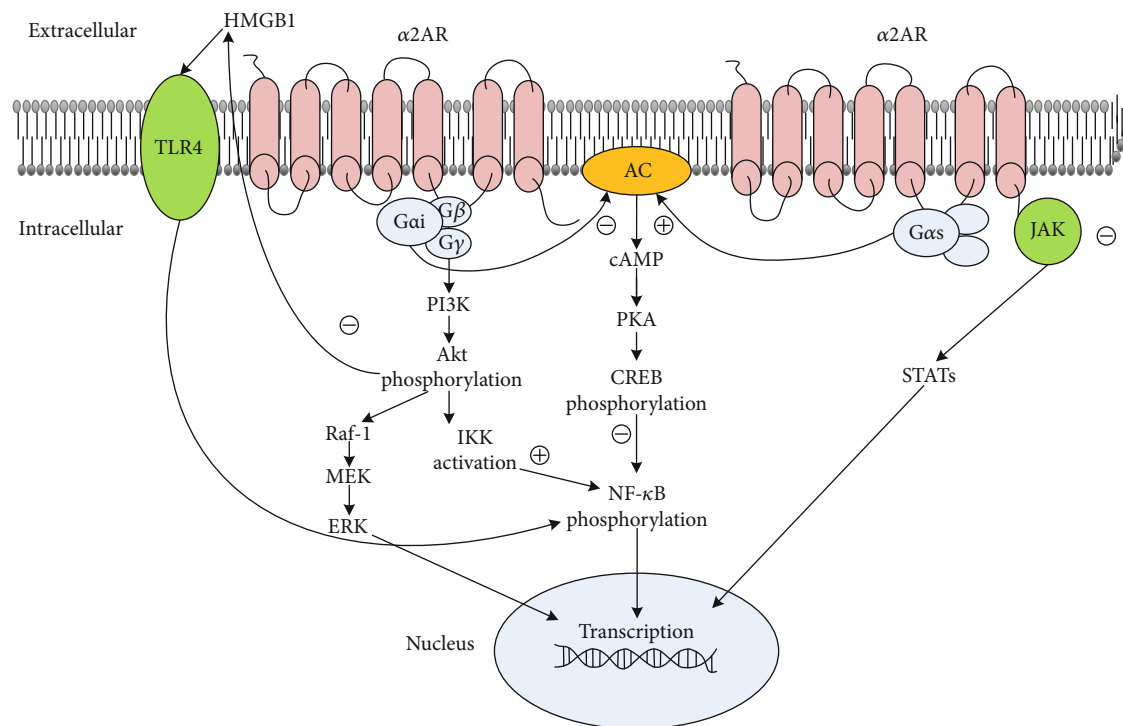


FIGURE 1: Main mechanisms of the organ-protective effects of $\alpha 2AR$ agonists. $\alpha 2AR$ s are classic inhibitory GPCRs (Gi). On the one hand, $\alpha 2AR$ s directly inhibit the AC-cAMP-PKA pathway through $G_{\alpha i}$ proteins; on the other hand, the separation of the $G_{\beta\gamma}$ subunit from $G_{\alpha i}$ activates the PI3K/Akt pathway and influences a series of downstream signaling including MEK/ERK, HGMB1/TLR4/NF- κ B, and IKK/NF- κ B. Incidentally, $\alpha 2AR$ agonists may inhibit JAK/STAT pathways. But when under high concentrations of an agonist and high receptor expression, $\alpha 2AR$ s may couple both physically and functionally to Gs, producing an opposite effect of inhibiting NF- κ B.

the Bax/cytochrome C/caspase pathway [15], and the ERK1/2 signaling pathway [18, 30], as well as inhibiting Notch/NF- κ B signaling pathways [31] and activating the mitochondrial ATP-sensitive K^+ (mitoKATP) channels (see Figure 1) [32, 33].

4. The Mechanism of Organ-Protective Effects of Dexmedetomidine

4.1. Nerve System Protection. In studies of the protective effects of DEX on organs, those focused on the nervous system were the earliest and deepest. Jiang et al. [34] first reported the protective effect of DEX on hypoxic-ischemic brain damage in 1991. In the past 20 years, people have mainly focused on three aspects: (1) protecting against cerebral ischemia/hypoxia injury and improving nervous system function after brain injury [35], (2) reducing the damage of anesthetics on developing neurons [36–38], and (3) decreasing the incidence of postoperative delirium or cognitive dysfunction [39, 40]. Currently, great progress has been made in research on the effects and mechanisms of DEX, suggesting that DEX has application values in newborns, children, patients with craniocerebral injury or stroke, and elderly patients with degraded cerebral function. Going forward, more efforts will be needed to validate laboratory research in the clinic.

Regarding the protective effect of DEX on the nervous system, it has five main functions: (1) inhibiting the excitability of sympathetic nerves and regulating the release of catecholamines, (2) regulating the release of central glutamate, (3) inhibiting cell apoptosis and release of inflammatory cytokines, (4) antioxidant stress, and (5) regulating synaptic plasticity and reducing neurotoxicity of anesthetics. The inhibition of cell apoptosis and release of inflammatory cytokines are considered to be paramount.

4.1.1. Regulates the Release of Catecholamine. Cerebral ischemia/hypoxia causes the brain to superfluently release catecholamines. This causes calcium overload in neurons, generates abundant neurotoxic free radicals, aggravates ischemia and hydrocephalus through severe cerebrovascular contraction, and increases the sensitivity of neurons to glutamate, exacerbating its destructiveness [41, 42]. DEX can effectively reduce the production of catecholamine, reducing cerebral vascular spasms and subsequent brain damage [16, 35].

4.1.2. Inhibits the Release of Glutamate. Glutamate, an excitatory neurotransmitter released during cerebral ischemia, excites receptors and causes neuronal damage. DEX dose-dependently inhibits the release of glutamate caused by multiple channels [43, 44], significantly reduces the hypoxia and depolarization-induced increase of extracellular glutamate

[45], and reduces the accumulation of glutamate by inhibiting the absorption of neurocyte to glutamate.

4.1.3. Anti-Inflammatory and Antiapoptotic Effects. Cerebral ischemia, traumatic injury, and postoperative cognitive dysfunction (POCD) are closely related to neuron inflammation and apoptosis. DEX has shown its anti-inflammatory and antiapoptotic effects in multiple animal models [46–51]. As we mentioned above, the anti-inflammatory effect of DEX is achieved by inhibiting the TLR4/NF- κ B [47], JAK2-STAT3 [25, 50], and NF- κ B/COX-2 pathways [27, 52]; activating the ERK1/2 pathway [53]; and releasing acetylcholine (ACh) through antisympathetic effects via the cholinergic pathway [13]. At the same time, DEX also reduces neuronal apoptosis through a variety of mechanisms that enhance the viability of the neurocyte. These include increasing the expression of antiapoptotic proteins Mdm-2 and Bcl-2, inhibiting proapoptotic Bax and p53, reducing the permeability of mitochondrial membranes, reducing the release of cytochrome C and apoptosis-inducing factors into the cytoplasm [54], activating the PI3K/Akt pathway and reducing cysteinyl aspartate proteinase (caspase-3) by promoting the phosphorylation of the focal adhesion kinase (FAK) [43], enhancing the phosphorylation of ERK1/2 by inhibiting neuronal sodium ions and delaying potassium ion influx [4, 55], and inhibiting the Notch/NF- κ B signaling pathway [31].

4.1.4. Antioxidant Stress. The brain is very sensitive to the destruction of oxygen-free radicals, and ischemia-reperfusion injuries produce an intracorporal antioxidant-peroxidation state imbalance. DEX eliminates the excessive free radicals in the body and reduces this pathological chain reaction by reducing malondialdehyde (MDA) and improving the activity of superoxide dismutase [56, 57].

4.1.5. Reduces Neurotoxicity of Anesthetics and Regulates Synaptic Plasticity. Many studies have confirmed that general anesthetics cause neurotoxicity in the developing brain, produce neural apoptosis, and inhibit the establishment of connections between synapses [36, 45]. Three large retrospective clinical studies showed that the general anesthesia of healthy children under 2 years of age had little correlation with postoperative neurodevelopmental hypogenesis. However, the risk in premature babies and those with congenital heart disease is greatly increased [58]. Based on this, in 2016, the FDA reiterated that repeated application of general anesthetics and sedatives to children under three years old and women in the last three months of pregnancy may affect child and fetus development.

DEX reduces the neurotoxicity of sevoflurane through many pathways: inhibiting apoptosis and autophagy [59], increasing the expression of tyrosine kinase B (TrkB) and BDNF, promoting neurocyte proliferation, maintaining nervous system function [60], inhibiting neuronal mitochondrial dynamin-related protein (Drp1) [37], and dose-dependently activating the bone morphogenetic protein (BMP)/Smad pathway to regulate self-renewal, differentiation, proliferation, migration, and apoptosis of the neuro-

cyte [61]. The multiple signal pathways we mentioned above show that DEX has played a significant role in neuroprotection during infant development, laying the foundation for the safe adhibition of DEX in children and pregnant women and solving the problem of general anesthesia drug selection for children.

Synaptic plasticity, the property of adjustable connection between synapses, is closely related to learning and memory since it controls synaptic information transmission. DEX pretreatment significantly improved the decline of the proliferative capacity and decreased neuronal plasticity in neonatal rats after hyperoxia induction [62]. The research on regulation of synaptic plasticity through DEX has important implications for neurodevelopmental protection and promotes the study of synaptic plasticity regulation. What is more, it is a meaningful breakthrough in the treatment of neurological diseases such as memory deficits.

4.2. Cardioprotective Benefits. Intraoperative patients are susceptible to stimuli such as surgical procedures and endotracheal intubation, which cause excitation in sympathetic nerves. This can lead to tachycardia, increased blood pressure, imbalance of myocardial blood oxygen supply and demand, and cardiac complications. The main pharmacological effects of DEX are reducing the excitability of the sympathetic nervous system, weakening the stress response, and stabilizing hemodynamics. Thus, it effectively prevents the occurrence of myocardial ischemia in the perioperative period. A large number of clinical observations have confirmed that DEX reduces postoperative mortality and myocardial infarction [63, 64].

We conclude that the cardioprotective mechanism of DEX is mainly reflected in the following three aspects:

- (1) Inhibition of norepinephrine neuron activity in the locus coeruleus, which suppresses sympathetic nerve excitation to reduce catecholamine levels in the blood, cardiac load, and myocardial oxygen consumption. At the same time, it prolongs diastolic perfusion time, increases left ventricular coronary blood flow, reduces myocardial lactic acid release, and improves myocardial resistance to ischemia and hypoxia
- (2) DEX directly inhibits cardiac norepinephrine release to reduce the occurrence of arrhythmias in high-risk patients
- (3) Anti-inflammation and antiapoptosis: DEX pretreatment activates some of the signal pathways through G protein like PI3K/Akt and MEK1-2-ERK1/2, sequentially reducing apoptosis and inflammatory response caused by ischemia-reperfusion and reducing the myocardial infarction area [65–67]. The downstream molecular mechanism is not completely clear at present

Through a review of laboratory and clinical research, a new perspective is gradually formed: rational use of DEX during the perioperative period may effectively reduce the risk of cardiovascular surgery [68, 69]. However, experiments

by Mimuro et al. [70] have questioned this. They found that during ischemia-reperfusion injury in mouse myocardium, DEX increases the myocardial infarction area without altering hemodynamics and coronary blood flow. This effect is antagonized by yohimbine, an α_2 AR antagonist. Although such objections are in the minority, they still need to be taken seriously. Therefore, the cardioprotective effects of DEX need to be further studied and discussed.

4.3. Pulmonary Protection. The lungs, as sensitive organs, are extremely vulnerable to systemic inflammation and remote organ ischemia-reperfusion injury. Many clinical practices—such as trauma, one-lung ventilation, extracorporeal circulation, and liver transplantation—cause lung damage through inflammation and apoptosis. Ventilation-associated lung injury (VALI) is also frequently associated with acute respiratory distress syndrome (ARDS) during treatment. In recent years, it has been observed that DEX has pulmonary protection benefits in many cases of lung injuries through its effect on the pulmonary vasoconstriction mechanism, pulmonary vascular ischemia-reperfusion injury, and release of inflammatory cytokine.

4.3.1. Relieves Inflammation, Apoptosis, and Oxidative Stress from Various Pathological Injuries. In models of acute lung injury caused by renal ischemia-reperfusion injury, DEX pre- and posttreatment significantly reduce pulmonary edema and inflammatory response by reducing myeloperoxidase (MPO) activity as well as downregulating intercellular adhesion molecule-1 (ICAM-1) and TNF- α mRNA expression [71, 72]. In the rat sepsis model [24], DEX inhibits inflammatory response in the lung by the TLR4/myeloid differentiation factor 88/NF- κ B pathway and reduces mortality by activating PI3K/Akt/mTOR pathways. In the rat chest trauma model, DEX also has a protective effect on pulmonary contusion [73], which reduces proinflammatory cytokines by inhibiting the activity of NF- κ B. Furthermore, DEX reduces mitochondrial dysfunction, oxidative stress, and apoptosis in LPS-induced acute lung injury [74]. Moreover, the pulmonary protection effect of DEX has a parabolic correlation with its concentration. It shows that 50 μ g/kg is the strongest concentration: 10 and 100 μ g/kg did have an effect, but it was weaker than at 50 μ g/kg [54, 75].

4.3.2. Reduces VALI and Hypoxic Pulmonary Vasoconstriction. On the one hand, VALI is caused by diffuse alveolocapillary membrane damage and increased permeability due to excessive airway pressure (volutrauma). On the other hand, intense mechanical stretching activates a variety of mediators involved in inflammation in the lung's inherent cells, promotes the transcription and expression of proinflammatory factors, triggers a waterfall of inflammation, and eventually leads to the occurrence of lung injury [76]. Yang et al. [77] used the high tidal volume ventilation (HVT) mode to induce lung injury in rats. When they intravenously injected ten times the clinical dose, DEX significantly improved the lung injury with respect to its pathological morphology, inflammatory cytokines, and chemokines.

In addition, DEX improves hypoxic pulmonary vasoconstriction (HPV) and oxygenation during one-lung ventilation. In an isolated lung, the imbalance of ventilator-flow ratios causes hypoxemia; in response, the body compensates for HPV by reducing the abnormal distribution of pulmonary blood flow. During anesthesia, HPV is often affected by anesthetics such as isoflurane, sevoflurane, and propofol [78]. The application of DEX indirectly affects HPV by reducing the medicinal dose of inhalation and intravenous anesthesia. At the same time [79], DEX directly enhances HPV and alters oxygenation by reducing oxidative stress and increasing nitric oxide release during one-lung ventilation.

4.4. Renal Protection. The renal blood supply accounts for 20% of cardiac output, and 90%–95% of this supply is distributed in the cortex. The perioperative shock, extracorporeal circulation, and usage of vasoactive drugs can easily lead to ischemia-reperfusion injury (I/R) in the renal parenchyma, especially the cortex [26, 80]. The renoprotective effects of DEX are as follows.

4.4.1. Improves Local Renal Blood Flow and Diuresis. Ischemia-reperfusion leads to an increase in systemic and local sympathetic activity along with intense vasoconstriction in the renal cortex. DEX improves renal ischemia damage by improving outer renal medullary blood flow through local renal vasodilation [75], increasing glomerular filtration, dampening the ability of arginine vasopressin in the collecting duct, inhibiting the expression of aquaporins along with the transport of Na⁺ and water [81], urination stimulation, and so on [82]. At the same time, DEX also reduces glomerular congestion, swelling in renal tubular epithelial cells, and luminal stenosis [83]. What is more, DEX has multiple effects during the perioperative period: in addition to analgesia, it reduces the accumulation of other analgesic and nonsteroidal anti-inflammatory drugs that increase kidney injury risk.

4.4.2. Inhibits Inflammation, Oxidative Stress, and Apoptosis. As we mentioned above, DEX blocks NF- κ B transcription by inhibiting the TLR4/NF- κ B and JAK/STAT pathways while activating α_7 nAChR via the cholinergic pathway, thus producing anti-inflammatory effects [13, 26, 84, 85]. As a synthetic iNOS promoter, obstruction of NF- κ B may reduce NO release, prevent oxidative stress, and reduce mitochondrial damage [86]. DEX also reduces oxidative stress by promoting the Keap1/Nrf2/ARE/HO-1 pathway [87]. Chen et al. [88] proposed that DEX exerts antiapoptotic functions by inhibiting the ROS/JNK signaling pathway, thus reducing the expression of Bax, cytochrome C, cleaved caspase-9 proteins, and cleaved caspase-3 proteins in the mitochondrial-dependent pathway.

4.4.3. Relieves Hypercoagulability. When sepsis or ischemia-reperfusion injury occurs, various inflammatory cytokines stimulate endotheliocytes to release inflammatory mediators and procoagulant substances. This activates the coagulation system, leading to a hypercoagulability state. Thereafter, the diffuse microthrombus is formed in the glomerulus (which causes perirenal blood stasis), and the glomerular filtration rate decreases. The inflammatory response interacts with

the abnormal coagulation, causing accumulation of the toxic and harmful metabolites, aggravating kidney damage, and ultimately leading to acute and chronic kidney disease. The antisympathetic effect of DEX weakens the stress response, thereby relieving the hypercoagulable state [89]. In addition, DEX can dilate blood vessels, accelerate blood flow, reduce erythrocyte aggregation, reverse blood stagnation, and reduce kidney damage caused by coagulopathy.

4.5. Hepatoprotective Effects. DEX also has hepatoprotective benefits due to its effects on inflammation, apoptosis, and oxidative stress. In animal experiments of hepatic ischemia reperfusion injury, intraperitoneal injection of DEX (10 or 100 $\mu\text{g}/\text{kg}$) 30 minutes before liver ischemia can increase the levels of superoxide dismutase, catalase, and glutathione to reduce liver tissue damage [90]. In lipopolysaccharide- (LPS-) induced oxidative stress and apoptosis experiments on rat liver, it was confirmed that DEX reduces symptoms by enhancing the GSK-3 β /MKP-1/Nrf2 pathway activity through α 2AR [91]. Wang et al. found that DEX protects rat liver from ischemia-reperfusion injury in relation to the TLR4/NF- κ B pathway [33]. In the LPS/D-galactosamine-induced mouse acute liver injury experiments by Yang et al., DEX inhibited the release of TNF- α , phosphorylation of c-jun-N-terminal kinase (JNK), and cleavage of caspase-3. By reducing the activity of caspase-3, caspase-8, and caspase-9, it helped relieve hepatocyte apoptosis [92]. But the molecular mechanism and clinical significance of this activity require further research and clarification.

4.6. Intestinal Protection. The intestinal barriers are important for the body's resistance to external pathogens and toxins, inflammation, stress, surgical trauma, and hypovolemia; however, ischemia-reperfusion injury can cause intestinal barrier damage [93, 94]. Thus, bacteria and toxins in the intestine can reach the mesenteric lymphoid tissues, lymph fluid, blood, and extraintestinal tissues and organs, causing gut-derived sepsis and eventually leading to multiple organ dysfunction syndrome (MODS) [95]. Attention to the protection of intestinal barrier functions under pathological conditions can reduce the incidence of gut-derived sepsis, improve the prognosis of patients, and reduce the mortality of critical patients. Therefore, in recent years, the protection of intestinal health during the perioperative period has been increasingly recognized.

4.6.1. Anti-Inflammation, Antioxidative Stress, and Antiapoptosis. The effects of DEX against inflammation, apoptosis, and oxidative stress that we have described above also function in intestinal protection. Zhang et al. [54] studied intestinal ischemia-reperfusion injuries in rats, administering DEX at different times and doses. They showed that DEX pretreatment was dose-dependent for resisting intestinal ischemia-reperfusion injury in a certain range. Their experiments suggested that in addition to the reduction of oxidative stress, inflammation indicators of malondialdehyde (MDA) and myeloperoxidase (MPO), serum levels of diamine oxidase (DAO), activity of caspase-3, ileal mucosa levels, and the apoptotic index of ileal mucosal cells were significantly

lower than in those rats without DEX. It was shown that the effect of DEX is maximal at 5 $\mu\text{g}/\text{kg}/\text{h}$, but has no effect in posttreatment. The mechanism of the difference in pre- and posttreatment needs further research.

In addition, some clinical trials have also highlighted the intestinal protective effect of DEX. DEX pretreatment relieves intestinal and liver damage in patients undergoing liver cancer resection who are afflicted by selective hepatic lobectomy and liver cirrhosis [96]. DEX also has significant preventive effects on postoperative abdominal adhesions [97], and its mechanism may relate to antioxidative stress effects and reduction of tissue inflammation.

4.6.2. Promotes Recovery of Intestinal Motility, Improves Intestinal Microcirculation, and Protects against Intestinal Epithelial Barrier Disruption. DEX promotes isolated rat ileum contraction [98]. In contrast, Herbert et al. [99] found that DEX dose-dependently inhibited the enterocinesia of guinea pigs' small intestines in vitro. In healthy volunteers, DEX also inhibits gastric emptying and enterocinesia [100]. These contradictory results may be related to the physiological state of the different subjects. Under normal physiological conditions, DEX may inhibit enterogastric peristalsis via enteric neurons. On the other hand, under pathological conditions such as infection, stress, trauma, and hypovolemia, DEX benefits intestinal microcirculation perfusion, protects the gut barrier, and restores gastrointestinal motility. It does the latter by reducing inflammation and stress reactions, maintaining hemodynamic stability, relieving postoperative pain, and reducing the dosage of postoperative opioids. In rat models, DEX protects against intestinal epithelial barrier disruption by recovering the density of small blood vessels perfused in the intestinal mucosa and muscles, attenuating intestinal microcirculatory dysfunction, and inhibiting inflammatory response, thus reducing mucosal cell death and tight junctional damage [56, 101].

5. Correlation of Anti-Inflammatory Effects with Timing and Dose

The anti-inflammatory effect of DEX has some correlation with its dose. In sepsis rats, Taniguchi et al. [102] found that the medium dose (5 $\mu\text{g}/\text{kg}/\text{h}$) and high dose (10 $\mu\text{g}/\text{kg}/\text{h}$) of DEX reduce plasma levels of TNF- α and IL-6, while the low-dose group (2.5 $\mu\text{g}/\text{kg}/\text{h}$) showed no decreasing effect. Similar experimental phenomena were observed in vitro [43, 103]. Lai et al. [104] believed that the anti-inflammatory effect of DEX had a parabolic relationship with its concentration. In their in vitro experiment, LPS-induced expression of inflammatory cytokines was treated with different concentrations of DEX. The result shows that while the addition of 0.01 $\mu\text{mol}/\text{L}$ of DEX had no impact, and the addition of 1 $\mu\text{mol}/\text{L}$ of DEX was significantly inhibited, 100 $\mu\text{mol}/\text{L}$ of DEX promoted the expression of nitric oxide synthase and nitric oxide synthesis; the effects of inflammatory cytokines such as prostaglandin E2, TNF- α , IL-1 β , IL-6, and IL-10 are consistent with the effects of nitric oxide. Some other scholars have also observed the same trend [54, 55].

In addition, Gu et al. believe that the protective effect of DEX on organs is related to the processing time, and the posttreatment conditioning is less than the pretreatment [11]. Zhang et al. believe that DEX posttreatment does not alleviate dilated reperfusion injury in the small intestine [54]. Based on the physiological characteristics of $\alpha 2AR$ described above, $\alpha 2AR$ -related AC regulation is affected by factors such as $\alpha 2AR$ density and AC activity at the time, while the latter two are related to the state of the body. So we speculate that there are two situations: (1) $\alpha 2AR$ density and AC activity may be affected by different stages of inflammation in the body or organs; (2) although DEX is mainly coupled with the Gi protein, in a certain concentration range, it may also be coupled with the Gs protein. The latter leads to a subtle two-way regulation effect on AC activity and even the downstream pathways. As a result, some scholars have observed dose-dependent changes in organ protection and differential results in pre- and posttreatment. Consequently, in the future, it is necessary to search for a more safe and effective concentration range and medication timing in the usage of DEX.

6. Perspective

In conclusion, the organ-protective effect of DEX is achieved in different pathological conditions by multiple mechanisms. However, a majority of the current DEX studies are based on animal experiments, and the mechanism is not fully elucidated. More intensive research and clinical trials are necessary for further verification. In addition, despite the mainstream belief that the organ-protective effect of DEX seems clear, there are conflicting conclusions about whether $\alpha 2AR$ agonism is protective or destructive. Therefore, while considering the sedative, analgesic, and organ-protective effects of DEX, we need to explore the different rates of timing, appropriate dosages, and medication profiles of this substance. This will help to promote realistic, significant clinical observations that validate the potential for using DEX in the future to protect organs.

Conflicts of Interest

The authors declare that there is no conflict of interest regarding the publication of this article.

Acknowledgments

This work was supported by the Science and Technology Research Project of the Liaoning Provincial Education Department (LK201651).

References

- [1] A. Paris and P. H. Tonner, "Dexmedetomidine in anaesthesia," *Current Opinion in Anaesthesiology*, vol. 18, no. 4, pp. 412–418, 2005.
- [2] A. J. Lewington, J. Cerda, and R. L. Mehta, "Raising awareness of acute kidney injury: a global perspective of a silent killer," *Kidney International*, vol. 84, no. 3, pp. 457–467, 2013.
- [3] E. F. Daher, G. B. Silva Junior, S. Q. Santos et al., "Differences in community, hospital and intensive care unit-acquired acute kidney injury: observational study in a nephrology service of a developing country," *Clinical Nephrology*, vol. 78, no. 6, pp. 449–455, 2012.
- [4] T. Kamibayashi and M. Maze, "Clinical uses of alpha2-adrenergic agonists," *Anesthesiology*, vol. 93, no. 5, pp. 1345–1349, 2000.
- [5] M. Maze, M. Maze, and M. Fujinaga, "Alpha 2 adrenoceptors in pain modulation: which subtype should be targeted to produce analgesia?," *Anesthesiology*, vol. 92, no. 4, pp. 934–936, 2000.
- [6] T. Taniguchi, Y. Kidani, H. Kanakura, Y. Takemoto, and K. Yamamoto, "Effects of dexmedetomidine on mortality rate and inflammatory responses to endotoxin-induced shock in rats," *Critical Care Medicine*, vol. 32, no. 6, pp. 1322–1326, 2004.
- [7] M. I. Simon, M. P. Strathmann, and N. Gautam, "Diversity of G proteins in signal transduction," *Science*, vol. 252, no. 5007, pp. 802–808, 1991.
- [8] K. K. Meldrum, K. Hile, D. R. Meldrum, J. A. Crone, J. P. Gearhart, and A. L. Burnett, "Simulated ischemia induces renal tubular cell apoptosis through a nuclear factor-kappaB dependent mechanism," *The Journal of Urology*, vol. 168, no. 1, pp. 248–252, 2002.
- [9] K. DONNAHOO, D. R. MELDRUM, R. SHENKAR, C. S. CHUNG, E. ABRAHAM, and A. H. HARKEN, "Early renal ischemia, with or without reperfusion, activates NFkappaB and increases TNF-alpha bioactivity in the kidney," *The Journal of Urology*, vol. 163, no. 4, pp. 1328–1332, 2000.
- [10] M. S. Hayden and S. Ghosh, "Signaling to NF-kappaB," *Genes & Development*, vol. 18, no. 18, pp. 2195–2224, 2004.
- [11] X. Y. Gu, B. L. Liu, K. K. Zang et al., "Dexmedetomidine inhibits tetrodotoxin-resistant Nav1.8 sodium channel activity through Gi/o-dependent pathway in rat dorsal root ganglion neurons," *Molecular Brain*, no. 1, article S13041-015-0105-2, p. 15, 2015.
- [12] H. Rong, Z. Zhao, J. Feng et al., "The effects of dexmedetomidine pretreatment on the pro- and anti-inflammation systems after spinal cord injury in rats," *Brain, Behavior, and Immunity*, vol. 64, article S0889159117300685, pp. 195–207, 2017.
- [13] J. Gu, P. Sun, H. Zhao et al., "Dexmedetomidine provides renoprotection against ischemia-reperfusion injury in mice," *Critical Care*, vol. 15, no. 3, p. R153, 2011.
- [14] B. Li, T. du, H. Li et al., "Signalling pathways for transactivation by dexmedetomidine of epidermal growth factor receptors in astrocytes and its paracrine effect on neurons," *British Journal of Pharmacology*, vol. 154, no. 1, pp. 191–203, 2008.
- [15] M. G. Eason, H. Kurose, B. D. Holt, J. R. Raymond, and S. B. Liggett, "Simultaneous coupling of alpha 2-adrenergic receptors to two G-proteins with opposing effects. Subtype-selective coupling of alpha 2C10, alpha 2C4, and alpha 2C2 adrenergic receptors to Gi and Gs," *The Journal of Biological Chemistry*, vol. 267, no. 22, pp. 15795–15801, 1992.
- [16] C. M. Fraser, S. Arakawa, W. McCombie, and J. C. Venter, "Cloning, sequence analysis, and permanent expression of a human alpha 2-adrenergic receptor in Chinese hamster ovary cells. Evidence for independent pathways of receptor coupling to adenylate cyclase attenuation and activation," *The*

- Journal of Biological Chemistry*, vol. 264, no. 20, pp. 11754–11761, 1989.
- [17] M. A. Daemen, B. de Vries, and W. A. Buurman, “Apoptosis and inflammation in renal reperfusion injury,” *Transplantation*, vol. 73, no. 11, pp. 1693–1700, 2002.
- [18] K. Pohjanoksa, C. Jansson, K. Luomala, A. Marjamäki, J. M. Savola, and M. Scheinin, “ α 2-Adrenoceptor regulation of adenylyl cyclase in CHO cells: Dependence on receptor density, receptor subtype and current activity of adenylyl cyclase,” *European Journal of Pharmacology*, vol. 335, no. 1, article S0014299997011540, pp. 53–63, 1997.
- [19] A. B. Sanz, M. D. Sanchez-Niño, A. M. Ramos et al., “NF- κ B in renal inflammation,” *Journal of the American Society of Nephrology*, vol. 21, no. 8, pp. 1254–1262, 2010.
- [20] S. Hofer, J. Steppan, T. Wagner et al., “Central sympatholytics prolong survival in experimental sepsis,” *Critical Care*, vol. 13, no. 1, p. R11, 2009.
- [21] H. Qiao, R. D. Sanders, D. Ma, X. Wu, and M. Maze, “Sedation improves early outcome in severely septic Sprague Dawley rats,” *Critical Care*, vol. 13, no. 4, article cc8012, p. R136, 2009.
- [22] A. S. Levey and M. T. James, “Acute kidney injury,” *Annals of Internal Medicine*, vol. 167, no. 9, pp. ITC66–ITC80, 2017.
- [23] L. Yang, G. Xing, L. Wang et al., “Acute kidney injury in China: a cross-sectional survey,” *Lancet*, vol. 386, no. 10002, article S014067361500344X, pp. 1465–1471, 2015.
- [24] N. H. Lameire, A. Bagga, D. Cruz et al., “Acute kidney injury: an increasing global concern,” *Lancet*, vol. 382, no. 9887, pp. 170–179, 2013.
- [25] Y. R. Lankadeva, S. Ma, N. Iguchi et al., “Dexmedetomidine reduces norepinephrine requirements and preserves renal oxygenation and function in ovine septic acute kidney injury,” *Kidney International*, vol. 96, no. 5, pp. 1150–1161, 2019.
- [26] Y. Si, H. Bao, L. Han et al., “Dexmedetomidine protects against renal ischemia and reperfusion injury by inhibiting the JAK/STAT signaling activation,” *Journal of Translational Medicine*, vol. 11, no. 1, article 1479-5876-11-141, p. 141, 2013.
- [27] H. Yao, X. Chi, Y. Jin et al., “Dexmedetomidine Inhibits TLR4/NF- κ B Activation and Reduces Acute Kidney Injury after Orthotopic Autologous Liver Transplantation in Rats,” *Scientific Reports*, vol. 5, no. 1, article BF5rep16849, 2015.
- [28] M. Miksa, P. Das, M. Zhou et al., “Pivotal role of the alpha (2A)-adrenoceptor in producing inflammation and organ injury in a rat model of sepsis,” *PLoS One*, vol. 4, no. 5, article e5504, 2009.
- [29] R. D. Ye, “Regulation of nuclear factor kappaB activation by G-protein-coupled receptors,” *Journal of Leukocyte Biology*, vol. 70, no. 6, pp. 839–848, 2001.
- [30] Y. M. Zhu, C. C. Wang, L. Chen et al., “Both PI3K/Akt and ERK1/2 pathways participate in the protection by dexmedetomidine against transient focal cerebral ischemia/reperfusion injury in rats,” *Brain Research*, vol. 1494, pp. 1–8, 2013.
- [31] M. S. Paller, J. R. Hoidal, and T. F. Ferris, “Oxygen free radicals in ischemic acute renal failure in the rat,” *The Journal of Clinical Investigation*, vol. 74, no. 4, pp. 1156–1164, 1984.
- [32] X. Chi, X. Wei, W. Gao et al., “Dexmedetomidine ameliorates acute lung injury following orthotopic autologous liver transplantation in rats probably by inhibiting toll-like receptor 4-nuclear factor kappa B signaling,” *Journal of Translational Medicine*, vol. 13, no. 1, article 554, 2015.
- [33] Y. Wang, S. Wu, X. Yu et al., “Dexmedetomidine Protects Rat Liver against Ischemia-Reperfusion Injury Partly by the α 2A-Adrenoceptor Subtype and the Mechanism Is Associated with the TLR4/NF- κ B Pathway,” *International Journal of Molecular Sciences*, vol. 17, no. 7, article ijms17070995, p. 995, 2016.
- [34] S. Jiang, J. Streeter, B. M. Schickling, K. Zimmerman, R. M. Weiss, and Miller FJ Jr, “Nox1 NADPH oxidase is necessary for late but not early myocardial ischaemic preconditioning,” *Cardiovascular Research*, vol. 102, no. 1, pp. 79–87, 2014.
- [35] U. Kunter, S. Daniel, M. B. Arvelo et al., “Combined expression of A1 and A20 achieves optimal protection of renal proximal tubular epithelial cells,” *Kidney International*, vol. 68, no. 4, pp. 1520–1532, 2005.
- [36] Y. T. Xuan, X. L. Tang, S. Banerjee et al., “Nuclear factor-kappaB plays an essential role in the late phase of ischemic preconditioning in conscious rabbits,” *Circulation Research*, vol. 84, no. 9, pp. 1095–1109, 1999.
- [37] Y. Shan, S. Sun, F. Yang, N. Shang, and H. Liu, “Dexmedetomidine protects the developing rat brain against the neurotoxicity wrought by sevoflurane: role of autophagy and Drp1-Bax signaling,” *Drug Design, Development and Therapy*, vol. 12, pp. 3617–3624, 2018.
- [38] J. Geng, Y. Liu, Y. Guo et al., “Correlation between TERT C228T and clinic-pathological features in pediatric papillary thyroid carcinoma,” *Science China. Life Sciences*, vol. 62, no. 12, article 9546, pp. 1563–1571, 2019.
- [39] A. Iida, H. Yoshidome, T. Shida et al., “Hepatocyte nuclear factor-kappa beta (NF-kappaB) activation is protective but is decreased in the cholestatic liver with endotoxemia,” *Surgery*, vol. 148, no. 3, pp. 477–489, 2010.
- [40] B. Dawn, Y. Guo, A. Rezazadeh et al., “Tumor necrosis factor-alpha does not modulate ischemia/reperfusion injury in naïve myocardium but is essential for the development of late preconditioning,” *Journal of Molecular and Cellular Cardiology*, vol. 37, no. 1, pp. 51–61, 2004.
- [41] J. Lutz, L. A. Luong, M. Strobl et al., “The A20 gene protects kidneys from ischaemia/reperfusion injury by suppressing pro-inflammatory activation,” *Journal of Molecular Medicine (Berlin, Germany)*, vol. 86, no. 12, article 405, pp. 1329–1339, 2008.
- [42] C. G. da Silva, E. R. Maccariello, S. W. Wilson et al., “Hepatocyte growth factor preferentially activates the anti-inflammatory arm of NF- κ B signaling to induce A20 and protect renal proximal tubular epithelial cells from inflammation,” *Journal of Cellular Physiology*, vol. 227, no. 4, pp. 1382–1390, 2012.
- [43] S. Bunte, F. Behmenburg, N. Majewski et al., “Characteristics of dexmedetomidine postconditioning in the field of myocardial ischemia-reperfusion injury,” *Anesthesia and Analgesia*, vol. 130, no. 1, pp. 90–98, 2020.
- [44] K. Nishina, H. Akamatsu, K. Mikawa et al., “The effects of clonidine and dexmedetomidine on human neutrophil functions,” *Anesthesia and Analgesia*, vol. 88, no. 2, pp. 452–458, 1999.
- [45] D. J. Pepperl and J. W. Regan, “Selective coupling of alpha 2-adrenergic receptor subtypes to cyclic AMP-dependent reporter gene expression in transiently transfected JEG-3 cells,” *Molecular Pharmacology*, vol. 44, no. 4, pp. 802–809, 1993.




- [46] D. M. Rosenbaum, S. G. Rasmussen, and B. K. Kobilka, "The structure and function of G-protein-coupled receptors," *Nature*, vol. 459, no. 7245, pp. 356–363, 2009.
- [47] A. V. Smrcka and I. Fisher, "G-protein $\beta\gamma$ subunits as multifunctional scaffolds and transducers in G-protein-coupled receptor signaling," *Cellular and Molecular Life Sciences*, vol. 76, no. 22, article 3275, pp. 4447–4459, 2019.
- [48] K. A. Meller, J. Calka, M. Kaczmarek, and B. Jana, "Expression of alpha and beta adrenergic receptors in the pig uterus during inflammation," *Theriogenology*, vol. 119, pp. 96–104, 2018.
- [49] D. Ma, N. Rajakumaraswamy, and M. Maze, " α 2-Adrenoceptor agonists: shedding light on neuroprotection?," *British Medical Bulletin*, vol. 71, no. 1, pp. 77–92, 2005.
- [50] H. Lavon, P. Matzner, A. Benbenishty et al., "Dexmedetomidine promotes metastasis in rodent models of breast, lung, and colon cancers," *British Journal of Anaesthesia*, vol. 120, no. 1, pp. 188–196, 2018.
- [51] W. X. Wang, Q. Wu, S. S. Liang et al., "Dexmedetomidine promotes the recovery of neurogenesis in aged mouse with postoperative cognitive dysfunction," *Neuroscience Letters*, vol. 677, pp. 110–116, 2018.
- [52] N. Bao, B. Tang, and J. Wang, "Dexmedetomidine preconditioning protects rats from renal ischemia–reperfusion injury accompanied with biphasic changes of nuclear factor-kappa B signaling," *Journal of Immunology Research*, vol. 2020, Article ID 3230490, 12 pages, 2020.
- [53] H. de Castro Abrantes, M. Briquet, C. Schmuziger et al., "The lactate receptor HCAR1 modulates neuronal network activity through the activation of $G\alpha$ and $G\beta\gamma$ subunits," *The Journal of Neuroscience*, vol. 39, no. 23, pp. 4422–4433, 2019.
- [54] X. Y. Zhang, Z. M. Liu, S. H. Wen et al., "Dexmedetomidine administration before, but not after, ischemia attenuates intestinal injury induced by intestinal ischemia-reperfusion in rats," *Anesthesiology*, vol. 116, no. 5, pp. 1035–1046, 2012.
- [55] V. Hanci, G. Yurdakan, S. Yurtlu, I. Ö. Turan, and E. Y. Sipahi, "Protective effect of dexmedetomidine in a rat model of α -naphthylthiourea-induced acute lung injury," *The Journal of Surgical Research*, vol. 178, no. 1, pp. 424–430, 2012.
- [56] Y. C. Yeh, C. Y. Wu, Y. J. Cheng et al., "Effects of dexmedetomidine on intestinal microcirculation and intestinal epithelial barrier in endotoxemic rats," *Anesthesiology*, vol. 125, no. 2, pp. 355–367, 2016.
- [57] Y. Li and S. Liu, "The effect of dexmedetomidine on oxidative stress response following cerebral ischemia-reperfusion in rats and the expression of intracellular adhesion molecule-1 (ICAM-1) and S100B," *Medical Science Monitor*, vol. 23, pp. 867–873, 2017.
- [58] M. R. Graham, "Clinical update regarding general anesthesia-associated neurotoxicity in infants and children," *Current Opinion in Anaesthesiology*, vol. 30, no. 6, pp. 682–687, 2017.
- [59] J. F. Perez-Zoghbi, W. Zhu, M. R. Grafe, and A. M. Brambrink, "Dexmedetomidine-mediated neuroprotection against sevoflurane-induced neurotoxicity extends to several brain regions in neonatal rats," *British Journal of Anaesthesia*, vol. 119, no. 3, pp. 506–516, 2017.
- [60] L. J. Bo, P. X. Yu, F. Z. Zhang, and Z. M. Dong, "Dexmedetomidine mitigates sevoflurane-induced cell cycle arrest in hippocampus," *Journal of Anesthesia*, vol. 32, no. 5, pp. 717–724, 2018.
- [61] Y. Shan, F. Yang, Z. Tang et al., "Dexmedetomidine ameliorates the neurotoxicity of sevoflurane on the immature brain through the BMP/SMAD signaling pathway," *Frontiers in Neuroscience*, vol. 12, p. 964, 2018.
- [62] S. Endesfelder, H. Makki, C. von Haefen, C. D. Spies, C. Bühner, and M. Sifringer, "Neuroprotective effects of dexmedetomidine against hyperoxia-induced injury in the developing rat brain," *PLoS One*, vol. 12, no. 2, article e0171498, 2017.
- [63] D. N. Wijeyesundera, J. S. Naik, and W. S. Beattie, "Alpha-2 adrenergic agonists to prevent perioperative cardiovascular complications: a meta-analysis," *The American Journal of Medicine*, vol. 114, no. 9, pp. 742–752, 2003.
- [64] B. M. Biccard, S. Goga, and J. de Beurs, "Dexmedetomidine and cardiac protection for non-cardiac surgery: a meta-analysis of randomised controlled trials," *Anaesthesia*, vol. 63, no. 1, pp. 4–14, 2008.
- [65] S. Sulaiman, R. B. Karthekeyan, M. Vakamudi, A. S. Sundar, H. Ravullapalli, and R. Gandham, "The effects of dexmedetomidine on attenuation of stress response to endotracheal intubation in patients undergoing elective off-pump coronary artery bypass grafting," *Annals of Cardiac Anaesthesia*, vol. 15, no. 1, pp. 39–43, 2012.
- [66] M. Ibacache, G. Sanchez, Z. Pedrozo et al., "Dexmedetomidine preconditioning activates pro-survival kinases and attenuates regional ischemia/reperfusion injury in rat heart," *Biochimica et Biophysica Acta*, vol. 1822, no. 4, article S0925443911002985, pp. 537–545, 2012.
- [67] W. Li, J. Yu, Z. Li, and W. B. Yin, "Rational design for fungal laccase production in the model host *Aspergillus nidulans*," *Science China. Life Sciences*, vol. 62, no. 1, pp. 84–94, 2019.
- [68] G. Wang, J. Niu, Z. Li, H. Lv, and H. Cai, "The efficacy and safety of dexmedetomidine in cardiac surgery patients: a systematic review and meta-analysis," *PLoS One*, vol. 13, no. 9, article e0202620, 2018.
- [69] D. Duncan, A. Sankar, W. S. Beattie, D. N. Wijeyesundera, and Cochrane Anaesthesia Group, "Alpha-2 adrenergic agonists for the prevention of cardiac complications among adults undergoing surgery," *Cochrane Database of Systematic Reviews*, 2018.
- [70] S. Mimuro, T. Katoh, A. Suzuki et al., "Deterioration of myocardial injury due to dexmedetomidine administration after myocardial ischaemia," *Resuscitation*, vol. 81, no. 12, pp. 1714–1717, 2010.
- [71] J. Gu, J. Chen, P. Xia, G. Tao, H. Zhao, and D. Ma, "Dexmedetomidine attenuates remote lung injury induced by renal ischemia-reperfusion in mice," *Acta Anaesthesiologica Scandinavica*, vol. 55, no. 10, pp. 1272–1278, 2011.
- [72] N. Bao and D. Dai, "Dexmedetomidine protects against ischemia and reperfusion-induced kidney injury in rats," *Mediators of Inflammation*, vol. 2020, Article ID 2120971, 8 pages, 2020.
- [73] X. Wu, X. Song, N. Li, L. Zhan, Q. Meng, and Z. Xia, "Protective effects of dexmedetomidine on blunt chest trauma-induced pulmonary contusion in rats," *Journal of Trauma and Acute Care Surgery*, vol. 74, no. 2, pp. 524–530, 2013.
- [74] C. Fu, X. Dai, Y. Yang, M. Lin, Y. Cai, and S. Cai, "Dexmedetomidine attenuates lipopolysaccharide-induced acute lung injury by inhibiting oxidative stress, mitochondrial dysfunction and apoptosis in rats," *Molecular Medicine Reports*, vol. 15, no. 1, pp. 131–138, 2017.

- [75] F. T. Billings, S. W. C. Chen, M. Kim et al., " α 2-Adrenergic agonists protect against radiocontrast-induced nephropathy in mice," *American Journal of Physiology-Renal Physiology*, vol. 295, no. 3, pp. F741–F748, 2008.
- [76] L. I. L. I. JIANG, L. LI, J. SHEN, Z. QI, and L. GUO, "Effect of dexmedetomidine on lung ischemia-reperfusion injury," *Molecular Medicine Reports*, vol. 9, no. 2, pp. 419–426, 2014.
- [77] C. L. Yang, P. S. Tsai, and C. J. Huang, "Effects of dexmedetomidine on regulating pulmonary inflammation in a rat model of ventilator-induced lung injury," *Acta Anaesthesiologica Taiwanica*, vol. 46, no. 4, pp. 151–159, 2008.
- [78] R. Xia, J. Xu, H. Yin et al., "Intravenous Infusion of Dexmedetomidine Combined Isoflurane Inhalation Reduces Oxidative Stress and Potentiates Hypoxia Pulmonary Vasoconstriction during One-Lung Ventilation in Patients," *Mediators of Inflammation*, vol. 2015, Article ID 238041, 7 pages, 2015.
- [79] E. Erturk, S. Topaloglu, D. Dohman et al., "The Comparison of the Effects of Sevoflurane Inhalation Anesthesia and Intravenous Propofol Anesthesia on Oxidative Stress in One Lung Ventilation," *BioMed Research International*, vol. 2014, Article ID 360936, 4 pages, 2014.
- [80] S. Andonian, T. Coulthard, A. D. Smith, P. S. Singhal, and B. R. Lee, "Real-time quantitation of renal ischemia using targeted microbubbles: in-vivo measurement of P-selectin expression," *Journal of Endourology*, vol. 23, no. 3, pp. 373–378, 2009.
- [81] A. J. Rouch, L. H. Kudo, and C. Hebert, "Dexmedetomidine inhibits osmotic water permeability in the rat cortical collecting duct," *The Journal of Pharmacology and Experimental Therapeutics*, vol. 281, no. 1, pp. 62–69, 1997.
- [82] A. Junaid, L. Cui, S. B. Penner, and D. D. Smyth, "Regulation of aquaporin-2 expression by the alpha (2)-adrenoceptor agonist clonidine in the rat," *The Journal of Pharmacology and Experimental Therapeutics*, vol. 291, no. 2, pp. 920–923, 1999.
- [83] M. Cakir, A. Polat, S. Tekin et al., "The effect of dexmedetomidine against oxidative and tubular damage induced by renal ischemia reperfusion in rats," *Renal Failure*, vol. 37, no. 4, pp. 704–708, 2015.
- [84] P. K. Chatterjee, Y. al-Abed, B. Sherry, and C. N. Metz, "Cholinergic agonists regulate JAK2/STAT3 signaling to suppress endothelial cell activation," *American Journal of Physiology. Cell Physiology*, vol. 297, no. 5, pp. C1294–C1306, 2009.
- [85] W. J. de Jonge, E. van der Zanden, F. O. The et al., "Stimulation of the vagus nerve attenuates macrophage activation by activating the Jak 2-STAT3 signaling pathway," *Nature Immunology*, vol. 6, no. 8, pp. 844–851, 2005.
- [86] Y. J. Ji, H. N. Liu, X. F. Kong et al., "Use of insect powder as a source of dietary protein in early-weaned piglets1," *Journal of Animal Science*, vol. 94, suppl_3, pp. 111–116, 2016.
- [87] X. Yu, X. Chi, S. Wu et al., "Dexmedetomidine Pretreatment Attenuates Kidney Injury and Oxidative Stress during Orthotopic Autologous Liver Transplantation in Rats," *Oxidative Medicine and Cellular Longevity*, vol. 2016, Article ID 4675817, 10 pages, 2016.
- [88] Y. Chen, X. Feng, X. Hu et al., "Dexmedetomidine Ameliorates Acute Stress-Induced Kidney Injury by Attenuating Oxidative Stress and Apoptosis through Inhibition of the ROS/JNK Signaling Pathway," *Oxidative Medicine and Cellular Longevity*, vol. 2018, Article ID 4035310, 12 pages, 2018.
- [89] Z. Chen, D. H. Shao, Z. M. Mao, L. L. Shi, X. D. Ma, and D. P. Zhang, "Effect of dexmedetomidine on blood coagulation in patients undergoing radical gastrectomy under general anesthesia: a prospective, randomized controlled clinical trial," *Medicine (Baltimore)*, vol. 97, no. 27, article e11444, 2018.
- [90] T. Sahin, Z. Begeç, H. İ. Toprak et al., "The effects of dexmedetomidine on liver ischemia-reperfusion injury in rats," *The Journal of Surgical Research*, vol. 183, no. 1, pp. 385–390, 2013.
- [91] J. Sha, H. Zhang, Y. Zhao et al., "Dexmedetomidine attenuates lipopolysaccharide-induced liver oxidative stress and cell apoptosis in rats by increasing GSK-3 β activity via the α 2 adrenergic receptor," *Toxicology and Applied Pharmacology*, vol. 364, article S0041008X18305763, pp. 144–152, 2019.
- [92] C. Yang, L. He, C. Wang et al., "Dexmedetomidine alleviated lipopolysaccharide/D-galactosamine-induced acute liver injury in mice," *International Immunopharmacology*, vol. 72, pp. 367–373, 2019.
- [93] K. Wang, Z. Wan, A. Ou et al., "Monofloral honey from a medical plant, *Prunella vulgaris*, protected against dextran sulfate sodium-induced ulcerative colitis via modulating gut microbial populations in rats," *Food & Function*, vol. 10, no. 7, pp. 3828–3838, 2019.
- [94] K. Wang, X. Jin, Q. Li et al., "Propolis from Different Geographic Origins Decreases Intestinal Inflammation and Bacteroides spp. Populations in a Model of DSS-Induced Colitis," *Molecular Nutrition & Food Research*, vol. 62, no. 17, article 1800080, 2018.
- [95] R. P. Dickson, "The microbiome and critical illness," *The Lancet Respiratory Medicine*, vol. 4, no. 1, article S2213260015004270, pp. 59–72, 2016.
- [96] Z. X. Wang, C. Y. Huang, Y. P. Hua, W. Q. Huang, L. H. Deng, and K. X. Liu, "Dexmedetomidine reduces intestinal and hepatic injury after hepatectomy with inflow occlusion under general anaesthesia: a randomized controlled trial," *British Journal of Anaesthesia*, vol. 112, no. 6, pp. 1055–1064, 2014.
- [97] S. Kuru, O. B. Bozkirli, A. M. Barlas et al., "The preventive effect of dexmedetomidine against postoperative intra-abdominal adhesions in rats," *International Surgery*, vol. 100, no. 1, pp. 87–95, 2015.
- [98] C. Aydin, I. Bagcivan, S. GURSOY, A. Altun, O. Topcu, and A. Koyuncu, "Altered spontaneous contractions of the ileum by anesthetic agents in rats exposed to peritonitis," *World Journal of Gastroenterology*, vol. 15, no. 13, pp. 1620–1624, 2009.
- [99] M. K. Herbert, S. Roth-Goldbrunner, P. Holzer, and N. Roewer, "Clonidine and dexmedetomidine potently inhibit peristalsis in the guinea pig ileum in vitro," *Anesthesiology*, vol. 97, no. 6, pp. 1491–1499, 2002.
- [100] T. Iirola, S. Vilo, R. Aantaa et al., "Dexmedetomidine inhibits gastric emptying and oro-caecal transit in healthy volunteers," *British Journal of Anaesthesia*, vol. 106, no. 4, pp. 522–527, 2011.
- [101] Y.-C. Yeh, W.-Z. Sun, W.-J. Ko et al., "Dexmedetomidine Prevents Alterations of Intestinal Microcirculation That Are Induced by Surgical Stress and Pain in a Novel Rat Model," *Anesthesia and Analgesia*, vol. 115, no. 1, pp. 46–53, 2012.
- [102] T. Taniguchi, A. Kurita, K. Kobayashi, K. Yamamoto, and H. Inaba, "Dose- and time-related effects of dexmedetomidine on mortality and inflammatory responses to

- endotoxin-induced shock in rats," *Journal of Anesthesia*, vol. 22, no. 3, pp. 221–228, 2008.
- [103] C. Xie, Z. Wang, J. Tang, Z. Shi, and Z. He, "The effect of dexmedetomidine post-treatment on the inflammatory response of astrocyte induced by lipopolysaccharide," *Cell Biochemistry and Biophysics*, vol. 71, no. 1, pp. 407–412, 2015.
- [104] Y. C. Lai, P. S. Tsai, and C. J. Huang, "Effects of Dexmedetomidine on Regulating Endotoxin-Induced Up-Regulation of Inflammatory Molecules in Murine Macrophages," *The Journal of Surgical Research*, vol. 154, no. 2, article S0022480408004654, pp. 212–219, 2009.

Review Article

Detection and Prognosis of Prostate Cancer Using Blood-Based Biomarkers

Wei Jin ¹, Xiang Fei,¹ Xia Wang,¹ Yan Song ¹ and Fangjie Chen ²

¹Department of Urology, Shengjing Hospital of China Medical University, Shenyang, Liaoning, China

²Department of Medical Genetics, School of Life Sciences, China Medical University, Shenyang, Liaoning, China

Correspondence should be addressed to Fangjie Chen; chenfj@cmu.edu.cn

Received 28 February 2020; Revised 24 March 2020; Accepted 27 April 2020; Published 4 May 2020

Guest Editor: Xiaolu Jin

Copyright © 2020 Wei Jin et al. This is an open access article distributed under the Creative Commons Attribution License, which permits unrestricted use, distribution, and reproduction in any medium, provided the original work is properly cited.

Prostate cancer (PCa) is second only to lung cancer as a cause of death. Clinical assessment of patients and treatment efficiency therefore depend on the disease being diagnosed as early as possible. However, due to issues regarding the use of prostate-specific antigen (PSA) for screening purposes, PCa management is among the most contentious of healthcare matters. PSA screening is problematic primarily because of diagnosis difficulties and the high rate of false-positive biopsies. Novel PCa biomarkers, such as the Prostate Health Index (PHI) and the 4Kscore, have been proposed in recent times to improve PSA prediction accuracy and have shown higher performance by preventing redundant biopsies. The 4Kscore also shows high precision in determining the risk of developing high-grade PCa, whereas elevated PHI levels suggest that the tumor is aggressive. Some evidence also supports the effectiveness of miRNAs as biomarkers for distinguishing PCa from benign prostatic hyperplasia and for assessing the aggressiveness of the disease. A number of miRNAs that possibly act as tumor inhibitors or oncogenes are impaired in PCa. These new biomarkers are comprehensively reviewed in the present study in terms of their potential use in diagnosing and treating PCa.

1. Overview

Prostate cancer (PCa), which manifests as solid tumors, is the most prevalent form of cancer in male individuals. PCa is second only to lung neoplasms in terms of mortality rate, and its incidence rises with age in numerous countries. In the US alone, around 2.8 million male individuals are diagnosed annually with PCa [1]. A marked increase has also been noted recently in the incidence of PCa in China due to factors such as lifestyle changes and more efficient diagnosis. The incidence of PCa may also differ due to different dietary habits. Dietary factors, like the consumption of protein, fat, carbohydrates, vitamins, and polyphenols, may have an important role in PCa pathogenesis [2, 3]. Adequate diet and physical activity trigger alterations in the serum factors that retard the development of androgen-reliant PCa cells and cause them to die [2, 4]. Conversely, PCa can be promoted by a high body mass index, hypertension, and a number of metabolic factors [5, 6]. PCa is characterized by a high degree of inhomogeneity, as it can manifest as either latent

forms or highly aggressive forms that lead to morbidity and death due to metastasis to other parts of the body [7–9].

PCa screening is based on the use of the prostate-specific antigen (PSA), a feature that has made this disease notably contentious within the healthcare field. PCa exhibited a staggering rise in incidence during the period from 1986–1991, when the PSA test first became available. However, subsequent prostate biopsies frequently revealed no correlation between elevated PSA levels and the presence of cancer in many cases. Indeed, PSA levels do not exceed 4.0 $\mu\text{g/L}$ in 20–25% of the cases with a PCa diagnosis [10]. The results of cytology or histopathology are the basis of a confirmed PCa diagnosis, especially in cases where the PSA levels lie between 4 and 10 $\mu\text{g/L}$ —the so-called “grey area.” By contrast, about one-quarter of the cases with PSA levels of 2–10 $\mu\text{g/L}$ has positive biopsies.

PSA is not an exclusive marker of cancer because it is produced by cancerous prostate cells and by healthy prostate cells. Therefore, factors such as a large prostate size, benign prostatic hyperplasia (BPH), or prostatitis can trigger false

positives and result in an incorrect PCa diagnosis and treatment [11]. The United States Preventive Services Task Force issued a recommendation in 2018 that PCa screening should not be performed on the basis of PSA levels in cases of male individuals refusing the procedure or in male individuals 70 years of age or older [12]. Furthermore, unimportant tumors may be excessively detected due to PSA-based screening, leading to unnecessary treatment. In addition, the possible positive outcomes of screening are no greater than the adverse outcomes of excessive detection and unnecessary treatment [13]. Diagnosis of PCa based only on PSA levels is therefore gradually losing its appeal as a clinical approach [14]; however, this has not put an end to the controversy surrounding screening [15, 16]. A recent study suggested that although discontinuation of PSA-based screening would eliminate excessive diagnoses, the lack of screening would lead to a complete failure to avoid preventable deaths and would increase the PCa-related mortality rate by 13–20% [17].

In recent times, various initiatives have been launched to identify novel subtypes of PSA that could make PSA-based screening more precise for diagnosing early PCa and formulating a prognosis for it. These initiatives have yielded several novel PCa biomarkers, including the PHI, a biomarker that has received the approval of the US Food and Drug Administration (FDA) for prostate cancer detection [18]. Another PCa biomarker is the 4Kscore, otherwise known as the 4-kallikrein panel, which screens for total PSA, fPSA, intact PSA (iPSA), and human kallikrein 2. MicroRNAs are another source of promising PCa biomarkers that have emerged as potential alternatives to PSA, owing to the progress being made in deep sequencing technology [19]. Taking all these aspects into account, the aim of the present study is to review the new understanding that has been achieved regarding PCa blood-based biomarkers and the role that they can play in diagnosing and treating early PCa.

2. The Prostate Health Index (PHI)

The importance of proPSA as a component of fPSA was highlighted in 1997 by the revelation that the serum of individuals with PCa contained truncated proPSA forms [20]. Preliminary findings confirmed that PCa could be detected based on proPSA isoforms, leading to fewer negative biopsies in cases with PSA levels in the “grey area.” A reliable immunoassay has since been made available on the market by Beckman Coulter to assess [-2] proPSA, and this immunoassay has been extensively investigated for its relevance for use in managing early PCa. Overall, PCa patients have a notably higher ratio of [-2] proPSA to fPSA (%p2PSA).

The [-2] proPSA immunoassay has now been integrated alongside fPSA and tPSA in the PHI test. This test is highly specific for PCa of clinical importance and has proven effective in detecting this disease [21, 22]. It enables differentiation between benign prostatic hyperplasia (BPH) and PCa in suspected cases, but it can also enhance the accuracy of detection of high-grade cancer, thereby preventing redundant biopsies. In June 2012, this biomarker received FDA approval for use in detecting PCa in male individuals 50 years

of age or older who had PSA levels of 4–10 $\mu\text{g/L}$ and had undergone a digital rectal examination (DRE) without abnormal outcomes. The National Comprehensive Cancer Network also endorses the PHI test in cases where a biopsy has not been conducted or has produced negative results, and the Network specifies that a significant risk of PCa is reflected by PHI results higher than 35 [23].

Prospective research conducted in multiple centers among a sample of 2499 men has indicated that the use of PHI values higher than 30 at 90% sensitivity for high-grade PCa (HGPC) (Gleason ≥ 7) could have prevented Gleason 6 PCa diagnoses in 33% of the cases and biopsies in 56% of the cases of Asian men. Similarly, the use of PHI higher than 40 at 90% HGPC sensitivity could have prevented Gleason 6 PCa diagnoses in 31% of the cases and biopsies in 40% of the cases of Caucasian men [24, 25]. Prediction of biopsy results based on PHI and the %p2PSA score has now been advocated by a number of researchers. The usefulness of these measurements in cases where the PSA levels fall between 2 and 10 $\mu\text{g/L}$ has been demonstrated by two studies conducted in multiple centers in 1362 and 646 patients. The %p2PSA was associated with an area under the curve (AUC) value of 0.72, while the PHI was associated with an AUC value of 0.74 [23]. Both biomarkers considered together were associated with an AUC value of 0.67 [26]. Chiu et al. suggested that PHI was effective in cancer risk stratification for both European and Asian subjects [25]. However, population-specific PHI reference ranges were different and should be used [25]. These findings support the relevance of the PHI test for identifying cases among Asian and Caucasian individuals with a high risk of PCa and thereby minimizing redundant biopsies and excessive PCa diagnosis.

When compared with the total PSA and %fPSA, the combination of %p2PSA and PHI provided a greater precision of PCa detection at biopsy [23, 27]. Furthermore, the two biomarkers were well-correlated with tumor aggressiveness, occurring at higher levels in cases of Gleason > 6 . These findings have been confirmed by two meta-analyses from 2013 and 2014, which indicated that %p2PSA and PHI were, respectively, associated with AUCs of 0.635–0.78 and 0.69–0.781 [28, 29]. These meta-analyses additionally highlighted the superior outcomes obtained with these two biomarkers compared with those obtained with PSA and %fPSA. The latter observation was reinforced by a later meta-analysis, which undertook a comparison between PHI and %fPSA in cases with total PSA levels of 2–10 $\mu\text{g/L}$. In that meta-analysis, PHI had an AUC value of 0.74, while %fPSA had an AUC value of 0.63 [30].

Some researchers have argued that PCa could be predicted clinically with greater accuracy by incorporating PHI and %p2PSA into multivariate models that take into account the integration of PSA and a range of clinical and demographic factors. For instance, the incorporation of PHI and %p2PSA into a multivariate model based on patient age, prostate volume, PSA, and %fPSA was reported to increase the AUC value from 0.762 to 0.802 or 0.815, depending, respectively, on whether a logistic regression analysis or an artificial neural network was applied [31]. Similarly, a different study on 112 patients with Gleason 6 who underwent

radical prostatectomy reported that the patients with a final histology upgrade to Gleason 7 or higher exhibited markedly increased PHI values [32]. Another study found that PHI had an AUC value of 0.815 for the detection of HGPC in cases of Gleason 7 or higher [33] and suggested that the ideal PHI cut-off point of 24 at 95% sensitivity for detection of aggressive PCa. The use of this cut-off point prevented redundant biopsies in 41% of the cases. By contrast, an active monitoring program involving 167 patients revealed that the baseline and longitudinal %p2PSA and PHI levels allowed better prediction of renewed biopsy categorization at follow-up, whereas total PSA level showed no similar correlation with renewed biopsy categorization [34].

3. The 4Kscore

Another test that can predict the likelihood of occurrence of high-risk PCa is the 4Kscore or 4-kallikrein panel. The 4Kscore consists of four kallikrein blood markers—total PSA, free PSA (fPSA), intact PSA (iPSA), and the human kallikrein-related peptide 2 (hK2)—and has received ample research attention. For example, researchers from the Memorial Sloan-Kettering Cancer Center have found an association between the 4Kscore and AUC values that exceeded not only the AUC values associated with a PSA-based model for the detection of all types of PCa (AUCs = 0.674 – 0.832) but also the AUC values for HGPC detection with Gleason of 7 or higher (AUCs = 0.793 – 0.870) [35, 36]. A comparison of the equivalent clinical models for high-risk PCa prediction yielded similar results. The model incorporating the variables of PSA, patient age, and DRE had AUC values of 0.709–0.868, whereas the addition of fPSA, iPSA, and hK2 to the model led to AUC values of 0.798–0.903 [37].

One major factor that PCa risk predictions typically take into account is prostate volume, as this factor has an impact on the levels of PSA in the serum. However, one study reported that the method used to perform the 4Kscore to detect PCa was unaffected by the prostate volume [38]. This was the conclusion reached from a biomarker investigation in two groups of patients ($n = 2914$, $n = 740$, respectively) with PSA levels of 3 $\mu\text{g/L}$ or higher. The inclusion of the prostate volume in a model underpinned by 4Kscore, patient age, and DRE led to an increase in AUC from 0.856 to 0.860 in the first group, whereas the inclusion or exclusion of the prostate volume made no difference to the AUC value in the second group (0.802).

The 4Kscore was made available on the market by Opko Diagnostics. It constitutes an algorithm that generates predictions about HGPC by integrating the 4-kallikrein panel with patient age, DRE, and history of previous biopsy. The US Food and Drug Administration FDA has not yet approved this test, but the National Comprehensive Cancer Network issued a recommendation in June 2015 that the 4Kscore could be employed to screen for HGPC in cases where biopsy had either not been conducted or where it had produced negative results [39, 40].

In a prospective study conducted in 26 urology centers throughout the US, the 4Kscore achieved an AUC value of 0.82 when it was used to assess 1012 male patients about to

undergo a prostate biopsy. The use of a 6% cut-off point was found to eliminate the necessity of a biopsy in 30% of the cases and deferred diagnosis in only 1.3% of the HGPC cases [41]. By contrast, a different study reported that the 4Kscore enabled the prediction of HGPC in cases with PSA levels exceeding 10 $\mu\text{g/L}$ or with a positive DRE [42]. This ability of the 4Kscore to decrease the number of biopsies without overlooking a significant proportion of HGPCs has been highlighted by a number of studies [43, 44]. The biopsy was deemed unnecessary in approximately half of the 262 cases scheduled for prostate biopsy because of PSA levels of 3 $\mu\text{g/L}$ or higher, but the diagnosis of aggressive PCa was overlooked in just 1% of these cases when the 4Kscore was used [45]. A different study on a sample of 740 male individuals who had been referred for biopsy due to high PSA levels reported comparable results [46].

The efficacy of the 4Kscore for predictions was demonstrated by a study initiated in 1986 in Sweden on a sample of patients of different ages (40, 50, and 60 years old) [47]. The patients were divided into two groups based on their 4Kscore outcomes at 50 and 60 years of age to determine how likely they were to develop remote metastasis after two decades. The study concluded that remote metastasis was more likely to develop in patients with a 4Kscore exceeding 5 at 50 years of age and with PSA levels of 2 $\mu\text{g/L}$ or higher, as well as in patients with a 4Kscore exceeding 7.5 at 60 years of age and PSA levels of 3 $\mu\text{g/L}$ or higher. Biopsy was considered unnecessary in cases that had moderate increases in PSA levels during midlife and a low risk of HGPC based on the 4Kscore. A different study on 1423 PCa patients showed that remote metastasis occurred in 235 patients with PSA levels exceeding 2 $\mu\text{g/L}$. However, metastasis was much better predicted by a prespecified model underpinned by the four kallikrein markers than by PSA alone [47]. On the whole, the available research results support the efficiency of the 4Kscore for use in early PCa diagnosis and prognosis.

One study compared the efficacy of the 4Kscore and PHI in a sample of 531 male individuals with PSA levels of 3–15 $\mu\text{g/L}$. Neither biomarker differed markedly in the detection of either any-grade PCa or HGPC. The 4Kscore had AUC values of 0.69 and 0.718, while the PHI had AUC values of 0.704 and 0.711 [48].

4. The Usefulness of MicroRNAs as PCa Biomarkers

4.1. miRNAs and PCa. Ample research has recently explored the function of protein-coding genes in oncogenesis. Transcription of the human genome to messenger RNA (mRNA) occurs in a proportion of 90%, but protein encoding is undertaken by just 2% of the genome. Therefore, many RNAs do not encode for any protein. According to the findings from the latest studies, a genome segment without protein encoding is involved in oncogenesis [49, 50].

The expression of genes is regulated by endogenously expressed small, noncoding, single-stranded RNAs known as microRNA (miRNAs). Adverse regulation of gene expression by miRNA genes occurs after transcription, with the miRNA genes attaching primarily to the 3' untranslated

region (3'-UTR) of the coding gene, thereby suppressing mRNA translation. In the case of PCa, this suppression also promotes pathways for PCa progression by triggering translational repression or mRNA deterioration [49, 50]. The types of miRNA complexes present in human plasma and serum were investigated in one study by differential centrifugation and size-exclusion chromatography of the miRNAs [51]. Most of the miRNAs were found in the plasma and serum in a form that did not undergo membrane binding, whereas a few were vesicle-associated miRNAs. A different study suggested that miRNAs from human serum, saliva, and other biological fluids could be made more sensitive through exosome isolation [52].

The physiological and pathological processes showing miRNA involvement include development, differentiation, metabolism, immunity, proliferation, apoptosis, senescence, cell identity, and stem cell maintenance [50, 53]. A number of miRNAs that participate in the development of human cancer have been identified, and these appear to act as oncogenic factors that prevent the activity of tumor-suppressing genes or as tumor-suppressing miRNAs that activate oncogenes [54].

Novel biomarkers for the diagnosis and prognosis of cancer can be discovered by investigating cancer-related abnormal miRNA expression profiles. Many methods have been used to detect miRNAs, including northern blotting, next-generation sequencing (or RNA sequencing, RNA-Seq), microarrays analysis, reverse transcription PCR (RT-PCR), highly sensitive biosensors, and computational prediction [55]. In 2008, the first circulating miRNA profile of the serum of patients with diffuse large B-cell lymphoma was published as an aid for cancer diagnosis [56]. In many human cancers, the processes of development, invasion, and progression occur through direct involvement of hundreds of miRNAs with modified expression, and the cancer-related genomic area contains approximately half of the miRNA genes. PCa development is promoted by this type of dysfunctional regulation through the upregulation of oncogene modulation or downregulation of tumor inhibitors [50].

The current findings indicate the notable feature that the classification of human cancer origins can be based on miRNA signatures [57]. Thus, metastatic cancers of unknown origin can be effectively identified with high tissue specificity based on their miRNAs. For instance, a study of 208 tumors consisting of 15 distinct histologies, including PCa, revealed successfully and estimated the primary tumor origin by profiling miRNA expression in paraffin-embedded tissue [58]. A novel algorithm formulated in that study also categorized the miRNAs with 85% general precision (CI: 79–89%). This algorithm was successful in determining the primary origin of 42 of 48 metastases (88% precision; CI: 75–94%). However, these results must be verified by further research.

Several studies have highlighted an association between PCa and the modifications observed in the expression of miRNAs, which are associated with dysfunctional cell proliferation, differentiation, progression, and other processes [59, 60]. Comprehending the mechanism by which miRNAs interact with their targets and the implications of those inter-

actions for PCa development is important for identifying the central part played by miRNAs in PCa [61]. This comprehension can also help in developing efficient treatment interventions, especially because aberrant miRNA expression is now viewed as a useful biomarker for diagnosing and classifying PCa and for determining its prognosis [62].

4.2. Oncogenic miRNAs and PCa. Cancer cell progression is promoted by miRNAs that serve as oncogenic miRNAs [63]. Calin and colleagues [64] were the first to investigate the correlation between miRNA dysregulation and cancer. Specifically, the authors observed that the dysregulation of miR-15 and miR-16 contributed to the development of chronic lymphocytic leukemia. PCa is typically associated with overexpression of miRNAs (e.g., miR-21, miR-32, miR-221, miR-222, miR-181, miR-18a, and miR-429) that have a crucial function in the regulation of PI3K/AKT, the epithelial-to-mesenchymal transition (EMT), cell proliferation, apoptosis, and androgen receptor (AR) expression [65, 66].

The androgen-regulated oncogenic miRNAs with expression in PCa include miR-21 and miR-32 [67]. MiR-21 regulates the expression of a large number of mRNA targets associated with microvascular proliferation and tumor invasiveness, and its expression is correlated with weak biochemical recurrence-free survival. Therefore, miR-21 expression can be used to estimate the probability of biochemical recurrence in PCa patients who have undergone radical prostatectomy [68]. The expression of miR-21 is also associated with castration resistance and metastasis, and its level increases linearly with clinical parameters such as the Gleason score and lymph node metastasis [59]. A study conducted on patients who had undergone radical prostatectomy revealed a close correlation between elevated miR-21 levels and advanced disease staging, lymph node metastasis, and poor patient outcomes. A multivariate analysis revealed that miR-21 expression was an independent estimator of biochemical recurrence after five years [69]. Hence, miR-21 can be used as a biomarker that anticipates cancer progression [70].

An additional miRNA with androgen regulation (via dihydrotestosterone [DHT] stimulation) is miR-32. This miRNA has a higher expression in castration-resistant prostate cancer (CRPC) cases than in benign prostatic cases. Its oncogenic activity includes targeting B-cell translocation gene 2 (BTG-2) as well as phosphoinositide-3-kinase interacting protein 1 (PIK3IP1). This miRNA suppresses apoptosis and encourages cells to proliferate by stimulating cell growth, as revealed by observations of miR-32 effects in the LNCaP PCa cell line. On the whole, miR-32 manifests its oncogenic activity by targeting the tumor-suppressing genes that control the ability of cells to proliferate, survive, and migrate [71, 72].

The oncogenic reprogramming of PCa-mobilized stem cells is believed to occur with the involvement of oncogenic miR-125b, miR-130b, and miR-155 [73, 74]. Mechanistic studies confirm that stem cell neoplastic reprogramming is likely triggered by miR-125b and miR-155 exosomal trafficking via targeted suppression of the sizable tumor-

suppressor homolog2 and programmed cell death by the neoplastic transformation suppressor protein 4 [75]. Furthermore, miR-125 has been observed to target apoptosis-promoting genes in PCa, thus functioning as an oncogene [76]. Apoptosis is suppressed and cell proliferation is intensified when miR-125b, a miRNA triggered by an androgen receptor, is activated in the LNCaP cells. Some evidence supports miR-125b targeting of the mediator of Mdm2 sequestration, p14^{ARF} and subsequent disruption of Mdm2 deterioration, and triggering of the p53 network [77].

The expression of p27^{Kip1}, which regulates the cell cycle, is susceptible to the effects of several miRNAs, such as miR-221, miR-222, and miR-429 [78]. Two of these, miR-221 and miR-222, are encoded on the X chromosome and share a seed sequence. Both of these miRNAs manifest their oncogenic effects by targeting a number of tumor-suppressing genes, and they both display overexpression in PCa. Abnormal expression of these two miRNAs can aid in prognosis because this expression has a close association with metastatic CRPC [78].

A modified miR-9 signature has been correlated with the progression and metastasis of PCa [79]. Similarly, miR-27a targets prohibition in PCa, thereby regulating AR processing [61]. PCa tissues and cell lines also show high expression of miR-18, which targets the tumor-suppressing serine/threonine-protein kinase 4, thereby functioning as an oncogenic miRNA [80]. One study showed that the inhibition of miR-18a slowed PCa cell and tumor growth by promoting apoptosis triggered by Akt dephosphorylation with STK4 mediation [80]. These findings support the use of the peripheral blood oncogenic miR-18a as a noninvasive PCa biomarker and for differentiating PCa from BPH [81].

Important stages in PCa progression are associated with poor prognosis; these include bone metastasis and events affecting the skeleton [82]. Extensive research has been conducted on the involvement of miRNAs in cancer metastasis. PCa has been associated with the upregulation of miR-96, miR-154, and miR-409-5p, which are likely very important promoters of cancer colonization of bone during metastasis [83–86]. Additional evidence produced by targeting major fibroblast-activating molecules has shown a correlation between PCa progression and increased expression of miR-133b, miR-409, and miR-210 [84, 85].

4.3. Tumor-Suppressing miRNAs and PCa. Tumor-suppressing gene action may be an additional function of miRNAs. Cancer cells generally exhibit downregulation of tumor-suppressing miRNAs, thereby promoting proliferation [87], the epithelial-mesenchymal transition (EMT), invasiveness, and metastasis. PCa progression could be monitored by evaluating the expression pattern of tumor-suppressing miRNA as a biomarker, and the same pattern could also be targeted by various treatment interventions [88].

Reduced expression of miRNA has been associated with cancer progression in a number of studies. PCa with castration resistance can develop through priming of AR and AR-V7 upregulation with hnRNPH1 mediation following dysregulation of miR-212 [89]. The PCa tumor promoter EGFR is targeted by miR-133 and miR-146a, thereby pre-

venting disease progression. Therefore, intensified EGFR signaling may explain the loss of these two biomarkers and the subsequent aggressive progression of PCa [90]. Evidence has also been produced to indicate that the LNCaP, DU145, and PC3 PCa cell lines, as well as PCa tissues, exhibit reduced expression of miR-335 [91]. Another miRNA that inhibits tumors is miRNA-30a, a miRNA that targets sine oculis homeobox homolog 1 to prevent cancerous cells from proliferating and invading other tissues [92].

PCa is also associated with the downregulation of miR-145, miR-200, miR-29b, miR-205, and miR-940, which leads to the upregulation of genes associated with the EMT. During the EMT, cells lose their attachment to other cells, and epithelial cells acquire the abilities of migration and invasion through conversion to mesenchymal stem cells capable of differentiation into various other cell types. Reduced expression of miR-29b and miR-130b in PCa is also correlated with extracellular matrix regulation through the targeting of matrix metalloproteinase 2 (MMP2) [93, 94]. EMT and cancer invasion are inhibited by miR-200 members through a direct suppression of the zinc-finger E-box binding homeobox 1 and 2 (ZEB1 and ZEB2) translation factors [95]. Both prostate tumors and cancer cell lines have been associated with miR-200b downregulation, and miR-200b expression contributes significantly to the regulation of tumor invasion, metastasis, and chemosensitivity [96]. Enhanced expression of miR-200b targets Bmi-1, thereby preventing the proliferation and migration of PCa cells, as well as increasing PCa cell chemosensitivity to docetaxel.

In general, hindering the EMT by miR-200c appears to support the maintenance of the “epithelialness” of cancer cells [97, 98]. According to one study, PCa was prevented from progressing by miR-205 downregulation that targets laminin-332, integrin- β 4, and MMP-2 to regulate the extracellular matrix [99]. In addition, miR-205 targets the Bcl-2 protein to suppress apoptosis. The loss of miR-205 is significant in androgen-autonomous expression equivalent to Bcl-2 upregulation and possibly in reduced sensitivity to docetaxel in PCa [100].

An association has been established between decreased expression of miR-146a in PCa and angiogenesis suppression through targeting of the epidermal growth factor receptor pathway [101]. The progression and metastasis of PCa are stimulated by miR-1 downregulation through targeting of Src and TWIST1 [102]. EMT regulation and PCa progression are also mediated by targeted downregulation through the loss of miR-154 due to stromal antigen 2 (STAG2), the loss of miR-203 due to tumor growth factor- α (TGF- α), and the loss of miR-224 due to Tribbles Pseudokinase 1 (TRIB1) [103, 104].

The original members of the family of tumor-suppressing miRNAs are miR-15a and miR-16. These two miRNAs are in charge of regulating the expression of numerous oncogenes, such as BCL2, MCL1, CCND1, and WNT3A. The effects of miR-15 and miR-16-1 on the BCL2 gene product trigger apoptosis [105–107]. By contrast, the loss of these two miRNAs elevates the levels of cyclin D1, an important regulator of the transition from the G1 to the S phase. The loss of these two miRNAs also activates the WNT3a gene and the

precancerous Wnt signaling pathway. Notably, cancer progression is stimulated by the cooperation between increased miR-21 expression and the loss of miR-15 and miR-16, as revealed by mouse models of PCa. One study found that some PCa patients exhibited deregulated miR-15/miR-16 and miR-21, and this deregulation was related to suboptimal prognosis and disease-free survival [108].

The expression and activity of the AR gene also seem to be targeted by a number of tumor-suppressing miRNAs. Proliferation is inhibited and apoptosis intensified by miR-488* [109], which can successfully reduce the expression of the AR protein in androgen-responsive as well as androgen-refractory PCa cells. PCa cells that overexpress miR-488* have also been shown to have lower PSA expression. Similarly, the direct downregulation of AR expression by excessive expression of miR-488* in PCa cells can prevent cell growth and enhance apoptosis [109].

AR expression is significantly affected by miRNAs like miR-125b, miR-135a, and miR-27a [76, 110]. Androgen-responsive PCa cells display the upregulation of miR-135a, which therefore seems to have a tumor-inhibiting effect. An androgen-responsive component is also demonstrated by miR-125b in the gene promoter area. Research on castrated mice revealed that the upregulation of miR-125b caused prostate tumor xenografts to exhibit androgen-independent growth, suggesting that the miRNA suppressed apoptosis [110].

AR expression regulates the expression of miR-27a as well. The expression of prohibitin, a tumor-suppressing gene, and AR corepressor, is downregulated when miR-27a expression is increased through androgen mediation. By facilitating a reduction in the expression of the prohibitin protein product, miR-27a upregulates the AR target gene expression and enhances the growth of PCa cells [111]. On the whole, the wide range of functions fulfilled by miRNAs in PCa development has received substantial attention in the search to understand how miRNAs aid and inhibit the disease process.

4.4. Exosomal miRNAs. The shortcomings of the existing protocols for PCa screening call for the discovery of novel biomarkers. Effective management of this disease and improvements in prognosis and survival can only come with protocols that will allow the detection and classification of prostate tumors as early as possible. Another potential source of biomarkers is exosomes. These nanovesicles measure 50–150 nm and are found in cells as early endosomes that contain miRNAs, mRNA, proteins, and lipids. Exosomes play a key role in intercellular communication and in the regulation of recipient cell biology, as well as in a range of physiological and pathological processes [112]. Some evidence now supports the idea that miRNA can be reliably sourced from blood-derived exosomes to identify disease biomarkers [113, 114].

In numerous tumor types, prognosis has been predicted based on exosomal miRNAs recovered from the blood [115]. The relevance of using the miRNAs found in exosomes to manage PCa was investigated in a few studies. Two of these studies have suggested that PCa could be differentiated based on miR-141 upregulation [116, 117]. Another study

reported that PCa was associated with the upregulation of both miR-141 and miR-375 and that disease progression was correlated with the serum levels of these miRNAs [118]. A correlation has also been established between poor survival outcomes and plasma levels of exosomal miR-1290 and miR-375. Better predictions were achieved when these novel biomarkers were included in a clinical prognostic model [119, 120]. miR-574-3p, miR-141-5p, and miR-21-5p were markedly upregulated in urinary exosomes from PCa patients extracted via lectin-based exosome agglutination [121]. By contrast, extraction of urinary exosomes by differential centrifugation revealed a marked increase only in the expression of miR-141. The presence of miR-19b was also examined in urinary exosomes extracted via differential centrifugation and revealed good potential for PCa detection [122].

Despite the inconsistencies in the reported results, the initial findings regarding exosomal biomarkers are encouraging. However, the determination of the usefulness of exosomes will first require standardization of the isolation and profiling methods and the performance of extensive clinical trials. Furthermore, miRNAs are not without their shortcomings and difficulties, just like other novel biomarkers for cancer. These shortcomings and difficulties stem from differences in how samples are selected, handled, processed, and prepared, as well as from disagreements regarding data normalization. Consequently, before miRNAs can be employed clinically, those shortcomings and difficulties must be addressed.

5. Conclusion

A great deal of inhomogeneity occurs in PCa. In some cases, the risk of disease progression is minimal, and the cancer-specific survival rates at a 15-year follow-up can be higher than 99%. Around 50–60% of new diagnoses are low-risk PCa [123]. However, aggressive PCa is associated with a significant reduction in survival rate. Therefore, detection of the disease as early as possible is vital, as is the effective treatment of these cases. These advances can only come about with the development of better methods of early diagnosis to improve the survival rate.

A number of novel biomarkers related to PCa aggressiveness have been recently shown to have great clinical potential. The outcomes of prospective studies conducted in multiple centers have indicated that the use of the PHI and 4Kscore biomarkers decrease the proportion of redundant biopsies in male individuals subjected to PSA screening. Various guidelines have advocated the use of these biomarkers [124, 125]. Nevertheless, comparative analysis of the usefulness of biomarkers requires large-scale prospective studies and stringent control of the bias caused by patient preselection based on the levels of PSA in the serum.

Several miRNAs with possible oncogene or tumor-suppressing functions are deregulated in PCa. As revealed by miRNA profiling research, mRNAs can regulate gene transcription either on their own or in conjunction with other transcription factors, with the end result being disrupted cellular processes in PCa tissues [18, 125]. Novel

approaches to PCa management could be identified by advances in the knowledge of the functions of miRNAs in controlling PCa development and progression [126, 127]. Research on the integrated function of biomarkers and combination with magnetic resonance imaging data is also worthwhile [128, 129]. Comparative analyses are also needed on the outcomes achieved with blood biomarkers and the encouraging data yielded using PSA or PHI. It should be known that none single biomarker has the capacity to perfectly detect PCa, and more detailed profiling of novel PCa biomarkers remains necessary.

Conflicts of Interest

The authors declare there is no conflict of interest.

Acknowledgments

This study was supported by the grant from the National Natural Science Foundation of China (Grant No. 81502208), and the grant funded by the Natural Science Foundation of Liaoning Province (Grant No. 20170541054).

References

- [1] H. Gronberg, "Prostate cancer epidemiology," *Lancet*, vol. 361, no. 9360, pp. 859–864, 2003.
- [2] M. Matsushita, K. Fujita, and N. Nonomura, "Influence of diet and nutrition on prostate cancer," *International Journal of Molecular Sciences*, vol. 21, no. 4, p. 1447, 2020.
- [3] S. F. Peisch, E. L. Van Blarigan, J. M. Chan, M. J. Stampfer, and S. A. Kenfield, "Prostate cancer progression and mortality: a review of diet and lifestyle factors," *World Journal of Urology*, vol. 35, no. 6, pp. 867–874, 2017.
- [4] S. Noh, E. Choi, C. H. Hwang, J. H. Jung, S. H. Kim, and B. Kim, "Dietary compounds for targeting prostate cancer," *Nutrients*, vol. 11, no. 10, p. 2401, 2019.
- [5] K. S. Sfanos, S. Yegnasubramanian, W. G. Nelson, and A. M. De Marzo, "The inflammatory microenvironment and microbiome in prostate cancer development," *Nature Reviews Urology*, vol. 15, no. 1, pp. 11–24, 2018.
- [6] A. M. De Marzo, E. A. Platz, S. Sutcliffe et al., "Inflammation in prostate carcinogenesis," *Nature Reviews Cancer*, vol. 7, no. 4, pp. 256–269, 2007.
- [7] C. Della Pepa, C. Cavaliere, S. Rossetti et al., "Predictive comprehensive geriatric assessment in elderly prostate cancer patients: the prospective observational scoop trial results," *Anti-Cancer Drugs*, vol. 28, no. 1, pp. 104–109, 2017.
- [8] A. Vecchia, O. Caffo, U. de Giorgi et al., "Clinical outcomes in octogenarians treated with docetaxel as first-line chemotherapy for castration-resistant prostate cancer," *Future Oncology*, vol. 12, no. 4, pp. 493–502, 2016.
- [9] R. D. Loberg, C. J. Logothetis, E. T. Keller, and K. J. Pienta, "Pathogenesis and treatment of prostate cancer bone metastases: targeting the lethal phenotype," *Journal of Clinical Oncology*, vol. 23, no. 32, pp. 8232–8241, 2005.
- [10] M. Salagierski and J. A. Schalken, "Molecular diagnosis of prostate cancer: PCA3 and TMPRSS2: ERG gene fusion," *The Journal of Urology*, vol. 187, no. 3, pp. 795–801, 2012.
- [11] R. J. Hendriks, I. M. van Oort, and J. A. Schalken, "Blood-based and urinary prostate cancer biomarkers: a review and comparison of novel biomarkers for detection and treatment decisions," *Prostate Cancer and Prostatic Diseases*, vol. 20, no. 1, pp. 12–19, 2017.
- [12] US Preventive Services Task Force, D. C. Grossman, S. J. Curry et al., "Screening for prostate cancer," *Journal of the American Medical Association*, vol. 319, no. 18, pp. 1901–1913, 2018.
- [13] K. J. L. Bell, C. Del Mar, G. Wright, J. Dickinson, and P. Glasziou, "Prevalence of incidental prostate cancer: a systematic review of autopsy studies," *International Journal of Cancer*, vol. 137, no. 7, pp. 1749–1757, 2015.
- [14] N. Sangster-Guity, B. Tu-Sekine, D. M. Raben, S. R. Denmeade, and S. A. Williams, "Mutational analysis of prostate-specific antigen defines the intrinsic proteolytic activity of the proPSA zymogen," *The Prostate*, vol. 76, no. 13, pp. 1203–1217, 2016.
- [15] S. V. Carlsson and M. J. Roobol, "What's new in screening in 2015?," *Current Opinion in Urology*, vol. 26, no. 5, pp. 447–458, 2016.
- [16] X. Filella, "Towards personalized prostate cancer screening," *Advances in Laboratory Medicine / Avances en Medicina de Laboratorio*, vol. 1, no. 1, 2020.
- [17] K. Fleshner, S. V. Carlsson, and M. J. Roobol, "The effect of the USPSTF PSA screening recommendation on prostate cancer incidence patterns in the USA," *Nature Reviews Urology*, vol. 14, no. 1, pp. 26–37, 2017.
- [18] P. H. Carroll and J. L. Mohler, "NCCN guidelines updates: prostate cancer and prostate cancer early detection," *Journal of the National Comprehensive Cancer Network*, vol. 16, no. 5S, pp. 620–623, 2018.
- [19] D. A. Sartori and D. W. Chan, "Biomarkers in prostate cancer: what's new?," *Current Opinion in Oncology*, vol. 26, no. 3, pp. 259–264, 2014.
- [20] S. D. Mikolajczyk, L. S. Grauer, L. S. Millar et al., "A precursor form of PSA (pPSA) is a component of the free PSA in prostate cancer serum," *Urology*, vol. 50, no. 5, pp. 710–714, 1997.
- [21] A. Lepor, W. J. Catalona, and S. Loeb, "The prostate health index: its utility in prostate cancer detection," *The Urologic Clinics of North America*, vol. 43, no. 1, pp. 1–6, 2016.
- [22] X. Filella, L. Foj, J. M. Auge, R. Molina, and J. Alcover, "Clinical utility of %p2PSA and prostate health index in the detection of prostate cancer," *Clinical Chemistry and Laboratory Medicine*, vol. 52, no. 9, pp. 1347–1355, 2014.
- [23] C. Stephan, S. Vincendeau, A. Houlgatte, H. Cammann, K. Jung, and A. Semjonow, "Multicenter evaluation of [-2] proprostate-specific antigen and the prostate health index for detecting prostate cancer," *Clinical Chemistry*, vol. 59, no. 1, pp. 306–314, 2013.
- [24] I. Heidegger and R. Pichler, "Re: Peter K.-F. Chiu, Chi-Fai Ng, Axel Semjonow, et al. A multicentre evaluation of the role of the prostate health index (PHI) in regions with differing prevalence of prostate cancer: adjustment of PHI reference ranges is needed for European and Asian settings. *Eur Urol* 2019;75:558–61," *European Urology*, vol. 75, no. 6, pp. e158–e159, 2019.
- [25] P. K.-F. Chiu, C.-F. Ng, A. Semjonow et al., "A multicentre evaluation of the role of the prostate health index (PHI) in regions with differing prevalence of prostate cancer: adjustment of PHI reference ranges is needed for European and Asian settings," *European Urology*, vol. 75, no. 4, pp. 558–561, 2019.

- [26] M. Lazzeri, A. Haese, A. de la Taille et al., "Serum isoform [-2]proPSA derivatives significantly improve prediction of prostate cancer at initial biopsy in a total PSA range of 2–10 ng/ml: a multicentric European study," *European Urology*, vol. 63, no. 6, pp. 986–994, 2013.
- [27] S. Loeb, M. G. Sanda, D. L. Broyles et al., "The prostate health index selectively identifies clinically significant prostate cancer," *The Journal of Urology*, vol. 193, no. 4, pp. 1163–1169, 2015.
- [28] W. Wang, M. Wang, L. Wang, T. S. Adams, Y. Tian, and J. Xu, "Diagnostic ability of %p2PSA and prostate health index for aggressive prostate cancer: a meta-analysis," *Scientific Reports*, vol. 4, p. 5012, 2015.
- [29] X. Filella and N. Gimenez, "Evaluation of [-2] pro PSA and prostate health index (phi) for the detection of prostate cancer: a systematic review and meta-analysis," *Clinical Chemistry and Laboratory Medicine*, vol. 51, pp. 729–739, 2012.
- [30] D. Bruzzese, C. Mazzeola, M. Ferro et al., "Prostate health index vs percent free prostate-specific antigen for prostate cancer detection in men with "gray" prostate-specific antigen levels at first biopsy: systematic review and meta-analysis," *Translational Research*, vol. 164, no. 6, pp. 444–451, 2014.
- [31] X. Filella, L. Foj, J. Alcover, J. M. Auge, R. Molina, and W. Jimenez, "The influence of prostate volume in prostate health index performance in patients with total PSA lower than 10 $\mu\text{g/L}$," *Clinica Chimica Acta*, vol. 436, pp. 303–307, 2014.
- [32] I. Heidegger, H. Klocker, R. Pichler et al., "ProPSA and the prostate health index as predictive markers for aggressiveness in low-risk prostate cancer—results from an international multicenter study," *Prostate Cancer and Prostatic Diseases*, vol. 20, no. 3, pp. 271–275, 2017.
- [33] C. de la Calle, D. Patil, J. T. Wei et al., "Multicenter evaluation of the prostate health index to detect aggressive prostate cancer in biopsy naïve men," *The Journal of Urology*, vol. 194, no. 1, pp. 65–72, 2015.
- [34] J. J. Tosoian, S. Loeb, Z. Feng et al., "Association of [-2]proPSA with biopsy reclassification during active surveillance for prostate cancer," *The Journal of Urology*, vol. 188, no. 4, pp. 1131–1136, 2012.
- [35] A. J. Vickers, A. M. Cronin, M. J. Roobol et al., "A four-kallikrein panel predicts prostate cancer in men with recent screening: data from the European Randomized Study of Screening for Prostate Cancer, Rotterdam," *Clinical Cancer Research*, vol. 16, no. 12, pp. 3232–3239, 2010.
- [36] A. J. Vickers, A. M. Cronin, G. Aus et al., "Impact of recent screening on predicting the outcome of prostate cancer biopsy in men with elevated prostate-specific antigen: data from the European Randomized Study of Prostate Cancer Screening in Gothenburg, Sweden," *Cancer*, vol. 116, pp. 2612–2620, 2010.
- [37] A. J. Vickers, A. Gupta, C. J. Savage et al., "A panel of kallikrein marker predicts prostate cancer in a large, population-based cohort followed for 15 years without screening," *Cancer Epidemiology, Biomarkers & Prevention*, vol. 20, no. 2, pp. 255–261, 2011.
- [38] S. V. Carlsson, M. T. Peltola, D. Sjoberg et al., "Can one blood draw replace transrectal ultrasonography-estimated prostate volume to predict prostate cancer risk?," *BJU International*, vol. 112, no. 5, pp. 602–609, 2013.
- [39] T. Chongqing, P. Liubao, Z. Xiaohui et al., "Cost-utility analysis of the newly recommended adjuvant chemotherapy for resectable gastric cancer patients in the 2011 Chinese National Comprehensive Cancer Network (NCCN) clinical practice guidelines in oncology: gastric cancer," *Pharmacoeconomics*, vol. 32, no. 3, pp. 235–243, 2014.
- [40] A. Nirenberg, N. K. Reame, K. D. Cato, and E. L. Larson, "Oncology nurses' use of National Comprehensive Cancer Network clinical practice guidelines for chemotherapy-induced and febrile neutropenia," *Oncology Nursing Forum*, vol. 37, no. 6, pp. 765–773, 2010.
- [41] D. J. Parekh, S. Punnen, D. D. Sjoberg et al., "A multi-institutional prospective trial in the USA confirms that the 4Kscore accurately identifies men with high-grade prostate cancer," *European Urology*, vol. 68, no. 3, pp. 464–470, 2015.
- [42] A. Vickers, E. A. Vertosick, D. D. Sjoberg et al., "Properties of the 4-kallikrein panel outside the diagnostic gray zone: meta-analysis of patients with positive digital rectal examination or prostate specific antigen 10 ng/ml and above," *The Journal of Urology*, vol. 197, 3 Part 1, pp. 607–613, 2017.
- [43] R. J. Bryant, D. D. Sjoberg, A. J. Vickers et al., "Predicting high-grade cancer at ten-core prostate biopsy using four kallikrein markers measured in blood in the ProtecT study," *Journal of the National Cancer Institute*, vol. 107, no. 7, 2015.
- [44] S. Carlsson, A. Maschino, F. Schroder et al., "Predictive value of four kallikrein markers for pathologically insignificant compared with aggressive prostate cancer in radical prostatectomy specimens: results from the European Randomized Study of Screening for Prostate Cancer section Rotterdam," *European Urology*, vol. 64, no. 5, pp. 693–699, 2013.
- [45] A. Benchikh, C. Savage, A. Cronin et al., "A panel of kallikrein markers can predict outcome of prostate biopsy following clinical work-up: an independent validation study from the European Randomized Study of Prostate Cancer screening, France," *BMC Cancer*, vol. 10, no. 1, p. 635, 2010.
- [46] A. J. Vickers, A. M. Cronin, G. Aus et al., "A panel of kallikrein markers can reduce unnecessary biopsy for prostate cancer: data from the European Randomized Study of Prostate Cancer Screening in Göteborg, Sweden," *BMC Medicine*, vol. 6, no. 1, p. 19, 2008.
- [47] P. Stattin, A. J. Vickers, D. D. Sjoberg et al., "Improving the specificity of screening for lethal prostate cancer using prostate-specific antigen and a panel of kallikrein markers: a nested case-control study," *European Urology*, vol. 68, no. 2, pp. 207–213, 2015.
- [48] T. Nordstrom, A. Vickers, M. Assel, H. Lilja, H. Gronberg, and M. Eklund, "Comparison between the four-kallikrein panel and prostate health index for predicting prostate cancer," *European Urology*, vol. 68, no. 1, pp. 139–146, 2015.
- [49] P. V. Nazarov, S. E. Reinsbach, A. Muller et al., "Interplay of microRNAs, transcription factors and target genes: linking dynamic expression changes to function," *Nucleic Acids Research*, vol. 41, no. 5, pp. 2817–2831, 2013.
- [50] X. Liu, Q. Chen, J. Yan et al., "MiRNA-296-3p-ICAM-1 axis promotes metastasis of prostate cancer by possible enhancing survival of natural killer cell-resistant circulating tumour cells," *Cell Death & Disease*, vol. 4, no. 11, article e928, 2013.
- [51] J. D. Arroyo, J. R. Chevillet, E. M. Kroh et al., "Argonaute2 complexes carry a population of circulating microRNAs independent of vesicles in human plasma," *Proceedings of the National Academy of Sciences of the United States of America*, vol. 108, no. 12, pp. 5003–5008, 2011.
- [52] A. Gallo, M. Tandon, I. Alevizos, and G. G. Illei, "The majority of microRNAs detectable in serum and saliva is

- concentrated in exosomes," *PLoS One*, vol. 7, no. 3, article e30679, 2012.
- [53] M. Jin, T. Zhang, C. Liu et al., "miRNA-128 suppresses prostate cancer by inhibiting BMI-1 to inhibit tumor-initiating cells," *Cancer Research*, vol. 74, no. 15, pp. 4183–4195, 2014.
- [54] H. Lan, H. Lu, X. Wang, and H. Jin, "MicroRNAs as potential biomarkers in cancer: opportunities and challenges," *BioMed Research International*, vol. 2015, Article ID 125094, 17 pages, 2015.
- [55] E. A. Hunt, D. Broyles, T. Head, and S. K. Deo, "MicroRNA detection: current technology and research strategies," *Annual Review of Analytical Chemistry*, vol. 8, no. 1, pp. 217–237, 2015.
- [56] C. H. Lawrie, S. Gal, H. M. Dunlop et al., "Detection of elevated levels of tumour-associated microRNAs in serum of patients with diffuse large B-cell lymphoma," *British Journal of Haematology*, vol. 141, no. 5, pp. 672–675, 2008.
- [57] J. Lu, G. Getz, E. A. Miska et al., "MicroRNA expression profiles classify human cancers," *Nature*, vol. 435, no. 7043, pp. 834–838, 2005.
- [58] R. Sokilde, M. Vincent, A. K. Moller et al., "Efficient identification of miRNAs for classification of tumor origin," *The Journal of Molecular Diagnostics*, vol. 16, no. 1, pp. 106–115, 2014.
- [59] S. Sakamoto, "Editorial comment to functional significance of aberrantly expressed microRNAs in prostate cancer," *International Journal of Urology*, vol. 22, no. 3, pp. 252–253, 2015.
- [60] Y. Goto, A. Kurozumi, H. Enokida, T. Ichikawa, and N. Seki, "Functional significance of aberrantly expressed microRNAs in prostate cancer," *International Journal of Urology*, vol. 22, no. 3, pp. 242–252, 2015.
- [61] X.-B. Shi, L. Xue, J. Yang et al., "An androgen-regulated miRNA suppresses Bak1 expression and induces androgen-independent growth of prostate cancer cells," *Proceedings of the National Academy of Sciences of the United States of America*, vol. 104, no. 50, pp. 19983–19988, 2007.
- [62] A. Srivastava, H. Goldberger, A. Dimtchev et al., "MicroRNA profiling in prostate cancer - the diagnostic potential of urinary miR-205 and miR-214," *PLoS One*, vol. 8, no. 10, article e76994, 2013.
- [63] S. Griffiths-Jones, R. J. Grocock, S. van Dongen, A. Bateman, and A. J. Enright, "miRBase: microRNA sequences, targets and gene nomenclature," *Nucleic Acids Research*, vol. 34, no. 9, pp. D140–D144, 2006.
- [64] G. A. Calin, C. D. Dumitru, M. Shimizu et al., "Nonlinear partial differential equations and applications: frequent deletions and down-regulation of micro-RNA genes miR15 and miR16 at 13q14 in chronic lymphocytic leukemia," *Proceedings of the National Academy of Sciences of the United States of America*, vol. 99, no. 24, pp. 15524–15529, 2002.
- [65] R. Kanwal, A. R. Plaga, X. Liu, G. C. Shukla, and S. Gupta, "MicroRNAs in prostate cancer: functional role as biomarkers," *Cancer Letters*, vol. 407, pp. 9–20, 2017.
- [66] Y. Yang, J. X. Guo, and Z. Q. Shao, "miR-21 targets and inhibits tumor suppressor gene PTEN to promote prostate cancer cell proliferation and invasion: an experimental study," *Asian Pacific Journal of Tropical Medicine*, vol. 10, no. 1, pp. 87–91, 2017.
- [67] S. E. Jalava, A. Urbanucci, L. Latonen et al., "Androgen-regulated miR-32 targets BTG2 and is overexpressed in castration-resistant prostate cancer," *Oncogene*, vol. 31, no. 41, pp. 4460–4471, 2012.
- [68] T. Li, R. S. Li, Y. H. Li et al., "miR-21 as an independent biochemical recurrence predictor and potential therapeutic target for prostate cancer," *The Journal of Urology*, vol. 187, no. 4, pp. 1466–1472, 2012.
- [69] E. K. Amankwah, E. Anegebe, H. Park, J. Pow-Sang, A. Hakam, and J. Y. Park, "miR-21, miR-221 and miR-222 expression and prostate cancer recurrence among obese and non-obese cases," *Asian Journal of Andrology*, vol. 15, no. 2, pp. 226–230, 2013.
- [70] A. Cannistraci, A. L. Di Pace, R. De Maria, and D. Bonci, "MicroRNA as new tools for prostate cancer risk assessment and therapeutic intervention: results from clinical data set and patients' samples," *BioMed Research International*, vol. 2014, Article ID 146170, 17 pages, 2014.
- [71] U. G. Lo, C. F. Lee, M. S. Lee, and J. T. Hsieh, "The role and mechanism of epithelial-to-mesenchymal transition in prostate cancer progression," *International Journal of Molecular Sciences*, vol. 18, no. 10, p. 2079, 2017.
- [72] U. G. Lo, D. Yang, and J. T. Hsieh, "The role of microRNAs in prostate cancer progression," *Translational andrology and urology*, vol. 2, no. 3, pp. 228–241, 2013.
- [73] A. A. Moustafa, M. Ziada, A. Elshaikh et al., "Identification of micro RNA signature and potential pathway targets in prostate cancer," *Experimental Biology and Medicine*, vol. 242, pp. 536–546, 2016.
- [74] G. L. Andriole, E. D. Crawford, R. L. Grubb et al., "Prostate cancer screening in the randomized prostate, lung, colorectal, and ovarian cancer screening trial: mortality results after 13 years of follow-up," *Journal of the National Cancer Institute*, vol. 104, no. 2, pp. 125–132, 2012.
- [75] Z. Y. Abd Elmageed, Y. Yang, R. Thomas et al., "Neoplastic reprogramming of patient-derived adipose stem cells by prostate cancer cell-associated exosomes," *Stem Cells*, vol. 32, no. 4, pp. 983–997, 2014.
- [76] X.-B. Shi, L. Xue, A. H. Ma, C. G. Tepper, H. J. Kung, and R. W. V. White, "miR-125b promotes growth of prostate cancer xenograft tumor through targeting proapoptotic genes," *The Prostate*, vol. 71, no. 5, pp. 538–549, 2011.
- [77] S. Amir, A. H. Ma, X. B. Shi, L. Xue, H. J. Kung, and R. W. Devere White, "Oncomir miR-125b suppresses p14ARF to modulate p53-Dependent and p53-independent apoptosis in prostate cancer," *PLoS One*, vol. 8, no. 4, article e61064, 2013.
- [78] T. Sun, M. Yang, S. Chen et al., "The altered expression of miR-221/-222 and miR-23b/-27b is associated with the development of human castration resistant prostate cancer," *The Prostate*, vol. 72, no. 10, pp. 1093–1103, 2012.
- [79] S. J. Seashols-Williams, W. Budd, G. C. Clark et al., "miR-9 acts as an oncomiR in prostate cancer through multiple pathways that drive tumour progression and metastasis," *PLoS One*, vol. 11, no. 7, article e0159601, 2016.
- [80] T. I. Hsu, C. H. Hsu, K. H. Lee et al., "MicroRNA-18a is elevated in prostate cancer and promotes tumorigenesis through suppressing STK4 *in vitro* and *in vivo*," *Oncogene*, vol. 33, no. 4, article e99, 2014.
- [81] G. Al-Kafaji, Z. T. Al-Naieb, and M. Bakhiet, "Increased oncogenic microRNA-18a expression in the peripheral blood of patients with prostate cancer: a potential novel non-

- invasive biomarker,” *Oncology Letters*, vol. 11, no. 2, pp. 1201–1206, 2016.
- [82] M. Norgaard, A. O. Jensen, J. B. Jacobsen, K. Cetin, J. P. Fryzek, and H. T. Sorensen, “Skeletal related events, bone metastasis and survival of prostate cancer: a population based cohort study in Denmark (1999 to 2007),” *The Journal of Urology*, vol. 184, no. 1, pp. 162–167, 2010.
- [83] W. Lou, J. Liu, Y. Gao et al., “MicroRNAs in cancer metastasis and angiogenesis,” *Oncotarget*, vol. 8, no. 70, pp. 115787–115802, 2017.
- [84] M. Gururajan, S. Jossion, G. C. Chu et al., “miR-154* and miR-379 in the DLK1-DIO3 microRNA mega-cluster regulate epithelial to mesenchymal transition and bone metastasis of prostate cancer,” *Clinical Cancer Research*, vol. 20, no. 24, pp. 6559–6569, 2014.
- [85] S. Jossion, M. Gururajan, P. Hu et al., “miR-409-3p/-5p promotes tumorigenesis, epithelial-to-mesenchymal transition, and bone metastasis of human prostate cancer,” *Clinical Cancer Research*, vol. 20, no. 17, pp. 4636–4646, 2014.
- [86] M. K. Siu, Y. C. Tsai, Y. S. Chang et al., “Transforming growth factor- β promotes prostate bone metastasis through induction of microRNA-96 and activation of the mTOR pathway,” *Oncogene*, vol. 34, no. 36, pp. 4767–4776, 2015.
- [87] D. Lin, F. Cui, Q. Bu, and C. Yan, “The expression and clinical significance of GTP-binding RAS-like 3(ARHI) and microRNA 221 and 222 in prostate cancer,” *The Journal of International Medical Research*, vol. 39, no. 5, pp. 1870–1875, 2011.
- [88] H. M. Lin, K. L. Mahon, C. Spielman et al., “Phase 2 study of circulating microRNA biomarkers in castration-resistant prostate cancer,” *British Journal of Cancer*, vol. 116, no. 8, pp. 1002–1011, 2017.
- [89] Y. Yang, D. Jia, H. Kim et al., “Dysregulation of miR-212 promotes castration resistance through hnRNPH1-mediated regulation of AR and AR-V7: implications for racial disparity of prostate cancer,” *Clinical Cancer Research*, vol. 22, no. 7, pp. 1744–1756, 2016.
- [90] E. R. Sherwood, J. L. Van Dongen, C. G. Wood, S. Liao, J. M. Kozlowski, and C. Lee, “Epidermal growth factor receptor activation in androgen-independent but not androgen-stimulated growth of human prostatic carcinoma cells,” *British Journal of Cancer*, vol. 77, no. 6, pp. 855–861, 1998.
- [91] Q. Fu, X. Liu, Y. Liu, J. Yang, G. Lv, and S. Dong, “MicroRNA-335 and -543 suppress bone metastasis in prostate cancer via targeting endothelial nitric oxide synthase,” *International Journal of Molecular Medicine*, vol. 36, no. 5, pp. 1417–1425, 2015.
- [92] Q. Zhu, H. Li, Y. Li, and L. Jiang, “MicroRNA-30a functions as tumor suppressor and inhibits the proliferation and invasion of prostate cancer cells by down-regulation of SIX1,” *Human Cell*, vol. 30, no. 4, pp. 290–299, 2017.
- [93] D. Ren, M. Wang, W. Guo et al., “Double-negative feedback loop between ZEB2 and miR-145 regulates epithelial-mesenchymal transition and stem cell properties in prostate cancer cells,” *Cell and Tissue Research*, vol. 358, no. 3, pp. 763–778, 2014.
- [94] Q. Chen, X. Zhao, H. Zhang et al., “MiR-130b suppresses prostate cancer metastasis through down-regulation of MMP2,” *Molecular Carcinogenesis*, vol. 54, no. 11, pp. 1292–1300, 2015.
- [95] C. P. Bracken, P. A. Gregory, Y. Khew-Goodall, and G. J. Goodall, “The role of microRNAs in metastasis and epithelial-mesenchymal transition,” *Cellular and Molecular Life Sciences*, vol. 66, no. 10, pp. 1682–1699, 2009.
- [96] J. Banyard, I. Chung, A. M. Wilson et al., “Regulation of epithelial plasticity by miR-424 and miR-200 in a new prostate cancer metastasis model,” *Scientific Reports*, vol. 3, no. 1, p. 3151, 2013.
- [97] J. H. Tseng, M. Bisogna, L. N. Hoang et al., “miR-200c-driven mesenchymal-to-epithelial transition is a therapeutic target in uterine carcinosarcomas,” *Scientific Reports*, vol. 7, no. 1, p. 3614, 2017.
- [98] J. Yu, Y. Lu, D. Cui et al., “miR-200b suppresses cell proliferation, migration and enhances chemosensitivity in prostate cancer by regulating Bmi-1,” *Oncology Reports*, vol. 31, no. 2, pp. 910–918, 2014.
- [99] P. Gandellini, V. Profumo, A. Casamicheli et al., “miR-205 regulates basement membrane deposition in human prostate: implications for cancer development,” *Cell Death and Differentiation*, vol. 19, no. 11, pp. 1750–1760, 2012.
- [100] B. Verdoodt, M. Neid, M. Vogt et al., “MicroRNA-205, a novel regulator of the anti-apoptotic protein Bcl 2, is down-regulated in prostate cancer,” *International Journal of Oncology*, vol. 43, no. 1, pp. 307–314, 2013.
- [101] B. Xu, N. Wang, X. Wang et al., “MiR-146a suppresses tumor growth and progression by targeting EGFR pathway and in a p-ERK-dependent manner in castration-resistant prostate cancer,” *The Prostate*, vol. 72, no. 11, pp. 1171–1178, 2012.
- [102] Y. N. Liu, J. Yin, B. Barrett et al., “Loss of androgen-regulated microRNA 1 activates SRC and promotes prostate cancer bone metastasis,” *Molecular and Cellular Biology*, vol. 35, no. 11, pp. 1940–1951, 2015.
- [103] M. K. Siu, W. Abou-Kheir, J. J. Yin et al., “Loss of EGFR signaling-regulated miR-203 promotes prostate cancer bone metastasis and tyrosine kinase inhibitors resistance,” *Oncotarget*, vol. 5, no. 11, pp. 3770–3784, 2014.
- [104] Z. Y. Lin, Y. Q. Huang, Y. Q. Zhang et al., “MicroRNA-224 inhibits progression of human prostate cancer by downregulating TRIB1,” *International Journal of Cancer*, vol. 135, no. 3, pp. 541–550, 2014.
- [105] K. Hanlon, C. E. Rudin, and L. W. Harries, “Investigating the targets of MIR-15a and MIR-16-1 in patients with chronic lymphocytic leukemia (CLL),” *PLoS One*, vol. 4, no. 9, p. e7169, 2009.
- [106] W. Jin, F. Chen, K. Wang, Y. Song, X. Fei, and B. Wu, “miR-15a/miR-16 cluster inhibits invasion of prostate cancer cells by suppressing TGF- β signaling pathway,” *Biomedicine & Pharmacotherapy*, vol. 104, pp. 637–644, 2018.
- [107] R. I. Aqeilan, G. A. Calin, and C. M. Croce, “_miR-15a_ and _miR-16-1_ in cancer: discovery, function and future perspectives,” *Cell Death and Differentiation*, vol. 17, no. 2, pp. 215–220, 2010.
- [108] M. Musumeci, V. Coppola, A. Addario et al., “Control of tumor and microenvironment cross-talk by miR-15a and miR-16 in prostate cancer,” *Oncogene*, vol. 30, no. 41, pp. 4231–4242, 2011.
- [109] K. Sikand, J. E. Slaibi, R. Singh, S. D. Slane, and G. C. Shukla, “miR 488* inhibits androgen receptor expression in prostate carcinoma cells,” *International Journal of Cancer*, vol. 129, no. 4, pp. 810–819, 2011.

- [110] A. Kroiss, S. Vincent, M. Decaussin-Petrucci et al., “Androgen-regulated microRNA-135a decreases prostate cancer cell migration and invasion through downregulating ROCK1 and ROCK2,” *Oncogene*, vol. 34, no. 22, pp. 2846–2855, 2015.
- [111] C. E. Fletcher, D. A. Dart, A. Sita-Lumsden, H. Cheng, P. S. Rennie, and C. L. Bevan, “Androgen-regulated processing of the oncomir miR-27a, which targets prohibitin in prostate cancer,” *Human Molecular Genetics*, vol. 21, no. 14, pp. 3112–3127, 2012.
- [112] A. Valentino, P. Reclusa, R. Sirera et al., “Exosomal microRNAs in liquid biopsies: future biomarkers for prostate cancer,” *Clinical & Translational Oncology*, vol. 19, no. 6, pp. 651–657, 2017.
- [113] L. Cheng, R. A. Sharples, B. J. Scicluna, and A. F. Hill, “Exosomes provide a protective and enriched source of miRNA for biomarker profiling compared to intracellular and cell-free blood,” *Journal of Extracellular Vesicles*, vol. 3, no. 1, 2014.
- [114] L. Cheng, X. Sun, B. J. Scicluna, B. M. Coleman, and A. F. Hill, “Characterization and deep sequencing analysis of exosomal and non-exosomal miRNA in human urine,” *Kidney International*, vol. 86, no. 2, pp. 433–444, 2014.
- [115] D. C. Yu, Q. G. Li, X. W. Ding, and Y. T. Ding, “Circulating microRNAs: potential biomarkers for cancer,” *International Journal of Molecular Sciences*, vol. 12, no. 3, pp. 2055–2063, 2011.
- [116] P. S. Mitchell, R. K. Parkin, E. M. Kroh et al., “Circulating microRNAs as stable blood-based markers for cancer detection,” *Proceedings of the National Academy of Sciences of the United States of America*, vol. 105, no. 30, pp. 10513–10518, 2008.
- [117] M. J. Lodes, M. Caraballo, D. Suci, S. Munro, A. Kumar, and B. Anderson, “Detection of cancer with serum miRNAs on an oligonucleotide microarray,” *PLoS One*, vol. 4, no. 7, p. e6229, 2009.
- [118] J. C. Brase, M. Johannes, T. Schlomm et al., “Circulating miRNAs are correlated with tumor progression in prostate cancer,” *International Journal of Cancer*, vol. 128, no. 3, pp. 608–616, 2011.
- [119] N. Mottet, J. Bellmunt, M. Bolla et al., “EAU-ESTRO-SIOG guidelines on prostate cancer. Part I: screening, diagnosis, and local treatment with curative intent,” *European Urology*, vol. 71, no. 4, pp. 618–629, 2017.
- [120] N. Mottet, J. Bellmunt, M. Bolla et al., “EAU guidelines on prostate cancer. Part II: treatment of advanced, relapsing, and castration-resistant prostate cancer,” *European Urology*, vol. 59, no. 4, pp. 572–583, 2011.
- [121] R. Samsonov, T. Shtam, V. Burdakov et al., “Lectin-induced agglutination method of urinary exosomes isolation followed by mi-RNA analysis: application for prostate cancer diagnostic,” *The Prostate*, vol. 76, no. 1, pp. 68–79, 2016.
- [122] O. E. Bryzgunova, M. M. Zaripov, T. E. Skvortsova et al., “Comparative study of extracellular vesicles from the urine of healthy individuals and prostate cancer patients,” *PLoS One*, vol. 11, no. 6, article e0157566, 2016.
- [123] L. Klotz, “Low-risk prostate cancer can and should often be managed with active surveillance and selective delayed intervention,” *Nature Clinical Practice Urology*, vol. 5, no. 1, pp. 2–3, 2008.
- [124] A. J. Vickers, J. A. Eastham, P. T. Scardino, and H. Lilja, “The memorial Sloan Kettering cancer center recommendations for prostate cancer screening,” *Urology*, vol. 91, pp. 12–18, 2016.
- [125] M. C. Sighinolfi and B. Rocco, “Reply to Alessia Cimadamore, Marina Scarpelli, Liang Cheng, et al’s Letter to the Editor, re: Maria Chiara Sighinolfi, Bernardo Rocco’s Words of Wisdom re: EAU Guidelines: Prostate Cancer 2019. Mottet N, van den Bergh RCN, Briers E, et al. <https://uroweb.org/guideline/prostate-cancer/>. *Eur Urol* 2019, 76:871,” *European Urology*, vol. 77, no. 5, pp. e128–e129, 2020.
- [126] S. C. Druskin, J. J. Tosoian, A. Young et al., “Combining Prostate Health Index density, magnetic resonance imaging and prior negative biopsy status to improve the detection of clinically significant prostate cancer,” *BJU International*, vol. 121, no. 4, pp. 619–626, 2018.
- [127] V. J. Gnanapragasam, K. Burling, A. George et al., “The prostate health index adds predictive value to multi-parametric MRI in detecting significant prostate cancers in a repeat biopsy population,” *Scientific Reports*, vol. 6, no. 1, p. 35364, 2016.
- [128] S. Washino, T. Okochi, K. Saito et al., “Combination of prostate imaging reporting and data system (PI-RADS) score and prostate-specific antigen (PSA) density predicts biopsy outcome in prostate biopsy naïve patients,” *BJU International*, vol. 119, no. 2, pp. 225–233, 2017.
- [129] P. J. L. De Visschere, A. Briganti, J. J. Fütterer et al., “Role of multiparametric magnetic resonance imaging in early detection of prostate cancer,” *Insights into Imaging*, vol. 7, no. 2, pp. 205–214, 2016.

Review Article

Regulation of Iron Homeostasis and Related Diseases

Yikun Li,^{1,2} Xiali Huang,¹ Jingjing Wang,^{1,3} Ruiling Huang¹ ,¹ and Dan Wan¹ 

¹Key Laboratory of Agro-Ecological Processes in Subtropical Region, Hunan Research Center of Livestock & Poultry Sciences, South-Central Experimental Station of Animal Nutrition and Feed Science in Ministry of Agriculture, Institute of Subtropical Agriculture, The Chinese Academy of Sciences, Changsha, Hunan 410125, China

²University of Chinese Academy of Sciences, Beijing 100049, China

³Department of Animal Nutrition and Feed Science, College of Animal Science and Technology, Huazhong Agricultural University, Wuhan 430070, China

Correspondence should be addressed to Ruiling Huang; huangrl@isa.ac.cn and Dan Wan; w.dan@isa.ac.cn

Received 26 February 2020; Accepted 23 March 2020; Published 2 May 2020

Guest Editor: Guan Yang

Copyright © 2020 Yikun Li et al. This is an open access article distributed under the Creative Commons Attribution License, which permits unrestricted use, distribution, and reproduction in any medium, provided the original work is properly cited.

The liver is the organ for iron storage and regulation; it senses circulating iron concentrations in the body through the BMP-SMAD pathway and regulates the iron intake from food and erythrocyte recovery into the bloodstream by secreting hepcidin. Under iron deficiency, hypoxia, and hemorrhage, the liver reduces the expression of hepcidin to ensure the erythropoiesis but increases the excretion of hepcidin during infection and inflammation to reduce the usage of iron by pathogens. Excessive iron causes system iron overload; it accumulates in never system and damages neurocyte leading to neurodegenerative diseases such as Parkinson's syndrome. When some gene mutations affect the perception of iron and iron regulation ability in the liver, then they decrease the expression of hepcidin, causing hereditary diseases such as hereditary hemochromatosis. This review summarizes the source and utilization of iron in the body, the liver regulates systemic iron homeostasis by sensing the circulating iron concentration, and the expression of hepcidin regulated by various signaling pathways, thereby understanding the pathogenesis of iron-related diseases.

1. Introduction

Iron is the maximum trace element in the body. As a transition metal, iron readily donates and accepts electrons to participate in biologic processes like oxygen transport, mitochondrial respiration, nucleic acid replication, intermediary, xenobiotic metabolism, and cell signaling [1]. Iron is so important is that its deficiency is one of the major risk factors for disability and death worldwide, and it is estimated to affect 2 billion people [2, 3]. On the other hand, excessive iron is harmful; it damages the liver and the brain, causing oxidative stress on the nerve to cause neurodegenerative diseases such as Parkinson's syndrome. Mutations in multiple iron-regulated pathways lead to heredity iron overload diseases like hereditary hemochromatosis (HH) and iron-refractory iron deficiency anemia (IRIDA) [4].

2. Absorption of Iron in the Food and Cellular Iron Acquisition

Dietary iron includes the heme iron and nonheme iron; 90% of them are nonheme iron, mainly present as the form of $\text{Fe}(\text{OH})_3$ complexation. Nonheme dietary iron is absorption at the brush border of duodenal enterocytes and exhibited diurnal rhythms [5]. The cytochrome b (Dcytb) on the duodenal enterocyte membrane reduced Fe^{3+} to Fe^{2+} , then the Fe^{2+} through the divalent metal transporter 1 (DMT1) on the membrane into the cell. The heme iron absorption mainly uptakes by the heme carrier protein 1 (HCP-1) [6, 7]. When the heme gets into the cell, it is degraded into iron, carbon monoxide, and biliverdin by heme oxygenase 1 or 2 (HO-1/2) [8]. Intracellular iron is efflux to the extracellular by the ferroportin1(FPN1), the only iron transmembrane

efflux protein in vertebrate cells [9–11]. Excess cellular iron is stored in ferritin, which has a large cavity to store thousands of iron atoms; it prevents dissociative iron from causing oxidative damage to cells [12]. After the Fe^{2+} efflux into the circulation, it oxidized to Fe^{3+} by the ferroxidases such as hephaestin (HEPH) or its homologue ceruloplasmin (CP) [13, 14] and succeedingly loaded onto the transferrin (Tf) and transported by the bloodstream.

The majority of the blood iron participates in hematopoiesis in the bone marrow, and a minor part transports to the liver. The liver is the essential organ for the body to store the iron, and the iron in hepatocytes is mainly stored in ferritin. For the excess iron, it is engulfed by the Kupffer cells of the reticuloendothelial system and deposited in the system as the form of hemosiderin [15].

Iron in the blood binds to the cell surface transferrin receptor (TfR), Tf-Fe/TfR complex sag, and endocytose into the cell, subsequently the conformational of the complex is changed triggered by the acidified endosomes [16, 17], which releases iron from the Tf [18]. The iron in the endosome is restored to Fe^{2+} by prostate six-transmembrane epithelial antigen of prostate 3 (STEAP3) and transported into the cytolymph by DMT1 [19]. The apo-Tf and TfR complex in the endosome are recycled to the cell surface. The sorting nexin 3 (SNX3) is one of the proteins of the phosphoinositide-binding protein family [20], is required for the recycling of Tf/TfR in endocytosis, and increases iron absorption by Tf recycling and bound ability [21]. We summarized the iron absorption and cellular iron acquisition in Figure 1.

2.1. Iron Cycle Is Associated with the Production and Clearance of Erythrocyte. In humans, 200 billion red blood cells are producing every day, requiring more than 2×10^{15} iron atoms per second to maintain erythropoiesis. The demand for iron is majorly obtained from recycling erythrocytes, so the production and clearance of erythrocytes are critical for iron homeostasis [22].

The erythropoiesis occurs in the erythroblastic island of the late fetal liver and adult bone marrow which surrounds a central macrophage, termed as nurse macrophage. The nurse macrophage promotes erythropoiesis in the erythroblastic island niche [23], phagocytosing the nuclei expelled from erythroid precursor cells in the late stage of erythropoiesis [24]. Other than that, macrophage in the erythroblastic island produces and releases ferritin by exocytosis [25]; then, the ferritin is endocytosed into the erythroblasts [26]. After entering the cell, iron releases from ferritin after acidification and proteolysis, which is used for heme production during the development of erythrocytes [27]. It seems that macrophages provide ferritin to nurture erythroblastic but have others also point out that the transferrin is the sole iron source during erythropoiesis; ferritin endocytosis is just a tiny force for the erythroblastic acquisition iron [28].

While the life of the erythrocyte is about to end or get irreparable damage, the bloodstream takes their last ride to the reticuloendothelial system in the splenic and hepatic. There, it is known that splenic red pulp macrophage cleans up senescent and damaged red blood cells then recycles iron

for erythropoiesis after hemoglobin catabolism [29]. There, firstly, the residential macrophage scrutinizes the passaged erythroid [30], then triggered engulf and digest the erythrocytes when macrophages contact to erythrocyte receptors and detect the specific markers on its surface [31], like phosphatidylserine and band 3 [32, 33]. Whereafter, the red blood cell is phagocytosed by macrophages into macrophage phagolysosome, causing hemoglobin breakdown and the heme release [34]. Subsequently, heme in phagolysosome is exported to the cytosol via the heme transporter (HRG1) and is decomposed into iron by HO-1/HO-2 [35, 36], then the iron is utilized by macrophages or effluxed extracellularly by FPN1. [8]. Macrophages for the iron cycle are shown in Figure 1.

Fe^{3+} in food is reduced to Fe^{2+} by Dcytb on the duodenal epithelium; it absorbs Fe^{2+} from the intestinal cavity through DMT1. HCP1 intakes heme in food, and HO-1 degrades it into Fe^{2+} in the cytoplasm. Excessive iron storage in the ferritin and other export into the blood through by FPN1; after that, Fe^{2+} is oxidized by CP and HEPH at the basolateral side then loads onto Tf.

Macrophage phagocytosed erythrocytes and releases heme in the phagolysosome. HRG1 exports heme from phagolysosome into the cytosol; then, HO-1 degrades heme into Fe^{2+} and efflux into the bloodstream by FPN1.

Tf-Fe combine with TfR on cytomembrane. SNX3 induce Tf-TfR sag and endocytose into the cell. Acidified endosomes release Fe^{3+} and restored to Fe^{2+} by STEAP3 and Fe^{2+} into the cytoplasm through the DMT1. Apo-Tf and TfR complex is recycled to the cell surface, and Tf is released into the blood.

The miR-Let-7d and miR-16 family decreases DMT1 expression. Hepcidin internalizes and degrades FPN1. miR-485-3p and miR-20b regulate the expression of FPN1. miR-200b induces downregulation of ferritin, and miR-320 suppresses the expression of TfR1.

2.2. Hepcidin-FPN1 Axis Sensing and Regulating the Systemic Iron Homeostasis in the Liver. Except for the storage of iron, the liver is the most important organ to regulate the systemic iron homeostasis by secreting the hepcidin. Hepcidin (HAMP) is a polypeptide that synthesizes regulatory hormone; it regulates iron homeostasis by combining FPN1 at extracellular to internalize and degrade FPN1 in the lysosome [37]. Iron in the blood loads on the Tf and transports with the bloodstream after being exported from the FPN1. While the concentration of circulating iron floats, hepatocytes sense and regulate hepcidin expression through the BMP/SMAD pathway to regulate the iron output from FPN1 [38]. This way, hepatocyte controls the amount of iron in circulation within the normal range, and unregulated hepcidin in the liver can cause iron deficiency or iron overload.

In the BMP/SMAD pathway, bone morphogenetic protein (BMP) and its coreceptor hemojuvelin (HJV) are the most critical hepcidin that regulate signaling pathway in quantitation [39]. BMP6 is predominantly secreted from liver endothelial cells [40]; its expression is regulated by iron [41], so it reflects the hepatic iron level [42, 43]. BMP6 and HJV together activate the BMP serine threonine kinase

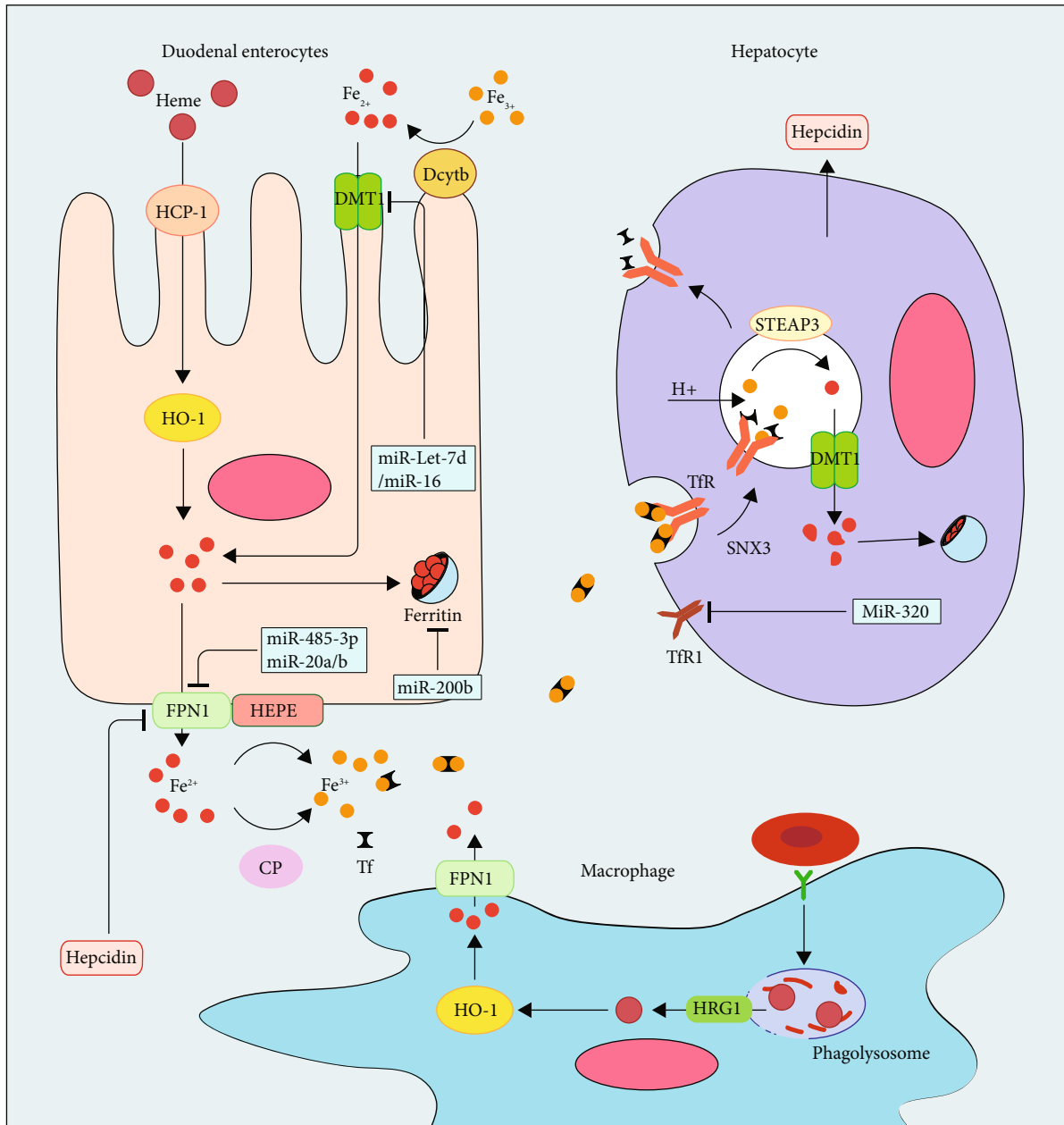


FIGURE 1: Systemic iron homeostasis.

receptor- (BMPR-) I/II complex [44, 45]. BMP6/HJV complex as a ligand combines with the BMPR I (Alk2 and Alk3) [46], and BMPR II (ActR2a and BMPR2) [47] promotes phosphorylation downstream BMP media such as SMAD1, SMAD5, and SMAD8 (SMAD1/5/8) [48]. Phosphorylated SMAD1/5/8 combines with the cytoplasmic SMAD4 as an active transcriptional complex and moves into the nucleus; the complex combines with the BMP reaction element (BMP-RE1 and BMP-RE2) and then activates transcription of the *HAMP* [49, 50]. MT-2 (matriptase-2, *TMPRSS6*, transmembrane protease serine 6) is ubiquitously expressed in the liver, invalid of MT-2 due to genetic mutation causes iron-refractory iron deficiency anemia (IRIDA) [51, 52], and MT-2 is also downregulated by iron and BMP6 [53, 54]. HJV is a glycosphosphatidylinositol- (GPI-) anchored protein

[55]; MT-2 cleaves the membrane HJV (m-HJV) to a form of soluble HJV (s-HJV) to decrease the affinity for BMP6 [56]; thus, the MT-2 expression increases during iron deficiency [57]. However, recent research shows that MT-2 independently cleaves HJV to regulate hepcidin expression, and it also cleaves other components in the BMP/SMAD pathway other than HJV [58]. The furin family of proprotein convertases expressed in the liver also produces s-HJV by cleaving the HJV, but different with MT-2; sHJV generated by furin negatively regulated BMP while the MT-2 only reduces the combination [56]; this process is regulated by iron deficiency or hypoxia [59]. Others like endofin, ATOH8, and SMAD7 also affect the signal transduction of the BMP/SMAD pathway [60–62], which is the perceptron and messenger of iron concentration.

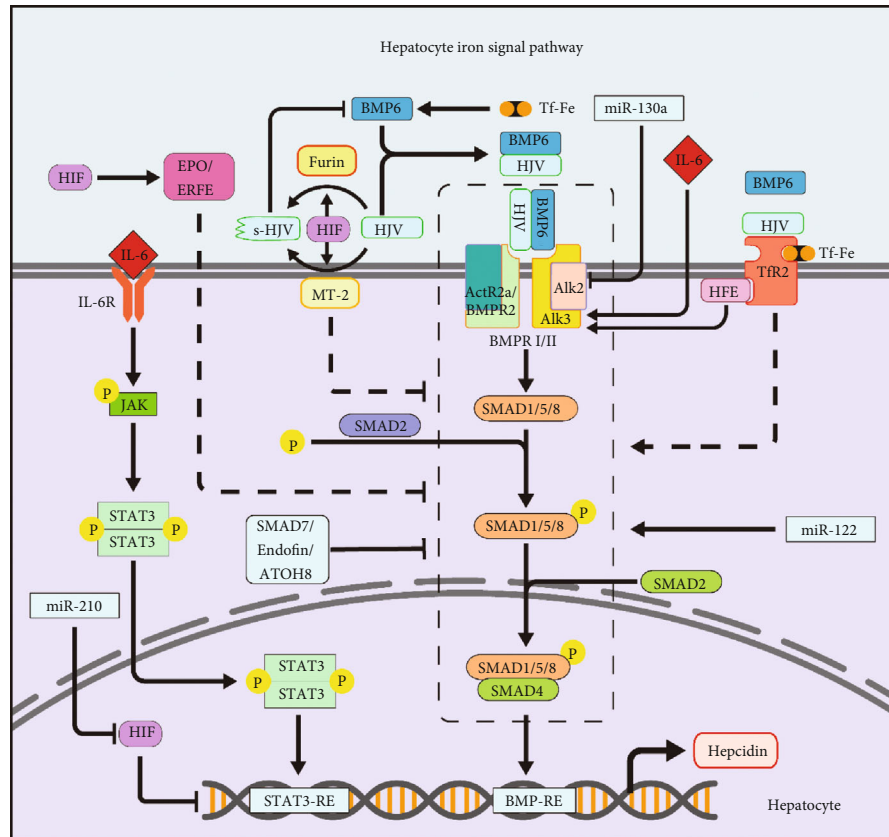


FIGURE 2: Hepatocyte pathways regulate iron homeostasis.

As the iron concentration in the blood, it is sensed by the liver through the Tf-Fe competing with HFE binding to TfR (TfR1/TfR2) on the hepatocyte cytomembrane [63]. The difference in the ability of Tf and HFE to bind to TfR transmits a signal of concentration of the blood iron in hepatocyte [64]. The capability of Tf-Fe combined with TfR1 is stronger than HFE, and Tf-Fe combined with TfR1 is far stronger than TfR2 [65]. While the systemic iron fluxes at a high concentration, the saturation of iron binding to TfR1 and the excessive Tf-Fe binding to TfR2, at the same time, the HFE having no choice but combining with TfR2 or free on the cell surface, both of these states transmit signals to stimulate the expression of hepcidin. While the systemic iron fluxes, the high concentration of the Tf-Fe saturated binding to all TfR1 and the rest excessive Tf-Fe saturated binding to TfR2, at the same time, the HFE only binds to TfR2 or dissociation on the cytomembrane, the combination of TfR2 with either Tf-Fe or HFE can transmit the signals to stimulate the expression of hepcidin [66]. When the iron in circulating decreases, TfR1 combines all of Tf-Fe and partial HFE, uncombined TfR2 weaken the effects of the stimulation and decreasing the expression of hepcidin to augment the intestinal iron absorption [55].

It is not completely clear how TfR2, HFE, and HJV affect hepcidin expression, but there have been experiments shown in *HFE* and *TfR2* knockout mice that the conduction of the BMP/SMAD signaling pathway was impaired [67, 68]. Recent research shows that the noncompetitive binding of HFE and TfR2 to HJV causes changes in hepcidin expression

[55]; in addition, HFE also has the ability to regulate the BMP/SMAD signaling pathway by binding to ALK3 [69]. Neogenin is also involved in the regulation of the hepcidin by being a scaffold of binding HJV and ALK3 [22, 70]; it increases the stability of the HJV protein and suppressing HJV secretion [71]. Besides that, neogenin inhibits the BMP-2-induced phosphorylation of the Smad1/5/8 [72] and facilitates the cleavage of HJV by matriptase-2 or furin [70, 73]. There are others pointout the HJV-neogenin interaction dose not only exist in the liver but also in other tissues [70]. Signal pathways in hepatocytes regulate hepcidin expression as shown in Figure 2.

BMP/SMAD signaling pathway: BMP6 and its coreceptor HJV activate BMPR I/II, leading to phosphorylation of SMAD (1/5/8) and complexes with SMAD4 as an active transcriptional complex. The complex combines with the BMP-RE on *HAMP* then activates transcription of the hepcidin. SMAD2 promotes the phosphorylation of SMAD (1/5/8). SMAD7, endofin, and ATOH8 reduce the signaling of BMP/SMAD. HJV is cleaved by MT-2 and furin to reduced binding capacity to BMP6. miR-130a and miR-122 inhibit AIL2 and BMP/SMAD to regulate the expression of hepcidin.

High concentrations of Tf-Fe induce HFE and Tf-Fe which combine with TfR2 and HJV together to promote BMP/SMAD signaling pathway. HFE interacts with ALK3 increasing hepcidin excrete.

Hypoxia induces the HIF-determined EPO/ERFE concentration in the blood circulation; all of them increase the systemic iron concentration through the BMP/SMAD

pathway. HIF promotes MT2 and furin to cleavage HJV, and miR-210 inhibits it to reduce hepcidin expression. Iron increases BMP6 expression.

In inflammation, IL-6 combines with its receptor IL-6R to activate the JAK, triggering the phosphorylates of STAT3 that forms as a complex move into the nucleus and promotes the transcription of *HAMP*. IL6 increases the BMP/SMAD pathway by promoting ALK3.

2.3. Role of Inflammation, Hypoxia, and MicroRNA in Iron Regulation. Infection and inflammation induce hepcidin production [74], which inhibits iron efflux from intestinal and promotes iron chelation in macrophages, thus reducing the concentration of blood iron [75]. During inflammation, the secretion of proinflammatory cytokines (such as IL-6) increases. Interleukin-6 (IL-6) is one kind of cytokine that regulates the transcription of hepcidin [76]. It combines with the IL-6 receptor (IL-6R) on the membrane, then activates JAK and phosphorylates STAT3 protein in hepatocytes. The phosphorylated STAT3 protein moves into the nucleus, regulating the expression of *HAMP* by binding to the STAT3-specific site [77]. IL-6 not only affects hepcidin expression through the JAK/STAT3 pathway but also combines one of the BMPR I receptor Alk3 [78]; this indicates that the JAK-STAT3 pathway has cross action with the BMP/SMAD pathway [79]. In acute inflammatory condition, the stimulation of Toll-like receptor reduces FPN1 in macrophages, blocking the iron excretion from macrophages which is recovered from red blood cells and rapidly induced hypoferrremia [80]. Then, the heme, required by the proerythroblast to complete its terminal differentiation stage, is exported from macrophages by FLVCR1 [81]. High hepcidin lowers the pathogens available in iron; it is a strategy to starve the pathogens to limit their growth [82]. But as one of the defensin-like peptide hormones, the innate immunity functions of hepcidin have a connection to antimicrobial peptides and inflammation; perhaps, the role of hepcidin in immunity could bypass iron and be directly related to hosting defense (Figure 2).

The body compensates for the oxygen content by intensifying the erythropoiesis when hypoxia, blood loss, or the other causes. In response to the erythropoiesis, erythropoietin (EPO) is secreted by the kidney. According to the severity of hypoxia, EPO has a hundred times of differing in serum [83], it controls iron absorption, erythroid progenitor cell proliferation, maturation, and survival [84, 85]. Erythroferrone (ERFE) is a soluble protein released by EPO-stimulated erythroid precursors; it suppresses the expression of hepcidin [86]. EPO and ERFE suppress the expression of hepcidin by BMP/SMAD pathway target genes [87–89]. But in the IRIDA, due to the MT-2 restriction, the EPO/ERFE-mediated hepcidin downregulation in the BMP/SMAD pathway is obstructed, the blocked signal transmission leads both the EPO and the ERFE, and hepcidin simultaneously maintained elevated levels even in the patients with anemia [90]. The hypoxia-inducible factor (HIF) is a transcription factor of EPO, and the content of the EPO is completely dependent on HIF-2 α [91]. HIF-2 α promotes erythropoiesis, including increases in the production of EPO, which enhances iron uptake and utilization [92]. Therefore, hypoxia increases

the demand for iron and reduces the expression of hepcidin by HIF and EPO [93]. Hepcidin promoter contains several HIF1 and HIF2 sites, regulating the hepcidin by the hypoxia-oxygen-sensing regulatory pathway [94]. Besides that, HIF participates in the BMP/SMAD pathway by affecting the MT-2 and increasing the furin mRNA level [95, 96] (Figure 2).

MicroRNAs are a class of small noncoding RNAs (~22 nt) that bind to the 3' untranslated region (3'UTR) of the target messenger RNA (mRNA), thereby negatively regulating gene expression, and many miRNAs are involved in posttranscriptional regulation of iron. miR-485-3p and miR-17 seed family member miR-20a and miR-20b, as the concurrent modulator to regulate the expression of FPN1 [97–99]. miR-Let-7d and miR-16 family (miR-15b, miR-16, miR-195, and miR-497) bind the 3'UTR of *DMT1*-IRE mRNA then decrease DMT1 expression levels, causing iron accumulation in the endosomes, or hoarded in ferritin or used for iron-related proteins [100–102]. MiR-320 is another microRNA related to cellular iron uptake, which inhibits TfR1 expression and prevents cell proliferation [103], and miR-200b induces downregulation of ferritin [104]. In the BMP-SMAD signaling, ALK2 as primary endogenous BMP type I receptors is involved in systemic iron regulation; miR-130a targets 3'UTR of *ALK2* to inhibit BMP-SMAD signaling and the expression of hepcidin; it was upregulated in the iron deficiency mice [105].

In the regulation of hypoxia, *HIF-1 α* hypoxia response element-binding site was identified in the promoter of miR-210; the miR-210 is specifically induced by HIF-1 α during hypoxia [106]. Iron-sulfur cluster scaffold protein (ISCU) is an iron homeostasis essential molecule; iron deficiency induces miR-210 expression through HIF-1 α , and miR-210 directly inhibits ISCU and TfR to maintain the systemic iron homeostasis [107]. miR-122 is a very important microRNA that is selectively expressed in the liver and participates in a variety of regulation, including maintaining iron homeostasis. It controls hepcidin mRNA transcription by inhibiting the expression of *Hfe*, *Hjv*, and *Bmpr1a* in the liver, thereby preventing iron deficiency [108], thus activating *Hamp* mRNA expression. miRNAs related to iron regulation are summarized in Figures 1 and 2.

2.4. Diseases Related to Disorders of Iron Metabolism

2.4.1. Iron Overload Causes Cell Oxidative Damaged-Ferroptosis. Ferroptosis is a form of regulated cell death; unlike other forms of regulated cell death, ferroptosis is unnecessary for the caspases [109]. Ferroptosis is characterized by the overwhelming iron-dependent oxidative injury and accumulation of lipid hydroperoxides to lethal levels. The excessive iron produces ROS (reactive oxygen species) by Fenton reaction in cells. In cells, the ROS has multiple sources; iron and its derivatives are essential for the ROS-producing enzymes.

Ferroptosis is related to amino acid metabolism. Glutathione (GSH) protects cells from oxidative stress damage, but the availability of cysteine limits the GSH biosynthesis [110]; therefore, the cysteine is contributed to protecting cells

TABLE 1: Genetic mutation causes iron metabolism disorders.

Protein	Gene	Mutation site	Downstream effect	Phenotype	Reference
HFE	HFE	C282Y	Iron concentration perception	Regulation hepcidin expression by binding TfR	[133]
TfR2	TFR2	Y250X	Tf, HFE receptor	C282Y homozygote modifier	[144]
HJV	HJV	G320V, etc.	Activate BMP-SMAD	Regulation hepcidin expression	[134]
MT2	TMPRSS6	A736V	Cleavage HJV	Determining protease activity, influences the hepcidin response to iron	[140]
FPN1	SLC40A1	C326S	Cellular iron effluxion	Resistance combine hepcidin	[145, 146]

from oxidative stress. Cysteine is produced by the reduction of cystine which is transported into cells by the cystine/glutamate reverse transport system xc^- , then for the GSH synthesis. Cells not only rely on the system xc^- to import cystine but also bypass the system xc^- by the transsulfuration pathway to biosynthesize the cysteine from methionine.

The depletion of GSH inactivation of the GSH peroxidase 4 (GPX4) ultimately causes the ferroptosis. Erastin, an oncogenic RAS-selective lethal small molecule [111], induces ferroptosis by inducing GSH depletion and inactivation of the phospholipid peroxidase GPX4 and inhibits import of cystine [112]. So amino acid metabolism is closely linked to ferroptosis [113]; furthermore, studies on the association of ferroptosis and various diseases have provided a new perspective and have become a new research aspect, such as Parkinson's disease, Alzheimer's disease, Huntington's disease, stroke, apoplexy, ischemia-reperfusion injury, cardiopathy, carcinogenesis, periventricular leukomalacia, and brain injury [110].

2.4.2. Parkinson's Disease. Parkinson's disease (PD) is a progressive neurological disorder, primarily from the death of dopaminergic neurons in the substantia nigra [114]. Studies have shown that Parkinson's disease is caused by biochemical abnormalities, including oxidative stress and mitochondrial dysfunction [115, 116], and in recently, some studies have also shown the correlation between PD and ferroptosis [117].

Iron accumulation in neurons induces oxidative stress by Fenton's reaction generating ROS. ROS induces iron release from mitochondrial iron-sulfur cluster protein and other iron storage proteins; it leads the further ROS generation through Fenton's reaction [118], then the ROS damage DNA and mtDNA by epigenetic mechanism and oxidize protein [118–120]. The most significant characteristic of Parkinson's disease is the progressive degeneration in the substantia nigra, but current research is still incomprehensible why neurodegeneration only exists in certain nuclei while the other iron-accumulation tissue remains unaffected and the mechanism of neurotoxicity [121].

Mitophagy, the spontaneous and selectively autophagic elimination of damaged or dysfunctional mitochondria, is regulated by accumulation of iron, Parkin, and PINK1 (PTEN-induced putative kinase protein 1) and mediated by autophagosomes. There are reports that show the loss of iron in neuronal triggering mitophagy in a PINK1/Parkin-independent manner [122, 123], and in contrast, the accumulation of cellular iron obstructed the mitophagy, so that the

cells unable to eliminate the damaged mitochondria to maintain normal physiological status.

PINK1 is stably localized on damaged mitochondria with low membrane potential [124], and the Parkin, an E3 ubiquitin ligase, is selectively recruited from cytosol to dysfunctional mitochondria [125] and liberates the activity of the E3 by the PINK1-dependent mitochondrial localization [124], then Parkin ubiquitination outer mitochondrial membrane proteins to trigger mitophagy [126]. So, the PINK1 and Parkin together sense the distress of mitochondria and selectively target them for degradation [127], and the mutations of PINK1 or Parkin fail to clear damaged mitochondria [128, 129], causing neuronal damage [130], leading to Parkinson's disease [131].

2.4.3. Hereditary Iron Disease. Hereditary hemochromatosis (HH) mainly in Western populations causes iron overloaded. HH is caused by multiple genetic defects like *HFE*, *TfR2*, *HJV*, *TMPRSS6*, *FPN1*, and *HAMP*. According to different mutant genes, HH is divided into HFE hemochromatosis (type1), juvenile hemochromatosis (type 2), TfR2 hemochromatosis (type 3), and ferroportin hemochromatosis.

The majority of the HH is typ1 and typ2; it is due to the homozygosity for the C282Y mutation in the *HFE* and G320V, etc. in the *HJV* genes [132–135]. *HFE* and *HJV* mutations alone or simultaneously affect the expression of hepcidin through the BMP/SMAD pathway. In type 3 HH, the mutation was identified on human chromosome 7q22 homozygous recessive Y250X in *TfR2* [136]; type 3 HH is less severe than typ1 and typ2 HH. Type 3 HH pathogenesis is demonstrated in the mutation experiment of mice; the mutation of TfR2 caused the inability of TF and HFE to bind to it, weakened the signal transmission, and resulted in the down-regulation of hepcidin expression [137], which ultimately caused iron overload in multiple organs. As a receptor for hepcidin, *FPN1* has C326 residue and is necessary for the binding of hepcidin [138]. Ferroportin hemochromatosis is associated with the mutation of C326 residue, it is an autosomal dominant genetic disease with similar clinical and phenotypic features to other HH, and the mutation of C326 suffices to cause *FPN1* resistance of hepcidin [138, 139]. The loss-of-function mutation of *TMPRSS6* causes IRIDA, and its molecular basis was first identified in 2008 [140, 141]. Microcytic hypochromic anemia, low Tf saturation, and excessive hepcidin are the main characteristic of IRIDA; however, oral iron supplementation is futile in relieving the symptoms. In the IRIDA, the most frequent mutation is S304L; besides that, 40 different mutations in the *TMPRSS6*

gene have been described including *K225E*, *K253E*, *G228D*, *R446W*, *V736A*, and *V795I* [142], but the latest research shows that *ALK2* gene mutation is also involved in the IRIDA [143]. Including the gene mutations mentioned above, we summarized the various genetic variations that caused hereditary iron disease in Table 1.

2.4.4. Perspectives. As one of the most important elements in the body, after the decades of research, we have been clear about the effect of the liver on iron metabolism and regulation, but we are still constantly discovering new methods to affect iron metabolism directly or indirectly. As the secretory organ of hepcidin, the study of microRNA and gene mutations has opened a new horizon for iron regulation in hepatocyte. The discovery of more potential regulators raises more awareness of iron metabolism, and more drugs can be developed to treat iron-related diseases, such as inhibitors or agonist of key genes. Due to the importance of iron in the body, the molecular mechanism of iron sensing and regulation and its interaction needed to fully comprehend.

Conflicts of Interest

The authors declare no conflict of interest, financial, or otherwise.

Acknowledgments

This work was supported by the National Key R&D Program of China (2016YFD0501201), the National Natural Science Foundation of China (31702127), the Young Elite Scientists Sponsorship Program by CAST (2018QNRC001), the Hunan Province Key Laboratory of Animal Nutritional Physiology and Metabolic Process (2018TP1031), and Yangzhou Science and Technology Bureau-Modern Agricultural Technology Project (SNY2017030037).

References

- [1] S. Dev and J. L. Babitt, "Overview of iron metabolism in health and disease," *Hemodialysis International*, vol. 21, pp. S6–S20, 2017.
- [2] L. Allen and B. D. Benoist, *WHO Guidelines on Food Fortification with Micronutrients*, WHO, 2006.
- [3] D. Wan, Q. Wu, H. Ni, G. Liu, Z. Ruan, and Y. Yin, "Treatments for iron deficiency (ID): prospective organic iron fortification," *Current Pharmaceutical Design*, vol. 25, no. 3, pp. 325–332, 2019.
- [4] A. Pietrangelo, "Ferroportin disease: pathogenesis, diagnosis and treatment," *Haematologica*, vol. 102, no. 12, pp. 1972–1984, 2017.
- [5] Y. Zhang, D. Wan, X. Zhou et al., "Diurnal variations in iron concentrations and expression of genes involved in iron absorption and metabolism in pigs," *Biochemical and Biophysical Research Communications*, vol. 490, no. 4, pp. 1210–1214, 2017.
- [6] M. Shayeghi, G. O. Latunde-Dada, J. S. Oakhill et al., "Identification of an intestinal heme transporter," *Cell*, vol. 122, no. 5, pp. 789–801, 2005.
- [7] P. Krishnamurthy, T. Xie, and J. D. Schuetz, "The role of transporters in cellular heme and porphyrin homeostasis," *Pharmacology & Therapeutics*, vol. 114, no. 3, pp. 345–358, 2007.
- [8] Y. Gottlieb, M. Truman, L. A. Cohen, Y. Leichtmann-Bardoogo, and E. G. Meyron-Holtz, "Endoplasmic reticulum anchored heme-oxygenase 1 faces the cytosol," *Haematologica*, vol. 97, no. 10, pp. 1489–1493, 2012.
- [9] M. B. Troadec, D. M. Ward, E. Lo, J. Kaplan, and I. de Domenico, "Induction of FPN1 transcription by MTF-1 reveals a role for ferroportin in transition metal efflux," *Blood*, vol. 116, no. 22, pp. 4657–4664, 2010.
- [10] A. Donovan, C. A. Lima, J. L. Pinkus et al., "The iron exporter ferroportin/Slc40a1 is essential for iron homeostasis," *Cell Metabolism*, vol. 1, no. 3, pp. 191–200, 2005.
- [11] A. Donovan, A. Brownlie, Y. Zhou et al., "Positional cloning of zebrafish ferroportin1 identifies a conserved vertebrate iron exporter," *Nature*, vol. 403, no. 6771, pp. 776–781, 2000.
- [12] P. M. Harrison and P. Arosio, "The ferritins: molecular properties, iron storage function and cellular regulation," *Biochimica et Biophysica Acta-Bioenergetics*, vol. 1275, no. 3, pp. 161–203, 1996.
- [13] H. Chen, Z. K. Attieh, T. Su et al., "Hephaestin is a ferroxidase that maintains partial activity in sex-linked anemia mice," *Blood*, vol. 103, no. 10, pp. 3933–3939, 2004.
- [14] N. E. Hellman and J. D. Gitlin, "Ceruloplasmin metabolism and function," *Annual Review of Nutrition*, vol. 22, pp. 439–458, 2002.
- [15] J. S. Hankins, M. P. Smeltzer, M. McCarville et al., "Patterns of liver iron accumulation in patients with sickle cell disease and thalassemia with iron overload," *European Journal of Haematology*, vol. 85, no. 1, pp. 51–57, 2010.
- [16] H. Kawabata, R. S. Germain, P. T. Vuong, T. Nakamaki, J. W. Said, and H. P. Koeffler, "Transferrin receptor 2-alpha supports cell growth both in iron-chelated cultured cells and in vivo," *Journal of Biological Chemistry*, vol. 275, no. 22, pp. 16618–16625, 2000.
- [17] J. Wally, P. J. Halbrooks, C. Vornrhein et al., "The crystal structure of iron-free human serum transferrin provides insight into inter-lobe communication and receptor binding," *Journal of Biological Chemistry*, vol. 281, no. 34, pp. 24934–24944, 2006.
- [18] A. M. Giannetti, P. J. Halbrooks, A. B. Mason, T. M. Vogt, C. A. Enns, and P. J. Björkman, "The molecular mechanism for receptor-stimulated iron release from the plasma iron transport protein transferrin," *Structure*, vol. 13, no. 11, pp. 1613–1623, 2005.
- [19] R. S. Ohgami, D. R. Campagna, E. L. Greer et al., "Identification of a ferrireductase required for efficient transferrin-dependent iron uptake in erythroid cells," *Nature Genetics*, vol. 37, no. 11, pp. 1264–1269, 2005.
- [20] P. J. Cullen and H. C. Korswagen, "Sorting nexins provide diversity for retromer-dependent trafficking events," *Nature Cell Biology*, vol. 14, no. 1, pp. 29–37, 2012.
- [21] C. Chen, D. Garcia-Santos, Y. Ishikawa et al., "Snx3 regulates recycling of the transferrin receptor and iron assimilation," *Cell Metabolism*, vol. 17, no. 3, pp. 343–352, 2013.
- [22] M. U. Muckenthaler, S. Rivella, M. W. Hentze, and B. Galy, "A red carpet for iron metabolism," *Cell*, vol. 168, no. 3, pp. 344–361, 2017.
- [23] T. Korolnek and I. Hamza, "Macrophages and iron trafficking at the birth and death of red cells," *Blood*, vol. 125, no. 19, pp. 2893–2897, 2015.

- [24] M. C. Bessis and J. Breton-Gorius, "Iron metabolism in the bone marrow as seen by electron Microscopy: a critical review," *Blood*, vol. 19, no. 6, pp. 635–663, 1962.
- [25] M. J. Leimberg, E. Prus, A. M. Konijn, and E. Fibach, "Macrophages function as a ferritin iron source for cultured human erythroid precursors," *Journal of Cellular Biochemistry*, vol. 103, no. 4, pp. 1211–1218, 2008.
- [26] J. M. Leimberg, E. Prus, G. Link, E. Fibach, and A. M. Konijn, "Iron-chelator complexes as iron sources for early developing human erythroid precursors," *Translational Research*, vol. 151, no. 2, pp. 88–96, 2008.
- [27] L. Li, C. J. Fang, J. C. Ryan et al., "Binding and uptake of H-ferritin are mediated by human transferrin receptor-1," *Proceedings of the National Academy of Sciences of the United States of America*, vol. 107, no. 8, pp. 3505–3510, 2010.
- [28] M. W. Hentze, M. U. Muckenthaler, B. Galy, and C. Camaschella, "Two to tango: regulation of mammalian iron metabolism," *Cell*, vol. 142, no. 1, pp. 24–38, 2010.
- [29] D. Z. de Back, E. B. Kostova, M. van Kraaij, T. K. van den Berg, and R. van Bruggen, "Of macrophages and red blood cells; a complex love story," *Frontiers in Physiology*, vol. 5, p. 11, 2014.
- [30] R. E. Mebius and G. Kraal, "Structure and function of the spleen," *Nature Reviews Immunology*, vol. 5, no. 8, pp. 606–616, 2005.
- [31] M. Knutson and M. Wessling-Resnick, "Iron metabolism in the reticuloendothelial system," *Critical Reviews in Biochemistry and Molecular Biology*, vol. 38, no. 1, pp. 61–88, 2003.
- [32] J. Connor, C. C. Pak, and A. J. Schroit, "Exposure of phosphatidylserine in the outer leaflet of human red blood cells. Relationship to cell density, cell age, and clearance by mononuclear cells," *Journal of Biological Chemistry*, vol. 269, no. 4, pp. 2399–2404, 1994.
- [33] P. Low, S. Waugh, K. Zinke, and D. Drenckhahn, "The role of hemoglobin denaturation and band 3 clustering in red blood cell aging," *Science*, vol. 227, no. 4686, pp. 531–533, 1985.
- [34] D. Bratosin, J. Mazurier, J. P. Tissier et al., "Cellular and molecular mechanisms of senescent erythrocyte phagocytosis by macrophages. A review," *Biochimie*, vol. 80, no. 2, pp. 173–195, 1998.
- [35] C. White, X. Yuan, P. J. Schmidt et al., "HRG1 is essential for heme transport from the phagolysosome of macrophages during erythrophagocytosis," *Cell Metabolism*, vol. 17, no. 2, pp. 261–270, 2013.
- [36] I. Yanatori, M. Tabuchi, Y. Kawai, Y. Yasui, R. Akagi, and F. Kishi, "Heme and non-heme iron transporters in non-polarized and polarized cells," *BMC Cell Biology*, vol. 11, no. 1, p. 39, 2010.
- [37] E. Nemeth, M. S. Tuttle, J. Powelson et al., "Hepcidin regulates cellular iron efflux by binding to ferroportin and inducing its internalization," *Science*, vol. 306, no. 5704, pp. 2090–2093, 2004.
- [38] I. Hollerer, A. Bachmann, and M. U. Muckenthaler, "Pathophysiological consequences and benefits of HFE mutations: 20 years of research," *Haematologica*, vol. 102, no. 5, pp. 809–817, 2017.
- [39] N. L. Parrow and R. E. Fleming, "Bone morphogenetic proteins as regulators of iron metabolism," in *Annual Review of Nutrition*, R. J. Cousins, Ed., vol. 34, pp. 77–94, Annual Reviews: Palo Alto, 2014.
- [40] S. Canali, K. B. Zumbrennen-Bullough, A. B. Core et al., "Endothelial cells produce bone morphogenetic protein 6 required for iron homeostasis in mice," *Blood*, vol. 129, no. 4, pp. 405–414, 2017.
- [41] E. Ramos, L. Kautz, R. Rodriguez et al., "Evidence for distinct pathways of hepcidin regulation by acute and chronic iron loading in mice," *Hepatology*, vol. 53, no. 4, pp. 1333–1341, 2011.
- [42] R. Daher, C. Kannengiesser, D. Houamel et al., "Heterozygous mutations in BMP6 pro-peptide lead to inappropriate hepcidin synthesis and moderate iron overload in humans," *Gastroenterology*, vol. 150, no. 3, pp. 672–683.e4, 2016.
- [43] C. Latour, C. Besson-Fournier, D. Meynard et al., "Differing impact of the deletion of hemochromatosis-associated molecules HFE and transferrin receptor-2 on the iron phenotype of mice lacking bone morphogenetic protein 6 or hemojuvelin," *Hepatology*, vol. 63, no. 1, pp. 126–137, 2016.
- [44] A. U. Steinbicker, T. B. Bartnikas, L. K. Lohmeyer et al., "Perturbation of hepcidin expression by BMP type I receptor deletion induces iron overload in mice," *Blood*, vol. 118, no. 15, pp. 4224–4230, 2011.
- [45] J. L. Babitt, F. W. Huang, D. M. Wrighting et al., "Bone morphogenetic protein signaling by hemojuvelin regulates hepcidin expression," *Nature Genetics*, vol. 38, no. 5, pp. 531–539, 2006.
- [46] P. B. Yu, C. C. Hong, C. Sachidanandan et al., "Dorsomorphin inhibits BMP signals required for embryogenesis and iron metabolism," *Nature Chemical Biology*, vol. 4, no. 1, pp. 33–41, 2008.
- [47] C. Mayeur, P. A. Leyton, S. A. Kolodziej, B. Yu, and K. D. Bloch, "BMP type II receptors have redundant roles in the regulation of hepatic hepcidin gene expression and iron metabolism," *Blood*, vol. 124, no. 13, pp. 2116–2123, 2014.
- [48] S. Canali, C. Vecchi, C. Garuti, G. Montosi, J. L. Babitt, and A. Pietrangelo, "The SMAD pathway is required for hepcidin response during endoplasmic reticulum stress," *Endocrinology*, vol. 157, no. 10, pp. 3935–3945, 2016.
- [49] G. Casanovas, K. Mleczo-Sanecka, S. Altamura, M. W. Hentze, and M. U. Muckenthaler, "Bone morphogenetic protein (BMP)-responsive elements located in the proximal and distal hepcidin promoter are critical for its response to HJV/BMP/SMAD," *Journal of Molecular Medicine*, vol. 87, no. 5, pp. 471–480, 2009.
- [50] C. Mayeur, S. A. Kolodziej, A. Wang et al., "Oral administration of a bone morphogenetic protein type I receptor inhibitor prevents the development of anemia of inflammation," *Haematologica*, vol. 100, no. 2, pp. E68–E71, 2015.
- [51] L. Silvestri, A. Pagani, A. Nai, I. de Domenico, J. Kaplan, and C. Camaschella, "The serine protease matriptase-2 (TMPRSS6) inhibits hepcidin activation by cleaving membrane hemojuvelin," *Cell Metabolism*, vol. 8, no. 6, pp. 502–511, 2008.
- [52] F. Béliveau, A. Tarkar, S. P. Dion et al., "Discovery and development of TMPRSS6 inhibitors modulating hepcidin levels in human hepatocytes," *Cell Chemical Biology*, vol. 26, no. 11, pp. 1559–1572.e9, 2019.
- [53] D. Meynard, V. Vaja, C. C. Sun et al., "Regulation of TMPRSS6 by BMP6 and iron in human cells and mice," *Blood*, vol. 118, no. 3, pp. 747–756, 2011.

- [54] N. Zhao, C. P. Nizzi, S. A. Anderson et al., "Low intracellular iron increases the stability of matriptase-2," *Journal of Biological Chemistry*, vol. 290, no. 7, pp. 4432–4446, 2015.
- [55] F. D'Alessio, M. W. Hentze, and M. U. Muckenthaler, "The hemochromatosis proteins HFE, TfR2, and HJV form a membrane-associated protein complex for hepcidin regulation," *Journal of Hepatology*, vol. 57, no. 5, pp. 1052–1060, 2012.
- [56] J. E. Maxson, J. Chen, C. A. Enns, and A. S. Zhang, "Matriptase-2- and proprotein convertase-cleaved forms of hemojuvelin have different roles in the down-regulation of hepcidin expression," *Journal of Biological Chemistry*, vol. 285, no. 50, pp. 39021–39028, 2010.
- [57] A. S. Zhang, S. A. Anderson, K. R. Meyers, C. Hernandez, R. S. Eisenstein, and C. A. Enns, "Evidence that inhibition of hemojuvelin shedding in response to iron is mediated through neogenin," *Journal of Biological Chemistry*, vol. 282, no. 17, pp. 12547–12556, 2007.
- [58] M. Wahedi, A. M. Wortham, M. D. Kleven et al., "Matriptase-2 suppresses hepcidin expression by cleaving multiple components of the hepcidin induction pathway," *Journal of Biological Chemistry*, vol. 292, no. 44, pp. 18354–18371, 2017.
- [59] L. Silvestri, A. Pagani, and C. Camaschella, "Furin-mediated release of soluble hemojuvelin: a new link between hypoxia and iron homeostasis," *Blood*, vol. 111, no. 2, pp. 924–931, 2008.
- [60] J. B. Goh, D. F. Wallace, W. Hong, and V. N. Subramaniam, "Endofin, a novel BMP-SMAD regulator of the iron-regulatory hormone, hepcidin," *Scientific Reports*, vol. 5, no. 1, p. 12, 2015.
- [61] S. Upanan, A. T. McKie, G. O. Latunde-Dada et al., "Hepcidin suppression in β -thalassemia is associated with the down-regulation of atonal homolog 8," *International Journal of Hematology*, vol. 106, no. 2, pp. 196–205, 2017.
- [62] D. Lai, F. Teng, S. Hammad et al., "Hepatic Smad7 overexpression causes severe iron overload in mice," *Blood*, vol. 131, no. 5, pp. 581–585, 2018.
- [63] H. Kawabata, "Transferrin and transferrin receptors update," *Free Radical Biology and Medicine*, vol. 133, pp. 46–54, 2019.
- [64] M. D. Kleven, S. Jue, and C. A. Enns, "Transferrin receptors TfR1 and TfR2 bind transferrin through differing mechanisms," *Biochemistry*, vol. 57, no. 9, pp. 1552–1559, 2018.
- [65] P. J. Schmidt, P. T. Toran, A. M. Giannetti, P. J. Bjorkman, and N. C. Andrews, "The transferrin receptor modulates Hfe-dependent regulation of hepcidin expression," *Cell Metabolism*, vol. 7, no. 3, pp. 205–214, 2008.
- [66] J. Gao, J. Chen, M. Kramer, H. Tsukamoto, A.-S. Zhang, and C. A. Enns, "Interaction of the hereditary hemochromatosis protein HFE with transferrin receptor 2 is required for transferrin-induced hepcidin expression," *Cell Metabolism*, vol. 9, no. 3, pp. 217–227, 2009.
- [67] D. F. Wallace, L. Summerville, E. M. Crampton, D. M. Frazer, G. J. Anderson, and V. N. Subramaniam, "Combined deletion of Hfe and transferrin receptor 2 in mice leads to marked dysregulation of hepcidin and iron overload," *Hepatology*, vol. 50, no. 6, pp. 1992–2000, 2009.
- [68] P. Kent, N. Wilkinson, M. Constante et al., "Hfe and HJV exhibit overlapping functions for iron signaling to hepcidin," *Journal of Molecular Medicine*, vol. 93, no. 5, pp. 489–498, 2015.
- [69] L. Traeger, C. A. Enns, J. Krijt, and A. U. Steinbicker, "The hemochromatosis protein HFE signals predominantly via the BMP type I receptor ALK3 in vivo," *Communications Biology*, vol. 1, no. 1, p. 7, 2018.
- [70] N. Zhao, J. E. Maxson, R. H. Zhang, M. Wahedi, C. A. Enns, and A.-S. Zhang, "Neogenin facilitates the induction of hepcidin expression by hemojuvelin in the liver," *Journal of Biological Chemistry*, vol. 291, no. 23, pp. 12322–12335, 2016.
- [71] D. H. Lee, L. J. Zhou, Z. Zhou et al., "Neogenin inhibits HJV secretion and regulates BMP-induced hepcidin expression and iron homeostasis," *Blood*, vol. 115, no. 15, pp. 3136–3145, 2010.
- [72] M. Hagihara, M. Endo, K. Hata et al., "Neogenin, a receptor for bone morphogenetic proteins," *Journal of Biological Chemistry*, vol. 286, no. 7, pp. 5157–5165, 2011.
- [73] C. A. Enns, R. Ahmed, and A. S. Zhang, "Neogenin interacts with matriptase-2 to facilitate hemojuvelin cleavage," *Journal of Biological Chemistry*, vol. 287, no. 42, pp. 35104–35117, 2012.
- [74] C. Y. Wang and J. L. Babitt, "Hepcidin regulation in the anemia of inflammation," *Current Opinion in Hematology*, vol. 23, no. 3, pp. 189–197, 2016.
- [75] T. Ganz and E. Nemeth, "Iron balance and the role of hepcidin in chronic kidney disease," *Seminars in Nephrology*, vol. 36, no. 2, pp. 87–93, 2016.
- [76] E. Nemeth, S. Rivera, V. Gabayan et al., "IL-6 mediates hypoferremia of inflammation by inducing the synthesis of the iron regulatory hormone hepcidin," *The Journal of Clinical Investigation*, vol. 113, no. 9, pp. 1271–1276, 2004.
- [77] D. M. Wrighting and N. C. Andrews, "Interleukin-6 induces hepcidin expression through STAT3," *Blood*, vol. 108, no. 9, pp. 3204–3209, 2006.
- [78] C. Mayeur, L. K. Lohmeyer, P. Leyton et al., "The type I BMP receptor Alk3 is required for the induction of hepatic hepcidin gene expression by interleukin-6," *Blood*, vol. 123, no. 14, pp. 2261–2268, 2014.
- [79] M. V. V. Falzacappa, G. Casanovas, M. W. Hentze, and M. U. Muckenthaler, "A bone morphogenetic protein (BMP)-responsive element in the hepcidin promoter controls HFE2-mediated hepatic hepcidin expression and its response to IL-6 in cultured cells," *Journal of Molecular Medicine*, vol. 86, no. 5, pp. 531–540, 2008.
- [80] C. Guida, S. Altamura, F. A. Klein et al., "A novel inflammatory pathway mediating rapid hepcidin-independent hypoferremia," *Blood*, vol. 125, no. 14, pp. 2265–2275, 2015.
- [81] S. B. Keel, R. T. Doty, Z. Yang et al., "A heme export protein is required for red blood cell differentiation and iron homeostasis," *Science*, vol. 319, no. 5864, pp. 825–828, 2008.
- [82] D. Vyoral and J. Petrak, "Therapeutic potential of hepcidin – the master regulator of iron metabolism," *Pharmacological Research*, vol. 115, pp. 242–254, 2017.
- [83] B. L. Ebert and H. F. Bunn, "Regulation of the erythropoietin gene," *Blood*, vol. 94, no. 6, pp. 1864–1877, 1999.
- [84] I. Artuso, M. Pettinato, A. Nai et al., "Transient decrease of serum iron after acute erythropoietin treatment contributes to hepcidin inhibition by ERFE in mice," *Haematologica*, vol. 104, no. 3, pp. E87–E90, 2019.
- [85] J. Rossert and K. U. Eckardt, "Erythropoietin receptors: their role beyond erythropoiesis," *Nephrology Dialysis Transplantation*, vol. 20, no. 6, pp. 1025–1028, 2005.

- [86] L. Kautz, G. Jung, E. V. Valore, S. Rivella, E. Nemeth, and T. Ganz, "Identification of erythroferrone as an erythroid regulator of iron metabolism," *Nature Genetics*, vol. 46, no. 7, pp. 678–684, 2014.
- [87] S. Aschemeyer, V. Gabayan, T. Ganz, E. Nemeth, and L. Kautz, "Erythroferrone and matriptase-2 independently regulate hepcidin expression," *American Journal of Hematology*, vol. 92, no. 5, pp. E61–E63, 2017.
- [88] J. Arezes, N. Foy, K. McHugh et al., "Erythroferrone inhibits the induction of hepcidin by BMP6," *Blood*, vol. 132, no. 14, pp. 1473–1477, 2018.
- [89] C. Y. Wang, A. B. Core, S. Canali et al., "Smad1/5 is required for erythropoietin-mediated suppression of hepcidin in mice," *Blood*, vol. 130, no. 1, pp. 73–83, 2017.
- [90] A. Nai, A. Rubio, A. Campanella et al., "Limiting hepatic Bmp-Smad signaling by matriptase-2 is required for erythropoietin-mediated hepcidin suppression in mice," *Blood*, vol. 127, no. 19, pp. 2327–2336, 2016.
- [91] P. P. Kapitsinou, Q. Liu, T. L. Unger et al., "Hepatic HIF-2 regulates erythropoietic responses to hypoxia in renal anemia," *Blood*, vol. 116, no. 16, pp. 3039–3048, 2010.
- [92] V. H. Haase, "Hypoxic regulation of erythropoiesis and iron metabolism," *American Journal of Physiology-Renal Physiology*, vol. 299, no. 1, pp. F1–F13, 2010.
- [93] G. Nicolas, C. Chauvet, L. Viatte et al., "The gene encoding the iron regulatory peptide hepcidin is regulated by anemia, hypoxia, and inflammation," *Journal of Clinical Investigation*, vol. 110, no. 7, pp. 1037–1044, 2002.
- [94] M. Safran and W. G. Kaelin Jr., "HIF hydroxylation and the mammalian oxygen-sensing pathway," *Journal of Clinical Investigation*, vol. 111, no. 6, pp. 779–783, 2003.
- [95] S. McMahon, F. Grondin, P. P. McDonald, D. E. Richard, and C. M. Dubois, "Hypoxia-enhanced expression of the proprotein convertase furin is mediated by hypoxia-inducible Factor-1," *Journal of Biological Chemistry*, vol. 280, no. 8, pp. 6561–6569, 2005.
- [96] S. Lakhal, J. Schödel, A. R. M. Townsend, C. W. Pugh, P. J. Ratcliffe, and D. R. Mole, "Regulation of type II transmembrane serine proteinase TMPRSS6 by hypoxia-inducible factors: new link between hypoxia signaling and iron homeostasis," *Journal of Biological Chemistry*, vol. 286, no. 6, pp. 4090–4097, 2011.
- [97] C. Sangokoya, J. F. Doss, and J. T. Chi, "Iron-responsive miR-485-3p regulates cellular iron homeostasis by targeting ferroportin," *PLoS Genetics*, vol. 9, no. 4, p. e1003408, 2013.
- [98] K. R. Babu and M. U. Muckenthaler, "miR-20a regulates expression of the iron exporter ferroportin in lung cancer," *Journal of Molecular Medicine*, vol. 94, no. 3, pp. 347–359, 2016.
- [99] S. Jiang, X. Fang, M. Liu, Y. Ni, W. Ma, and R. Zhao, "MiR-20b down-regulates intestinal ferroportin expression in vitro and in vivo," *Cell*, vol. 8, no. 10, p. 1135, 2019.
- [100] I. Andolfo, L. de Falco, R. Ascì et al., "Regulation of divalent metal transporter 1 (DMT1) non-IRE isoform by the microRNA let-7d in erythroid cells," *Haematologica*, vol. 95, no. 8, pp. 1244–1252, 2010.
- [101] W. Hou, Q. Tian, N. M. Steuerwald, L. W. Schrum, and H. L. Bonkovsky, "The let-7 microRNA enhances heme oxygenase-1 by suppressing Bach1 and attenuates oxidant injury in human hepatocytes," *Biochimica Et Biophysica Acta-Gene Regulatory Mechanisms*, vol. 1819, no. 11–12, pp. 1113–1122, 2012.
- [102] S. Jiang, S. Guo, H. Li, Y. Ni, W. Ma, and R. Zhao, "Identification and functional verification of microRNA-16 family targeting intestinal divalent metal transporter 1 (DMT1) in vitro and in vivo," *Frontiers in Physiology*, vol. 10, p. 11, 2019.
- [103] D. G. Schaar, D. J. Medina, D. F. Moore, R. K. Strair, and Y. Ting, "miR-320 targets transferrin receptor 1 (CD71) and inhibits cell proliferation," *Experimental Hematology*, vol. 37, no. 2, pp. 245–255, 2009.
- [104] S. I. Shpyleva, V. P. Tryndyak, O. Kovalchuk et al., "Role of ferritin alterations in human breast cancer cells," *Breast Cancer Research and Treatment*, vol. 126, no. 1, pp. 63–71, 2011.
- [105] K. B. Zumbrennen-Bullough, Q. Wu, A. B. Core et al., "MicroRNA-130a is up-regulated in mouse liver by iron deficiency and targets the bone morphogenetic protein (BMP) receptor ALK2 to attenuate BMP signaling and hepcidin transcription," *Journal of Biological Chemistry*, vol. 289, no. 34, pp. 23796–23808, 2014.
- [106] R. Kulshreshtha, M. Ferracin, S. E. Wojcik et al., "A microRNA signature of hypoxia," *Molecular and Cellular Biology*, vol. 27, no. 5, pp. 1859–1867, 2007.
- [107] Y. Yoshioka, N. Kosaka, T. Ochiya, and T. Kato, "Micromanaging iron homeostasis hypoxia-inducible micro-RNA-210 suppresses iron homeostasis-related proteins," *Journal of Biological Chemistry*, vol. 287, no. 41, pp. 34110–34119, 2012.
- [108] M. Castoldi, M. Vujic Spasic, S. Altamura et al., "The liver-specific microRNA miR-122 controls systemic iron homeostasis in mice," *Journal of Clinical Investigation*, vol. 121, no. 4, pp. 1386–1396, 2011.
- [109] J. C. Reed and M. Pellicchia, "Ironing out cell death mechanisms," *Cell*, vol. 149, no. 5, pp. 963–965, 2012.
- [110] B. R. Stockwell, J. P. Friedmann Angeli, H. Bayir et al., "Ferroptosis: a regulated cell death nexus linking metabolism, redox biology, and disease," *Cell*, vol. 171, no. 2, pp. 273–285, 2017.
- [111] S. J. Dixon, K. M. Lemberg, M. R. Lamprecht et al., "Ferroptosis: an iron-dependent form of nonapoptotic cell death," *Cell*, vol. 149, no. 5, pp. 1060–1072, 2012.
- [112] W. S. Yang, R. SriRamaratnam, M. E. Welsch et al., "Regulation of ferroptotic cancer cell death by GPX4," *Cell*, vol. 156, no. 1–2, pp. 317–331, 2014.
- [113] J. P. F. Angeli, R. Shah, D. A. Pratt, and M. Conrad, "Ferroptosis inhibition: mechanisms and opportunities," *Trends in Pharmacological Sciences*, vol. 38, no. 5, pp. 489–498, 2017.
- [114] W. Dauer and S. Przedborski, "Parkinson's disease: mechanisms and models," *Neuron*, vol. 39, no. 6, pp. 889–909, 2003.
- [115] A. H. V. Schapira, "Mitochondria in the aetiology and pathogenesis of Parkinson's disease," *Lancet Neurology*, vol. 7, no. 1, pp. 97–109, 2008.
- [116] J. T. Greenamyre and T. G. Hastings, "BIOMEDICINE: Parkinson's—Divergent causes, convergent mechanisms," *Science*, vol. 304, no. 5674, pp. 1120–1122, 2004.
- [117] B. Do Van, F. Gouel, A. Jonneaux et al., "Ferroptosis, a newly characterized form of cell death in Parkinson's disease that is regulated by PKC," *Neurobiology of Disease*, vol. 94, pp. 169–178, 2016.
- [118] R. Ward, F. A. Zucca, J. H. Duyn, R. R. Crichton, and L. Zecca, "The role of iron in brain ageing and

- neurodegenerative disorders," *The Lancet Neurology*, vol. 13, no. 10, pp. 1045–1060, 2014.
- [119] J. P. M. Melis, H. van Steeg, and M. Luijten, "Oxidative DNA damage and nucleotide excision repair," *Antioxidants & Redox Signaling*, vol. 18, no. 18, pp. 2409–2419, 2013.
- [120] J. B. J. Kwok, "Role of epigenetics in Alzheimer's and Parkinson's disease," *Epigenomics*, vol. 2, no. 5, pp. 671–682, 2010.
- [121] D. J. Hare and K. L. Double, "Iron and dopamine: a toxic couple," *Brain*, vol. 139, Part 4, pp. 1026–1035, 2016.
- [122] G. F. G. Allen, R. Toth, J. James, and I. G. Ganley, "Loss of iron triggers PINK1/Parkin-independent mitophagy," *EMBO Reports*, vol. 14, no. 12, pp. 1127–1135, 2013.
- [123] R. M. Ivatt and A. J. Whitworth, "The many faces of mitophagy," *EMBO Reports*, vol. 15, no. 1, pp. 5–6, 2014.
- [124] N. Matsuda, S. Sato, K. Shiba et al., "PINK1 stabilized by mitochondrial depolarization recruits Parkin to damaged mitochondria and activates latent Parkin for mitophagy," *Journal of Cell Biology*, vol. 189, no. 2, pp. 211–221, 2010.
- [125] D. Narendra, A. Tanaka, D. F. Suen, and R. J. Youle, "Parkin is recruited selectively to impaired mitochondria and promotes their autophagy," *Journal of Cell Biology*, vol. 183, no. 5, pp. 795–803, 2008.
- [126] A. M. Pickrell and R. J. Youle, "The roles of PINK1, Parkin, and mitochondrial fidelity in Parkinson's disease," *Neuron*, vol. 85, no. 2, pp. 257–273, 2015.
- [127] D. P. Narendra, S. M. Jin, A. Tanaka et al., "PINK1 is selectively stabilized on impaired mitochondria to activate Parkin," *PLoS Biology*, vol. 8, no. 1, p. e1000298, 2010.
- [128] D. F. Suen, D. P. Narendra, A. Tanaka, G. Manfredi, and R. J. Youle, "Parkin overexpression selects against a deleterious mtDNA mutation in heteroplasmic cybrid cells," *Proceedings of the National Academy of Sciences of the United States of America*, vol. 107, no. 26, pp. 11835–11840, 2010.
- [129] C. Vives-Bauza, C. Zhou, Y. Huang et al., "PINK1-dependent recruitment of Parkin to mitochondria in mitophagy," *Proceedings of the National Academy of Sciences of the United States of America*, vol. 107, no. 1, pp. 378–383, 2010.
- [130] E. M. Valente, P. M. Abou-Sleiman, V. Caputo et al., "Hereditary early-onset Parkinson's disease caused by mutations in PINK1," *Science*, vol. 304, no. 5674, pp. 1158–1160, 2004.
- [131] R. J. Youle and D. P. Narendra, "Mechanisms of mitophagy," *Nature Reviews Molecular Cell Biology*, vol. 12, no. 1, pp. 9–14, 2011.
- [132] L. Valenti, A. L. Fracanzani, R. Rametta et al., "Effect of the A736V TMPRSS6 polymorphism on the penetrance and clinical expression of hereditary hemochromatosis," *Journal of Hepatology*, vol. 57, no. 6, pp. 1319–1325, 2012.
- [133] L. De Falco, R. Tortora, N. Imperatore et al., "The role of TMPRSS6 and HFE variants in iron deficiency anemia in celiac disease," *American Journal of Hematology*, vol. 93, no. 3, pp. 383–393, 2018.
- [134] X. Kong, L. Xie, H. Zhu et al., "Genotypic and phenotypic spectra of hemojuvelin mutations in primary hemochromatosis patients: a systematic review," *Orphanet Journal of Rare Diseases*, vol. 14, no. 1, p. 171, 2019.
- [135] A. Pietrangelo, A. Caleffi, J. Henrion et al., "Juvenile hemochromatosis associated with pathogenic mutations of adult hemochromatosis genes," *Gastroenterology*, vol. 128, no. 2, pp. 470–479, 2005.
- [136] C. Camaschella, A. Roetto, A. Cali et al., "The gene *TFR2* is mutated in a new type of haemochromatosis mapping to 7q22," *Nature Genetics*, vol. 25, no. 1, pp. 14–15, 2000.
- [137] H. Kawabata, R. E. Fleming, D. Gui et al., "Expression of hepcidin is down-regulated in Tfr2 mutant mice manifesting a phenotype of hereditary hemochromatosis," *Blood*, vol. 105, no. 1, pp. 376–381, 2005.
- [138] A. Fernandes, G. C. Preza, Y. Phung et al., "The molecular basis of hepcidin-resistant hereditary hemochromatosis," *Blood*, vol. 114, no. 2, pp. 437–443, 2009.
- [139] R. L. Sham, P. D. Phatak, C. West, P. Lee, C. Andrews, and E. Beutler, "Autosomal dominant hereditary hemochromatosis associated with a novel ferroportin mutation and unique clinical features," *Blood Cells, Molecules & Diseases*, vol. 34, no. 2, pp. 157–161, 2005.
- [140] A. Nai, A. Pagani, L. Silvestri et al., "TMPRSS6 rs855791 modulates hepcidin transcription in vitro and serum hepcidin levels in normal individuals," *Blood*, vol. 118, no. 16, pp. 4459–4462, 2011.
- [141] K. E. Finberg, M. M. Heeney, D. R. Campagna et al., "Mutations in TMPRSS6 cause iron-refractory iron deficiency anemia (IRIDA)," *Nature Genetics*, vol. 40, no. 5, pp. 569–571, 2008.
- [142] E. Beutler, C. van Geet, D. M. W. M. te Loo et al., "Polymorphisms and mutations of human TMPRSS6 in iron deficiency anemia," *Blood Cells Molecules and Diseases*, vol. 44, no. 1, pp. 16–21, 2010.
- [143] A. Pagani, S. Colucci, R. Bocciardi et al., "A new form of IRIDA due to combined heterozygous mutations of TMPRSS6 and ACVR1A encoding the BMP receptor ALK2," *Blood*, vol. 129, no. 25, pp. 3392–3395, 2017.
- [144] A. Roetto, A. Totaro, A. Piperno et al., "New mutations inactivating transferrin receptor 2 in hemochromatosis type 3," *Blood*, vol. 97, no. 9, pp. 2555–2560, 2001.
- [145] S. Altamura, R. Kessler, H. J. Gröne et al., "Resistance of ferroportin to hepcidin binding causes exocrine pancreatic failure and fatal iron overload," *Cell Metabolism*, vol. 20, no. 2, pp. 359–367, 2014.
- [146] M. Theurl, D. Song, E. Clark et al., "Mice with hepcidin-resistant ferroportin accumulate iron in the retina," *FASEB Journal*, vol. 30, no. 2, pp. 813–823, 2016.

Research Article

Dexmedetomidine Protects against Ischemia and Reperfusion-Induced Kidney Injury in Rats

Naren Bao ¹ and Di Dai ²

¹Department of Anesthesiology, The First Hospital of China Medical University, 155 Nanjing North Street, Shenyang, China

²Department of Laboratory Medicine, The First Hospital of China Medical University, 155 Nanjing North Street, Shenyang, China

Correspondence should be addressed to Di Dai; diana_dd@126.com

Received 5 March 2020; Accepted 24 March 2020; Published 3 April 2020

Guest Editor: Hongmei Jiang

Copyright © 2020 Naren Bao and Di Dai. This is an open access article distributed under the Creative Commons Attribution License, which permits unrestricted use, distribution, and reproduction in any medium, provided the original work is properly cited.

Acute kidney injury (AKI), a clinical syndrome, is a sudden onset of kidney failure that severely affects the kidney tubules. One potential treatment is dexmedetomidine (DEX), a highly selective α_2 -adrenoreceptor agonist that is used as an anesthetic adjuvant. It also has anti-inflammatory, neuroprotective, and sympatholytic qualities. The aim of this study was to establish whether DEX also offers protection against ischemia and reperfusion- (I/R-) induced AKI in rats. An intraperitoneal injection of DEX (25 μ g/kg) was administered 30 min prior to the induction of I/R. The results indicate that in the I/R rats, DEX played a protective role by reducing the damage to the tubules and maintaining renal function. Furthermore, in response to I/R, the DEX treatment reduced the mRNA expression of TNF- α , IL-1 β , IL-6, and MCP-1 in the kidney tissues and the serum levels of TNF- α , IL-1 β , IL-6, and MCP-1. DEX also reduced the levels of oxidative stress and apoptosis in the tubular cells. These results indicate that in response to I/R kidney injury, DEX plays a protective role by inhibiting inflammation and tubular cell apoptosis, reducing the production of reactive oxygen species, and promoting renal function.

1. Introduction

Acute kidney injury (AKI) can be a consequence of major surgery. It significantly increases the risks for morbidity and mortality [1]. AKI can result in arrhythmia, cerebral edema, hyperkalemia, renal insufficiency, and water intoxication. All of these conditions pose a risk of death [2]. Few studies have reported on acute stress-induced AKI; thus, research into the underlying mechanisms and effective treatments is needed.

AKI can be initiated by ischemia and reperfusion (I/R). During I/R, the renal tubular epithelial cells experience disturbed cell polarity and cytoskeletal integrity, disrupted cell-cell and cell-matrix interactions, mitochondrial damage, and increased reactive oxygen species (ROS) synthesis [3–5]. Oxidative stress resulting from acute restraint stress has been determined to lead to hippocampal and hepatic damage [6]. Because oxidative stress can promote apoptosis, it also has the capacity to cause AKI. Indeed, a number of pathological kidney injuries have been attributed to apoptosis [6]. This

finding has stimulated inquiries into the role of oxidative stress and apoptosis in the pathological process of I/R-induced kidney injury.

Dexmedetomidine (DEX) possesses several properties that are potentially beneficial for treating AKI. It is a potent and highly selective α_2 adrenergic agonist with analgesic, sedative, and antisympholytic characteristics [7, 8]. The distal and proximal tubules of the kidney, as well as the peritubular vasculature, are rich in α_2 -adrenoceptors [7, 8]. Using animal models, studies have explored the effects of DEX following I/R injury. As well as being beneficial for tubular architecture and function and tubular epithelial cell apoptosis, DEX reduces the synthesis of ROS and inhibits the secretion of proinflammatory cytokines [9]. Despite DEX's capacity to alleviate renal I/R injury following surgery, the mechanism by which it acts in AKI has yet to be elucidated.

The purpose of this study was to explore DEX's protective effects against renal I/R injury in rats. In addition, it is aimed at identifying the mechanisms by which DEX modulates apoptosis, inflammatory cytokines, and ROS.

2. Materials and Methods

2.1. Animals and Experimental Design. The study observed the China Medical University's guidelines for the use of laboratory animals. Approval was sought from and granted by the Ethics Committee on Animal Experiments of The First Hospital of China Medical University.

Eighteen healthy 7–8-week-old male Sprague-Dawley rats weighing 220–270 g were used. They were accommodated in a laboratory (22°C ± 1°C, 12–12 h light-dark cycle) in pathogen-free housing for one week prior to the experiment. Food and water were provided ad libitum until 12 h before the experiment. The food was then withdrawn; however, the water was available.

The rats were sedated and analogized with 10% chloral hydrate (0.3 ml/100 g) and 10 µg/kg sufentanil citrate (Renfu Pharmaceutical, China, Lot 81A06031) injected intraperitoneally (i.p.). To improve perioperative analgesia, 0.2% ropivacaine (AstraZeneca AB, Sweden) was used for local infiltration before surgical incision and after suture. The rats' temperatures were measured, and they were sustained at 37°C (±1°C) with a heat pad. The heart rates were monitored with subcutaneous electrodes. Arterial pressure was invasively monitored by a 24 G trocar that was placed in the left femoral artery. The exclusion criteria were applied to the rats that had heart rates slower than 200 beats per min (bpm) for more than 5 min or mean blood pressures (MAP) less than 55 mmHg. To induce renal I/R injury, the right renal pedicle was clamped for 45 min, and the left was surgically removed.

After the removal of the arterial clip, the color of the remaining kidney was observed. A change from dark purple to reddish brown within 5 min signaled the successful restoration of blood perfusion. Each rat was administered a 0.5 ml saline i.p. injection every 2 h until it awoke or the specimen was collected. The animals were euthanized at 24 h after the I/R, and abdominal aortic blood samples were collected immediately. To remove the cellular elements, the blood samples were left on ice for 2 h and then centrifuged for 15 min (3,000 g, 4°C). The serum was stored at –80°C. The kidneys were harvested following transcardial perfusion with ice-cold heparinized saline. A part of the renal tissue sections were fixed in paraformaldehyde and embedded in paraffin wax; 4 µm sections were removed and stained with hematoxylin and eosin. In addition, a terminal deoxynucleotidyl transferase deoxyuridine triphosphate nick-end labeling (TUNEL) assay was performed. The remainder of the renal tissue was maintained at –80°C until further analysis.

The rats were randomly assigned to one of three groups ($n = 6$ per group):

Group 1. Sham control (Sham): The rats received 0.5 ml saline i.p. injections prior to sham surgery. The renal vessels were not clamped.

Group 2. Renal I/R group (I/R): The surgery was performed as previously described.

Group 3. DEX+I/R group (DEX+I/R): At 30 min prior to the initiation of renal ischemia, 25 µg/kg of DEX was administered by i.p. injection.

TABLE 1: Primers used in this study.

Primers	Sequences
TNF- α	Forward, 5'-CCC GGA ATG TCG ATG CCT GAGTG-3'
	Reverse, 5'-CGC CCC GGC CTT CCA AAT AAAT-3'
IL-1 β	Forward, 5'-GCC CAT CCT CTG TGA CTC AT-3'
	Reverse, 5'-AGG CCA CAG GTA TTT TGT CG-3'
IL-6	Forward, 5'-TCT CGA GCC CAC CAG GAA CGA-3'
	Reverse, 5'-AGG GAA GGC AGT GGC TGT CA-3'
MCP-1	Forward, 5'-AGC ATC CAC GTG CTG TCT C-3'
	Reverse, 5'-GAT CAT CTT GCC AGT GAA TGAG-3'
GAPDH	Forward, 5'-AGG TCG GTG TGA ACG GAT TTG-3'
	Reverse, 5'-TGT AGA CCA TGT AGT TGA GGTC-3'

2.2. Renal Histology. The kidneys were postfixed with 10% buffered formalin, dehydrated in graded ethanol solutions, embedded in paraffin, sectioned, and stained with hematoxylin and eosin. Acute tubular necrosis was graded on a 0 to 4 scale on the basis of the damage to the cortex or outer medulla: 0 = normal, 1 = minimal damage (<5% involvement), 2 = mild damage (5–25% involvement), 3 = moderate damage (25–75% involvement), and 4 = severe damage (>75% involvement) [10].

2.3. Renal Function. Serum creatinine (CREA) and serum urea nitrogen were quantified with a UniCel Dx800 Synchron device (Beckman, USA). Standard enzyme immunoassay kits (BioPorto Diagnostics, Gentofte, Denmark) were used to establish the serum concentrations of the neutrophil gelatinase-associated lipocalin (NGAL) and cystatin C.

2.4. Reverse Transcription Polymerase Chain Reaction. Reverse transcription polymerase chain reaction (RT-PCR) was used to determine the expression levels of TNF- α , IL-1 β , IL-6, and MCP-1 in the kidneys. The total cellular RNA was extracted with TRIzol (Invitrogen), and the cDNA was synthesized with a Moloney murine leukemia virus (M-MLV) reverse transcription kit (Promega). Quantitative real-time PCR was performed through the use of an IQ SYBR Green Supermix reagent (Bio-Rad, USA) with a Bio-Rad real-time PCR machine. The manufacturer's instructions were followed. The data were analyzed by the use of the $-\Delta\Delta CT$ method. Glyceraldehyde 3-phosphate dehydrogenase (GAPDH) was used as a housekeeping gene against which the expression levels of the target genes were normalized. Table 1 presents the primer sequences.

2.5. Kidney Oxidative Stress Analysis. A homogenate of the kidney tissue was made to measure the concentration of glutathione (GSH) and malondialdehyde (MDA). The homogenate was also used to identify superoxide dismutase (SOD) antioxidant enzyme activity. The manufacturer's instructions for the corresponding assay kit (Nanjing Jiancheng Bioengineering Institute, Nanjing, China) were followed.

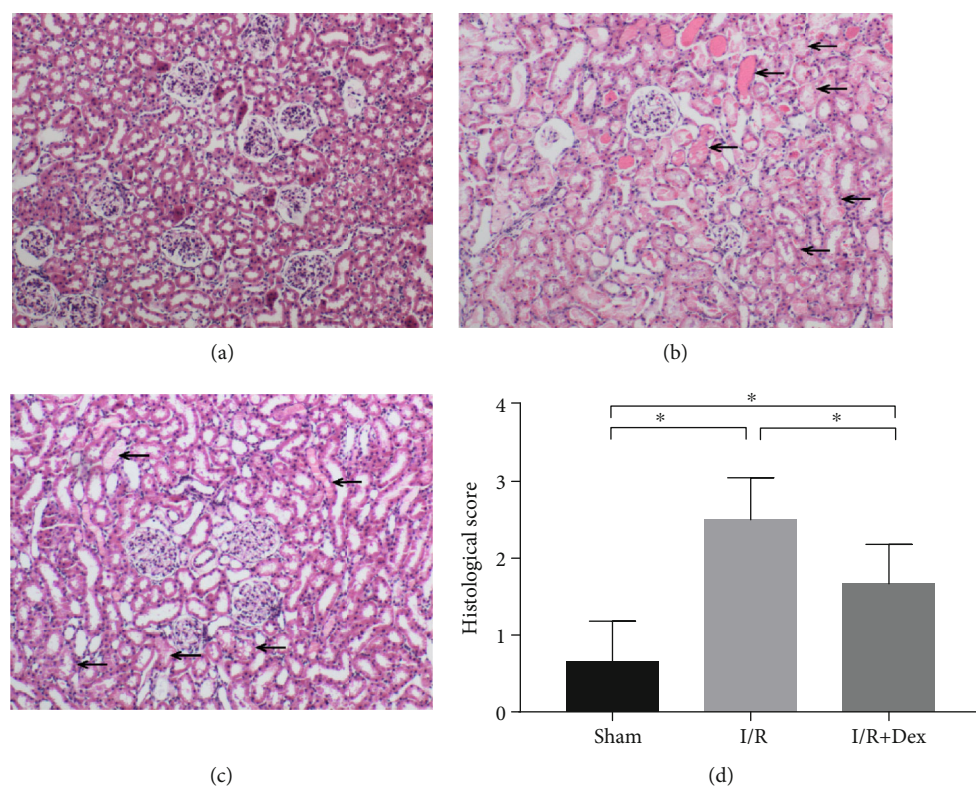


FIGURE 1: Dexmedetomidine (DEX) preconditioning showed renoprotective effects histologically (10x). Renal injury was inflicted in the experimental group by removing the left kidney and clamping the right renal artery for 45 min (renal ischemia-reperfusion (I/R)). In the sham control group, both renal pedicles were dissected without occlusion. DEX was administered 30 min prior to ischemia. Representative microphotographs were taken from (a) the sham control group, (b) the I/R group, (c) the DEX (25 $\mu\text{g}/\text{kg}$)+I/R group, and (d) the quantification of the histological scores following I/R in rats. The histological damages were indicated by black arrows. The data are the mean \pm SD ($n = 6$). * $p < 0.05$.

2.6. Serum Inflammatory Cytokine Analysis. The serum inflammatory cytokines were measured through the use of a commercial enzyme-linked immunosorbent assay (ELISA) kit from Nanjing Jiancheng Bioinstitute (Nanjing, Jiangsu, China) and a microplate reader at 450 nm (Thermo Scientific, Waltham, MA). The manufacturer's guidelines were followed.

2.7. Terminal Deoxynucleotidyl Transferase Deoxyuridine Triphosphate Nick-End Labeling (TUNEL) Assay. To detect the apoptotic tubular epithelial cells, an in situ TUNEL assay was used in accordance with the manufacturer's instructions (In Situ Cell Death Detection Kit, POD, Roche, Switzerland). The sections that had been fixed in paraffin were dewaxed. They were then rehydrated with xylene and a graded series of ethanol and double-distilled water. The sections were treated with proteinase K (20 $\mu\text{g}/\text{ml}$) at room temperature for 15 min before being rinsed twice with phosphate buffer saline (PBS). After the slide was dried, 50 μl of TUNEL reaction mixture was applied. The slides were incubated at 37°C in a humidified chamber for 60 min and then rinsed three times with PBS. Converter-POD (50 μl) was added to the specimen, and a coverslip was applied before incubation at 37°C in a humidified chamber for 30 min. The samples were again rinsed three times with PBS and then stained with a diaminobenzidine (DAB) substrate (Zhongshan, Beijing,

China). After 10 min, the DAB was removed by being rinsed three times with PBS. Hematoxylin or methyl green stains were applied and then rinsed with tap water almost immediately. ImageJ software (version 1.38; National Institutes of Health, Rockville, MD) was used for counting the number of TUNEL-positive cells in an objective grid in regions of 10 randomly selected sections. A 40x objective lens was used for the counts, which were performed by a researcher who was blinded to the experiment aims. The data from the average of these 10 counts were analyzed.

2.8. Statistical Analysis. The data were analyzed in IBM SPSS Statistics for Windows, version 22.0 (SPSS Inc., Chicago, IL, USA). The results are presented as means and standard deviation (SD). One-way analysis of variance (ANOVA) was used to compare multiple sets of data. Statistical significance was set at $p < 0.05$. The graphs were created in GraphPad Prism 7.00 (GraphPad Inc., San Diego, CA, USA).

3. Results

To confirm the effects of DEX on I/R-induced renal injury, 25 $\mu\text{g}/\text{kg}$ of DEX was administered by i.p. injection 30 min before I/R. Figure 1 presents the histological images through which kidney injury was determined. The evidence provided by the hematoxylin and eosin (H&E) stains indicates that the

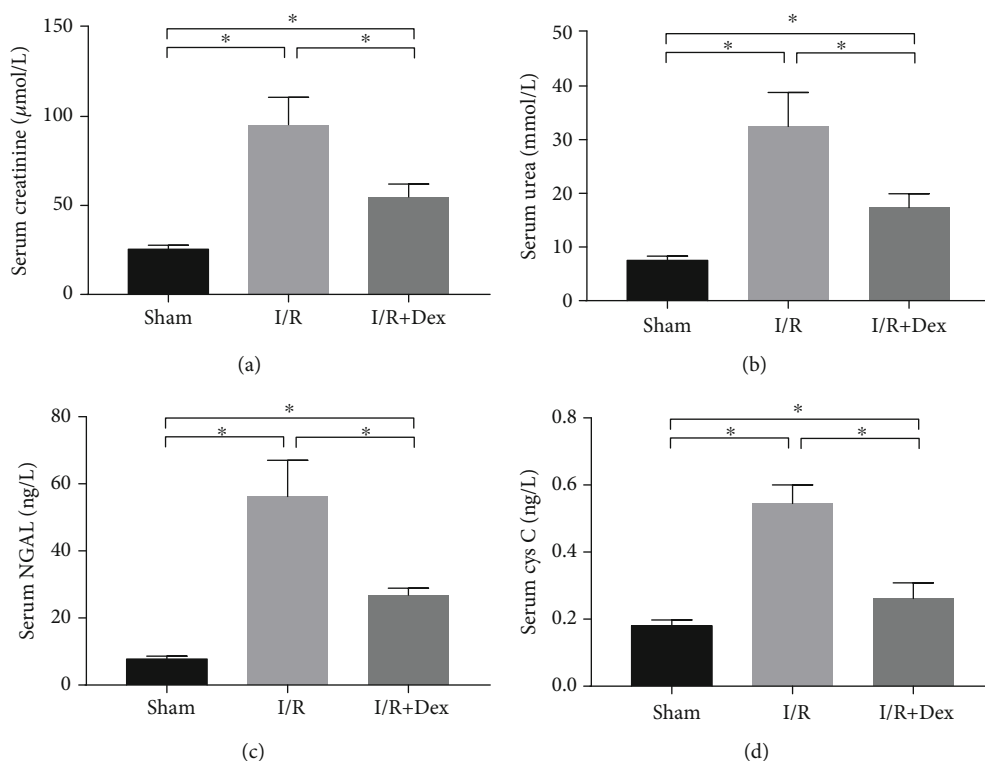


FIGURE 2: Renal function in rats subjected to the sham procedure, untreated ischemia-reperfusion (I/R), or I/R with dexmedetomidine (DEX) treatment. Levels of (a) serum creatinine, (b) serum urea nitrogen, (c) serum neutrophil gelatinase-associated lipocalin (NGAL), and (d) cystatin C (Cys C) in the sham control, I/R, and DEX (25 µg/kg)+I/R groups. The data are the mean ± SD ($n = 6$). $*p < 0.05$.

histological injuries to the I/R rats' kidneys included focal renal hemorrhage, focal tubular necrosis, neutrophil infiltration, and vacuolar degeneration of the renal tubular epithelial cells ($p < 0.05$). The histological damage in the DEX-treated rats was lesser ($p < 0.05$) than that in the I/R rats.

As is shown in Figure 2, the marked increase in serum CREA ($p < 0.05$) and urea nitrogen ($p < 0.05$) was indicative of I/R-induced renal dysfunction. However, these serum markers were significantly lower ($p < 0.05$) in the DEX-treated rats than in the I/R rats. This suggests that the renal function in the DEX-treated rats was maintained to some extent after I/R induction. Furthermore, the serum NGAL and cystatin C levels in the I/R-induced rats were significantly higher ($p < 0.05$) than those in the sham group. However, they were significantly lower ($p < 0.05$) in the DEX-treated rats than in the I/R-induced rats (Figure 2).

The effects of DEX on oxidative stress were also evaluated. As is illustrated in Figure 3, the MDA concentrations in the I/R-induced rats were significantly higher ($p < 0.05$) than those in the sham group. However, in the I/R rats treated with DEX, the levels of oxidative stress were lower ($p < 0.05$) than those in the I/R rats. The GSH and SOD activity levels in the I/R group were significantly lower ($p < 0.05$) than those in the sham controls. Indeed, the GSH concentrations and SOD activity levels in the I/R group treated with DEX were significantly higher ($p < 0.05$) than those in the I/R group.

The effects of DEX on the expression of proinflammatory cytokines were evaluated. The RT-PCR results for the kidney

samples indicated that the expression levels of IL-1 β , IL-6, MCP-1, and TNF- α mRNA were significantly higher ($p < 0.05$) in the I/R-induced rats than in the controls (Figure 4). However, DEX exerted a modulatory effect. The mRNA expression of IL-1 β , IL-6, MCP-1, and TNF- α ($p < 0.05$) in the kidney tissues of the rats that received DEX treatment was lower than that in the I/R-induced rats. The serum levels of IL-1 β , IL-6, MCP-1, and TNF- α in the I/R rats were considerably higher than those in the DEX-treated I/R rats ($p < 0.05$). The serum levels of IL-1 β , IL-6, MCP-1, and TNF- α ($p < 0.05$) in the rats that received DEX treatment were lower than those in the I/R-induced rats. This suggests that in the case of I/R injury, DEX exerts an inhibitory effect on the expression of inflammatory cytokines.

The available evidence suggests that the pathogenesis of I/R injury is aggravated by the apoptosis of the tubular cells. Thus, the effect of DEX on tubular epithelial cell apoptosis in the I/R-induced rats was explored. The results of the TUNEL assay revealed that I/R injury was associated with a significant increase ($p < 0.05$) in the level of apoptosis in these epithelial cells. In contrast, there were fewer apoptotic cells in the kidney samples from the DEX-treated rats ($p < 0.05$) than in those from the I/R group (Figure 5).

4. Discussion

A sequela of cardiovascular and transplant surgery or shock is renal I/R injury that causes AKI. This results in longer hospital stays and even death [11]. The present study has

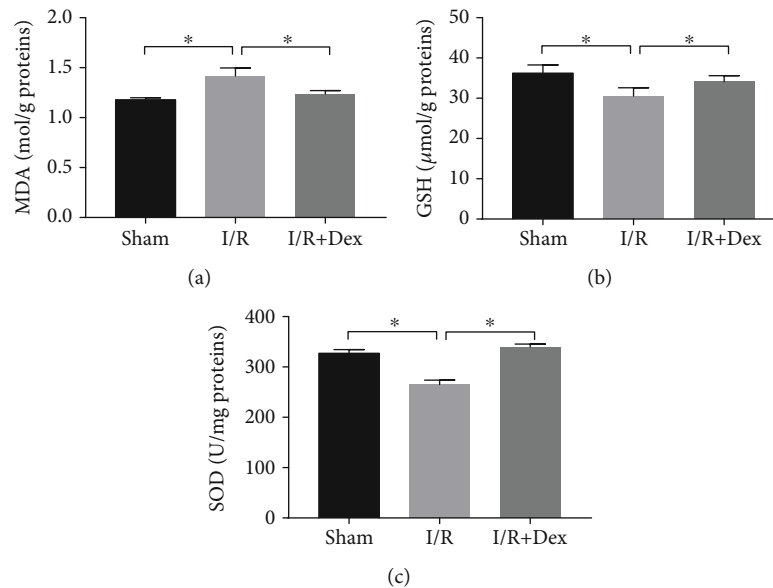


FIGURE 3: Extent of oxidative stress in rats subjected to the sham procedure, untreated ischemia-reperfusion (I/R), or I/R with dexmedetomidine (DEX) treatment. Levels of (a) malondialdehyde (MDA), (b) glutathione (GSH), and (c) superoxide dismutase (SOD) in the sham control, I/R, and DEX (25 μ g/kg)+I/R groups. The data are the mean \pm SD ($n = 6$). * $p < 0.05$.

demonstrated that pretreatment with DEX helps to maintain renal morphology and function in cases of I/R injury. When kidney I/R occurred, the levels of inflammatory mediators circulating in the blood were reduced, and the kidneys experienced less oxidative stress as a consequence of the administration of DEX. These findings suggest that DEX might be an appropriate pharmaceutical intervention to reduce acute injury-induced kidney damage.

Among the qualities of DEX are its anesthetic-sparing effect and facilitation of hemodynamic stability. Consequently, DEX is frequently administered as a sedative in perioperative and intensive care medicine. It is also applied as an anesthetic adjuvant [12]. DEX has wide clinical applications because its analgesic, hemodynamic, sedative, and sympatholytic qualities make it particularly useful for perioperative patients.

Other features are its anti-inflammation, antioxidant, and antiapoptotic effects on the brain, heart, lungs, and kidneys [13, 14]. The results of several animal model studies indicate that DEX also offers protection against I/R injury to the kidney [12, 15]. Other studies have highlighted the beneficial role of DEX in preventing renal injury in patients undergoing cardiovascular and other major surgical procedures [16]. These findings supplement those of earlier studies that reported significant increases in the CREA and BUN levels following I/R injury. This suggests impaired renal function. An examination of the histopathological evidence indicates that I/R causes kidney injury; however, DEX pretreatment can be mitigative.

A surfeit of oxygen-free radicals is produced by organisms in a state of stress. This disrupts the delicate balance between the oxidation and antioxidant systems [17]. The results of this study indicate that the MDA levels, an important biomarker of oxidative damage, are reduced and the

GSH and SOD levels are increased by DEX. MDA is a useful indirect indicator of the extent of free radical-induced damage [18]. In contrast, GSH and SOD are important antioxidants [19]. The results suggest that I/R diminished the antioxidant defense system by increasing the MDA levels and reducing the GSH and GSH enzyme activity. This suggests that I/R could induce oxidative stress, which might be significant in the pathogenesis of AKI. The DEX treatment helped to protect against oxidative stress suggesting that it has antioxidative effects [20]. Therefore, DEX could provide protection against I/R-induced AKI.

Another manifestation of I/R injury is a heightened inflammatory response [21, 22]. This response aggravates the conditions because the macrophages, T cells, and other inflammatory mediators are recruited to the tissues injured by I/R [21, 22]. As the results of the tissue samples obtained from the kidneys of I/R-injured rats in this study have demonstrated, the expression of IL-1 β , IL-6, MCP-1, and TNF- α mRNA was elevated. In contrast, the renal tissue samples from the rats that had received DEX following I/R exhibited lower IL-1 β , IL-6, MCP-1, and TNF- α mRNA expression. Relationships among renal morphology, the serum levels of inflammatory mediators, and the state of cell apoptosis were found. The pathogenesis and progression of I/R injury are influenced by the proinflammatory cytokines, including IL-1 β , IL-6, MCP-1, and TNF- α [23, 24]. DEX not only acts locally on the kidney's α_2 -adrenoceptors but also influences the anti-inflammatory reactions, thereby mitigating the damaging effects of I/R on the kidney.

Apoptosis, also known as programmed cell death, is a critical mechanism for maintaining cell stability; however, too much can damage the body [25]. Usually, apoptosis, an early event in kidney I/R injury, interacts with the subsequent inflammation and kidney injury [26]. In the present study, a

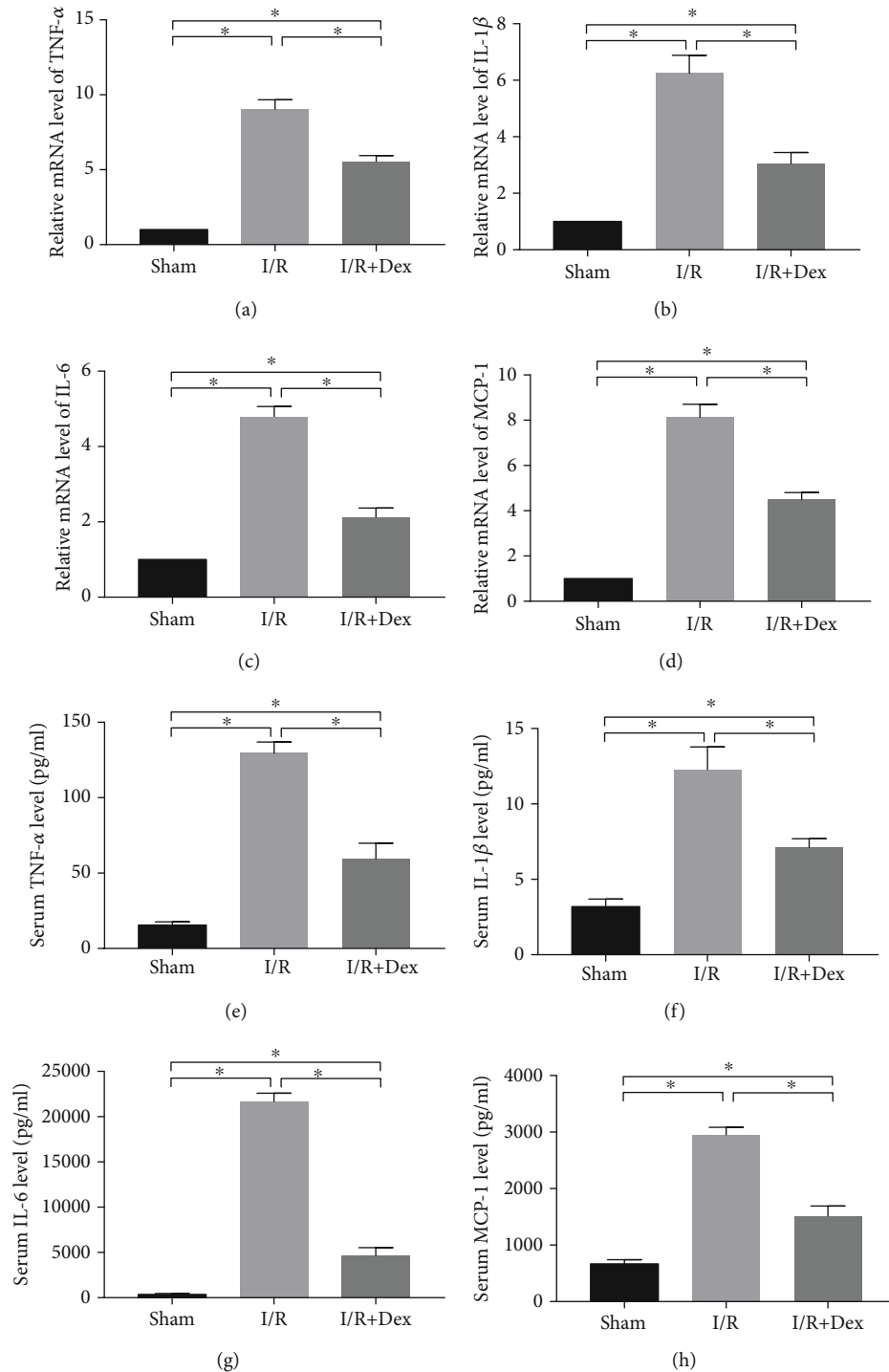


FIGURE 4: The mRNA levels of the inflammatory mediators in the rat kidneys or the serum levels of the inflammatory mediators subjected to the sham procedure, ischemia-reperfusion (I/R), or I/R with dexmedetomidine (DEX) treatment. Reverse transcription polymerase chain reaction (RT-PCR) tests of the mRNA levels of (a) IL-1 β , (b) IL-6, (c) MCP-1, and (d) TNF- α in the kidney tissues from the sham control, I/R, and DEX (25 μ g/kg)+I/R groups. Enzyme-linked immunosorbent assay (ELISA) of the levels of (e) IL-1 β , (f) IL-6, (g) MCP-1, and (h) TNF- α in the sera from the sham control, I/R, and DEX (25 μ g/kg)+I/R groups. The data are the mean \pm SD ($n = 6$). * $p < 0.05$.

significantly higher number of TUNEL-positive cells were retrieved from the rats with the I/R-injured kidneys than from those that received the DEX intervention. Studies have found that TNF- α causes injury to the kidneys [27, 28]. DEX

might protect against AKI following I/R by stimulating an antiapoptotic effect.

The data obtained from this study demonstrate that DEX exerts a protective effect against I/R injury in rats by

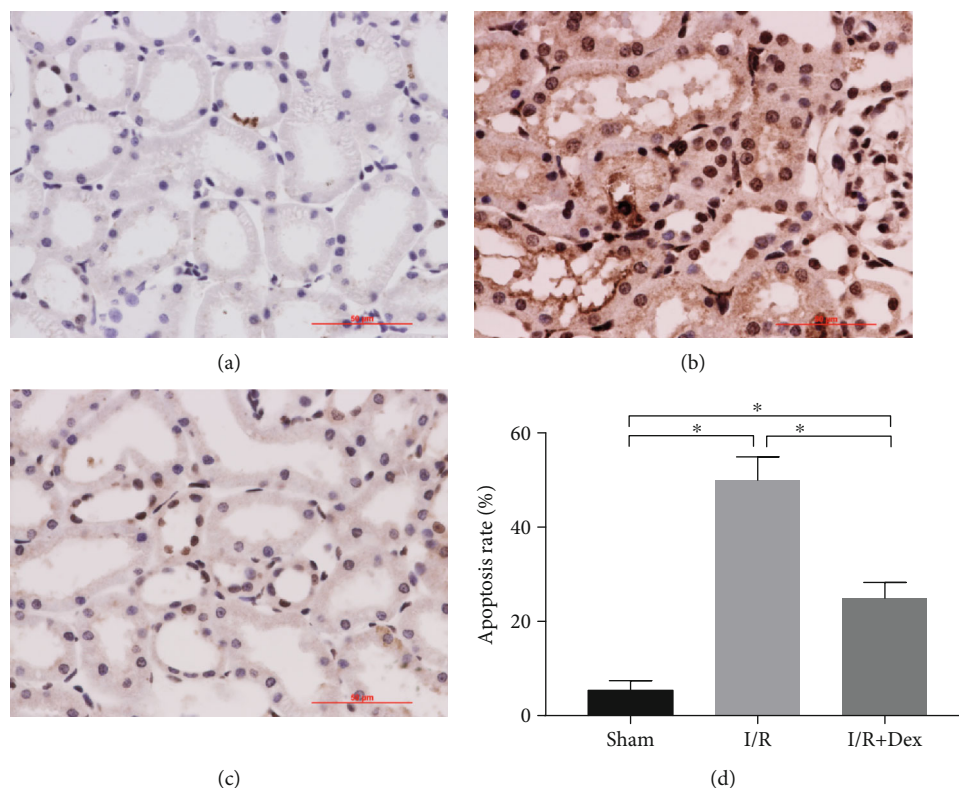


FIGURE 5: Apoptosis was detected in the rat kidneys via terminal deoxynucleotidyl transferase deoxyuridine triphosphate nick-end labeling (TUNEL) staining (40x) in rats subjected to the sham procedure, untreated ischemia-reperfusion (I/R), or I/R with dexmedetomidine (DEX) treatment. Representative microphotographs were taken from (a) the sham control group, (b) the I/R group, (c) the DEX (25 $\mu\text{g}/\text{kg}$)+I/R group, and (d) the apoptosis rate following I/R in the rats. The data are the mean \pm SD ($n = 6$). $*p < 0.05$.

inhibiting tubular cell apoptosis and inflammation, lowering ROS production, and promoting renal function. These results suggest that DEX may play a role in the treatment of I/R-initiated AKI. However, DEX is not without side effects; through parasympathetic activation, it can contribute to bradycardia. How DEX can be best exploited to protect vital organs has yet to be established. Further research into its applications is justified.

Data Availability

The data used to support the findings of this study are available from the corresponding author upon request.

Conflicts of Interest

The authors declare that there is no conflict of interest regarding the publication of this article.

Authors' Contributions

Naren Bao finished the first draft of the manuscript; Di Dai critically revised the manuscript. All the authors approved the submission of the manuscript.

Acknowledgments

This work was supported by the Science and Technology Research Project of Liaoning Provincial Education Department (LK201651).

References

- [1] C. Hobson, T. Ozrazgat-Baslanti, A. Kuxhausen et al., "Cost and mortality associated with postoperative acute kidney injury," *Annals of Surgery*, vol. 261, no. 6, pp. 1207–1214, 2015.
- [2] M. V. Wohlaer, A. Sauaia, E. E. Moore, C. C. Burlew, A. Banerjee, and J. Johnson, "Acute kidney injury and post-trauma multiple organ failure," *Journal of Trauma and Acute Care Surgery*, vol. 72, no. 2, pp. 373–380, 2012.
- [3] B. Khoundabi, A. Kazemnejad, M. Mansourian, S. M. Hashemian, and M. Kazemipoor Dizaji, "Acute kidney injury risk factors for ICU patients following cardiac surgery: the application of joint modeling," *Trauma Monthly*, vol. 21, no. 4, article e23749, 2016.
- [4] N. M. Abogresha, S. M. Greish, E. Z. Abdelaziz, and W. F. Khalil, "Remote effect of kidney ischemia-reperfusion injury on pancreas: role of oxidative stress and mitochondrial apoptosis," *Archives of Medical Science*, vol. 12, no. 2, pp. 252–262, 2016.
- [5] Q. Ma, Y. Xu, L. Tang et al., "Astragalus polysaccharide attenuates cisplatin-induced acute kidney injury by suppressing oxidative damage and mitochondrial dysfunction," *BioMed*

- Research International*, vol. 2020, Article ID 2851349, 12 pages, 2020.
- [6] S. N. Amin, A. A. el-Aidi, M. B. Zickri, L. A. Rashed, and S. S. Hassan, "Hepatoprotective effect of blocking *N*-methyl-d-aspartate receptors in male albino rats exposed to acute and repeated restraint stress," *Canadian Journal of Physiology and Pharmacology*, vol. 95, no. 6, pp. 721–731, 2017.
 - [7] K. Kang, Y. Gao, S. C. Wang et al., "Dexmedetomidine protects against lipopolysaccharide-induced sepsis-associated acute kidney injury via an $\alpha 7$ nAChR-dependent pathway," *Biomedicine & Pharmacotherapy*, vol. 106, pp. 210–216, 2018.
 - [8] J. S. Cho, J. K. Shim, S. Soh, M. K. Kim, and Y. L. Kwak, "Perioperative dexmedetomidine reduces the incidence and severity of acute kidney injury following valvular heart surgery," *Kidney International*, vol. 89, no. 3, pp. 693–700, 2016.
 - [9] Q. Zhang, D. Wu, Y. Yang, T. Liu, and H. Liu, "Dexmedetomidine alleviates hyperoxia-induced acute lung injury via inhibiting NLRP3 inflammasome activation," *Cellular Physiology and Biochemistry*, vol. 42, no. 5, pp. 1907–1919, 2017.
 - [10] P. Jablonski, B. O. Howden, D. A. Rae, C. S. Birrell, V. C. Marshall, and J. Tange, "An experimental model for assessment of renal recovery from warm ischemia," *Transplantation*, vol. 35, no. 3, pp. 198–204, 1983.
 - [11] C. Ponticelli, "Ischaemia-reperfusion injury: a major protagonist in kidney transplantation," *Nephrology, Dialysis, Transplantation*, vol. 29, no. 6, pp. 1134–1140, 2014.
 - [12] J. Gu, P. Sun, H. Zhao et al., "Dexmedetomidine provides renoprotection against ischemia-reperfusion injury in mice," *Critical Care*, vol. 15, no. 3, article R153, 2011.
 - [13] J. W. Sleight, S. Vacas, A. M. Flexman, and P. O. Talke, "Electroencephalographic arousal patterns under dexmedetomidine sedation," *Anesthesia and Analgesia*, vol. 127, no. 4, pp. 951–959, 2018.
 - [14] M. Mahmoud, S. Sadhasivam, S. Salisbury et al., "Susceptibility of transcranial electric motor-evoked potentials to varying targeted blood levels of dexmedetomidine during spine surgery," *Anesthesiology*, vol. 112, no. 6, pp. 1364–1373, 2010.
 - [15] M. Le Guen, N. Liu, F. Tounou et al., "Dexmedetomidine reduces propofol and remifentanyl requirements during bispectral index-guided closed-loop anesthesia: a double-blind, placebo-controlled trial," *Anesthesia and Analgesia*, vol. 118, no. 5, pp. 946–955, 2014.
 - [16] H. Qiao, R. D. Sanders, D. Ma, X. Wu, and M. Maze, "Sedation improves early outcome in severely septic Sprague Dawley rats," *Critical Care*, vol. 13, no. 4, p. R136, 2009.
 - [17] J. D. Moreira, L. Pernomian, M. S. Gomes et al., "Enhanced nitric oxide generation from nitric oxide synthases as the cause of increased peroxynitrite formation during acute restraint stress: effects on carotid responsiveness to angiotensinergic stimuli in type-1 diabetic rats," *European Journal of Pharmacology*, vol. 783, pp. 11–22, 2016.
 - [18] T. Halder, G. Upadhyaya, C. Basak, A. Das, C. Chakraborty, and S. Ray, "Dehydrins impart protection against oxidative stress in transgenic tobacco plants," *Frontiers in Plant Science*, vol. 9, p. 136, 2018.
 - [19] H. Yaribeygi, M. T. Mohammadi, and A. Sahebkar, "PPAR- α agonist improves hyperglycemia-induced oxidative stress in pancreatic cells by potentiating antioxidant defense system," *Drug Research*, vol. 68, no. 6, pp. 355–360, 2018.
 - [20] Z. Chen, T. Ding, and C. G. Ma, "Dexmedetomidine (DEX) protects against hepatic ischemia/reperfusion (I/R) injury by suppressing inflammation and oxidative stress in NLRC5 deficient mice," *Biochemical and Biophysical Research Communications*, vol. 493, no. 2, pp. 1143–1150, 2017.
 - [21] Y. Nozaki, K. Kinoshita, S. Hino et al., "Signaling rho-kinase mediates inflammation and apoptosis in T cells and renal tubules in cisplatin nephrotoxicity," *American Journal of Physiology Renal Physiology*, vol. 308, no. 8, pp. F899–F909, 2015.
 - [22] S. Malik, K. Suchal, N. Gamad, A. K. Dinda, D. S. Arya, and J. Bhatia, "Telmisartan ameliorates cisplatin-induced nephrotoxicity by inhibiting MAPK mediated inflammation and apoptosis," *European Journal of Pharmacology*, vol. 748, pp. 54–60, 2015.
 - [23] C. Z. Li, H. H. Jin, H. X. Sun et al., "Eriodictyol attenuates cisplatin-induced kidney injury by inhibiting oxidative stress and inflammation," *European Journal of Pharmacology*, vol. 772, pp. 124–130, 2016.
 - [24] N. M. Elsherbiny, M. A. Eladl, and M. M. Al-Gayyar, "Renal protective effects of arjunolic acid in a cisplatin-induced nephrotoxicity model," *Cytokine*, vol. 77, pp. 26–34, 2016.
 - [25] B. G. Zhou, H. M. Zhao, X. Y. Lu et al., "Erzhi pill® repairs experimental liver injury via TSC/mTOR signaling pathway inhibiting excessive apoptosis," *Evidence-based Complementary and Alternative Medicine*, vol. 2017, Article ID 5653643, 15 pages, 2017.
 - [26] H. Tian, Y. Lu, S. P. Shah, Q. Wang, and S. Hong, "14S,21R-Dihydroxy-docosahexaenoic acid treatment enhances mesenchymal stem cell amelioration of renal ischemia/reperfusion injury," *Stem Cells and Development*, vol. 21, no. 7, pp. 1187–1199, 2012.
 - [27] M. D. Sanchez-Niño, A. Benito-Martin, S. Gonçalves et al., "TNF superfamily: a growing saga of kidney injury modulators," *Mediators of Inflammation*, vol. 2010, Article ID 182958, 11 pages, 2010.
 - [28] Y. Wang, R. Wang, B. Yao et al., "TNF- α suppresses sweat gland differentiation of MSCs by reducing *FTO*-mediated m⁶A-demethylation of *Nanog* mRNA," *Science China Life Sciences*, vol. 63, no. 1, pp. 80–91, 2020.

Research Article

The Enlargement of Abdominal Lymph Nodes Is a Characteristic of Autoimmune Liver Disease

Yongjuan Wang ^{1,2}, Xiuxiu Xu,¹ Maojuan Ran,¹ Xiaopei Guo,¹ Lu Zhou ¹, Xi Wang,¹ Bangmao Wang,¹ and Jie Zhang ¹

¹Department of Gastroenterology and Hepatology, General Hospital, Tianjin Medical University, Tianjin Institute of Digestive Disease, Tianjin 300052, China

²Department of Gastroenterology and Hepatology, The Second Affiliated Hospital of Hebei Medical University, Hebei, China

Correspondence should be addressed to Jie Zhang; zhangjie_xhk@tmu.edu.cn

Received 17 February 2020; Accepted 13 March 2020; Published 21 March 2020

Guest Editor: Hongmei Jiang

Copyright © 2020 Yongjuan Wang et al. This is an open access article distributed under the Creative Commons Attribution License, which permits unrestricted use, distribution, and reproduction in any medium, provided the original work is properly cited.

Background. The enlargement of lymph nodes is a common clinical sign in connective tissue disease (CTD) and viral hepatitis. In this research, we evaluated the incidence of enlarged lymph nodes in autoimmune liver diseases (AILD). Moreover, we identified the clinical significance of abdominal lymph node enlargement in AILD. **Methods.** The characteristics of abdominal lymph nodes, including their morphology and distribution, were assessed by ultrasonography and computed tomography in 125 patients with AILD, 54 with viral hepatitis, 135 with CTD, and 80 healthy controls. The pathological and laboratory results of 106 AILD patients were collected to analyze the association between lymphadenectasis and disease activity. **Results.** Enlargement of abdominal lymph nodes was found in 69.6% of patients with AILD, 63% of patients with viral hepatitis, 29.6% of patients with CTD, and 2% of healthy controls. Alkaline phosphatase (ALP), glutamate transpeptidase (GGT), and immunoglobulin M (IgM) levels were significantly increased in AILD patients with lymphadenectasis (LA) in contrast to patients without lymphadenectasis (NLA) ($P < 0.05$). The pathological characteristics of inflammation, cholestasis, and focal necrosis were more common in the LA group than in the NLA group ($P < 0.05$). As shown by multivariate logistic regression analysis, interface hepatitis (OR = 3.651, $P < 0.05$), cholestasis (OR = 8.137, $P < 0.05$), and focal necrosis (OR = 5.212, $P < 0.05$) were related to LA. **Conclusions.** The percentage of abdominal lymph node enlargement in AILD subjects was significantly higher than that in CTD subjects. Therefore, the enlargement of lymph nodes can represent a noninvasive indicator of histological and biochemical inflammation activity in AILD.

1. Introduction

Autoimmune liver disease (AILD) is a common cause of chronic hepatitis that leads to liver cirrhosis due to occult onset [1]. The categories of AILD include autoimmune hepatitis (AIH), primary biliary cholangitis (PBC), primary sclerotic cholangitis (PSC), and overlap syndrome. At present, AILD remains a major diagnostic and therapeutic challenge due to the lower incidence of disease and heterogeneous subtypes [2, 3].

Inflammatory response in organs usually leads to hyperplasia of regional lymph nodes. Enlarged abdominal lymph nodes are a common finding in patients with chronic active hepatitis [4, 5], especially in those caused by autoimmune

[6, 7] or viral infection [8–10]. In addition, a higher incidence of enlarged abdominal lymph nodes in PBC (74–100%) and AIH (13–73%) has been reported [6].

The existing research shows that the enlargement of lymph nodes in multiple parts of the body is a shared clinical manifestation in connective tissue diseases (CTD) [11, 12]. CTD comprises a group of immune system diseases involving the connective tissues of the body. Patients with CTD can have positive antinuclear antibodies (ANA) and increased IgG levels, which can also be found in AILD patients [11]. Furthermore, it has been reported that enlarged lymph nodes are associated with disease activity in CTD. Researchers also found that enlarged abdominal lymph nodes in chronic hepatitis C (CHC) subjects are associated

with serum parameters of viremia, a high frequency of serum CD8 levels, and severe histological damage [13, 14]. However, the characteristics of enlarged lymph nodes in CTD, CHC, and AILD have not been studied. In addition, the association between the enlargement of lymph nodes and AILD activity is still unclear.

We speculated that lymphoid hyperplasia was the response of an altered immune system to an undefined antigenic stimulus. In the present study, we analyzed the incidence of enlarged lymph nodes in CTD, viral hepatitis, and AILD. Then, we evaluated their association with disease activity by comparing them with biochemical, immunological, and pathological results in AILD subjects. In addition, we assessed the distribution of abdominal lymph nodes in CTD, viral hepatitis, and three subtypes of AILD. The results indicated that the enlargement of lymph nodes is a noninvasive indicator of histological and biochemical inflammation activity in AILD.

2. Methods

2.1. Patients. For the study, 225 individuals with AILD were recruited from October 2008 to May 2016. The diagnosis of AILD was made according to EASL guidelines (AIH), AASLD guidelines (PBC), and the Paris standard (AIH-PBC) [15, 16]. All patients were negative for neoplasm, lymphadenoma, and intestinal tuberculosis. Exclusion criteria were applied, with the following results: 46 patients were excluded for a history of viral hepatitis, alcoholic liver disease, drug-induced liver disease, or CTD; 54 patients were excluded for incomplete data. Ultimately, 125 AILD subjects were enrolled in the study, 106 of whom underwent liver biopsies. Additionally, 135 patients with CTD, as diagnosed by the American College of Rheumatology (ACR) and the European League Against Rheumatism (EULAR) [17–19], were enrolled in the study from October 2008 to May 2016. All patients were negative for a history of neoplasm, lymphadenoma, intestinal tuberculosis, and multifarious liver diseases. Moreover, 54 patients with viral hepatitis, as diagnosed by EASL guidelines, were also investigated [20, 21]. As a control group, 80 healthy volunteers were recruited for the study. The study was approved by the ethics committee of Tianjin Medical University General Hospital. All patients and control volunteers were at least 18 years old and provided informed consent to participate in the study.

2.2. Serologic and Pathological Laboratory Tests. Laboratory tests were performed on AILD subjects: alanine amino transferase (ALT), aspartate amino transferase (AST), alkaline phosphatase (ALP), glutamate transpeptidase (GGT), and total bilirubin (TBIL); IgG, IgM, and IgA; and anti-nuclear antibody (ANA), smooth muscle antibody (SMA), anti-liver kidney microsomal antibody (Anti-LKM), anti-mitochondrial antibody (AMA), and anti-mitochondrial antibody 2 (AMA2). All the above-mentioned parameters were detected before treatment. Within the lobular parenchyma, the following morphological changes were evaluated: hepatocyte edema, interface hepatitis, focal necrosis, and hepatic fibrosis. All

liver biopsy specimens were checked independently by two experienced pathologists.

2.3. Computed Tomography Image Analysis. Celiac lymph nodes of the liver and abdominal organs were assessed for echotexture by ultrasonography and computed tomography. Abdominal lymph nodes larger than 5 mm in the shortest diameter were counted, and the size of each lymph node was measured in the longest axis (a) and in the corresponding perpendicular axis (b) using ALOKA ultrasound and TSX-032A computed tomography, respectively. Examinations were performed by two experienced radiologists, and patients with consistent evaluation results were included in the study. The maximum cross-sectional area was recorded as the result after multiple measurements.

2.4. Statistics. Statistical analysis was completed with SPSS 7.5 for Windows (SPSS Inc., Chicago, IL, USA). Demographic characteristics of patients were expressed as median range or mean \pm SD. Statistical significance between two groups of normally distributed quantitative data was analyzed by a *t*-test. The Mann-Whitney *U* test was used for categorical and nonnormal continuous data. For qualitative data, comparisons among the groups were conducted using the χ^2 test or Fischer's exact test. Multivariate logistic regression analysis was used to identify factors that were independently associated with the presence of abdominal lymph nodes. A *P* value < 0.05 was considered statistically significant.

3. Results

3.1. The Frequency of Abdominal Lymph Nodes in AILD Is Higher Than That in CTD. As shown in Table 1, the baseline demographic data of all the patients were listed, and the frequency of abdominal lymph nodes was detected (Figure 1). The proportion of gender at the time of the study was the only demographic parameter which differed significantly among all the groups ($P < 0.05$). Enlarged lymph nodes occurred in all groups, and a significantly higher proportion of lymph nodes was found in AILD subjects than in control group subjects ($P < 0.001$). Abdominal lymph nodes tended to be more prevalent in patients with AILD (69.6%) and viral hepatitis (63%), whereas enlarged lymph nodes were only infrequently observed in patients with CTD and in control patients (29% and 2%, respectively). The positive proposition of abdominal lymph node enlargement in the subjects with AIH, PBC, and overlap syndrome was 56%, 86.2%, and 73.9%, respectively ($P = 0.014$), while the positive rate of lymph node enlargement in PBC subjects was significantly higher than that in AIH subjects ($P = 0.006$).

3.2. The Enlargement of Abdominal Lymph Nodes Is Positively Correlated with Disease Activities in AILD. As shown in Table 2, there were no significant differences in age or in the proportion of females in the LA group and NLA group. In addition, the levels of ALP and GGT in the LA group were higher than those in the NLA group: 181 U/L (126 U/L, 367 U/L) vs. 132 U/L (92.8 U/L, 166 U/L); 199 U/L (124 U/L, 416 U/L) vs. 104.5 U/L (55.3 U/L, 180 U/L), $P < 0.05$, respectively; meanwhile, there were no significant differences in other

TABLE 1: Baseline demographics and positive rates of abdominal lymphadenopathy in patients and healthy controls.

Diseases	Number	F/M	Mean age (y)	Patients with lymphadenopathy	<i>P</i>
AILD	125	(114/11)	59 ± 0.99	87 (69.6%)	—
AIH	50	(45/5)	62 ± 1.46	28 (56%)	
PBC	29	(28/1)	59.1 ± 1.8	25 (86.2%)	0.006**
AIH-PBC	46	(41/5)	58 ± 1.6	34 (73.9%)	
Viral hepatitis	54	(28/26)	55 ± 2.54	34 (63%)	0.306*
CTD	135	(103/32)	52.5 ± 2.38	40 (29.6%)	<0.001*
Healthy	80	(48/32)	48 ± 6.27	1 (2%)	<0.001*

The positive rate of abdominal lymph node enlargement in different groups was compared by the χ^2 test. *The AILD group was compared with the viral hepatitis, CTD, and health groups, respectively, and $P < 0.05$ was statistically significant. **The PBC group was compared with the AIH group. AILD: autoimmune liver disease; AIH: autoimmune hepatitis; PBC: primary biliary cholangitis; AIH-PBC: overlap syndrome; CTD: connective tissue diseases.

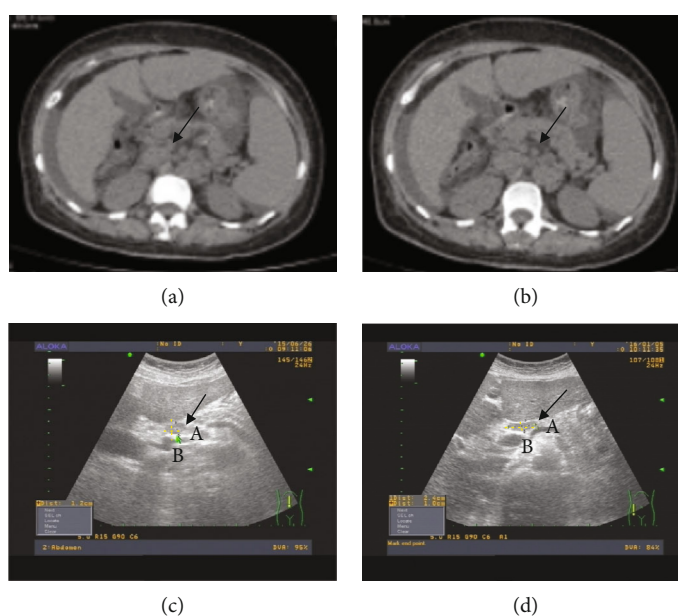


FIGURE 1: Enlarged lymph node (LN) was detected in autoimmune liver disease (AILD). (a) Abdominal CT examination indicated the enlargement of para-aortic lymph nodes. (b) Abdominal CT examination showed the enlargement of pancreatic lymph nodes. (c) Abdominal ultrasonography showed round enlarged lymph nodes around the pancreas. (d) Abdominal ultrasonography revealed oval enlarged lymph nodes around the pancreas. Abdominal lymph nodes larger than 5 mm but at their shortest diameter were counted. The arrow points to the lymph node: (A) longest axis and (B) perpendicular axis.

liver function test results. The patients in the LA group were observed to have a higher level of IgM (294 mg/dL (137 mg/dL, 474 mg/dL) vs. 247.5 mg/dL (98.8 mg/dL, 361 mg/dL)) than those in the NLA group ($P < 0.05$). It was also observed that interface hepatitis occurred in 22.2% of patients without lymph node enlargement, whereas up to 48.6% of those with lymph node enlargement presented with interface hepatitis ($P = 0.009$). Cholestasis was found in 30% of LA group subjects and 5.6% of NLA group subjects ($P = 0.004$), and focal necrosis was found in 31.4% of LA group subjects and 5.6% of NLA group subjects ($P = 0.003$). Meanwhile, no statistical significance in terms of inflammation of the portal area and hepatic fibrosis was found ($P > 0.05$). It was indicated that histological damage, including interface hepatitis, focal necrosis, and cholestasis, was more severe in the LA group than in the NLA group ($P < 0.05$). As liver biopsy specimens

showed, patients with lymph node enlargement presented with interface hepatitis, leukomonocyte infiltrates, cholestasis, focal necrosis, and hepatic rosette formation (Figure 2(b)), whereas patients without lymph node enlargement only presented with leukomonocyte infiltrates and focal necrosis (Figure 2(a)).

The correlations between biochemical and pathological characteristics and lymph nodes in AILD were assessed (Table 3). The enlargement of lymph nodes was not found to be correlated with serum levels of AST ($P = 0.468$), ALP ($P = 0.337$), or GGT ($P = 0.167$). In contrast, significant positive associations were observed between lymph nodes and interface hepatitis ($P = 0.019$), cholestasis ($P = 0.011$), and focal necrosis ($P = 0.044$).

The volume of abdominal lymph nodes in AILD was greater than that in viral hepatitis.

TABLE 2: Univariate analysis of demographic, biochemical, immunological, and pathological characteristics in 106 cases of AILD subjects.

	LA ($n = 70$)	NLA ($n = 36$)	P
Demography			
Age (years)	59.67 \pm 1.3	58.53 \pm 1.9	0.609
Female	64 (91.4%)	33 (91.7%)	0.999
Biochemistry			
ALT (U/L)	72 (36, 154)	57 (31, 146.25)	0.620*
AST (U/L)	81 (41, 136)	50.5 (28.75, 110)	0.073*
ALP (U/L)	181 (126, 367)	132 (92.8, 166)	0.001*
GGT (U/L)	199 (124, 416)	104.5 (55.3, 180)	0.000*
TBIL (mol/L)	20.5 (13.1, 47.6)	19.8 (11.6, 31.9)	0.334*
Immunology IgG (mg/dL)	1610 (1360, 1840)	1620 (1337, 1875)	0.942*
IgM (mg/dL)	294 (137, 474)	247.5 (98.8, 361)	0.035*
IgA (mg/dL)	327 (233, 454)	298 (228.8, 405)	0.733*
Histopathology			
Portal area inflammation	58 (82.9%)	26 (72.2%)	0.201**
Interface hepatitis	34 (48.6%)	8 (22.2%)	0.009**
Cholestasis	21 (30%)	2 (5.6%)	0.004**
Focal necrosis	22 (31.4%)	2 (5.6%)	0.003**

The data are presented as medians and quartiles. *The analysis of the biochemical parameters in the LA and NLA groups in AILD was performed by the Mann-Whitney test. **The analysis of the pathological parameters in the LA and NLA groups in AILD was conducted by the χ^2 test, with $P < 0.05$ being considered statistically significant. AILD: autoimmune liver disease; LA: lymphadenectasis; NLA: nonlymphadenectasis; ALT: alanine amino transferase; AST: aspartate amino transferase; ALP: alkaline phosphatase; GGT: glutamate transpeptidase; TBIL: total bilirubin.

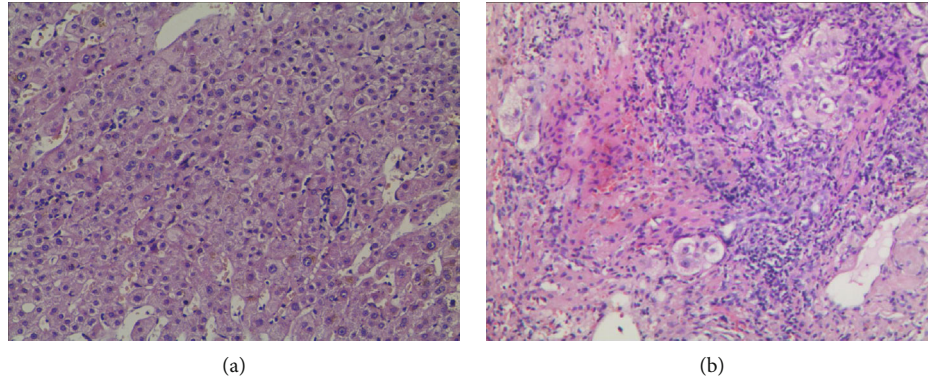


FIGURE 2: Typical liver biopsy from patients with or without lymph node enlargement. (a) In patients with lymph node enlargement, leukomonocyte infiltrates and focal necrosis are present. (b) In patients with lymph node enlargement, interface hepatitis, leukomonocyte infiltrates, cholestasis, focal necrosis, and hepatic rosette formation are present.

The morphological characteristics of lymph nodes, which have a circular or oval shape with clear boundaries and no fusion phenomena, can be detected by abdominal ultrasound and abdominal CT (Figure 1). The size of lymph nodes in AILD patients was found to be larger in comparison with that of lymph nodes in viral hepatitis patients. As shown in Table 4, ultrasound testing revealed that abdominal lymphadenopathy appeared in 50 of 87 (57.5%) cases of AILD and 21 of 34 (61.8%) cases of viral hepatitis. The number of abdominal lymph nodes was more than 1 in 46 cases (92%) of AILD patients and 19 cases (90.5%) of viral hepatitis patients, which was not significant ($P = 0.999$). Similarly, the aspect ratio (a/b) of lymph nodes greater than 2 presented

in 13 cases (26%) of AILD and 6 cases (28.6%) of viral hepatitis, and there was no significant difference between the two groups ($P = 0.823$). Moreover, the maximum cross-sectional area of lymph nodes in AILD patients was larger than that in patients with viral hepatitis (1.34 cm^2 (0.82 cm^2 , 2.07 cm^2) vs. 0.96 cm^2 (0.68 cm^2 , 1.32 cm^2), $P = 0.017$).

3.3. *The Distribution of Lymph Nodes in AILD Was More Common in the Periphery of the Pancreas and Porta Hepatis, Especially in Patients with AIH.* The distribution of lymph nodes in different liver injury diseases was determined (Table 5). In AILD, the frequencies of lymphadenopathy in the periphery of the pancreas, porta hepatis, abdominal

TABLE 3: Factors associated with the presence of abdominal lymph nodes in patients with AILD: multivariate analysis.

Variable	Odds ratio (95% CI)	*P
AST (IU/L)	1.001 (0.998, 1.004)	0.468
ALP (IU/L)	1.002 (0.998, 1.007)	0.337
GGT (IU/L)	1.003 (0.999, 1.007)	0.167
Interface hepatitis	3.651 (1.231, 10.3)	0.019
Cholestasis	8.137 (1.606, 41.232)	0.011
Focal necrosis	5.212 (1.046, 25.96)	0.044

*Analysis of the correlation between biochemical and pathological indexes and LN in AILD using logistic regression. The data are presented as medians and quartiles. $P < 0.05$ was considered statistically significant. AILD: autoimmune liver disease; AST: aspartate amino transferase; ALP: alkaline phosphatase; GGT: glutamate transpeptidase.

TABLE 4: The morphological characteristics of lymph nodes in patients with AILD and viral hepatitis.

Features	AILD ($n = 50$)	Viral hepatitis ($n = 21$)	P
Number			
=1	4 (8%)	2 (9.5%)	0.999*
>1	46 (92%)	19 (90.5%)	
Aspect ratio (a/b)			
<2	37 (74%)	15 (71.4%)	0.823*
≥ 2	13 (26%)	6 (28.6%)	
The maximum cross-sectional area of LN (cm^2)	1.34 (0.82, 2.07)	0.96 (0.68, 1.32)	0.017**

Number: lymph node number. Aspect ratio: longest axis (a)/perpendicular axis (b). Maximum cross-sectional area of LN: $a \times b$. *The analysis of the number and aspect ratio of LN between AILD and viral hepatitis was completed by the χ^2 test. **The analysis of the maximum cross-sectional area of LN between AILD and viral hepatitis was performed using the F test. $P < 0.05$ was considered statistically significant. AILD: autoimmune liver disease; LN: lymph nodes.

aorta, gastrohepatic ligament, and mesenteric roots were 37.9%, 33.3%, 32.2%, 17.2%, and 2.3%, respectively, while in CTD patients, these frequencies were 5%, 17.5%, 85%, 10%, and 47.5%, respectively. Abdominal lymph nodes appeared more often in the periphery of the pancreas ($P < 0.001$) and porta hepatis ($P = 0.014$) in AILD patients than in patients with CTD, while abdominal lymph nodes were commonly found in the abdominal aorta and mesenteric roots in CTD patients ($P < 0.001$). Compared to viral hepatitis, in AILD, lymph nodes occurred mainly in the periphery of the pancreas ($P = 0.005$) and gastrohepatic ligament ($P = 0.006$).

The distributions of lymph nodes in different subtypes of AILD were also analyzed (Table 5). In patients with AIH, the frequencies of lymphadenopathy in the periphery of the pancreas, porta hepatis, abdominal aorta, gastrohepatic ligament, and mesenteric roots were 53.6%, 50%, 25%, 10.7%, and 0%, respectively, while in PBC patients, these frequencies were 5%, 17.5%, 85%, 10%, and 47.5%, respectively (Table 5). In patients with AIH-PBC, the frequencies of lymphadenopathy in the periphery of the pancreas, porta hepatis, abdominal

aorta, gastrohepatic ligament, and mesenteric roots were 41.2%, 17.6%, 26.5%, 14.7%, and 0%, respectively. Abdominal lymph nodes mainly appeared in the periphery of the pancreas in AIH and AIH-PBC; meanwhile, in PBC, lymph nodes were mainly found in the abdominal aorta (Table 5).

4. Discussion

One study showed a higher incidence of enlarged lymph nodes in PBC (74–100%) and AIH (13–73%) [6]. In addition, abdominal lymph node enlargement could be the only imaging manifestation in patients with AILD [14]. It was reported that lymph nodes in patients with CTD were not limited to the body surface, but were in fact also distributed in the abdominal cavity [22]. However, in our study, abdominal lymph nodes tended to be most prevalent in patients with AILD (69.6%), significantly higher than in CTD patients (29.6%). We speculated that lymphoid hyperplasia was the response of an altered immune system to an undefined antigenic stimulus. It was reported that the lymph nodes in CTD were more commonly found on the body surface, which may be because CTD is an immune system disease involving connective tissues [23, 24]. The enlargement of lymph nodes in AILD was mainly found in the abdominal cavity, since AILD is an immune-related liver disease [6].

The sizes of the noticeable lymph nodes seemed to be histologically and serologically correlated with disease activity in patients with AILD [14]. The enlargement of perihepatic lymph nodes in chronic hepatitis C was shown to be related to liver histology and hepatitis C virus viremia, which in turn reflects the inflammatory activities and immunological responses of the host [25]. Previous studies have shown that enlarged regional lymph nodes are significantly correlated with the elevation of ALP and GGT, which is more common in chronic liver diseases [26]. In our study, the levels of ALP and GGT were significantly higher in the LA group than in the NLA group, which might indicate the persistence of inflammation. Several studies have suggested that regional lymph node enlargement is significantly correlated with ALT, AST, ALP, serum bilirubin, serum anti-mitochondrial antibodies, and IgG, reflecting hepatocellular damage, cholestasis, and humoral immunoreactivity in PBC. The increase of ALT and AST indicated that inflammatory damage to the liver persists; likewise, the increase of ALP and serum bilirubin indicated inflammatory damage to the bile duct [13, 26]. In our research, abdominal lymphadenopathy in subjects with AILD was related to histopathological severity, including interface inflammation, focal necrosis, and cholestasis. This study showed that patients with abdominal lymph node enlargement should undergo liver biopsy to analyze the activity and severity of liver inflammation and that timely treatment should be considered in these patients.

Nakanishi et al. observed enlarged lymph nodes in 77–91% of patients with CHC and 96% of patients with CHB [27]. In our study, abdominal lymph nodes tended to be prevalent both in patients with AILD (69.6%) and in those with viral hepatitis. The ultrasound results showed that the size of lymph nodes in subjects with AILD was larger than that in subjects with viral hepatitis. This finding is important,

TABLE 5: Frequency of lymphadenopathy detected in various organs in patients with AILD, CTD, and viral hepatitis.

Disease	Pancreatic N (%)	Hepatic N (%)	Para-aorta N (%)	Hepatogastric N (%)	Mesentery N (%)
AILD ($n = 87$)	33 (37.9)	29 (33.3)	28 (32.2)	15 (17.2)	2 (2.3)
AIH ($n = 28$)	15 (53.6)	14 (50)	7 (25)	3 (10.7)	0 (0)
PBC ($n = 25$)	4 (16)	9 (36)	12 (48)	7 (28)	2 (8)
AIH-PBC ($n = 34$)	14 (41.2)	6 (17.6)	9 (26.5)	5 (14.7)	0 (0)
CTD ($n = 40$)	2 (5)	7 (17.5)	34 (85)	4 (10)	19 (47.5)
Viral hepatitis ($n = 34$)	4 (11.8)	10 (29.4)	25 (73.5)	14 (41.2)	17 (50)

* $P < 0.05$ was considered statistically significant. AILD: autoimmune liver disease; AIH: autoimmune hepatitis; PBC: primary biliary cholangitis; AIH-PBC: overlap syndrome; CTD: connective tissue diseases.

as it might contribute to the identification of AILD and viral hepatitis.

It has been demonstrated that swelling of the mediastinal lymph node may be involved in patients with rheumatoid arthritis (RA), systemic lupus erythematosus (SLE), and mixed connective tissue disease (MCTD) [28]. The distribution of lymph nodes was extensive in SLE, including the axillary, cervical, supraclavicular, and inguinal regions; in RA, however, a lymph node often occurred in the lymphatic drainage of involved joints. In our study, abdominal lymph nodes were frequently found in the periphery of the pancreas and porta hepatis in patients with AILD; in contrast, abdominal lymph nodes were more common in the para-aorta and mesenteric roots in patients with CTD.

In our study, the distribution of lymph nodes in different subtypes of AILD was analyzed as well. The abdominal lymph nodes mainly appeared in the periphery of the pancreas and porta hepatis in AIH patients ($P < 0.05$); in patients with PBC, abdominal lymph nodes were more commonly found in the abdominal aorta. It has been reported that pancreatic lymph nodes can be divided into two groups—a pancreatic head group and the posterior wall of the pancreatic head group—and can both be considered “interchange stations” in the abdominal lymphatic system between the hepatic lymph nodes and the mesenteric lymph nodes [29]. We speculate that lymph nodes play a vital role in the pathogenesis of AIH at the periphery of the pancreas and porta hepatis. Efe et al. reported that the proportion of PBC patients with AIH features was high in an extended follow-up period [29]. This study showed that when pancreatic lymph nodes were found in PBC patients, these patients appeared to have AIH features as well. Therefore, the pathogenesis of different subtypes of AILD and abdominal lymph nodes warrants further research.

There were several limitations to our study. First, errors may have occurred because even though 106 of 125 individuals underwent liver biopsy and subsequent assessment of pathological features, this number of cases has little statistical significance. We also did not attempt to correlate disease activity with actual nodal size, only with lymph node enlargement.

In conclusion, the enlargement of perihepatic lymph nodes in AILD subjects can act as a good indicator, one that reflects the histological and biochemical inflammatory activities of the liver. Abdominal lymph nodes mainly appeared in the periphery of the pancreas in patients with AILD, while in

CTD and viral hepatitis patients, abdominal lymph nodes frequently occurred in the abdominal aorta and mesenteric roots. Future studies with larger groups of patients are needed to further analyze the effects and mechanisms of abdominal lymph nodes in AILD. Toward this end, we will explore whether changes in the size of lymph nodes can predict a sustained response of AILD therapy.

Data Availability

All the data are available at the correspondence author upon request.

Conflicts of Interest

None of the authors have any potential conflicts of interest related to this article to declare, and the results of this report have been produced, analyzed, and interpreted without any outside participation.

Authors' Contributions

Yongjuan Wang, Xiuxiu Xu, and Maojuan Ran contributed equally to this work.

Acknowledgments

This work was supported by the National Key R&D Program of China (2019YFC0119505) and the National Science Foundation of China (81860109 and 81500397). Thanks are due to Yujie Zhang for assistance with the pathology and to Haoran Song for guidance in iconography.

References

- [1] K. V. S. H. Kumar, A. K. Pawah, and M. Manrai, “Occult endocrine dysfunction in patients with cirrhosis of liver,” *Journal of Family Medicine and Primary Care*, vol. 5, no. 3, pp. 576–580, 2016.
- [2] Y. Wang, X. Guo, G. Jiao et al., “Splenectomy promotes macrophage polarization in a mouse model of concanavalin A-(ConA-) induced liver fibrosis,” *BioMed Research International*, vol. 2019, Article ID 5756189, 12 pages, 2019.
- [3] M. Carbone and J. M. Neuberger, “Autoimmune liver disease, autoimmunity and liver transplantation,” *Journal of Hepatology*, vol. 60, no. 1, pp. 210–223, 2014.

- [4] H. Hikita, H. Nakagawa, R. Tateishi et al., "Perihepatic lymph node enlargement is a negative predictor of liver cancer development in chronic hepatitis C patients," *Journal of Gastroenterology*, vol. 48, no. 3, pp. 366–373, 2013.
- [5] M. Sato, H. Hikita, S. Hagiwara et al., "Potential associations between perihepatic lymph node enlargement and liver fibrosis, hepatocellular injury or hepatocarcinogenesis in chronic hepatitis B virus infection," *Hepatology Research*, vol. 45, no. 4, pp. 397–404, 2015.
- [6] H. Fujii, N. Ohnishi, K. Shimura et al., "Case of autoimmune hepatitis with markedly enlarged hepatoduodenal ligament lymph nodes," *World Journal of Gastroenterology*, vol. 19, no. 11, pp. 1834–1840, 2013.
- [7] S. Hiramatsu, H. Nebiki, A. Ueno et al., "A case of primary biliary cirrhosis with systemic lymph node enlargement," *Nihon Shokakibyō Gakkai Zasshi*, vol. 109, no. 10, pp. 1784–1790, 2012.
- [8] J. Shu, J. N. Zhao, F. G. Han et al., "Chronic hepatitis B: enlarged perihepatic lymph nodes correlated with hepatic histopathology," *World Journal of Radiology*, vol. 5, no. 5, pp. 208–214, 2013.
- [9] Y.-L. Ko, C. S. Sun, K. M. Chung et al., "Manifestations of perihepatic lymph nodes in acute flare of chronic hepatitis B: association with HBeAg status and with HBeAg seroconversion," *PLoS One*, vol. 10, no. 2, article e0117590, 2015.
- [10] D. Schreiber-Dietrich, M. Pohl, X. W. Cui, B. Braden, C. F. Dietrich, and L. Chiorean, "Perihepatic lymphadenopathy in children with chronic viral hepatitis," *Journal of ultrasonography*, vol. 15, no. 61, pp. 137–150, 2015.
- [11] Y. Asano and S. Sato, "Connective tissue diseases: new criteria improve recognition of early systemic sclerosis," *Nature Reviews Rheumatology*, vol. 11, no. 1, pp. 3–4, 2015.
- [12] J. Varga and M. Hinchcliff, "Connective tissue diseases: systemic sclerosis: beyond limited and diffuse subsets?," *Nature Reviews Rheumatology*, vol. 10, no. 4, pp. 200–202, 2014.
- [13] F. Cassani, P. Valentini, M. Cataleta et al., "Ultrasound-detected abdominal lymphadenopathy in chronic hepatitis C: high frequency and relationship with viremia," *Journal of Hepatology*, vol. 26, no. 3, pp. 479–483, 1997.
- [14] P. Muller, C. Renou, A. Harafa et al., "Lymph node enlargement within the hepatoduodenal ligament in patients with chronic hepatitis C reflects the immunological cellular response of the host," *Journal of Hepatology*, vol. 39, no. 5, pp. 807–813, 2003.
- [15] A. W. Lohse, O. Chazouilleres, G. Dalekos et al., "EASL Clinical Practice Guidelines: autoimmune hepatitis," *Journal of Hepatology*, vol. 63, no. 4, pp. 971–1004, 2015.
- [16] K. D. Lindor, M. E. Gershwin, R. Poupon et al., "Primary biliary cirrhosis," *Hepatology*, vol. 50, no. 1, pp. 291–308, 2009.
- [17] D. Aletaha, T. Neogi, A. J. Silman et al., "2010 rheumatoid arthritis classification criteria: an American College of Rheumatology/European League Against Rheumatism collaborative initiative," *Arthritis and Rheumatism*, vol. 62, no. 9, pp. 2569–2581, 2010.
- [18] G. Bertsias, J. P. Ioannidis, J. Boletis et al., "EULAR recommendations for the management of systemic lupus erythematosus. Report of a Task Force of the EULAR Standing Committee for International Clinical Studies Including Therapeutics," *Annals of the Rheumatic Diseases*, vol. 67, no. 2, pp. 195–205, 2008.
- [19] C. H. Shiboski, S. C. Shiboski, R. Seror et al., "2016 American College of Rheumatology/European League Against Rheumatism classification criteria for primary Sjögren's syndrome: a consensus and data-driven methodology involving three international patient cohorts," *Arthritis & Rheumatology*, vol. 69, no. 1, pp. 35–45, 2017.
- [20] European Association for the Study of the Liver, "EASL clinical practice guidelines: Management of chronic hepatitis B virus infection," *Journal of Hepatology*, vol. 57, no. 1, pp. 167–185, 2012.
- [21] European Association for the Study of the Liver, "EASL recommendations on treatment of hepatitis C 2014," *Journal of Hepatology*, vol. 61, no. 2, pp. 373–395, 2014.
- [22] D. Shrestha, A. K. Dhakal, S. R. KC, A. Shakya, S. C. Shah, and H. Shakya, "Systemic lupus erythematosus and granulomatous lymphadenopathy," *BMC Pediatrics*, vol. 13, no. 1, 2013.
- [23] G. Redlarski, A. Palkowski, and M. Krawczuk, "Body surface area formulae: an alarming ambiguity," *Scientific Reports*, vol. 6, article 27966, 2016.
- [24] J.-P. Hsin and J. L. Manley, "The RNA polymerase II CTD coordinates transcription and RNA processing," *Genes & Development*, vol. 26, no. 19, pp. 2119–2137, 2012.
- [25] Y.-M. Lin, M. J. Sheu, H. T. Kuo et al., "The early on-treatment perihepatic lymph node response predicts sustained viral response of anti-hepatitis C virus therapy," *European Journal of Gastroenterology & Hepatology*, vol. 23, no. 11, pp. 990–996, 2011.
- [26] C. Hu, C. Deng, G. Song et al., "Prevalence of autoimmune liver disease related autoantibodies in Chinese patients with primary biliary cirrhosis," *Digestive Diseases and Sciences*, vol. 56, no. 11, pp. 3357–3363, 2011.
- [27] S. Nakanishi, K. Shiraki, K. Sugimoto et al., "Clinical significance of ultrasonographic imaging of the common hepatic arterial lymph node (no. 8 LN) in chronic liver diseases," *Molecular Medicine Reports*, vol. 3, no. 4, pp. 679–683, 2010.
- [28] H. AL-Jahdali, P. Rajiah, C. Allen, S. S. Koteyar, and A. N. Khan, "Pictorial review of intrathoracic manifestations of progressive systemic sclerosis," *Annals of Thoracic Medicine*, vol. 9, no. 4, pp. 193–202, 2014.
- [29] C. Efe, E. Ozaslan, A. Heurgué-Berlot et al., "Sequential presentation of primary biliary cirrhosis and autoimmune hepatitis," *European Journal of Gastroenterology & Hepatology*, vol. 26, no. 5, pp. 532–537, 2014.

Review Article

The Therapeutic Potential of MicroRNAs in Atrial Fibrillation

Xiaona Xu , Zhiqiang Zhao, and Guangping Li 

Tianjin Key Laboratory of Ionic-Molecular Function of Cardiovascular Disease, Department of Cardiology, Tianjin Institute of Cardiology, The Second Hospital of Tianjin Medical University, Tianjin 300211, China

Correspondence should be addressed to Guangping Li; tic_tjcardiol@126.com

Received 28 January 2020; Accepted 3 March 2020; Published 12 March 2020

Guest Editor: Hongmei Jiang

Copyright © 2020 Xiaona Xu et al. This is an open access article distributed under the Creative Commons Attribution License, which permits unrestricted use, distribution, and reproduction in any medium, provided the original work is properly cited.

One of the most globally prevalent supraventricular arrhythmias is atrial fibrillation (AF). Knowledge of the structures and functions of messenger RNA (mRNA) has recently increased. It is no longer viewed as solely an intermediate molecule between DNA and proteins but has come to be seen as a dynamic and modifiable gene regulator. This new perspective on mRNA has led to rising interest in it and its presence in research into new therapeutic schemes. This paper, therefore, focuses on microRNAs (miRNAs), which are small noncoding RNAs that regulate posttranscriptional gene expression and play a vital role in the physiology and normative development of cardiovascular systems. This means they play an equally vital role in the development and progression of cardiovascular diseases. In recent years, multiple studies have pinpointed particular miRNA expression profiles as being associated with varying histological features of AF. These studies have been carried out in both animal models and AF patients. The emergence of miRNAs as biomarkers and their therapeutic potential in AF patients will be discussed in the body of this paper.

1. Introduction

It is well known that RNA can be edited and modified, that RNA can form both secondary and tertiary structures, and that RNA experiences a dynamic, tight, and occasionally reversible posttranscriptional regulation through various RNA-binding proteins. Because of this knowledge, biotechnology companies are currently undertaking the clinical development of RNA-targeting therapies. It is in the companies' interests to increase the number of "drug-able" targets. One such target biotechnological research has been the endogenous regulators of gene silencing, microRNAs (miRNAs). They have been investigated due to their potential as therapeutic agents [1]. Initially found in *Caenorhabditis elegans* (*C. elegans*) in 1993, miRNAs are known for using messenger RNA (mRNA) degradation and translational repression to inhibit their target genes [2]. miRNAs regulate gene expression on a posttranscriptional level. They are short, noncoding RNAs, which can bind mRNAs and regulate gene expression through either mRNA degradation or translational repression [3]. mRNA degradation and the blockage of mRNA translation are the two potential mechanisms for miRNA

repression of gene expression [4]. Additionally, more than one miRNA has arrhythmogenic potential, and there are always different miRNAs acting within different types of atrial fibrillation (AF) [5]. Thus, to be stable, specific, and potent and have low levels of toxicity, RNA-targeting therapeutic modalities require different chemical modifications.

AF is the most common cardiac arrhythmia, correlated with increased morbidity and mortality rates [6]. Although multiple novel molecular concepts of AF pathophysiology have been in development throughout the previous decade, most of the therapeutic approaches presently available have major limitations. These include a lack of potency and negative side effects, such as malignant arrhythmias in the ventricle [7]. The genetic programming of miRNA regulations, both downregulation and upregulation, has been shown to affect developmental changes [8]. However, AF and other multiple cardiovascular diseases, which lead to myocardial remodeling, have been associated with changes (due to altered miRNA expression levels) in circulating blood and in cardiovascular tissues [9, 10]. miRNAs have been identified as active elements in multiple cardiovascular diseases. This is what motivates further research into their role in AF

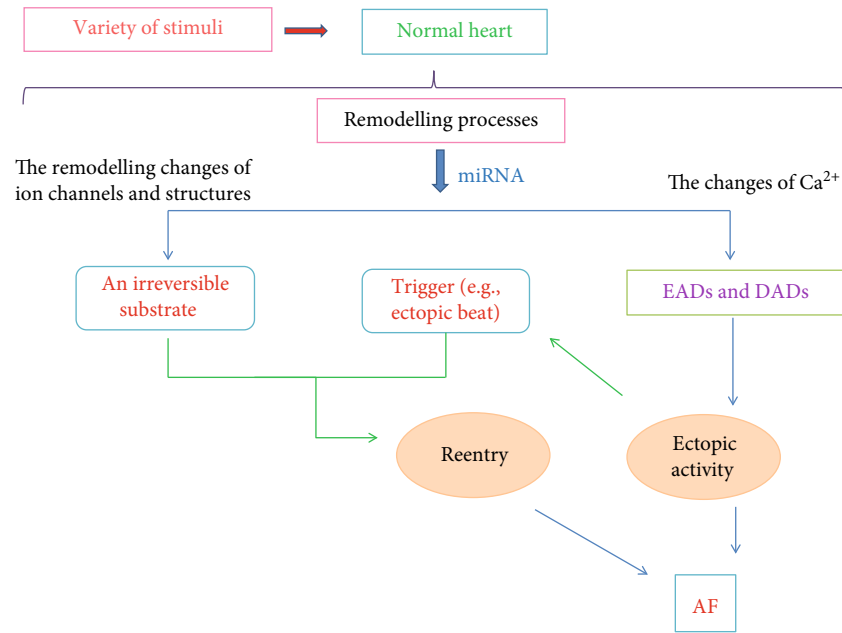


FIGURE 1: Illustration of AF mechanisms. Reentrant activity and ectopic activity are contained within the pathogenesis. Both the structure and function of the atrial tissue will be altered after the normal heart is stimulated. A substrate for reentrant AF is created by atrial remodeling through the alteration of ion-channel function or the introduction of tissue fibrosis. The likelihood of ectopic activity can be increased by remodeling through the production of Ca^{2+} in cell handling, which can cause triggered activity. Abbreviations—EADs: early afterdepolarizations; DADs: delayed afterdepolarizations; AF: atrial fibrillation.

pathophysiology, as the study of miRNAs could lead to the successful development of safer treatment options with higher efficacy [11, 12].

This review is aimed at providing a summary of the most recent developments in miRNA research based on both human and animal models. Firstly, the studies currently available, which have investigated the role of miRNAs in AF, will be described. This will provide a basis for suggestions as to the extent to which miRNAs might have the capacity to positively affect therapeutic strategies. Once an expression profile of miRNA on the development of AF is given, taking into consideration both human and animal studies, the potential roles of miRNA in AF regulation will be discussed. Following this, the potential function of miRNAs in AF's pathophysiological processes will be considered in accordance with the available experimental evidence. In this way, the possible future clinical applications of miRNAs in AF will be expressed.

2. Pathomechanisms of AF

The most widely accepted pathomechanisms of AF are reentry and ectopic activity (Figure 1) [7, 13]. Both of these pathomechanisms are frequently the result of alterations in atrial tissue structure and function (or atrial remodeling), which can be induced by the disease or by AF itself. These pathomechanisms aid the progression towards increasingly persistent forms of AF [14, 15]. Abnormal local spontaneous discharges from overactive ectopic pacemakers cause ectopic activity. In normal atrial tissue, enhanced ectopy or reentry is rare, and these are often caused by the remodeling that takes

place when cardiac diseases act on the tissue [15]. Delayed or early afterdepolarizations (repolarization failure) have also been suggested as the cause of ectopic activity [14]. Delayed afterdepolarizations (DADs) are caused by the simultaneous release of diastolic Ca^{2+} from the sarcoplasmic reticulum. This release generally occurs due to an overload of the sarcoplasmic reticulum Ca^{2+} release channels [17–19]. Early afterdepolarizations (EADs) occur in response to excessive prolongation of action potential duration, which creates afterdepolarizations in the mechanisms that rely on Ca^{2+} . EADs can also occur when short-duration action potential (or a parasympathetic effect) combines with prolonged transients of Ca^{2+} . This is known as a sympathetic effect and occurs in response to sympathovagal discharge [20].

There are two methods of thinking about reentry. Allesie et al. [20] developed the leading circle concept, which theorizes that centripetal waves maintain this latter refractory through movement towards the center. The shortest circuit is the shortest distance an impulse travels in the refractory period, and it is in the shortest circuit through which a functional reentry is established. Following from the leading circle concept, a functional reentry depends on a balance between the speed of conduction and the refractory capabilities of the cells. The chances of simultaneous conduction occurring in a potential reentry area increase when there is a short refractory capacity or slow conduction speed. A spiral wave reentry, or a “rotor,” is another way in which reentry can take place. In this specific type, the reentry occurs in a particular region when a curved wavefront and wavetail come together at a point of a singularity. Additionally, this singularity's

tissue must not be refractory [21]. In a spiral wave reentry, the reentry is achieved through rapid circulation around a central core by a rotor with a wavefront. To determine the size of the spiral wave, the excitability and refractoriness of the tissue of this reentry will be measured. If the tissue has a short refractory capacity and is highly excitable, rotor maintenance is achievable and can be stabilized, as these factors permit the spiral wave to rotate rapidly around a core.

The chances of reentry or ectopic firing are increased by remodeling (Figure 1). Remodeling encourages ectopic firing due to its alternating cardiomyocyte handling of Ca^{2+} , which it does to encourage DADs or EADs to develop. Remodeling may be carried out electrically, but due to its rapid atrial rates, such as those seen when AF takes place, atrial refractoriness will be shortened by electrical remodeling through reduced action potential duration [21, 22]. AF has long-term effects on cellular structure, which remains remodeled (cardiomyocyte hypertrophy and glycogen accumulation). There is a possibility that assist rapid atrial activation promotes atrial fibrosis [23]. Atrial fibrosis may inhibit atrial conduction. If this occurs, an irreversible substrate for AF might be created.

Many pathologies are associated with AF, and a common feature amongst them is atrial fibrosis, which appears to play a central role in AF pathogenesis. Additionally, two features shared by many associated disorders—atrial strength and atrial enlargement—are key contributors to AF development. AF may be suppressed by an antiarrhythmic intervention, depending on whether or not the intervention has the capacity to suppress underlying mechanisms [23, 24].

3. miRNAs in AF

miRNAs have the potential to be appropriate disease biomarkers due to their tissue-specific and pathology-specific expressions. miRNAs are stable in plasma because of their ability to mingle with microparticles, such as exosomes, macrovesicles, and apoptotic bodies [25–27], and because they are frequently tied to proteins and high-density lipoproteins, which protect them from RNase activity. miRNAs also have high sensitivity and specificity and are detectable in both plasma and serum. Biomarkers can provide vital insight post-diagnosis [28]. When AF has been diagnosed, biomarkers can reveal atrial cardiomyopathies at the root of AF, which can have a widespread implication for prognosis and treatment. Such insights would certainly enhance patient care, making it more individually tailored. Numerous studies support the involvement of miRNAs in AF-related remodeling processes and have also suggested that miRNAs are likely to play vital roles in signaling during AF pathogenesis [29, 30].

3.1. Electrical Disturbances. Evidence suggests that increases in K^+ current (I_{K1}) and decreases in L-type Ca^{2+} currents (I_{CaL}) are two of the most important ionic current changes at the base of AF-induced electrical remodeling. Multiple miRNAs have been identified in these types of remodeling, as well as in other components of electrical atrial remodeling [11]. miR-1 was first identified, in coronary artery disease, as having arrhythmogenic potential. It was also found to have a proarrhythmic effect in ischemic models

because of the targeting of the gap-junction channel gene *GJA1* (encoding gap junction $\alpha 1$ protein) [31]. Furthermore, it has been shown that miR-1 is a regulator for Ca^{2+} -handling proteins—for example, protein phosphatase 2A (PP2A), the $\text{Na}^+/\text{Ca}^{2+}$ exchanger 1, and calmodulin. However, additional studies are necessary to reveal whether AF is associated with miR-1-dependent regulation of Ca^{2+} handling. Another complication lies in the fact that the data implicates miR-26 as a regulator in AF changes in I_{K1} [32]. The calcium-/calmodulin-/calcineurin-regulated nuclear factor of activated T cells (NFAT) pathway has a negative control on the transcription of miR-26. Enriched NFAT nuclear translocation has been found in both dogs and in patients with AF [33]. This is likely to contribute to the reduction of miR-26. Still, these are not the only miRNAs involved in AF regulation. For instance, miR-208a is a crucial miRNA for cardiac hypertrophic responses. Spontaneous AF has been found to be frequent in miR-208a-knockout mice [34]. Furthermore, miR-328 has been found to be upregulated in AF patients [35], whilst miR-499 has been found to be upregulated through a miRNA expression study of atrial tissue in AF patients. This study compared AF patients with control participants [36].

3.2. Structural Remodeling. The trademark of structural remodeling in AF is atrial fibrosis. It is believed to have a crucial pathophysiological role in the condition, and miRNAs are considered to be potential regulators of the fibrotic remodeling that occurs in AF [11]. Of these miRNAs, miR-21 has a high expression of fibroblasts, and it has been intensively investigated through rodent models of cardiac hypertrophy. It is thought to target and repress the translation of the protein sprout homologue 1 (SPRY1) by encoding the protein. SPRY1 is a negative regulator of the extracellular signal-regulated kinase (ERK) pathway. Similarly, miR-26 may play an important role in AF-related electrical remodeling, but it is also thought to contribute to atrial fibrotic remodeling. It may participate in this remodeling by regulating the expression of transient receptor potential channel 3 (TRPC3) [32]. Furthermore, miR-29 is known to target multiple extracellular matrix genes, including collagen, fibrillin, and elastin [37]. miR-29b has been shown to be downregulated in the atria of dogs with heart failure. An inverse correlation has been found in its expression between its extracellular matrix protein levels and AF development [38]. In ventricular fibrosis during cardiac hypertrophy, miR-30 and miR-133 have been shown to be downregulated through the derepression of a vital profibrotic protein. Transforming growth factor- ($\text{TGF-}\beta$) $\beta 1$ and $\text{TGF-}\beta$ receptor type-2 (TGFR-2) have also been discovered as profibrotic factors shown to be upregulated in nicotine-treated dogs. Reduced expressions of miR-133 and miR-590 (miRNAs that target $\text{TGF-}\beta 1$ and TGFR-2) are also found in nicotine-treated dogs [39].

4. miRNAs as Potential Therapeutic Targets in AF

Recently, tissue-specific miRNAs have been studied in both humans and animals. These studies have implicated miRNAs

as contributors to structural and electrical remodeling in AF [13, 40]. Changes in the expressions of miR-21, miR-26, miR-29b, miR-30c, miR-133, and miR-590 have been identified as having a relationship with AF structural remodeling. They are thought to regulate the signaling cascades related to atrial fibrosis. The changes in these miRNAs have also been found to be in relationship with electrical remodeling. miR-1 and miR-26, when downregulated, may help increase the basal inward rectifier current I_{K1} . On the other hand, when miR-21 and miR-328 are upregulated, they appear involved in reducing L-type Ca^{2+} currents (I_{CaL}) in the myocytes of patients with AF [35, 41]. Several relevant studies suggest that miRNAs are dysregulated in various AF forms, demonstrated by research in patients and animals.

4.1. Treatment of AF: The Role Played by Specific miRNAs, as Shown by Animal Studies. Tissue-specific miRNAs have been studied in animals, and various researchers have indicated that miRNAs play a crucial role in AF processes. *In vivo* manipulation of miRNAs in AF has been achieved, and the results suggest that particular miRNA therapeutics could be developed for atrial cardiomyopathies. Lu et al. [35] have discovered that antogomir-328 may successfully reverse AF susceptibility in ATP dogs through the *in vivo* adenoviral-mediated forced expression of miR-328. The capacity of miR-1 to reduce AF susceptibility has also been demonstrated by Jia et al. [42]. In this study, LNA-based antimir-1 was administered and found to prolong the atrial effective refractory period (AERP) and reduce AF susceptibility and duration in rabbits [43]. Furthermore, *in vivo* experiments in dogs and mice showed decreased Cav1.2, Cav β 1, and I_{CaL} , as well as shortening of the action potential duration and enhanced AF susceptibility [43]. The cluster of miR-106b-25 has been shown to be downregulated through upregulating ryanodine receptor 2 (RYR2) protein expression in patients with continual AF. Additionally, miR-106b-25 knockout mice have displayed a steady rise in Ca^{2+} release with RYR2, a known contributor to AF vulnerability [8]. Evidence shows that miR-29b expression is reduced in the atrial tissues of AF patients. These findings are supported by the observation of a miR-29b downregulation in the atrial tissues of canines undergoing ventricular tachypacing to induce congestive heart failure (CHF) and following AF [44].

4.2. Human Studies and What They Show about the Function of Particular miRNAs in AF Treatment. Various tissue-specific miRNA studies on human patients suggest that miRNAs play an important role in AF processes. When looking at the left atria (LA) of AF patients, a higher expression of miRNA-21 was seen compared to the LA of patients in sinus rhythm. A positive correlation was found between increased miRNA-21 expression and atrial collagen content. This relates to the reduced protein expression of SPRY1 and the increased expression of connective tissue growth factor (CTGF), lysyl oxidase, and Rac1-GTPase [45]. A recent study has shown that miR-21 and miR-150 have a relationship with AF, comparing 112 AF patients with 99 AF-free people [46]. In this study, the plasma levels of 86 miRNAs were measured.

AF atrial remodeling pathogenesis was carried out for each miRNA by quantitative reverse transcription polymerase chain reaction (qRT-PCR). The levels of plasma in miR-21 and miR-150 were found to be noticeably lower amongst AF patients [46]. Another study was carried on both local and systemic plasma levels and found that miRNAs positively correlate with AF. Studies with atrial substrate properties suggest that miR-328 plays a vital role in atrial remodeling processes in AF patients [47]. miR-328 is locally produced in the LA. This may affect atrial remodeling in AF patients, as miR-328 plasma levels were higher in AF patients than in control patients. These levels were also measured as higher in the LA appendage than in the pulmonary vein (PV) or the periphery [47]. A study by Dawson et al. (2013) revealed that, in AF or congestive heart failure (CHF), patients' plasma exhibited a noticeable reduction of miR-29b and miR-21 expressions. This study further demonstrated that miR-29b was yet further decreased in AF and CHF patients [48]. CHF can cause fibrotic atrial remodeling and contribute to AF maintenance. Therefore, both of these miRNAs could be crucial biomarkers for atrial remodeling [5].

5. miRNA-Mediated Regulation of Inflammatory Cytokines in AF

Several studies have indicated that inflammatory mediators play a mechanistic role in AF pathophysiology. Inflammatory mediators such as C-reactive protein (CRP), interleukins, TNF- α , TGF- β , and MCP-1 were reported as having higher blood serum levels in AF patients than in control subjects. When miR-21 is upregulated, it promotes both AF and susceptibility to AF [8]. This is due to STAT3 phosphorylation or inhibition of the TGF- β pathway and downregulation of Smad7 [49]. Yet it is noteworthy that, *in vivo*, the control of miR-21 using anti-miR-21 has been shown to reduce AF and fibrosis in animals [50]. The CRP is also crucial to systemic inflammation. Additionally, a correlation of some strength is observed between miR-150 and CRP levels. When miR-150 is downregulated, it can aid AF growth through targeting genes that have a role in the inflammation [51]. Thus, it is a predictive biomarker for AF. Different cytokines—for example, TNF- α , TGF- β , IL-6, and IL-18 from macrophages and monocytes—are secreted in response to inflammatory stimuli. These produce increased plasma CRP production in AF patients but do not produce an increase in healthy subjects.

6. Prospective Future for miRNAs as Therapeutics

Research has demonstrated that there is a correlation between AF and quantifiable alterations in miRNA expression levels. Nonetheless, it cannot be ignored that differential miRNA expression levels, which have been measured through blood and tissue samples in the left and right atria, depend on the cardiac disease's severity or type. Furthermore, the phase and type of AF will impact the differential expression of miRNAs. These variables, alongside the methodologies used, should be considered when evaluating

research. This must be done before miRNAs can be brought into clinical application [8, 43].

Despite the strength of the data supporting the effect of miRNAs in AF, the limitations of these studies cannot be overlooked. There are various inconsistencies, which are likely due to small sample sizes and variables (e.g., sex, age, drug therapies, and concomitant conditions). All these have influenced the studies to date. To clearly identify which miRNAs are dysregulated in clinical AF, further research is required. Further research is also required to determine what level of miRNA changes depends on the base pathology and the stage of the disease. Microarray techniques have been crucial to all studies profiling miRNA. These techniques are semiquantitative and are known for producing false-positive and false-negative results. Inarguably, future research using more quantitative methods, including high-throughput qPCR, is necessary. Research might also benefit from a fresh approach, such as deep sequencing, which would help researchers develop miRNA expression profiles in AF with precision and detail.

There are multiple concerns as to the safety of miRNA therapeutics, which would need to be addressed before miRNA-based therapy could be utilized in clinical practice. One of the primary concerns is miRNAs' ability to target multiple pathways. miRNAs might interfere with physiological pathways as a high number of miRNA mimics may be delivered to an organ that is not the target organ or a pathway not within the target tissue. Further research must be carried out to confirm the safety of miRNAs, as well as their therapeutic potential. Future research should, therefore, focus on the *in vivo* effects of cardiovascular miRNA therapeutics.

Conflicts of Interest

The authors declare there is no conflict of interest to report.

Acknowledgments

This study was supported by National Natural Science Foundation of China (Nos. 81700304 and 81370300), Tianjin Science and Technology Committee (18JCYBJC92200), Tianjin Natural Science Foundation Project (17JCQNJC11400), and Key Laboratory Science Foundation of Second Hospital of Tianjin Medical University (2017ZDSYS05).

References

- [1] A. Laina, A. Gatsiou, G. Georgiopoulos, K. Stamatelopoulos, and K. Stellos, "RNA therapeutics in cardiovascular precision medicine," *Frontiers in Physiology*, vol. 9, p. 953, 2018.
- [2] R. C. Lee, R. L. Feinbaum, and V. Ambros, "The *C. elegans* heterochronic gene *lin-4* encodes small RNAs with antisense complementarity to *lin-14*," *Cell*, vol. 75, no. 5, pp. 843–854, 1993.
- [3] C. Schulte, M. Karakas, and T. Zeller, "microRNAs in cardiovascular disease - clinical application," *Clinical Chemistry and Laboratory Medicine*, vol. 55, no. 5, pp. 687–704, 2017.
- [4] H. O. Iwakawa and Y. Tomari, "The functions of microRNAs: mRNA decay and translational repression," *Trends in Cell Biology*, vol. 25, no. 11, pp. 651–665, 2015.
- [5] A. M. da Silva, J. N. de Araujo, R. C. de Freitas, and V. N. Silbiger, "Circulating microRNAs as potential biomarkers of atrial fibrillation," *BioMed Research International*, vol. 2017, Article ID 7804763, 7 pages, 2017.
- [6] J. Andrade, P. Khairy, D. Dobrev, and S. Nattel, "The clinical profile and pathophysiology of atrial fibrillation: relationships among clinical features, epidemiology, and mechanisms," *Circulation Research*, vol. 114, no. 9, pp. 1453–1468, 2014.
- [7] J. Heijman, N. Voigt, S. Nattel, and D. Dobrev, "Cellular and molecular electrophysiology of atrial fibrillation initiation, maintenance, and progression," *Circulation Research*, vol. 114, no. 9, pp. 1483–1499, 2014.
- [8] S. Komal, J. J. Yin, S. H. Wang et al., "MicroRNAs: emerging biomarkers for atrial fibrillation," *Journal of Cardiology*, vol. 74, no. 6, pp. 475–482, 2019.
- [9] C. R. Wyndham, "Atrial fibrillation: the most common arrhythmia," *Texas Heart Institute Journal*, vol. 27, no. 3, pp. 257–267, 2000.
- [10] E. M. Small, R. J. A. Frost, and E. N. Olson, "MicroRNAs add a new dimension to cardiovascular disease," *Circulation*, vol. 121, no. 8, pp. 1022–1032, 2010.
- [11] X. Luo, B. Yang, and S. Nattel, "MicroRNAs and atrial fibrillation: mechanisms and translational potential," *Nature Reviews Cardiology*, vol. 12, no. 2, pp. 80–90, 2015.
- [12] G. Santulli, G. Iaccarino, N. De Luca, B. Trimarco, and G. Condorelli, "Atrial fibrillation and micro RNAs," *Frontiers in Physiology*, vol. 5, p. 15, 2014.
- [13] C. E. Molina and N. Voigt, "Finding Ms or Mr Right: which miRNA to target in AF?," *Journal of Molecular and Cellular Cardiology*, vol. 102, pp. 22–25, 2017.
- [14] D. Dobrev and S. Nattel, "New antiarrhythmic drugs for treatment of atrial fibrillation," *The Lancet*, vol. 375, no. 9721, pp. 1212–1223, 2010.
- [15] S. Nattel, B. Burstein, and D. Dobrev, "Atrial remodeling and atrial fibrillation: mechanisms and implications," *Circulation: Arrhythmia and Electrophysiology*, vol. 1, no. 1, pp. 62–73, 2008.
- [16] Y. H. Yeh, R. Wakili, X. Y. Qi et al., "Calcium-handling abnormalities underlying atrial arrhythmogenesis and contractile dysfunction in dogs with congestive heart failure," *Circulation: Arrhythmia and Electrophysiology*, vol. 1, no. 2, pp. 93–102, 2008.
- [17] M. G. Chelu, S. Sarma, S. Sood et al., "Calmodulin kinase II-mediated sarcoplasmic reticulum Ca^{2+} leak promotes atrial fibrillation in mice," *Journal of Clinical Investigation*, vol. 119, no. 7, pp. 1940–1951, 2009.
- [18] J. A. Vest, X. H. T. Wehrens, S. R. Reiken et al., "Defective cardiac ryanodine receptor regulation during atrial fibrillation," *Circulation*, vol. 111, no. 16, pp. 2025–2032, 2005.
- [19] D. Dobrev and S. Nattel, "Calcium handling abnormalities in atrial fibrillation as a target for innovative therapeutics," *Journal of Cardiovascular Pharmacology*, vol. 52, no. 4, pp. 293–299, 2008.
- [20] A. Burashnikov and C. Antzelevitch, "Reinduction of atrial fibrillation immediately after termination of the arrhythmia is mediated by late phase 3 early afterdepolarization-induced triggered activity," *Circulation*, vol. 107, no. 18, pp. 2355–2360, 2003.
- [21] S. Nattel, F. Xiong, and M. Aguilar, "Demystifying rotors and their place in clinical translation of atrial fibrillation

- mechanisms," *Nature Reviews Cardiology*, vol. 14, no. 9, pp. 509–520, 2017.
- [22] N. C. Denham, C. M. Pearman, J. L. Caldwell et al., "Calcium in the pathophysiology of atrial fibrillation and heart failure," *Frontiers in Physiology*, vol. 9, p. 1380, 2018.
- [23] M. Miragoli and A. V. Glukhov, "Atrial fibrillation and fibrosis: beyond the cardiomyocyte centric view," *BioMed Research International*, vol. 2015, Article ID 798768, 16 pages, 2015.
- [24] S. Nattel, "Molecular and cellular mechanisms of atrial fibrosis in atrial fibrillation," *JACC: Clinical Electrophysiology*, vol. 3, no. 5, pp. 425–435, 2017.
- [25] M. R. Ladomery, D. G. Maddocks, and I. D. Wilson, "MicroRNAs: their discovery, biogenesis, function and potential use as biomarkers in non-invasive prenatal diagnostics," *International Journal of Molecular Epidemiology and Genetics*, vol. 2, no. 3, pp. 253–260, 2011.
- [26] T. L. Whiteside, "The potential of tumor-derived exosomes for noninvasive cancer monitoring," *Expert Review of Molecular Diagnostics*, vol. 15, no. 10, pp. 1293–1310, 2015.
- [27] R. U. Takahashi, M. Prieto-Vila, A. Hironaka, and T. Ochiya, "The role of extracellular vesicle microRNAs in cancer biology," *Clinical Chemistry and Laboratory Medicine*, vol. 55, no. 5, pp. 648–656, 2017.
- [28] C. Ricci, C. Marzocchi, and S. Battistini, "MicroRNAs as biomarkers in amyotrophic lateral sclerosis," *Cells*, vol. 7, no. 11, p. 219, 2018.
- [29] Y. Li, Z. Yin, J. Fan, S. Zhang, and W. Yang, "The roles of exosomal miRNAs and lncRNAs in lung diseases," *Signal Transduction and Targeted Therapy*, vol. 4, no. 1, p. 47, 2019.
- [30] Y. Cui, X. Zhang, M. Yu, Y. Zhu, J. Xing, and J. Lin, "Techniques for detecting protein-protein interactions in living cells: principles, limitations, and recent progress," *Science China Life Sciences*, vol. 62, no. 5, pp. 619–632, 2019.
- [31] B. Yang, H. Lin, J. Xiao et al., "The muscle-specific microRNA miR-1 regulates cardiac arrhythmogenic potential by targeting GJA1 and KCNJ2," *Nature Medicine*, vol. 13, no. 4, pp. 486–491, 2007.
- [32] X. Luo, Z. Pan, H. Shan et al., "MicroRNA-26 governs profibrillatory inward-rectifier potassium current changes in atrial fibrillation," *The Journal of Clinical Investigation*, vol. 123, no. 5, pp. 1939–1951, 2013.
- [33] M. Oh-hora and A. Rao, "The calcium/NFAT pathway: role in development and function of regulatory T cells," *Microbes Infect*, vol. 11, no. 5, pp. 612–619, 2009.
- [34] T. E. Callis, K. Pandya, H. Y. Seok et al., "MicroRNA-208a is a regulator of cardiac hypertrophy and conduction in mice," *The Journal of Clinical Investigation*, vol. 119, no. 9, pp. 2772–2786, 2009.
- [35] Y. Lu, Y. Zhang, N. Wang et al., "MicroRNA-328 contributes to adverse electrical remodeling in atrial fibrillation," *Circulation*, vol. 122, no. 23, pp. 2378–2387, 2010.
- [36] T. Y. Ling, X. L. Wang, Q. Chai et al., "Regulation of the SK3 channel by microRNA-499—Potential role in atrial fibrillation," *Heart Rhythm*, vol. 10, no. 7, pp. 1001–1009, 2013.
- [37] A. J. Kriegel, Y. Liu, Y. Fang, X. Ding, and M. Liang, "The miR-29 family: genomics, cell biology, and relevance to renal and cardiovascular injury," *Physiological Genomics*, vol. 44, no. 4, pp. 237–244, 2012.
- [38] S. V. Pandit and A. J. Workman, "Atrial electrophysiological remodeling and fibrillation in heart failure," *Clinical Medicine Insights Cardiology*, vol. 10s1, Supplement 1, pp. CMC.S39713–CMC.S39746, 2016.
- [39] S. Clauss, M. F. Sinner, S. Kääh, and R. Wakili, "The role of microRNAs in antiarrhythmic therapy for atrial fibrillation," *Arrhythmia & Electrophysiology Review*, vol. 4, no. 3, pp. 146–155, 2015.
- [40] A. Briasoulis, S. Sharma, T. Telila et al., "MicroRNAs in atrial fibrillation," *Current Medicinal Chemistry*, vol. 26, no. 5, pp. 855–863, 2019.
- [41] A. Barana, M. Matamoros, P. Dolz-Gaitón et al., "Chronic atrial fibrillation increases MicroRNA-21 in human atrial myocytes decreasing L-type calcium current," *Circulation: Arrhythmia and Electrophysiology*, vol. 7, no. 5, pp. 861–868, 2014.
- [42] X. Jia, S. Zheng, X. Xie et al., "MicroRNA-1 accelerates the shortening of atrial effective refractory period by regulating KCNE1 and KCNB2 expression: an atrial tachypacing rabbit model," *PloS One*, vol. 8, no. 12, pp. e85639–e85639, 2013.
- [43] N. W. E. van den Berg, M. Kawasaki, W. R. Berger et al., "MicroRNAs in atrial fibrillation: from expression signatures to functional implications," *Cardiovascular Drugs and Therapy*, vol. 31, no. 3, pp. 345–365, 2017.
- [44] L. T. Weckbach, U. Grabmaier, S. Clauss, and R. Wakili, "MicroRNAs as a diagnostic tool for heart failure and atrial fibrillation," *Current Opinion in Pharmacology*, vol. 27, pp. 24–30, 2016.
- [45] K. H. Shi, H. Tao, J. J. Yang, J. X. Wu, S. S. Xu, and H. Y. Zhan, "Role of microRNAs in atrial fibrillation: New insights and perspectives," *Cell Signal*, vol. 25, no. 11, pp. 2079–2084, 2013.
- [46] D. D. McManus, K. Tanriverdi, H. Lin et al., "Plasma microRNAs are associated with atrial fibrillation and change after catheter ablation (the miRhythm study)," *Heart Rhythm*, vol. 12, no. 1, pp. 3–10, 2015.
- [47] T. Soeki, T. Matsuura, S. Bando et al., "Relationship between local production of microRNA-328 and atrial substrate remodeling in atrial fibrillation," *Journal of Cardiology*, vol. 68, no. 6, pp. 472–477, 2016.
- [48] K. Dawson, R. Wakili, B. Ördög et al., "MicroRNA29," *Circulation*, vol. 127, no. 14, pp. 1466–1475, 2013, 1475e1461-1428.
- [49] R. B. Luwor, B. Baradaran, L. E. Taylor et al., "Targeting Stat3 and Smad7 to restore TGF- β cytoskeletal regulation of tumor cells *in vitro* and *in vivo*," *Oncogene*, vol. 32, no. 19, pp. 2433–2441, 2013.
- [50] J. Zhang, J. Jiao, S. Cermelli et al., "miR-21 inhibition reduces liver fibrosis and prevents tumor development by inducing apoptosis of CD24+ progenitor cells," *Cancer Research*, vol. 75, no. 9, pp. 1859–1867, 2015.
- [51] X. Li, L. Chen, W. Wang, F.-B. Meng, R.-T. Zhao, and Y. Chen, "MicroRNA-150 inhibits cell invasion and migration and is downregulated in human osteosarcoma," *Cytogenetic and Genome Research*, vol. 146, no. 2, pp. 124–135, 2015.

Research Article

Serine Deficiency Exacerbates Inflammation and Oxidative Stress via Microbiota-Gut-Brain Axis in D-Galactose-Induced Aging Mice

Fenggen Wang,¹ Hongbin Zhou,² Ligang Deng,¹ Lei Wang,¹ Jingqing Chen ,³
and Xihong Zhou ⁴

¹Institute of Quality Standard & Testing Technology for Agro-Products, Shandong Academy of Agricultural Sciences, Jinan 250100, China

²Dalian Chengsan Husbandry Co., Ltd., Dalian, China

³State Key Laboratory of Animal Nutrition, China Agricultural University, Beijing 100193, China

⁴Key Laboratory of Agro-ecological Processes in Subtropical Region, Institute of Subtropical Agriculture, Chinese Academy of Sciences, Changsha 410125, China

Correspondence should be addressed to Jingqing Chen; cjq9512@163.com and Xihong Zhou; xhzhou@isa.ac.cn

Received 17 January 2020; Accepted 18 February 2020; Published 2 March 2020

Guest Editor: Hongmei Jiang

Copyright © 2020 Fenggen Wang et al. This is an open access article distributed under the Creative Commons Attribution License, which permits unrestricted use, distribution, and reproduction in any medium, provided the original work is properly cited.

Inflammation and oxidative stress play key roles in the process of aging and age-related diseases. Since serine availability plays important roles in the support of antioxidant and anti-inflammatory defense system, we explored whether serine deficiency affects inflammatory and oxidative status in D-galactose-induced aging mice. Male mice were randomly assigned into four groups: mice fed a basal diet, mice fed a serine- and glycine-deficient (SGD) diet, mice injected with D-galactose and fed a basal diet, and mice injected with D-galactose and fed an SGD diet. The results showed that D-galactose resulted in oxidative and inflammatory responses, while serine deficiency alone showed no such effects. However, serine deficiency significantly exacerbated oxidative stress and inflammation in D-galactose-treated mice. The composition of fecal microbiota was affected by D-galactose injection, which was characterized by decreased microbiota diversity and downregulated ratio of *Firmicutes/Bacteroidetes*, as well as decreased proportion of *Clostridium XIVa*. Furthermore, serine deficiency exacerbated these changes. Additionally, serine deficiency in combination with D-galactose injection significantly decreased fecal butyric acid content and gene expression of short-chain fatty acid transporters (*Slc16a3* and *Slc16a7*) and receptor (*Gpr109a*) in the brain. Finally, serine deficiency exacerbated the decrease of expression of phosphorylated AMPK and the increase of expression of phosphorylated NFκB p65, which were caused by D-galactose injection. In conclusion, our results suggested that serine deficiency exacerbated inflammation and oxidative stress in D-galactose-induced aging mice. The involved mechanisms might be partially attributed to the changes in the microbiota-gut-brain axis affected by serine deficiency.

1. Introduction

The population of aging people is increasing rapidly worldwide, and aging is considered as being the major factor for the development of age-related diseases. Consequently, revealing the mechanisms involved in age-related diseases is critically important. Free radical theory is one of the accepted mechanisms by researchers, as increased reactive oxygen species are accumulated in the brains and they attack many

kinds of biomolecules during the process of age-related diseases [1]. Additionally, inflammation has been considered to contribute to the pathogenesis of age-related disorders, and the condition often referred to as “inflammaging” [2]. Recently, increasing evidences indicated that the changes in microbiota composition have been associated with oxidative and inflammatory processes in the aging brain, as there are bidirectional communications between the brain and the gut microbiota, termed the microbiota-gut-brain axis, which

enables gut microbes to communicate with the brain [3, 4]. However, studies are still needed to elucidate how the microbiota-gut-brain axis works in these processes.

Generally, diets were considered to play important roles in brain aging through the modulation of gene and protein expression [5]. Recent researchers suggested that diet-induced changes of gut microbiota also affected age-related pathogenesis [6]. Serine is a nutritionally nonessential amino acid, but it is a major substrate for the synthesis of glutathione. Recent studies demonstrated that dietary supplementation with serine showed strong anti-inflammatory and antioxidative abilities in certain mouse models [7–10]. Moreover, serine exerted beneficial effects on microbiota composition and alleviated inflammatory responses in a dextran sulfate sodium-induced colitis model in mice [11]. Importantly, the offspring mice from dams fed a serine- and glycine-deficient diet were vulnerable to oxidative stress [12]. Consequently, we conducted the present study to explore whether serine deficiency affects inflammatory and oxidative status in the brain in an aging mouse model induced by chronic D-galactose treatment, which had a similar characteristic as natural aging rodents did. Furthermore, whether and how the microbiota-gut-brain axis is involved in these effects were also explored.

2. Materials and Methods

2.1. Animals and Experimental Design. Thirty-two male C57BL/6J mice at the age of 9 weeks were purchased from SLAC Laboratory Animal Central (Changsha, China). The mice were maintained in plastic cages under standard conditions and were free to access feed and water. After an acclimatization of 2 weeks, all animals were randomly assigned into 4 groups ($n = 8$): Control group, mice were fed a basal diet and injected with saline; SGD group, mice were fed a serine- and glycine-deficient (SGD) diet and injected with saline; D-gal group, mice were fed a basal diet and injected with D-galactose; and D-SGD group, mice were fed a serine- and glycine-deficient diet and injected with D-galactose. Mice were subcutaneously injected with 1.2 g per kg body weight/day D-galactose (D-galactose solution, 0.15 g/mL). The basal diet and the serine- and glycine-deficient diet were purchased from Research Diets (New Brunswick, NJ, USA). The experiment lasted two months. The experimental protocol was approved by the Protocol Management and Review Committee of Institute of Subtropical Agriculture, and mice were treated according to the animal care guidelines of the Institute of Subtropical Agriculture (Changsha, China). At the end of the experiments, fresh feces were collected for the analysis of microbiota composition and short-chain fatty acid (SCFA) concentrations. After the mice were sacrificed, the blood samples were collected and serum were separated and stored at -20°C until analysis. The brain was also collected and immediately frozen in liquid nitrogen and stored at -80°C until analysis.

2.2. Biochemical Assays. Concentrations of advanced glycation end products (AGEs), malondialdehyde (MDA), tumor necrosis factor (TNF- α), interleukin 1 β (IL-1 β), and IL-6,

as well as activities of superoxide dismutase (SOD), glutathione peroxidase (GSH-Px), catalase (CAT), and glutathione content were measured using commercially available kits (Meimian, Jiangsu Yutong Biological Technology Co., Ltd, Nanjing, China) based on absorption according to the manufacturer's instructions.

2.3. qRT-PCR. Total RNA was isolated from whole brain tissue using the TRIZOL reagents (Invitrogen, Shanghai, China). The RNA was reverse transcribed into cDNA using a cDNA Reverse Transcription Kit (Takara, Dalian, China) according to the manufacturer's instructions. RT-qPCR was performed with SYBR Green mix (Takara) as previously described [13]. The primers used to amplify the mRNA are listed in Supplementary Table 1.

2.4. Microbiota Profiling. DNA was extracted from fecal samples using the QIAamp DNA Stool Mini Kit (Qiagen) as previously described [14]. Bacterial 16S rRNA gene sequences (V3–V4 region) were amplified, and then, PCR were performed in a total volume of 50 μL consisting of 12.5 μL of Phusion High-Fidelity PCR Master Mix (New England BioLabs Inc., Beverly, MA, United States), 1 μL of each primer, 50 ng of template DNA, and PCR-grade water. The purified 400–450 bp PCR products were used for MiSeq Illumina sequencing performed using the Illumina HiSeq 2500 platform (Illumina Inc., San Diego, CA, United States). Followingly, the obtained paired-end reads were merged and then assigned to each sample according to their unique barcodes. High-quality clean tags were clustered into operational taxonomic units (OTUs) using USEARCH according to the QIIME quality-controlled process based on 97% sequence similarity. Further analysis was performed with representative OTUs using the Greengenes database with the RDP algorithm.

2.5. Determination of SCFA Concentrations. Fresh fecal pellets were mixed with deionized ice-cold water intermittently on a vortex mixer for 2 min. After maintained on ice for 20 min, the samples were centrifuged at 4800 g for 20 min at 4°C . The supernatant was collected and analyzed by injection onto the chromatographic system as previously described [15].

2.6. Western Blotting Analysis. Total proteins extracted from brain samples were used for western blotting determination as previously described [16]. Briefly, 20 μg protein per lane was separated by SDS-PAGE and then blotted onto PVDF membranes. After blocked with skim milk, the membrane was incubated with primary antibodies against AMPK, phosphorylated AMPK, NF κB p65, and phosphorylated NF κB p65 (Cell Signaling, Danvers, MA, USA) overnight at 4°C . Then, after incubating with the secondary antibody at $22 \pm 2^{\circ}\text{C}$ for 1 h, the membrane was detected using the EZ-ECL (Biological Industries, Cromwell, CT, USA).

2.7. Statistical Analysis. Statistical analysis was performed using the *t*-test or one-way ANOVA with the data statistics software SPSS 18.0. $P < 0.05$ was considered statistically

TABLE 1: Effects of serine deficiency on levels of AGEs and MDA in D-galactose-treated mice.

Index	Control	SGD	D-gal	D-SGD
AGEs (pg/mL)	304 ± 25 ^a	350 ± 30 ^a	562 ± 37 ^b	693 ± 32 ^c
MDA in serum (nmol/mL)	2.05 ± 0.17 ^a	2.49 ± 0.26 ^a	3.79 ± 0.33 ^b	5.86 ± 0.57 ^c
MDA in brain (nmol/mg protein)	2.42 ± 0.28 ^a	3.05 ± 0.41 ^a	5.44 ± 0.53 ^b	7.13 ± 0.49 ^c

^{a,b,c}Mean values within a row with unlike superscript letters were significantly different ($P < 0.05$). $n = 8$.

TABLE 2: Effects of serine deficiency on levels of serum inflammatory cytokines in D-galactose-treated mice.

Index	Control	SGD	D-gal	D-SGD
TNF- α (pg/mL)	114.2 ± 7.9 ^a	120.3 ± 6.8 ^a	143.5 ± 11.2 ^b	177.8 ± 14.4 ^c
IL-1 β (pg/mL)	57.3 ± 3.6 ^a	60.7 ± 4.1 ^a	87.8 ± 3.1 ^b	112.4 ± 6.3 ^c
IL-6 (pg/mL)	145.3 ± 12.3 ^a	158.9 ± 13.6 ^a	209.4 ± 19.4 ^b	283.8 ± 20.1 ^c

^{a,b,c}Mean values within a row with unlike superscript letters were significantly different ($P < 0.05$). $n = 8$.

TABLE 3: Effects of serine deficiency on activities of antioxidant enzymes and GSH concentration in the serum of D-galactose-induced aging mice.

Index	Control	SGD	D-gal	D-SGD
SOD (U/mL)	34.1 ± 2.3 ^a	32.5 ± 2.1 ^a	24.9 ± 1.5 ^b	18.4 ± 1.3 ^c
CAT (U/L)	23.1 ± 2.3 ^a	19.8 ± 2.5 ^a	14.3 ± 2.0 ^b	7.5 ± 1.7 ^c
GSH-Px (U/mL)	31.0 ± 3.7 ^a	26.1 ± 2.3 ^a	19.3 ± 1.6 ^b	7.9 ± 1.9 ^c
GSH (nmol/mL)	615.3 ± 36.3 ^a	552.2 ± 29.4 ^a	421.4 ± 25.0 ^b	228.2 ± 27.6 ^c

^{a,b,c}Mean values within a row with unlike superscript letters were significantly different ($P < 0.05$). $n = 8$.

significant. All the measurement data are expressed as the means ± standard error (SEM).

3. Results

3.1. Serine and Glycine Deficiency Exacerbated the Accumulation of AGEs and MDA in D-Galactose-Treated Mice. As shown in Table 1, no significant difference was observed in AGE content in serum and MDA content in both serum and brain between the mice in the Control group and the SGD group. However, AGE content in serum and MDA content in both serum and brain were significantly higher in the D-gal group than those in the Control group. Moreover, the mice in the D-SGD group had the highest contents of AGEs and MDA, which were significantly higher than the mice in the other three groups.

3.2. Serine and Glycine Deficiency Exacerbated Inflammation and Oxidative Stress in D-Galactose-Treated Mice. As shown in Table 2, no significant difference in TNF- α , IL-1 β , and IL-6 contents in serum was observed between the mice in the Control group and the SGD group. However, the contents of these inflammatory cytokines were significantly higher in the D-gal group than those in the Control group. Moreover, the mice in the D-SGD group had significantly higher concentration of these inflammatory cytokines than those in the other three groups.

As shown in Table 3, no significant difference was observed in serum activities of SOD, CAT, GSH-Px, and GSH content between the mice in the Control group and

the SGD group. However, activities of these antioxidant enzymes and GSH content were significantly lower in the D-gal group than those in the Control group. Moreover, the mice in the D-SGD group had significantly lower activities of antioxidant enzymes and lower GSH content than those in the other three groups.

As shown in Figure 1, serine and glycine deficiency did not affect the mRNA expression of *TNF- α* , *IL-1 β* , *IL-6*, *Cat*, *Sod1*, *Sod2*, and *Gpx1* in the brain of mice without D-galactose treatment. However, under D-galactose treatment, the mRNA expression of *TNF- α* , *IL-1 β* , and *IL-6* was significantly increased, while the mRNA expression of *Cat*, *Sod1*, *Sod2*, and *Gpx1* was significantly decreased in mice fed SGD diet when compared with the mice fed the basal diet.

3.3. Serine and Glycine Deficiency Exacerbated Structure Change of Microbiota and Decreased SCFA Levels in D-Galactose-Treated Mice. As shown in Table 4, among the bacterial α -diversity, there was no significant difference between the groups regarding Simpson index. However, the Shannon H and observed species indexes decreased significantly in the D-gal and SGD groups when compared with the Control group. These two α -diversity indexes were further decreased in the D-SGD group when compared with either the D-gal group or the SGD group.

Furthermore, we compared distinct community profiles at different taxonomic levels among the groups. At the phylum level, the results showed that the ratio of *Firmicutes/Bacteroidetes* was not significantly affected by serine and glycine deficiency (Figure 2(a)). However, under D-

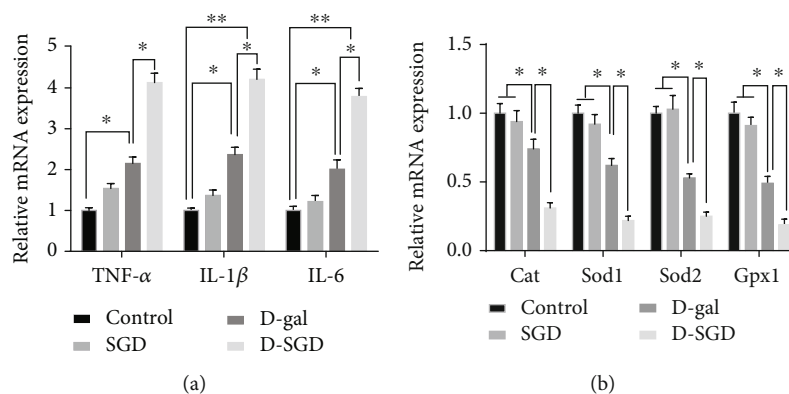


FIGURE 1: Effects of serine deficiency on the mRNA expression of genes encoding inflammatory cytokines and antioxidant enzymes in D-galactose-treated mice. (a) Relative mRNA expression of *TNF-α*, *IL-1β*, and *IL-6* in the brain; (b) relative mRNA expression of *Cat*, *Sod1*, *Sod2*, and *Gpx1* in the brain. Data were expressed as mean \pm SEM, $n = 8$. * $P < 0.05$, ** $P < 0.01$.

TABLE 4: Effects of serine deficiency on α -diversity indexes of microbiota in D-galactose-induced aging mice.

Index	Control	SGD	D-gal	D-SGD
Shannon H	6.72 \pm 0.52 ^a	5.13 \pm 0.39 ^b	4.62 \pm 0.57 ^b	3.09 \pm 0.30 ^c
Simpson	0.84 \pm 0.11	0.75 \pm 0.09	0.71 \pm 0.10	0.66 \pm 0.18
Observed species	317.3 \pm 25.8 ^a	269.9 \pm 27.4 ^b	248.1 \pm 19.3 ^b	201.7 \pm 22.3 ^c

^{a,b,c}Mean values within a row with unlike superscript letters were significantly different ($P < 0.05$). $n = 8$.

galactose treatment, the ratio of *Firmicutes/Bacteroidetes* was significantly decreased in mice fed SGD diet when compared with the mice fed the basal diet. At the genus level, D-galactose injection significantly decreased the proportion of *Clostridium XIVa* (Figure 2(b)). Moreover, serine and glycine deficiency exacerbated the decrease of the proportion of *Clostridium XIVa* resulted from D-galactose injection.

Then, we determined the levels of SCFA in fresh feces. As shown in Figure 2(c), among the treatment groups, there were no significant difference regarding the levels of acetic acid and propionic acid. However, although serine and glycine deficiency or D-galactose injection alone did not change the level of butyric acid, SGD diet in combination of D-galactose injection significantly decreased the level of butyric acid. Additionally, mRNA expression of SCFA transporters and receptor in the brain was determined. The results showed that mRNA expression of *Slc16a3*, *Slc16a7*, and *Gpr109a* was significantly decreased in the D-SGD groups when compared with the other three treatment groups (Figure 2(d)).

3.4. Serine and Glycine Deficiency Inhibited the AMPK-NFκB Signaling Pathway in D-Galactose-Treated Mice. As shown in Figure 3, no significant difference was observed in the protein expression of pAMPK and pNFκB p65 between the Control group and the SGD group. However, the protein expression of pAMPK was significantly decreased while pNFκB p65 were significantly increased in the D-gal group when compared with the Control group. Furthermore, the changes of

expression of these two phosphorylated proteins were much more significant in the D-SGD group when compared with those in the D-gal group.

4. Discussion

Chronic D-galactose exposure is a common model for exploring the mechanisms of age-related diseases. In this model, the formation of AGEs is considered as a trigger for the initiation of age-related diseases [17]. In the present study, we detected increased AGE content in the circulation of mice treated with D-galactose, suggesting that the aging model was successfully built and the mice were under the condition of high risks of developing age-related diseases. Accumulated AGEs are often associated with increased oxidative stress and inflammation as abnormal D-galactose metabolism results in the overproduction of reactive oxygen species (ROS) [18, 19]. ROS reacts with lipids to produce more stable products such as malondialdehyde (MDA), which further damage nucleic acids and proteins in the brain and lead to inflammatory aging [20]. In the present study, we found increased MDA content in both serum and brain, as well as increased serum contents of inflammatory cytokines and decreased activities of antioxidant enzymes in mice after chronic treatment with D-galactose. Moreover, genes encoding inflammatory cytokines were increased while genes encoding antioxidant enzymes were decreased in the brain. These results further confirmed the oxidative and inflammatory responses by D-galactose exposure, which were in line with previous results [17, 21]. Serine is a major substrate

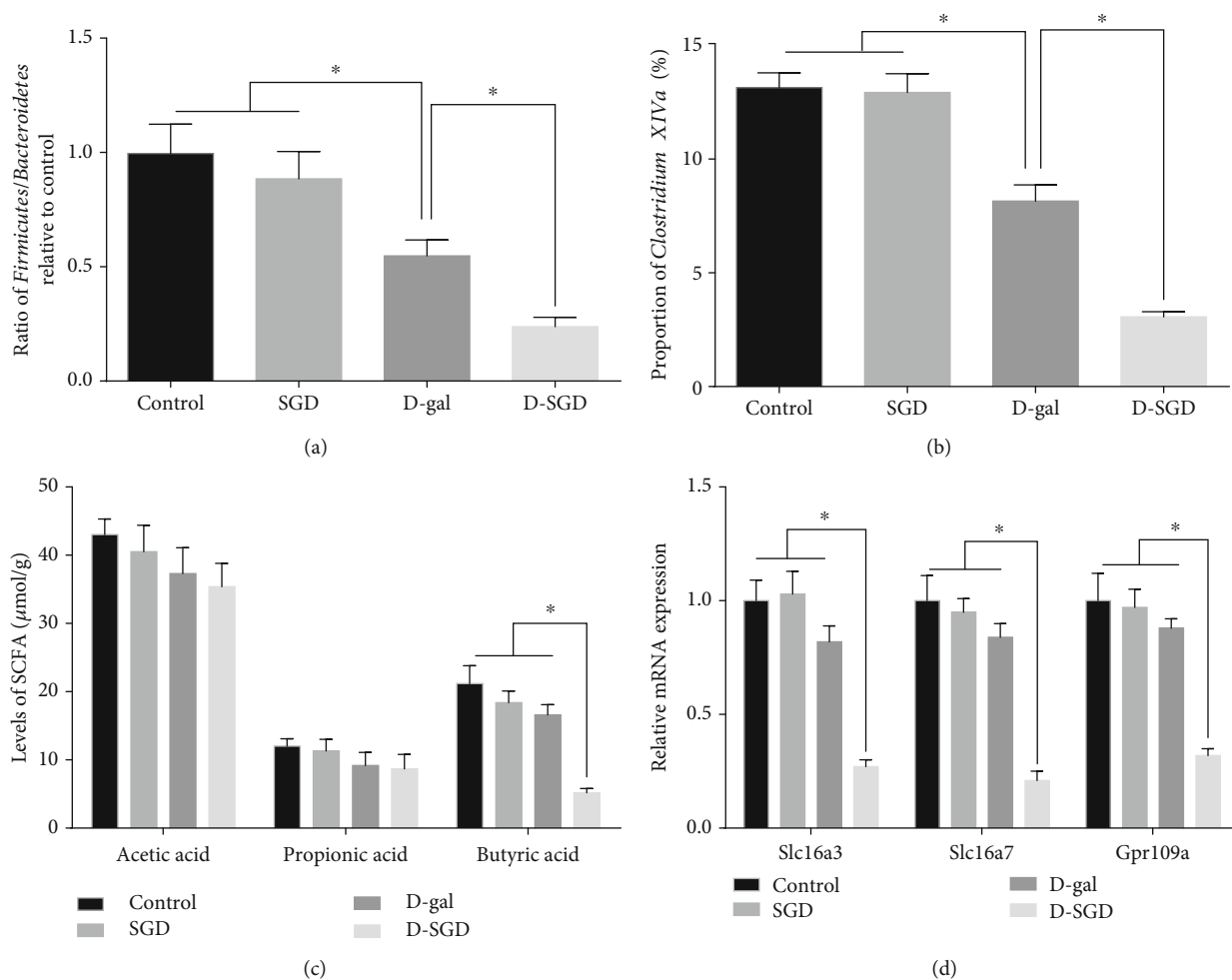


FIGURE 2: Serine deficiency exacerbated structure change of microbiota and decreased SCFA levels in D-galactose-treated mice. (a) Ratio of Firmicutes/Bacteroidetes in fecal microbiota; (b) proportion of Clostridium XIVa; (c) levels of short-chain fatty acids (SCFA) in feces; (d) relative mRNA expression of Slc16a3, Slc16a7, and Gpr109a in the brain. Data were expressed as mean ± SEM, n = 8. *P < 0.05.

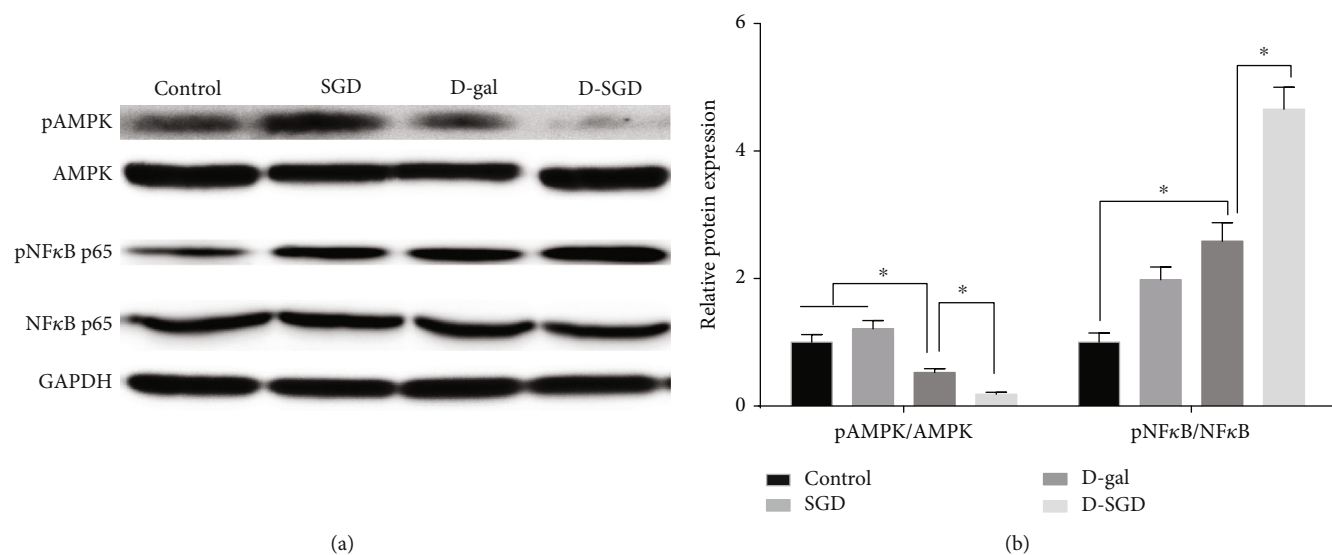


FIGURE 3: Effects of serine deficiency on AMPK and NFκB expression in D-galactose-treated mice. (a) Protein expression of AMPK, pAMPK, NFκB p65, and pNFκB p65; (b) Relative expression of pAMPK/AMPK and pNFκB p65 according to the results of (a). Data were expressed as mean ± SEM, n = 3. *P < 0.05.

for the synthesis of GSH and NADPH [22, 23], suggesting that its availability plays a key role in the support of the antioxidant systems. Serine deficiency was previously proved to exacerbate oxidative stress [12]. In accordance with this report, our results showed that serine deficiency also exacerbates oxidative and inflammatory responses in the brain of aging mice. Our results suggested that the availability of serine might be important for aging individuals although whether extra serine supplementation might be beneficial for the prevention of age-related diseases remains to be explored.

Generally, the major species of the microbiota was proved to remain unchanged in older individuals, except that there is a reduced microbiota diversity [3]. We found that Shannon H and observed species were significantly decreased in mice treated with D-galactose, suggesting a reduction of richness of gut microbiota [24]. Moreover, we observed a significant decrease of the *Firmicutes* to *Bacteroidetes* ratio, which is considered as the most remarkable changes in older individuals [25]. Surprisingly, the α -diversity of microbiota and the *Firmicutes* to *Bacteroidetes* ratio were further decreased when the mice were fed a serine- and glycine-deficient diet. These results indicated that serine deficiency affected the microbiota composition in older individuals.

Recently, increasing evidences suggested that the microbiota could regulate brain function through the microbiota-gut-brain axis which enables microbes to communicate with the brain [26]. We found a decrease of the proportion of *Clostridium XIVA* at the genus level in mice treated with D-galactose, and its proportion was further decreased when the mice were fed a serine- and glycine-deficient diet. *Clostridium XIVA* is one of the producers of butyric acids [27]. In accordance with this, we determined the content of SCFAs in the feces and found a decrease of butyric acid in these mice. SCFAs were a bunch of microbial metabolites which could mediate the communication between microbes and the brain [28]. They can reach the brain since they are able to cross the blood-brain barrier according to the results of a cell culture model [29]. In association with the decreased content of butyric acid in the feces, we also found that the expression of its transporters and receptor was decreased in mice treated with D-galactose and a serine- and glycine-deficient diet. These results suggested that serine deficiency may reduce the communications between the gut microbiota and the brain through decreasing the production of butyric acid. SCFAs could enter the mitochondrial citric acid cycle and then generate energy [30]. Since AMPK is the key energy sensor, the AMPK-NF κ B signaling pathway was supposed to mediate the effects of SCFAs, as SCFA could activate AMPK and inhibit NF κ B activation [31]. Our results showed that D-galactose exposure inhibited AMPK phosphorylation while increased NF- κ B phosphorylation in the brain. Moreover, these changes were much more significant in mice treated with both D-galactose and a serine- and glycine-deficient diet. These results suggested that the AMPK-NF κ B signaling pathway also play a role in modulating oxidative and inflammatory responses which was exacerbated by serine deficiency.

In conclusion, our results showed that serine deficiency exacerbated oxidative and inflammatory status in an aging mouse model induced by chronic D-galactose treatment. Furthermore, our results suggested that the interactions between the microbiota and the brain through microbiota-gut-brain axis might mediate the abovementioned changes. To be specific, serine deficiency decreased the gut butyrate producer *Clostridium XIVA* and resulted in decreased production of butyric acid. Subsequently, the decreased butyric acid affected the phosphorylation of AMPK which promotes NF κ B activation and the accumulation of its downstream targets.

Data Availability

The data used to support the findings of this study are included with the article.

Conflicts of Interest

The authors declared that there are no conflicts of interest.

Acknowledgments

This work was supported by the “Huxiang Young Talents Plan” Project of Hunan Province (2019RS2046) and the Youth Innovation Promotion Association CAS. We would like to thank Dalian Chengsan Husbandry Co., Ltd. for their help with the determination of SCFA concentrations.

Supplementary Materials

Supplementary Table 1: sequences of primers used for RT-qPCR in the experiments. Supplementary Table 2: components of the control diet and serine- and glycine-deficient (SGD) diet used in the experiments. These two diets were purchased from Research Diets (New Brunswick, NJ, USA). (*Supplementary Materials*)

References

- [1] H. F. Poon, V. Calabrese, G. Scapagnini, and D. A. Butterfield, “Free radicals: key to brain aging and heme oxygenase as a cellular response to oxidative stress,” *The Journals of Gerontology. Series A, Biological Sciences and Medical Sciences*, vol. 59, no. 5, pp. M478–M493, 2004.
- [2] M. S. Spychala, V. R. Venna, M. Jandzinski et al., “Age-related changes in the gut microbiota influence systemic inflammation and stroke outcome,” *Annals of Neurology*, vol. 84, no. 1, pp. 23–36, 2018.
- [3] T. G. Dinan and J. F. Cryan, “Gut instincts: microbiota as a key regulator of brain development, ageing and neurodegeneration,” *The Journal of Physiology*, vol. 595, no. 2, pp. 489–503, 2017.
- [4] C. Garcia-Pena, T. Alvarez-Cisneros, R. Quiroz-Baez, and R. P. Friedland, “Microbiota and aging. A review and commentary,” *Archives of Medical Research*, vol. 48, no. 8, pp. 681–689, 2017.
- [5] P. Castrogiovanni, G. Li Volti, C. Sanfilippo et al., “Fasting and fast food diet play an opposite role in mice brain aging,” *Molecular Neurobiology*, vol. 55, no. 8, pp. 6881–6893, 2018.

- [6] Q. Jiang, C. Lu, T. Sun et al., "Alterations of the brain proteome and gut microbiota in d-galactose-induced brain-aging mice with krill oil supplementation," *Journal of Agricultural and Food Chemistry*, vol. 67, no. 35, pp. 9820–9830, 2019.
- [7] L. He, J. Long, X. Zhou, Y. Liu, T. Li, and X. Wu, "Serine is required for the maintenance of redox balance and proliferation in the intestine under oxidative stress," *The FASEB Journal*, 2020.
- [8] X. Zhou, L. He, C. Wu, Y. Zhang, X. Wu, and Y. Yin, "Serine alleviates oxidative stress via supporting glutathione synthesis and methionine cycle in mice," *Molecular Nutrition & Food Research*, vol. 61, no. 11, p. 1700262, 2017.
- [9] X. Zhou, L. He, S. Zuo et al., "Serine prevented high-fat diet-induced oxidative stress by activating AMPK and epigenetically modulating the expression of glutathione synthesis-related genes," *Biochimica et Biophysica Acta - Molecular Basis of Disease*, vol. 1864, no. 2, pp. 488–498, 2018.
- [10] X. Zhou, Y. Zhang, L. He et al., "Serine prevents LPS-induced intestinal inflammation and barrier damage via p53-dependent glutathione synthesis and AMPK activation," *Journal of Functional Foods*, vol. 39, pp. 225–232, 2017.
- [11] H. Zhang, R. Hua, B. Zhang, X. Zhang, H. Yang, and X. Zhou, "Serine alleviates dextran sulfate sodium-induced colitis and regulates the gut microbiota in mice," *Frontiers in Microbiology*, vol. 9, p. 3062, 2018.
- [12] L. He, H. Zhang, and X. Zhou, "Weanling offspring of dams maintained on serine-deficient diet are vulnerable to oxidative stress," *Oxidative Medicine and Cellular Longevity*, vol. 2018, Article ID 8026496, 10 pages, 2018.
- [13] G. Guan, S. Ding, Y. Yin, V. Duraipandiyani, N. A. Al-Dhabi, and G. Liu, "Macleaya cordata extract alleviated oxidative stress and altered innate immune response in mice challenged with enterotoxigenic *Escherichia coli*," *Science China Life Sciences*, vol. 62, no. 8, pp. 1019–1027, 2019.
- [14] K. Wang, X. Jin, M. You et al., "Dietary propolis ameliorates dextran sulfate sodium-induced colitis and modulates the gut microbiota in rats fed a Western diet," *Nutrients*, vol. 9, no. 8, p. 875, 2017.
- [15] J. Y. Sha, Y. D. Zhou, J. Y. Yang et al., "Maltol (3-hydroxy-2-methyl-4-pyrone) slows d-galactose-induced brain aging process by damping the Nrf2/HO-1-mediated oxidative stress in mice," *Journal of Agricultural and Food Chemistry*, vol. 67, no. 37, pp. 10342–10351, 2019.
- [16] G. Liu, S. Chen, G. Guan et al., "Chitosan modulates inflammatory responses in rats infected with enterotoxigenic *Escherichia coli*," *Mediators of Inflammation*, vol. 2016, Article ID 7432845, 6 pages, 2016.
- [17] X. Zhang, C. Jin, Y. Li, S. Guan, F. Han, and S. Zhang, "Catalpol improves cholinergic function and reduces inflammatory cytokines in the senescent mice induced by D-galactose," *Food and Chemical Toxicology*, vol. 58, pp. 50–55, 2013.
- [18] E. S. Cannizzo, C. C. Clement, R. Sahu, C. Follo, and L. Santambrogio, "Oxidative stress, inflamm-aging and immunosenescence," *Journal of Proteomics*, vol. 74, no. 11, pp. 2313–2323, 2011.
- [19] R. D. Semba, E. J. Nicklett, and L. Ferrucci, "Does accumulation of advanced glycation end products contribute to the aging phenotype?," *The Journals of Gerontology Series A: Biological Sciences and Medical Sciences*, vol. 65A, no. 9, pp. 963–975, 2010.
- [20] S. Gawel, M. Wardas, E. Niedworok, and P. Wardas, "Malondialdehyde (MDA) as a lipid peroxidation marker," *Wiadomości Lekarskie*, vol. 57, no. 9–10, pp. 453–455, 2004.
- [21] B. Li, S. E. Eviwie, J. Lu et al., "Lactobacillus helveticus KLDS1.8701 alleviates d-galactose-induced aging by regulating Nrf-2 and gut microbiota in mice," *Food & Function*, vol. 9, no. 12, pp. 6586–6598, 2018.
- [22] O. D. K. Maddocks, C. F. Labuschagne, P. D. Adams, and K. H. Vousden, "Serine metabolism supports the methionine cycle and DNA/RNA methylation through de novo ATP synthesis in cancer cells," *Molecular Cell*, vol. 61, no. 2, pp. 210–221, 2016.
- [23] X. Zhou, H. Zhang, L. He, X. Wu, and Y. Yin, "Long-term l-serine administration reduces food intake and improves oxidative stress and Sirt1/NFκB signaling in the hypothalamus of aging mice," *Frontiers in Endocrinology*, vol. 9, 2018.
- [24] G. Guan, H. Wang, S. Chen et al., "Dietary chitosan supplementation increases microbial diversity and attenuates the severity of *Citrobacter rodentium* infection in mice," *Mediators of Inflammation*, vol. 2016, Article ID 9236196, 7 pages, 2016.
- [25] S. Saraswati and R. Sitaraman, "Aging and the human gut microbiota—from correlation to causality," *Frontiers in Microbiology*, vol. 5, p. 764, 2014.
- [26] J. A. Foster, M. Lyte, E. Meyer, and J. F. Cryan, "Gut Microbiota and Brain Function: An Evolving Field in Neuroscience: Table 1," *International Journal of Neuropsychopharmacology*, vol. 19, no. 5, pp. pyv114–pyv117, 2016.
- [27] M. Vital, A. Karch, and D. H. Pieper, "Colonic butyrate-producing communities in humans: an overview using omics data," *mSystems*, vol. 2, no. 6, 2017.
- [28] B. Dalile, L. Van Oudenhove, B. Vervliet, and K. Verbeke, "The role of short-chain fatty acids in microbiota-gut-brain communication," *Nature Reviews Gastroenterology & Hepatology*, vol. 16, no. 8, pp. 461–478, 2019.
- [29] R. W. Mitchell, N. H. On, M. R. del Bigio, D. W. Miller, and G. M. Hatch, "Fatty acid transport protein expression in human brain and potential role in fatty acid transport across human brain microvessel endothelial cells," *Journal of Neurochemistry*, vol. 117, no. 4, pp. 735–746, 2011.
- [30] P. Schonfeld and L. Wojtczak, "Short- and medium-chain fatty acids in energy metabolism: the cellular perspective," *Journal of Lipid Research*, vol. 57, no. 6, pp. 943–954, 2016.
- [31] A. Clark and N. Mach, "The crosstalk between the gut microbiota and mitochondria during exercise," *Frontiers in Physiology*, vol. 8, p. 319, 2017.

Research Article

Effects of Shikonin on the Functions of Myeloid Dendritic Cells in a Mouse Model of Severe Aplastic Anemia

Mengying Zheng , Bingnan Liu , Yuanyuan Shao , Luogang Hua , Rong Fu ,
Huaquan Wang , Ting Wang , Weiwei Qi, Zonghong Shao , and Chunyan Liu 

The Department of Hematology, General Hospital of Tianjin Medical University, Tianjin, China

Correspondence should be addressed to Chunyan Liu; liuchunyan_1981@tmu.edu.cn

Received 30 December 2019; Accepted 6 February 2020; Published 20 February 2020

Guest Editor: Hongmei Jiang

Copyright © 2020 Mengying Zheng et al. This is an open access article distributed under the Creative Commons Attribution License, which permits unrestricted use, distribution, and reproduction in any medium, provided the original work is properly cited.

This study is aimed at investigating the effects of shikonin, a pyruvate kinase M2 (PKM2) inhibitor, on the functions of myeloid dendritic cells (mDCs) in a mouse model of severe aplastic anemia (AA) generated by total body irradiation and lymphocyte infusion. Flow cytometry and qPCR were used to determine the proportions of PKM2+ mDCs and other immune indicators in the AA mice. Glucose consumption level, pyruvate generation level, and ATP content were used to determine the level of glycolytic metabolism in the mDCs. The survival rates of AA mice were evaluated after the administration of shikonin or the immunosuppressive agent cyclosporin A. The AA mice displayed pancytopenia, decreased CD4+/CD8+ cell ratio, increased perforin and granzyme levels in CD8+ cells, increased costimulatory CD80 and CD86 expressions, and inadequate regulatory T cell number. *In vivo* animal experiments showed that the shikonin-mediated inhibition of the PKM2 expression in mice was associated with high survival rates. In addition, the administration of cyclosporin A or shikonin decreased the expression of cytotoxic molecules and costimulatory CD80 and CD86 on CD8+ cells. Taken together, the results of this study indicated that shikonin could inhibit the activation and proliferation of mDCs as well as the activation of downstream cytotoxic T cells by reducing the PKM2 level in mDCs.

1. Introduction

Severe aplastic anemia (SAA) is a class of highly heterogeneous hematological diseases with complex etiology and pathogenesis [1]. Its clinical symptoms are often characterized by fatal anemia, bleeding, and infection. Immunosuppressive therapy with antithymocyte globulin and cyclosporin A (CsA) is considered a standard treatment approach for SAA patients and is known to improve prognosis. SAA patients exhibit abnormally high levels of activated myeloid dendritic cells (mDCs) that secrete inflammatory factors involved in the generation and activation of T cells. This overactivation of mDCs and T lymphocytes leads to the failure of bone marrow hematopoietic function [2, 3].

Shikonin is an active ingredient in the commonly used Chinese medicinal herb *Lithospermum erythrorhizon* and has been receiving increased attention as a new pyruvate kinase M2 (PKM2) inhibitor [4–6]. Because of its highly

selective inhibitory effect on PKM2 instead of PKM1 and pyruvate kinase-L, shikonin is considered the most potent and specific inhibitor of PKM2 identified to date [7]. Recently, the anticancer role of shikonin has also attracted widespread research attention. Studies have shown that shikonin exerts anticancer effects by inhibiting the proliferation of different cancer cells and inducing their apoptosis and autophagy. Shikonin has also been shown to inhibit liver cancer by causing mitochondrial dysfunction and increasing the oxidative stress level in tumor cells [8]. Apart from its antitumor activity, shikonin has been shown to have therapeutic effects against HIV infection, psoriasis, and other autoimmune diseases, but their underlying mechanisms are still unclear. Our previous research revealed that the PKM2 protein levels were elevated in the mDCs of SAA patients and that mDC activation is associated with increased intracellular PKM2 level. PKM2 regulates the immune status of SAA patients by enhancing the functions of mDCs and

downstream cytotoxic T lymphocytes (CTLs) to prevent the aggravation of immune imbalance [9]. Hence, in this study, we focused on investigating the effect of shikonin on the immune status of SAA.

This study used an aplastic anemia (AA) mouse model obtained by inducing an autoimmune attack with total body irradiation (TBI) plus lymphocyte infusion. The AA mice were then treated with shikonin or CsA, and the results showed that shikonin affected the function of mDCs and CTLs *in vivo*. In addition, the high survival rates and blood counts in the AA mice were found to be associated with the shikonin-mediated downregulation of PKM2 levels.

2. Materials and Methods

2.1. Study Subjects

2.1.1. Animals. The AA mouse models were obtained from Beijing Weitong Lihua Experimental Animal Technology Co. Ltd. To generate these AA mice, the first filial generation of inbred C57BL/6 mice and Balb/c mice was used as recipient mice (CB6F1, strain code: 303, 8 weeks old, SPF). These mice were major histocompatibility complex- (MHC-) heterozygous hybrids carrying H2^{b/d} with a high complement level. Allogeneic donor lymphocytes were obtained from C57BL/6 mice (H2^{b/b}). Homologous wild-type C57BL/6 mice (strain code: 213, 8 weeks old, SPF) were used as the control mice. After the infusion of donor lymphocytes with MHC mismatch, T lymphocyte immune-mediated bone marrow destruction occurred in the CB6F1 mice, with pathogenesis mimicking that of human AA.

The obtained mice were bred and maintained at the Animal Center, Institute of Radiation Medicine, Chinese Academy of Medical Sciences. All animal-related studies were approved by the Tianjin Medical University intramural animal care and use committee.

2.1.2. Induction of Bone Marrow Failure. Axillary and inguinal lymph nodes (LNs) were collected from C57BL/6 donors and then ground into homogenates, washed, centrifuged, and filtered. Their cell number was counted and adjusted to 10⁷/100 μ L.

The mice were divided into three groups: a normal control group (NC, $n = 10$), a TBI group ($n = 10$), and an AA model group ($n = 17$). The NC group contained CB6F1 mice. The TBI mice were given 4 Gy TBI using a cesium-137 gamma source. The AA model mice were also preirradiated with 4 Gy TBI using the same cesium-137 gamma source. After 4–6 h, diluted LN cells were injected through the retro-orbital sinus into the recipient AA group mice (CB6F1) at 10 \times 10⁶ cells/recipient in a 100 μ L lymphocyte separation solution (Solarbio, Beijing, China).

2.1.3. Administration of Immunosuppressive Agents to the AA Mice. We divided the CB6F1 mice into three groups: CsA, shikonin, and normal saline (NS) groups. After infusion with donor lymphocytes for 1 h, the three groups were administered CsA (50 μ g/g/d, $n = 10$), shikonin (Sigma-Aldrich, USA) (100 μ g/g/d, $n = 10$), or normal saline (NS, $n = 10$), respectively, through the peritoneal cavity for 10 days. All

mice were fed a healthy diet and then bled on the 17th day (see the specific operational steps in Table S1).

2.2. Blood Counts and Immune Index

2.2.1. Blood Counts. Blood samples were collected from the retro-orbital sinuses of mice and anticoagulated with EDTA. Blood counts were determined using an automatic blood cell analyzer (MEK-722, Nihon Kohden).

2.2.2. Flow Cytometry. Peripheral blood samples obtained by the above-described method were incubated with red blood cell lysate solution (BD Biosciences, USA) for 20 min to lyse the red blood cells (RBCs). The lysates were stained with antibodies and analyzed using a flow cytometer (FACSCalibur, BD Biosciences, USA).

Monoclonal antibodies against murine CD3, CD4, CD8, CD11c, CD80, CD86, Foxp3, PKM2, CD25, MHC II, CD107a, and CD107b were obtained from BD Biosciences (San Diego, CA, USA).

2.2.3. Determination of Glucose Consumption, Pyruvate Generation, and ATP Content. After eyeball extraction, the peripheral blood samples of the mice were collected and anticoagulated with EDTA. The mDCs were sorted and counted using a mouse mDC immunomagnetic sorting kit (Miltenyi Biotec, Germany). The supernatant of the cell culture was used to measure the amount of glucose consumption using a Glucose Assay Kit (Nanjing Institute of Biological Engineering, Nanjing, China) according to the kit's instructions. The pyruvate and ATP concentrations in the cells were measured using a Pyruvate Assay Kit (Nanjing Institute of Biological Engineering, Nanjing, China) and an ATP Assay Kit (Beyotime Biotechnology, Shanghai, China), respectively, according to the kit instructions. The optical densities at 505 nm for glucose measurement and pyruvate generation, and at 636 nm for ATP content, were read using an ELISA reader (BioTek Instruments, Inc., USA).

2.2.4. Quantitative RT-PCR (qRT-PCR). The CD8+ T cells from the mice were sorted by immunomagnetic separation. Total RNA was extracted and subjected to reverse transcription.

qRT-PCR was performed in an iQ5 PCR system (Bio-Rad, Hercules, CA, USA) under the following thermal cycling conditions: initial denaturation at 95°C for 2 min, followed by 40 cycles of amplification (95°C for 10 s, indicated annealing temperature for 35 s, 72°C for 30 s, and 65°C for 10 s). The primer sequences were as follows: Perforin, F: 5'-CAGGTCACATAGGCATGCACG-3' and R: 5'-GAACAGCAGGACGTTAATGGAG-3'; Granzyme B, F: 5'-GAAACGCTACTAATACTACAGG-3' and R: 5'-CCACTGAGCTAAGAGGT-3'; and β -actin, F: 5'-TTGCCGACACGATGCAGAA-3' and R: 5'-GCCGATCCACACCGTGTACT-3'. The relative expression levels of genes of interest were calculated.

2.2.5. Survival Rates. The survival rates of the mice from the NC ($n = 10$), TBI ($n = 10$), AA model ($n = 5$), shikonin ($n = 5$), CsA ($n = 5$), and NS ($n = 5$) groups for 90 days or

until death were calculated and compared. Blood counts were determined at days 17, 30, and 90 after the induction of AA.

2.2.6. Statistical Analysis. Data are presented as mean \pm standard deviation. Statistical analyses were performed using the chi-square test, followed by the nonparametric unpaired *t*-test. *p* values < 0.05 were considered to indicate significance. One-way analysis of variance was performed for the comparison of three independent groups.

3. Results

3.1. Blood Counts Detected in NC, TBI, and AA Model Groups. The counts of white blood cells (WBCs), RBCs, hemoglobin (Hb), and platelets (PLTs) in the peripheral blood samples of the CB6F1 mice were $7.89 \pm 1.21 \times 10^9/L$, $10.24 \pm 0.93 \times 10^{12}/L$, 166.9 ± 8.14 g/L, and $720.3 \pm 80.39 \times 10^9/L$, respectively, in the NC group; $2.71 \pm 0.63 \times 10^9/L$, $9.74 \pm 0.28 \times 10^{12}/L$, 145 ± 10.79 g/L, and $648.4 \pm 144.2 \times 10^9/L$, respectively, in the TBI group; and $1.18 \pm 0.84 \times 10^9/L$, $4.47 \pm 1.13 \times 10^{12}/L$, 89.58 ± 16.17 g/L, and $156.1 \pm 80.29 \times 10^9/L$, respectively, in the AA model group. The peripheral blood tests of the AA model group showed pancytopenia compared with those of the NC and TBI groups (Table 1, Figure 1) ($p < 0.0001$).

3.2. PKM2+ mDCs Increased in the AA Mice and Decreased after Shikonin Treatment. The proportion of PKM2+ mDCs (PKM2+CD11c+/CD11c+) was higher in the AA group ($33.76 \pm 10.21\%$) compared with those in the NC group ($20.54 \pm 6.22\%$) and the TBI group ($24.81 \pm 4.28\%$) ($p < 0.05$). The proportion was not significantly different between the NC and TBI groups ($p > 0.05$). After the treatments, the PKM2 levels in the mDCs decreased in the shikonin ($18.33\% \pm 2.81\%$, $n = 10$) and CsA ($22.25 \pm 2.21\%$, $n = 10$) groups compared with that in the NS group ($30.44 \pm 2.14\%$, $n = 10$) ($p < 0.05$). The levels were not significantly different between the shikonin and CsA groups ($p > 0.05$) (Figure 2).

3.3. The Expression of mDC Costimulatory Molecules CD80 and CD86 Increased in the AA Mice and That of CD86 Decreased after Shikonin Treatment. To verify whether PKM2 overexpression was responsible for the activation of mDCs, the expressions of costimulatory molecules CD86 and CD80 on the mDCs were evaluated. The percentages of mDCs in the peripheral blood samples of NC, TBI, AA, shikonin, CsA, and NS groups were $12.32 \pm 2.61\%$, $14.02 \pm 3.73\%$, $14.64 \pm 4.67\%$, $15.09 \pm 2.90\%$, $13.36 \pm 4.48\%$, and $14.92 \pm 3.53\%$, respectively, indicating that the differences between the six groups were not significant ($p > 0.05$, Figure S1).

The proportions of CD86+ mDCs in the NC, TBI, AA, shikonin, CsA, and NS groups were $8.68 \pm 1.96\%$, $13.87 \pm 5.39\%$, $20.27 \pm 8.41\%$, $13.21 \pm 4.35\%$, $14.06 \pm 4.96\%$, and $19.21 \pm 5.73\%$, respectively. Notably, the proportion was significantly higher in the AA group than those in the NC and TBI groups ($p < 0.05$). After the treatments, the CD86 expression in the shikonin and CsA groups decreased significantly compared with that in the AA group ($p < 0.05$, Figure 3(a)).

TABLE 1: Blood counts in the NC, TBI, and AA model groups.

	NC group ($n = 12$)	TBI group ($n = 10$)	AA group ($n = 10$)
WBC ($\times 10^9/L$)	$7.89 \pm 1.21^*$	$2.71 \pm 0.63^\#$	$1.18 \pm 0.84^{* \#}$
NEU ($\times 10^9/L$)	$0.52 \pm 0.11^*$	$0.38 \pm 0.15^\#$	$0.24 \pm 0.11^{* \#}$
LYM ($\times 10^9/L$)	$6.67 \pm 0.56^*$	$1.97 \pm 0.37^\#$	$0.79 \pm 0.25^{* \#}$
RBC ($\times 10^{12}/L$)	$10.24 \pm 0.93^*$	$9.74 \pm 0.28^\#$	$4.47 \pm 1.13^{* \#}$
HGB (g/L)	$166.9 \pm 8.14^*$	$145 \pm 10.79^\#$	$89.58 \pm 16.17^{* \#}$
PLT ($\times 10^9/L$)	$720.3 \pm 80.39^*$	$648.4 \pm 144.2^\#$	$156.1 \pm 80.29^{* \#}$

*The peripheral blood tests of the AA group showed pancytopenia compared with the NC group ($p < 0.0001$). [#]The peripheral blood tests of the AA group showed pancytopenia compared with the TBI group ($p < 0.0001$).

The percentages of CD80+ mDCs in the NC, TBI, AA, shikonin, CsA, and NS groups were $7.3 \pm 4.24\%$, $9.65 \pm 3.11\%$, $11.42 \pm 5.77\%$, $8.72 \pm 3.95\%$, $6.69 \pm 4.08\%$, and $10.28 \pm 3.13\%$, respectively. The percentage of CD80+ mDCs in the AA group was elevated compared with that in the NC group ($p < 0.05$). After the treatments, the CD80 expression in the CsA group decreased significantly compared with that in the AA group ($p < 0.05$). However, no statistically significant difference was observed in the CD80 expression between the shikonin and AA groups (Figure 3(b)).

3.4. The Glucose Consumption Level, Pyruvate Level, and ATP Content in mDCs Increased in the AA Mice and Decreased after Shikonin Treatment. We measured the glucose consumption level, pyruvate generation level, and ATP content to determine the level of glycolytic metabolism in the mDCs of each group. The glucose consumption levels of mDCs in the NC, TBI, AA, shikonin, CsA, and NS groups were 1.79 ± 0.67 , 2.38 ± 0.47 , 3.94 ± 1.19 , 1.83 ± 0.31 , 2.11 ± 0.55 , and 4.15 ± 0.81 , respectively. Notably, the level in the AA group was significantly higher than those in the TBI and NC groups ($p < 0.05$). After the treatments, the glucose consumption levels of mDCs in the shikonin and CsA groups reduced significantly compared with that in the AA group ($p < 0.05$, Figure 3(c)).

The pyruvate generation levels of mDCs in the NC, TBI, AA, shikonin, CsA, and NS groups were 1.80 ± 0.62 , 2.29 ± 0.69 , 3.97 ± 1.07 , 2.02 ± 0.66 , 2.43 ± 0.77 , and 3.68 ± 1.00 , respectively. Notably, the level in the AA group was significantly higher than those in the TBI and NC groups ($p < 0.05$). After the treatments, the pyruvate generation levels of mDCs in the shikonin and CsA groups reduced significantly compared with that in the AA group ($p < 0.05$, Figure 3(d)).

The ATP contents of mDCs in the NC, TBI, AA, shikonin, CsA, and NS groups were 1.99 ± 0.75 , 2.38 ± 0.68 , 3.25 ± 0.79 , 2.12 ± 0.53 , 1.68 ± 0.40 , and 3.08 ± 0.75 , respectively. Notably, the ATP content in the AA group was significantly higher than those in the TBI and NC groups ($p < 0.05$). After the treatments, the ATP contents of mDCs in the shikonin

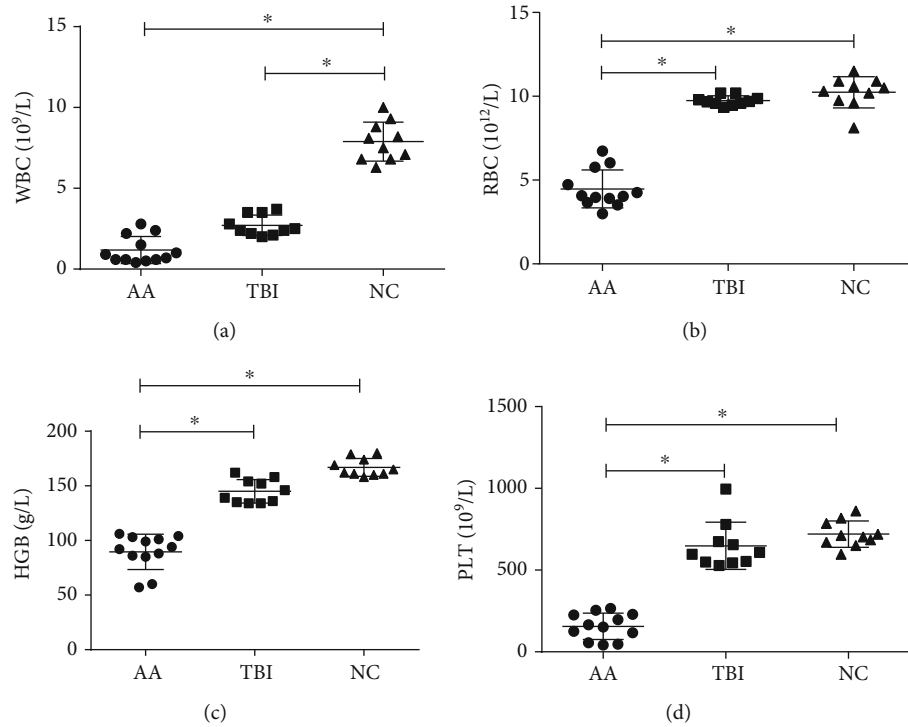


FIGURE 1: The peripheral blood tests of the AA group CB6F1 mice showed aleukocytosis (a), anemia (b, c), and thrombocytopenia (d) compared with the NC group and TBI group ($*p < 0.01$). AA: aplastic anemia ($n = 12$); TBI: total body irradiation ($n = 10$); NC: normal control ($n = 10$).

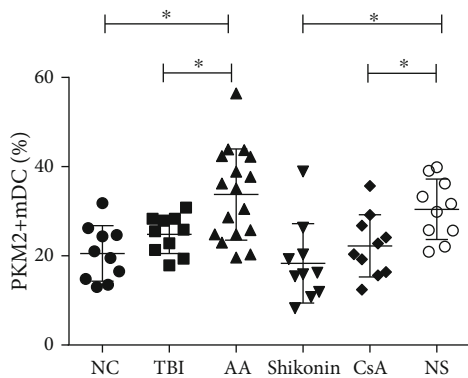


FIGURE 2: The PKM2+mDC proportion of mDCs (PKM2+CD11c+/CD11c+) in the AA group was higher than those of the NC and TBI groups ($n = 10$, $p < 0.05$). There was no significant difference between the NC and TBI groups ($n = 10$, $p > 0.05$). The PKM2 level is decreased in mDCs of the shikonin and CsA groups compared with the NS group ($n = 10$, $p < 0.05$). There was no significant difference between the shikonin and CsA groups ($p > 0.05$). AA: aplastic anemia ($n = 17$); TBI: total body irradiation ($n = 10$); NC: normal control ($n = 10$); shikonin ($n = 10$); CsA: cyclosporin A ($n = 10$); NS: normal saline ($n = 10$) ($*p < 0.05$).

and CsA groups decreased significantly compared with that in the AA group ($p < 0.05$, Figure 3(e)).

3.5. The mRNA Expression of Granzyme B in CD8+ Cells Increased in the AA Mice and Decreased after Shikonin

Treatment. The granzyme B mRNA expression in the CD8+ cells of the AA group (1.79 ± 0.61) was significantly higher than that in the CD8+ cells of the NC group (0.97 ± 0.48 , $p < 0.05$). Notably, the expressions in the shikonin (1.20 ± 0.57) and CsA (1.16 ± 0.37) groups was lower than those in the AA and NS groups (1.82 ± 0.70) ($p < 0.05$, Figure 4(a)). However, the perforin mRNA expression in the CD8+ cells showed no significant difference between the six groups ($p > 0.05$, Figure 4(b)).

We further investigated the degranulation levels of CTLs. The ratio of CD107a+CD8+/CD8+ cells (expressed as a percentage) was significantly higher in the AA group ($72.4 \pm 7.41\%$) compared with that in the NC group ($20.73 \pm 3.71\%$) ($p < 0.05$) but showed no significant difference between the NC and TBI groups ($p > 0.05$). After the treatments, the CD107a levels in the CD8+ cells decreased significantly in the shikonin ($45.08 \pm 5.96\%$) and CsA ($33.56 \pm 5.74\%$) groups compared with that in the NS group ($71.65 \pm 7.33\%$) ($p < 0.05$). Notably, the difference in the CD107a levels between the shikonin and CsA groups was not significantly different ($p > 0.05$). The ratios of CD107b+CD8+/CD8+ cells (expressed as a percentage) in the NC, TBI, AA, shikonin, CsA, and NS groups were $14.94 \pm 1.44\%$, $23.03 \pm 6.1\%$, $45.54 \pm 8.56\%$, $19.39 \pm 2.43\%$, $25.88 \pm 2.12\%$, and $41.54 \pm 3.99\%$, respectively. The ratio in the AA group was significantly higher than that in the NC group ($p < 0.05$). After the treatments, the ratio in the shikonin and CsA groups reduced significantly compared with that in the AA group ($p < 0.05$, Figure 4(c)).

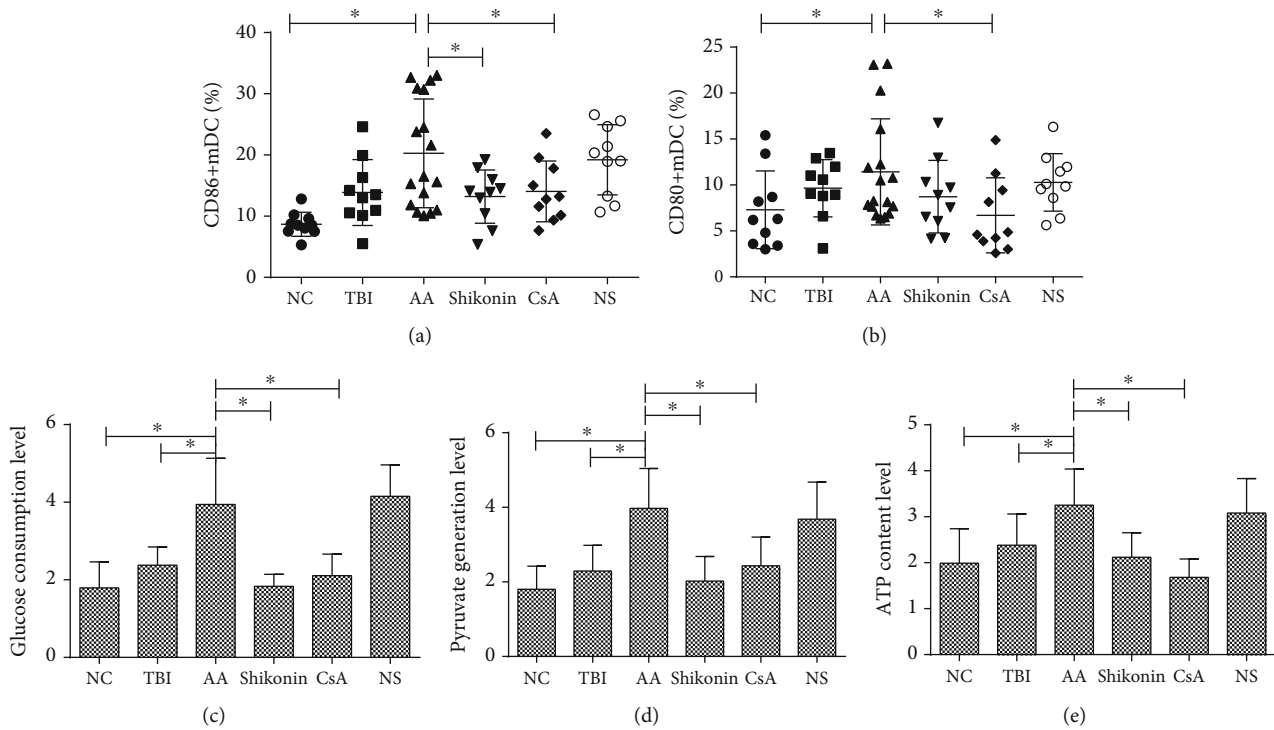


FIGURE 3: (a) The CD86+ mDCs in the AA group significantly increased compared with those of the NC and TBI groups ($p < 0.05$). After the treatments, the CD86 levels in the shikonin and CsA groups decreased significantly compared with that in the AA group ($p < 0.05$). (b) The CD80+ mDCs in the AA group significantly increased compared with those in the NC group ($p < 0.05$). The CD80 levels in the CsA group decreased compared with those in the AA group ($p < 0.05$). (c) The glucose consumption levels in mDCs of the AA group were significantly higher than those in the TBI and NC groups, while those in the shikonin and CsA groups were significantly lower than those in the AA group ($p < 0.05$). (d) The pyruvate levels in mDCs of the AA group were significantly higher than those in the TBI and NC groups, while those in the shikonin and CsA groups were significantly lower than those in the AA group ($p < 0.05$). (e) The ATP contents in mDCs in the AA group were significantly higher than those in the TBI and NC groups, while those in the shikonin and CsA groups were significantly lower than those in the AA group ($p < 0.05$). AA: aplastic anemia ($n = 17$); TBI: total body irradiation ($n = 10$); NC: normal control ($n = 10$); shikonin ($n = 10$); CsA: cyclosporin A ($n = 10$); NS: normal saline ($n = 10$) (* $p < 0.05$).

3.6. The Influence of PKM2 Inhibition on Other Immune Cells. We also explored the effects of PKM2 on other immune cells in addition to mDCs. The ratio of CD4+/CD8+ cells in the AA group (1.41 ± 0.78) was significantly lower than those in the TBI (2.21 ± 0.71 , $p < 0.05$), NC (2.46 ± 0.84 , $p < 0.05$), shikonin (2.09 ± 0.57 , $p < 0.05$), and CsA (2.42 ± 0.80 , $p < 0.05$) groups (Figure 5(a)).

The ratio of CD4+CD25+Foxp3+ cells (Treg) in the AA group (3.96 ± 1.94) was significantly lower than those in the TBI (5.36 ± 2.04 , $p < 0.05$), NC (6.94 ± 1.66 , $p < 0.05$), shikonin (5.57 ± 1.39 , $p < 0.05$), and CsA (5.64 ± 1.80 , $p < 0.05$) groups (Figure 5(b)).

3.7. The Effect of Shikonin on the Survival Rates of the AA Mice. Mice from the NC, TBI, AA model, shikonin, CsA, and NS groups were housed to evaluate their 90-day survival rates. The findings revealed that 90% (9/10) of the NC group, 100% (10/10) of the TBI group, 0% (0/5) of the AA model group, 60% (3/5) of the shikonin group, 60% (3/5) of the CsA group, and 20% (1/5) of the NS group survived to day 90. At day 46, 60% of the mice from the shikonin and CsA groups were alive, and all survived until they were euthanized at the end of the experiment, but only one mouse in the NS

group survived to day 46. Meanwhile, none of the mice in the AA model group survived till day 32. As shown in Figure 6, 90 days after the first administration of shikonin or CsA, the survival rates in the shikonin and CsA groups were higher than those in the AA model and NS groups ($p < 0.05$). The survival rates were not significantly different between the TBI and NC groups.

The blood counts of the mice from the TBI group reached close to normal levels by day 90. The TBI plus lymphocyte infusion led to unrecoverable reduction in the WBC counts. Until the time of death, the blood counts of the mice in the AA model and NS groups showed no improvement, whereas those of the mice in the shikonin and CsA groups, especially leukocyte counts, gradually recovered. Figure 7 shows the WBC, Hb, and PLT counts in mice from different groups.

4. Discussion

SAA is a hematological disease characterized by bone marrow hematopoietic failure. Although its etiology and pathogenesis are complex, recent data suggest that AA is an immune-mediated disease [1]. According to recent research, dysfunctional mDCs play a role in SAA pathogenesis [3].

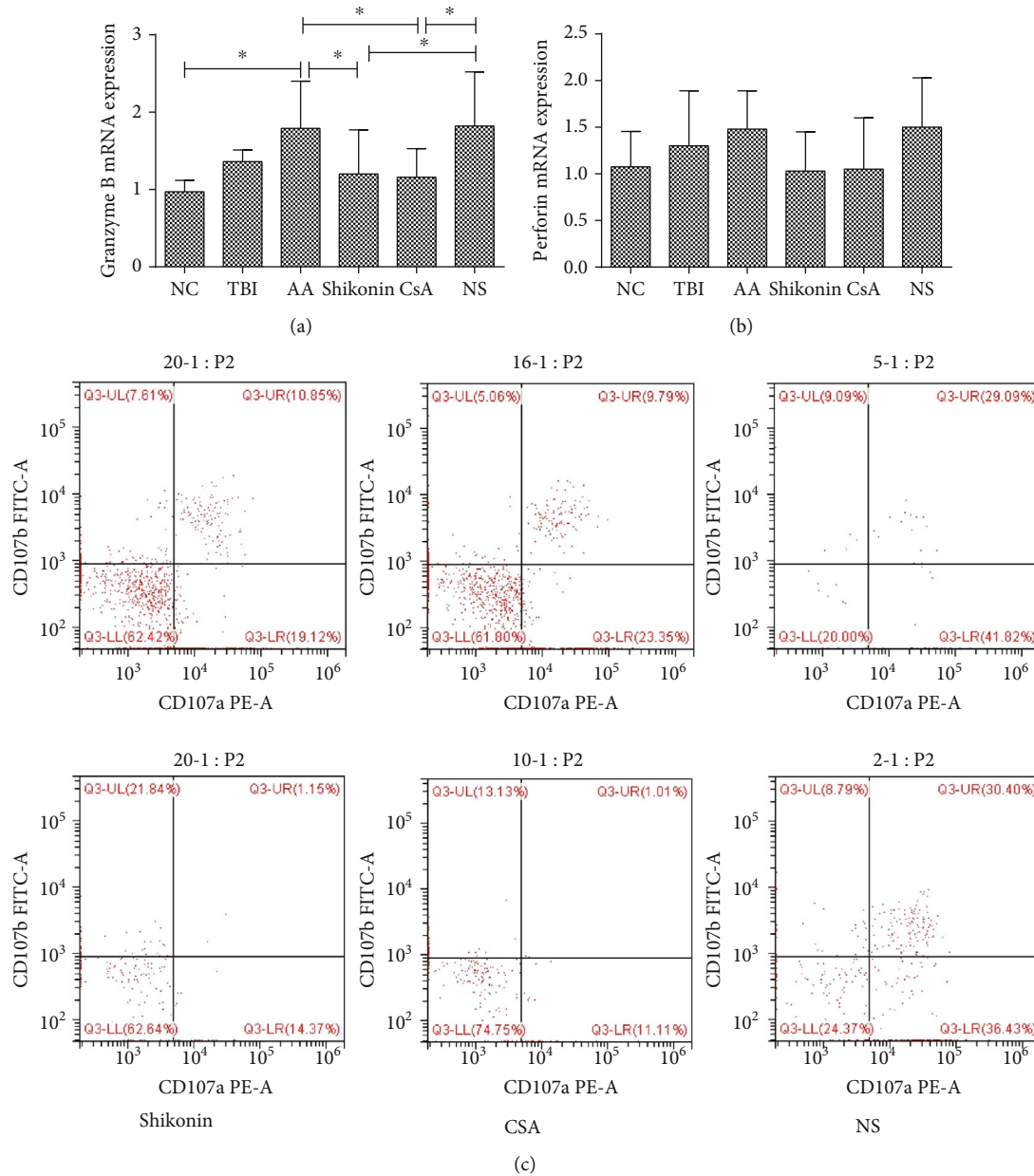


FIGURE 4: (a) The granzyme B mRNA expression of CD8⁺ cells in the AA group was significantly higher than that in the NC group, while those in the shikonin and CsA groups were significantly decreased compared with the AA and NS groups ($p < 0.05$). (b) The level of perforin mRNA expression in CD8⁺ cells did not show a statistically significant difference among the six groups ($p > 0.05$). (c) The ratio of CD107a⁺CD8⁺/CD8⁺ cells and CD107b⁺CD8⁺/CD8⁺ cells in the AA group was increased compared with that in the NC group, while those in the shikonin and CsA groups were significantly decreased compared with that in the NS group ($p < 0.05$). AA: aplastic anemia ($n = 17$); TBI: total body irradiation ($n = 10$); NC: normal control ($n = 10$); shikonin ($n = 10$); CsA: cyclosporin A ($n = 10$); NS: normal saline ($n = 10$).

However, the mechanisms of mDC activation and of the resulting induction of a series of autoimmune damage processes are still unclear.

Shikonin is a major active chemical component extracted from the traditional Chinese medicinal herb *L. erythrorhizon*. Studies have proven that shikonin is a highly specific PKM2 inhibitor and plays an important role in suppressing breast cancer, hepatocellular carcinoma, and other tumors. In

recent years, research on the roles of shikonin in human health has gradually deepened. Accumulating evidence suggests that shikonin can suppress tumor growth and overcome the resistance to chemotherapy drugs in tumor cells [10]. Tang et al. [11] suggested that shikonin can significantly inhibit the proliferation of esophageal cancer cells by regulating the HIF1 α /PKM2 signaling pathway. Shikonin can also suppress the inflammatory immune response by

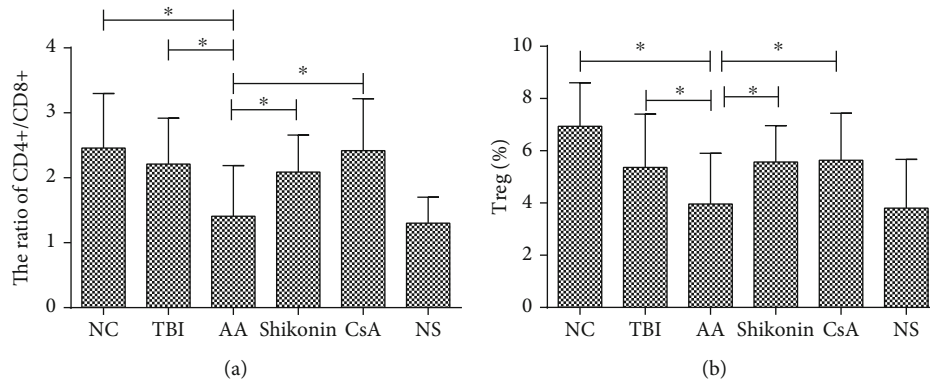


FIGURE 5: (a) The ratio of CD4+/CD8+ in the AA group was significantly lower than those in the TBI, NC, shikonin, and CsA groups ($p < 0.05$). (b) The frequency of Treg in the AA group was significantly lower than those in the TBI, NC, shikonin, and CsA groups ($p < 0.05$). AA: aplastic anemia ($n = 17$); TBI: total body irradiation ($n = 10$); NC: normal control ($n = 10$); shikonin ($n = 10$); CsA: cyclosporin A ($n = 10$); NS: normal saline ($n = 10$) (* $p < 0.05$).

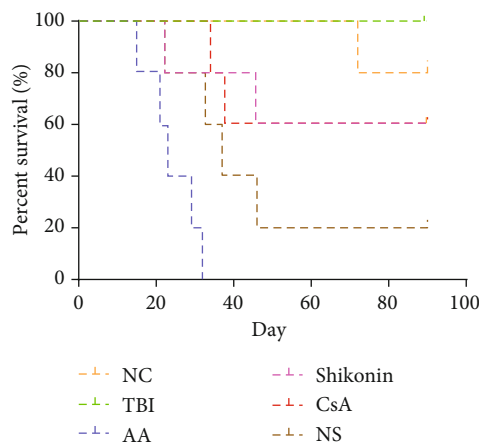


FIGURE 6: The survival rates of the mice from the NC ($n = 10$), TBI ($n = 10$), AA model ($n = 5$), shikonin ($n = 5$), CsA ($n = 5$), and NS ($n = 5$) groups were examined and compared for 90 days or until death. The mice from the Shikonin and CsA groups had a higher survival rate than the AA model and NS groups ($p < 0.05$). No significant difference was observed between the TBI and NC groups. AA: aplastic anemia; TBI: total body irradiation; NC: normal control; CsA: cyclosporin A; NS: normal saline.

blocking inflammatory signals, thereby delaying the progression of inflammatory diseases such as sepsis. Furthermore, it has been reported to inhibit T lymphocyte activation by inhibiting IKK β activity and JNK signaling and is thus expected to play a therapeutic role as a potential immunosuppressant in autoimmune diseases [12]. Given the extensive therapeutic effects of shikonin against immunological diseases, inflammation, and tumors, in this study, we attempted to investigate the therapeutic role of shikonin against SAA pathogenesis.

DCs are the only antigen-presenting cells that can activate naïve T cells. They can be divided into several subsets based on their origin, location, and function. mDCs play a unique role in the generation of T lymphocyte-mediated immune responses [13]. The ability of mDCs to activate T cells depends on their maturation and functional differentia-

tion status and is also affected by environmental factors such as microbial products, cytokines, oxygenase, metabolites, and immunosuppressive agents [14, 15]. mDCs can regulate the function and proliferation of T cells and promote the activation of Th1 and CD8+ T cells in immune responses. mDCs also play a role in the regulation of Treg differentiation by modulating the expression of programmed cell death ligand 1 and T cell costimulatory molecules [16]. In mice, monocytes can differentiate to mDCs under inflammatory conditions *in vivo* or *in vitro* after stimulation with granulocyte macrophage colony-stimulating factor and interleukin 4 [17]. mDCs highly express CD11c, MHC-II, and DC-specific transcription factors [18]. Our previous study showed that the mDCs of newly diagnosed SAA patients exhibit elevated PKM2 protein levels and that this protein is involved in the activation of mDC function [8].

In this study, shikonin and CsA were used to treat AA model mice to observe their effect on the immune status of these mice. CB6F1 mice were used to generate AA mouse models of bone marrow failure by inducing autoimmune attack. The parental lines of the CB6F1 mice were Balb/C mice (H2^{d/d}) and C57BL/6 mice (H2^{b/b}). Because CB6F1 mice are MHC-heterozygous hybrids carrying H2^{b/d}, they could easily initiate autoimmune reaction with high complement level. In a previous study, a lethal dose of irradiation was found to damage the hematopoietic tissue of the bone marrow microenvironment in CB6F1 mice. At this point, the C57BL/6 mouse (H2^{b/b}) lymphocytes, which are MHC-mismatched, could induce sustained hematopoietic impairment of the immune bone marrow [19]. In our study, the SAA model mice showed a decrease in blood counts. A decreased ratio of CD4+/CD8+ cells, increased expressions of CD80 and CD86 on mDCs, increased levels of CTL degranulation, and inadequate Treg number were also detected. The state of immune dysfunction in these AA mice was similar to that in SAA patients. We found that the proportion of PKM2+ mDCs in the AA mice was elevated and was significantly positively correlated to the function of mDCs and CTLs. PKM2 activation in mDCs was confirmed in *in vivo* mice experiments, but the PKM2 levels in mDCs

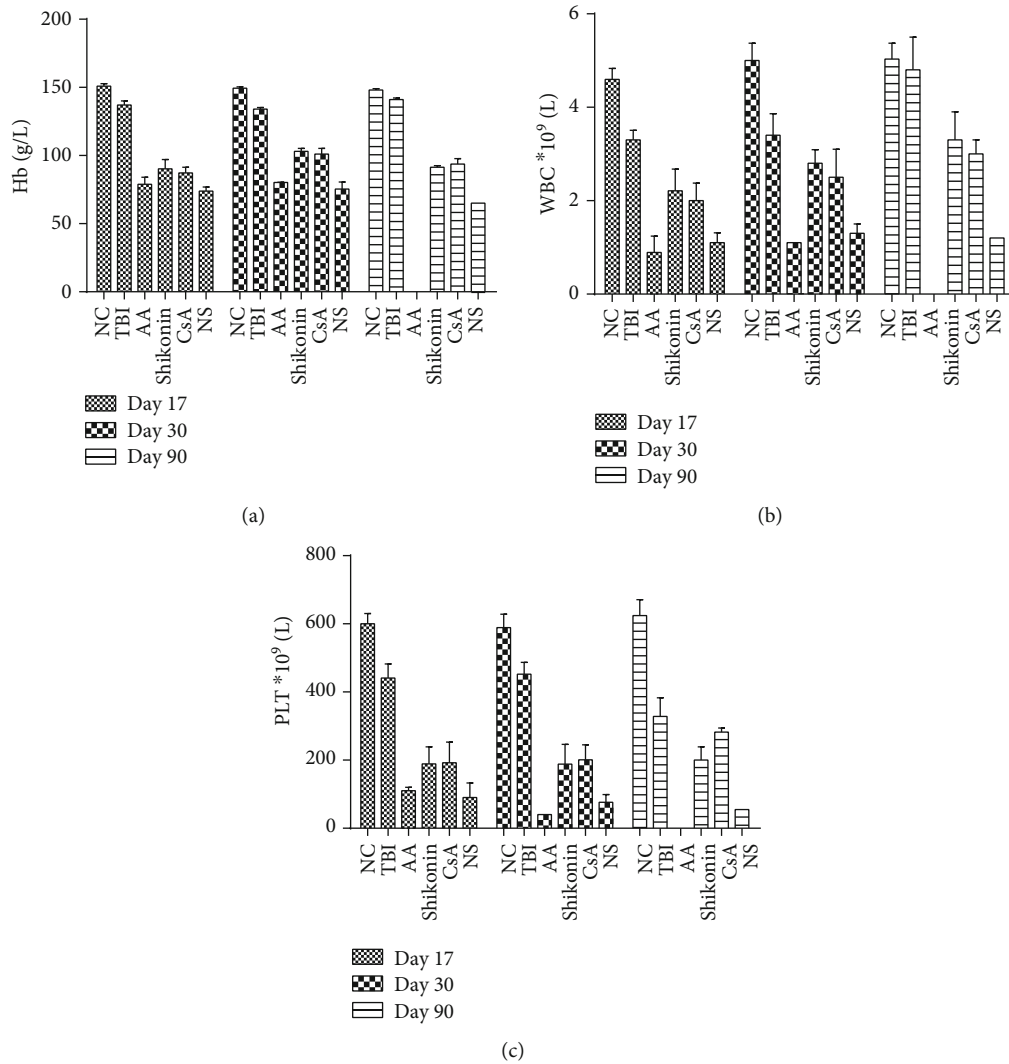


FIGURE 7: Mice peripheral blood counts at day 17, day 30, and day 90. Until the time of death, no improvement was observed in (a) Hb, (b) WBC, and (c) PLT in the mice from the AA model and NS groups, whereas the blood counts from the shikonin and CsA groups gradually recovered over time, especially leukocytes ($p < 0.05$). AA: aplastic anemia ($n = 17$); TBI: total body irradiation ($n = 10$); NC: normal control ($n = 10$); shikonin ($n = 10$); CsA: cyclosporin A ($n = 10$); NS: normal saline ($n = 10$).

decreased after shikonin or CsA treatment. The expression of mDC co-stimulatory molecules CD80 and CD86 increased in the AA mice and that of CD86 decreased after shikonin treatment. This finding suggests that shikonin reduced the expression of mDC costimulatory molecules by reducing PKM2 levels, which inhibited mDC activation, rather than reducing the number of mDCs. The glucose consumption level, pyruvate generation level, and ATP content were also increased in the mDCs of the AA mice. This finding suggests that shikonin blocked cell glycolytic metabolism to some extent, thereby inhibiting the activation and proliferation of mDCs. The level of glycolysis in the mDCs also decreased after shikonin and CsA treatments.

During antigen presentation, mDCs gradually mature and express high levels of the costimulatory molecules CD80 and CD86 [20]. CTLs are activated through the combination of mDCs and numerous cellular signals, which initi-

ates an immune response. As the main effector cells with cytotoxic function CTLs are closely related to SAA pathogenesis, so we also explored the effect of shikonin on CTLs in the AA mice. Our data showed that shikonin decreased the level of the cytotoxic molecule granzyme B in CD8⁺ T cells and could regulate the ratio of CD4⁺/CD8⁺ cells and the Treg count in the AA mice. The effects of shikonin were similar to those of CsA. The expression of CD107a/b on the surface of CD8⁺ T cells in the AA group increased relative to that in the controls but reduced after shikonin or CsA administration. CD8⁺ T cells store most of the cytotoxic molecules in cytotoxic granules, which degranulate upon contact with the target cell. As a lysosomal-associated membrane glycoprotein, CD107a/b is expressed on the surface of CD8⁺ T cells [21]. When CD8⁺ T cells come in contact with target cells, the costimulatory molecules fuse with the target cell membrane; this causes the release of the cytotoxic molecules

from the T cell granules, eventually leading to the death of the target cells [22]. The upregulation of CD107a/b expression on CTLs observed in our study was consistent with the increase in granzyme B secretion. Thus, the results above indicate that the CTL activity in the AA group was significantly increased relative to that in the controls but reduced after administering shikonin or CsA. We speculate that the changes in CTL function were due to shikonin-mediated inhibition of PKM2 levels in mDCs, which in turn regulated the expression of mDC costimulatory molecules and inflammatory factors. Recently, the role of Treg cell population in SAA pathogenesis has attracted much research attention [10]. Tregs are believed to control the progression of autoimmunity in AA by suppressing overactive T cells and preventing the antigen presentation process of mDCs [23]. Our data showed inadequate numbers of Tregs in the AA mice. When treated with shikonin or CsA, the number of Tregs increased, which is consistent with the insufficient Tregs found in human AA that cannot inhibit the autologous effector T cells, eventually leading to T cell-mediated bone marrow failure. After shikonin treatment reduced the activity of mDCs, the inhibitory effect of mDCs on Tregs also decreased.

Additionally, we evaluated the survival rates and peripheral blood counts of mice at different time points to explore the effects of shikonin and the immunosuppressant CsA. Our SAA mouse model generated by the combined use of TBI plus lymphocyte infusion exhibited a mortality rate of almost 100% within 32 days. However, treatment with shikonin or CsA reduced the mortality rate to 40%. The survival rate increased and PKM2 expression decreased after shikonin administration in the shikonin group compared with those in the AA model and NS groups. The finding demonstrated that the high survival rates in mice treated with shikonin were associated with shikonin-induced inhibition of PKM2 expression. After a short period of bone marrow suppression, the blood counts of the TBI group quickly returned to the normal levels. However, the blood counts of the AA model and NS groups showed no improvement until the time of death, whereas those, especially leukocyte counts, of the shikonin and CsA groups gradually recovered. This finding indicates that the mice experienced partial remission in blood counts after shikonin or CsA treatment compared with the AA model and NS groups. This result is consistent with our previous finding in *in vitro* studies using human cell lines that the PKM2 expression level in the mDCs is significantly associated with SAA progression [9]. Shikonin administration in AA mice was conducive to disease recovery, which again confirmed the therapeutic significance of shikonin against SAA pathogenesis.

In summary, shikonin could inhibit the activation and proliferation of mDCs and inhibit the activation of their downstream immune effector cells by reducing PKM2 levels in mDCs. Thus, shikonin is a potential new drug target for SAA immunotherapy.

Data Availability

The data used to support the findings of this study are available from the corresponding author upon request.

Ethical Approval

All applicable international, national, and/or institutional guidelines for the care and use of animals were followed. All procedures performed in studies involving animals were in accordance with the ethical standards of the institution or practice at which the studies were conducted.

Conflicts of Interest

The authors confirm that there are no conflicts of interest.

Authors' Contributions

All authors listed have contributed to conception, design, gathering, analysis or interpretation of data and have contributed to the writing and intellectual content of the article. All authors gave informed consent to the submission of this manuscript. Mengying Zheng, Bingnan Liu, Yuanyuan Shao, and Luogang Hua contributed equally to this work.

Acknowledgments

This work was supported by the National Natural Science Foundation of China (81570106, 81570111, 81400085, and 81400088), Tianjin Municipal Natural Science Foundation (14JCYBJC25400, 15JCYBJC24300, and 12JCZDJC21500), and Tianjin Science and Technology support key project plan (20140109).

Supplementary Materials

Figure S1: the percentage of mDCs in the peripheral blood of mice in the NC, TBI, AA, PKM2-i, CsA, and NS groups were tested by FCM. Among mononuclear cells, mDCs were identified as CD11c+MHC II+. There was no significant difference among the six groups. ($p > 0.05$). Table S1: specific operational steps in mice. (*Supplementary Materials*)

References

- [1] C. Arieta Kuksin, G. Gonzalez-Perez, and L. M. Minter, "CXCR4 expression on pathogenic T cells facilitates their bone marrow infiltration in a mouse model of aplastic anemia," *Blood*, vol. 125, no. 13, pp. 2087–2094, 2015.
- [2] C. Liu, W. Sheng, R. Fu et al., "Differential expression of the proteome of myeloid dendritic cells in severe aplastic anemia," *Cellular Immunology*, vol. 285, no. 1-2, pp. 141–148, 2013.
- [3] F. V. Filipp, "Cancer metabolism meets systems biology: pyruvate kinase isoform PKM2 is a metabolic master regulator," *Journal of Carcinogenesis*, vol. 12, no. 1, p. 14, 2013.
- [4] Z. Zhang, Q. Liu, Y. Che et al., "Antigen presentation by dendritic cells in tumors is disrupted by altered metabolism that involves pyruvate kinase M2 and its interaction with SOCS3," *Cancer Research*, vol. 70, no. 1, pp. 89–98, 2010.
- [5] X. Ning, H. Qi, R. Li et al., "Discovery of novel naphthoquinone derivatives as inhibitors of the tumor cell specific M2 isoform of pyruvate kinase," *European Journal of Medicinal Chemistry*, vol. 138, pp. 343–352, 2017.
- [6] W. Li, J. Liu, and Y. Zhao, "PKM2 inhibitor shikonin suppresses TPA-induced mitochondrial malfunction and

- proliferation of skin epidermal JB6 cells,” *Molecular Carcinogenesis*, vol. 53, no. 5, pp. 403–412, 2014.
- [7] J. Chen, J. Xie, Z. Jiang, B. Wang, Y. Wang, and X. Hu, “Shikonin and its analogs inhibit cancer cell glycolysis by targeting tumor pyruvate kinase-M2,” *Oncogene*, vol. 30, no. 42, pp. 4297–4306, 2011.
- [8] F. Ni, X. Huang, Z. Chen, W. Qian, and X. Tong, “Shikonin exerts antitumor activity in Burkitt’s lymphoma by inhibiting C-MYC and PI3K/AKT/mTOR pathway and acts synergistically with doxorubicin,” *Scientific Reports*, vol. 8, no. 1, p. 3317, 2018.
- [9] C. Liu, M. Zheng, T. Wang et al., “PKM2 is required to activate myeloid dendritic cells from patients with severe aplastic anemia,” *Oxidative Medicine and Cellular Longevity*, vol. 2018, Article ID 1364165, 9 pages, 2018.
- [10] J. Fang, L. Lin, Y. Wang et al., “Regulatory T cells and CD20⁺ B cells in pediatric very severe aplastic anemia: possible clinical markers for evaluating the therapeutic efficacy and prognosis,” *Hematology*, vol. 23, no. 10, pp. 823–827, 2018.
- [11] J. C. Tang, J. Zhao, F. Long et al., “Efficacy of shikonin against esophageal cancer cells and its possible mechanisms *in vitro* and *in vivo*,” *Journal of Cancer*, vol. 9, no. 1, pp. 32–40, 2018.
- [12] T. Li, F. Yan, R. Wang, H. Zhou, and L. Liu, “Shikonin suppresses human T lymphocyte activation through inhibition of IKK β activity and JNK phosphorylation,” *Evidence-based Complementary and Alternative Medicine*, vol. 2013, Article ID 379536, 13 pages, 2013.
- [13] Q. Lin, Z. Liu, M. Luo et al., “Visualizing DC morphology and T cell motility to characterize DC-T cell encounters in mouse lymph nodes under mTOR inhibition,” *Science China. Life Sciences*, vol. 62, no. 9, pp. 1168–1177, 2019.
- [14] C. M. Krawczyk, T. Holowka, J. Sun et al., “Toll-like receptor-induced changes in glycolytic metabolism regulate dendritic cell activation,” *Blood*, vol. 115, no. 23, pp. 4742–4749, 2010.
- [15] C. Kong, R. Gao, X. Yan et al., “Alterations in intestinal microbiota of colorectal cancer patients receiving radical surgery combined with adjuvant CapeOx therapy,” *Science China Life Sciences*, vol. 62, no. 9, pp. 1178–1193, 2019.
- [16] B. Kumar and R. N. Bamezai, “Moderate DNA damage promotes metabolic flux into PPP via PKM2 Y-105 phosphorylation: a feature that favours cancer cells,” *Molecular Biology Reports*, vol. 42, no. 8, pp. 1317–1321, 2015.
- [17] R. Kushwah and J. Hu, “Role of dendritic cells in the induction of regulatory T cells,” *Cell & Bioscience*, vol. 1, no. 1, p. 20, 2011.
- [18] H. P. Morgan, I. McNae, M. W. Nowicki et al., “Allosteric mechanism of pyruvate kinase from *Leishmania mexicana* uses a rock and lock model,” *The Journal of Biological Chemistry*, vol. 285, no. 17, pp. 12892–12898, 2010.
- [19] S. Nakao, “Guest editorial: advances in the management of acquired aplastic anemia,” *International Journal of Hematology*, vol. 97, no. 5, pp. 551–552, 2013.
- [20] Y. Huang, Y. Yin, Y. Gu et al., “Characterization and immunogenicity of bone marrow-derived mesenchymal stem cells under osteoporotic conditions,” *Science China Life Sciences*, pp. 1–14, 2019.
- [21] P. Wolint, M. R. Betts, R. A. Koup, and A. Oxenius, “Immediate cytotoxicity but not degranulation distinguishes effector and memory subsets of CD8⁺ T cells,” *The Journal of Experimental Medicine*, vol. 199, no. 7, pp. 925–936, 2004.
- [22] G. de Saint Basile, G. Ménasché, and A. Fischer, “Molecular mechanisms of biogenesis and exocytosis of cytotoxic granules,” *Nature Reviews Immunology*, vol. 10, no. 8, pp. 568–579, 2010.
- [23] G. Guan, S. Ding, Y. Yin, V. Duraipandiyar, N. A. al-Dhabi, and G. Liu, “*Macleaya cordata* extract alleviated oxidative stress and altered innate immune response in mice challenged with enterotoxigenic *Escherichia coli*,” *Science China Life Sciences*, vol. 62, no. 8, pp. 1019–1027, 2019.